SEDIMENTOLOGY AND DIAGENESIS OF MIDDLE AND UPPER CAMBRIAN PLATFORM CARBONATES AND SILICICLASTICS, PORT AU PORT PENINSULA, NEWFOUNDLAND

NANCY CHOW

SEDIMENTOLOGY AND DIAGENESIS OF MIDDLE AND UPPER CAMBRIAN PLATFORM CARBONATES AND SILICICLASTICS, PORT AU PORT PENINSULA, WESTERN NEWFOUNDLAND

by

© Nancy Chow, B.Sc.

A thesis submitted to the School of Graduate Studies, in partial fulfillment of the requirements for the degree of Doctor of Philosophy

Department of Earth Sciences
Memorial University of Newfoundland

September 1985

St. John's Newfoundland

"Exhilaration is that feeling you get just after a great idea hits you and just before you realize what's wrong with it."

(Unknown)

ABSTRACT

The Port au Port Group is an outer shelf, peritidal carbonate and siliciclastic platform deposit composed of six lithofacies: (1) parted limestone; (2) grey and variegated shale; (3) ooid calcarenite; (4) carbonate laminite; (5) stromatolite and thrombolite mound; and (6) mixed glauconitic sandstone and oolite. Ooid calcarenites, carbonate laminites, and variegated shales together were deposited as a series of carbonate sand shoals in which the shallow-subtidal and intertidal zones were each regimes of in situ ooid formation and accumulation. Parted limestones and grey shales were deposited on muddy tidal flats leeward of the carbonate shoals. Both muddy tidal flats and carbonate sand shoals were sites of stromatolite and thrombolite mound growth. Siliciclastic sands and silts represent eolian deposits and reworking of nearshore siliciclastics.

The lithofacies occur in two types of meter-scale assemblages: (1) predictable meter-scale, shallowing-upward cycles of parted limestone and shale deposited in the muddy tidal flats, which were largely controlled by variable rates of sedimentation; and (2) unpredictable meter-scale assemblages of ooid calcarenite and carbonate laminite, which resulted from the sporadic but frequent migration of the carbonate shoals. These two assemblages together form Grand Cycles that reflect the complex interplay of sea-level eustasy and regional variations in sedimentation and environmental conditions. These Grand Cycles are distinct from western North American cycles because they are composed almost entirely of peritidal sediments; thinness of the cycles; and restricted areal occurrence. These differences may reflect narrower

shelf widths; lower rates of sedimentation; and lower amplitudes of relative sea-level rise on the northeastern margin of the North American craton compared to the western margin.

Concentric ooids in intertidal brown oolites were originally bimineralic: aragonitic laminae are now blocky calcite and laminae of fibrous and micritic Mg calcite have altered to calcite with well-preserved fabrics. Radial ooids in subtidal grey oolite were Mg calcite only and underwent progressive alteration during burial to give rise to a variety of cortical fabrics, ranging from radial to blocky calcite. The facies-specific nature of ooid mineralogy and morphology suggests that local environmental conditions strongly influenced ooid formation, particularly turbulence and sea floor topography.

The spectrum of calcite cements, mudstones and dolomites represents a protracted history of diagenesis, which includes: (1) synsedimentary peritidal lithification, erosion and dolomitization; (2) possible shallow-burial meteoric lithification and alteration of metastable carbonates; (3) deep-burial lithification and dolomitization; and (4) cementation and dedolomitization related to uplift. Peritidal lithification and dolomitization, along with minor shallow-burial lithification, determined the final appearance of the rocks; deeper burial and re-exposure events resulted in only a diffuse overprinting of all lithofacies.

ACKNOWLEDGEMENTS

My greatest appreciation is extended to my thesis supervisor, N. P. James, for suggesting this project and his advice, encouragement, text editing and endless enthusiasm. I am also grateful for the opportunity to do field work in the Canadian Rockies and western U.S.A.. I thank R. K. Stevens for providing Chateau Picadilly on the Port au Port Peninsula as living accommodations for much of the field work. H. Wood, S. Scott and A. Pye provided capable and tolerant field assistance.

This study was financed by a Texaco Canada Resources research grant and Natural Sciences and Engineering Research Council funding to N. P. James. My financial support was provided by a Natural Sciences and Engineering Research Council postgraduate scholarship and Memorial University Fellowship.

I also thank the following people for their assistance and advice during the course of this study: J. Aitken for his hospitality and discussions of Grand Cycles during the field trip to the Rockies; D. Boyce for his trilobite identifications; L. Coniglio for editing and proof-reading the final draft, help in assembling of the final copies and providing "break-times"; M. Coniglio for thorough criticism of Chapters 1, 5, 6, 7, 8, and 9, advice in unravelling the mysteries of "Perfect Writer" and designing a tractor-feed; A. Desrochers for discussion of various aspects of the study; C. Emerson for assistance on the SEM; R. Hiscott for constructive criticism of Chapter 4; I. Knight for showing me sections at Canada Bay and thorough editing of Chapter 4;

T. Lane for discussions of ideas in Chapter 8; W. Marsh for photographic services, technical advice and darkroom facilities; P. Myrow for constructive criticisms of Chapter 4; G. Narbonne for discussion of trace fossils and providing a copy of N. Richards' B.Sc. thesis; L. Nolan and W. Howell for drafting advice; A. Pye for plate reproduction; A. Rowell and M. Rees for their hospitality and discussions during the visit to Lawrence, Kansas; S. Rowland for his hospitality and discussions during the field trip to Nevada; R. Smyth for discussion of White Bay outcrops; Texaco Canada Resources and Amoco Canada for making thin-sections; F. Thornhill, L. Warford, G. Ford and R. Soper for making most of the thin sections and providing numerous rock saw belts and facilities for polishing and slabbing; Westfield Minerals for data on the Goose Arm section; Mr. P. Periwinkle, Esq. for his company during long nights of word processing.

Finally, I thank my parents for their constant support and encouragement and the Coniglios (and their circus) for taking me in.

TABLE OF CONTENTS

LIST OF FIGURES

LIST OF TABLES

LIST OF PLATES

Chapter 1

INTRODUCTION

1.1 PROLOGUE

The accessibility of shallow-marine carbonate systems, both modern and ancient, and the occurrence of some of the world's largest hydrocarbon reservoirs in Paleozoic shelf carbonates have prompted investigations of these sediments worldwide. The plethora of depositional and diagenetic models, based largely upon classic modern examples such as the Bahamian Platform and Persian Gulf have guided the interpretation of most Phanerozoic shallow-water carbonate sequences.

In North America, well-exposed Cambrian strata provide excellent opportunities for detailed sedimentologic and diagenetic studies of ancient platform carbonates. Cambrian outcrop belts occur as far south as New Mexico; as far north as the Northwest Territories; to the west in the Canadian Rockies and Great Basin; and in the Appalachian region in the east (Holland, 1971). Yet, there are surprisingly few comprehensive investigations of these rocks.

The mixed carbonate and siliciclastic sequence of Middle to Late Cambrian age in western Newfoundland is one of the most complete and

best exposed deposits of such rocks in eastern North America. Outcrops of these strata are found at numerous locations - from the Port au Port Peninsula in the south to Lower Cove near the northern tip of the Great Northern Peninsula. This study is an analysis of paleoshelf conditions, and depositional and diagenetic structures and processes in this mixed sediment sequence.

1.2 GEOLOGIC SETTING

Middle and Upper Cambrian platform sediments in western Newfoundland outcrop in a discontinuous fringe around the flanks of the Precambrian Long Range, forming a belt approximately 400 km long by 75 km wide. Generally trending southwest-northeast to west-east, the most complete sequences are present in the readily-accessible coastal exposures on the Port au Port Peninsula; the northern and southern shores of Goose Arm; the south shore of Bonne Bay; Little Coney Arm in White Bay; Canada Bay; and along the St. Barbe coast (Fig. 1.1). Inland from these coastal sections, outcrops are sporadic and poorly exposed due to dense vegetation.

The eastern part of the outcrop belt is either covered by Carboniferous rock or disappears into White Bay. The western side passes under the Gulf of St. Lawrence and/or is tectonically overlain by allochthonous rocks. Equivalent sections in Quebec and Ontario are predominantly sandstone and conglomerate; the exception being one tiny problematical exposure of Middle and Upper Cambrian limestones and

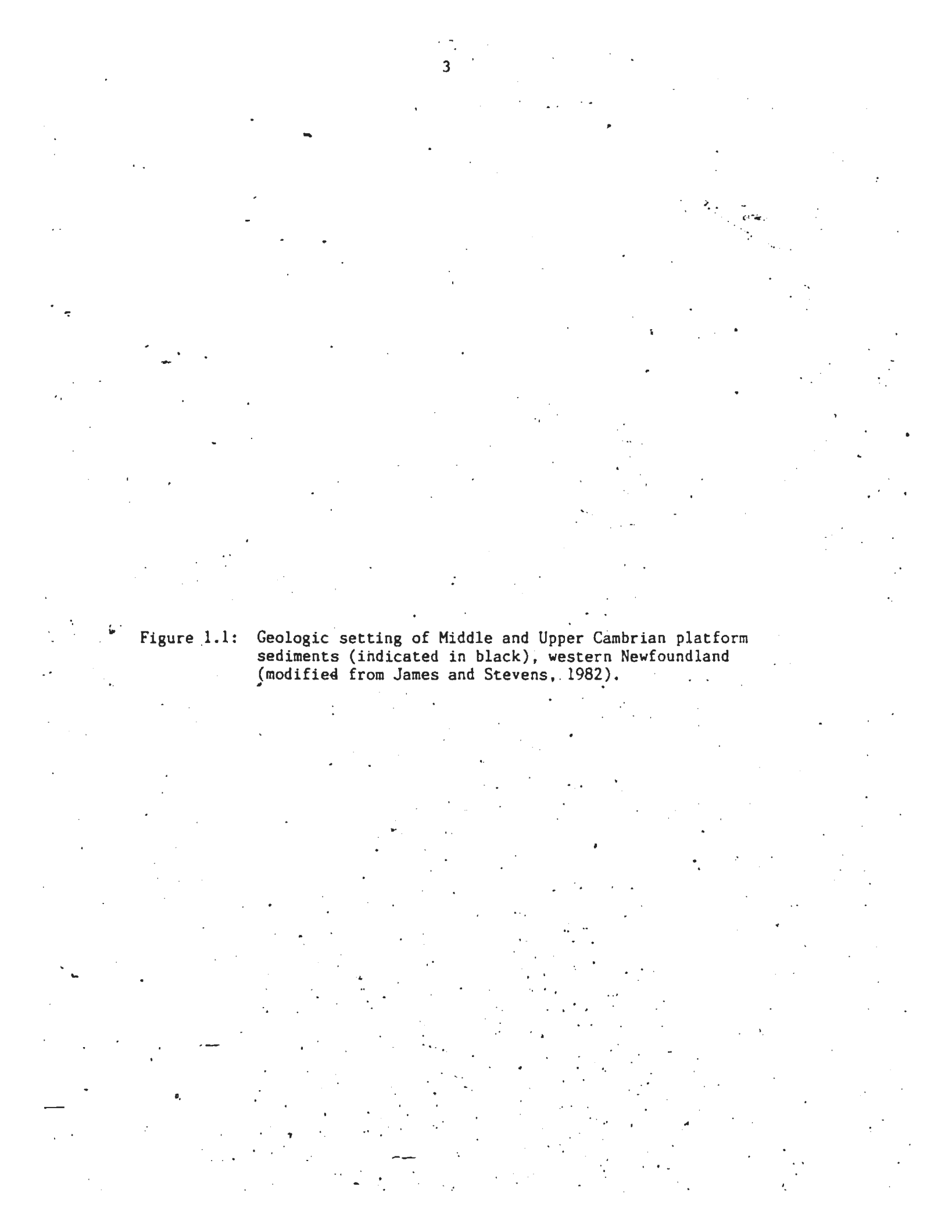

Figure 1.1: Geologic setting of Middle and Upper Cambrian platform sediments (indicated in black), western Newfoundland (modified from James and Stevens, 1982).

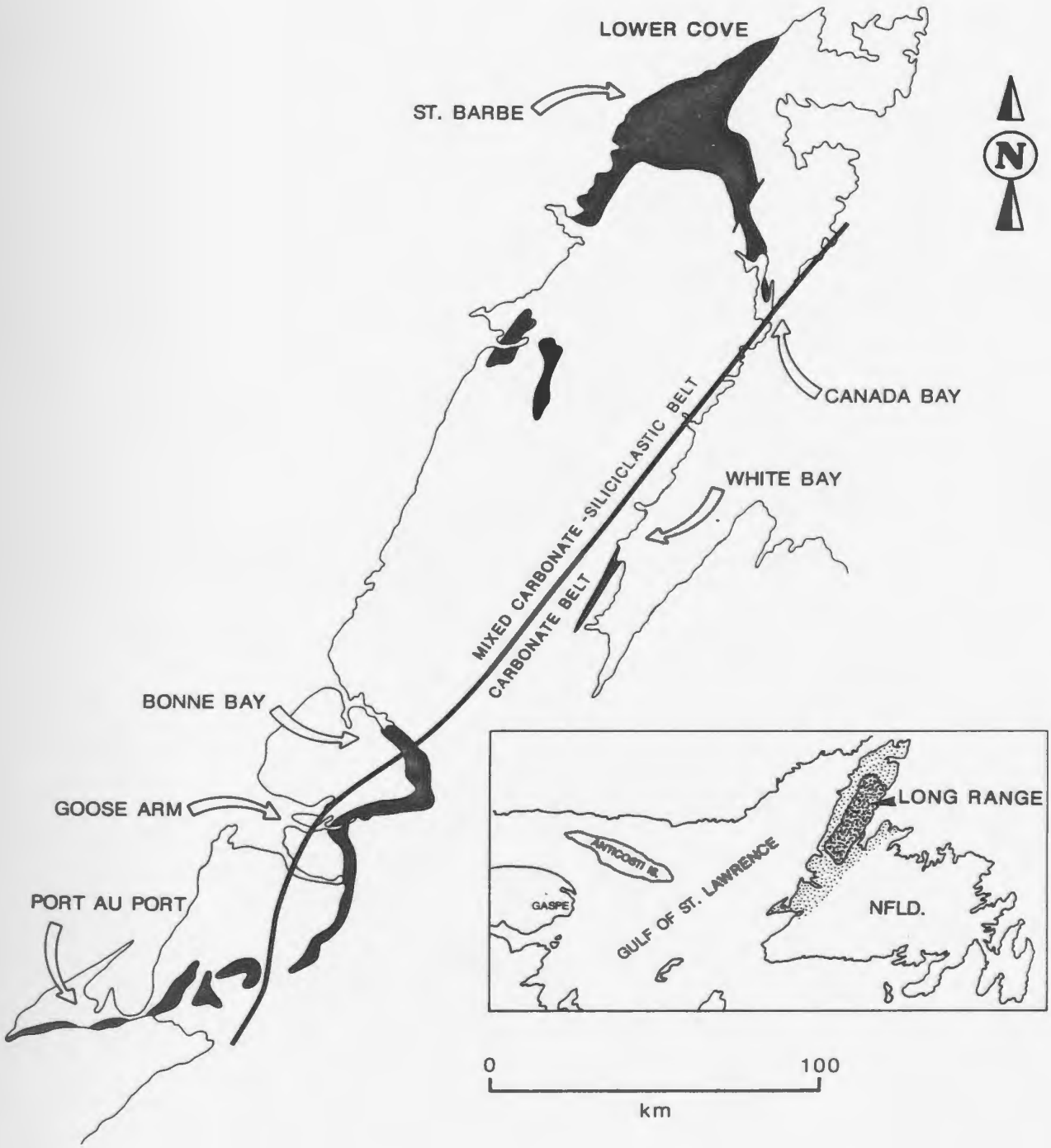
LOWER COVE
ST. BARBE
N
CANADA BAY
WHITE BAY
MIXED CARBONATE -SILICICLASTIC BELT
CARBONATE BELT
BONNE BAY
GOOSE ARM
PORT AU PORT
LONG RANGE
ANTICOSTI IS.
GASPE
GULF OF ST. LAWRENCE
NFLD.
0
100
km

shales in eastern Gaspe (Corner-of-the-Beach and Murphy Creek Formations -- North, 1971; Fritz, 1972).

The Middle and Upper Cambrian shallow-marine strata of this study is part of the tectono-stratigraphic Humber Zone of the Appalachian Orogen (Williams, 1976; 1979) which records the growth and demise of a continental margin of Iapetus. These strata represent sediments on the outer part of the stable shelf, which paleogeographic reconstructions suggest was at approximately 25 degrees S latitude, within the sub-tropical climate zone (Scotese et al., 1979). They comprise part of an eastward-thickening prism of Lower Cambrian to Middle Ordovician volcanics, siliciclastics and carbonates which rest unconformably on Grenvillian crystalline basement (Rodgers, 1968; Williams and Stevens, 1974; James and Stevens, 1982). This package is characterized by a gradual transition from siliciclastics (Lower Cambrian Hawke Bay Formation) to carbonates (Lower Ordovician St. George Group).

Foundering and destruction of the margin (Taconic Orogeny) is reflected in the upward-deepening part of the autochthonous Table Head Group of Middle Ordovician age (Klappa et al., 1980) and overlying easterly-derived siliciclastic flysch (Rodgers and Neale, 1963; Stevens, 1970). Slope and basin sediments (Cow Head and Curling Groups), coeval with the shelf deposits, occur as part of an allochthonous package which was emplaced over the shelf sediments during orogenesis (Stevens, 1970; Coniglio, 1985; James and Stevens, in prep.). The shelf-slope transition was obliterated by tectonics or obscured by rock cover. The allochthonous rocks are capped by a neoautochthonous sequence of Middle Ordovician to (?) Devonian shallow water and terrestrial carbonates and

siliciclastics (Rodgers, 1965; James and Stevens, 1982). Uplift, faulting, and exposure on the Port au Port Peninsula during the Late Devonian Acadian orogeny resulted in the development of karst topography on the exposed Cambrian and Ordovician carbonates (Dix, 1981).

The Cambrian sediments of this study are part of the extensive Cambro-Ordovician shallow shelf sequence developed on both sides of the North American continent, forming a mirror image across the craton (Holland, 1971). In the west the sequence is exposed from Mexico to the Northwest Territories in a belt at least 1100 km wide. Studies of particular interest have been conducted by Aitken (1966, 1978) in the southern Canadian Rockies and Palmer and Halley (1979) and Mount and Rowland (1981) in the Great Basin of the western United States. In the east a narrower belt generally less than 700 km wide can be traced from Alabama to Newfoundland (e.g., Palmer, 1971; Markello and Read, 1981; Pfeil and Read, 1981; Demicco, 1982). The western Newfoundland succession, in addition to being the most northerly in the Appalachians, is one of the best exposed in eastern North America. Study of exposures in the central and southern Appalachians in comparison is hampered by discontinous exposure caused by extensive glacial and soil cover; greater structural deformation; and a paucity of Cambrian fossils. Comparison of these North American Cambrian outcrops reveals lithologic differences on a detailed scale, especially between eastern and western North America, but striking similarities in the style of cyclicity and overall depositional patterns.

1.3 PREVIOUS STUDIES

The first extensive study of the geology of western Newfoundland was conducted in 1861 to 1863 by James Richardson of the Geological Survey of Canada, the results of which were published in Logan (1863).

Schuchert and Dunbar (1934), incorporating the work of Richardson, completed the first comprehensive stratigraphic study of western Newfoundland, which in turn has provided the framework for much of the later work on Lower Paleozoic strata. They proposed the name, March Point formation, for Upper Cambrian strata on the southern shore of the Port au Port Peninsula between Cape St. George and Big Cove Brook (Fig. 1.2), including within this sequence sediments now recognized to be of Middle and Late Cambrian age. A structurally-repeated Middle to Upper Cambrian section from Jerrys Nose to east of the Gravels was included in their type section of the Lower Ordovician "St. George series".

On the basis of trilobites collected by Schuchert and Dunbar (1934), Lochman (1938) subsequently divided the March Point formation into the Middle Cambrian March Point formation and the Upper Cambrian Petit Jardin formation.

Later mapping projects in western Newfoundland helped delineate the distribution of Middle and Upper Cambrian strata but contributed very little to refining the stratigraphy and correlating between areas. Betz (1939) defined the Middle Cambrian Cloud Rapids and Treyton Pond Formations in the Canada Bay area and correlated them with the March Point formation of Schuchert and Dunbar (1934). Troelsen (1947) later

Figure 1.2: Outcrop localities on Port au Port Peninsula, western Newfoundland (modified from Levesque, 1977; Schillereff and Williams, 1979; James and Stevens, 1982).

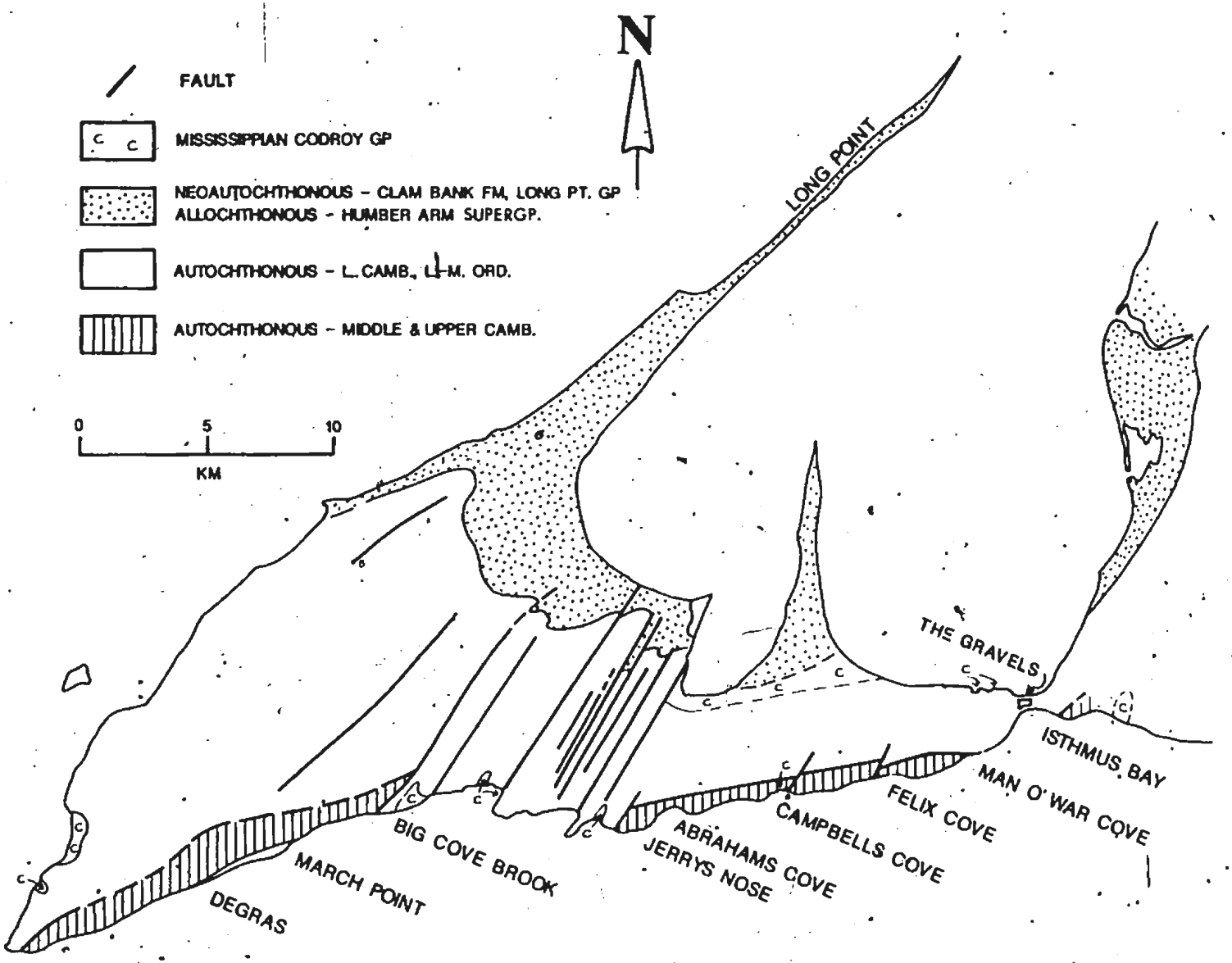
N
FAULT
MISSISSIPPIAN CODROY GP
NEOAUTOCHTHONOUS – CLAM BANK FM, LONG PT. GP
ALLOCHTHONOUS – HUMBER ARM SUPERGP.
AUTOCHTHONOUS – L. CAMB., L–M. ORD.
AUTOCHTHONOUS – MIDDLE & UPPER CAMB.
0
5
10
KM
LONG POINT
THE GRAVELS
ISTHMUS BAY
MAN O' WAR COVE
FELIX COVE
CAMPBELLS COVE
ABRAHAMS COVE
JERRYS NOSE
BIG COVE BROOK
MARCH POINT
DEGRAS

examined the geology of the Bonne Bay area and proposed the name, East Arm Formation, for Upper Cambrian limestone, dolostone and shale exposed along the southwest shore of East Arm. Walthier (1949) in his re-examination of the Cambrian and Ordovician type sections of Schuchert and Dunbar (1934) considered the lower 145 m of the St. George series to be part of the Middle Cambrian March Point and Upper Cambrian Petit Jardin Formations. Lilly (1961) in mapping the Cambro-Ordovician strata along the Humber Gorge and in Goose Arm proposed the name, Penguin Cove Formation, to describe probable Lower Cambrian sediments exposed in Goose Arm and the Reluctant Head Formation for Upper Cambrian strata in the Humber Gorge. Lock (1969) in his examination of Lower Paleozoic strata in the White Bay area reinterpreted the Cambro-Ordovician Doucers Formation (Heyl, 1937) to be intermediate between the autochthonous platform carbonates and the allochthonous slope sediments (Cow Head Group).

Kindle and Whittington (1965) and Whittington and Kindle (1966, 1969) recognized new exposures of Cambrian strata based on trilobite discoveries on the Port au Port Peninsula and along the Strait of Belle Isle. Their work indicated that much of the St. George type section as defined by Schuchert and Dunbar (1934) is really of Late Cambrian age and that strata along the Strait of Belle Isle previously thought to be part of the St. George series (Schuchert and Dunbar, 1934) were of Middle Cambrian age.

Smit (1971) and Swett and Smit (1972) re-examined the Cambro-Ordovician shallow-marine sequence and presented the first account of the sedimentology and diagenesis of the units. They

recognized the predominance of shallow subtidal to supratidal sediments and proposed the following diagenetic history based primarily on oolitic carbonates on the Port au Port Peninsula: (1) recrystallization; (2) first dolomitization; (3) silicification; (4) calcitization; and (5) second dolomitization. Comparison of the sequence in western Newfoundland with correlative sections in northwest Scotland and central Greenland revealed stratigraphic, sedimentologic, geochemical and diagenetic similarities suggesting common depositional and diagenetic histories for these three regions.

More recent studies of the Cambro-Ordovician succession have concentrated on detailed mapping and determining the basic sedimentology of the sequence. The Newfoundland Department of Mines and Energy have undertaken a stratigraphic mapping program of Lower Paleozoic rocks on the Great Northern Peninsula, particularly along the St. Barbe coast (Knight, 1977; Knight, 1978; Knight, 1980a; Knight, 1980b); Canada Bay (Knight, 1979; Knight, 1980b; Knight and Saltman, 1980; Stouge, 1981); and White Bay (Smyth, 1981; Smyth and Schillereff, 1982). A new Cambrian stratigraphy, incorporating trilobite data collected by Boyce (1977), was proposed consisting of five informal units (Knight, 1977): the Micrite Formation which is correlative with the March Point Formation; and the overlying Lower Dolostone, Middle Stromatolite, Upper Dolostone and Cherty Dolomite Members.

Researchers at Memorial University have conducted detailed investigations of Lower Cambrian to Middle Ordovician sediments throughout western Newfoundland (Lower Cambrian -- James and Kobluk, 1978; James and Klappa, 1983; Middle Cambrian to Lower Ordovician

Levesque, 1977; Lower Ordovician -- Pratt, 1979; Middle Ordovician, Klappa et al., 1980).

Levesque (1977) summarized most of the pertinent literature on the autochthonous Cambro-Ordovician platform sediments and presented the first detailed descriptions, correlations and sedimentologic interpretations of the sequence since the work of Schuchert and Dunbar (1934). He recognized the cyclic and "high energy" features of the Middle and Upper Cambrian sequence and proposed a revised stratigraphy: the March Point and overlying Petit Jardin Formations on the Port au Port Peninsula; the Wolf Brook and Blue Cliff Formations at Goose Arm; the South Head and East Arm Formations at Bonne Bay; and the upper Hawke Bay Formation at Hawkes Bay.

1.4 APPROACH TO STUDY

1.4.1 Objectives and Database

The objectives of this project are twofold: (1) a detailed facies analysis of the Middle and Upper Cambrian shallow-marine sediments and (2) an evaluation of the diagenetic history of the sequence on the Port au Port Peninsula, with specific emphasis on diagenetic products and processes in oolites and lime mudstones.

On the Port au Port Peninsula, accessible sea cliffs and wave-cut platforms along the southern shore expose a nearly continuous sequence of Middle and Upper Cambrian limestones, dolostones and siliciclastics

which show considerable diversity of sedimentary textures (Fig. 1.2). Textural preservation is excellent with the sections subjected to only gentle folding and minor faulting during Acadian orogenesis. Outcrops in areas north and east of the Port au Port Peninsula, particularly Goose Arm, White Bay and Canada Bay, exhibit increasing dolomitization and deformation, and decreasing lithological diversity. For these reasons, the outcrops of the Port au Port Peninsula have been selected as the type area and are the main database for this study. Information from other Cambrian outcrops in western Newfoundland, however, is also utilized in the study.

An integration of field and petrographic evidence provides the basis for this study and is supplemented by cathode luminescence; scanning electron microscopy; and stable isotopic analyses. Field work was carried out in three summers from 1982 to 1984. Stratigraphic sections were measured in seven areas in western Newfoundland: Degras, March Point, Abrahams Cove, Campbells Cove, Felix to Man O' War Coves on the Port au Port Peninsula; east of Isthmus Bay; and Little Coney Arm in White Bay (see Appendix B; Figs. B.1 to B.7). Reconnaissance work was conducted along the St. Barbe coast (from St. Barbe Bay to Lower Cove), Goose Arm and Canada Bay. Selected outcrops in the Canadian Rockies and Great Basin (central Utah and Nevada) were also briefly examined.

Each of the seven sections was measured using a range pole. Detailed descriptions of colour, lithology, and sedimentary structures were made, using the classification of Dunham (1962). Particular attention was paid to unstylolitized lithologic contacts, especially between fine-grained limestone and dolostone, and the nature of vertical facies changes.

Approximately 600 hand samples were collected and slabbed. 550 thin sections were examined after being stained with Alizarin Red-S and potassium ferricyanide to differentiate calcite from dolomite and qualitatively determine iron content[1]. 90 of these thin sections were polished and examined with cathode luminescence; 35 samples were analyzed for their stable isotope content; 10 samples were examined using scanning electron microscopy (SEM).

1.4.2 Organization

Division of this thesis into Parts "A" (Chapters 2-4) and "B" (Chapters 5-9) reflects the twofold objective of the study. Part A includes the stratigraphy of the sequence and a description of the provisional lithostratigraphic units. It also deals with various aspects of the sedimentology of mixed carbonates and siliciclastics, including major lithofacies, their arrangement into facies sequences, possible depositional mechanisms, and comparison with other North American examples. Part B uses the sedimentologic framework to evaluate carbonate diagenesis on the basis of field, petrographic, cathode luminescence and stable isotope data. This part focuses on: the lithification of fine- and coarse-grained lithofacies, particularly early lithification; the nature of ooid precipitation and alteration; the origin of parted limestones; mechanical and chemical compaction; and dolomitization.

---

1. Ferroan and non-ferroan are used herein to indicate whether iron staining occurs in stained thin sections.

PART A: STRATIGRAPHY AND SEDIMENTOLOGY

INTRODUCTION

This section is a compilation of the physical aspects of the Middle and Upper Cambrian platform sequence in western Newfoundland, based primarily on sections on the Port au Port Peninsula and supplemented by reconnaissance work in specific areas on the Great Northern Peninsula, Canadian Rockies, Utah and Nevada.

Description of the provisional stratigraphic nomenclature used in this study is provided in Chapter 2. The lithostratigraphy and biostratigraphy of the type area along the southern shore of the Port au Port Peninsula are detailed. Lithologic correlations between the type area and outcrops in Goose Arm, Bonne Bay, White Bay, Canada Bay and along the St. Barbe coast are also included.

Chapter 3 is a documentation of the spectrum of shallow-marine, mixed carbonate and siliciclastic sediments. Six lithofacies, named on the basis of the most abundant rock type are recognized: (1) parted limestone; (2) shale; (3) ooid calcarenite; (4) carbonate laminite; (5) stromatolite and thrombolite mound; and (6) glauconitic sandstone and oolite. The origin of parted limestones cannot be completely explained by depositional processes and is further discussed in Chapter 6. A detailed description of the variety of ooids is given in Chapter 7 and provides additional information regarding precipitation, deposition and

alteration of these particles.

The lithofacies are arranged into vertical sedimentary assemblages, which are described in Chapter 4. Study of meter-scale assemblages and large-scale cycles (Grand Cycles) allows interpretation of possible mechanisms of formation which in turn yield information regarding the complex interplay of sedimentation, eustasy and subsidence on a mixed carbonate and siliciclastic platform. Comparisons of the large-scale cycles are made with selected Cambrian platform sequences in the Canadian Rockies; southern Great Basin of Nevada; and the southern Appalachians.

TERMINOLOGY

This section defines some of the terminology used in the first part of this thesis. Further discussion of the following terms is provided in Pettijohn (1975), Folk (1974b), and Fairbridge and Bourgeois (1978).

Bedding

Beds are the smallest lithostratigraphic units and are distinguishable from units above and below on the basis of colour, mineralogy, texture and other physical characteristics. They are distinct from laminae, which are less than 1 cm in thickness, and partings which are laminae present between thicker strata of different lithology. Thin-bedded units are greater than 1 cm but less than 10 cm in thickness whereas thick-bedded units are greater than 10 cm in thickness. Planar beds have a constant thickness and are laterally extensive. Laterally discontinuous beds are nodular or lenticular and those of variable

thickness are wavy (Reineck and Wunderlich, 1968). "Nodular" and "lenticular" have no genetic connotations.

The Wentworth grain-size scale is used to describe the dimensions of siliciclastic grains and abiotic carbonate particles. Silt-size siliciclastics (4-62.5 μm in diameter) and sand-size (up to 2 mm in diameter) siliciclastics, bioclasts and ooids are common components. The terms calcarenite and calcirudite are also used to describe grainy limestones, the former referring to sediment of sand-size calcite particles and the latter to sediment of calcite particles larger than sand size.

Carbonate beds are composed of limestone and/or dolostone. Limestones vary from lime mudstone to floatstone (sensu Dunham, 1962). Muds and mudstones (also "muddy") in this thesis refer to carbonate muds; unlithified and lithified, mud-size siliciclastics are designated siliciclastic muds and shales respectively. Usage of the term "mudstone" in this study departs from Dunham's (1962) original definition and has been broadened to include limestones composed of crystalline calcite with less than 10 % particles. The term neospar is applied to crystalline calcite formed by neomorphism of finer-textured carbonate (Nichols, 1967) which, according to Folk (1965), can be divided into micrite (less than 4 μm), microspar (4-30 μm) and pseudospar (greater than 30 μm). The same approach was used by Coniglio (1985) to describe fine-grained carbonates in the Cambro-Ordovician Cow Head Group in western Newfoundland.

Thin-bedded to laminated limestone interbedded with shale and/or

dolostone partings to thin-beds are volumetrically important. In this study, the term parted limestone (Aitken, 1966) is used to describe these rocks and has no connotation of relative limestone, shale and dolostone thicknesses. This definition includes fitted, nodular and ribbon carbonates.

Depositional Environments and Paleogeography

Interpretations of depositional environments and paleogeography presented in the first part of this thesis require clarification of some terms. The following definitions, except for shelf and tidal flat, are also used by Aitken (1978).

Shelf is that part of a continental margin situated between the cratonic shoreline and the slope and does not imply water depth. It is generally tectonically stable and undergoing slow subsidence. Platform is a depositional term, referring to a region of the shelf which has remained under shallow-water conditions.

Ancient carbonate platforms have three commonly recognized components. Carbonate sand shoal complexes include subtidal, intertidal and supratidal carbonates deposited in a high-energy area. Lower-energy tidal flats may be deposited in the lee of these shoals or at the cratonic shoreline (see James, 1984). Tidal flat deposits include a spectrum of genetically-related shallow subtidal, intertidal and supratidal, generally fine-grained sediments. Similar sediments are also deposited in intrashelf or inshore basins which lie between the shoal complexes and the cratonic shoreline (e.g., Aitken, 1978; Markello and Read, 1981).

Chapter 2

STRATIGRAPHIC FRAMEWORK

2.1 INTRODUCTION

The Middle and Upper Cambrian platform sediments in western Newfoundland have long been viewed as a complex package of strata fraught with stratigraphic and correlation problems. Recognizing these difficulties, past workers have generally proposed a separate stratigraphic terminology for each study area with few attempts at regional correlation. Several different stratigraphic classifications have been proposed since the work of Schuchert and Dunbar (1934; reviewed in Appendix A) but have not been formalized and do not conform with guidelines set out in the North American Stratigraphic Code (1983). Consequently, considerable confusion still exists regarding the stratigraphy of these rocks; the criteria for establishing stratigraphic boundaries and nomenclature; and the degree of correlation between outcrops.

Synthesis of studies conducted by the Newfoundland Department of Mines and Energy in the Great Northern Peninsula, work by Memorial University in south-central western Newfoundland (refer to "Previous Studies") and research from this study on the Port au Port Peninsula enables

refinement of the existing stratigraphic nomenclature.

The following is a description of the provisional lithostratigraphic units used in this study and is eventually intended to be a formal proposal of revised stratigraphic nomenclature.

2.2 PROPOSED STRATIGRAPHY

The autochthonous strata of Early Cambrian to Middle Ordovician age have been divided into four groups: (1) Lower Cambrian Labrador Group (Schuchert and Dunbar, 1934); (2) Middle to Upper Cambrian Port au Port Group (provisional, this study); (3) St. George Group of mainly Early Ordovician age (Schuchert and Dunbar, 1934; Knight and James, in prep.); and (4) Table Head Group of Middle Ordovician age (Klappa et al., 1980).

2.2.1 Lithostratigraphy

The Port au Port Group is composed of two repeated lithologic packages: (a) a recessive, thin-bedded sequence of silty limestone and dolostone with shales present as thin beds or partings in the carbonates and (b) a resistant sequence of thick-bedded limestones and dolostones composed mainly of ooid grainstones and laminated dolostones. These distinct lithotopes provide the basis for the subdivision of the group on the Port au Port Peninsula.

The succession is divided into three formations (Fig. 2.1) which in ascending order are: (1) the March Point Formation, a unit recognized in

Figure 2.1: Composite stratigraphic section of the Port au Port Group type section from the Port au Port Peninsula, western Newfoundland. Trilobite zones are indicated on right (references provided in text). Arrows point to approximate location of trilobite samples.

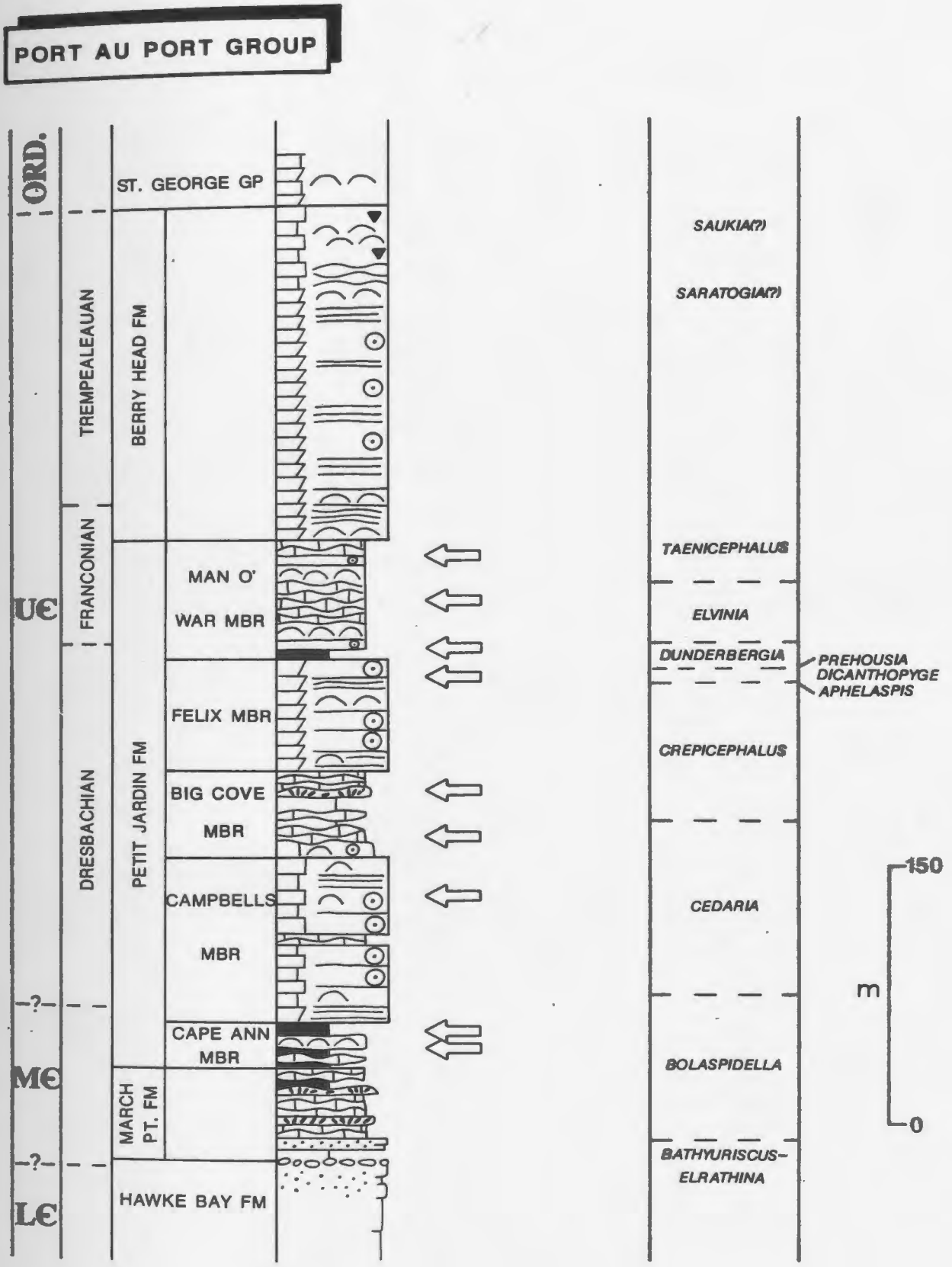
PORT AU PORT GROUP
ORD.
UC
MC
?
?
LC
TREMPEALEAUAN
FRANCONIAN
DRESBACHIAN
ST. GEORGE GP
BERRY HEAD FM
PETIT JARDIN FM
MARCH PT. FM
HAWKE BAY FM
MAN O' WAR MBR
FELIX MBR
BIG COVE MBR
CAMPBELLS MBR
CAPE ANN MBR
SAUKIA(?)
SARATOGIA(?)
TAENICEPHALUS
ELVINIA
DUNDERBERGIA
PREHOUSIA
DICANTHOPYGE
APHELASPIS
CREPICEPHALUS
CEDARIA
BOLASPIDELLA
BATHYURISCUS-ELRATHINA
150
m
0

all areas and composed of distinctive, grey and tan weathering, mudstones and dolostones, with minor grey shales, ooid grainstones and glauconitic sandstones; (2) the Petit Jardin Formation, a complex sequence of ooid grainstones, laminated dolostones and stromatolites with interbeds of mudstones, dolostones and shales that varies greatly from area to area; and (3) the laterally extensive Berry Head Formation, composed of interbedded dolomitized oolites and stromatolites, and laminated dolostones. The terms "March Point" and "Petit Jardin" have been used and revised by previous workers but are more strictly defined in this new nomenclature. A historical review of the stratigraphy is given in Appendix A and Table 2.1.

On the Port au Port Peninsula, the Petit Jardin Formation is further divisible into five members which in ascending order are: (1) the Cape Ann Member -- thin-bedded mudstones and shales punctuated by stromatolites and thrombolites and minor ooid grainstones; (2) the Campbells Member -- ooid grainstones to packstones interbedded with laminated dolostones and stromatolite and thrombolite mounds; (3) the Big Cove Member -- thin-bedded mudstones and shales and minor ooid grainstones; (4) the Felix Member -- dolomitized ooid grainstones and packstones and laminated dolostones punctuated by algal mounds and (5) the Man O' War Member -- thin-bedded mudstones and dolostones with abundant flat pebble conglomerate horizons and stromatolite and thrombolite mounds.

2.2.2 Biostratigraphy

Trilobites collected by various workers since the study by Schuchert

TABLE 2.1: SUMMARY OF PREVIOUS WORK

AUTHOR	Logan 1863	Schuchert & Dunbar 1934		Heyl 1937	Lochman 1938	Betz 1939	Troelson 1947	Walthier 1949	Lilly 1964		Whittington & Kindle 1965, 1969		Lock 1969	Smit 1971	Knight 1977	Knight & Saltman 1980	Smyth & Schillereff 1982
AREA	W.Nfld.	W.Nfld.		White Bay	Port au Port	Canada Bay	Bonne Bay,	Port au Port	Goose Arm	Humber Gorge	S.W.Nfld.	N.W.Nfld.	White Bay	W.Nfld.	St. Barbe Coast	Canada Bay	White Bay
STRATIGRAPHY (thickness in m)	Lower Silurian	Upper Cambrian	March Point Fm. 360+	Doucers fm.	Petit Jardin fm. 103	Disconformity	East Arm Fm 162	Petit Jardin Fm. 37	Unconformity	Reluctant Head Fm. 244	Petit Jardin Fm. 107	unnamed shaly dolomite	Doucers Fm.	St. George Fm.	Dolomite fm. 450	Dolomite fm. 430	Dolostone fm.
	Potsdam Group	Middle Cambrian	Non-sedimentation nterval		March Point fm. 259	Treytown Pond Fm. 183	Cover	March Point Fm. 259			March Point Fm. 267	Cloud Rapids Fm.	Cooey Arm Group	Petit Jardin Fm. 36			
						Cloud Rapids Fm. 91								March Point Fm. 280	Micrite fm. 50	Limestone fm. 40	
														Hawke Bay Fm.			

TABLE 2.1 (cont'd)

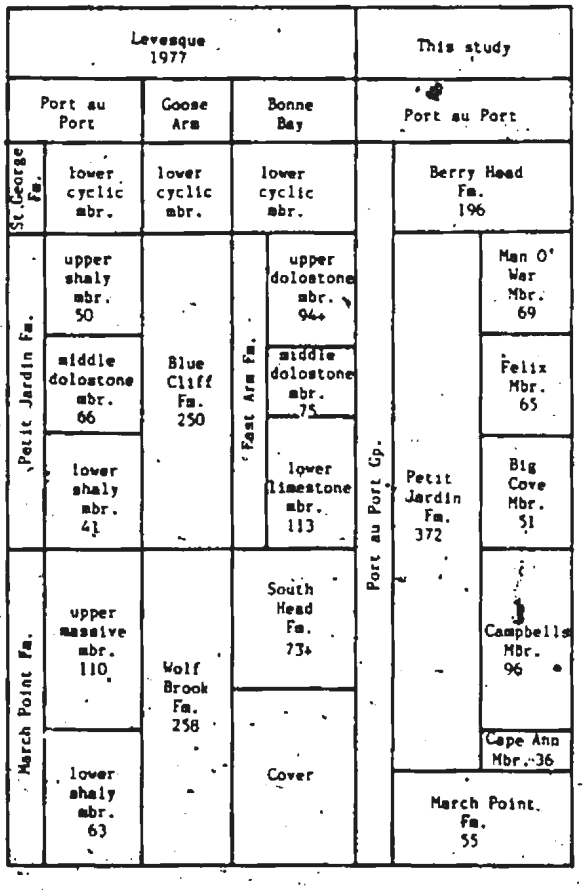

and Dunbar (1934) have permitted the Port au Port Group to be dated more precisely (Fig. 2.1; Appendix A). Lochman (1938) recognized that all the trilobites represented belong to the North American faunal province and could be correlated with standard North American faunal zones. Studies by subsequent workers (Kindle and Whittington, 1965; Whittington and Kindle, 1969; Palmer, 1969; Boyce, 1977, 1979; Levesque, 1977; Stouge and Boyce, 1983) have shown the strata to be of late Middle Cambrian to Late Cambrian age and have provided sufficient information to date the various components of the sequence.

The March Point Formation and Cape Ann Member contain trilobites of the Bathyuriscus-Elrathina and Bolaspidella zones indicating a late Middle Cambrian age (Lochman, 1938; Levesque, 1977; Boyce, 1977; Boyce, pers. comm., 1984). Trilobites collected from the lower half of the underlying Hawke Bay Formation indicate a latest Early Cambrian age Bonnia-Olenellus zone (Boyce, 1977; Levesque, 1977). To date, no fossils from the intervening Plagiura-Poliella, Albertella or Glossopleura zones (early to middle Middle Cambrian) have been discovered suggesting that either the upper part of the Hawke Bay sandstones is partly of Middle Cambrian age or a hiatus (the Hawke Bay Event) is represented by the Hawke Bay-March Point contact as suggested by Palmer and James (1979).

Trilobites collected from the Petit Jardin Formation range from the Cedaria to Taenicephalus zones of Upper Cambrian Dresbachian to early Franconian stages (Lochman, 1938; Troelsen, 1947; Levesque, 1977). Five of the ten zones (the top of the Crepicephalus zone; the Aphelaspis, Dicanthopyge and Prehousia zones; and the base of the Dunderbergia zone; Levesque, 1977) are condensed into an 8 to 12 m interval near the top of

the Felix Member indicating that a significant depositional break and/or interval of condensed sedimentation occurs near the Dresbachian-Franconian boundary.

No zone fossils have been collected from the Berry Head Formation to date. The uppermost beds of the unit, however, have yielded conodonts indicating a latest Late Cambrian age (F. O'Brien, pers. comm., 1983).

2.3 REGIONAL VARIATIONS AND CORRELATION

The three formations of the Port au Port Group as defined on the Port au Port Peninsula can be correlated between outcrop areas along the west coast of Newfoundland (Fig. 2.2) based upon evidence from this study; work of the Newfoundland Department of Mines and Energy in the Great Northern Peninsula; and detailed stratigraphic, sedimentologic and paleontologic studies by Memorial University (see "Previous Studies").

The March Point and Berry Head Formations are recognizable in all examined areas, from the Port au Port Peninsula to Canada Bay and the St. Barbe coast. The March Point Formation has a relatively uniform lithology, with the exception of the section at Goose Arm where it is composed mainly of oolitic and oncolitic limestone. The Berry Head Formation shows no significant lateral variation in lithology but does show a thickening of approximately 50 m at the White Bay section.

The Petit Jardin Formation, however, is more complex and members that are recognized in one area cannot be correlated with members identified

Figure 2.2: Correlation of stratigraphic sections of the Port au Port Group. Legend of symbols is given in Appendix B.

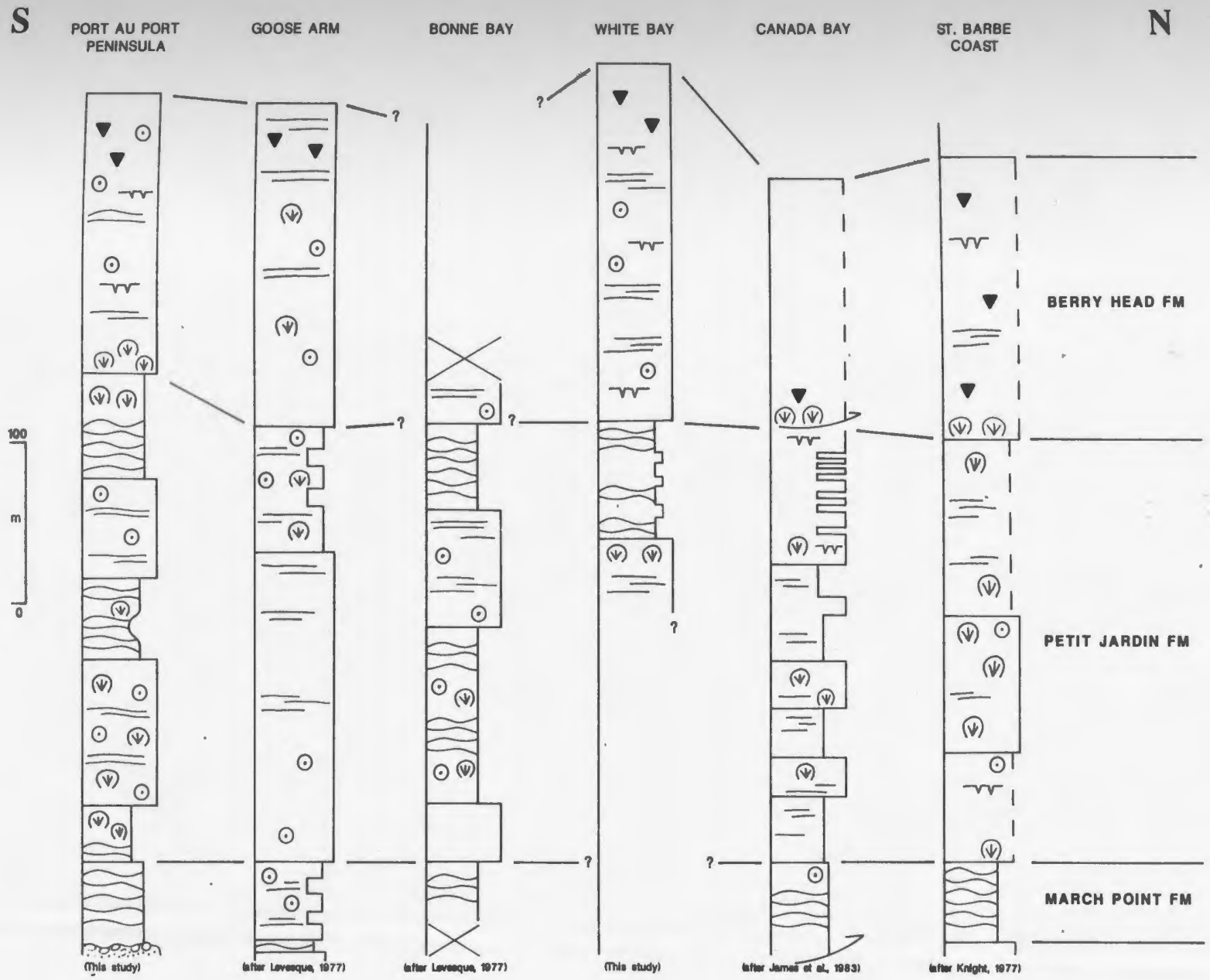
S
N
PORT AU PORT PENINSULA
GOOSE ARM
BONNE BAY
WHITE BAY
CANADA BAY
ST. BARBE COAST
100
m
0
BERRY HEAD FM
PETIT JARDIN FM
MARCH POINT FM
(This study)
(after Lavesque, 1977)
(after Lavesque, 1977)
(This study)
(after James et al., 1983)
(after Knight, 1977)

in another area. The five members defined on the Port au Port Peninsula, for example, cannot be traced to Bonne Bay or Canada Bay, although the formation in all three areas contains the same two large-scale lithologic assemblages.

2.3.1 Bonne Bay

Similar to the Port au Port Peninsula the Petit Jardin Formation at Bonne Bay consists of two recurring assemblages: (1) thinly bedded mudstone and argillaceous dolostone interbedded with ooid-intraclast grainstone, flat-pebble conglomerate, stromatolites and shale (up to 114 m thick); and (2) massive to thick-bedded dolomitized oolite and laminated dolostone with occasional stromatolites, intraformational conglomerate and shale partings (35 to 75 m thick). The thin-bedded assemblage at Bonne Bay, however, is much thicker than that on the Port au Port Peninsula.

2.3.2 Canada Bay (Shelly Whites Point Section)

The Petit Jardin Formation at Canada Bay is also composed of two alternating assemblages: thin-bedded dolostone and dolomitic shale (30-60 m thick); and thick-bedded, mottled dolostone and dolomitized stromatolite horizons with minor laminated dolostone and shale (25-30 m thick). The first is arranged in small cycles, 3-5 m in thickness, which from base to top are: (a) grey dolarenite and mottled dolostone; (b) tan weathering, thin-bedded dolostone; (c) laminated dolostone, commonly cryptalgal; and (d) black shale. Subaerial features such as desiccation cracks and fenestral porosity are common in the upper part

of each assemblage. The cyclical nature of these two assemblages is reminiscent of that documented on the Port au Port Peninsula and at Bonne Bay (detailed descriptions are given in Chapter 4).

2.3.3 St. Barbe Coast

The section of the Petit Jardin Formation along the St. Barbe coast, 65 km (present day) to the northwest of Canada Bay, consists of discontinuous coastal exposures from St. Barbe to Lower Cove. The formation is composed of thin-bedded dolostones, dolomitic shales, extensive stromatolite horizons, oolitic and intraclastic dolarenites and mottled dolostones. Desiccation cracks, fenestral porosity, ripple cross-laminations and bioturbation are common.

2.3.4 White Bay

At the Little Coney Arm section in White Bay only the upper 330 m of the Port au Port Group is well exposed: the Berry Head Formation and the uppermost part of the Petit Jardin Formation. The Berry Head Formation is approximately 255 m thick, 50 m thicker than in most sections to the south and west. The sequence is composed predominantly of light grey, massive to laminated dolostone with abundant mudcracks and ripple marks. Mottled and patterned dolostones are also common along with minor stromatolitic horizons. Phyllitic and shaly beds of the Petit Jardin Formation are present in the lower 75 m of well-exposed strata. The underlying rocks are poorly exposed and appear to be mainly dolostone.

2.3.5 Goose Arm

The Petit Jardin Formation is composed of massive to laminated, medium- to coarse-crystalline dolostones showing some relic oolite textures and minor cryptalgal mounds. Cyclical assemblages occasionally interrupt the sequence and are composed of: (a) basal dark grey, ooid-intraclast grainstone, 0.5-1.0 m thick; (b) thin-bedded mudstone and dolostone, 0.5 m thick, which shows an upward change from flaser to wavy to lenticular bedding; or stromatolite and thrombolite mounds; and (c) brown-tan weathering, laminated to thin-bedded, mudcracked dolostone, 0.5-1.0 m thick.

Based on these six areas, outcrops of the Petit Jardin Formation can be divided into two parallel southwest-northeast trending facies belts (Fig. 1.1): (1) an easterly, predominantly carbonate belt which includes outcrops from White Bay and Goose Arm and (2) a westerly belt of mixed carbonate and siliciclastic sediments containing sections from the Port au Port Peninsula, Bonne Bay, Canada Bay and the St. Barbe coast.

Chapter 3

DEPOSITIONAL SYSTEM

3.1 INTRODUCTION

The succession of carbonate and siliciclastic sediments of the Port au Port Group has been interpreted in previous studies as representing deposition on wide tidal flats and adjacent shallow subtidal to supratidal carbonate shoals (Swett and Smit, 1972; Levesque, 1977; Knight, 1980b). This study agrees with these interpretations but detailed examination further reveals that the sequence is composed of a spectrum of depositional features that records a complex interplay of submarine and subaerial conditions on the Cambrian platform. On the basis of lithology, the rocks are divided into two assemblages that reflect two distinct styles of sedimentation: one consists of thinly interbedded, fine-grained siliciclastics and carbonates and the other consists predominantly of thick-bedded carbonates (lithofacies are summarized in Table 3.1). This two-fold division provides the framework for analysis of the sedimentology and the development of facies models for mixed carbonate and siliciclastic sediments in general. This analysis in turn yields information regarding the nature of tidal activity; eolian processes; climatic and weather conditions (especially

TABLE 3.1: SUMMARY OF LITHOFACIES

LITHOFACIES	PARTED LIMESTONE	SHALE	OOID CALCARENITE	CARBONATE LAMINITE	STROMATOLITE & THROMBOLITE MOUNDS	GLAUCONITIC SANDSTONE & OOLITE
STRATIGRAPHIC OCCURRENCE	March Point, Cape Ann, Big Cove, Man O' War Mbrs.	Grey: Cape Ann, Big Cove Mbrs. Variegated: Campbells, Felix Mbrs.; Berry Head Fm.	Campbells, Felix Mbrs.; Berry Head Fm.	Campbells, Felix Mbrs.; Berry Head Fm.	Throughout Port au Port Gp.	March Point Fm.; Campbells, Felix Mbrs.; Berry Head Fm.
LITHOLOGY	Parted limestone, flat-pebble conglomerate, minor ooid & bioclast calcarenite.	Calcareous or dolomitic shale; commonly micaceous.	Grey oolite; brown oolite.	Laminated dolostone and mudstone, patterned dolostone.	Limestone or dolomitized mounds.	Glauconitic, calcareous quartz-arenite and sub-arkose; arenaceous calcarenite. Local occurrences of glauconite & quartz sand grains. Ubiquitous siliciclastic silt.
THICKNESS	1-2 m packages of parted limestone; conglomerate and calcarenite, up to 30 cm.	0.05-1.0 m thick.	Grey oolite: 0.3-0.5 m thick; brown oolite: 0.5-3.0 m thick.	0.5-1.0 m thick.	0.1-1.0 m in height; 0.1-2.0 m in width.	0.1-1.6 m thick beds.
BEDDING & STRUCTURES	Nodular to thin-bedded. Upward changes from ripple cross-laminated to flaser, wavy, & lenticular bedding. Gutter casts, mudcracks, and trace fossils.	Fissile; mudcracks, trace fossils.	Ripple to mega-ripple forms, herringbone cross-bedding. Intraclasts and mudcracked beds in brown oolite.	Laminated to thin-bedded. Mudcracks, prism cracks, tepees, fenestrae.	Variable mound morphology: hemispherical to digitate forms.	Interference ripples, ripple cross-bedding, runzelmarken, trace fossils.
BIOTA	Echinoderms, trilobites, phosphatic brachiopods.		Echinoderms, trilobites, phosphatic brachiopods.		Echinoderms, trilobites, *Girvanella*, *Renalcis*(?).	
DIAGENESIS	Hardgrounds, dolomitization.	Compaction.	Hardgrounds, dolomitization, silicification.	Karst, dolomitization.	Karst, dolomitization, silicification.	Lithification.
INTERPRETATION	Muddy tidal flat.		Shoal Sand Shoal Complex.			

storm activity); and water circulation and chemistry on the Cambrian platform.

3.2 PARTED LIMESTONES

3.2.1 Description

This lithofacies includes two interbedded lithologies which exhibit similar textural features (Fig. 3.1): type (1) — thinly interbedded limestone and dolostone (Plate 1a, b) and type (2) -- intimately interlaminated to interbedded limestone, dolostone and shale (Plate 1c). The term, parted limestone, is a convenient epithet used in the field to describe these rock types (Aitken, 1966) and is synonymous with the term, ribbon rocks, commonly used to describe the Cambrian of the southern and central Appalachians (Wanless, 1979; Demicco, 1982). The rocks range from thin beds of argillaceous limestone with shale or dolomitic partings to shale or dolostone with some minor limestone lenses. Also included within this lithofacies are thin-bedded, ripple cross-laminated limestones which lack shale or dolostone thin-beds and partings. These carbonates and shales comprise 1-2 m thick packages which have dominantly limestone at the base and grade upwards to shale and/or dolostone at the top (refer to Chap. 4; Plate 2a, b). Detailed petrography of parted limestones is presented in Chapter 7.

The grey-weathering limestones vary from relatively continuous thin beds to very discontinuous horizons composed of irregularly shaped lenses and nodules, up to 5 cm thick. They are mudstone to peloidal

Figure 3.1: Schematic diagram of type 1 and type 2 parted limestones, and types of bedding in parted limestone.

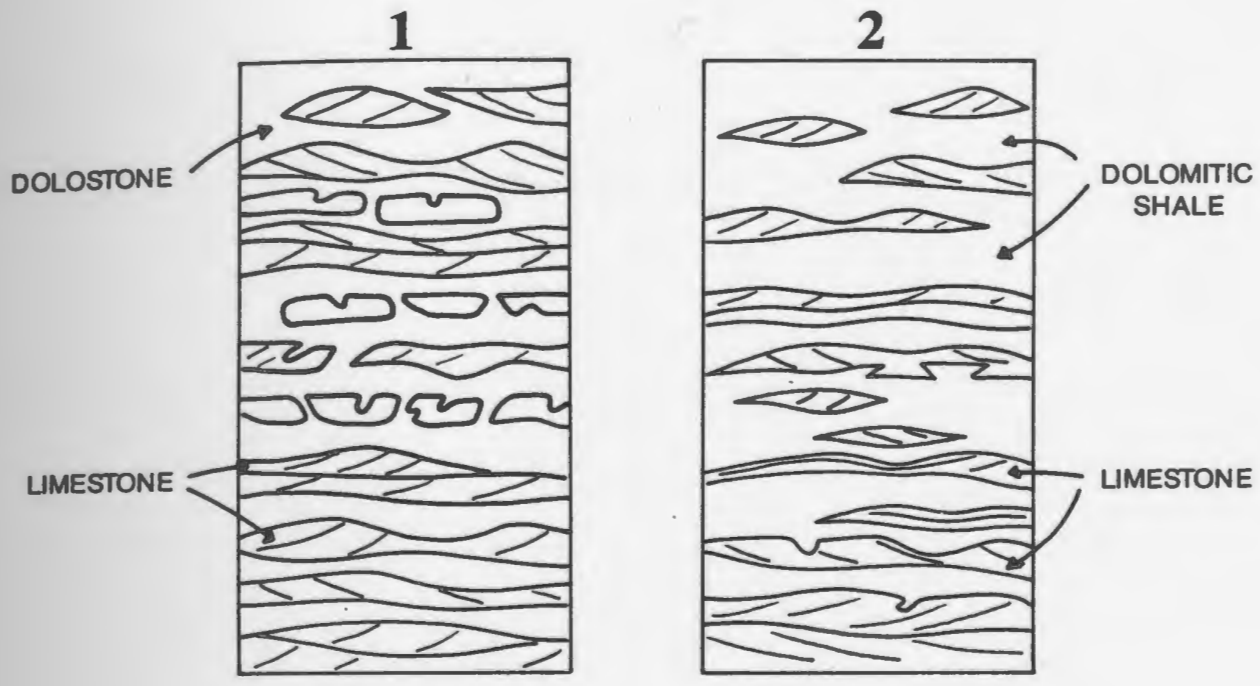
1
2
DOLOSTONE
LIMESTONE
DOLOMITIC SHALE
LIMESTONE

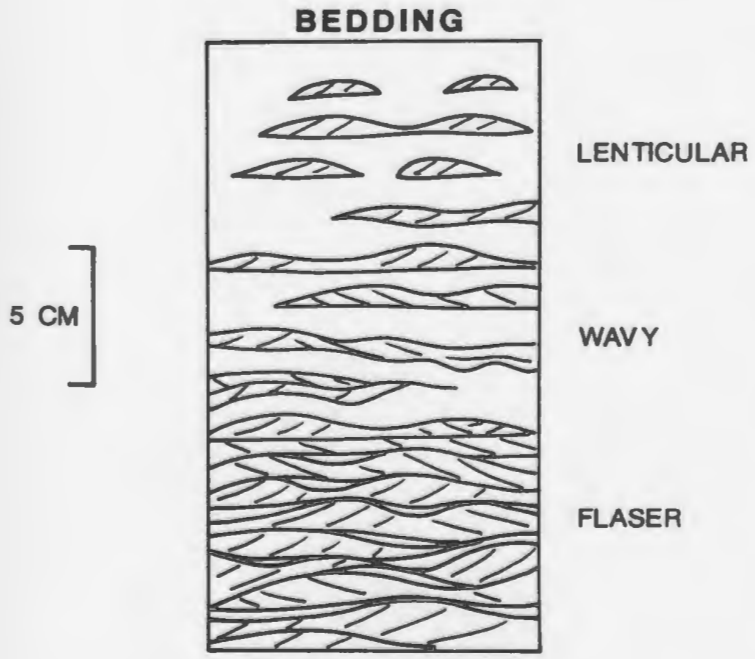
BEDDING
LENTICULAR
5 CM
WAVY
FLASER

wackestone and packstone with ubiquitous angular, silt-sized quartz grains and minor glauconite particles and micas. Planar to ripple cross-laminations; symmetrical ripple forms; load and gutter casts; compaction features; and mudcracks can be seen in cross-section. Bedding plane features include interference ripples, runzelmarken and desiccation polygons. A variety of ichnofossils, mainly horizontal and vertical burrows, surface traces and possible vertical borings (refer to Chap. 7; Richards, 1984) are also commonly preserved (Plate 1e).

Shaly and dolomitic interbeds are up to 5 cm in thickness and due to differential weathering commonly impart a platy appearance to the parted limestone. These interbeds are laterally continuous, draping over limestone beds and nodules. Shale beds are dark grey on fresh surfaces and are commonly calcareous. The dolomitic beds, medium grey in colour on fresh surfaces, weather a distinctive tan colour and are generally composed of ferroan dolomite in an argillaceous matrix. The shales and dolostones, which have abundant quartz and feldspar silt, are generally laminated and also drape over the limestone layers. Mudcracks and delicate trace fossils are commonly preserved on both top and bottom surfaces.

Sequences of parted limestone beds are frequently punctuated by stromatolite and thrombolite horizons (Plate 6a, c); conglomerates; ooid calcarenites (Plate 3d); and lenses and thin beds of bioclast calcarenites and calcirudites containing trilobite, echinoderm, and phosphatic brachiopod fragments, and rare oncoids.

Conglomerates are the next most abundant lithology in this lithofacies

after parted limestone. They are interbedded with all types of parted limestone and occasionally with grey oolite. The most common type is flat-pebble conglomerate, which occurs in thin beds and lenses, up to several tens of meters in lateral extent (Plate 1a; 12a, b). Beds characteristically have planar bases and convex upward top surfaces, although some have erosional bases. They are composed of angular to well rounded, tabular clasts up to 20 cm in diameter and 2 cm in width. Clasts are of variable composition, ranging from laminated mudstone and peloidal packstone to bioclast-intraclast packstone to wackestone and occasional algal boundstone. They are edgewise to horizontally disposed and are commonly cracked and bored. Although generally enclosed in bioclast-intraclast packstone to wackestone matrix and rarely in dolomitized silty mudstone, grain-supported conglomerates commonly show excellent shelter porosity that is now occluded by coarse calcite cement. Matrix-supported conglomerates with angular, equant clasts are rare.

Parted limestones are the major elements of the "shaly" members: the March Point Formation, and the Cape Ann, the Big Cove and the Man O' War Members. Each unit, however, has distinct textural features.

March Point Formation. Parted limestones in the March Point Formation are primarily of type 1 and are characterized by a uniform sequence of interbedded to interlaminated layers or nodular beds of limestone and partings to thin beds of tan weathering dolostone. Only minor horizons of type 2 parted limestone, 2 to 5 cm thick, are present. Excellent horizontal to vertical trace fossils are preserved (Richards, 1984) and only minor mudcracks are observed. The formation is generally

characterized by the absence of algal mounds, although one thin horizon is seen in the vicinity of Campbells Cove on the Port au Port Peninsula.

Cape Ann Member. Parted limestones of this unit are mainly type 2, thin-bedded limestone and dolostone with thin beds to partings of calcareous black shale. All variations from dominantly limestone beds to dominantly shale are present. Excellent limestone stromatolite and thrombolite horizons (e.g., up to 8 m in height at the Cape St. George section) are well preserved. Runzelmarken, mudcracks and red and green shales present in the upper 7-8 m of the member accompany a decrease in the grey shale content of the parted limestone.

Big Cove Member. Parted limestones of the Big Cove Member are mainly type 2 but are characterized by a variation in composition from the base of the member to the top. The lower third of the unit is parted limestone interbedded with ooid grainstone, algal mound horizons and flat-pebble conglomerates showing the gradual transition from the underlying Campbells Member. Parted limestone in the middle third of the unit, poorly exposed because of scree, is a range of lithologies from dominantly limestone to dominantly shale. Abundant runzelmarken and skip and bounce casts are present and glauconite, phosphatic and quartz sand grains are common. A significant decrease in the percentage of shale occurs in the upper portion of the member, resulting in parted limestone composed of interbedded limestone and dolostone with only minor argillaceous partings (type 1) and well developed gutter casts and mudcracks. This upper limestone gradually becomes more lenticularly bedded upwards with an increase in the proportion of dolostone interbeds.

Man O' War Member. The Man O' War Member, characterized by type 1 parted limestones, exhibits a wide range of lithologies varying from dominantly dolostone with minor limestone lenses to dominantly limestone with dolostone partings. Runzelmarken preserved on bedding planes, and mudcracks are common. Frequent interbeds of grainstones, large algal mounds and thick flat-pebble conglomerates give rise to a highly varied assemblage.

Minor horizons of parted limestone, less than 1 m in thickness, are present in the upper half of the Campbells and Felix Members. Those in the Felix Member are identical to the above described rocks; those in the Campbells Member have the same fabrics but are composed of interlaminated oolitic quartzarenite to arenaceous ooid calcarenite and dolomitic mudstone. Mudcracks are abundant throughout.

3.2.2 Interpretation

In the interpretation of parted limestones, the relationship between the limestone and dolostone of type 1 must first be considered. There are two possible interpretations: (1) the thin-bedded nature of parted limestones is predominantly a primary sedimentary feature (e.g., Levesque, 1977; Pratt, 1982; Demicco, 1982) and (2) the limestone and dolostone beds are the result of secondary diagenetic processes unrelated to depositional textures, such as pressure solution, which concentrated insoluble components and precipitated dolomite to form thin-bedded strata from originally homogeneous limestone (Logan and Semeniuk, 1976; Wanless, 1979).

The first interpretation appears to be the more plausible in light of the following observations: (1) sedimentary structures such as ripple forms, planar and ripple cross-laminations and gutter casts are preserved in cross-section in the limestone beds; (2) delicate structures such as runzelmarken and horizontal trace fossils can often be seen on bedding planes; (3) mudcracks and burrows are commonly preferentially dolomitized; (4) dolostone beds or partings in which planar to wavy laminations are preserved show draping over ripple forms and infilling of troughs in the limestone beds; (5) interbedded limestone and dolostone beds exhibit textures similar to interbedded limestone and shale horizons; and (6) only vertical changes in the composition of the parted limestones have been observed. Similar evidence is presented by Levesque (1977) and Demicco (1983).

Parted limestones are texturally identical to flaser, wavy and lenticular bedding in modern siliciclastic sand and mud tidal flat sequences (Reineck and Wunderlich, 1968) and thus are interpreted to be their carbonate equivalents (Fig. 3.1): (1) flaser bedding -- ripple cross-laminated sand in which mud streaks are preserved in the troughs but incompletely or not at all on the crests; (2) wavy bedding -- interbedded mud and ripple-cross-laminated sand in which the mud layers cover the ripple troughs and crests; mud generally fills in the troughs; and (3) lenticular bedding -- similar to above forms but in which the ripples or lenses are vertically and laterally discontinuous. Other workers, such as Levesque (1977) and Demicco (1983), have drawn similar conclusions. Demicco (1983) provided a detailed description of Upper

Cambrian tidal flat deposits and comparison with the North Sea. The March Point Formation is composed mainly of wavy-bedded limestones whereas the Cape Ann, Big Cove and Man O' War Members show wavy and lenticular bedding and only minor flaser bedding and ripple cross-laminated limestone.

Type 1 and 2 parted limestones show similar sedimentary features and are often intimately interbedded sugges ing that both lithofacies were deposited by the same processes. The absence or presence of shale reflects varying siliciclastic input and does not appear to affect the style of sedimentary structures.

Flaser, wavy and lenticular bedding are interpreted to be tidal features in which alternating layers of sand-size particles and mud were deposited during alternating periods of tidal current activity and quiescence. Tidal flats of the North Sea are an excellent modern analogue (Reineck and Singh, 1980). The ripple cross-laminated limestones, interpreted to have been deposited under peak ebb and flood tidal currents, are now mainly mudstone. Sediment transport mechanisms, however, dictate that ripple formation occurs in fine silt to coarse sand (Harms et al., 1975). This suggests that the limestone beds were originally grainy and that the grains were destroyed during compaction and/or later diagenesis (Shinn and Robbin, 1983).

In contrast, the fine grained dolostones and shales show laminations draping over ripples and filling in irregularities in the limestone beds, suggesting that they settled out of suspension during periods of high slack tide (Reineck and Singh, 1980). The dolostone beds were

originally mudstone horizons that were subsequently dolomitized with fabric preservation. Hawley (1981), however, indicated that mud deposition by tidal activity could not completely account for the thickness and erosional resistance of mud beds in flaser bedding. Demicco (1983) suggested that mudstone interbeds may have been in large part originally peloidal muds that were deposited during slack tide.

The different types of bedding in the parted limestone lithofacies contain evidence for varying degrees of subaerial exposure. Ripple cross-laminated limestone and flaser bedding generally show no evidence of subaerial exposure and therefore are interpreted as subtidal to lowest intertidal features. Wavy bedding is of relatively uniform character with abundant trace fossils but may exhibit subaerial exposure textures. For example, few mudcracks are present in the March Point Formation whereas mudcracks and runzelmarken are well developed in the Man O' War Member. These are interpreted as upper subtidal to lower intertidal, and intertidal sediments respectively. The lenticular bedded horizons, which commonly grade up from flaser and wavy bedding, have dessication cracks, runzelmarken, and other subaerial exposure fabrics and so are interpreted to be uppermost intertidal to supratidal deposits.

In modern tidal flats, flaser, wavy and lenticular bedding have been observed in many tidal flats that have a mesotidal (2 to 4 m; e.g. North Sea, Reineck and Singh, 1980) to macrotidal (greater than 4 m; Mont Saint-Michel Bay in France, Larsonneur, 1975) tidal range. It is also notable that bedding in many modern tidal flats is often destroyed by bioturbation and only in the subtidal is the sand-mud layering

preserved (Weimer et al., 1982). Applying these observations to the Port au Port Group, it is proposed that: (1) the 1-2 m thick packages of parted limestones suggest at least a mesotidal tidal range (see "Discussion") and (2) bioturbation was not extensive as evidenced by the preservation of bedding in subtidal, intertidal and supratidal sediments. Bioturbation, however, may have been instrumental in the disruption of some type 1 parted limestones to produce nodular limestone layers (refer to Chap. 7).

The relationship between types of bedding and the subtidal, intertidal and supratidal areas of a tidal flat is not well defined in modern siliciclastic environments; lenticular and flaser bedding, for example, may be common to both subtidal and intertidal facies (Reineck, 1975). Bedding is strongly influenced by sediment supply and energy range, indicating that siliciclastic sand and mud percentages may not be indicative of specific facies (Weimer et al., 1982). In carbonate environments, a more continuous supply of carbonate sand and carbonate mud (when there is a paucity of siliciclastic mud) from a probable subtidal source (Ginsburg, 1971; James, 1984) suggests that varying sand/mud ratios reflect to a greater extent energy conditions and thus are more indicative of tidal flat subenvironments.

The lack of evidence for tidal channels or channel-fill in parted limestone suggests that channels in the Cambrian tidal flat were either not preserved or never existed. Tidal flats of northwest Andros Island in the Bahamas are cut by extensive channels that comprise approximately 14 % of the entire complex (Shinn, Lloyd and Ginsburg, 1969; Hardie and Garrett, 1977a, b). Tidal flat complexes of the Trucial coast

embayment in the Persian Gulf are similarly dissected by tidal channels (Bathurst, 1975; Schneider, 1975). Reworking of channel deposits by tidal processes suggests that the preservation potential of these deposits is poor. Siliciclastic tidal flats in the Gulf of California, in contrast, are characterized by the relative absence of tidal chanels. Thompson (1975) interpreted the lack of channelling to be related to the insignificant development of barrier islands, which permit tidal currents to flow uniformly and unrestricted over the flats. This results in deposits lacking both significant upward-fining sequences, and lenticular, wavy and flaser bedding. Comparing these modern tidal systems to the Port au Port Group, it is suggested that the Bahamas and Persian Gulf are the best modern analogues and that the Cambrian tidal flat was cut by channel systems that were not preserved in the rock record.

Flat-pebble conglomerate beds and lenses in parted limestone generally lack an erosive lower contact and thus cannot be interpreted as channel deposits. The presence of these conglomerates sporadically throughout the tidal flat sediments in association with different lithologies suggests that they are storm-derived deposits (detailed discussion is presented in Chap. 4 on "storm deposits"). The generally large size of the clasts and the lithologic similarity between the clasts, adjacent beds and matrix indicate that they were not transported far and were likely derived from the erosion of nearby beds. Local round-pebble conglomerates are also considered to have originated from storm deposition but were subsequently subject to further abrasion and reworking.

3.3 SHALES

3.3.1 Description

Shale beds are present throughout the sequence. There are two types of shale: (1) common grey shale which occurs mainly with type 2 parted limestones in the Cape Ann and Big Cove Members and as minor, decimeter-thick interbeds in the March Point Formation and Man O' War Member and (2) less common, variegated red and green shales in the Campbells and Felix Members and the Berry Head Formation. Variegated shales are generally interbedded with carbonate laminites and brown oolites (described later in this section) and are rarely thicker than 5 to 10 cm. Mudcracks are common.

The shales are commonly calcareous or dolomitic and locally contain silt-size quartz, glauconite and feldspar grains. Illite and chlorite are the main clay minerals (Wood, 1983).

3.3.2 Interpretation

Shales are interbedded with other lithofacies which record deposition in the intertidal to supratidal zones. As previously interpreted, the grey shales of the parted limestone lithofacies are interpreted to represent periods of slack water and subsequent subaerial exposure in tidal flat deposits. Similarly the variegated red and green shales, which are volumetrically minor components of the predominantly carbonate

members, represent the subaerial end-member of migrating carbonate shoals (discussed below). In western Newfoundland, there is no evidence for a subtidal shale basin as described by Markello and Read (1981) in the Cambrian of the southern Appalachians and Aitken (1978) in the Canadian Rockies (refer to Chap. 4).

The sporadic occurrence of shale in parted limestone can be explained in several ways: (1) the absence of a sufficient siliciclastic source; (2) insufficient energy to disperse the clastics platformward; or (3) winnowing out of the fine sediments on a high energy platform. The second mechanism is unlikely, given the apparent frequency of storm events on the platform and the obvious influence of significant tidal activity. The last mechanism is not feasible, given that carbonate mud is still present when there is a paucity of siliciclastic mud. Similar sedimentary structures in shales and carbonate mudstones and the intimate interbedding of type 1 and 2 parted limestone indicate that the overall energy of the tidal flats did not vary sufficiently with time to account for variations in shale content. Instead the balance between siliciclastic and carbonate muds appears to be a function of the amount of siliciclastic mud available to the system rather than reflecting a change in environment. A diminution of siliciclastic mud influx permits deposition of lime sediments. This argument is also applicable to variegated shales.

In addition to vertical variations in shale content in parted limestone, a lateral change is also possible. Similarity with siliciclastic tidal flat sediments suggests that the Cambrian tidal flat probably exhibited a lithologic change from dominantly grainy limestone

near the low water line to mainly siliciclastic and/or carbonate muds near the high water line. This characteristic sediment distribution is attributed to both the transport mechanism and energy conditions (Reineck and Singh, 1980). Energy conditions tend to be greater in the shallow subtidal and lower intertidal zones than higher up in the complex resulting in the deposition of sands and the winnowing of muds. Mud deposition takes place near the high water line due to low wave and current activity and the fact that the time of slack water allowing mud to settle out of suspension is much longer during high tide than low tide (Postma, 1961). This accumulation of muds was probably easily remobilized by high energy conditions or rising relative sea level and provided the source for subsequent mud deposition.

3.4 OOID CALCARENITES

3.4.1 Description

. Two types of oolite are present and can easily be differentiated in the field as: (1) a dark grey coloured oolite and (2) a buff to dark brown coloured oolite. They are the main lithologies of the Campbells and Felix Members and probably the dolomitized Berry Head Formation as well. Minor beds of grey oolite are also present in the upper part of the Cape Ann and Big Cove Members. Detailed petrographic description and interpretation of grey and brown oolites are given in Chapter 6.

3.4.1.1 Grey Oolite

These rocks are thin beds of ooid grainstone and minor packstone. Upper surfaces of beds frequently exhibit megaripples that commonly have silicified crests or thin, mudcracked lime mudstone drapes in the troughs (Plate 3b). Herringbone cross-bedding is rare, but does occur. The oolites are commonly interbedded with brown oolites and laminated dolostone to dolomitic limestone (discussed below) and are occasionally associated with parted limestones (Plate 3a, d). No lateral gradations between these lithofacies are observed, although this may be a function of outcrop limitations. Bed boundaries are generally stylolitized and thicknesses of individual beds may vary laterally.

The grains are well-sorted, medium to coarse sand-size (Plate 3c) and occur with common intraclasts of dark grey oolite (Plate 4a) and occasional lime mudstone clasts. Ooids have radial-fibrous cortices; nuclei may be peloids, intraclasts or bioclastic fragments but are commonly obscured.

3.4.1.2 Brown Oolite

The thick, buff to dark brown coloured ooid packstone to grainstone beds are characterized by abundant dolostone and limestone intraclasts and thin, laminated beds of the same lithology (1 to 5 cm thick) that are mudcracked and laterally discontinuous (Plate 4b, c). Herringbone cross-bedding is pronounced and occasional symmetrical ripple forms and oolite intraclasts are present.

Ooids are medium sand size with peloid nuclei and either well-developed concentric cortices or superficial (thickness of cortex is less than one-half the radius of the nucleus; Illing, 1954) radial-fibrous cortices. Coarser radial-fibrous ooids of the grey oolite type, oolitic and micritic intraclasts, peloids, bioclastic fragments and quartz and feldspar silt are common accessory components. The variability in grain, matrix and cement components results in colour variations in brown oolite from dark grey-brown to buff. Darker-coloured oolite tends to be better sorted, have more coarse-grained ooids and contains less micrite and siliciclastic silt than light-coloured oolite.

3.4.2 Interpretation

The ooid calcarenites associated with the carbonate laminite lithofacies (to be discussed in the following section) appear to be part of a "genetic package" in which deposition of the two lithofacies is related. These lithofacies in the the Campbells and Felix Members and the Berry Head Formation are interpreted to represent deposition in a heterogeneous, carbonate sand shoal complex. The sand shoal is composed of grey oolite, buff-brown oolite and laminated dolostone and limestone.

Grey oolites lack evidence of subaerial exposure and are interpreted to be the subtidal component of the shoal. The abundance of lime mud matrix in associated brown oolites suggests that the paucity of mud in grey oolites was due to sufficiently high energy conditions inhibiting mud deposition or causing winnowing of the mud, rather than the lack of a mud source in the subtidal. The consistent dark grey colouration

(possibly related to organic content) of the oolites further suggests that little reworking and subaerial exposure took place subsequent to deposition.

Brown oolites contain sedimentary structures indicating intermittent subaerial exposure and are interpreted to be intertidal deposits which were subject to frequent fluctuations in energy. The lighter colour of these oolites relative to grey oolites may reflect a greater degree of sediment reworking and oxidation of organic material.

Ooid sand shoals, comprised of long and narrow or spill-over type bars and tidal channels, along the platform margin of the Bahamas Banks have long been considered to be a modern analogue for ancient oolite deposits (Ball, 1967; Harris, 1979). This does not appear to be applicable for oolites of the Port au Port Group as indicated by their thinness (generally less than 2 m); the absence of cross-bedded lobate bodies of spill-over bars; and the two distinct types of oolite. Instead, the Joulters Cay ooid shoal on the windward margin of Great Bahama Bank, is a more likely analogue to these Cambrian oolites. Detailed study of the area by Harris (1979) shows the shoal to be an intertidal sand flat, 400 sq km, that is flanked on the windward sides by mobile ooid sands in a belt 1 to 2 km wide. Ooid grainstone is found in the mobile fringe, which is the active zone of ooid formation, whereas the sand flat is a mixture of micritized ooids derived from the mobile fringe, other grain types and mud.

Comparison with Joulters Cay suggests that the grey oolite of the Port

au Port Group is analogous to the mobile fringe ooids and brown oolite to the sand flat sediments. The difference in size and internal morphology of the the ooid grains in each of these oolites, however, indicates that both these shoal areas were zones of ooid formation in the Cambrian.

3.5 CARBONATE LAMINITES

3.5.1 Description

This lithofacies is tan to reddish-mauve weathering, grey to buff, laminated dolostone and limestone and minor massive dolostone. Thick-bedded laminite is an important constituent of the Campbells, Felix and Man O' War Members and Berry Head Formation. The term, laminite, first suggested by Knopf (in Sander, 1951, p.135) is used here as a nongeneric term to describe finely laminated limestones and dolostones. Petrography of dolomitic laminites (dololaminites) is presented in Chapter 8.

Three rock types are included within the laminite lithofacies: type 1 -- centimeter-scale, planar laminated dolostones and limestones with abundant mudcracks and minor low angle cross-laminations, scour marks, tepee structures, and laminated intraclasts (Plate 5a); type 2 -- millimeter-scale laminated dolostone and limestone composed of slightly wavy and crenulated laminite with occasional large prism cracks and rip-up clasts, possible fenestrae (Plate 5c, d); and type 3 -- patterned

dolostones composed of patches of light-coloured and dark-coloured dolostone (Dixon, 1976; Plate 5b).

Type 1 and 2 laminites are interbedded with oolite beds whereas only type 1 is also associated with the parted limestones. Type 3, patterned dolostones, are found in association with type 1 and 2 only in the Berry Head Formation and are minor constituents of the brown oolites.

Laminites may be capped by thin (usually less than 5 cm thick), rust-stained, dolomitic siltstone or shale. Although the upper bed boundaries are generally planar or stylolitized, several other types of boundaries are observed in cross section: (1) smooth, scalloped surfaces which have vertical relief on the order of centimeters to tens of centimeters; (2) smooth meter-scale depressions along bedding planes; and (3) locally developed lenses of breccia blocks that are commonly encrusted with stromatolites and thrombolites.

3.5.2 Interpretation

Textural features preserved in the laminite lithofacies suggest very shallow water conditions with extensive periods of subaerial exposure, ie. a supratidal environment. Type 1 laminite interbedded with parted limestones is interpreted to be the supratidal end-member of the parted limestone lithofacies which is in turn interpreted to represent deposition on a muddy tidal mud flat (refer to the previous discussion on parted limestones). Type 1 and 2 laminites associated with the oolite lithofacies are part of a "genetic package", deposited in a peritidal carbonate shoal complex, as described previously. These

laminites are generally interbedded with mudcracked, variegated shales and represent the supratidal crest of the shoal complex.

Type 2 limestone and dolostone laminites have features suggesting the influence of sediment binding by blue-green algal mats or cyanobacteria. Aitken (1967) has referred to these as cryptalgalaminites. Modern analogues have been documented in the intertidal to supratidal mud flats of the Persian Gulf (Kendall and Skipwith, 1968); the Bahamas (Hardie and Ginsburg, 1977); and Shark Bay (Davies, 1970).

The presence of patterned dolostones with the other types of laminites support the interpretation of a supratidal to highest intertidal depositional environment. The dark areas of the dolostone are commonly concentrations of pyrite (particularly well developed in the Little Coney Arm section at White Bay). Dixon (1976) proposed that these small pyrite accumulations are early diagenetic products formed in sulphate-rich, reducing environments, such as may be found in tidal and supratidal regimes. Longman (1982), has carried this interpretation further based upon similar structures in burrowed micrite of the Middle Ordovician Bromide Formation of Oklahoma. He proposed that they are oxidation marks or bleached rims along desiccation cracks and fractures that formed by air or percolating water oxidizing organic matter and pyrite shortly after deposition in a tidal flat environment.

Bed boundaries that are not obscured by stylolitization are highly irregular and sculptured. These features are interpreted as carbonate dissolution features or paleokarst resulting from extensive subaerial

exposure (see Chapter 5). Angular breccia blocks occasionally associated with these structures are likely due to collapse of oversteepened flanks on paleokarst pits or depressions.

3.6 STROMATOLITE AND THROMBOLITE MOUNDS

3.6.1 Description

These mounds are present throughout and vary considerably in their external morphology, internal composition and associated lithofacies. A stromatolite has been defined as a fixed body with definite limits and characterized by macroscopic laminations inferred to be due to blue-green algal activity (Aitken, 1967) and/or cyanobacteria (Bauld, 1981) and will be described using the classification of Logan et al. (1964). A thrombolite was originally defined by Aitken (1967) as a non-laminated body with definable boundaries, characterized by an internal clotted fabric and occasional calcareous algae. The term, thrombolite, has been the subject of much discussion and redefinition by numerous workers (e.g. Ahr, 1971; Lohmann, 1977; Pratt & James, 1982; Read and Pfeil, 1983); it is used in this study only as a descriptive field term for non-laminated mounds with a clotted fabric.

The stromatolites vary in external morphology and have different associated sediments. Based upon field observations, there are three types: (1) hemispherical to bulbous-shaped forms, 0.1 to 1.0 m in height and 1.0 to 2.0 m in diameter (Plate 7c); (2) branching to fan-shaped heads, 0.1 to 2.0 m in diameter and up to 1.0 m in height (Plate 7b);

and (3) lamellar or stratiform types, 1-5 cm in height (Plate 14e). The first type is the commonest and has an internal morphology that ranges from low-relief, concentric laminations to discrete, vertically-stacked hemispheroids (SH stromatolites) associated with close-linked hemispheroids (LLH-C stromatolites). Some of the larger type 1 stromatolite mounds appear to be composed of columnar-shaped heads flanked by parted limestones, laminites or ooid-peloid grainstones to packstones (Plate 14e). The smaller, relatively rare type 2 stromatolites are composed of LLH-C to SH-V stromatolites and associated with brown oolites or laminites.

Thrombolite mounds vary considerably in size and shape ranging from hemispherical heads, 0.2 to 1.0 m in height and 0.3 to 1.0 m in diameter to centimeter-thin lenses (Plate 6b, c; 7a). Larger forms are commonly capped by LLH-C stromatolites and rooted upon flat-pebble conglomerates. Inter-mound sediments can be parted limestone, carbonate laminite or ooid calcarenite. Internally, thrombolites are composed of millimeter-sized, dark grey clots arranged in an upward branching network of digits (refer to Chapter 5). Clots are separated by patches of white to light grey limestone with abundant trilobite and brachiopod fragments and irregular areas of silty limestone, Girvanella and (?)Renalcis are occasionally present.

Bioherms and biostromes composed of both stromatolites and thrombolites occur in the sequence. In one exceptional example in the Cape Ann Member of the Petit Jardin Formation near Cape St. George on the Port au Port Peninsula, the mounds attain a thickness of approximately 8 m and are composed of both stromatolites and

thrombolites (Plate 6a).

3.6.2 Interpretation

On the basis of their lithofacies associations, these Cambrian stromatolites and thrombolites appear to have developed in a number of different environments, ranging from peritidal sand shoal to muddy tidal flat settings.

The morphology of modern stromatolites depends on energy conditions, desiccation, sedimentation rate and stability of the substrate (Logan et al., 1964; Hoffman, 1976). Larger hemispherical mounds tend to develop in subtidal or lower intertidal zones. With increasing energy conditions of the tidal regime, columnar and domal stromatolites form, passing in turn upward into stratiform stromatolites of the upper intertidal to supratidal zone (summarized in James, 1984).

Thrombolites have been documented in numerous studies on the Cambro-Ordovician platform (e.g. Aitken, 1967; Ahr, 1971; Lohmann, 1977; Pratt, 1979; Demicco, 1982). Holocene subtidal mounds in Shark Bay, western Australia (Logan et al., 1974) share many similarities with ancient thrombolites (e.g. Read and Pfeil, 1983). Many of these studies have postulated that thrombolite mounds may have been rigid framework algal reefs formed in an open subtidal shelf environment. Thrombolite mounds of the Port au Port Group appear to be similar to these thrombolites, at least on a macroscopic scale. Based upon their association with intertidal and shallow subtidal sediments, however, it is further suggested that they were algal patch reefs, with up to 1.0 to

1.5 m of synoptic relief, which developed in both intertidal and shallow subtidal zones.

3.7 GLAUCONITIC SANDSTONES AND OOLITES

3.7.1 Description

This lithofacies is uncommon but is important when deciphering the depositional history of the Port au Port sequence and so has been treated separately.

Glauconite-rich, calcareous quartzarenites to subarkoses (Folk et al., 1970) to arenaceous limestones, composed of rounded, medium- to coarse-grained quartz grains with minor phosphatic clasts, are present in the basal 20 m of the [redacted]ch Point Formation (Plate 8a). Beds are up to 1.5 m thick at the base and thin upwards, passing gradationally into parted limestones at the top of the interval (Plate 8b, c). Thin, reddish-brown interlayers of silty shale are also present. Interference ripples, straight ripple marks, and runzelmarken may occur on bedding surfaces, and high angle cross-bedding and compacted mudcracks are seen in cross-section. The upper parts of the siliciclastic sandstone beds are well burrowed (Skolithos is particularly common) and occasionally have thin caps of rust-stained dolomitic sandstone.

These basal sandstones are the best-developed siliciclastic sand units in the Port au Port Group. Higher in the section, siliciclastic sand accumulations are uncommon and occur as: (1) thin beds of glauconitic

quartzarenite interbedded with brown oolite and dololaminite in the Felix Member and (2) rounded, coarse to medium sand-size quartz and glauconite grains (up to 20 %) in brown oolite in the Campbells and Felix Members and Berry Head Formation and only rarely in parted limestones. In contrast angular, silt-size to very fine-grained sand-size quartz and feldspar grains are pervasive in all the previously described carbonates but are most common and abundant in carbonate laminites and parted limestones.

3.7.2 Interpretation

The siliciclastics at the base of the March Point Formation contain only rare subaerial exposure features and rest directly upon quartzites of the Hawke Bay Formation. These beds record the change from shallow marine, siliciclastic deposition during the Early Cambrian (Levesque, 1977) to mixed carbonate and siliciclastic deposition in Middle Cambrian time. Whether this was a continuous transition or one interrupted by a hiatus at the Hawke Bay-March Point contact is uncertain. Regardless, the similarity in size and composition of clastic grains across the contact suggests that the siliciclastic sands of the March Point were probably derived from the remobilization and reworking of Hawke Bay sandstones in a shallow subtidal environment. The presence of abundant glauconite and phosphate grains indicate considerable reworking and a relatively slow rate of deposition (Van Houten and Purucker, 1984).

Minor beds and localized concentrations of siliciclastics above the March Point Formation are more difficult to interpret. The bimodal grain-size distribution of rounded, coarse- to medium-grained quartz and

feldspar sand, and angular silt-sized quartz and feldspar appears to be a common phenomenon on Cambro-Ordovician carbonate shelves (e.g. Dott and Byers, 1980). This is also seen in equivalent Cambro-Ordovician slope deposits of the Cow Head Group (N.P. James, pers. comm., 1983). The nature of the siliciclastic delivery system is still much debated and various studies have proposed mechanisms ranging from eolian processes to progradation of siliciclastics during lowering of sea level (e.g. Dott and Byers, 1980).

Siliciclastic sands above the March Point Formation in the Port au Port Group are most commonly associated with brown oolites present throughout the sequence, suggesting that: (1) the latest deposition of these grains was by mechanisms that were more facies-selective than eolian processes (cf. Koopman et al., 1979; Dott and Byers, 1980), although earlier reworking by winds is not precluded and (2) the transport mechanism was not directly related to either high or low sea-level stands. No conclusive interpretation of the origin of these siliciclastics, however, can be made with the available information. One possible explanation may be that high-energy events such as storm activity or extreme tides remobilized and transported siliciclastic sands seaward from some nearshore source (not observed in western Newfoundland). Carbonate shoal complexes may have trapped some of these siliciclastics that were then further distributed by longshore currents. The common association of glauconite particles and siliciclastic sand suggests that reduced carbonate sedimentation rates, possibly during low sea-level stands, enabled reworking and concentration of these grains in the shoal complex.

In contrast, the pervasiveness of siliciclastic silts in the sequence suggests that their main tranport mechanism was areally extensive and most likely eolian. The lack of rounded grains is merely a function of grain size, silt-size particles being more difficult to abrade than sand-size particles.

3.8 SUMMARY OF LITHOFACIES INTERPRETATIONS

Parted Limestones: Thinly interbedded to interlaminated limestones, dolostones and shales are muddy tidal flat deposits that are texturally similar to some modern siliciclastic tidal flat sediments. Limestones were deposited by peak ebb and flood tidal currents; dolostones and shales settled out of suspension during slack high tide. Flaser, wavy, and lenticular bedding represent shallow subtidal, intertidal and supratidal deposition respectively. Interbedded flat-pebble conglomerates are interpreted to be storm deposits.

Shales: Components of this lithofacies are interpreted to be upper intertidal to supratidal deposits: (1) grey shales represent periods of high slack tide in muddy tidal flats and (2) variegated red and green shales are supratidal deposits of carbonate shoal complexes. The sporadic occurrence of shales in the carbonate-dominated sequences is interpreted to represent reworking and remobilization of a nearshore supply of siliciclastic mud by high energy events (e.g. storms) or rising relative sea level.

Ooid Calcarenites. Grey oolite and brown oolite are interpreted to be

subtidal mobile fringe and intertidal sand flat deposits respectively of a high energy, carbonate sand shoal complex. The differences in ooid morphology between the two types of oolite suggest that the intertidal and subtidal zones of the shoal complex were distinct zones of *in situ* ooid formation and deposition.

Carbonate Laminites. This lithofacies contains abundant evidence for extensive subaerial exposure and represents supratidal deposition. Dololaminites interbedded with parted limestones are interpreted as supratidal deposits of muddy tidal flats. Limestone and dolostone laminites interbedded with ooid calcarenites represent deposits of the supratidal crest of carbonate sand shoal complexes.

Stromatolite and Thrombolite Mounds. A plethora of stromatolite and thrombolite mounds with variable shapes and internal composition occur throughout the sequence. Stromatolite morphology and inter-mound lithologies suggest that they developed in shallow subtidal, intertidal and supratidal zones of both sand shoal complexes and muddy tidal flats. Thrombolites are interpreted as rigid framework patch reefs that developed in shallow subtidal to intertidal zones.

Glauconitic Sandstones and Oolites. A bimodal distribution of rounded siliciclastic sands and angular silts is present throughout. Ubiquitous silt-size quartz and feldspar are interpreted to be eolian in origin. Glauconitic, siliciclastic sandstones at the base of the sequence represent reworking of ?Lower Cambrian Hawke Bay sandstones in a shallow subtidal environment. Sand-size quartz and feldspar in the limestones and dolostones above occur most commonly in brown oolite. They are

interpreted to have been reworked from a nearshore environment by storms or extreme high tides and trapped in the carbonate sand shoal complexes.

3.9 DISCUSSION

3.9.1 Lateral and Vertical Lithofacies Relationships

The six lithofacies in the Port au Port Group represent platform deposition in the shallow subtidal, intertidal or supratidal zones. In outcrop, few lateral gradations between lithofacies are observed so that determination of the lateral relationship of lithofacies must be inferred. Vertical lithofacies associations are described in Chapter 4 on facies sequences.

Close inspection of the succession reveals that these lithofacies can be divided into two distinct vertical packages which share few common characteristics except that they each contain subtidal, intertidal and supratidal components. The first package is composed of predominantly parted limestones, which represent shallow subtidal to supratidal deposition, and minor glauconitic sandstones of subtidal origin. The second consists of thick-bedded subtidal grey oolites, intertidal brown oolites and supratidal carbonate laminites and variegated shales.

This prominent vertical packaging of lithofacies is interpreted to indicate two laterally adjacent, mega-environments on the platform: a muddy tidal flat and a carbonate shoal. The vertical relationship of

the lithofacies within each package indicates that sedimentation in the subtidal, intertidal and supratidal zones occurred essentially coevally within each environment.

3.9.2 Summary of Environmental Conditions

Examination of lithofacies allows a preliminary estimate of some of the environmental parameters present on the Port au Port platform. Additional information is gleaned by analysis of meter-scale assemblages, large-scale cycles, and storm deposits which are described in Chapter 4.

Tidal Range. The occurrence of flaser, wavy and lenticular bedding in parted limestone indicate a mesotidal (2 to 4 m) to macrotidal tidal range (greater than 4 m) as indicated by studies of modern tidal flats (for e.g. Reineck and Singh, 1980). This is in accord with Demicco (1983) who postulated a tidal range of 1 to 8 m for a late Cambrian tidal flat in the central Appalachians.

Klein (1971) presented a model for siliciclastic tidal flat sediments in which the thickness of fining-upward intertidal sequences coincides with the mean tidal range. Application of this model to carbonate sediments, however, provides only minimum ranges because of the considerable effects of variable sedimentation rates, compaction and pressure solution. The 1 to 2 m thick packages of tidal flat sediments in the Port au Port Group indicate at least a mesotidal range.

The effects of tidal currents are also observed in ooid calcarenites. Brown oolite and rarely grey oolite show excellent herringbone

cross-bedding and intermittent subaerial exposure.

Shelf Circulation. The variability of energy conditions on the shelf is indicated by the different lithofacies. The abundance of ooid and bioclastic calcarenites, which commonly show herringbone cross-bedding and a paucity of mud, indicate high energy conditions. The presence of carbonate and siliciclastic mud in virtually all lithofacies, however, implies that energy conditions were at least periodically sufficiently low to allow mud deposition. No evidence has been found for prolonged periods of quiescence during which extensive subtidal mud was deposited.

Well-developed bedding structures in parted limestones, interpreted to be products of tidal processes, also indicate periodic high energy conditions in the tidal flat and good circulation with the open ocean. In addition, the abundance of flat pebble conglomerates and the minor beds of ooid and bioclastic grainstones interbedded with parted limestone represent episodic high energy events in the tidal flat.

Climate. The absence of evidence of evaporites and the frequent occurrence of sedimentary structures that are interpreted to be paleokarst features, such as pitted surfaces, suggest that the climate was humid rather than arid.

Water Depth. Lithofacies indicate deposition of the Port au Port Group occurred in shallow subtidal to supratidal conditions. The lack of extensive deep subtidal or open shelf sedimentation is indicated by: (1) the absence of hummocky cross-stratification, which is widely interpreted to have formed by storm processes below normal wave base

(Walker, 1984; Dott and Bourgeois, 1982), in sediments which have undergone obvious storm reworking; (2) the paucity of bioturbated muds lacking mudcracks; and (3) the pervasiveness of mudcracks throughout the sequence and the common occurrence of paleokarst surfaces.

Chapter 4

FACIES SEQUENCES

4.1 INTRODUCTION

The Port au Port Group on the Port au Port Peninsula is characterized by prominent, layer-cake architecture. Detailed field observations reveal that it is comprised of three scales of sedimentary assemblages[1]: large-scale cycles (Grand Cycles; Aitken, 1966) on the order of hundreds of meters in thickness that are each divisible into two half-cycles (Aitken, 1966) composed of meter-scale assemblages. The utility of examining carbonate rocks in terms of such facies sequences has been clearly demonstrated in numerous studies (e.g. James, 1984) and has prompted considerable speculation as to the possible mechanisms of cycle formation.

This chapter examines: (1) small- and large-scale assemblages in the Port au Port Group, based in large part on the Port au Port Peninsula section and supplemented by sections on the Great Northern Peninsula; (2) storm deposits which punctuate these assemblages on the Port au Port

---

1. The term, "assemblage", is used herein to describe a vertical succession of lithofacies; those assemblages which are rhythmically repeated are termed "cycles".

Peninsula; and (3) comparison with western North American Grand Cycles. Detailed study of sequences in the Port au Port Group demonstrates the complex interplay of carbonate and siliciclastic sedimentation on the Cambrian platform and contributes to the understanding of the effects of sedimentation, eustasy and crustal movements on platform sequences.

4.2 METER-SCALE ASSEMBLAGES

Two distinct types are recognized in the Port au Port Group: (1) mixed-sediment cycles composed of parted limestone and shale and (2) oolite-laminite assemblages which lack a sequential arrangement of lithofacies.

4.2.1 Parted Limestone-Shale Cycles

4.2.1.1 Description

These cycles are prominent in the Cape Ann, Big Cove and Man O' War Members. A cycle is composed of a basal ripple-laminated limestone, which grades transitionally upwards into parted limestone, which in turn is capped by carbonate laminite and/or shale (Fig. 4.1; Plate 2a, b). Parted limestones exhibit upward changes from flaser bedding to wavy bedding to lenticular bedding. Flat-pebble conglomerates, skeletal wackestone and packstone, grey oolite and horizons of algal mounds randomly punctuate the cycles.

The cycles, 1 to 2 m in thickness, are characterized by their

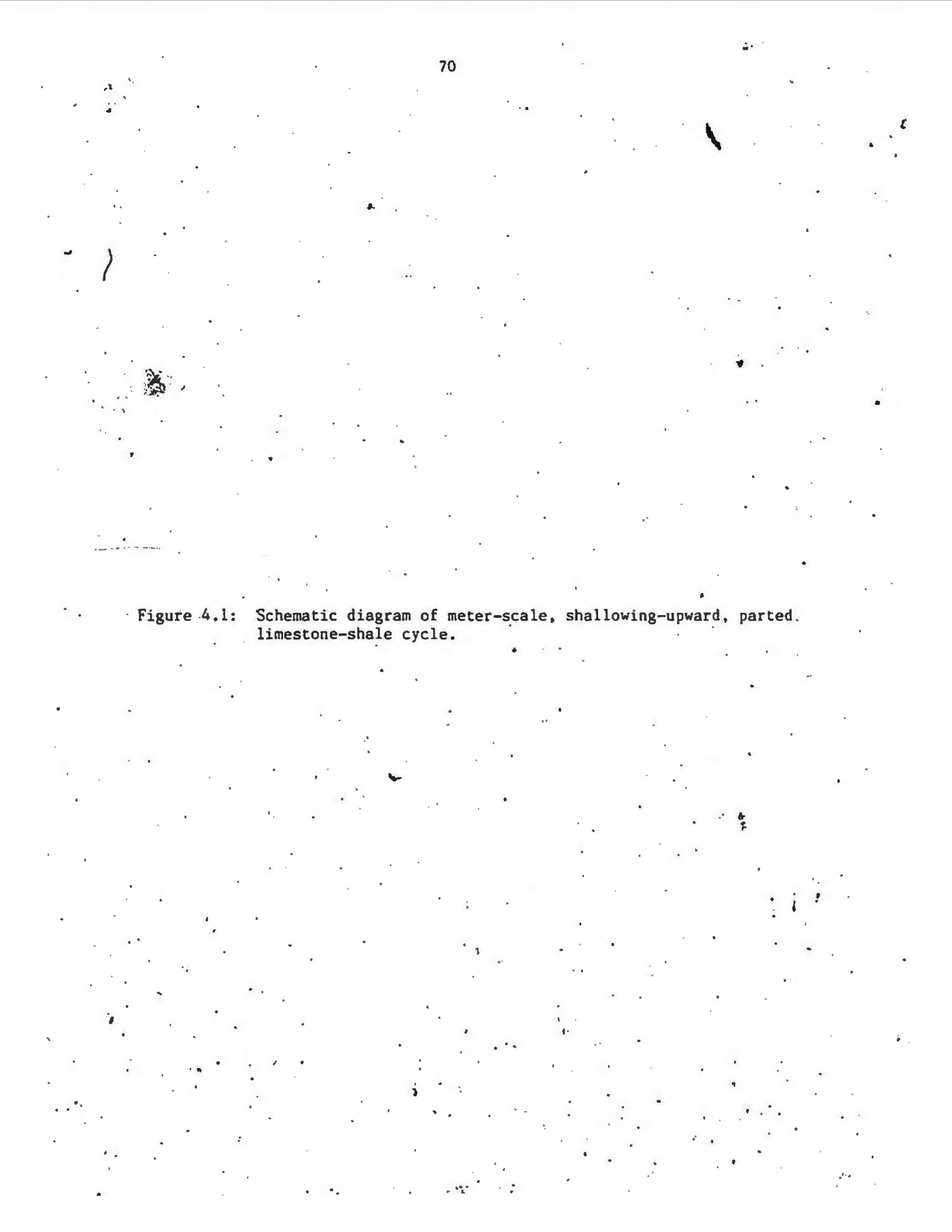

Figure 4.1: Schematic diagram of meter-scale, shallowing-upward, parted limestone-shale cycle.

PARTED LIMESTONE-SHALE CYCLE

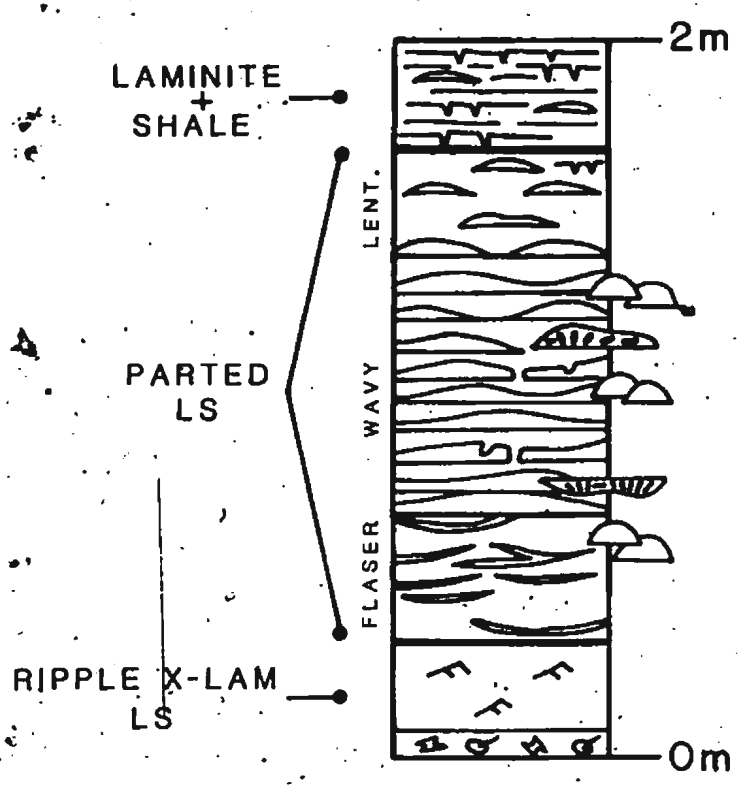

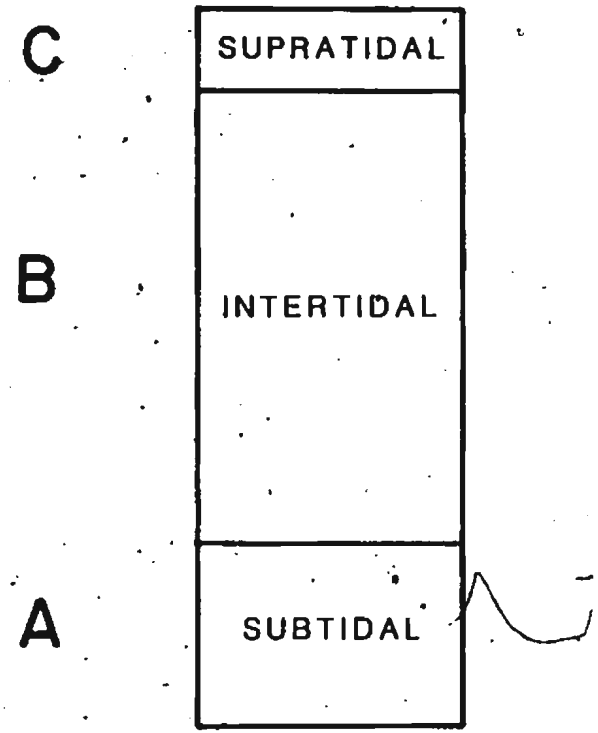

consistent lithological asymmetry and lateral extent; individual cycles can be correlated between outcrops tens of kilometers apart (Fig. B.8), but not with other outcrop areas in western Newfoundland. The style of cyclicity and frequency of occurrence, however, differs within each stratigraphic unit.

Cape Ann Member. Parted limestone is mainly thinly bedded to nodular, silty limestone with thin beds or partings of calcareous black shale and minor dolostone (type 2). Cycles consist of an upward change from: (1) dominantly ripple cross-laminated limestone with load casts to (2) flaser bedded limestone with minor black argillaceous partings to (3) wavy bedding composed of irregular beds of limestone (preserving load casts, gutter casts, isolated ripple forms) with thin beds of black shale to (4) lenticular bedding with limestone lenses in dominantly black shale to (5) mainly black shale. Runzelmarken, mudcracks, trace fossils and skip and bounce marks are common in shalier horizons. A decrease in shale content toward the top of the Cape Ann Member results in thinly bedded limestone and dolostone in the upper part which lack obvious meter-scale cyclicity.

Big Cove Member. The upper two-thirds of this member is similar in composition to the Cape Ann Member but meter-scale cyclicity is less obvious. Toward the top of the Big Cove, there is a predominance of interbedded limestone and dolostone (type 1 parted limestone) with abundant mudcracks and gradual decrease in the thickness and abundance of shale beds.

Man O' War Member. Parted limestones are mainly type 1, with minor

argillaceous horizons and well developed meter-scale cycles. Each cycle consists of: (1) a lower, wavy- to flaser-bedded parted limestone (dominantly limestone with minor partings of dolostone) passing transitionally upward to (2) lenticular bedding composed of lenses of limestone in dolostone and (3) an upper horizon of dominantly laminated dolostone. Very thin variegated shale beds may cap the cycle and minor ooid and bioclastic calcarenites may be present in the lower part.

4.2.1.2 Interpretation

As previously discussed in Chapter 3, parted limestone-shale cycles are identical to pure siliciclastic tidal flat models both in terms of style of cyclicity and sedimentary structures. These carbonate-siliciclastic cycles are similarly interpreted to be shallowing-upward events (ie. shallow subtidal to intertidal to supratidal) in a tidal flat.

Meter-scale, shallowing-upward cycles have been well documented in ancient platform carbonate sequences and proven to be one of the most useful concepts in interpreting platform carbonates (James, 1984). The mechanism for such cyclity, however, is still a topic of considerable debate. Numerous hypotheses have been proposed and include changes in the rate of subsidence; sea-level changes; variations in rates of sea-level fluctuation; and changes in the rate of carbonate sedimentation related to such factors as climatic changes and variations in the carbonate source area (reviewed by Wilson, 1975). Possible mechanisms for the development of parted limestone-shale cycles must explain the following observations: (1) the presence of only

asymmetrical shallowing-upward cycles; (2) their lateral traceability over tens of kilometers; and (3) their vertical scale (a 1-2 m thick cycle formed over an estimated 100,000 yr period, based on an estimated 15 my period for a single Grand Cycle [refer to the discussion at the end of the chapter]).

Wilkinson (1982) has incorporated proposed mechanisms for carbonate shallowing-upward cycles into two end-member models: (1) an extrinsically controlled or allocyclic model in which rapid changes in relative sea-level are accompanied by constant carbonate production and sedimentation and (2) an autocyclic model (Ginsburg, 1971; Matti and McKee, 1976; Mossop, 1979; Wong and Oldershaw, 1980) in which cyclicity is intrinsically controlled by rates of carbonate production and deposition. Both models may produce similar prograding sequences and are based upon the premise that the rate of shelf carbonate accumulation generally exceeds the rate of subsidence of the shelf, which allows deposits to build up to sealevel and above (James, 1984).

The autocyclic model for carbonates is considered by many workers to be most compelling because it does not require rapid small-scale changes in sea-level or subsidence, nor global-scale cyclicity (James, 1984). It may offer the most plausible explanation for parted limestone-shale cycles. Under conditions of gradual subsidence and/or sea-level rise, water depth and size of the sediment source area control sedimentation rates. In parted limestone-shale cycles, the textural similarities between the carbonate components of the supratidal, intertidal and subtidal sediments indicate a common carbonate source area -- probably the subtidal environment (Ginsburg, 1971; James, 1984). Sediment

transport and deposition form sediment wedges which continuously prograde across the tidal flat. Sedimentation ceases when the subtidal source area becomes too deep or too small and does not resume again until the platform becomes deep enough to begin depositing the next cycle (Fig. 4.2). Cycles resulting from the autocyclic mechanism are: (1) laterally extensive, diachronous units, which may be bounded by submarine discontinuity surfaces; (2) complete, shallowing-upward sequences; and (3) lacking in extensive vadose diagenesis (Grotzinger, 1985).

In spite of the apparent feasibility of the autocyclic model, it suffers from several pitfalls. Firstly, demise of the sediment source area, which is the key to autocyclicity, would be unlikely in that dynamic equilibrium between sediment production rates, sediment dispersal and relative sea-level rise would be attained before the source area became too small or too deep to provide sediment (Pratt and James, in press; Grotzinger, 1985). Secondly, subsidence rates on passive margins (e.g., 2-4 cm/1000 yr, Pitman, 1978; 5-10 cm/1000 yr, Grotzinger, 1985) are too low to drown platform sediments in a reasonable period of time (Grotzinger, 1985).

An allocyclic model is most attractive for explaining large-scale cycles (James, 1984) and its applicability to meter-scale cycles cannot be discounted. Anderson and Goodwin (1980) and Anderson et al. (1984), for example, in their studies of some Upper Paleozoic sequences proposed that shallowing-upward cycles produced by "geologically instantaneous base-level rises" (Anderson et al., 1984, p.120) gave rise to basin-wide, time-stratigraphic units. They applied the term "punctuated

Figure 4.2: Schematic diagram illustrating formation of parted limestone-shale cycles by progradation of sediment wedges and subsidence. Eustatic or autocyclic mechanisms are not implied.

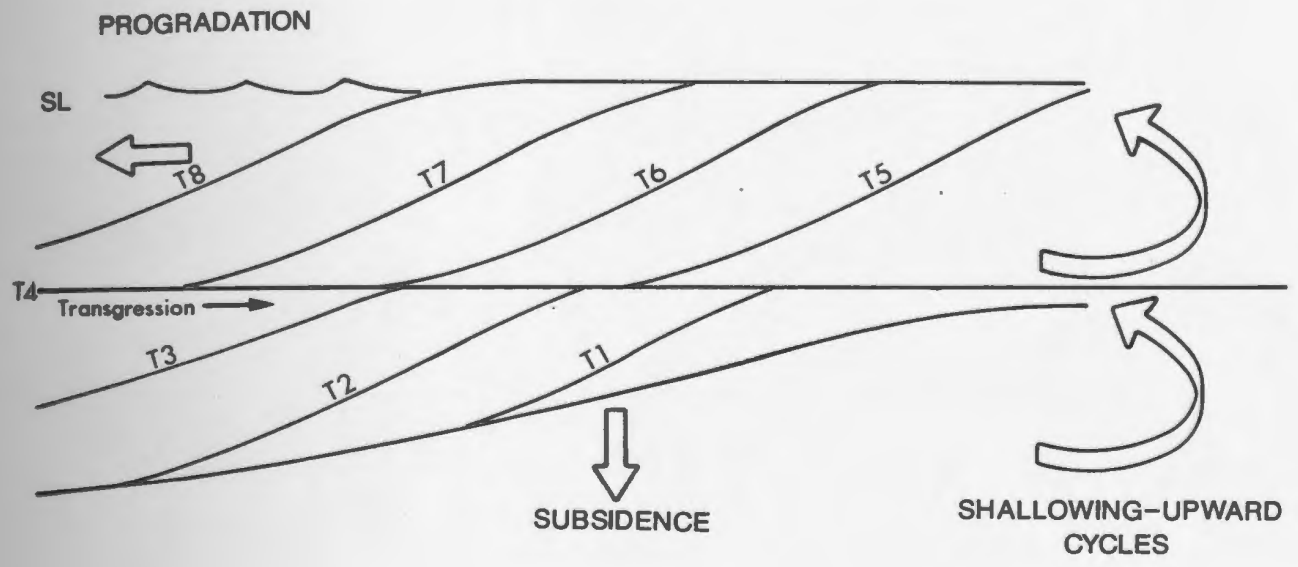
PROGRADATION
SL
T8
T7
T6
T5
T4
Transgression
T3
T2
T1
SUBSIDENCE
SHALLOWING-UPWARD
CYCLES

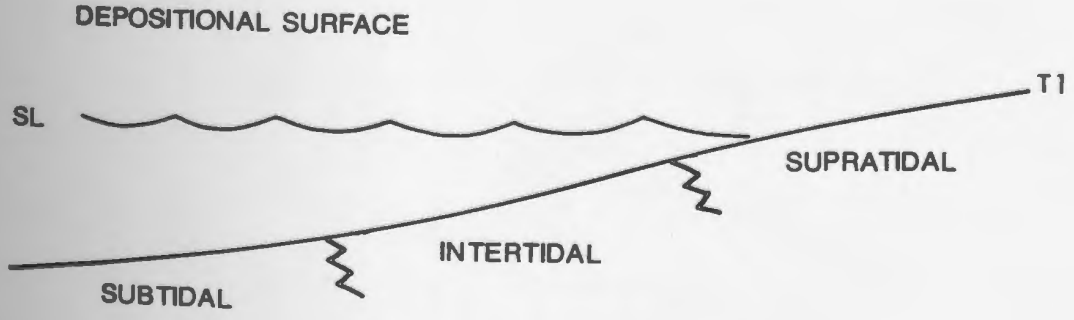
DEPOSITIONAL SURFACE
SL
T1
SUPRATIDAL
INTERTIDAL
SUBTIDAL

aggradational cycles" (PACs) to these episodic features. Their interpretations, however, are suspect as they are based upon some unsubstantiated evidence: (1) sharp non-depositional cycle boundaries are attributed to abrupt base-level rises without considering the possibility of other mechanisms, such as changing rates of sediment production and deposition and (2) no evidence is provided for the lateral synchroneity of their cycles, a criterion which is intrinsic to PACs. Furthermore, a generic term like "PAC" has little application to the description of other cycles in the rock record, in which the mechanism(s) of formation is uncertain.

In the study by Grotzinger (1985), 1-15 m thick shallowing-upward cycles, correlative over 100 km across and 200 km parallel to depositional strike, were documented in the lower Proterozoic Rocknest Formation in the Northwest Territories. He showed that eustatic changes in sea-level, specifically those resulting from fluctuations in global ice-volume and geoidal effects (further discussed in "Grand Cycles"), could be of (1) asymmetrical nature, permitting slow progradation and rapid transgression and (2) small enough scale to generate meter-scale cycles (periods of 10,000-100,000 yr). This allocyclic model can account for vadose diagenesis in the cycles and the occurrence of incomplete cycles, which cannot be explained by autocyclic models. Grotzinger also noted that because of geoidal eustasy, eustatic changes differ regionally or locally (in periodicity, amplitude and direction) and suggested that a eustatic mechanism for small-scale cycles (and large-scale ones) does not require that they be globally or even regionally correlative.

It is apparent that observations from parted limestone-shale cycles do not unequivocally support either a eustatic or autocyclic mechanism. These cycles, however, lack substantial vadose diagenesis (e.g. paleokarst), contain numerous hardgrounds (refer to Chap. 7), and are generally complete cycles -- evidence which suggests a predominantly autocyclic mechanism.

4.2.2 Oolite-Laminite Assemblages

4.2.2.1 Description

Interbedded grey and brown oolites and carbonate laminite, which occur repeatedly throughout the Campbells and Felix Members and Berry Head Formation, are characterized by the absence of consistent and predictable upward changes in lithofacies (Plate 3a). Basal grey oolite overlain by brown oolite which is in turn capped by laminite is a common arrangement as is the reverse change from laminite to grey oolite (Fig. 4.3). Field observations of the non-sequential nature of these lithofacies is supported by Markov chain analysis (Powers and Easterling, 1982; Hiscott, pers. comm., 1984) of the Campbells Member of the March Point section on the Port au Port Peninsula.

All three lithofacies are not always present. Brown oolite is the only recurring lithology; for simplification of subsequent discussions the bases of these oolite beds are arbitrarily designated as "assemblage boundaries". These individual assemblages, 1 to 2 meters in thickness, can be traced the extent of the outcrop (tens to hundreds of meters); however, they cannot be correlated between outcrops only tens of

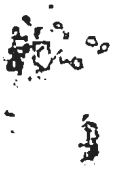

Figure 4.3: Composite of oolite-laminite assemblages illustrating the variety of vertical changes in lithofacies (gy. = grey; bn. = brown).

OOLITE-LAMINITE ASSEMBLAGE

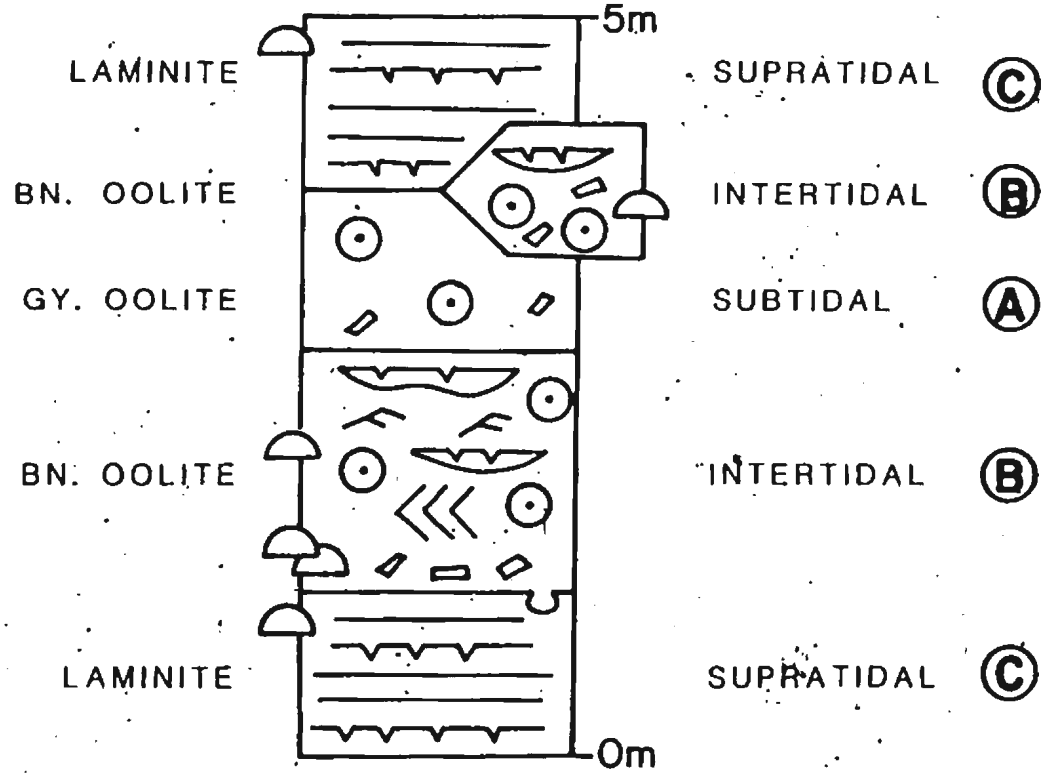

kilometers apart. Stromatolite and thrombolite mounds; peloidal and bioclastic calcarenites; and variegated shales occur throughout though not in any specific position in the assemblages.

Lithologic contacts are generally stylolitic but appear to follow original sedimentary bedding boundaries. Where bedding contacts are present, they are generally gradational, particularly the upward transition from brown oolite to grey oolite and from brown oolite to carbonate laminite.

Individual brown oolite beds also occasionally have asymmetrical, decimeter-scale sequences. They are composed of (from base to top): (1) oolite with herringbone cross-bedding; (2) ripple cross-bedded oolite (with symmetrical ripple forms); and (3) laterally discontinuous, mudcracked, dolomitic mudstone beds (up to 10 cm thick).

4.2.2.2 Interpretation

Oolite-laminite assemblages record the evolution of the subtidal mobile fringe (grey oolite); intertidal sand flat (brown oolite) and supratidal cap (carbonate laminite) of a carbonate sand shoal complex (refer to Chap. 3). Unlike many platform carbonates, however, these assemblages are rarely shallowing-upward cycles. Any mechanisms proposed for their formation must account for the following observations: (1) the unpredictable vertical arrangement of lithofacies; (2) the common absence of subtidal or supratidal components; (3) the thinness of individual assemblages; (4) the large number of assemblages; and (5) the inability to correlate individual assemblages between

adjacent outcrops.

Neither the eustatic nor autocyclic models reviewed by Wilkinson (1982) for consistently shallowing-upward cycles successfully explains the nature of these assemblages. Instead, they are most reasonably explained as products of vertical accretion and frequent, rapid migration of the subtidal, intertidal and supratidal components of the carbonate shoal on a subsiding platform (Fig. 4.4). The shoal components accrete to sea-level largely by means of in situ sediment production; intertidal and subtidal zones are sediment source areas as well as sediment sinks. The irregularity of the assemblages reflects the variable configuration and geographic extent of the shoal complex which change dynamically in response to varying sediment production and dispersal rates, and such hydrographic conditions as tidal variations and storm activity. The effects of relative sea level fluctuation and rates of sea level change are not important factors in this model.

A similar model has been proposed by Pratt and James (in press) for the Lower Ordovician St. George Group in western Newfoundland. Their "island tidal flat" model for epeiric seas consists of a mosaic of islands surrounded by open water in which cyclic sedimentation is governed not by eustatic mechanisms but rather by regional or local hydrography.

4.3 STORM DEPOSITS

The cyclic nature of platform carbonate sequences has been well

Figure 4.4: (A) Schematic diagram of carbonate sand shoal complex; and (B) postulated mechanism of formation involving vertical accretion and frequent, rapid migration of the various components of the shoal complex in a subsiding platform.

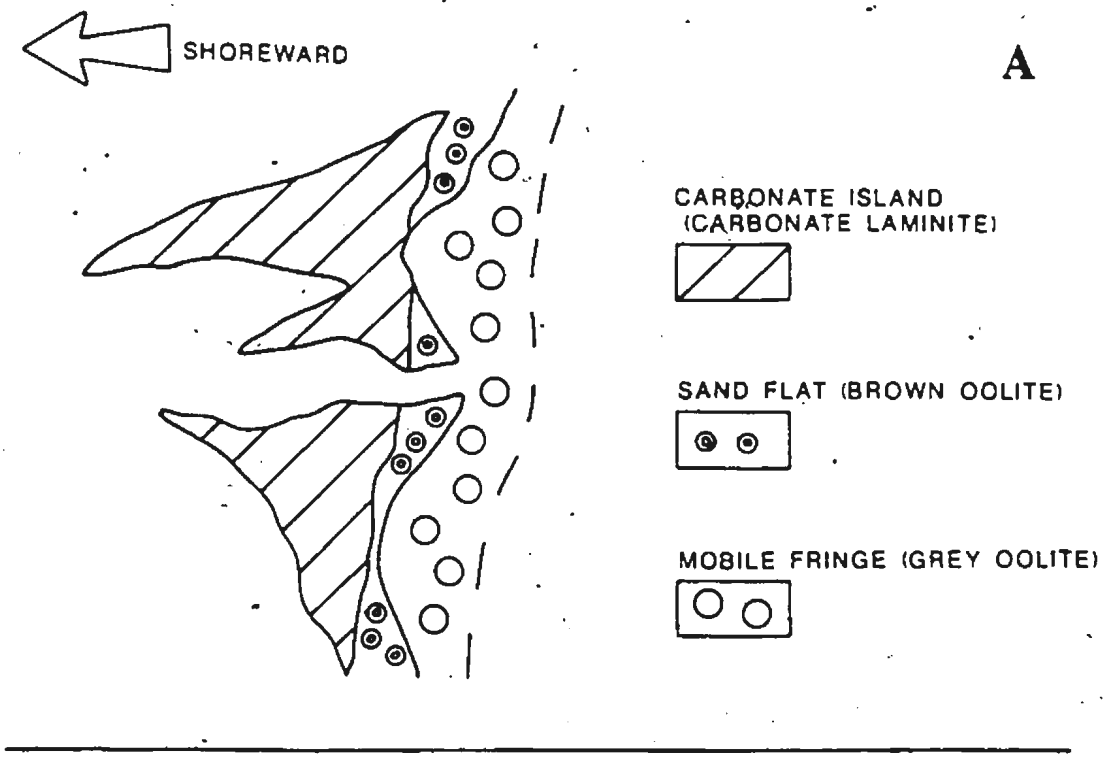
SHOREWARD
A
CARBONATE ISLAND
(CARBONATE LAMINITE)
SAND FLAT (BROWN OOLITE)
MOBILE FRINGE (GREY OOLITE)

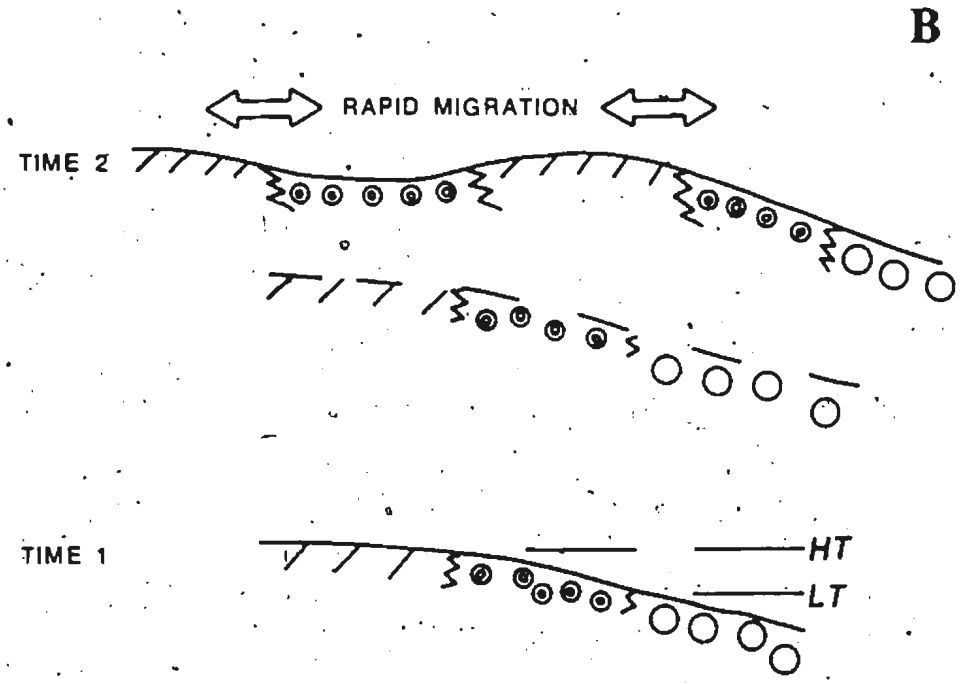
B
RAPID MIGRATION
TIME 2
TIME 1
HT
LT

documented (refer to James, 1984). In contrast, the importance of deposits which record "rare events" (Seilacher, 1982; Dott, 1983) has only recently become more apparent. Storm deposits or "tempestites" (Ager, 1974) appear to be common event deposits on Paleozoic platforms and consist of depositional and erosional features that record the beginning, climax and waning of the storm event (Kreisa and Bambach, 1982). Typical sedimentologic features are: (1) beds with erosional bases and gradational or burrowed tops; (2) lateral thickening and thinning of beds and lenticular beds; (3) hummocky cross-stratification; (4) vertical changes in sedimentary structures that represent transition from higher to lower flow regimes; (5) gutter and pot casts; (6) reworking of fauna; and (7) sediment infiltration fabrics (e.g. Kreisa, 1981, and references cited therein; Aigner, 1982; Seilacher, 1982).

In the Port au Port Group, there are several notable sedimentary structures interpreted to be related to storm activity on the platform. In other studies, similar structures have been used to substantiate a variety of interpretations, ranging from strandline to turbidite deposits. In the Port au Port Group, however, constraints set by the interpretation of lithofacies and paleogeographic setting indicate that the episodic features are most reasonably interpreted in a tempestite model. The most common is <u>flat-pebble conglomerate</u>, which is interbedded with parted limestone and composed mainly of clasts derived from adjacent beds (refer to Chap. 3 and 5). Conglomerates with oolitic clasts are also occasionally present in association with oolites and carbonate laminites. These conglomerates randomly punctuate the meter-scale assemblages and are not restricted to any one lithofacies.

They vary from laterally extensive planar beds to more areally restricted lensoid horizons with planar to slightly convex-downward bases.

The conglomerates are interpreted to be tempestites formed by the erosion and redeposition of already-lithified sediments in supratidal to shallow subtidal environments. Sepkoski (1982) has likewise interpreted flat-pebble conglomerates in Cambrian carbonates in western North America. Other workers (e.g. Donaldson and Ricketts, 1979) have frequently interpreted similar types of conglomerates as beach deposits formed by energetic reworking of the sediment. High energy deposits, however, do not necessarily reflect very shallow water conditions; they only indicate that the area was above storm wave-base. Interpretation of Port au Port conglomerates solely as beach deposits is precluded by: (1) the absence of subaerial exposure features and (2) the occurrence of identical parted limestones overlying and underlying a conglomerate bed, suggesting no prolonged changes in the depositional environment.

Parted limestones also commonly contain centimeter-scale, erosional groove casts or channels. These are termed gutter casts by Whitaker (1973) and may also be of storm origin. The casts are interpreted to be erosional features caused by high energy, possibly helical currents (Whitaker, 1973) or scours produced around obstacles (Aigner and Futterer, 1978). Various workers (Aigner, 1982 ; Kreisa, 1981) have proposed that these gutter casts are storm features that record an episodic increase in energy on the sea floor during peak storm conditions.

Two oolite facies have been identified as possible tempestites. The first consists of 10-30 cm thick beds of grey oolite that are associated with parted limestones and flat-pebble conglomerates in the upper parts of the Cape Ann, Big Cove and Man O' War Members. Radial ooids, which comprise these oolites, probably did not form in a muddy tidal flat environment (see Chap. 3). A more plausible interpretation is that ooids were derived from the sand shoal complex and swept by storms into the tidal flat. This is substantiated by the association of the oolites with storm-derived conglomerates and the morphologic similarity between the ooids in tidal flat deposits and those in sand shoal deposits of the Campbells and Felix Members. The second facies includes decimeter-scale sequences that occasionally occur in brown oolite. The sequences, which are composed of herringbone cross-bedded oolite overlain by ripple cross-laminated oolite and topped by mudcracked mudstone beds, are interpreted to reflect waning energy conditions following storm erosion. Similar tempestite sequences in bioclastic limestones have been documented by Aigner (1982), who also commented on their similarity to Bouma sequences.

Although tempestites are present throughout the Port au Port Group, flat-pebble conglomerates and thin beds of ooid and bioclastic grainstones to packstones are more abundant in the Man O' War Member. This suggests that storm events became more frequent in the younger part of the sequence. The thickness of the conglomerates (up to 30 cm) and the large size of the tabular clasts (up to 10 cm in diameter) also tend to indicate storms of longer duration and higher energy respectively than recorded by conglomerates in the older part of the sequence.

4.4 GRAND CYCLES

4.4.1 Introduction

The Port au Port Group on the Port au Port Peninsula is characterized by three large-scale, asymmetrical cycles (100 to 250 m thick). These are distinct from meter-scale assemblages and from the larger scale, unconformity-bounded, craton-wide sequences described by Sloss (1963). Each cycle spans at least several trilobite zones and is divisible into two components, each 50 to 150 m in thickness. The two components, first documented by Levesque (1977) and termed large-scale megarhythms, include: (1) a recessive weathering, lower shaly half-cycle composed of parted limestone-shale cycles and (2) a resistant weathering, upper carbonate half-cycle composed of oolite-laminite assemblages.

Large-scale cycles (90 to 600 m thick) are also the dominant sedimentary features in the Cambrian of the Canadian Cordillera (Aitken, 1966, 1978) and the Great Basin of the western United States (Palmer and Halley, 1979; Mount and Rowland, 1981). These have been termed "Grand Cycles" by Aitken (1966). As outlined by Aitken (1981), these Grand Cycles characteristically consist of a lower unit of interbedded siliciclastic mudstone and limestone and/or sandstone (shaly half-cycle) which passes gradationally upward into an upper unit of predominantly limestone and dolomitized limestone (carbonate half-cycle). Grand Cycle boundaries are generally abrupt stratigraphic contacts and each cycle includes two or more trilobite zones. In eastern North America, no

Grand Cycles have been well documented in Cambrian sections. There has only been cursory examination of cycles in the southern Appalachians by Aitken (1981) and Palmer (1971).

Although there are significant differences in the detailed sedimentology, large-scale cycles in the Port au Port Group possess all the essential characteristics of Grand Cycles and hence are considered to be Grand Cycles comparable to those elsewhere in North America. In western Newfoundland, they are best preserved in the Port au Port Peninsula sections. Cambrian sequences at Bonne Bay and Canada Bay are also composed of these large cycles but they are not as well developed or exposed. The predominantly carbonate sections at Goose Arm and White Bay lack obvious Grand Cycles.

Grand Cycles have been interpreted to be features of passive continental margins, particularly continental shelves, in which carbonate-dominated sedimentation alternated with siliciclastic-influenced sedimentation (Aitken, 1981). Cycles containing shaly half-cycles which represent slope deposition do occur but are not well known and will be not be considered further in this discussion (Aitken, 1966; Palmer, 1971). The concept of Grand Cycles provides a useful approach for an analysis of Cambrian platform sediments and forms the framework for depositional and diagenetic models in this study. As will be shown in this section, use of the term "Grand Cycle" does not imply specific lithofacies assemblages or depositional processes; cycles may vary considerably between regions and even within specific regions.

4.4.2 Grand Cycles in Western Newfoundland

Grand Cycles are reflected in the revised stratigraphy of the Cambrian platform sequence (refer to Chapter 2, Appendix A) and can be traced over an east-west distance of approximately 45 km on the Port au Port Peninsula. They are, from base to top: Grand Cycle "A" consisting of the March Point Formation, Cape Ann Member and Campbells Member; Grand Cycle "B" composed of the Big Cove and Felix Members; and Grand Cycle "C" consisting of the Man O' War Member and the Berry Head Formation (Fig. 4.5). The lower shaly half-cycle and upper carbonate half-cycle of each Grand Cycle represent two distinctly different styles of sedimentation and form the basis for detailed examination of the Port au Port Group (Fig. 4.6).

4.4.2.1 Shaly Half-Cycle

Each shaly half-cycle (50-90 m thick) is represented by thinly interbedded fine-grained carbonates and siliciclastics (March Point Formation, and Cape Ann, Big Cove and Man O' War Members). It is characterized by the meter-scale parted limestone-shale cycles which are randomly interrupted by skeletal wackestone and packstone, algal boundstone and flat pebble conglomerate. Angular quartz silt is ubiquitous; rounded, medium to coarse sand size quartz is rare.

The base of each half-cycle is marked by the abrupt appearance of grey or variegated shale and generally appears to be conformable with the underlying thick-bedded carbonates. Shales grade rapidly into parted

Figure 4.5: Stratigraphic section showing the three Grand Cycles in the Port au Port Group, Port au Port Peninsula.

GRAND CYCLES

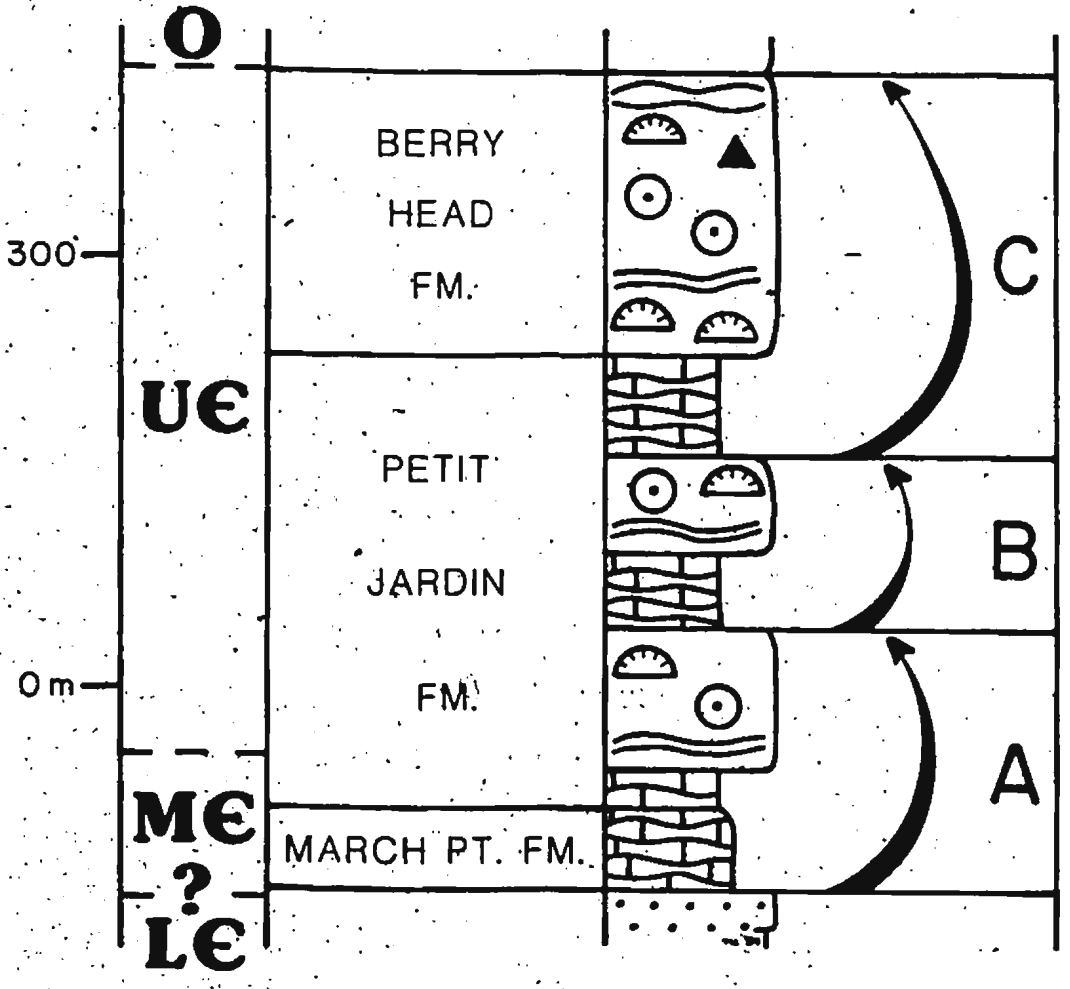

Figure 4.6: Schematic diagram illustrating the components of a Grand Cycle, based on the March Point Formation, and Cape Ann and Campbells Members of the Petit Jardin Formation on the Port au Port Peninsula.

SCHEMATIC

GRAND CYCLE

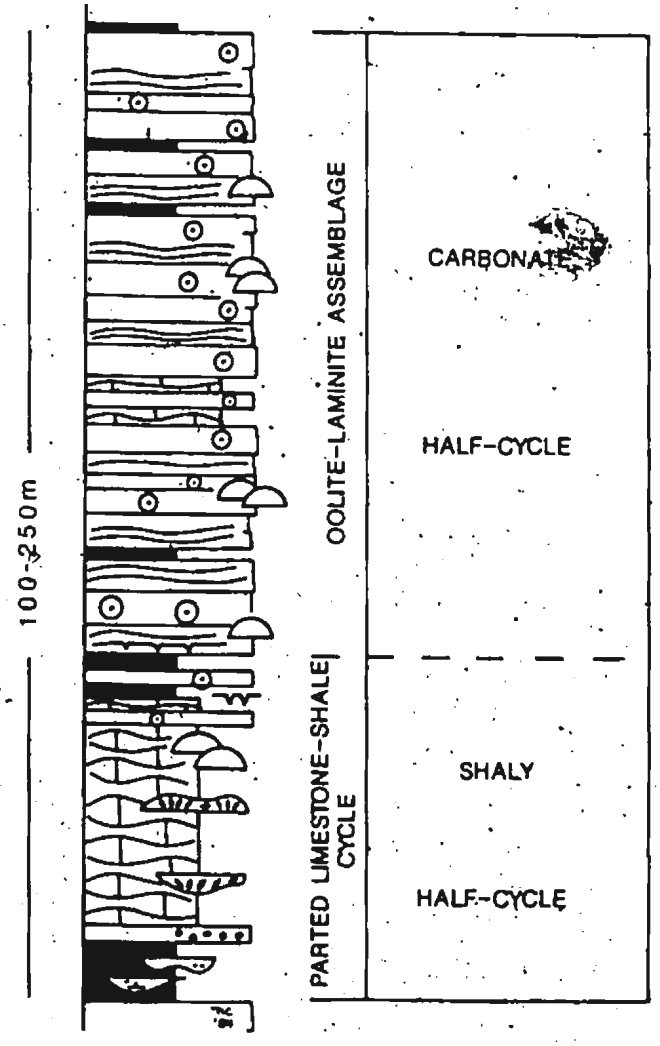

limestones and minor ooid calcarenites in the upper part of the half-cycle. Although the three shaly half-cycles of the Port au Port Group generally exhibit the above elements, the half-cycles are not identical (Fig. B.9).

Grand Cycle A. The March Point/Cape Ann/Campbells cycle begins with the abrupt appearance of fine-grained siliciclastics and limestones above thick-bedded sandstones of the Lower Cambrian Hawke Bay Formation. The basal 20 m is composed of interbedded calcareous siltstone to silty lime mudstone; glauconitic sandstone and limestone; and dark grey shale. Above the basal interval, quartzose sandstone and intervals with abundant quartz sand are rare in the shaly half-cycle. These siliciclastic-rich beds pass gradationally upward into type 1 parted limestone (limestone and dolostone) with rare desiccation cracks. In the Cape Ann Member grey shale becomes abundant, comprising up to 50% of the parted limestone (type 2). In the upper part of the half-cycle, type 1 parted limestone again predominates; ie. shale disappears and the section is composed predominantly of dolostone with limestone lenses and abundant mudcracks and prism cracks.

Grand Cycle B. In contrast to the above described shaly half-cycle, the Big Cove Member lacks basal siliciclastic-dominated beds with interbedded parted limestone. Some minor thin beds of glauconitic silty limestone, however, do occur near the base. The Big Cove Member, in particular the upper two-thirds, is similar to the Cape Ann Member and exhibits the same upward transitions.

Grand Cycle C. The Man O' War Member is distinct from the underlying

shaly half-cycles in that it has a greater diversity of lithologies. Abundant algal-mound horizons; grey oolites; bioclastic calcarenites; and flat-pebble conglomerates occur throughout. As in the other shaly half-cycles, the base of the Man O' War Member is marked by the abrupt appearance of siliciclastics. The basal 10 m is composed of interbedded dark grey shale, oolite and laminite with several meter-thick, dolomitized algal mound horizons. The shale and thick-bedded carbonate quickly disappear upward in the member and are replaced by type 1 parted limestone with prominent meter-scale cycles; grey shale in this part of the unit is uncommon. Runzelmarken and mudcracks are common, particularly in the upper portion of the member.

4.4.2.2 Transitional Interval

In contrast to the relatively abrupt lower boundary of the shaly half-cycle, the transition to the carbonate half-cycle is gradational (Plate 2c). The base of the carbonate half-cycle is arbitrarily placed at the first occurrence of thick-bedded carbonates.

The onset of carbonate half-cycle deposition is heralded by: the appearance of thin beds of grey oolite within parted limestone at the top of the shaly half-cycle; (2) the gradual development of carbonate laminite from underlying and adjacent parted limestone; and (3) the gradual disappearance of grey shale in parted limestone. Variegated shale in beds up to 1 m thick may be interbedded with the basal laminites. This transition occurs over an interval of 10 to 15 m.

4.4.2.3 Carbonate Half-Cycle

Carbonate half-cycles are composed of meter-scale assemblages of thickly interbedded ooid calcarenite and carbonate laminite. The Campbells Member is predominantly limestone whereas the Felix Member and Berry Head Formation are dolostone. Stromatolite and thrombolite mound horizons punctuate the meter-scale assemblages and minor recessive horizons of parted limestone and red and green shale are present throughout.

The base of each half-cycle is characterized by interbedded brown oolite and laminite, the latter often showing well developed prism cracks. Grey oolite is uncommon until the upper portion of the cycle where it is interbedded with laminite and brown oolite. Minor calcareous sandstone, composed of medium- to coarse-grained quartz sand, and local concentrations of rounded quartz sand and angular silt are present, particularly in the Felix Member.

The upper boundary of each Grand Cycle is marked by the abrupt appearance of thick beds of siliciclastic mud of the overlying cycle. The change, however, is a rapidly gradational transition occurring over an interval of approximately 5 to 7 m. In this interval, thin beds of variegated shale and parted limestone are interbedded with carbonate beds near the top of the carbonate half-cycle; minor beds of ooid calcarenite and carbonate laminite occur in the basal part of the next shaly half-cycle.

4.4.2.4 Boundaries

Critical to the understanding of Grand Cycles is the nature of the boundaries. Are they disconformities? Are they time-synchronous horizons?

In the Port au Port Group both conformable and disconformable cycle boundaries occur. The boundary between Grand Cycles A and B, B and C, and the top of Grand Cycle C appear to be conformable. This is supported by the available biostratigraphic data and the absence of subaerial exposure horizons. A possible disconformable boundary has been noted at the boundary of the upper Middle Cambrian March Point Formation with the underlying Lower Cambrian to lower Middle Cambrian (?) Hawke Bay Formation (Palmer and James, 1979).

Within each Grand Cycle the strata appear to be generally conformable, although hardgrounds and subaerial exposure horizons are common throughout the sequence. These diastems appear to represent hiatuses of relatively short duration, at least shorter than that detectable by trilobite biostratigraphy. There are no major changes in lithologies above and below the diastems. The notable exception is revealed by biostratigraphy and involves a condensed interval present just below the top of Grand Cycle B. Here several Upper Cambrian trilobite zones (Aphelaspis, Dicanthopyge, Prehousia and Dunderbergia) are concentrated in an 8 to 12 m interval (refer to Chapter 2; Levesque, 1977). The interval consists of interbedded carbonate laminite and glauconitic, arenaceous brown oolite which is also suggestive of reduced sedimentation rates.

Although Grand Cycle boundaries are either relatively abrupt or rapidly gradational, determination of the synchroneity or diachroneity of cycle boundaries in western Newfoundland is beyond the resolution of the biostratigraphy currently available. Studies of other North American Grand Cycles, however, provide sedimentologic and biostratigraphic evidence regarding cycle boundaries. Aitken (1966, 1981), from his work in the Canadian Cordillera, proposed that the bases of Grand Cycles are approximately time-synchronous horizons. Palmer and Halley (1979), on other hand, proposed that Grand Cycle boundaries of the Middle Cambrian Carrara Formation of the Great Basin are slightly diachronous. Aitken (1981), however, points out that this diachroneity is inherent in their model and is not supported by faunal or sedimentologic evidence.

In contrast, the transitional intervals between the shaly half-cycles and the overlying carbonate half-cycles have been documented to be diachronous, younging toward the craton, in both the Canadian Rockies and the Great Basin (Aitken, 1966; 1978; Palmer and Halley, 1979; Mount and Rowland, 1981). In western Newfoundland there is some biostratigraphic evidence, albeit scant, that the transitional interval between Grand Cycles A and B is also diachronous. On the Port au Port Peninsula, the upper part of the Campbells Member is in the Cedaria zone, whereas the lithologically correlative interval at Bonne Bay probably belongs in the younger Crepicephalus zone (Levesque, 1977; D. Boyce, pers. comm., 1983).

4.4.2.5 Great Northern Peninsula Outcrops

Of the sections examined along the Great Northern Peninsula only those at Bonne Bay and Canada Bay exhibit the same style of large-scale cyclicity as documented on the Port au Port Peninsula (Fig. 4.7). Field descriptions of the sections in each area are given in Chapter 2. The half-cycles are similar in lithology but differ considerably in unit thicknesses between the different areas. In the Bonne Bay section, there are two nearly complete Grand Cycles and a third one that is mostly obscured by talus. They are correlative with cycles "A", "B", and "C" on the Port au Port Peninsula, but have thicker shaly half-cycles. In Canada Bay, there are four Grand Cycles (60-120 m thick) of which the lower two are considerably thinner than Port au Port Peninsula cycles. Lithologically, "A" may be correlative with the lower two cycles in Canada Bay, and "B" and "C" with the two upper cycles.

Grand Cycles are not recognized in Goose Arm and White Bay. Sequences in these two areas are predominantly dolostone and are similar to carbonate half-cycles documented in the other areas. Directly below the Berry Head Formation in both areas is a 75-80 m interval of shale, parted limestone and stromatolite/thrombolite mounds. It is similar to shaly half-cycles and may be correlative with the Man O' War Member on the Port au Port Peninsula.

Outcrops along the St. Barbe coast contain lithologies that are similar to equivalent strata in other areas in western Newfoundland. Discontinuous coastal exposures, however, preclude assessment of the

Figure 4.7: Stratigraphic cross-section of the Port au Port Group, western Newfoundland with lithologic correlations. Goose Arm and White Bay sections (right) are included in the carbonate belt. Bonne Bay, Canada Bay, and Port au Port Peninsula sections are included in the more leeward (westward), mixed carbonate-siliciclastic belt (refer to Fig. 1.1).

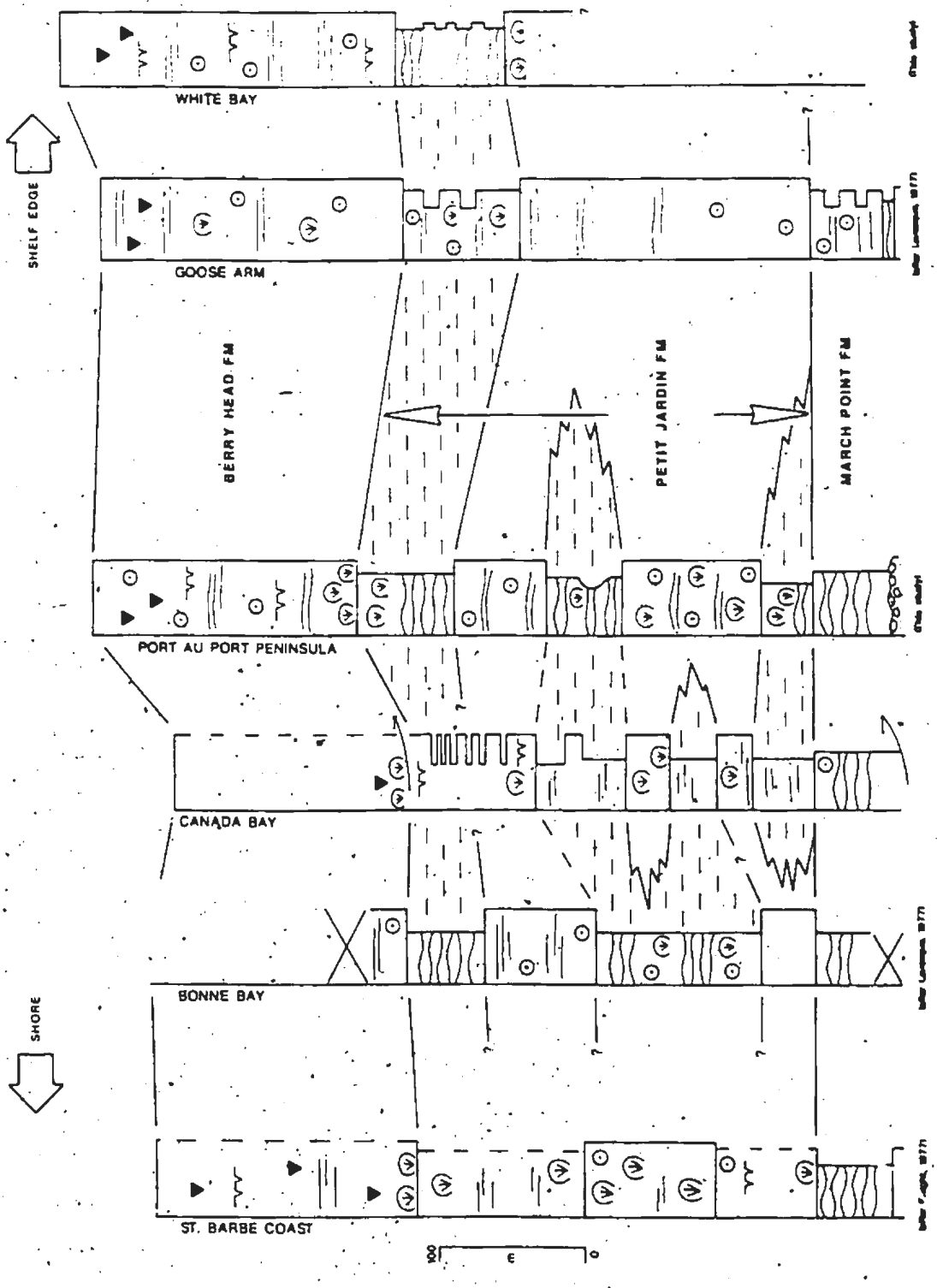
WHITE BAY
SHELF EDGE
GOOSE ARM
BERRY HEAD FM
PETIT JARDIN FM
MARCH POINT FM
PORT AU PORT PENINSULA
CANADA BAY
BONNE BAY
SHORE
ST. BARBE COAST

lithofacies in terms of Grand Cycles; there are extensive covered intervals in the Petit Jardin and Berry Head Formations.

4.4.3 Other North American Grand Cycles

Grand Cycles documented in other North American Cambrian sections by various workers bear all the essential characteristics of Grand Cycles as defined by Aitken (1981), but vary in their detailed sedimentology. The following section is only a simplified summary of the various cycles because no cycle is identical to any other one in the same region.

4.4.3.1 Southern Canadian Rocky Mountains

Detailed study of two contrasting types of Grand Cycles was conducted by Aitken (1966, 1978): the Middle Cambrian Stephen-type cycle and the Upper Cambrian Sullivan-type cycle. Both are interpreted to represent deposits of an inshore basin on the order of 1900 km long, 700 to 1100 km wide and greater than 8 to 12 m deep (shaly half-cycle) confined behind a platform-rim carbonate shoal complex (carbonate half-cycle).

In the Stephen-type cycle, the shaly half-cycle (Stephen Formation) is composed predominantly of parted limestones (type 1), with an increase in the proportion of greenish-grey shales approximately halfway through the half-cycle. This grades upward into a carbonate half-cycle (Eldon Formation) that is a monotonous sequence of parted limestones and mottled lime mudstones with minor dolomitic laminites and grainstones. Aitken (1978) interpreted this type of Grand Cycle as the record of deposition only in a quiet subtidal basin which underwent a transition

from predominantly terrigenous-mud deposition (shaly half-cycle) to carbonate-mud deposition (carbonate half-cycle). A narrow carbonate shoal (less than 20 km wide), not represented in this cycle, was situated to the west and laterally discontinuous, thus permitting tidal exchange across the barrier. This resulted in only rare "high energy" sediments in the shaly half-cycle.

Meter-scale cycles are present in both half-cycles. The lower 24 m of the Stephen Formation contain two laterally extensive cycles, each composed of (from base to top): (a) argillaceous lime mudstone; (b) parted limestone; and (c) cryptalgalaminated carbonate. The Eldon Formation commonly exhibits the following meter-scale cycle (from base to top): (a) burrow-mottled limestone and dolostone; (b) white pellet grainstone; and (c) cryptalgalaminated carbonate.

In contrast, shales are the predominant lithology in the shaly half-cycle (Sullivan Formation) of the Sullivan-type Grand Cycle. They are interbedded with abundant calcarenites; parted limestones (type 1); conglomerates; and carbonate laminites. The overlying carbonate half-cycle (Lyell Formation) is composed of ooid grainstones; parted limestones; dolomitic laminites; and conglomerates. These half-cycles record a relatively unbreached, broad carbonate shoal (up to 400 km wide) which separated a muddy intrashelf basin from the open ocean (Aitken, 1978).

The upper part of the Lyell Formation also has meter-scale cycles composed of (from base to top): (a) parted limestone, wavy bedding and flaser bedding; (b) parted limestone, lenticular bedding; and (c)

laminated dolostone, commonly with quartz sand at the top.

4.4.3.2 Great Basin

Palmer and Halley (1979) examined in detail the Lower and Middle Cambrian Carrara Formation of the southern Great Basin. The formation contains three complete Grand Cycles and one partial cycle, each 100 to 150 m thick. Each cycle consists of a lower shaly half-cycle of shales and siltstones with thin beds of siliciclastic or carbonate silt to fine-grained sand. Lower siliciclastic beds are occasionally graded and contain flute casts. Toward the top of the half-cycle, limestone beds become more abundant and pass gradationally upwards into the carbonate half-cycle, composed of subtidal lime mudstone facies (commonly peloidal limestones and oncoid-skeletal packstones) and ooid grainstone, and intertidal and supratidal algal boundstone. Siliciclastic rocks predominate in the east and carbonates predominate in outcrops to the west and northwest.

Palmer and Halley (1979) interpreted these cycles to represent: (1) a shoreward zone of predominantly siliciclastics deposited in a broad shelf lagoon (maximum depth of approximately 100 m) which was bordered on the east by the cratonic shoreline and (2) a carbonate platform to the west of the lagoon which consisted of carbonate islands (mainly in westernmost areas) and a subtidal platform-interior ooid sand blanket situated eastward of a protected subtidal platform dominated by carbonate mud deposition. The similarity between these Carrara Grand Cycles and those of Middle Cambrian age in the Canadian Rockies has been noted by both Palmer and Halley (1979) and Aitken (1981).

Meter-scale cycles are not described by Palmer and Halley (1979). My own field observations indicate that cycles identical to those in the Middle and Upper Cambrian of the Canadian Rockies are also present in carbonate half-cycles of the Carrara Formation. No cycles are apparent in shaly half-cycles.

4.4.3.3 Southern Appalachians

The concept of Grand Cycles has not been used to described Cambrian strata in this region. Aitken (1981), however, briefly stated that at least the Middle Cambrian is also a sequence of Grand Cycles that are virtually identical to those of the Canadian Rockies and Great Basin.

Based on Palmer (1971), Middle and Upper Cambrian platform sediments of the Conasauga Group in the northern sector of the southern Appalachians (Virginia, Tennessee) are composed of interbedded limestone and dolostone, 150 to 450 m in thickness, and variegated shale, 70 to 200 m thick. The carbonates (carbonate half-cycle) which are composed of massive limestones; oolitic dolostone and limestone; stromatolites; and flat-pebble conglomerates pinchout to the west into the Conasauga Shale. Similarly, the variegated shales (shaly half-cycles) pinchout eastward into the Honaker Dolomite and Elbrook Formation carbonates.

Palmer (1971) interpreted this succession of sediments to represent a carbonate shoal and a leeward shallow marine environment dominated by siliciclastics. Markello and Read (1981) provide a detailed description of the Upper Cambrian Nolichucky Formation (shaly half-cycle), interpreting it to have been deposited within and peripheral to a

subtidal intrashelf basin.

4.4.4 Facies Models

Examination of Grand Cycles is facilitated by their bipartite nature. In western Newfoundland, these large-scale cycles represent two different depositional environments that left records of shaly and carbonate half-cycles now vertically superimposed in the rock record. The following is a summary of the sequences in each type of Newfoundland half-cycle and their interpretation, compiled from detailed descriptions presented in Chapter 3 and in the previous section on "meter-scale assemblages".

The shaly half-cycle exhibits an overall shallowing-upward change. Ideally each shaly half-cycle is composed of a basal subtidal-dominated interval; an intermediate intertidal-dominated portion; and an upper supratidal-dominated interval (Fig. 4.8). Each interval is on the order of tens of meters thick. In turn, each shallowing-upward shaly half-cycle is composed of parted limestone-shale cycles which consist of basal subtidal sediments that grade upward into intertidal and supratidal sediments. The style of these smaller shallowing-upward cycles varies vertically within the half-cycle. Shallowing-upward cycles in the subtidal-dominated interval are characterized by thick subtidal sediments. Similarly, intertidal- and supratidal-dominated intervals are composed of cycles which contain thick intertidal and supratidal components, respectively, and minor beds of the other two

Figure 4.8: Schematic diagram of shaly half-cycle indicating the overall shallowing-upward change (right) that is also reflected in nature of the meter-scale, shallowing-upward parted limestone-shale cycles (left). Details provided in text.

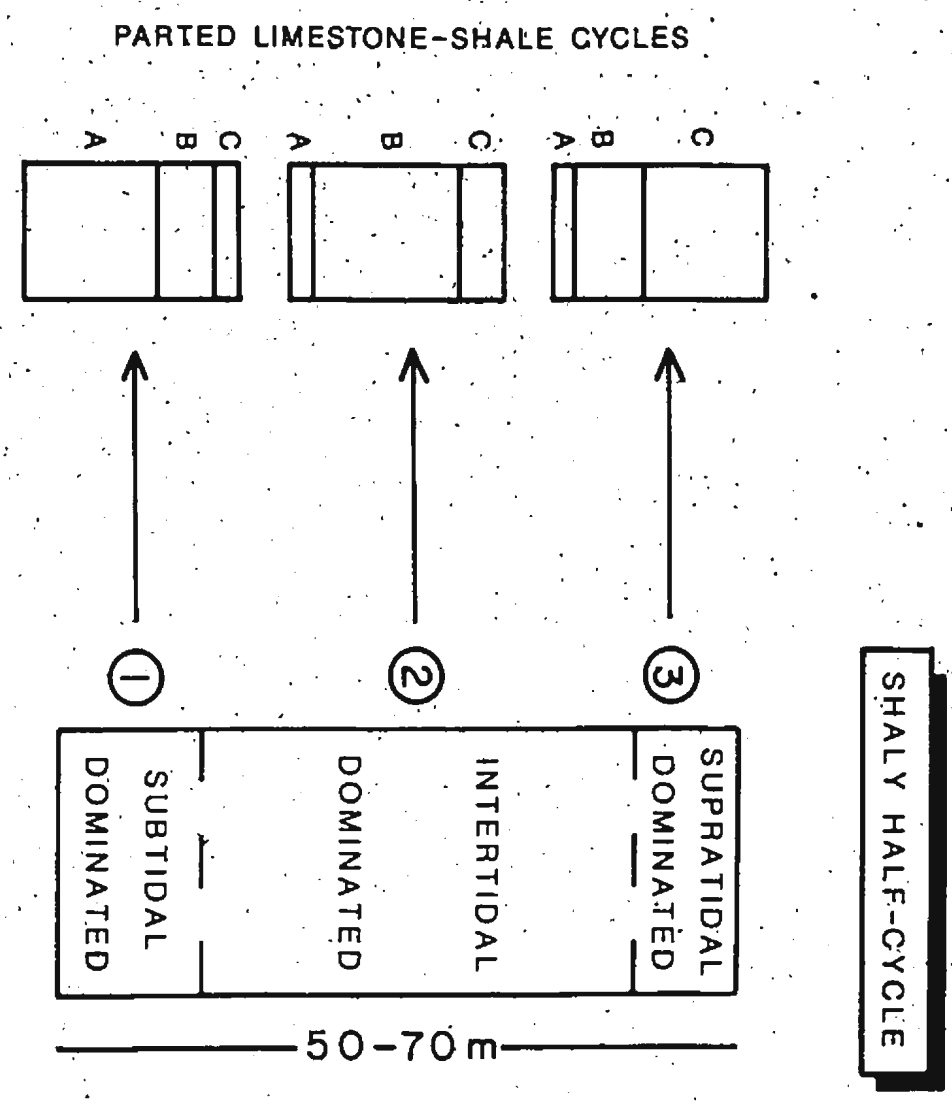
PARTED LIMESTONE-SHALE CYCLES
A
B
C
A
B
C
A
B
C
1
2
3
SUBTIDAL DOMINATED
DOMINATED
INTERTIDAL
SUPRATIDAL DOMINATED
50-70 m
SHALY HALF-CYCLE

components.

A shaly half-cycle represents deposition in muddy tidal flats which developed leeward of carbonate sand shoal complexes. Two depositional models are possible: (1) the tidal flat which developed in the lee of a carbonate shoal complex was separated from the shore by a subtidal basin (e.g. southern Appalachians -- "intrashelf basin" of Markello and Read, 1981; Canadian Rockies -- "inshore basin" of Aitken, 1978) and (2) the tidal flat passed westward (landward) into prograding terrestrial sediments of the cratonic shoreline. The applicability of these models to the Port au Port sequence is considered in the following discussion of "facies belts".

Unlike the shaly half-cycle, no overall shallowing- or deepening-upward changes are present in the carbonate half-cycle. The only large-scale vertical variation observed is the absence of subtidal grey oolites in the basal part of the half-cycle. Meter-scale, oolite-laminite sequences occur throughout.

Each carbonate half-cycle represents sedimentation in an carbonate sand shoal complex. The absence of vertical variations in lithology substantiate the interpretation that the complexes developed by rapid vertical and lateral migration of the laterally discontinuous components. These complexes, however, probably only formed poor barriers between the shoreward tidal flat and the open ocean. This interpretation is supported by the absence of evaporites; the frequent storm deposits; and the development of tidal-generated structures in shaly half-cycles.

Although Port au Port Grand Cycles are composed of vertically repeated shaly and carbonate half-cycles, they do not necessarily record migrations of persistent depositional environments. Instead they are interpreted to reflect the development of two laterally adjacent mega-environments, ooid shoal complex and muddy tidal flat, that varied in both time and space in response to environmental changes. There are three styles of platform sedimentation:

(1) The March Point Formation records widespread, muddy subtidal conditions over much of the platform.

(2) Shaly half-cycles of the Cape Ann and Big Cove Members contain no evidence of contemporaneous carbonate shoals in the lower three-quarters of the units. The consistent appearance of grey oolite storm deposits, derived from more seaward shoal complexes, in only the upper beds suggests that the carbonate shoal did not exist in the immediate vicinity of the mixed belt until the later stages of shaly half-cycle deposition. The extensive dolostones of White Bay and Goose Arm in the carbonate belt, however, indicate the virtually continuous presence of a carbonate shoal complex further to the east.

(3) In contrast, the Man O' War Member of the Petit Jardin Formation is punctuated throughout by grey oolite and thus interpreted to have been deposited in the lee of a persistent carbonate shoal. The member appears to be traceable between the examined sections in western Newfoundland (with the exception of the St. Barbe outcrops) but whether it is a synchronous or diachronous unit cannot be determined due to insufficient biostratigraphic control.

4.4.5 Facies Belts

As described in Chapter 2, the six outcrop areas of the Port au Port Group can be divided into an easterly carbonate belt, which contains White Bay and Goose Arm outcrops, and a westerly, mixed carbonate and siliciclastic belt, which includes sections from the Port au Port Peninsula, Bonne Bay, Canada Bay and the St. Barbe coast. Grand Cycles are variably developed in the mixed sediment belt. They appear to disappear eastward or towards the shelf margin into the carbonate belt by the pinchout of the shaly half-cycles into predominantly carbonates. Based upon western North American models, Newfoundland Grand Cycles probably disappear westward or cratonward by the pinchout of the carbonate half-cycles into predominantly fine-grained siliclastics and carbonates; this, however, cannot be verified. The restricted lateral extent of Grand Cycles on the platform has been well documented in other North American Cambrian outcrops and is considered to be an essential characteristic of typical Grand Cycles (Aitken, 1981).

The position of western Newfoundland outcrops relative to the shoreline and platform edge is uncertain. Based upon the thicknesses and interpreted pinchouts of the carbonate and shaly half-cycles and comparison with western North American examples, it is proposed that:

1. The carbonate belt represents an area of maximum development of an extensive carbonate shoal complex that probably formed on the outer part of the platform, probably near the platform edge. Placement of this belt near the platform edge cannot be substantiated as the shelf-slope

transition is not seen in Newfoundland, although the shelf edge has been postulated to be near the eastern flank of the Great Northern Peninsula (Knight, 1980b; James, 1981).

2. The mixed sediment belt records deposition of carbonates on the leeward flank of the carbonate shoal complex, and mixed carbonates and siliciclastics of an adjacent tidal flat. The relative paleogeographic positions of the various outcrop areas can be determined within the mixed belt. The sequence at Canada Bay, with its generally thinner carbonate half-cycles, is interpreted to be situated cratonward of the sequence on the Port au Port Peninsula. The Peninsula section is in turn considered to be situated farther from the craton than the thick shaly half-cycles and reduced carbonate half-cycles of Bonne Bay (Fig. 4.7). There is an overall thickening seaward from the most cratonward section at Bonne Bay to the Port au Port Peninsula which has the best developed Grand Cycles and the thickest section; a slight thinning is seen seaward of the Peninsula toward Goose Arm and White Bay.

It is important to note that the Berry Head Formation, traceable in all examined areas in western Newfoundland, does not exhibit this east-west facies change. Instead, it is a relatively uniform unit that consists of a blanket of dolomitized peritidal carbonates, including dololaminites, grainy (oolitic?) dolostone and algal mounds. The March Point Formation, formed predominantly of muddy subtidal sediments, also shows a poor facies differentiation; the preponderance of oolites and oncolites in the Goose Arm section, however, does support its placement in the outer area of the Cambrian platform.

Given the thickness and lithologic uncertainty of the covered intervals on the St. Barbe coast, the position of these outcrops on the Cambrian platform and their relation to Grand Cycles cannot be evaluated. Knight (1980b) proposed that the Port au Port Group in the northern and western areas of the Great Northern Peninsula (i.e., St. Barbe coast) is an inner platform deposit and that equivalent strata in Canada Bay are part of the platform margin. Comparison of exposed St. Barbe outcrops with more southerly Newfoundland areas, however, reveals lithologic similarities with both outer (Goose Arm, White Bay) and more inner platform deposits (Port au Port Peninsula, Bonne Bay).

Outcrop limitations to the west, imposed by the Gulf of St. Lawrence, complicate the placement of Port au Port strata relative to the paleoshoreline. The closest fossiliferous Middle and Upper Cambrian platform sediments are limestones and shales of the Corner-of-the-Beach and Murphy Creek Formations (Fritz, 1972) on the Gaspe Peninsula, Quebec. These formations are depositionally on strike with Port au Port rocks. Locations directly west of Newfoundland (200-300 km nonpalinspastically) and depositionally across strike have Ordovician rocks which rest directly upon Precambrian basement (e.g., the Quebec North Shore and Anticosti Island; North, 1971). These observations imply that the shoreline during Port au Port deposition was situated within what is now the Gulf of St. Lawrence and suggest a shelf width on the order of 200 km. Furthermore, the absence of evidence for an intrashelf basin (refer to Chap. 3), along with an insufficient shelf width to contain a basin of the dimensions proposed by Aitken (1978) and Markello and Read (800 km long by 300-400 km wide; 1981), suggest that tidal

flats connected the carbonate shoal complex with the craton.

The concept of facies belts has been used previously for Cambrian platform sediments by Robison (1960), Palmer (1960, 1972) and Palmer and Halley (1979) for the Great Basin and by Aitken (1966, 1978) for the Canadian Cordillera. Three belts were recognized which represent the areal distribution of lithofacies at a given time: (1) an inner detrital belt of dominantly siliciclastics (shaly half-cycle); (2) a middle carbonate belt (carbonate half-cycle); and (3) an outer detrital belt. The facies belts defined in this study take into consideration both the vertical and lateral distribution of lithofacies. Limited biostratigraphic control above the March Point Formation precludes unequivocal determination of time-equivalent outcrops.

4.4.6 Sequence of Formation

The following sequence is postulated for the formation of a single ideal Grand Cycle of the Port au Port Group:

(1) Marine transgression[2], putting most of the region under shallow subtidal conditions in which mixed deposition of carbonate sediments and siliciclastic mud prevailed. A narrow carbonate shoal may have persisted in the outer platform.

(2) Increased deposition of siliciclastic muds with continuing transgression and advent of relatively high energy conditions.

---

2. The term "transgression" is used here with no genetic connotations. A discussion of possible mechanisms for Grand Cycle formation is presented at the end of this chapter.

(3) Establishment or lateral expansion of a carbonate sand shoal near the platform edge as transgression slowed or stillstand was reached.

(4) Continued development and lateral migration of the shoal (carbonate half-cycle) forming a protective barrier which still allowed circulation with the open ocean. Muddy tidal flat conditions developed in the lee of the shoal (shaly half-cycle). The platform did not stagnate as indicated by the lack of abundant supratidal carbonates and widespread, subaerial exposure horizons at the top of the Grand Cycle.

(5) Relatively rapid, renewed transgression, marking the beginning of the next cycle.

Only the March Point Formation in Grand Cycle A contains evidence of extensive subtidal conditions (events 1 and 2). Most of the cycles record a narrow range of events (events 3 to 5) which, as discussed in a following section, is in contrast to other Cambrian Grand Cycles in North America.

It must be emphasized that mixed carbonate and siliciclastic deposition in Grand Cycles in western Newfoundland appears to be in contrast to shelf sedimentation models for pure siliciclastics or carbonates. In most models, transgression results in: (1) drowning of carbonate reefs or platforms, or promotion of carbonate platforms capable of keeping up with relative sea level rises and (2) drowning of siliciclastic sources (Kendall and Schlager, 1981). To the contrary, transgressive events in the above Grand Cycle model favour widespread distribution of siliciclastic sediments. The siliciclastic muds were

likely derived from sediment sinks that developed near the shoreline during a period when there was insufficient energy to transport them seaward. With transgression, these sediments were remobilized and transported seaward into the tidal flat. This explanation has also been suggested by various workers for western North American Grand Cycles (Aitken, 1978; Mount and Rowland, 1981).

4.4.7 Discussion

4.4.7.1 Regional Comparisons

The eastern and western flanks of the craton each possess a heterogenous carbonate shoal complex and a more shoreward belt of mixed carbonate and siliciclastic sedimentation. From the previous discussion, however, it is apparent that there are significant differences in the arrangement and distribution of lithologies between western Newfoundland and western North American Grand Cycles:

(1) Shaly and carbonate half-cycles in western Newfoundland contain shallow subtidal, intertidal and supratidal sediment; shaly half-cycles in western North America are predominantly subtidal.

(2) Shaly half-cycles in western Newfoundland record deposition of a muddy tidal flat rather than a shaly intrashelf basin as in western North America and the southern Appalachians.

(3) Intertidal and supratidal sediments of the carbonate half-cycles are not concentrated in the upper portions of the cycles in western Newfoundland whereas in the western North America there is a progressive

shallowing upward to supratidal carbonates.

(4) Lithofacies and meter-scale cycles within shaly half-cycles in western Newfoundland are distinct from those in carbonate half-cycles, unlike in western North America where there is considerable overlap of lithofacies.

(5) Individual Grand Cycles within each region record deposition on different parts of the platform as shown (Fig. 4.9). Cycles in western Newfoundland and the southern Great Basin contain no record of the platform edge whereas, in the Canadian Rockies (Kicking Horse Rim), the location of the carbonate shoal at the platform edge has been well documented.

(6) Half-cycles in western Newfoundland and the Great Basin consistently record deposition in two distinct mega-environments. In the Canadian Rockies, however, a Grand Cycle may record deposition in only an intrashelf basin (e.g. Stephen-type cycle).

(7) Karst surfaces are common in western Newfoundland carbonate half-cycles whereas, in western North America, evidence of extensive karst has not been observed except near the Kicking Horse Rim in the Canadian Rockies.

(8) Port au Port Grand Cycles are generally thinner than those in the Canadian Rockies.

(9) The areal distribution of Cambrian platform sediments flanking the North American craton is unequal. In western Newfoundland, discontinuous Cambrian exposures extend over 100 km across strike and

Figure 4.9: Composite diagram of Cambrian platform based on the following selected North American outcrops: southern Great Basin (Palmer and Halley, 1979; Mount and Rowland, 1981); Canadian Rockies (Aitken, 1978); and western Newfoundland (this study).

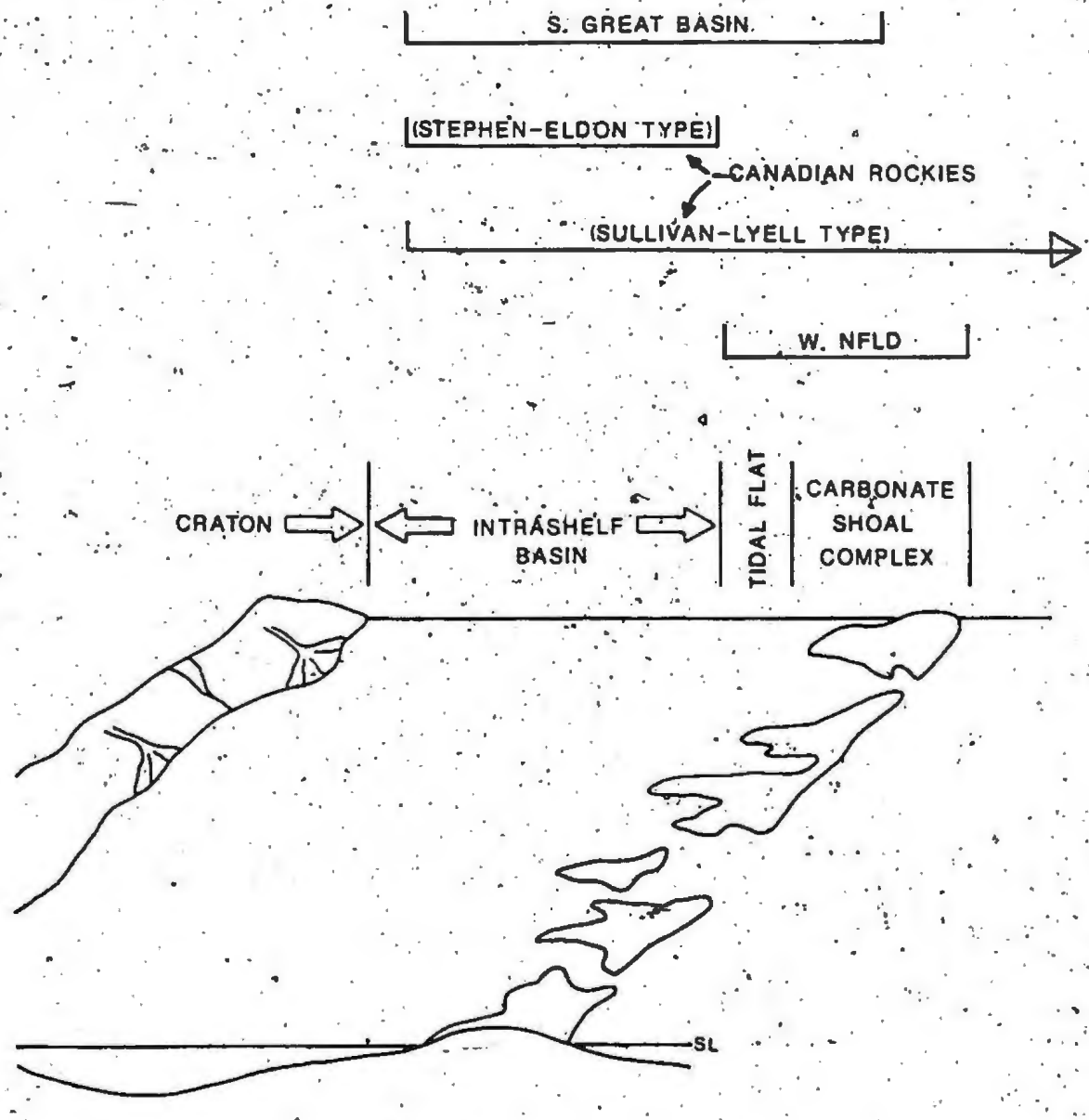
S. GREAT BASIN
(STEPHEN-ELDON TYPE)
CANADIAN ROCKIES
(SULLIVAN-LYELL TYPE)
W. NFLD
CRATON
INTRASHELF BASIN
TIDAL FLAT
CARBONATE SHOAL COMPLEX
SL

are interpreted to be part of an estimated 200 km wide shelf. In the west, Cambrian outcrop and subcrop can be traced continuously over a distance of at least 1100 km across strike. North (1971) proposed that these differences were related to variations in the Precambrian basement that have given rise to: (a) a narrower margin in the east that would have effected abrupt lateral variations in Cambrian sediments and (b) a wide, gently dipping platform in the west on which gradual lateral variations in facies were developed.

In spite of these differences (possible causes are examined later in this chapter), the sequence of events postulated for the formation of Grand Cycles in the various regions is similar. Interpretations by Aitken (1978) for the Canadian Rockies and Mount and Rowland (1981) in the southern Great Basin are basically in agreement with that proposed for western Newfoundland; the key points of which are: (1) a marine transgression produced an influx of shoreward-derived siliciclastic muds across the underlying carbonate shoal and (2) the gradual establishment and growth of a carbonate shoal accompanying a diminishing siliciclastic supply and slower transgression. Palmer and Halley (1979) suggested a minor variation in which siliciclastic influx arose through an "autocyclic" mechanism. They proposed that the subtidal-carbonate source area became too small to provide sufficient sediment for progradation of the carbonate platform; shoreward siliciclastics continued to migrate seaward and eventually covered part or all of the carbonate shoal. Aitken (1981), however, pointed out that there is no evidence for diachronous boundaries in Carrara Grand Cycles as are required for this interpretation and suggested that this model is open

to challenge.

4.4.7.2 Regional Correlations

In the past, correlations of Cambrian Grand Cycles in western and eastern North America have been precluded by poor faunal control; the variability in the definition of Grand Cycles; and the lack of well documented examples in the east. In light of more recent studies and several review papers on Grand Cycles, at least first order determinations of cycle correlations are now possible.

Based on detailed lithologic and biostratigraphic correlations in the Canadian Rockies, the relatively abrupt boundaries of Grand Cycles appear to be essentially isochronous (Aitken, 1966; 1981). Palmer (1981a) has used this to correlate the tops of Grand Cycles in Cambrian strata examined in North America. Included in his study are sections from the Canadian Cordillera, Great Basin, southern Appalachians, Montana, Wyoming, and northern Mexico. Plotting the Grand Cycle boundaries on a correlation chart using trilobite zones, he was able to show some degree of correlation between the various regions, particularly those in the west. This analysis is summarized in Figure 4.10. Numerous cycle tops can be traced 2500 km from Mexico to the Canadian Cordillera; this is in accord with conclusions reached by Fritz (1975) for Lower Cambrian sequences in the same regions. Some distinctive cycles present in the Great Basin region, however, are not correlative with any in the Cordillera. In contrast, only minor ties exist between cycles in the west and those in the southern Appalachians on the other side of the craton. In Palmer's (1981a) appraisal, it must

Figure 4.10: Correlation chart of Grand Cycle boundaries for the Port au Port Peninsula, western Newfoundland (this study); and other selected North American Cambrian examples (after Palmer, 1981 and references cited therein). Trilobite zones are shown on left. Solid lines indicate boundaries present in most sections in the outcrop region; dotted lines indicate boundaries present in only few sections in the region.

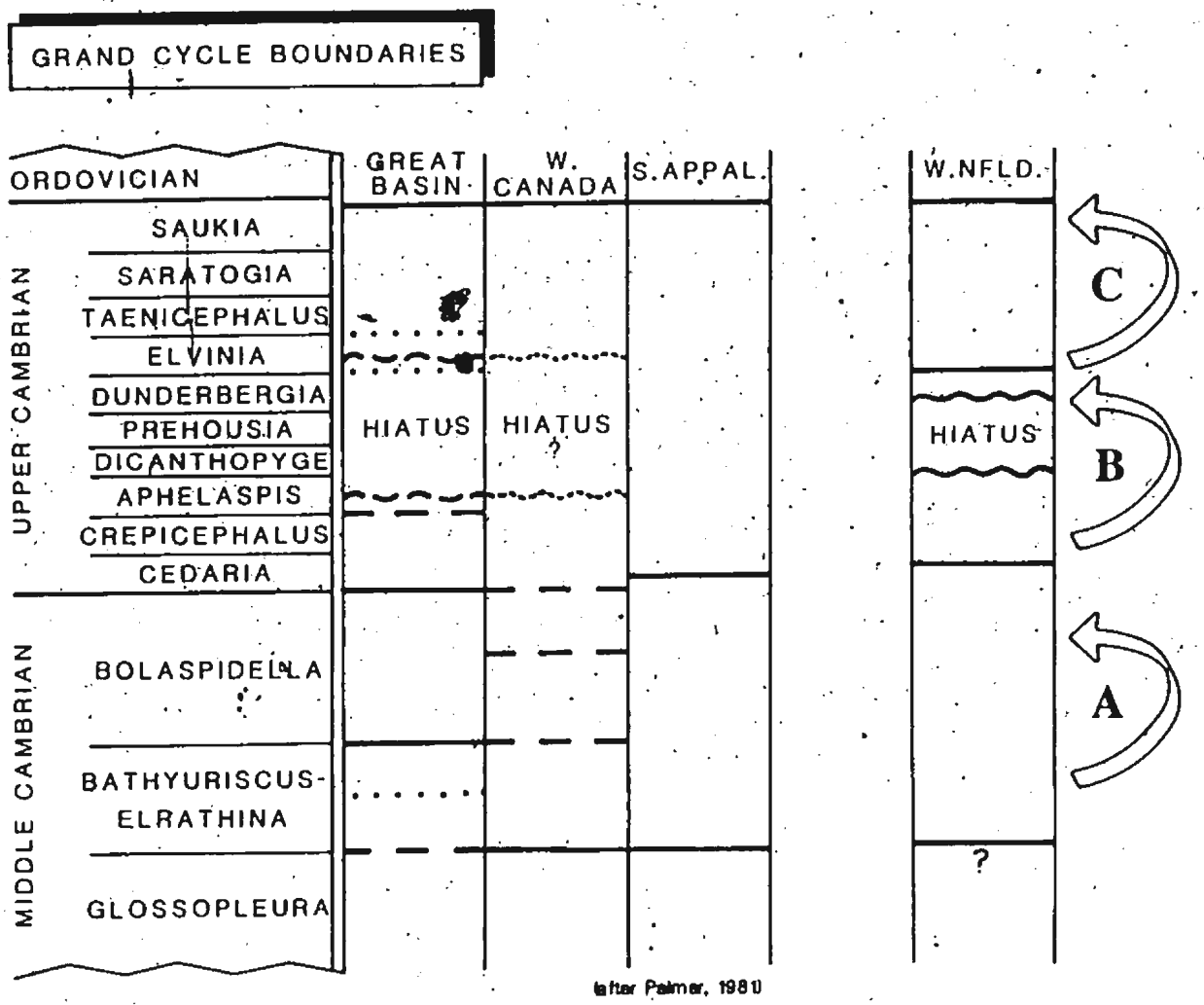
GRAND CYCLE BOUNDARIES
ORDOVICIAN
UPPER CAMBRIAN
SAUKIA
SARATOGIA
TAENICEPHALUS
ELVINIA
DUNDERBERGIA
PREHOUSIA
DICANTHOPYGE
APHELASPIS
CREPICEPHALUS
CEDARIA
MIDDLE CAMBRIAN
BOLASPIDELLA
BATHYURISCUS-
ELRATHINA
GLOSSOPLEURA
GREAT BASIN
W. CANADA
S.APPAL.
HIATUS
HIATUS
?
W.NFLD.
HIATUS
?
C
B
A
after Palmer, 1981

be noted that the data control is poor in the southern Appalachians, Northwest Territories and northern Mexico; he included only one section from each region.

Tentative correlations may be made between the three Grand Cycles recognized on the Port au Port Peninsula and those examined by Palmer (1981a) in the Great Basin and Canadian Rockies. Although there is uncertainty as to the age of some cycle boundaries on the Port au Port Peninsula, the scarce trilobite data available indicates only slight boundary differences from those in western North America. Furthermore, the interval of condensed sedimentation in the upper part of the Felix Member near the Dresbachian and Franconian boundary, herein termed the sub-Elvinia unconformity (refer to Chapter 2; Palmer and James, 1979), corresponds to regional disconformities seen in the Canadian Cordillera, Montana and parts of the northern Great Basin region (Palmer, 1981a, 1981b).

4.4.7.3 Proposed Mechanisms

Numerous mechanisms have been postulated for the formation of Grand Cycles ranging from widespread processes, such as eustasy, to more restricted processes, such as variations in rates or direction of tectonic movements or climatic fluctuations (Aitken, 1966). Any proposed hypotheses must account for the following observations:

(1) Geographic Extent -- Grand Cycles are recognized on both sides of the North American craton but appear to be more laterally extensive in the west.

(2) Correlation -- Cycle boundaries can be correlated between the various regions in western North America and some degree of correlation exists between sequences on either side of the continent.

(3) Period -- Based on an estimated time interval of 45 million years for the Middle and Late Cambrian (Cowie and Cribb, 1978), the three Grand Cycles in western Newfoundland were each deposited in about 15 million years. This is a very simplistic treatment that does not consider such factors as the sub-Elvinia unconformity or differences in cycle thicknesses. Aitken (1966) estimated periods on the order of 9 million years for Grand Cycles in the Canadian Cordillera. These large-scale cycles are on the scale of Vail et al.'s (1977) second-order cycles.

(4) Coupling Effect -- Grand Cycles in the Canadian Cordillera and the Great Basin are overall shallowing-upward cycles. Intertidal and supratidal carbonates at the top of carbonate half-cycles are abruptly overlain by subtidal shales suggesting that siliciclastic deposition was initiated by relative deepening of the shelf (Aitken, 1966, 1978; Palmer and Halley, 1979). Subtidal shales are not present in cycles in western Newfoundland.

(5) Boundaries -- The abrupt to rapidly gradational contacts of Grand Cycles are interpreted as isochronous surfaces. The transition between the two half-cycles, however, is diachronous tending to "young" in age toward the craton (Aitken, 1981; Palmer and Halley, 1979; Mount and Rowland, 1981).

(6) Meter-Scale Sequences -- Half-cycles are composed of smaller

repeated sequences. Shaly half-cycles on the Port au Port Peninsula are commonly composed of meter-scale, shallowing-upward cycles; carbonace half-cycles are composed of irregular sequences of limited lateral extent.

Platform sequences and their cyclicity are controlled by the rate and direction of relative sea-level changes (Wilson, 1975). These fluctuations in turn are governed by the balance of three controls: (1) sea-level eustasy (sea-level changes regardless of cause as redefined by Morner, 1976); (2) subsidence; and (3) rates and types of sedimentation (Kendall and Schlager, 1981).

Eustatic Model

Consideration of the geographic extent and degree of correlation of Grand Cycles in North America suggests that global or, at least, continental-scale processes controlled Grand Cycle formation. Eustatic sea-level change appears the most feasible. Dynamic regional factors, such as margin morphology, rates of subsidence and sedimentation, however, may have been in large part responsible for the different sedimentation styles and the imperfect correlation of cycle boundaries between regions (Morner, 1983).

Eustatic changes have been postulated by various workers to control large-scale cyclicity by absolute sea-level rise or fall and by changes in the rate of sea-level rise or fall. Vail et al. (1977) proposed that the first component created asymmetric global cycles that recorded gradual sea-level rises interrupted by sudden falls in sea-level. James (1984) suggested an alternative model that invoked essentially

symmetrical sea-level rise and fall to produce similar cycles.

The importance of the second component was demonstrated by Pitman (1978). He postulated that transgressive or regressive events at passive margins are caused by changes in the rate of sea-level rise or fall. This hypothesis has been employed for Grand Cycles by Aitken (1978, 1981), Palmer and Halley (1979) and Mount and Rowland (1981). Since the Cambrian was a period of widespread sea-level rise (Holland, 1971), they proposed that differential rates of relative sea-level rise were the causitive factor in cycle formation. The basal interval of a Grand Cycle reflected a rapid rise in relative sea-level which initiated a widespread influx of fine-grained siliciclastics onto the carbonate platform. The transition interval represented the gradual decrease in the rate of relative sea-level rise which allowed development of a carbonate shoal on the outer shelf and landward migration of the shoal. A new phase of rapid relative rise triggered the next cycle.

As previously described, the upper part of Grand Cycle B (Felix Member) in the Port au Port Group contains a condensed zone of glauconitic, arenaceous oolite; carbonate laminite; and quartzose sandstone which is correlative with the sub-Elvinia unconformity recognized elsewhere in North America. The occurrence of a hiatus within a cycle, instead of at cycle boundaries, appears to be incompatible with the concept of Grand Cycles and prompts re-examination of the necessity for rapid sea-level changes and the nature of sediment response.

A simplified model based on the Port au Port sequence is developed using the approach taken by James (1984; and references cited therein).

This model shows that an asymmetrical, large-scale cycle containing unconformities or condensed intervals may be developed by gradual and relatively symmetrical changes in the rates of sea-level rise (SLR). Rates of sedimentation and subsidence are assumed to be constant. As outlined in Figure 4.11, the sequence of events are:

(1) A rapid increase in SLR floods much of the platform and remobilizes shoreline-derived siliciclastic muds. Subtidal conditions persist during this stage (e.g. March Point Formation). More commonly, however, sedimentation in the muddy tidal flat keeps up with SLR resulting in meter-scale, shallowing-upward cycles with a thick subtidal component.

(2) As the increase in SLR slows, the shallowing-upward cycles become more prominent and develop thicker intertidal and supratidal components.

(3) The decrease in SLR is initially slow. Carbonate deposition in the high energy shoal complex is re-established and gradually expands toward the adjacent tidal flat.

(4) SLR decreases more rapidly and sedimentation in the shoal complex readily keeps up with or outpaces sea level. Meter-scale oolite-laminite assemblages form in response to migrating shoal components and contain abundant coastal paleokarst features.

(5) Sedimentation outpaces the slowest rate of SLR resulting in either: (a) very shallow water conditions with intermittent intervals of subaerial exposure (mudcracks) and reduced rates of carbonate sedimentation so that accumulations of siliciclastic sands are

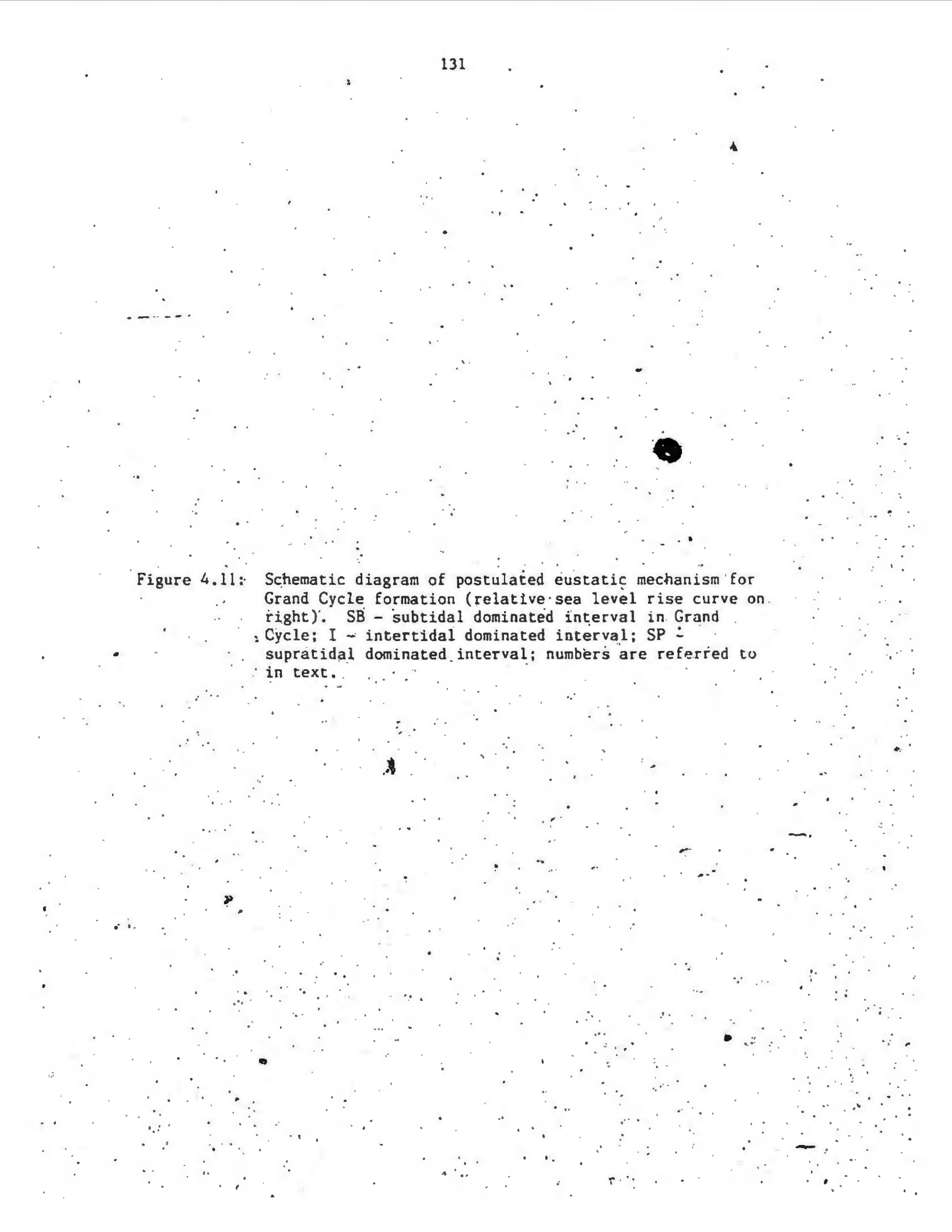

Figure 4.11: Schematic diagram of postulated eustatic mechanism for Grand Cycle formation (relative sea level rise curve on right). SB - subtidal dominated interval in Grand Cycle; I - intertidal dominated interval; SP - supratidal dominated interval; numbers are referred to in text.

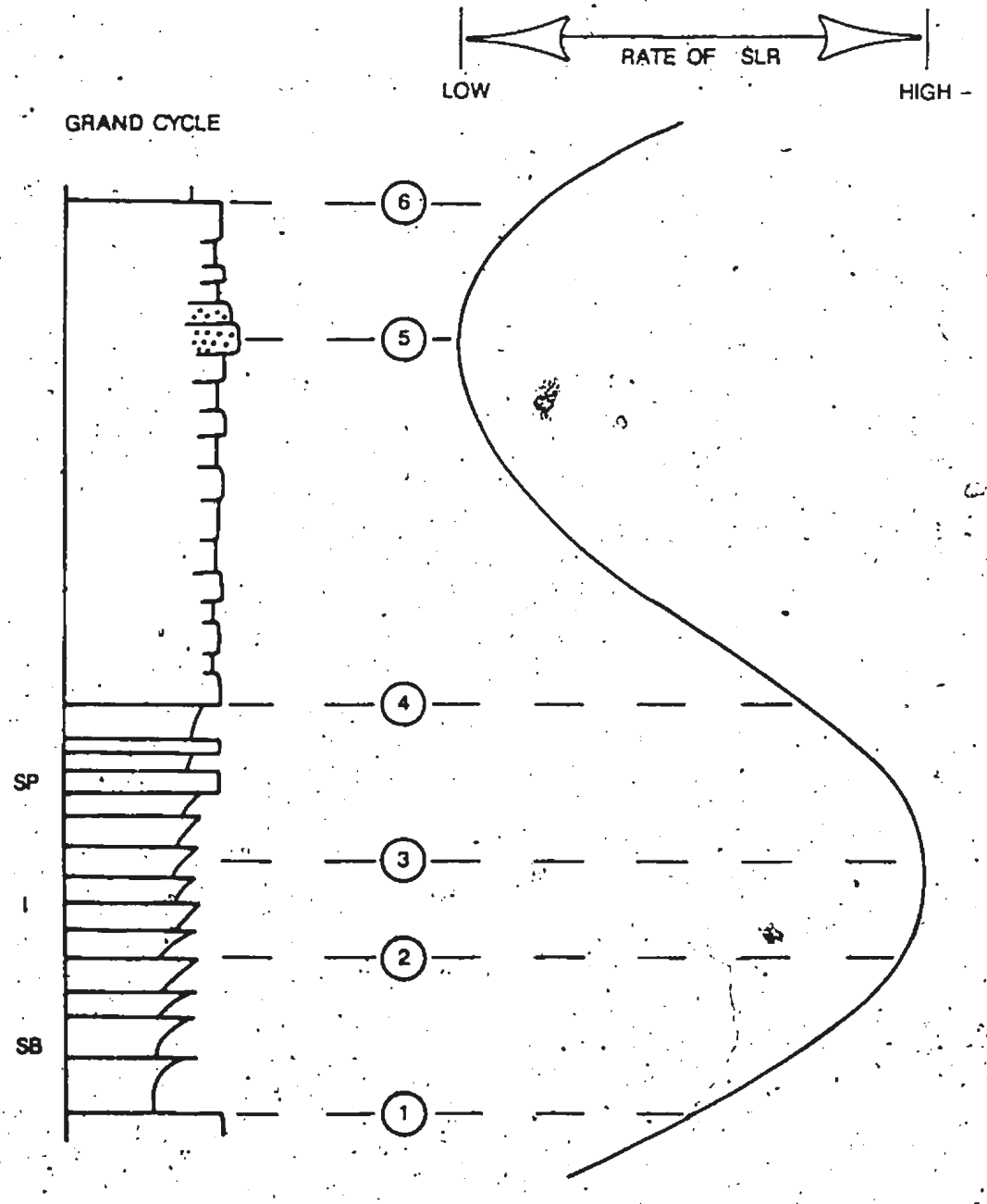
RATE OF SLR
LOW
HIGH
GRAND CYCLE
6
5
4
SP
3
I
2
SB
1

concentrated (e.g. sub-Elvinia of Felix Member of Port au Port Group) or (b) widespread subaerial exposure as sea level recedes below the platform margin (e.g. sub-Elvinia unconformity of western North American Grand Cycles).

(6) Slow increases in SLR re-establish carbonate shoal deposition.

Although a very simplified treatment, the above model illustrates several key points about the mechanics of Grand Cycle formation that have generally been overlooked. Firstly, cycle boundaries may have lagged behind periods of maximum and minimum rates of SLR, indicating that supposedly "anomalous" intervals of reduced or non-sedimentation within a cycle are in fact compatible with Grand Cycle mechanisms. The nature of cycle boundaries may have been strongly influenced by localized environmental conditions and thus varied between regions whereas "intracycle" discontinuity surfaces probably reflect major eustatic changes. It is not surprising, therefore, that regional correlations based on cycle boundaries are poor. Secondly, the widespread peritidal nature of Port au Port shaly and carbonate half-cycles may be explained by (1) tidal flat and shoal sedimentation that was able to keep up with SLR and (2) possibly lower amplitudes of SLR than in western North American cycles, which have subtidal shaly half-cycles and lack extensive subaerial exposure features. Maximum SLR was sufficient to reactivate shoreward-ponded muds which were then concentrated during deposition in upper intertidal and supratidal zones and represent the shallowest component of the shaly half-cycle.

Eustatic Causes

Eustatic fluctuations may be controlled by: (1) changes in the volume of ocean water through glacial processes -- glacial eustasy; (2) changes in the distribution of ocean water due to rotational and gravitational fluctuations -- geoidal eustasy; and (3) changes in the volume of ocean basins related to tectonics (isostasy or orogenesis) -- tectono-eustasy (Morner, 1976; Grotzinger, 1985). The last two controls may involve long-period changes (1-100 my; summarized in Morner, 1983) and may be applicable to Grand Cycles; glacial eustasy involves shorter-period events on the scale of meter-scale cycle periods (Grotzinger, 1985). Of particular importance is the influence of geoidal eustasy. Due to geoidal changes, eustasy is not globally synchronous and is valid only regionally or locally (Morner, 1976; 1983). This may partially account for the imperfect global correlation of Grand Cycles and suggests that the poor correlation of Grand Cycles between eastern and western North America does not necessarily preclude a primary eustatic mechanism (refer to Palmer, 1981a).

4.5 SUMMARY

Repeated sedimentary assemblages are the dominant sedimentary features in the Port au Port Group on the Port au Port Peninsula.

Predictable meter-scale, shallowing-upward cycles of parted limestone and shale, deposited in muddy tidal flats, are best explained by an autocyclic mechanism by which cyclicity is controlled by rates of

carbonate sedimentation. This model, however, has several possible pitfalls, such as insufficient rates of platform subsidence, suggesting that an allocyclic model involving changes in relative sea-level cannot be discounted. In contrast, meter-scale oolite-laminite assemblages, deposited in carbonate sand shoal complexes, are characterized by unpredictable lithofacies sequences. These assemblages are most reasonably explained by vertical accretion and frequent, rapid migration of the shoal complex in response to such factors as tidal variations and storm activity. Both these assemblages are punctuated by deposits interpreted to be storm derived; they include: (1) flat-pebble conglomerates and gutter casts in parted limestones; (2) grey oolites in parted limestones; and (3) occasional "waning energy" sequences in brown oolite.

Grand Cycles are composed of a lower shaly half-cycle, composed of parted limestone-shale cycles, and an upper carbonate half-cycle of oolite-laminite assemblages. Integrating detailed observations from the Port au Port Peninsula, where these cycles are best preserved, with information from outcrops on the Great Northern Peninsula, each Grand Cycle is interpreted to represent deposition on the leeward flank of an extensive carbonate shoal complex, probably situated near the platform edge, and an adjacent muddy tidal flat. The interpreted sequence of Grand Cycle formation involves: (1) a rapid marine transgression which flooded the platform with shoreward-derived siliciclastic muds and (2) the gradual development of a carbonate shoal and leeward tidal flat accompanying the waning of siliciclastics and slowed transgression.

Tentative correlations and the overall lithologic similarity between

Grand Cycles in the Canadian Rockies, Great Basin and western Newfoundland suggest a eustatic mechanism, possibly involving changes in the rate of relative sea-level rise, for the formation of Grand Cycles. Unlike these western North American examples, Grand Cycles in western Newfoundland are composed of pervasive, peritidal sediments and lack evidence for an intrashelf basin. They are also thinner and have a smaller areal extent than the other North American cycles. These differences emphasize the variable nature of Grand Cycles and may be attributed to such factors as narrower shelf widths; lower rates of sedimentation; and lower amplitudes of relative sea-level changes on the northeastern flank of the North American craton relative to the western flank.

PART B: DIAGENESIS

INTRODUCTION

This section is a documentation of diagenetic aspects of carbonates in the Port au Port Group on the Port au Port Peninsula. Calcite and dolomite are volumetrically the most important components in the sequence, and their fabric variability suggests that they are the joint products of deposition and diagenesis. Other authigenic minerals, such as silica and fluorite, are of minor importance and are not considered in any detail.

Chapter 5 includes description and interpretation of intergranular and intragranular cements, conglomerates, and erosion surfaces, which suggest a range of lithification processes. The sequence of lithification and evidence for early lithification in fine-grained carbonates set the "diagenetic stage" for subsequent chapters, providing critical evidence for the interpretation of ooid alteration, dolomitization and particularly the origin of parted limestones.

Examination of the variety of calcareous ooids in Chapter 6 provides evidence regarding ooid genesis and deposition under varying environmental conditions in sand shoal complexes. Study of these abiotic particles also enables speculation as to the nature of mineralogical transformations with burial, and secular trends in carbonate depositional mineralogy.

Chapter 7 deals with the origin of parted limestones which, as suggested from field observations, is not solely depositional. Cathode luminescence (CL), in conjunction with evidence from mudstone conglomerates and hardgrounds in parted limestones, is used to determine the influence of diagenetic processes, particularly early lithification, mechanical compaction and pressure solution. This interpretation is applicable for similar strata throughout the rock record.

Dolomites, examined in Chapter 8, are described using mainly CL properties, enabling interpretation of the sequence of dolomitization and the effects of depositional conditions and early limestone lithification.

Chapter 9 is a synthesis of the sequence of carbonate diagenesis and examines carbon and oxygen isotopic analyses of calcites in light of previously described field, petrographic and CL evidence. Depositional interpretations and interpreted diagenesis are also briefly reviewed in order to determine a depositional-diagenetic model.

The distinctive luminescence of both sediments and cements in this study enables extensive use of CL. In conjunction with standard petrography, CL is used to: (1) examine microfabrics, particularly in ooids, that cannot be discerned by other methods; and (2) delineate compositional zoning within calcite cements, dolomites, mudstones and calcareous particles that enables qualitative estimates of the spacial and temporal variations in pore-water chemistry (e.g., Sommer, 1972; Carpenter and Oglesby, 1976; Richter et al., 1981; Amieux, 1982).

TERMINOLOGY

In the following chapters, calcite and dolomite microfabrics are described, requiring the definition of some terms.

CL colours of calcites in this study are variable intensities of yellow-orange, brown, or black; these colours are designated bright and moderate luminescence; dull luminescence; and non-luminescence respectively. Dolomites have a similar range of CL colours but also have red CL.

Crystal sizes of both calcite and dolomite are described using the classification of Folk (1974b):

aphanocrystalline	less than 4 μm
very finely crystalline	4-15 μm
finely crystalline	15-62 μm
medium crystalline	62-250 μm
coarsely crystalline	0.25-1.0 mm
very coarsely crystalline	1.0-4.0 mm
extremely coarsely crystalline	greater than 4.0 mm

Calcite and dolomite crystals may be euhdral, subhedral, or anhedral as defined for igneous rocks (Bates and Jackson, 1980). Idiotopic, hypidiotopic, and xenotopic refer to crystal mosaics in which most of the crystals are euhdral, subhedral or anhedral, respectively.

Chapter 5

LITHIFICATION

5.1 INTRODUCTION

Two major phases of lithification are recognized in the Port au Port sequence: an early facies-specific phase and a later non-facies-specific phase. The spectrum of early cements and sedimentary structures reflects variability in the shallow marine environment, whereas the later cements exhibit little variation and are common to almost all rock types in the Port au Port Group. The first section of this chapter is a description and interpretation of the different types of cements and the matrix sediment, based on thin-section petrography and staining techniques, and CL. The second section of this chapter examines conglomerate horizons, hardgrounds and emersion surfaces, providing additional evidence for early lithification.

5.2 CEMENT PETROGRAPHY

Most intergranular and intragranular pores in calcarenites and calcirudites are occluded by a variety of cements that are now calcite.

Similar cements are also present in stromatolite-thrombolite bioherms and biostromes, where they are intimately associated with organic and lime mud components. Five types of cement are recognized: (1) fibrous calcite; (2) micritic calcite (isopachous and meniscus); (3) syntaxial calcite overgrowths; (4) prismatic clear calcite; and (5) blocky calcite.

5.2.1 Fibrous Calcite

This generally non-ferroan calcite occurs in intergranular pores in grainy sediments and as encrustations in bioherms and biostromes.

Radially oriented (perpendicular to substrate) fibrous calcite is the most pervasive cement in calcarenites and calcirudites, particularly in grey oolite (Plate 16c, d). It is generally the first generation of cement and may occlude all original porosity. Fibrous cement is also found in brown oolite (Plate 21b,e), flat-pebble conglomerates and bioclastic calcarenites and calcirudites, but is volumetrically less than the micritic matrix. This cement occurs as isopachous rinds, 25-50 μm in thickness, around particles but may thicken up to 100-125 μm away from grain contacts to form polygonal sutures (Plate 16a; cf. Shinn, 1975). Two luminescence stages comprise these cement rinds: (1) moderate-luminescent, isopachous, inclusion-rich calcite; and (2) dull-luminescent, inclusion-poor calcite crystals with non-luminescent cores. These crystals are in optical continuity with trilobites and radial ooids.

In biostromes and bioherms, fibrous calcite lines sediment-filled

cavities, and also occurs as rinds and botryoids interlaminated with micrite and cryptalgal structures. These calcites have patchy dull to moderate luminescence similar to fibrous calcite cement in calcarenites. Indistinct zoning, 50-100 μm wide, of alternating dull and moderate luminescence occasionally occurs. Two types of fibrous calcite, which often occur together in the same cryptalgal structure as separate cement generations, are recognized (Fig. 5.1).

Type 1. Fan-like arrays of fibrous calcite of variable size (from 100-200 μm in width and length) and orientation are present throughout stromatolites and thrombolites (Plate 9a, b). In hand specimens, these fans appear as black clots. They are composed of single or multiple-tiered layers of radiating, cone-shaped bundles, up to 0.5 mm in width and height. Cones have a turbid appearance imparted by abundant inclusions, and curved, convex-outward, twin lamellae. Inclusions are occasionally concentrated in zones, up to 50 μm wide, that parallel cone terminations.

Cones are composed of diverging crystals, which are approximately 20-40 μm in width and up to 1-2 mm in length. Crystals are characterized by sweeping extinction and distally divergent optic axes. Intercrystalline boundaries are straight to consertal but are commonly indistinct, and marginal crystals either parallel cone margins or abut against adjacent cones. In two dimensions, crystal terminations are generally scalenohedral or square-ended. This type of calcite has also been termed fascicular-optic calcite by Kendall (1977).

Type 2. This calcite consists of brown-coloured, fans or spherulites

Figure 5.1: Schematic diagram of early cements in biohermal and biostromal limestones.

BIOHERM-BIOSTROME CEMENTS

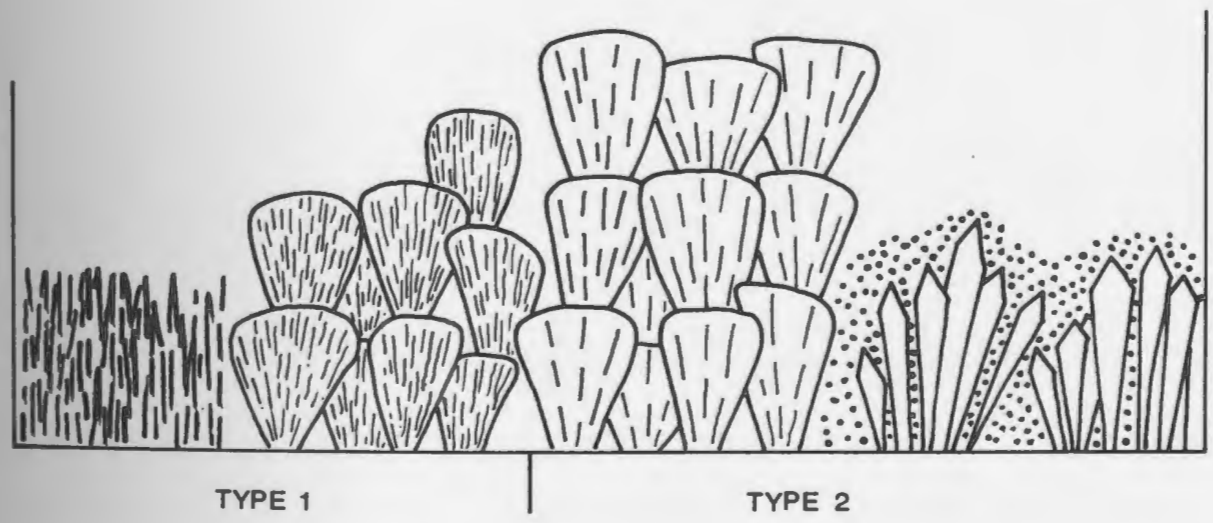

which grade laterally and vertically into arcuate to wavy-planar laminae. These arrays are composed of prismatic crystals, which distinguish this type from type 1 fascicular-optic calcite (Plate 9c,d). These prismatic crystals are inclusion-rich and up to 500-600 μm in length and 200-300 μm in width. Intercrystalline boundaries are generally consertal and crystal terminations are scalenohedral to square-ended. Unlike type 1 calcites, prismatic calcites have straight to only slightly undulose extinction and straight to slightly-curved twin lamellae. They are in optical continuity with echinoderm fragments and their syntaxial calcite overgrowths, and with radial ooids. Individual crystals or bundles of crystals are commonly overlain by silty micrite (Plate 9d), although some crystals project into overlying micritic laminae (cf. James and Ginsburg, 1979; Mazzullo and Cys, 1979 and other references cited therein).

Laminar arrays, 200-300 μm thick, typically have prismatic crystals with upward-directed crystal terminations and are intimately interlaminated with silty micrite laminations of similar thickness. Cement-micrite laminations may be continuous or discontinuous within stromatolites and can be traced between adjacent stromatolites. This laminated calcite also encrusts the surfaces of micritic laminae and intraclasts in sediment adjacent to biohermal and biostromal structures.

5.2.2 Micritic Calcite

Micritic calcite forming rinds, up to 50 μm in thickness, around ooids is present in ooid calcarenites (Plate 16b; 21c). Rinds may be

isopachous (cf. Bricker, 1971; James et al., 1976; Macintyre, 1977) or may thicken near grain contacts ("meniscus calcite" of Dunham, 1971). This calcite may either precede or succeed fibrous calcite cement and generally forms a separate rim of cement; in rare instances isopachous micrite passes laterally into isopachous fibrous calcite. Micrite cement can be differentiated from lime mud matrix by its moderate luminescence. Isopachous micrite is common in grey oolite, whereas meniscus micrite is rare, occurring only in irregular patches in brown oolite and in oolitic intraclasts composed of concentric ooids.

5.2.3 Prismatic Clear Calcite

This cement occludes intergranular pores in bioclast calcirudites and flat-pebble conglomerates, and in vugs and burrows in parted limestones and cryptalgal structures (Plate 10a-d). It occurs either as the first stage of cementation, which completely or partially rims grains, or the second stage after isopachous fibrous or micritic calcite cements or micritic matrix. Blocky calcite and some syntaxial calcite overgrowths occlude remaining pore space (Plate 10d). Prismatic calcite may form a single fringe of crystals, or tiered, fan-like crystal arrays. In coarser grained lithologies, perched sediment composed of micrite, peloids and siliciclastic silts generally inhibits cement precipitation on the top surfaces of large grains so that the best development of prismatic calcite is in shelter pores. No micritic sediment has been deposited subsequent to prismatic calcite precipitation. This cement is never present in calcarenite intraclasts.

Individual crystals reach up to 2 mm in length and 1.0 mm in width and

generally have straight intercrystalline boundaries and scalenohedral crystal terminations (Plate 10a, b). Numerous twin lamellae, which may be curved concave or convex toward the substrate impart a turbid appearance to crystals. Prismatic calcite exhibits uniform extinction between crossed polars and may syntaxially overgrow trilobite fragments. From CL, two optically continuous stages are recognizable:

(1) The proximal stage is a sub-isopachous fringe of inclusion-poor, ferroan calcite with patchy, dull luminescence. Crystals habits range from acicular (100-200 μm in length) in medium crystalline mosaics to prismatic (50-200 μm in width and 200-800 μm in length) in very coarsely crystalline mosaics. They have sharp, straight boundaries and well-developed scalenohedral terminations.

(2) The distal stage of moderate-luminescent, generally non-ferroan calcite encloses the proximal stage and generally occludes any remaining porosity. Inclusions are concentrated in 200-300 μm thick rinds at crystal margins. Some occurrences of this distal stage have scalenohdral terminations displaying moderate-dull luminescence which pass gradationally into moderately to brightly luminescent blocky calcite cement (Plate 11c).

Similar prismatic calcites have been documented by James and Klappa (1983) in Lower Cambrian Forteau (southern Labrador) biostromes and bioherms and coarse-grained calcarenites.

5.2.4 Syntaxial Calcite

Echinoderm particles and their syntaxial calcite overgrowths, forming

optically single crystals, are ubiquitous features in all rock types (Plate 11a). Overgrowths only partially occlude interstitial voids and are not developed on particles with micrite rims. Overgrowths are generally non-ferroan and always have a dull to moderate luminescence, whereas echinoderm particles are ferroan or non-ferroan and exhibit dull or patchy, dull to moderate luminescence. Fibrous and prismatic calcite cements adjacent to clear calcite overgrowths may have well-developed crystal terminations or more rarely, fibrous calcite abuts against the overgrowths along a sub-planar contact. In matrix-rich sediment, overgrowths are commonly absent, but when they occur they tend to be poorly-developed, inclusion-rich rinds, up to 50 μm thick.

5.2.5 Blocky Calcite

This cement is present in all lithofacies occluding any remaining primary porosity in calcarenites and calcirudites (Plate 11b; 21c); it is volumetrically the most important cement in some brown oolites and flat-pebble conglomerates. Blocky calcite also typically occludes: (1) ooid and skeletal molds, vugs and burrows (Plate 11c, d; 27b, d); (2) voids created by mechanical grain deformation (Plate 17b); and (3) fractures that cross-cut all grains and earlier cements.

Blocky calcite ranges in size from 50-200 μm, and shows an increase in size away from the substrate. Two separate luminescent stages are recognized but not always developed (Plate 11c): (1) a widely-developed, proximal stage of inclusion-rich, ferroan and non-ferroan calcite, which exhibits moderate and dull luminescence and (2) a later stage of non-ferroan calcite, characterized by moderate and bright luminescence.

This last stage is less common and is the last cement in the Port au Port sequence. It is present only in large intergranular cavities and bioclast molds, some fractures, and replaces dolomite rhombs (refer to "dedolomites" in Chapter 8).

5.2.6 Micrite Matrix

Although cements are the most important interparticle material in grainy sediments, micrite matrix containing bioclasts and silt-size quartz and feldspar grains is also present in some grey oolites (Plate 17a-f). This matrix is also the most pervasive interparticle component of brown oolite (Plate 21e, f) and flat-pebble conglomerates (Plate 12c). Matrix is of variable abundance and occurrence: (1) partially or completely occluding void space; (2) occuring as perched sediment on top of larger grains; and (3) present as a geopetal fill in large voids.

Micrite matrix tends to inhibit cementation, but when interparticle cements are developed, it may postdate or predate fibrous and micritic calcites and some syntaxial echinoderm overgrowths, but predates prismatic and blocky calcites.

5.3 INTERPRETATION: Sequence and Environments of Cementation

Comparison of the spacial and temporal distribution of cements in all rock types reveals a recurring cement sequence in both subtidal and intertidal sediments. The following interpretation is based largely upon grey and brown oolites, which best display the various types of

cements and their distribution. Data from flat-pebble conglomerates, bioclastic calcarenites and bioherm and biostrome carbonates supplement this interpretation.

Phase 1 involved precipitation of facies-specific cements that were commonly succeeded by matrix deposition: fibrous, isopachous micritic, meniscus micritic and some syntaxial calcite overgrowths. Phase 2 included limestone dissolution, forming moldic porosity, and prismatic calcite precipitation. Phase 3 involved fracturing, and precipitation of blocky calcite and the remaining syntaxial calcite overgrowths, not included in phases 1 or 2. In contrast to phase 1, these later phases are non-fabric specific, affecting all limestone lithofacies.

5.3.1 Phase 1 -- Subtidal and Intertidal Cementation

5.3.1.1 Ooid Calcarenites

Fibrous, isopachous micritic and meniscus calcite cements are interpreted to be synsedimentary in origin; ie. they were precipitated under the influence of shallow-marine waters, contemporaneous with or shortly after sediment deposition. Fibrous and isopachous micritic calcites, which are well developed in grey oolites of subtidal origin (Chap. 3) are interpreted to have precipitated under submarine conditions (shallow-marine phreatic zone; James and Choquette, 1983). This is based on: (1) their occurrence in subtidal sediments which lack evidence of subaerial exposure; (2) their association with fossiliferous micrite matrix, interpreted as marine internal sediment; (3) their occurrence in intraclasts; and (4) their similarity to modern submarine

cements — Mg calcite occurs as micrite-sized, and acicular or bladed crystals in rinds or completely filling pores, whereas aragonite consists of micrite-size crystals or acicular crystals in isopachous rinds, intergranular meshes or botryoids (e.g. James and Choquette, 1983; and references cited therein). Fibrous calcite also rarely occurs in brown oolite and may have precipitated in these intertidal sediments (Chap. 3) during periods of submergence.

Meniscus micritic calcite is restricted to intertidal brown oolite that is poorly cemented by the above-described submarine cements. The preferential occurrence of micritic calcite at grain contacts suggests precipitation in partially water-filled pores to form marine beachrock (Dunham, 1971), as would be expected in the intertidal zone. Modern mixed-water vadose zones commonly have meniscus cements, which have a patchy distribution (e.g. James and Choquette, 1983).

5.3.1.2 Bioherms and Biostromes

Fibrous calcites in biohermal and biostromal carbonates are interpreted to be synsedimentary cements that were precipitated during and shortly after the growth of these subtidal and intertidal structures but prior to deposition of overlying sediments. Modern reefs are commonly characterized by concomitant reef growth and cementation by fibrous and botryoidal aragonite, and micritic or bladed Mg calcite (e.g. James et al., 1976; James and Ginsburg, 1979). A similar interplay is envisaged for the Port au Port structures, in which fibrous calcite was a constructional component forming on growth surfaces, rather than just a void-filling precipitate. This interpretation is based on the

following observations:

(1) They are similar to isopachous fibrous calcite cement in ooid calcarenites, which is interpreted to be of synsedimentary subtidal origin.

(2) The direction of crystal growth is consistently upward as indicated by (a) the radially oriented, elongate crystals; (b) the increase in crystal width away from the substrate; and (c) the development of crystal terminations directed away from the substrate.

(3) Silty micrite interlaminated with fibrous calcite commonly filtered downward into intercrystalline pores of the underlying fibrous calcite isolating individual crystals or bundles of crystals.

Although fibrous calcite cements are clearly components of biohermal and biostromal carbonates, the degree of organic influence on cementation and the causes for different cement morphologies in such close spacial association to each other have not yet been determined.

Mazzullo and Cys (1979) have similarly interpreted masses of radial calcite cement in the core of Permian phylloid algal mounds, New Mexico, to have precipitated on the sea floor. Growth of these cements, accompanied by void-filling marine sediments and cements, resulted in an inorganic boundstone which later provided the foundation for the growth of algal mounds.

Synsedimentary cements in grainy sediments, bioherms and biostromes are extensive. These cements, which reflect precipitation in intertidal

and adjacent subtidal and supratidal (meteoric) zones, are genetically related and are here collectively termed peritidal cements (Fig. 5.2).

3.4.3 Phase 2 -- Early Meteoric Dissolution and Cementation.

The only precipitate during this stage appears to be prismatic calcite cement (Fig. 5.2). Its absence in intraclasts, the lack of overlying internal marine sediment, and its occurrence in fossil molds and between obvious synsedimentary and burial cements (discussed below) indicate precipitation in the near-surface zone. Furthermore, the generally clear and non-ferroan nature and moderate luminescence of the distal stage suggest prismatic calcite formed in large part in an early meteoric setting (e.g. Frank et al., 1982; Grover and Read, 1983; James and Klappa, 1983). The proximal stage, however, may be a mixed marine-phreatic and meteoric cement based on: (1) its occurrence between synsedimentary marine cements and the above early meteoric cement and (2) its ferroan nature and dull luminescence (cf. Meyers and Lohmann, 1978 ; James and Klappa, 1983).

The absence of prismatic calcite cement in fine calcarenites and their limited occurrence in coarse calcarenites, calcirudites and large voids suggest that either: (1) synsedimentary cements occluded much of the pore space so that later meteoric cementation was ineffective; or (2) the sediment was not subjected to extensive meteoric cementation.

Figure 5.2: Distribution of early cements in ooid and bioclastic calcarenites and calcirudites. Diagenetic zones are from James and Choquette (1984).

EARLY CEMENTS

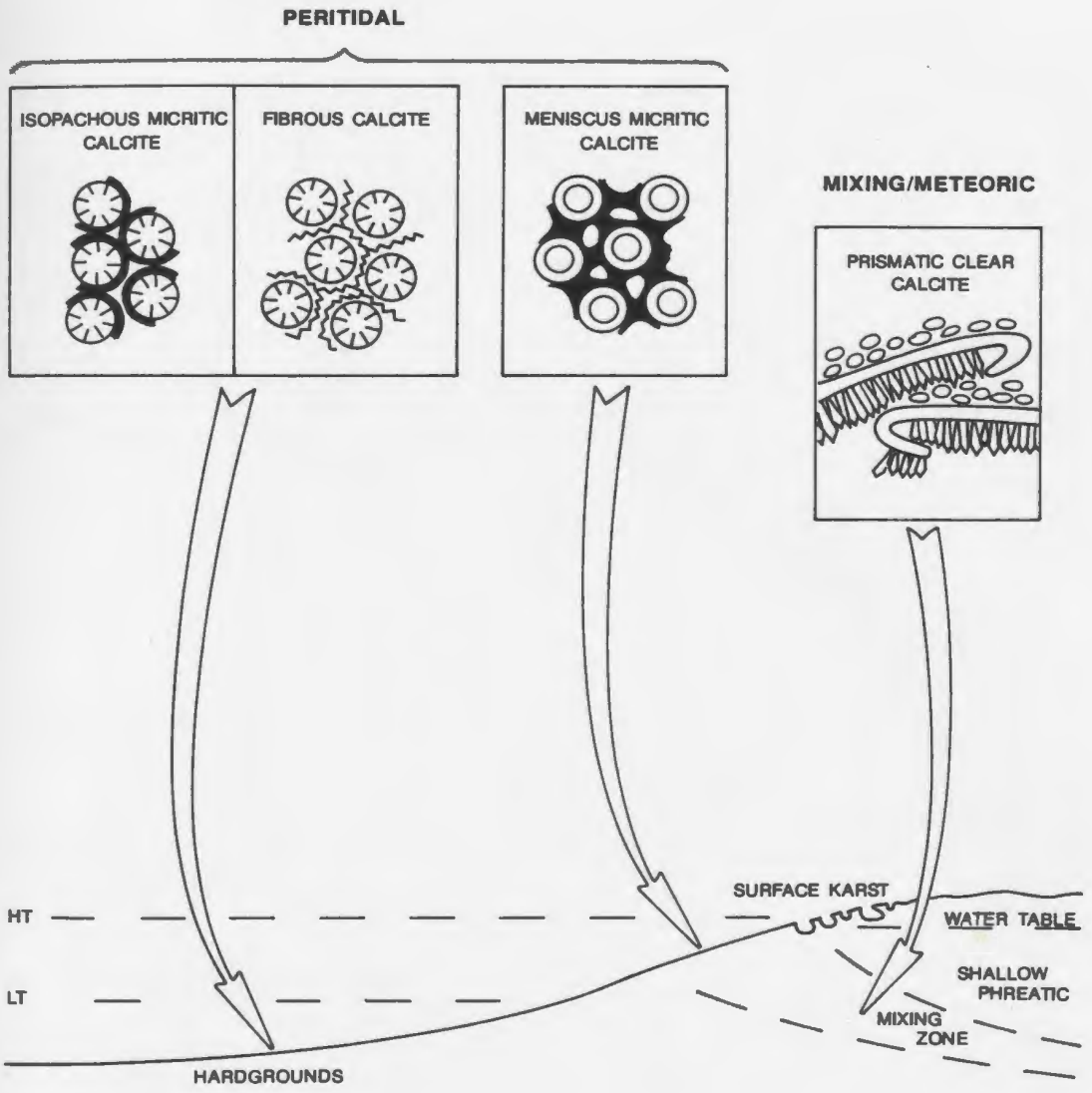

The occurrence of molds of such bioclasts as inarticulate brachiopods and gastropods (refer to Chap. 6) indicates that dissolution of metastable carbonates also occurred during this stage. These molds are generally occluded by dull-luminescent blocky calcite and rarely by prismatic calcite, suggesting that this fabric-specific dissolution, in large part, postdated prismatic calcite but predated blocky calcite precipitation.

5.3.3 Phase 3 -- Burial Cementation

Blocky calcites are the last cements and are interpreted to be post-compactional features precipitated under burial conditions[1], based on their occurrence in fractures that crosscut particles and phase 1 and 2 cements. The first stage of blocky calcite shows a transition from moderate to dull luminescence and an increasing iron content in the youngest zones, which reflect precipitation under progressively more reducing and presumably deeper burial conditions ([redacted] Meyers, 1974; Frank et al., 1982; Glover and Read, 1983; James and Klappa, 1983). This cement occludes most voids, which remained open or developed after early lithification, formation of fossil molds and fracturing.

The rarer, brightly luminescent second stage of blocky calcite, which crosscuts all lithologies, strongly suggests precipitation from meteoric fluids under shallower burial conditions than the first stage (e.g.

---

1. Diagenesis under "burial" conditions is herein considered to include processes that occur between the near-surface zone and the zone of metamorphism (Scholle and Halley, 1985); ie. the mesogenetic zone of Choquette and Pray (1970).

Meyers, 1974; Glover and Read, 1983); ie. the "telogenetic stage" of Choquette and Pray (1970). It is probably related to uplift and faulting of the Cambro-Ordovician sequence on the Port au Port Peninsula during the Late Devonian Acadian Orogeny, development of karst topography prior to Upper Mississippian sedimentation (Dix, 1981), and possibly post-Mississippian alteration (refer to Chap. 8).

Clear, syntaxial echinoderm overgrowths are contemporaneous with the first stage of blocky calcite. This is evidenced by the dull to moderate luminescence of the overgrowths, which is identical to that of blocky calcite. Cloudy syntaxial echinoderm overgrowths, however, may be of synsedimentary origin, based on the following evidence: (1) they are overlain by internal marine sediment; (2) they inhibited formation of adjacent fibrous calcite cements; and (3) they are truncated by erosion surfaces interpreted to be synsedimentary features (discussed below in "erosion surfaces"). Syntaxial echinoderm overgrowths have not yet been reported in modern marine environments (James and Choquette, 1983). Abundant calcite overgrowths in the fossil record, however, have been interpreted to be marine precipitates, based on the same type of evidence used above (e.g., Lohmann and Meyers, 1977; Wilkinson et al., 1982; Wilkinson et al., 1985).

5.3.4 Discussion

5.3.4.1 Cement Stratigraphy

In recent years, compositional zoning within calcite cements has been used extensively in cement stratigraphy, which involves correlation of

crystal zones within a stratigraphic section and between outcrops (Meyers, 1974, 1978; Grover and Read, 1983). Although CL reveals compositional zones in cements of the Port au Port Group, analysis of these cements using cement stratigraphy cannot be done due to: (1) the predominance of aphano- to finely crystalline, facies-specific cements which have indistinct zoning or homogeneous luminescence; (2) the lack of pervasive, well-developed compositional zoning in any of the easily-observed blocky calcite cements; and (3) the relatively rare occurrences of zoned, prismatic calcite cements. The uniform nature and stratigraphically-widespread occurrence of blocky calcite, however, suggest that either they were precipitated in a single, widespread event or the sequence was subjected to a number of similar events over time.

5.3.4.2 Original Mineralogy

Consideration of modern shallow marine cements suggests that synsedimentary marine cements of the Port au Port Group were originally aragonite or Mg calcite. Fibrous calcite cement in grainy, biohermal and biostromal carbonates is interpreted to have been Mg calcite, based upon: (1) petrographic similarities with modern Mg calcite cements (e.g., Bricker, 1971; James et al., 1976); (2) syntaxy with trilobite and echinoderm fragments and ooids interpreted to be Mg calcite (refer to the detailed discussion of ooid mineralogy in Chap. 6); and (3) good microfabric preservation. Microdolomite inclusions (Lohmann and Meyers, 1977) are not apparent in fibrous calcite; their absence, however, does not preclude a Mg calcite composition. Isopachous and meniscus micritic calcites were probably also Mg calcite. This interpretation is

compatible with the preservation of crypto- to microcrystalline fabrics, which are morphologically identical to modern micritic cements of Mg calcite (e.g., Bricker, 1971). There is little evidence for aragonite cements (refer to Chap. 6 for discussion of evidence for aragonite).

Blocky and prismatic calcites have sharp CL zoning and well-preserved microfabrics, suggesting that their mineralogy has remained unaltered from calcite (cf. Coniglio, 1985; Scholle and Halley, 1985). Syntaxial echinoderm overgrowths, which have the same petrographic characteristics as these calcites, may also have been precipitated as calcite (e.g. Bathurst, 1975; Longman, 1980; Wilkinson et al., 1982). Examples of echinoderm overgrowths interpreted as early Mg calcite cements, however, have been reported (e.g. Lohmann and Meyers, 1977; Meyers and Lohmann, 1978).

5.4 FEATURES OF SYNSEDIMENTARY LITHIFICATION

In addition to the calcite cements interpreted to be of peritidal origin, the Port au Port sequence contains other physical features which further substantiate the importance of synsedimentary diagenesis in both submarine and subaerial environments. The following sections describe conglomerates, hardgrounds and surface karst features, and discuss their implications for early lithification. Flat-pebble conglomerates and hardgrounds in parted limestone sequences are of particular importance as they provide the only unequivocal evidence for synsedimentary lithification of parted limestone.

5.4.1 Conglomerates

As described in Chapter 3, parted limestone cycles and oolite-laminite assemblages are punctuated by conglomerates, 3-30 cm thick, composed of clasts of similar lithologies. This close association of bedded and conglomeratic carbonates indicates a synsedimentary origin for the conglomerates.

5.4.1.1 Clasts

The well-rounded to subrounded clasts in conglomerates include four compositional types:

(1) Tabular to equidimensional ooid calcarenite clasts in oolite-laminite assemblages as scattered clasts or thin beds. These clasts are packstones to grainstones composed of radial, concentric or superficial radial ooids (described in Chapter 6; Plate 4a; 12d).

(2) Flat-pebble conglomerates are composed of tabular clasts of silty mudstone to packstone that occur throughout parted limestones (Plate 12a-c; e). The clasts contain variable percentages of bioclasts (trilobite and echinoderms), peloids, intraclasts and siliciclastic silt in a muddy matrix.

(3) Aphanocrystalline dolomite and dolomitized oolitic clasts are common constituents of oolite-laminite assemblages but are absent in parted limestones. These clasts are discussed in Chapter 8 on dolomites.

(4) Intermound sediments in biohermal and biostromal structures contain abundant clasts of algal boundstone compositionally identical to the adjacent mounds. These clasts are also present in overlying beds.

Calcarenite clasts tend to be well-cemented by syntaxial echinoderm overgrowths, fibrous calcite, or micritic calcite. These cements, along with the particles, are truncated at clast boundaries (Plate 12d). Blocky and prismatic calcite cements are noticeably absent.

Clasts in flat-pebble conglomerates contain abundant micrite matrix. The surfaces of these clasts are commonly pockmarked by pits and possible borings, 2-5 mm deep, which are filled with matrix sediment (Plate 12b). These pitted clasts also have opaque mineralization, composed primarily of pyrite, which occurs: (1) as concentric bands in the outermost 1-2 mm of the clasts and (2) disseminated throughout the clasts. Similar mineralization does not occur in oolitic clasts.

5.4.1.2 Matrix and Cement

The composition of the matrix can vary within and between conglomerate beds, and is often similar to that of the clasts. Oolitic conglomerates generally have a matrix of ooid-intraclast-bioclast grainstone, whereas conglomerates in parted limestone vary from mudstone to intraclast-bioclast grainstone (Plate 12c, d).

Cements occlude the remaining interparticle porosity, which is generally only shelter porosity formed under umbrellas of horizontal to gently inclined tabular clasts (Plate 11b). The main cement types are: an initial stage of prismatic calcite and a later stage of non-ferroan

and ferroan blocky calcite.

5.4.1.3 Implications for Synsedimentary Lithification

Compositional similarities between conglomerate clasts and matrix, and the overlying and underlying beds of ooid calcarenite or parted limestone indicate that: (1) the clasts need not have been extensively transported and (2) the beds from which they were derived were deposited in an environmental setting similar to that in which the conglomerates were deposited. The large and relatively undeformed conglomerate clasts clearly formed from the disruption of well-lithified beds rather than unlithified, cohesive sediment; this interpretation can also be applied to smaller, compositionally-identical clasts. Based on the following field and petrographic evidence, sediment lithification is interpreted to be of synsedimentary origin, occurring in subtidal and intertidal environments:

(1) Only synsedimentary cements are found in calcarenite clasts.

(2) Particles and synsedimentary cements within clasts are truncated by clast boundaries.

(3) The occurrence of undeformed micrite-rich clasts throughout parted limestone sequences is key evidence for early lithification of parted limestones. The compositional differences between these micritic clasts and the coarser neospar mosaics in limestone beds and nodules in parted limestone suggest that (a) clasts were derived from synsedimentary lithified beds and were not subjected to later aggradational neomorphism and (b) limestones with coarser neospar mosaics were later lithified;

the significance of this observation is fully discussed in Chapter 7.

Additional evidence for multiple phases of synsedimentary lithification is provided by the eroded upper surfaces of some conglomerate beds, which truncate both clasts, matrix and some calcite cements. This is discussed below in the section on "hardgrounds".

5.4.2 Erosion Surfaces

Numerous planar to scalloped erosion surfaces occur throughout the Port au Port sequence. Planar to sub-planar surfaces are well developed on parted limestone, grey oolite and conglomerate, whereas highly sculptured surfaces are found on carbonate laminites. These features are readily recognizable in outcrop and thin section, and they exhibit clear evidence of having formed on well-lithified sediment.

Two types of erosion surfaces are recognized, submarine hardgrounds and surface paleokarst. These provide additional evidence for synsedimentary lithification and erosion prior to deposition of overlying beds. Each type is distinct but does not exhibit features strictly diagnostic of diagenesis in subtidal, intertidal, supratidal or subaerial environments. Integrating environmental interpretations of the overlying and underlying sediments with the types of synsedimentary cements, however, permits interpretation of the environments in which these surfaces formed.

5.4.2.1 Hardgrounds

A hardground is a discontinuity surface at which synsedimentary

submarine cementation has formed a well-lithified sea floor (Bromley, 1975 and references cited therein). Hardgrounds are generally identified by such characteristics as eroded upper surfaces, encrusting fauna, borings, mineral crusts, the absence of compaction features and the inclusion of clasts derived from lithified sediment in overlying beds (Bromley, 1978). As will be shown in the following sections, however, these features are not consistently developed nor are they restricted to hardgrounds.

Parted limestone in the March Point Formation and Man O' War Member, and grey oolite in the Campbells Member, which are interpreted as predominantly subtidal sediments, have well developed discontinuity surfaces. The lack of evidence for subaerial exposure and the similarity in lithologies below and above the surfaces support the interpretation that these surfaces were hardgrounds that formed and were eroded under submarine conditions. These field observations are of particular importance for the origin of parted limestone hardgrounds and conglomerates, which due to their very fine grained nature lack conclusive petrographic evidence for a submarine origin.

These surfaces are geographically sporadic in occurrence, and multiple surfaces are commonly developed over short stratigraphic intervals (Fig. 5.3). They are traceable across individual outcrops (tens to hundreds of meters) but cannot be traced between adjacent outcrops that are tens of kilometers apart.

Grey Oolite

Hardgrounds on grey oolites are flat with abundant small pits forming

Figure 5.3: Vertical distribution of erosion surfaces in the Campbells and Felix Members of the Petit Jardin Formation, Port au Port Peninsula (K = surface paleokarst; H = hardground; C = condensed interval).

EROSION SURFACES

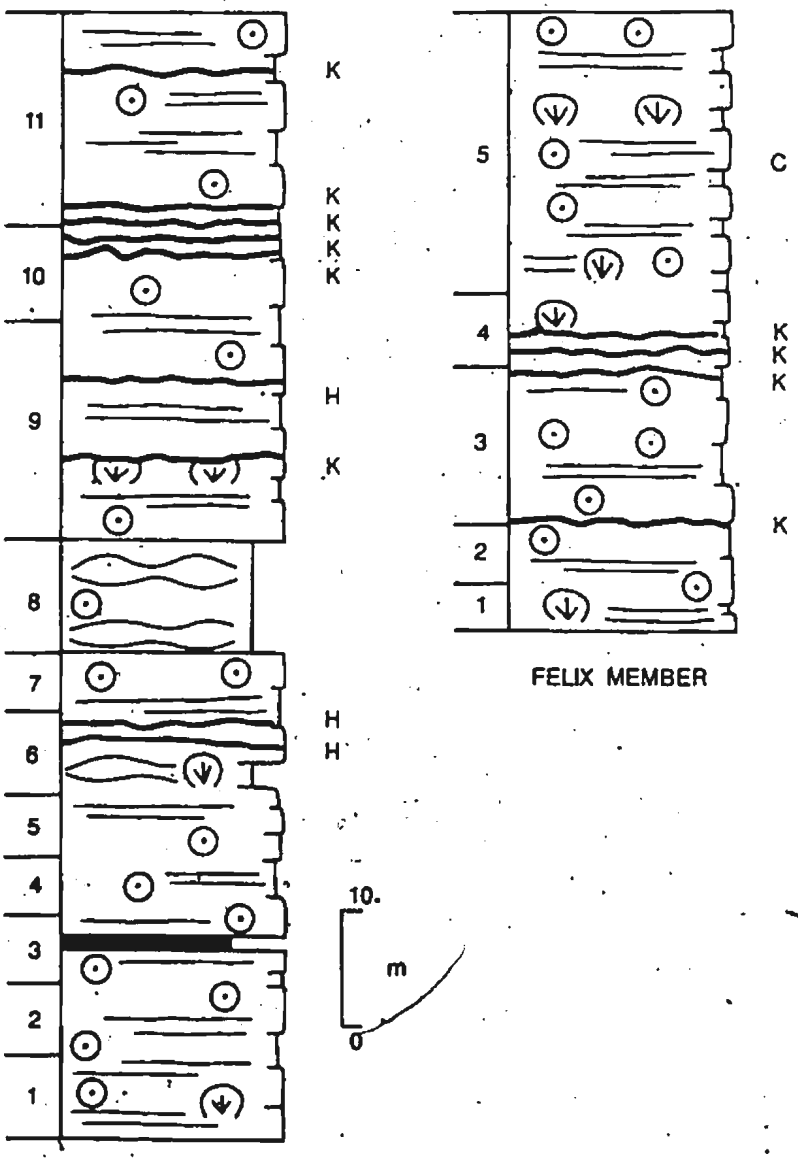

microrelief on the scale of hundreds of micrometers (Plate 13d). Mineralized crusts are rare (discussed in parted limestone hardgrounds) and no obvious borings have been observed. Multiple hardgrounds are common, occurring within centimeters of each other and merging into underlying hardgrounds. Ooids and syndepositional cements (fibrous calcite, isopachous micritic calcite and some syntaxial overgrowths) are truncated by the surfaces. These hardgrounds are generally overlain by grey oolite similar in composition to underlying beds, but stromatolite-thrombolite horizons are occasionally developed on the surfaces.

Rare occurrences of veneers (0.05 to 1.5 mm thick) of irregularly interlaminated fibrous calcite and silty micrite are found directly on top of oolitic hardgrounds (Plate 13d). Calcite crystals are oriented perpendicular to the substrate and contain minor amounts of opaque grains and inclusions that form indistinct laminations parallel to the substrate. Similar encrustations, interpreted as synsedimentary precipitates, have been documented by Purser (1973) on the Trucial Coast, Persian Gulf.

Parted Limestones and Conglomerates

Hardgrounds in parted limestones are subtle features due to the fine-grained nature of the sediment, which makes recognition of truncated surfaces and borings difficult. The abundance of interbedded flat-pebble conglomerates, however, with limestone clasts interpreted to be derived from adjacent parted limestones indicates that synsedimentary lithification and erosion of parted limestones were common processes.

Numerous resistant-weathering horizons (10-30 cm thick) of parted limestone, sporadically interbedded with more recessive beds of identical lithology, are interpreted to be hardground horizons (Plate 18a-c). The upper surfaces of these horizons are planar or hummocky and are always developed in limestone beds. These surfaces have microrelief created by abundant irregularly shaped, millimeter- to centimeter-sized pits which are generally filled by flat-pebble conglomerate. Burrows are well preserved and uncompacted, but borings and superposed borings, which are common criteria for hardground identification, are rare; they are only recognized by their crosscutting relationship with surfaces already interpreted to be hardgrounds. Limestone beds are homogeneous mudstone (discussed in detail in Chap. 7) and laminations and thin beds are not well developed.

Parted limestone hardgrounds are characterized by a pervasive impregnation of black opaque minerals, predominantly pyrite with minor glauconite (herein termed "pyrite"), that impart a distinctive bluish-grey colouration to weathered and fresh surfaces. Pyritized zones typically have sharp upper or outer boundaries, and lower or inner boundaries that are gradational with unmineralized sediment. These impregnations are similar to those rarely found in oolitic hardgrounds and occur in several modes, which have also been widely documented in other examples of ancient (e.g., Lindstrom, 1979; Bathurst, 1975) and Recent hardgrounds (e.g., Bathurst, 1975):

(1) continuous or discontinuous rinds at the upper surface of the hardground or developed approximately 100-200 μm below the surface; they are thin or non-existent under overhangs and at vertical margins of

irregularly-shaped pits, and are generally not truncated by micropits (Plate 13b, c).

(2) nested bands that developed below and subparallel to the hardground surface, similar in appearance to Liesegang rings.

(3) disseminated grains occurring in isolated patches or stringers throughout the parted limestone.

(4) haloes lining burrows below the hardground surface.

(5) partial replacement of carbonate grains by disseminated pyrite that is particularly well developed in radial ooids and bioclasts (Plate 25c).

Mineralized hardground surfaces are also developed on some flat-pebble conglomerates that punctuate parted limestone sequences (Plate 13e). Truncated or exhumed clasts are obvious at the upper surface of the conglomerate and circumgranular mineral impregnation of clasts, identical to that seen in hardground surfaces, is present throughout.

Implications of Hardgrounds

The occurrence of two distinct types of hardgrounds in grey oolites and parted limestones in the Port au Port sequence reflects the differences in depositional environments which control the nature of early lithification processes.

Hardgrounds developed on mudstone beds in parted limestone sequences are characterized by pervasive mineralization and are commonly overlain by sediment containing glauconite and phosphatic grains. These features

suggest that sea-floor sediments suffered intermittent periods of low sedimentation or non-deposition under relatively low energy conditions. The hummocky and micropitted surfaces and associated burrows further imply that lithification was sufficiently rapid to preserve the irregular topography of the bioturbated sea bottom (Bromley, 1975) or that the lithified surface was later eroded. This interpretation is based on modern examples documented by Taft et al. (1968) in the Bahamas and by Shinn (1969) in the Persian Gulf. They recognized three conditions, in addition to seawater chemistry, necessary for hardground formation: (1) sufficiently low sedimentation rates; (2) reduced energy conditions; and (3) stable bottom sediments.

Parted limestone hardgrounds are identical to Cretaceous Chalk hardgrounds of northwestern Europe (e.g. Bromley, 1967; Bathurst, 1975 and references cited therein). Chalk hardgrounds have upper surfaces that have been eroded and bored, and coated and replaced by phosphorite and glauconite. They have been interpreted by various workers to have formed at ocean depths greater than 50 m as a result of temporary periods of reduced sedimentation rates and/or non-deposition (Bathurst, 1975).

In contrast to hardgrounds in parted limestones, those on grey oolites are interpreted to have formed in the subtidal mobile fringe of a high-energy shoal complex in which there was active ooid precipitation and deposition. Synsedimentary subtidal cementation was intense and the major process in the formation of these hardgrounds; this is further substantiated by the absence of hardgrounds in intertidal brown oolite which generally has poorly developed synsedimentary cements.

Characteristics of oolitic hardgrounds are incompatible with a mechanism of formation which involves widespread hiatuses or reduced rates of sedimentation, as proposed for parted limestone hardgrounds. Incorporating evidence from oolite-laminite assemblages (refer to Chapter 4), it is suggested that localized variations in shoal topography and hydrography, caused by the rapid migration of shoal components, provided conditions conducive to the formation of oolitic hardgrounds. Fluctuating energy conditions resulted in local, and probably short-lived, periods of stable sediment conditions, which permitted sediment lithification, alternating with periods of turbulence during which ooid formation, reworking and hardground erosion took place.

Hardgrounds in the Port au Port sequence are similar to modern oolitic hardgrounds in Bahamian oolitic sands (Dravis, 1979). The Bahamian hardgrounds are forming in a high energy tidal bar environment that is characterized by a high sedimentation rate and strong sediment agitation. Dravis (1979) proposed that local topographic depressions and surficial algal mats provide sufficient sediment stability to allow synsedimentary lithification and the formation of hardgrounds.

Rare "pelagosite-like" encrustations that are developed on oolitic hardgrounds in the Port au Port Group can be interpreted in several ways. In the Persian Gulf, Holocene pelagosites of strontium-rich aragonite are interpreted by Purser (1973) to have precipitated during intervals of subaerial exposure which interrupted synsedimentary marine deposition and lithification. The absence of other evidence for subaerial exposure in Port au Port encrustations, however, suggests that

those in the Persian Gulf are not good modern analogues. These Cambrian encrustations may instead be of submarine origin as suggested by their morphological similarity with fibrous calcite cements in algal mounds and grey oolite. Similar cements in Permian algal mounds and adjacent sediments (New Mexico) have been interpreted by Mazzullo and Cys (1979) to have been precipitated on the sea floor.

5.4.2.2 Surface Paleokarst

Planar and scalloped erosion surfaces are found on many carbonate laminite beds in the Campbells and Felix Members, and rarely in the Man O' War Member (Fig. 5.3). Features such as truncated grains, pits with overhanging walls, and clasts that are presumably derived from beds underlying erosion surfaces indicate that these surfaces formed on synsedimentary lithified sediment. Furthermore, the consistent occurrence of these erosion surfaces on carbonate laminites (interpreted in Chapter 3 to be supratidal to highest intertidal sediments), the smoothly-sculpted shapes of the pits, and the absence of tools for mechanical erosion suggest that these surfaces are synsedimentary corrosion features formed during subaerial exposure; ie. surface paleokarst (cf. Sweeting, 1972; James and Choquette, 1984).

Surface Morphology

The following descriptions are based upon cliff exposures on the Port au Port Peninsula which present well-exposed, cross-sectional views of the paleokarst surfaces. Three recurring types are recognized (Fig. 5.4): (1) fractured and brecciated surfaces; (2) scalloped surfaces; and

Figure 5.4: Schematic diagram of the types of surface paleokarst in the Port au Port Group.

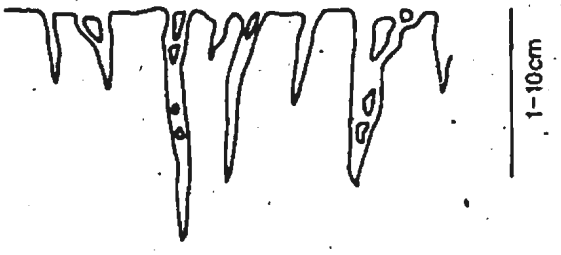
FRACTURES & BRECCIA
1-10cm


SCALLOPED SURFACES
2-50 cm


PLANAR SURFACES
1-10 mm

(3) planar surfaces. The first two are laterally intergradational; whereas no lateral variations have been observed in planar surfaces on an outcrop scale. These surfaces are sharp boundaries separating underlying carbonate laminites from overlying beds. Mineralized zones of what are now iron oxides are generally restricted to scalloped and planar surfaces and are present only in the upper 1-3 cm of the surfaces.

Fractured and Brecciated Surfaces (Grikes; Sweeting, 1972). Vertical to steeply dipping fractures occur in beds with nearly flat, upper surfaces and extend down to tens of centimeters, typically forming an anastomosing pattern in cross-section (Plate 14a). Fractures are up to a centimeter in width and are filled with sediment from overlying beds, commonly brown oolite.

Scalloped Surfaces (Kaminitzas; Sweeting, 1972). Pits and ridges, centimeters to decimeters in scale, form a series of closely spaced, concave-upward arcs (Plate 14d; 15a) or isolated stacks up to 30-40 cm in relief (Plate 15b). The irregularly spaced pits have smooth surfaces with curved, steeply sloping to oversteepened walls and flat to highly curved bottoms; the depths of the pits vary within individual surfaces. Intervening ridges typically vary from knife-edged pinnacles to flat-topped pinnacles with sharp overhanging flanges (Plate 15c). The consistent cross-sectional shape of the pits and ridges suggests that they are basins rather than cross-sections of runnels or grooves.

These scalloped surfaces are invariably overlain by either low-relief algal biostromes or intraclast floatstone to rudstone. Most of the

intraclasts are angular to subrounded and appear to have originated from the breakup of underlying beds. Erosion surfaces occasionally occur in sediments that fill the pits, suggesting multiple events of synsedimentary lithification.

An exceptional example of a scalloped surface is found in the lower part of the Berry Head Formation in the Isthmus Bay East section where a depression, 6 m wide and up to 1 m deep, is developed on dolostone laminite (Plate 14c). The depression is flat-bottomed with a rounded, overhanging margin, and is filled with conglomerates, dolostone laminite and stromatolite mounds that are best developed on the flanks.

In addition to these more sculptured surfaces are larger hummocky surfaces, composed of rounded ridges and narrow depressions up to 2 m in width and up to 0.5 m relief (Plate 14b). Hummocky surfaces are developed on carbonate laminites and are overlain by conglomerates or algal horizons as described above, or occasionally by grey oolite. The smaller-scale scalloped surfaces are commonly superimposed on these larger features. Examples of well-developed hummocky surfaces are present in the upper 20 m of the Felix Member, where several occur within a meter-interval.

Planar Surfaces. These surfaces contain millimeter-size pits that impart microrelief to otherwise relatively flat bedding surfaces. They are developed on the upper surfaces of: (1) carbonate laminites that are overlain by sediment which is identical to that overlying scalloped surfaces and (2) stromatolite and thrombolite horizons, truncating mounds and intermound sediments, that are overlain by thin lamellar

stromatolites (Plate 14e). Planar surfaces are traceable the extent of the outcrop (tens to hundreds of meters) but cannot be correlated between outcrops.

An exceptional planar surface is developed on top of the bioherm complex in the Cape Ann Member of the Degras section, Port au Port Peninsula and is one of the rare bedding plane exposures of erosion surfaces (Plate 14f). In the March Point section, 10 km to the east, the bioherm is not developed and the planar surface correlates with a meter-thick bed of variegated shale and dolostone laminite.

Petrographic Evidence for Surface Paleokarst

Petrographic examination of the paleokarst surfaces generally does not reveal diagnostic fabrics of early lithification and dissolution, such as truncation of particles and early cements, due to the fine-grained composition and dolomitization of carbonate laminites, and the abundance of stylolites at lithologic breaks. Several surfaces in the upper half of the Campbells Member at the March Point section, however, are developed on laminite that is only partially dolomitized. The upper part of these particular limestone laminites can be divided into two zones (Plate 15d, e):

(1) The upper zone, up to 1 cm in thickness, is a mosaic of micrite and microspar that is truncated by conglomerate-filled pits. Abundant borings, filled with microspar and pseudospar, pierce conglomerate clasts and the upper surface of the zone. CL of calcite in the borings is identical to that of the lower zone; the carbonate laminite and overlying conglomerate clasts, however, have neospar crystals of dull

luminescence with thin rims of moderate luminescence.

(2) The lower zone of microspar is rapidly gradational with the underlying layer and is composed of microspar crystals with small dull-luminescing cores and thick rims of moderate luminescence.

CL of these zones in which progressively younger calcites are precipitated away from the paleokarst surface indicates lithification from the surface downward. The upper zone was lithified shortly after deposition based on the abundance of borings and the occurrence of mudstone clasts of identical character in overlying beds. The lower zone and sediment fill of the borings were progressively lithified during later diagenesis as indicated by younger CL zones. This lower zone is similar to marginally aggraded mudstones in parted limestones (discussed in Chap. 7) in which lithification occurred during shallow burial.

Origin of Surface Paleokarst

Surface paleokarst in the Port au Port Group is identical to surface karst features (Karren) in modern karst terrains (Sweeting, 1972; Ritter, 1978) and hence substantiates the interpretation of these ancient surfaces as primarily the products of early lithification and carbonate dissolution during subaerial exposure. This interpretation is further supported by the rare occurrence of tepee structures (Assereto and Kendall, 1977) in carbonate laminites. Tepees are interpreted to have formed as a result of dessication contraction and expansive carbonate cementation in highest intertidal to supratidal environments (Shinn, 1969; Davies, 1970; Assereto and Kendall, 1971).

Along many modern tropical and subtropical marine coasts, grikes and kaminitzas are developed on bare carbonate rocks in supratidal environments (Sweeting, 1972) and on carbonates subaerially exposed in the intertidal zone (Kaye, 1959). Supratidal surface karst formed primarily by ponding of meteoric water on near-horizontal surfaces. Sediment below these supratidal contacts exhibits such features as vadose silts, solution vugs, moldic porosity, and early pendent cements. Intertidal surface karst is attributed to corrosion by both meteoric and marine waters, and exhibits features such as borings, encrusting organisms, occurrence beneath subtidal sediments and high rates of corrosion relative to supratidal erosion. Both supratidal and intertidal kaminitzas grade into planed off platforms (tidal terraces) due to the lateral widening and coalescence of adjacent solution basins.

In the Port au Port sequence, the absence of conclusive evidence supporting either supratidal or intertidal dissolution precludes definitive interpretation of the paleokarst surfaces. Although they typically occur on supratidal carbonate laminites that are overlain by intertidal-subtidal conglomerates, corrosion could have proceeded in the supratidal or intertidal environment, or under fluctuating intertidal and supratidal conditions. The occurrence of these surfaces in oolite-laminite assemblages, which are interpreted to be the products of rapidly migrating subtidal, intertidal and supratidal components of a shoal complex, indicates that all three interpretations are probable. The term <u>peritidal paleokarst</u> therefore is used to describe these surfaces.

Similar paleokarst surfaces have been observed in other Paleozoic carbonates but in general have received little attention. Several examples, however, have been well documented in recent years, especially in Ordovician and Silurian rocks (Read and Grover, 1977; Kobluk et al., 1977; Cherns, 1982; Kobluk, 1984). Many of these surfaces have been interpreted to have developed in the spray zone of the supratidal environment (e.g., Kobluk, 1984) and/or in tidal zones (e.g., Read and Grover, 1977). These are also considered as peritidal paleokarst.

5.4.2.3 Discussion

Alteration at Paleokarst Surfaces

Peritidal paleokarst surfaces in the Port au Port Group are characterized by well-developed brecciated and pitted surfaces. They are not associated with calcrete horizons and speleothem deposits that are typical of many modern karst horizons (Sweeting, 1972). Furthermore, they lack the extensive boring and subsurface leaching that have been reported in other Lower Paleozoic examples of coastal paleokarst (Kobluk, 1984).

The restriction of subaerial processes to surface alteration has significant environmental implications. Modern calcretes typically form in arid or semi-arid environments with high evaporation rates (James, 1972; Read, 1976; Esteban and Klappa, 1983). The absence of calcretes in the Port au Port sequence may reflect one or more of the following conditions: (1) a humid climate with low evaporation rates -- evaporites or their replacements have not been found in the sequence; (2) paucity

of land vegetation -- vascular land plants are not known in the Cambrian (Edwards et al., 1979), although the effects of such plants as fungi and algae in the Cambrian are uncertain; or (3) intensive subaerial exposure was not involved in paleokarst formation. The last condition may be of importance in light of the interpretation of Port au Port surface paleokarst as peritidal features formed under fluctuating tidal conditions.

The absence of extensive borings and subsurface leaching may be a function of the poor fabric preservation in carbonate laminites, particularly those that are dolomitized or stylolitic, or a primary feature due to such factors as tightly-cemented rock, short exposure periods, or the peritidal origin of the paleokarst.

Differentiation of Erosion Surfaces

None of the characteristics of hardgrounds and surface paleokarst in the Port au Port Group are unique to either type of surface (Table 5.1). Differentiation of these erosion surfaces has relied largely upon circumstantial evidence provided by the position of the surfaces within parted limestone and oolite-laminite assemblages. These shallow marine assemblages, however, represent laterally-adjacent peritidal environments that were subject to rapid environmental fluctuations caused by tidal processes, migrating shoal components and storm activity. The variability of environmental conditions complicates the interpretation of erosion surfaces. Oolitic hardgrounds, for example, which have clear evidence of submarine lithification, could have been eroded under subaerial or submarine conditions or both.

TABLE 5.1: COMPARISON OF HARDGROUNDS AND SURFACE PALEOKARST
Port Au Port Group

	HARDGROUNDS	SURFACE PALEOKARST
Occurrence	-grey oolite -parted limestone -flat-pebble conglomerate	-carbonate laminite -stromatolite-thrombolite mounds
	-lithologies above and below surface are similar	-abrupt lithologic changes across surface
Morphology	-near-planar with millimeter-scale relief -multiple horizons (2-3 within decimeter interval are common).	-highly sculptured surfaces with smooth-sided pits and overhanging ridges; planar surfaces; fractures and breccia -multiple horizons common
Mineralization	-rare in grey oolite -disseminated pyrite coats and penetrates below surface of parted limestone and conglomerate	-commonly pyrite or Fe-oxide at surface
Alteration	-truncated grains and synsedimentary cements -borings	-rare truncated grains -borings

From the above discussion, it is apparent that the separation of erosion surfaces into hardgrounds and paleokarst may be an artificial division in shallow marine deposits. In the Port au Port sequence, these surfaces occur in close stratigraphic proximity in sediments that record widely fluctuating environmental conditions. Although these so-called "hardgrounds" and "karst" were probably formed primarily by submarine and subaerial processes respectively, the similar characteristics of both types of surfaces suggests that subaerial and submarine lithification and erosion may have variably affected both types. It is proposed that "peritidal erosion surfaces" (after Bromley, 1975) be used to denote such surfaces that have been physically and chemically denuded, and "peritidal omission surfaces" (after Heim, 1924, in Bromley, 1975) when there is little or no evidence of erosion.

Relation to Grand Cycles

Peritidal erosion surfaces are present throughout the Grand Cycles of the Port au Port Group and are not restricted to either shaly or carbonate half-cycles. These surfaces are clearly facies-specific indicating that local environmental factors directly controlled their formation. Eustatic or basin subsidence mechanisms postulated for Grand Cycles governed the nature of environmental conditions but little affected the distribution of erosion surfaces.

Hardgrounds have been noted in other Cambrian platform sequences, notably in the intrashelf basin (shaly-half cycles) in the Canadian Rockies (Aitken, 1978) and in the Nolichucky Formation in the Virginia Appalachians (Markello and Read, 1981). Paleokarst surfaces, however,

have not been well documented in these regions nor in the Great Basin (Carrara Formation, Southern Great Basin; Palmer and Halley, 1979); they have been noted only in the area of the shelf rim (Aitken, pers. comm., 1984). The abundance of paleokarst in the Port au Port Group relative to other Cambrian sequences suggests that either: (1) surface paleokarst has not been recognized or has been obscured in these other sequences or (2) deposits of the Port au Port Group were subjected to greater synsedimentary lithification and corrosion. The thinner carbonate and shaly half-cycles in the Port au Port Group relative to those in other North American examples (refer to Chap. 4) supports the latter proposal and suggests that the Port au Port Group underwent more or longer periods of reduced sedimentation and exposure.

5.5 SUMMARY: Importance of Early Lithification

Cements in the Port au Port Group indicate a prolonged and convergent cementation history. Sediment lithification involved a progression from: (1) synsedimentary peritidal cementation, which is facies-specific and resulted in the formation of hardgrounds and surface paleokarst; to (2) early meteoric cementation and accompanying fabric-specific dissolution; to (3) pervasive burial cementation.

In ancient shallow marine deposits, the importance of the collective influence of submarine and subaerial processes, ie. peritidal diagenesis, has generally been underestimated. It tends to be overshadowed by more obvious seafloor and meteoric diagenesis (reviewed

in James and Choquette, 1983; 1984). In this study, however, the importance of peritidal lithification is apparent as evidenced by: (1) peritidal cements which occlude most original pores and (2) the widespread occurrence of temporally- and spacially-associated erosion surfaces, which may be the joint products of submarine and subaerial lithification and diagenesis. In many peritidal fabrics, the influence of submarine and subaerial processes often cannot be separated, emphasizing the inapplicability of many diagenetic terms, such as hardground or karst sensu stricto, which have specific environmental connotations.

Peritidal lithification, as would be expected, is strongly controlled by depositional settings and in turn modifies the original sediment framework. The distribution and extent of this early lithification in Port au Port sediments appear to be the key factors governing the direction and extent of subsequent diagenesis, particularly compaction and dolomitization (refer to Chap. 7 and 8 respectively).

Chapter 6

ORIGIN AND DIAGENESIS OF OOIDS

6.1 INTRODUCTION

Ooids [1] are common constituents of modern and ancient shallow marine carbonates and commonly exhibit an array of nuclei and cortical fabrics. These enigmatic spheroids have been the topic of much controversy and fascination since the 19th century but few unequivocal conclusions have been drawn to explain their formation and diagenesis (refer to Appendix C). Considerable uncertainty still remains as to the relationship between cortical fabrics and mineralogies, mechanisms of formation, environmental conditions and diagenetic alterations, and the relationship between modern and ancient ooids. In spite of these problems, the apparent abiotic origin of these particles have resulted in their use in more recent studies to evaluate long-term trends in marine carbonate precipitation and hence variations in depositional and diagenetic conditions during geologic history (e.g., Sandberg, 1975; Pigott and Mackenzie, 1979; Wilkinson, 1982).

---

1. The term, ooid, is used as in Kalkowsky (1908) and Teichert (1970) to describe the individual spheroidal or sub-spheroidal grains that comprise an oolite.

Oolites of intertidal and subtidal origin are major constituents of the Port au Port Group and have important implications for ooid formation and diagenesis in the rock record. These deposits contain largely *in situ* ooids which display a range of cortical morphologies that are well preserved in the Campbells Member on the Port au Port Peninsula due to early lithification and the absence of extensive dolomitization. Detailed field, petrographic and CL examinations suggest that the various diagenetic fabrics present in the cortex are the products of only two types of ooids, those with an original Mg calcite cortex and those with a bimineralic cortex, that have undergone progressive diagenesis. In addition, application of these interpretations to carbonate mineralogy trends in the rock record supports the importance of local environmental conditions over eustatic controls in controlling ooid morphology and mineralogy.

6.2 DEPOSITIONAL ENVIRONMENTS

As described in Chapters 3 and 4, two types of oolite, identifiable on both outcrop and microscopic scale, are present in the Port au Port Group. Grey oolite and brown oolite represent two separate regimes in carbonate sand shoal complexes, a subtidal mobile fringe and an intertidal sand flat respectively, of *in situ* ooid precipitation and deposition (Table 6.1). Occurrences of ooids typical of grey oolite as grains or ooid nuclei in brown oolite and vice versa indicate that there was some transportation of ooids between the two environments. The shoal complexes are interpreted to have been situated leeward of the

TABLE 6.1: OOID CALCARENITES

	GREY OOLITE	BROWN OOLITE
Interpretation	-subtidal mobile fringe	-intertidal sand flat
Colour	-dark grey	-buff to dark brown
Bed Thickness	-0.3-0.5 m	-0.5-3.0 m
Sedimentary Structures	-large-scale ripples, herringbone cross-bedding	-thin mudcracked layers, ripple cross-bedding, herringbone cross-bedding
Particles	-radial ooids (0.2-0.6 mm diameter; 10-20 um cortex) -radial-concentric ooids (0.5-1.0 mm diameter; rarely up to 4 mm) -oolitic intraclasts	-micritic intraclasts, peloids -concentric and superficial radial ooids (20-30 um) -oolitic intraclasts bioclasts, quartz sand
Matrix	-rare micrite	-abundant micrite
Synsedimentary Cement	-fibrous calcite, isopachous micrite	-minor fibrous calcite, meniscus micrite

platform edge, with beach ridges (brown oolite and supratidal carbonate laminites) which separated and protected adjacent muddy tidal flats from the open ocean. Tidal structures in tidal flat deposits, however, indicate active exchange with the open ocean, suggesting that the shoal complexes were laterally discontinuous. These complexes are distinct from modern oolite examples, notably the "classic" platform-rim shoals of the Bahamas (e.g. Ball, 1967; Bathurst, 1975) and alongshore oolite deposits of the Persian Gulf (Purser and Loreau, 1973).

Oolites in the Port au Port Group, together with supratidal carbonate laminites, comprise "genetic packages" of repeated, meter-scale assemblages, which lack predictable upward changing sequences (refer to Chap. 4). The variability of the packages suggests that evolution of the shoals took place through vertical accretion and rapid migration of the shoal components in response to changing environmental conditions.

6.3 OOID PETROGRAPHY

6.3.1 Grey Oolite

The characteristically uniform nature of grey oolite in outcrop is also reflected on a microscopic scale. Normal ooids (those in which the cortex is greater than half the radius of the ooid; Illing, 1954) with well developed radial fabrics are the main components. Three major types of ooids, based upon their cortical fabrics, are recognized: radial, radial-concentric and asymmetrical (Fig. 6.1). Peloids are the most common nuclei. Trilobite and echinoderm fragments, quartz silt and

Figure 6.1: Schematic summary of the various types of ooids in ooid calcarenites of the Port au Port Group.

TYPES OF OOIDS

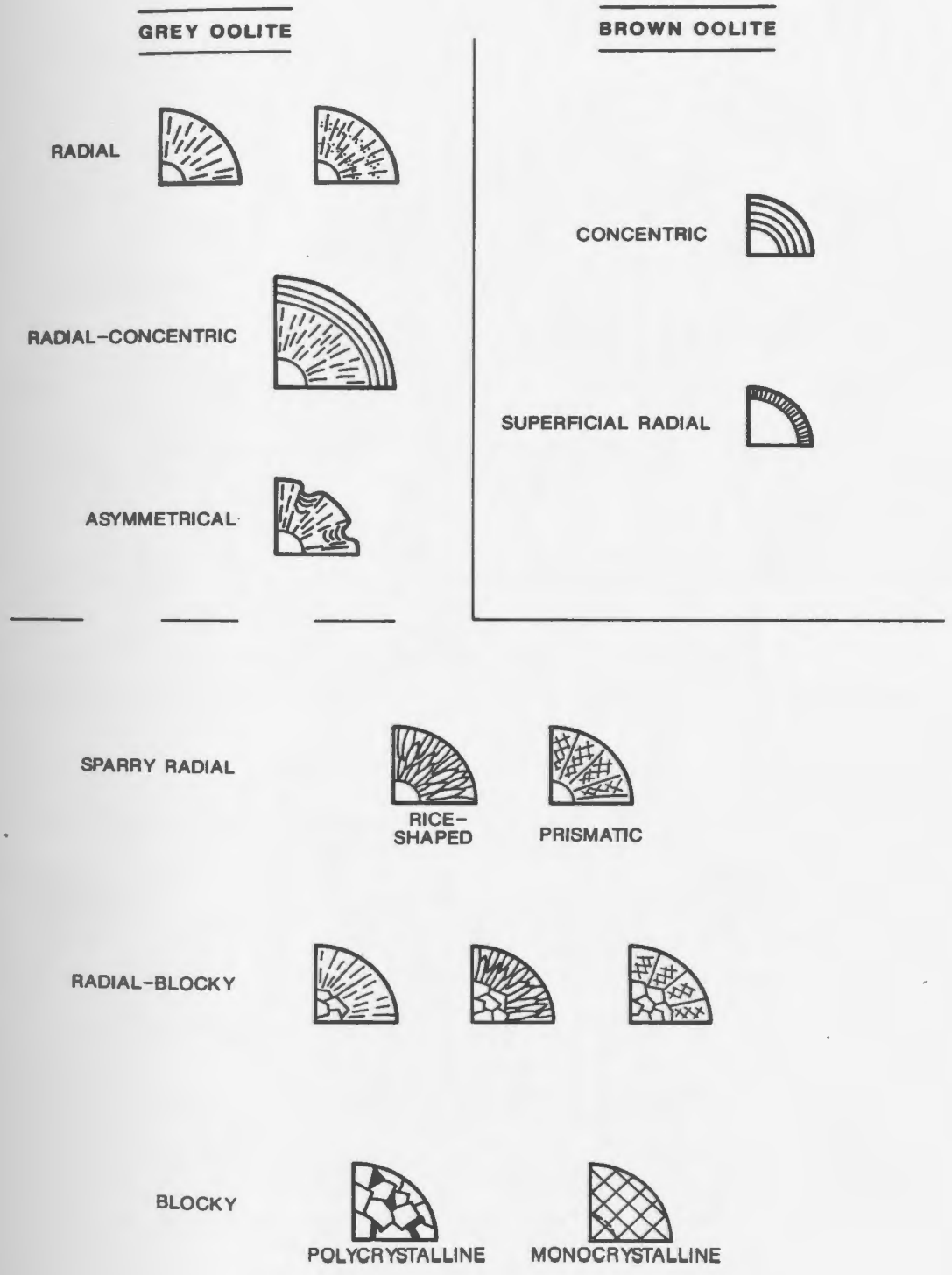

sand, broken and whole ooids, and micritic and oolitic intraclasts may be nuclei as well. The type of nuclei governs ooid shape but does not determine the type of cortex except where trilobite and echinoderm nuclei influence crystallite orientation. Similarly, sedimentary structures and microfabrics, such as cement types and matrix, are not specific to the type of ooid.

6.3.1.1 Radial Ooids

The most common type of ooid is medium to coarse sand-size and has a cortex of radially oriented calcite crystallites (Plate 16a-d). The cortex has a distinctive brown colouration in thin section and is rich in inclusions that are commonly arranged in a radiating pattern. Crystallites have fibrous to prismatic (wedge-shaped) and columnar habits, which are up to 30 to 40 μm in width and may extend the width of the cortex. SEM reveals that fibrous cortices are micron-size, equant to elongate crystallites and that inclusions are equidimensional to slightly elongate holes within the crystallites (Plate 16c). Some ooids contain dark brown micritic rays which may extend the entire width of the cortex (Plate 17d).

A few concentric bands may occur randomly spaced in the cortex but tend to be best developed in the inner and outer parts of the cortex (Plate 16a). Composed of a concentration of inclusions (and possibly some organic material and clays) individual bands rarely exceed 10 to 15 μm in thickness. Radial calcite crystals are commonly in optical continuity on either side of these bands. CL reveals additional concentric zones of dull and moderate luminescence that do not coincide

with inclusion-rich bands observable under light microscope (Plate 16d).

Ooid cortices enclosing nuclei of trilobite or echinoderm particles are in complete or partial optical continuity with those bioclasts which do not have micritic rims (cf. Marshall and Davies, 1975). Broken radial ooids are also common nuclei and have a distinctive wedge shape resulting from fracture surfaces that invariably parallel the radially oriented crystals of the cortex (cf. Halley, 1977).

Fabric preservation on a microscopic scale is commonly excellent and deformed ooids are rare. Ooids of sparry calcite and/or ferroan dolomite, however, are frequently associated with well-preserved ooids.

6.3.1.2 Radial-Concentric Ooids

Also commonly termed compound ooids (e.g. James and Klappa, 1983), these are normal ooids with cortices composed of two distinct fabrics, an inner band of radial fibrous calcite and an outer band of concentric laminae (Plate 17a-d). They are volumetrically important components of grey oolite and are up to 4 mm in diameter (pisoids according to Donahue, 1978). Nuclei may be radial ooids, peloids, trilobite or echinoderm fragments, but are commonly not identifiable; often only microspar is preserved.

The inner portion of the cortex is similar in colour and composition to the radial ooids described above and comprises approximately the central 60-70 μm of the cortex. Micritic rays, 20 to 30 μm wide, are common and may extend into the outer concentric zone resulting in deformation or truncation of the laminae (Plate 17c). This inner zone

occasionally consists of several whole radial ooids that are cemented together by radial fibrous calcite or isopachous micrite with minor micritic matrix (Plate 17d).

The outer part of the cortex is alternating concentric laminae of micrite and radially oriented fibrous calcite with minor blocky calcite laminae. Each lamina is of uniform composition and may be either a complete concentric ring (micritic and fibrous laminae) or discontinuous and lunate (blocky calcite laminae). This zone varies from 20-500 μm in width, with individual laminae generally less than 20 μm thick. Any irregularities in shape in the inner radial zone are "smoothed out" by thickening of the concentric laminae.

Smaller radial ooids, less than 60 μm in diameter, are commonly associated with radial-concentric ooids (Plate 17d). This bimodal distribution of grains is particularly well developed in the Man O' War Member and has been documented in other studies (e.g. Heller et al., 1980; Tucker, 1984).

Radial-concentric ooids generally have good fabric preservation and are rarely associated with ooids of sparry calcite. No oomoldic porosity is observed but unlike radial ooids, distorted radial-concentric ooids are common and are of two types: those in which the external shape of grains is altered and those which retain their original shape. In the first type of distorted ooid, the main deformation occurs in the outer concentric zone, which results in distortion of the external ooid shape and adjacent synsedimentary fibrous calcite cements (Plate 17b, c). The radial core is rarely

disrupted but may be slightly displaced and/or have an outer rim that is embayed by micrite or micritic rays; minor dissolution is also common. These ooids are commonly notched and stretched (spalled ooids, according to Wilkinson et al., 1985), and may occur as a series of grains linked in long zigzag chains (called elephantine by Wilkinson et al., 1985). Porosity created by ooid deformation is occluded by dull-luminescent blocky calcite. This distortion is due to the physical separation of outer laminae from cortex interiors and collapse into the ooid interior, or detachment of laminae away from the grain during mechanical compaction.

The second type of distorted ooid has a nucleus that is displaced from its central position and an undeformed outer shell (Plate 20c). Nuclei have commonly dropped into the lower half of the ooid (half-moon ooids, Carozzi, 1963; geopetal ooids, Mazzullo, 1977) but they have also been displaced into the upper part of the ooid or to the side, or not displaced at all. In contrast to the first type of distorted ooids, cortical preservation is poor, having been replaced by ferroan or non-ferroan blocky calcite and/or dolomite, and in rare cases aphanocrystalline quartz. These half-moon ooids are associated with fractures filled by blocky calcite.

6.3.1.3 Asymmetrical Ooids

Radial and radial-concentric ooids are the main components of grey oolites. Several other types of ooids are also present in lesser abundance but are important to ooid interpretation.

Cerebroid Ooids. These ooids are present only in oomicrites in the Man

O' War Member and have an irregular shape and mottled appearance due to the numerous zones of micrite in the cortex. This micrite characterizes cerebroid ooids and varies in morphology from irregular patches with no particular disposition to radiating cones (wedge-shaped rays with circular transverse sections) that have their widest end directed toward or away from the nucleus (Plate 17e). Most of these patches and rays, however, contain concave laminae that are continuous with concentric bands in radial-concentric areas of the cortex. The non-micritic portions of cortices adjacent to the micrite bulge outwards contributing further to the asymmetry of the grains.

Regenerated and Complex Ooids. These are commonly associated with both radial and radial-concentric ooids and are distinguished by their oolitic nuclei, which may be whole particles (radial, radial-concentric or concentric); broken radial fragments; or multiple ooids (Plate 17f). Cortices of broken and multiple ooid nuclei are often identical to those of the younger ooids. Multiple ooid nuclei may be oosparites or oomicrites but consistently have a first stage cement of fibrous calcite.

6.3.1.4 Micritized and Silicified Ooids

Ooids composed of micrite in grey oolite are rare. They commonly have vague radial structure and are associated with peloids.

Ooids replaced by silica are rare and are found only in the Man O' War Member and in the Berry Head Formation (Plate 17b). Ooid fabrics appear to be preserved on a microscopic scale under plane light but crossed

nicols reveal mosaics of aphanocrystalline to very finely crystalline quartz.

6.3.1.5 Dolomitized Ooids

Partial dolomitization of grey oolite is common and may impart a mottled to layered appearance to oolites. Dolomitization is generally fabric-specific to ooids and has partially or completely altered the particles. Three types of dolomite replace ooids: (1) aphanocrystalline dolomite; (2) ferroan dolomite; and (3) non-ferroan dolomite (described in detail in Chap. 8). Undolomitized and partially dolomitized ooids also have numerous small dolomite rhombs, 5-20 μm in size, ie. microdolomite (cf. Lohmann and Meyers, 1977).

Aphanocrystalline dolomite is highly fabric specific in grey oolite and relatively uncommon. This type of dolomitization is characterized by excellent preservation of ooid fabrics. Ferroan dolomite is the most common type and consists of finely to coarsely crystalline dolomite rhombs with a cloudy core and an outer zone of inclusion-poor, ferroan dolomite (Plate 20d; 28a). Fabric preservation is poor and the extent of dolomitization is variable. These dolomitized ooids are occasionally restricted to thin horizons forming alternating beds of dolomitized oolite and calcitic oolite. Non-ferroan dolomite is very finely to finely crystalline and has fabric preservation similar to ferroan dolomite.

6.3.2 Brown Oolite.

Two types of medium sand-size ooids are recognized on the basis of cortical fabrics, concentric and superficial radial (Fig. 6.1). The nuclei are micritic or oolitic intraclasts, broken or whole ooids, or peloids; echinoderm and trilobite grains are rare. Concentric and radial ooids rarely occur in the same bed, but no obvious spacial or temporal distribution can be discerned. Normal radial ooids, typical of grey oolite, are present in this lithofacies as isolated grains or in oolitic intraclasts.

6.3.2.1 Concentric Ooids

These ooids have cortices up to 60 μm in thickness, which are composed of concentric laminae, approximately 5 μm in width. Three distinct types of laminae are recognized and may occur within the same ooid (Plate 21b): (1) micrite laminae (commonly dolomitized) with moderate luminescence; (2) radial-fibrous calcite laminae with dull luminescence; and (3) laminae of finely to medium crystalline, inclusion-poor ferroan calcite with dull luminescence. The outermost lamina in any ooid grain; however, is generally micritic or dolomitized micrite. SEM microphotographs show that laminae have highly irregular boundaries, particularly those of blocky calcite, and that micritic laminae are composed of elongate to equant crystallites with no preferred orientation.

The most common nuclei are peloids and unbroken or broken radial ooids

(0.1 to 0.2 mm in diameter). Ooids with unidentifiable nuclei that have been replaced by microspar or pseudospar are also abundant. Echinoderm and trilobite nuclei are rare but when present, generally have micritic rims and are not syntaxial with the cortex.

6.3.2.2 Superficial Radial Ooids

These are characterized by a cortex of fibrous to prismatic calcite oriented radially to the nucleus (Plate 21e, f). The cortex is approximately 10 to 40 μm in thickness and when composed of fibrous calcite has a distinctive brown colouration identical to radial ooids in grey oolite. Dark micrite rays are common and concentric bands of micrite are occasionally developed in ooid cores. Cathode luminescence reveals concentric zones of alternating dull and moderate luminescence; up to 5 zones have been observed within a single ooid.

6.3.2.3 Distorted Ooids

Distorted concentric ooids are abundant in brown oolites that are cemented by only blocky calcite or poorly developed fibrous and meniscus calcite cements. Overcompacted and flattened ooids, which have elongated axes parallel to bedding, tend to occur in irregular, centimeter-thick layers parallel to bedding or in irregular patches (Plate 21a); elephantine and spalled ooids, typical of deformed grey oolites, are not present. Flattening of the ooids creates a "fitted grain" texture with no extensive brittle fracturing or partial removal of the cortices or nuclei. Most deformation is concentrated in the concentric laminae and in micritic or microspar nuclei. Radial ooids

and echinoderm particles present as ooid nuclei and distinct grain components are generally not flattened but have sutured grain contacts.

In comparison to concentric ooids, distortion of superficial radial ooids is minimal. Sutured grain contacts and minor brittle crushing of particles give rise to a slightly overcompacted fabric.

6.3.2.4 Blocky Calcite and Micritized Ooids

These ooids are the same size and shape as those previously described but lack good preservation of cortical and/or nuclear fabrics. Blocky calcite ooids are composed of inclusion-rich, very finely to finely crystalline crystals that commonly become more ferroan toward the ooid centers, and minor nonferroan, finely crystalline dolomite. Relict concentric fabrics are occasionally retained but generally only a micritic rim outlining the spherical shape of each ooid is preserved. No leached ooids or oomoldic porosity is present in calcareous brown oolite, but minor oomoldic porosity occurs in dolomitized oolite.

Micritized ooids are only recognizable from sand size petoids when vague concentric bands or radial fabrics are retained. These particles are rare and may be associated with either concentric or superficial radial ooids. As discussed by Wilkinson et al. (1985), these ambiguous grains may have originated by excessive grain abrasion, boring by microendolithic organisms or a combination of the two.

6.3.2.5 Dolomitized Ooids

All brown oolites in the Campbells Member of the Petit Jardin

Formation, which is predominantly limestone, exhibit some degree of dolomitization (also refer to Chapter 8). Three types of dolomitized ooids, similar to those in grey oolite, are recognized: (1) nonferroan and ferroan, aphanocrystalline dolomite with excellent fabric preservation; (2) ferroan, finely to coarsely crystalline dolomite in which gross ooid shapes are retained but not detailed fabrics; and (3) finely to medium crystalline, nonferroan dolomite which may preserve ooid fabrics.

Type 1 dolomite is most common and is best developed in the lower part of the Campbells Member where brown oolites are interbedded with carbonate laminites. The concentric and superficial radial ooids are partially or completely dolomitized and have well-preserved nuclear and cortical fabrics (Plate 21b). Other components of brown oolites, such as the micritic matrix, cements and oolitic and micritic intraclasts are often altered in a similar fashion. Oomoldic and vuggy porosity, up to 10%, and half-moon ooids are sometimes present. The resulting voids may be partially occluded by coarse ferroan dolomite and blocky calcite.

Comparatively, type 2 is rare in brown oolite. It occurs preferentially in ooid nuclei and is best developed in compacted sediments of the Campbells Member. Type 3 dolomite is rare in brown oolites in the Campbells Member but is common in the Felix Member.

6.4 OOID GENESIS

The facies-specific nature of the various ooid types in the sequence

strongly supports the previously proposed interpretation of *in situ* intertidal and subtidal ooid precipitation and deposition (Fig. 6.2).

6.4.1 Subtidal Ooids

Ooids in grey oolite exhibit a correlation between ooid size and the composition of the cortex, which suggests the importance of physical processes, particularly hydrodynamic, in ooid formation. The smaller ooids typically have a radial cortex whereas the larger ooids have cortices that become progressively more laminated (radial-concentric) toward the margin. This fabric is identical to those described in the Jurassic Twin Creek formation, Wyoming (Medwedeff and Wilkinson, 1983) and upper Cambrian Warrier Formation, Pennsylvania (Heller et al., 1980). As suggested by Heller et al. (1980), the smaller ooids were kept mainly in suspension under high energy conditions, which permitted the accretion of a radial cortex without severe grain abrasion. With increasing grain size (threshold of 600 μm), bedload transport became more important resulting in increased abrasion and grain collisions which caused growth of concentric laminae and grain breakage.

Tucker (1984), however, negated the importance of grain abrasion and suggested that water turbulence and turbidity were the main factors governing formation of the cortex. He proposed that smaller radial ooids formed under less turbulent and more turbid conditions than larger ooids, which formed in a mud-free environment by incremental ooid precipitation under high energy conditions. The above hydrodynamic interpretation is more feasible for Port au Port ooids than Tucker's proposal as suggested by: (1) the lack of correlation between the amount

Figure 6.2: Summary diagram of the formation and distribution of ooids in the Port au Port Group. Radial ooids formed in suspension under subtidal conditions and were: (1) deposited in the subtidal; (2) "nuclei" for the formation of subtidal radial-concentric ooids in bedload transport; or (3) transported into the intertidal environment, where they were (a) deposited as superfical radial ooids, or (b) nuclei for concentric ooids. Synsedimentary cementation of all ooid types is common.

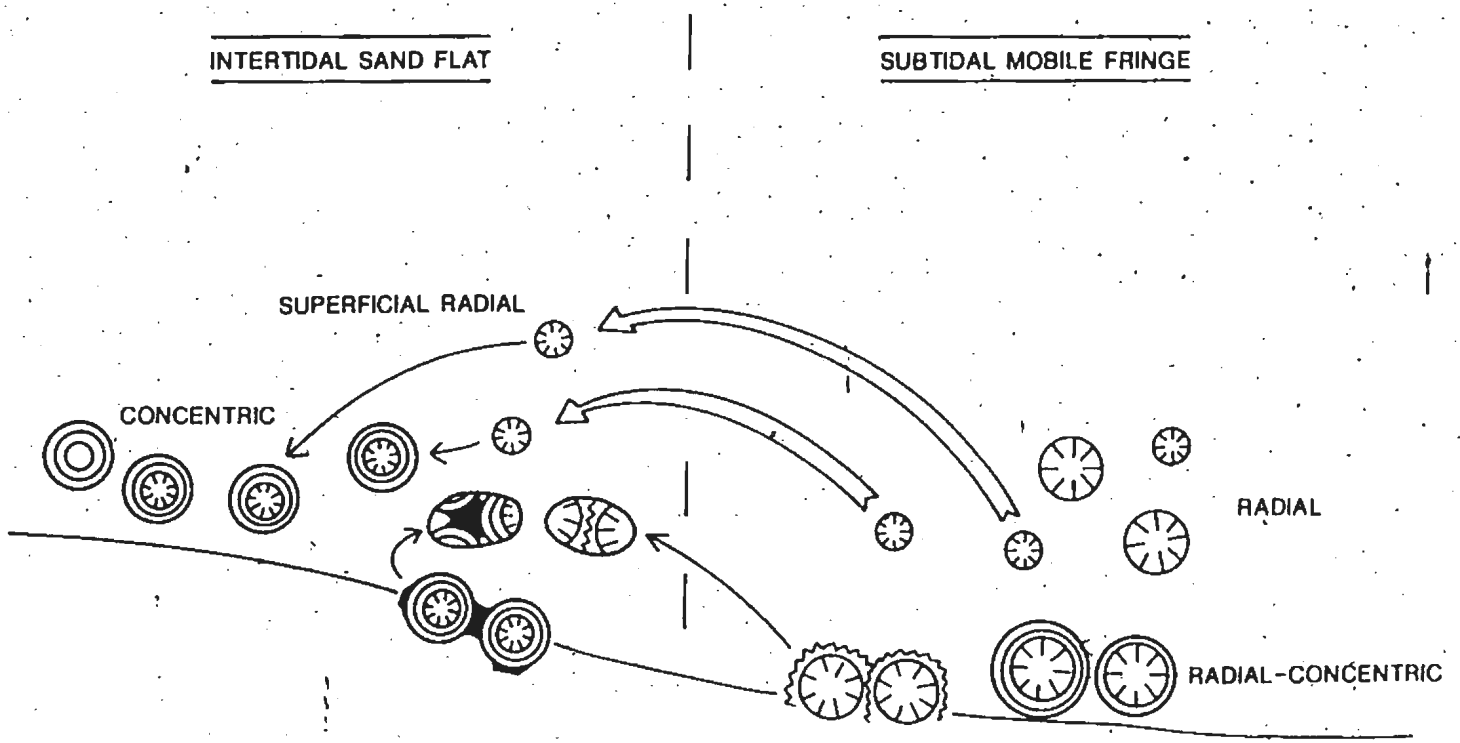
INTERTIDAL SAND FLAT
SUBTIDAL MOBILE FRINGE
SUPERFICIAL RADIAL
CONCENTRIC
RADIAL
RADIAL-CONCENTRIC

of micritic matrix and the size of ooids; (2) the similarity in structure and size between radial ooids and the radial inner cortex of radial-concentric ooids; and (3) the consistent size of the radial inner cortex in all radial-concentric ooids.

Minor occurrences of cerebroid ooids with micritic zones in grey oolite indicate the importance of localized controls on cortex formation. The formation of micritic areas in the cortex has been ascribed to a variety of processes which include: (1) dissolution and precipitation by bacteria (Kahle, 1974); (2) inhibition of ooid growth by microorganisms or lime mud (Richter, 1980; and (3) algal borings (Newell et al., 1960). The variable nature of cerebroid ooids in the Port au Port Group suggests that any one or all of these processes could have been active during ooid generation. The presence of cerebroid ooids, however, in which concave laminae in cone-shaped micritic areas can be traced into radial and radial-concentric areas of the cortex suggests that inhibition of cortex growth, possibly by microorganisms, was important in subtidal ooids.

6.4.2 Intertidal Ooids

Based upon the different types of modern ooids (e.g. Trucial Coast, Loreau and Purser, 1973; Baffin Bay, Land et al., 1979), concentric ooids in brown oolite are interpreted to reflect more turbulent conditions than subtidal grey oolite. The abundance of a lime mud matrix, thin mudcracked beds and the poorly sorted assemblage of grains, however, suggest that high energy conditions (during which ooid growth took place) alternated periodically with lower energy conditions (which

permitted mud deposition). Numerous equivocal mechanisms of cortical accretion have been proposed and are reviewed in Simone (1981).

The two types of concentric ooids, those with peloidal or unidentifiable nuclei and those with an inner cortex which is identical to subtidal radial ooids, indicate two pathways for the growth of concentric ooids. The first type is interpreted to have nucleated, grown and been deposited wholely within the intertidal sand flat, without significant transportation of ooids. The bipartite composition of the second type, in contrast, may reflect changing environmental conditions or the transportation of ooids between environments. The sharp boundary between the inner radial cortex and the outer concentric laminae support the latter interpretation; small radial ooids which formed in the subtidal mobile fringe were swept into the intertidal sand flat where they nucleated the growth of a concentric cortex. The occurrence of superficial radial ooids in brown oolite further suggests that some of these "baby" radial ooids did not undergo further accretion in the sand flat. This interpretation could also be applied to radial-concentric ooids in grey oolite, but the absence of these ooids in intertidal oolites suggests that they formed independently of the above concentric ooids and primarily under subtidal conditions.

6.5 OOID MORPHOLOGY AND MINERALOGY

Ooids of the Port au Port Group are now calcitic and exhibit a range of cortical fabrics. Based upon modern marine ooids, the original

morphology of the ooid cortices may have been: (1) tangential -- concentric laminae of needles or batons arranged tangentially to the nucleus, and laminae of subspherical, anhedral crystals with no discerible preferred orientation (Newell et al., 1960) and/or (2) radial-fibrous — long axes of elongate crystals radially oriented perpendicular to the ooid surface (Rusnak, 1960). Their original mineralogy may have been calcite, magnesium calcite or aragonite.

Cortices of undolomitized concentric and superficial ooids in brown oolite show little variation from the fabrics described earlier in this chapter. In contrast, undolomitized radial and radial-concentric ooids in grey oolite exhibit varying styles and degrees of cortical preservation, which have important implications for original ooid morphology and mineralogy.

6.5.1 Styles Of Preservation of Radial and Radial-Concentric Ooids

Radial ooids and the radial core of radial-concentric ooids exhibit several modes of cortical preservation. On a microscopic scale, two styles are recognized, fine and coarse preservation, which commonly occur within the same grey oolite bed and even within the same thin section. Preservation of the nucleus is dependent upon the type of particle and is unrelated to the preservation style of the cortex. Finely preserved ooids retain excellent fibrous fabrics on the scale of the light microscope and are as described earlier in this chapter. Under the SEM, however, cortices are seen to be composed of equant and elongate, micrometer-size crystallites oriented perpendicular to ooid surfaces, which have many tiny holes and microdolomite.

The style of coarse cortical preservation, in contrast, varies within any given grey oolite bed and within individual ooids (Plate 18a). There are three types of coarsely preserved ooids: sparry radial, radial-blocky, and blocky ooids.

6.5.1.1 Sparry Radial Ooids

Similar to well-preserved radial and radial-concentric ooids, these ooids have dominantly radial cortices but are composed of radially disposed crystals of: (1) rice-shaped calcite, 10-20 μm in size (Plate 18b) and (2) prismatic calcite, commonly twinned, 20 to 50 μm wide with crystal lengths that extend the entire width of the cortex. An intercrystalline matrix of pyrite, clays, and possibly organic material (herein referred to as argillaceous matrix) is poorly developed. Abundant inclusions, present throughout but concentrated near the elongate crystal edges, impart a brownish or cloudy appearance to the cortex, similar to that in finely preserved ooids. Under the SEM, these inclusions are seen to be predominantly holes, representing possible original micropores or removed mineral matter or fluids (Plate 18c). Moderate- and dull-luminescent concentric zones, identical to those observed in well preserved ooids, occur in most sparry radial ooids but are best developed in those with rice-shaped calcite cortices and poorly defined in prismatic calcite cortices (Plate 19b).

6.5.1.2 Radial-Blocky Ooids

This type of ooid encompasses a range of cortical structures that are

composed of two basic fabrics, blocky calcite and radially-disposed calcite (Plate 19a, b). The dull-luminescent blocky calcite tends to be concentrated in the inner part of the cortex and is of very finely to medium crystalline size. It is inclusion-poor with an abundant intercrystalline argillaceous matrix. Crystals increase in size toward the core of the ooid and tend to become more equant and ferroan.

The radial zone, well developed in the outer part of the cortex, is composed of inclusion-rich crystals that vary from fibrous calcite to finely to medium crystalline, rice-shaped and prismatic calcites, as described previously. This zone still retains the distinctive brownish colouration, and relict concentric bands are commonly preserved. The arrangement of an outer zone of radial calcite and an inner zone of blocky calcite is relatively consistent, although there are rare occurrences of blocky calcite and radial calcite in alternating concentric rings or patchy developments of blocky calcite. Ooids which have thick zones of radial calcite have very small cores of fine blocky calcite whereas those with thin radial zones have larger and coarser blocky calcite cores.

6.5.1.3 Blocky Ooids

Ooids with cortices of predominantly equant calcite of finely to coarsely crystalline size are abundant (Plate 20a, c). Blocky calcite is generally restricted to within ooid particles, but crystals cross-cutting ooid boundaries are occasionally present. Crystals characteristically decrease in size away from the core of the ooid, and are inclusion-poor and commonly ferroan. They display dull

luminescence, with occasional CL zoning, and tend to be associated with ferroan dolomite (Plate 20b, c). Crystals are occasionally twinned and have an abundant intercrystalline matrix. Blocky ooids are commonly associated with fractures filled by dull-luminescent blocky calcite; peloidal nuclei in these ooids are occasionally preserved and may be displaced from ooid centers (Plate 20c).

Fabric preservation is generally poor, apart from the retention of grain outlines by aligned inclusions and the frequent preservation of a thin outer rim of radial-fibrous calcite. Rare ooids with good fabric preservation under low magnification but composed of blocky calcite (visible only under crossed polarizers) are present. Relict radial and radial-concentric structures and nuclei in these ooids are preserved as inclusions in the blocky calcite crystals. This degree of preservation has only been found in ooids adjacent to abundant echinoderm particles and syntaxial calcite overgrowths; ooid cortices are partially or completely syntaxial with these bioclasts.

6.5.2 Interpretation of Ooid Structure

Ooids in both brown and grey oolites commonly have cortices which show well preserved radial, concentric or radial-concentric structures. In accord with other studies of ancient ooids (e.g. Sandberg, 1975; Wilkinson and Landing, 1978), the excellent preservation of cortical structures and the similarity with modern marine ooids (refer to Appendix C) suggest that these finely preserved Port au Port ooids have been little altered by diagenesis and so have retained much of their

primary cortical structure. Associated coarsely preserved ooids are interpreted to have originated from the same primary ooids as finely preserved ooids but to have been variably affected by diagenesis.

6.5.2.1 Brown Oolite

Concentric and superficial radial ooids that are not dolomitized or silicified exhibit a relatively consistent style of preservation. Concentric ooids have a cortex of alternating concentric micritic and radial-fibrous laminae that always exhibit fine fabric preservation and thus are interpreted as primary. Laminae of blocky calcite, which never preserve relict structures, are interpreted to be secondary or altered fabrics. Cortices of superficial radial ooids are texturally similar to radial-fibrous laminae in concentric ooids and the cortices of radial ooids in grey oolite, and are also considered to have retained most of their primary fabrics. Radial prismatic crystals that commonly occur in these superficial ooids may have resulted from the coalescence of originally acicular crystals.

Although distorted ooids are not abundant in brown oolite, they are notable for their unusual style of deformation. The "fitted grain texture", formed by concentric ooids plastically flattened parallel to bedding, is interpreted to have resulted from the mechanical compaction of unhardened cortices when early cements and matrix were not abundant; evidence of brittle fracturing of micritic and radial-fibrous laminae is rare. There appear to be two possible explanations: firstly, ooids were precipitated as soft particles and were lithified subsequent to particle compaction and secondly, they were hardened ooids that were altered

during later diagenesis to soft particles that were readily deformed.

No "soft ooids" have been reported in modern oolite environments and even experimentally precipitated ooids have hard cortices (Davies et al., 1978; Ferguson et al., 1978). The lack of a modern analogue does not preclude the possibility of "soft ooids" in the Cambrian. Robinson (1967), however, noted in his study of Recent and Pleistocene oolites from the Bahamas and southern Florida that aragonite ooids take on a soft friable texture when partially altered to calcite. Studies of aragonitic bioclasts (e.g., James, 1974; Pingitore, 1976) have also proposed that alteration to calcite involves an intermediate "chalky" stage (discussed in the following section). Thus it is suggested that the "fitted" concentric ooids of the Port au Port Group may be the products of mechanical compaction of partially dissolved, "chalky" ooids during burial.

6.5.2.2 Grey Oolite

Finely preserved radial, radial-concentric and asymmetrical ooids have retained detailed cortical structures, at least on the scale of the light microscope. As for radial and micritic fabrics in ooids of brown oolite, the preservation of fine fabrics and the similarity with modern radial ooids suggest that the present structure of these ooids in grey oolite is similar, if not identical, to original ooid fabrics. The presence of broken ooids as grain components or as ooid nuclei, which have fracture planes that are parallel to the radial fabric of the cortices, further supports a primary origin for radial coatings (Halley, 1977).

Coarsely preserved sparry radial, radial-blocky, and blocky ooids exhibit a range of cortical fabrics. Poor preservation of cortical structures and the fabric variability indicate that these ooids have been altered. The common retention of gross radial structures in the cortices of coarse-fabric ooids; their similarity in particle size; and close association with finely preserved ooids further suggest that they were derived from the same primary radial and radial-concentric ooids as the well preserved grains. They are not alteration products of ooids that are morphologically and/or mineralogically different. The relict concentric bands and radial structures in these altered ooids further indicate that they are neomorphic products and that wholesale dissolution and precipitation of the ooids generally did not occur. Minor occurrences of half-moon and blocky ooids adjacent to fractures, and CL zoning suggest localized occurrences of late-stage ooid dissolution.

There are several possibilities for the relationship between the various ooid types and their sequence(s) of alteration: (1) ooid diagenesis occurred in a single sequence in which all the previously described types of ooids reflect various stages of alteration; (2) there were several diagenetic pathways that ultimately resulted in the alteration of primary ooid fabrics to blocky calcite; and (3) the finely preserved radial and radial-concentric ooids, and the varieties of coarsely preserved ooids were completely unrelated alteration products. Based upon the above interpretation that finely and coarsely preserved ooids originated from the same type of primary ooid, the latter two cases are improbable. A single alteration sequence that gives rise to

progressively more altered ooid fabrics is the simplest and most feasible explanation.

It is proposed that blocky ooids and finely preserved radial and radial-concentric ooids are the two endmembers of the sequence and that the other coarsely preserved ooids are fossilized intermediate stages. Alteration of predominantly radial fabrics to blocky calcite occurred by: (1) the progressive loss of radial structures, due to aggradation and/or coalescence of acicular crystals, to form sparry radial cortices and (2) the outward development of blocky calcite to form radial-blocky and blocky cortices. Based primarily upon the cortical fabrics of the two endmembers and the assumed loss of radial fabrics with ooid alteration, the postulated diagenetic sequence is given in Figure 6.3. This is an idealized sequence in that all alteration phases are not always present. A systematic variation in ooid preservation styles, either temporally or spacially, has not been discerned.

The variety of ooid fabrics and associated dolomites and calcite cements suggest that ooid alteration was a protracted process, which spanned early and late diagenesis and involved either a single continuous event or multiple stages of alteration. Primary ooids probably stabilized to grains with finely preserved fabrics during shallow burial, prior to dolomitization, grain dissolution, and mechanical compaction. Subsequent modification to coarsely preserved ooids (ultimately blocky ooids) took place during later diagenesis and progressive sediment burial. Crosscutting relationships with early diagenetic dolomite (refer to Chap. 8) suggest that coarsely preserved fabrics were present prior to dolomitization but that some ooid

Figure 6.3: Schematic diagram of the sequence of alteration of primary radial and radial-concentric ooids to blocky ooids during progressive burial of the Port au Port Group.

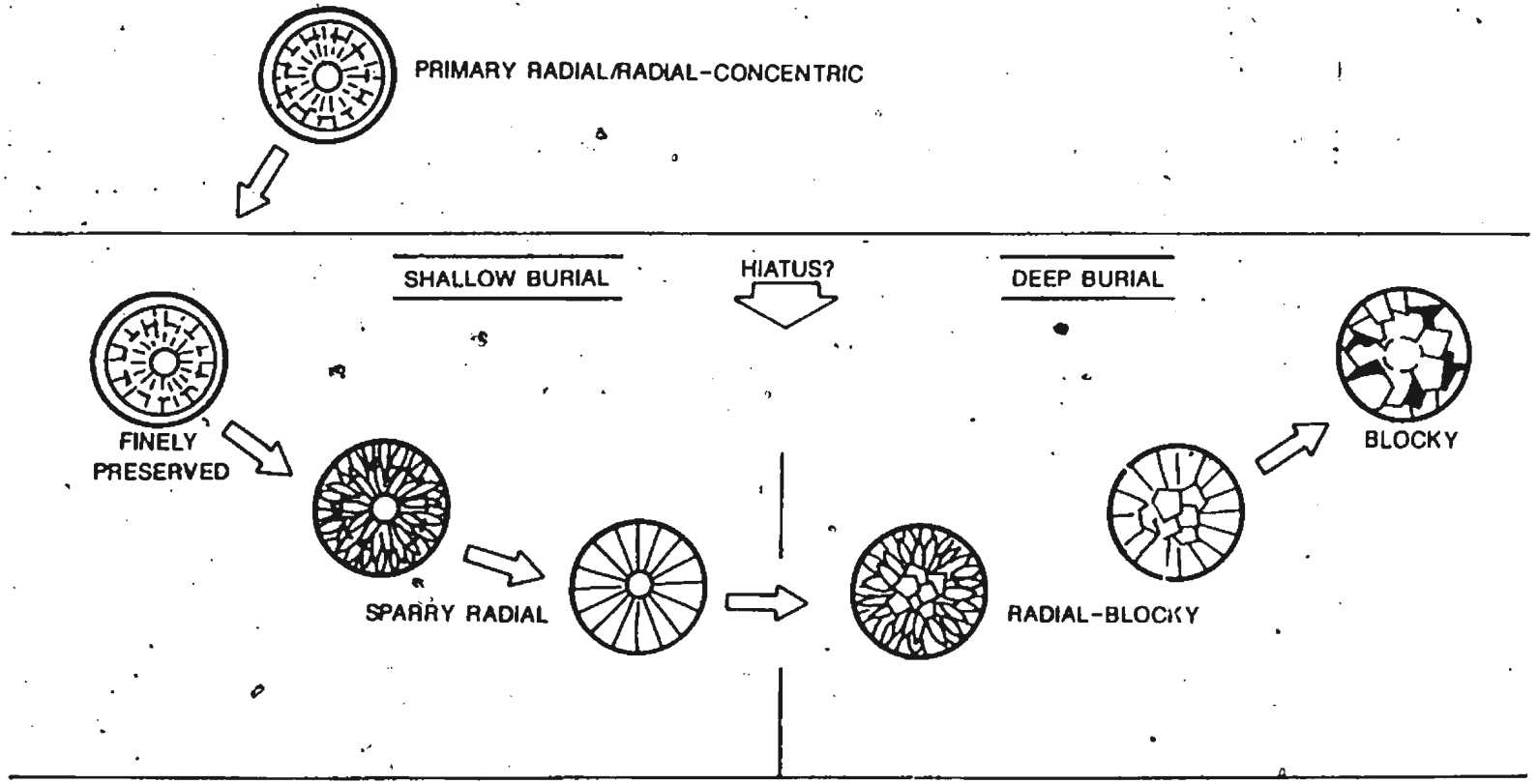
PRIMARY RADIAL/RADIAL-CONCENTRIC
SHALLOW BURIAL
HIATUS?
DEEP BURIAL
FINELY PRESERVED
SPARRY RADIAL
RADIAL-BLOCKY
BLOCKY

alteration took place after dolomitization.

Cathode luminescence data provide evidence, albeit equivocal, supporting the modification of cortices in several stages. Finely preserved radial and radial-concentric ooids, and coarsely preserved sparry radial ooids all have moderate to dull luminescence in concentric zones; a progressive loss of CL zoning occurs from rice-shaped to prismatic calcite cortices. Similarity in luminescence properties suggests that the alteration of finely preserved cortices to sparry radial ones was a gradual process or at least occurred under similar diagenetic conditions.

Blocky calcite in blocky and radial-blocky ooids, however, has uniformly dull luminescence and crosscuts radial structure, suggesting that alteration to blocky calcite was a much later event. Precipitation of this calcite may have been in part concomitant with precipitation of blocky calcite cement, as suggested by: (1) CL of blocky ooids is similar to that of blocky calcite cements, which commonly occlude intergranular and moldic porosity and late fractures, and are interpreted to be precipitated during deep burial (refer to Chap. 5) and (2) the occurrence of blocky ooids adjacent to blocky calcite filled fractures. Rare ooids with prismatic calcite that has bright-luminescent, scalenohedral crystal terminations projecting into adjacent blocky calcite further suggest that some of these blocky calcites may be late stage void-filling cements (Plate 19b).

6.5.3 Interpretation of Ooid Mineralogy

As previously mentioned, ooids on the Port au Port sequence may have originally been aragonite, calcite or Mg calcite or bimineralic. Ooids with radial and radial-concentric cortices in grey oolite and those with concentric and superficial radial cortices in brown oolite commonly show little evidence of extensive alteration. This excellent fabric preservation, in conjunction with the absence of leached ooids or oomoldic porosity, suggests that these ooid cortices were predominantly calcite or magnesium calcite with only minor, if any, aragonitic laminae. Interpretation of radial ooid mineralogies also has application for associated synsedimentary fibrous calcite cements (see Chap. 5).

In addition, studies of biogenic components and their styles of preservation and mineralogy have frequently been applied to the determination of original mineralogies and morphologies of fossil abiotic components. Strict application of biogenic alteration fabrics to ooids poses several problems in the Port au Port Group and warrants further discussion.

6.5.3.1 Application of Bioclast Diagenesis to Ooid Mineralogy

In the Port au Port Group, the main bioclastic components are trilobites, inarticulate brachiopods and echinoderms, and very minor gastropods. The style of preservation in each of these fossil skeletons is relatively constant and is identical to those seen later in the rock

record.

Trilobites. These bioclasts are generally well preserved and are composed of non-ferroan calcite crystals that are oriented perpendicular to the skeletal surface. No extensive neomorphism or dissolution has been observed, indicating that the original mineralogy was either calcite or Mg calcite. As discussed by James and Klappa (1983), some trilobites may have been Mg calcite (Lowenstam, 1963; Teiglar and Towe, 1975; Richter and Fuchtbauer, 1978) and others may have been calcite (Stehli, 1965).

Echinoderms. Only fragments of echinoderms are preserved in the sequence but they are the most abundant bioclasts. Echinoderm particles behave optically as single calcite crystals and have ubiquitous syntaxial overgrowths and intraparticle cements. The calcite is generally non-ferroan but there are occasional ferroan echinoderm clasts with non-ferroan calcite overgrowths.

The fabric and optical properties of these Cambrian echinoderms and overgrowths are consistent with younger examples. Modern echinoderms are Mg calcite (Bathurst, 1975) and studies of Pleistocene examples (Land, 1967; Richter, 1974) provide information regarding their preservation mechanism. Echinoderm fragments, which subsequently lose their magnesium content, undergo gradual calcite cementation of (1) intraparticle pores and (2) the precipitation of progressively thicker rinds of syntaxial calcite; all cements are in optical continuity with the particle. Lowenstam (1963) examined well-preserved Pennsylvanian echinoderms and found they were composed of either calcite or Mg

calcite. James and Klappa (1983) proposed that the mineralogy of extant forms and those as old as Mississippian age strongly argue for Cambrian echinoderms of Mg calcite.

Calcareous brachiopods. Most brachiopod fossils preserved in the Port au Port Group are phosphatic, though calcareous inarticulate brachiopods of inclusion-poor blocky calcite (fine crystalline) do exist. Only gross shell outlines are maintained.

The consistent lack of microstructure suggests that these brachiopod shells were originally aragonite (Williams and Wright, 1970; James and Klappa, 1983). Furthermore, CL and the preservation of shell outlines as inclusions in blocky calcite indicate that neomorphic alteration and/or cementation of dissolution molds by blocky calcite took place, usually within the same bioclast.

Gastropods. Gastropods are found in the upper part of the sequence, particularly in the Man O' War Member of the Petit Jardin Formation. They are composed of finely crystalline blocky calcite which obliterated all original microstructure. Two stages of calcite are developed: an initial stage of non-ferroan calcite and a later (inner) stage of inclusion-rich, ferroan calcite. Similar to brachiopods, consistently poor preservation of gastropod fabrics suggests an original aragonitic composition, and CL zoning indicates that the blocky calcite occluded gastropod molds.

From the above descriptions, it is apparent that the original mineralogy of these bioclasts influenced their present fabrics;

trilobite and echinoderm taxa with preserved microstructure were originally calcitic (most likely Mg-calcite) whereas brachiopod and gastropod debris now of blocky calcite were originally aragonitic. This relationship of shell mineralogy and microstructure preservation appears to apply to most fossil skeletons and provides a criterion for determining the original mineralogy of both biotic and abiotic components (e.g., Sorby, 1879; Sandberg, 1975; James and Klappa, 1983). This is particularly applicable to ooids which originally had a significant organic content (Newall et al., 1960).

Comparison of neomorphic fabrics of Cenozoic ooids and biogenic components with ancient ooids (e.g., Sandberg, 1975; Tucker, 1984; Wilkinson et al., 1984) indicates that diagenesis of aragonite ooids should result in the destruction of fine fabrics whereas calcitic ooids should retain detailed microstructures with diagenesis. Applying this to ooids of the Port au Port Group, radial and superficial radial ooids are interpreted to be originally calcitic (high or low Mg); concentric and radial-concentric ooids are interpreted to have an original bimineralic (aragonite and calcite) composition with a predominance of calcite (high or low Mg).

6.5.3.2 Concentric Ooid Fabrics

Concentric ooids in brown oolite and the concentric rim of radial-concentric ooids in grey oolite have fabrics which suggest a primary two-phase or bimineralic composition. Laminae of well preserved radial-fibrous and micritic calcite were originally calcite (probably Mg calcite). Evidence for this is provided in the following discussion of

"radial ooid fabrics". In contrast, laminae of blocky calcite, which have no microstructure preservation, are interpreted as originally composed of aragonite. Although there is no unequivocal evidence for original aragonite (e.g. aragonite relicts; Sandberg, 1983), the occurrence of distorted ooids (half-moon, elephantine, spalled ooids and lunate laminae) supports this interpretation. It is suggested that these ooids were altered by the dissolution of more soluble aragonite laminae and the collapse or detachment of less soluble calcitic laminae, accompanied by minor compaction (Wilkinson and Landing, 1978; Wilkinson et al., 1984; Wilkinson et al., 1985).

Bimineralic cortices have been recognized in Holocene ooids from Baffin Bay, Texas (Land et al., 1979) and consist of radial Mg calcite coatings and tangential and micritic coatings of aragonite. In addition, synsedimentary cements of coexisting Mg calcite and aragonite have been documented in modern seas (e.g. Land and Moore, 1980) and have been interpreted in studies of ancient carbonates (e.g. Davies, 1977; Sandberg and Popp, 1981).

The transformation of aragonite to calcite is widely considered to occur by an aragonite dissolution-calcite precipitation process of varying scales, which is governed by the rate and amount of water flow (James, 1974; Pingitore, 1976, 1978; James and Choquette, 1984). In the Port au Port Group, ooids with undistorted laminae of blocky calcite occur together with those that have lunate blocky calcite laminae and distorted laminae of fibrous and micritic calcite. This suggests that the alteration of aragonite laminae occurred under variable conditions prior to the mechanical compaction of ooids (ie. during shallow

burial). Two alteration processes appear to be applicable to these ooids:

(1) In ooids unaffected by mechanical compaction or lacking displaced nuclei, aragonite alteration occurred by concomitant aragonite dissolution and calcite precipitation ("neomorphism" of Folk, 1965; Bathurst, 1975; Dickson, 1983). The lack of fabric preservation suggests that this process took place where there was a large volume of fluid phase, such as in the meteoric phreatic zone (Pingitore, 1976; 1982).

(2) In ooids with displaced nuclei or distorted cortices, complete dissolution of the ooid or specific laminae under meteoric conditions created molds which were later occluded by post-mechanical compaction blocky calcite cement (macroscopic alteration; James and Choquette, 1984).

6.5.3.3 Radial and Coarsely Preserved Ooid Fabrics

The highly variable styles of ooid preservation in grey oolite pose problems for the interpretation of original cortical mineralogy. Two possibilities exist: (1) that the different preservation styles indicate different original mineralogies - aragonite, calcite or Mg calcite and (2) that these ooids had cortices of the same original mineralogy but were altered differently.

As previously described, recent studies of ancient ooids have placed much emphasis on the relationship between microstructure preservation and original mineralogy in abiotic and biotic components. Following this thinking, the diverse assemblage of coarsely preserved ooids in

grey oolite of the Port au Port Group should be interpreted as a heterogeneous array of primary aragonite and calcite (high or low Mg) ooids.

A more critical examination of the ooids and consideration of criteria for ancient aragonite and calcite (Sandberg, 1983; James and Klappa, 1983), however, indicate that these ooids contradict current dogma. Evidence provided in the previous section demonstrates that they originally had a common cortical morphology that gave rise to a range of preservation styles. The precipitation and deposition of ooids with identical morphology but differing mineralogy in spacial proximity seems intuitively improbable. Although modern marine ooids with coexisting aragonite and Mg calcite coatings have been documented (Baffin Bay, Texas; Land et al., 1979), no examples of aragonite ooids mixed with calcite or Mg calcite ooids of the same morphology have been reported. Thus finely and coarsely preserved ooids in the Port au Port grey oolites are interpreted to be diagenetic products of ooids with not only the same type of radial and radial-concentric cortex but with the same mineralogy.

Tucker (1984) in his study of mid-Proterozoic ooids in Montana recognized a similar variety of ooid types within the same oolite bed and even within the same thin section. He interpreted, however, those composed of calcite spar, with or without relics of original structure, and columnar calcite as originally aragonite. Ooids with excellent fabric preservation (radial and radial-concentric) were considered to have primary calcitic cortices. Yet in spite of the differences in preservation style, interpreted calcitic and aragonitic ooids are often

strikingly similar, both in size and gross cortical structure. Acceptance of a such a polymineralic interpretation poses problems in explaining the close association of such a variety of mineralogies and diagenetic fabrics. Proposed explanations have included extensive reworking and transport of ooids of different mineralogies, and changes in physical and chemical conditions in the area of ooid formation (Tucker, 1984; Wilkinson et al., 1984). The "monomineralic" interpretation of Port au Port ooids, however, provides a much simpler explanation.

Three possibilities exist as to the original mineralogy of the finely and coarsely preserved ooids: aragonite, Mg calcite and calcite.

Aragonite versus Calcite. In spite of the poor preservation fabrics of many of the ooids, there is no unequivocal evidence for aragonite in grey oolite. Sandberg (1983) summarized criteria for recognition of primary aragonite and ranked them according to their reliability. The presence of aragonite relicts is considered to be the most reliable criterion; coarse calcite mosaics (with or without relict structures) on their own are suspect indicators of aragonite and must be qualified by additional evidence. Radial ooid cortices in grey oolite were probably not aragonite for the following reasons:

(1) No relict aragonite has been found; several thin sections treated with Fiegl stain (e.g. Lasemi and Sandberg, 1984) also did not reveal any aragonite relicts.

(2) The absence of oomolds and deformed radial ooids in grey oolite limestone indicates little wholesale dissolution.

(3). Ooid cortices are in optical continuity with nuclei of originally calcitic trilobites or echinoderms, which indicate that the cortices were not aragonite.

(4) Rare ooids with originally aragonitic nuclei (brachipods and gastropods) still have well preserved cortices whereas the nuclei are now blocky calcite. If the entire ooid was aragonitic then two different preservation styles would not be expected (Sandberg, 1983) or the cortex would at least show partial replacement.

(5) Syntaxial calcite cement forms on echinoderm fragments and ooids. This type of cement has been shown to precipitate on calcitic particles during early meteoric diagenesis (Land, 1967; MacQueen et al., 1974), suggesting that the ooids were not aragonite.

Calcite versus Mg Calcite. Eliminating the possibility of an aragonite mineralogy, ooids and syntaxial fibrous calcite cements (Chap. 5) were either calcite or Mg calcite. The following evidence supports an original Mg-calcite composition:

(1) Radial cortices are partially or completely syntaxial with trilobite and echinoderm nuclei. Strong evidence indicates that these bioclasts were Mg-calcite which supports a similar mineralogy for the ooid cortices.

(2) Microdolomite inclusions are found in ooid cortices (Lohmann and Meyers, 1977).

(3) Stained thin sections indicate that ooid cortices are commonly

ferroan calcite which suggests an original composition of Mg calcite (Richter and Fuchtbauer, 1978).

(4) Port au Port ooids are similar to radial Mg calcite coatings of modern ooids in Baffin Bay, Texas (Land et al., 1979) and relict ooids on the Amazon Shelf (Milliman and Barreto, 1975) and off the Great Barrier Reef (Marshall and Davies, 1975).

Based upon the preceding arguments, the diagenesis of Mg-calcite radial and radial-concentric ooids is interpreted to have resulted in two related styles of preservation: one in which there is excellent preservation of microstructures and the other in which coarse preservation may occasionally retain relict fabrics. This interpretation, however, is contrary to our current understanding of Mg-calcite stabilization. The transformation of Mg calcite to calcite is believed to occur by an incongruent dissolution-precipitation reaction in which there is generally no obvious microscopic fabric change (summarized in James and Choquette, 1984); under the SEM, it is obvious that there is a slight coarsening of crystals (Sandberg, 1975; Towe and Hemleben, 1976). Although the exact nature of Mg calcite alteration is not well known, it has been suggested that dissolution of $MgCO_3$-rich zones occurred first and was accompanied by calcite precipitation that was syntaxial with adjacent calcites (Benson and Matthews, 1971; James and Choquette, 1984).

Recent studies, however, have revealed exceptions to this generalization. Firstly, molds interpreted as resulting from meteoric alteration of Mg calcite particles and cements have been documented

(e.g. Quaternary beachrock, Kenya; Schroeder, 1979). As noted by James and Klappa (1983), alteration of Mg calcite particles under conditions of rapid water flow and continuous undersaturation could result in a loss of structure. Secondly, evidence from foraminifera (Towe and Hemleben, 1976) suggests that the "stable" calcite, formed from the loss of Mg, is further altered during later diagenesis. Several other studies (e.g. Wilkinson et al., 1985; Sandberg, 1983) have noted coarse preservation textures in ooids interpreted to have been originally low magnesium calcite. Figure 6.4 summarizes the possible products of Mg calcite alteration.

Towe and Hemleben (1976) recognized three stages in the meteoric Mg-calcite diagenesis of foraminifera. Stage 1 involved a loss of magnesium to form calcite with no alteration in the fibrous texture. Stage 2 resulted in enlargement of fibrous calcite into a mosaic of equant grains with retention of relict structures; the concomitant disappearance of intercrystalline organic matter may have created sufficient voids for grain growth. Stage 3 involved the development of even coarser crystals that obliterated original structures. These three stages are parallel to the interpreted sequence of ooid alteration in grey oolite in the Port au Port Group. The first stage corresponds to the alteration of primary Mg calcite ooids into finely preserved calcite ooids in which cortical crystallites were morphologically unaltered. The second and third stages correspond to the transformation of the finely preserved ooids into coarsely preserved ooids through the progressive loss of organic material (a loss of the brownish colouration) and radial structure, and the development of progressively

Figure 6.4: Postulated diagenetic pathways for alteration of Mg calcite ooids in the Port au Port Group to: (a) calcite-filled ooid molds; and (b) finely and coarsely preserved ooids.

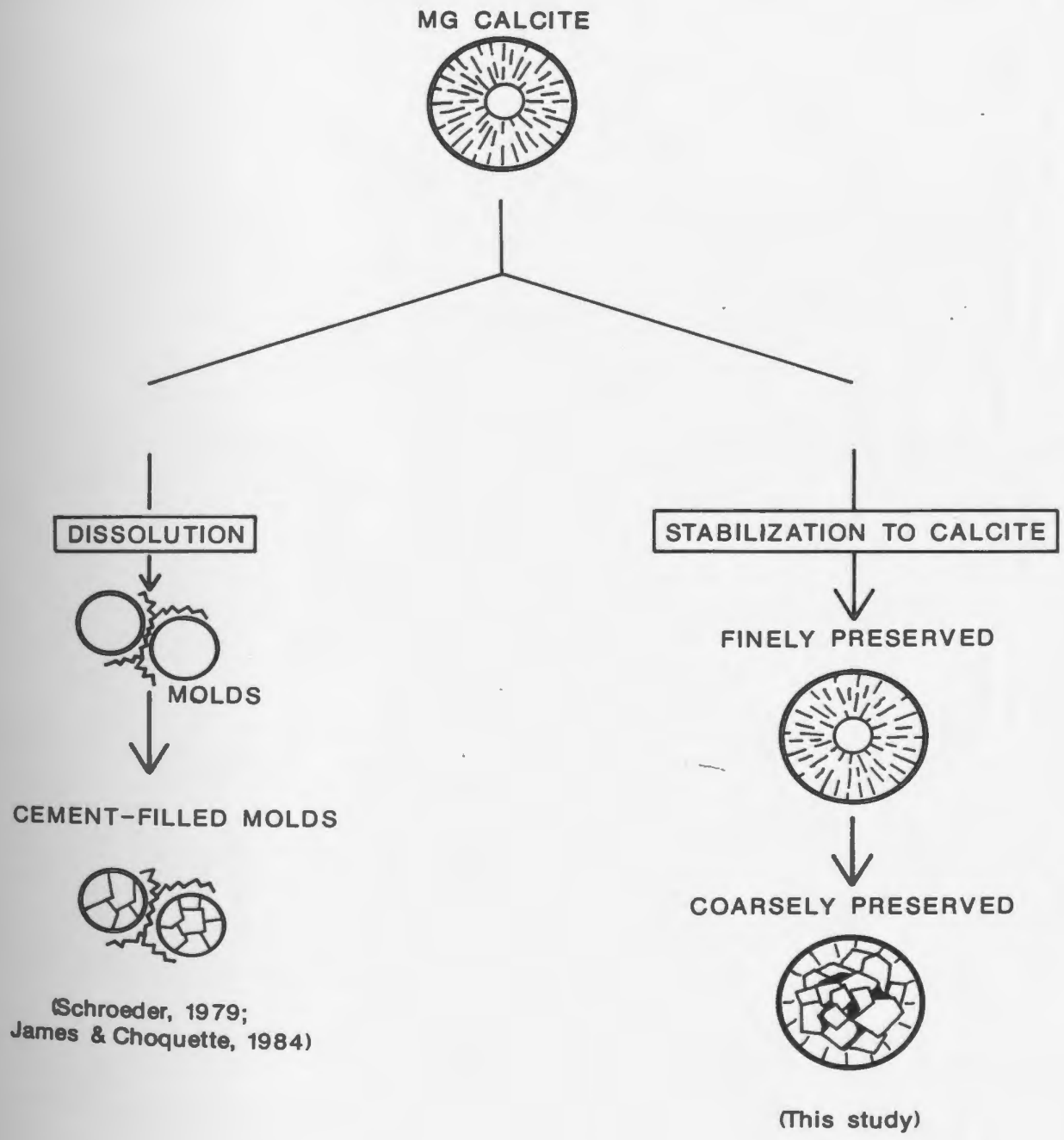
MG CALCITE
DISSOLUTION
MOLDS
CEMENT-FILLED MOLDS
(Schroeder, 1979;
James & Choquette, 1984)
STABILIZATION TO CALCITE
FINELY PRESERVED
COARSELY PRESERVED
(This study)

coarser mosaics of blocky calcite. These last two stages are of particular importance in that they suggest that calcite produced by the loss of magnesium (stage 1) is not necessarily protected from later diagenesis.

Whether the results of such studies of bioclastic components are applicable to abiotic particles, such as ooids, is a matter of contention. Nevertheless they do indicate that current concepts of Mg calcite alteration should be re-evaluated and that Mg calcite has indeed been subjected to diagenetic processes that resulted in varying but related styles of fabric preservation.

6.6 DISCUSSION

In recent years, two problems have received considerable attention: the relationship between ooid precipitation and the depositional environment, and the trend of ooid mineralogies and structures in the rock record.

6.6.1 Environmental Controls

Ancient ooids were formerly considered to have been similar in morphology and mineralogy to the modern tangential ooids developing in Bahamian carbonate shoals. It is now widely recognized that ancient ooids may have formed in a variety of different environments that gave rise to a complex assemblage of cortical fabrics and mineralogies, as are now documented for modern ooids. Due to the poor understanding of

the environmental parameters which influence the precipitation of modern ooids and the uncertainty regarding the effects of diagenesis, difficulties arise in the use of modern oolites as analogues for ancient deposits and the determination of the conditions under which ancient ooids formed.

There appear to be four criteria for natural ooid formation in modern environments (Bathurst, 1975) that probably apply to ancient ooids as well: (1) supersaturation with respect to calcium carbonate; (2) available nuclei; (3) sufficient agitation of grains; and (4) topography that retains grains in the system and offers areas of both high and low energy turbulence. The resulting fabrics and mineralogies are controlled by variations in the physical and/or chemical conditions within the environment of formation. As summarized in several studies and review articles (e.g., Simone, 1981; Wilkinson et al., 1984), numerous environmental factors have been proposed with few conclusive findings being made: (1) seawater chemistry, in particular Mg/Ca ratios; (2) sea floor topography; (3) water turbulence and related flow velocities through interparticle pores; (4) organic matter; (5) temperature; and (6) atmospheric conditions, in particular carbon dioxide levels.

The facies-specific distribution of the different types of ooids in the Port au Port Group supports the interpretation that cortical morphology and mineralogy were strongly controlled by environmental conditions. The intimate association of originally Mg calcite ooids and bimineralic ooids further suggests that widespread chemical conditions, atmospheric and hydrospheric, were not the primary factors governing

ooid formation. Instead, the influence of physical conditions within an environment and between adjacent environments (e.g. turbulence, sea floor topography and water flux) probably prevailed. Physical controls in turn governed such kinetic factors as rates of crystal growth, porosity and permeability of sediments, fluid flow velocities through pores, and fluid shear at crystal growth surfaces (Wilkinson et al., 1984; Given and Wilkinson, 1985). Changes in these kinetic factors created short-lived, mini-environments that permitted variable ooid formation. Over larger areas, however, seawater and atmospheric chemistry may have been important. The effect of organic material also cannot be negated but considerable uncertainty remains as to its importance even in modern ooids (Mitterer, 1968; Suess, 1970; Davies et al., 1978).

Other occurrences of bimineralic ooids have been reported in the rock record (e.g. Pennsylvanian Plattsburg Limestone - Kansas, Mississippian Bangor Limestone - Georgia; Wilkinson et al., 1984) and in a few Holocene environments (Baffin Bay, Texas, Land et al., 1979) in which the importance of local physical conditions on ooid morphology and mineralogy has been emphasized. In many modern examples, however, environmental changes appear to have influenced only the structure of the cortex, leaving the mineralogy unchanged (e.g. tangential and radial aragonite ooids of the Persian Gulf - Loreau and Purser, 1973; normal and superficial Bahamian aragonite ooids - Bathurst, 1975). The perfect correlation between original mineralogy, texture and environment of formation, which has been interpreted for ooids of the Port au Port Group, is absent in these modern ooids. This suggests that

facies-specific, physical controls were of greater importance in the Cambrian and perhaps at other times in the rock record than they are now and that more widespread controls on ooid growth, such as organic substances and chemical variables, prevail in modern environments.

6.6.2 Global Eustasy

Studies of ooid mineralogy have formed much of the foundation for the evaluation of temporal changes in non-skeletal carbonate mineralogy in the geologic record. Sandberg (1975; 1983) and Mackenzie and Pigott (1981) have postulated a cyclical pattern of physicochemical carbonate precipitation for the Phanerozoic, which in spite of the uncertainties in the estimation of global sea levels (e.g., Vail et al., 1977; Hallam, 1977), shows good correlation with trends of global eustasy. Aragonite precipitation dominated during intervals of eustatic sea level lowstand; during eustatic sea level highstands, calcite dominated.

Two factors have been widely proposed to relate global eustasy to ooid mineralogy: atmospheric-hydrospheric carbon dioxide (Mackenzie and Pigott, 1981; Sandberg, 1983) and oceanic Mg/Ca ratios (Folk, 1974a; Sandberg, 1975; Wilkinson, 1979). Available evidence currently favours variations in carbon dioxide levels which fluctuate during periods of submergence and emergence (Sandberg, 1983; Wilkinson et al., 1985). It has been postulated that times of low sea-level result in lower carbon dioxide levels ("icehouse mode"; Fischer, 1981) and promote aragonite and Mg calcite precipitation due to: (1) reduced rates of sea floor spreading and subduction zone metamorphism; (2) increased rates of weathering of carbonates and siliciclastic sediments; and (3) increased

photosynthesis. Periods of elevated sea-level promote higher carbon dioxide levels ("greenhouse mode"; Fischer, 1981) and result in predominantly calcite precipitation due to: (1) increased spreading and subduction zone metamorphism rates; (2) decreased rates of deposition and weathering of continental siliclastic sediments; and (3) increased areas of carbonate precipitation.

The interpretation of ooid and cement mineralogy in the Port au Port Group is in agreement with the proposed eustasy-ooid mineralogy trend discussed above. The Mg calcite and aragonite components of this Middle and Upper Cambrian sequence formed during an interval of progressive sea-level rise that culminated in the Silurian-Devonian (Vail et al., 1977). As discussed by James and Klappa (1983), much of the Cambrian succession could be interpreted as the transition phase between Precambrian carbonates (now predominantly dolomite) and middle Paleozoic carbonates precipitated (as mainly calcite?) during high-stand conditions.

6.7 SUMMARY

Detailed petrographic and CL study of oolites of the Port au Port Group reveals four types of facies-specific ooids which represent deposition in carbonate sand shoal complexes. Radial and radial-concentric ooids in grey oolite are interpreted to have been precipitated and deposited in a subtidal mobile fringe. Ooid size and the nature of grain transport (suspension versus bedload transport) were

probably the main factors determining the morphology of these ooids. Concentric and superficial radial ooids in brown oolite were precipitated and deposited in an intertidal sand flat. Radial ooids transported from the mobile fringe were also important constituents in the sand flat.

Concentric ooids and concentric laminae in radial-concentric ooids are interpreted to have originally had a bimineralic composition. Aragonitic laminae are now blocky calcite whereas laminae of fibrous and micritic Mg calcite are well preserved as calcite. Radial ooids and radial inner cortices of radial-concentric ooids, in contrast, are interpreted to have originally been Mg calcite and to have progressively altered to a variety of preservation styles. Mg calcite ooids were altered to radial calcite during shallow burial which in turn underwent further diagenesis with deeper burial. This interpretation disagrees with current dogma regarding calcite and aragonite diagenesis and suggests that the criterion commonly used to determine original mineralogy, ie. fabric preservation, may be misleading. The results of this study suggest that re-evaluation of other ooids in the rock record is in order and that the use of more unequivocal evidence for original aragonite or calcite (e.g. Sandberg, 1983) be promoted.

The correlation between ooid mineralogy and morphology and the interpreted environment of formation in the Port au Port Group indicates the importance of local environmental conditions on ooid formation, particularly physical factors such as turbulence and sea floor topography. These local conditions are ultimately governed by global eustasy that effects secular changes in carbonate precipitation, as

suggested by global eustasy-ooid mineralogy trends.

Chapter 7

ORIGIN OF PARTED LIMESTONES

7.1 INTRODUCTION

The parted limestones described in Chapter 3 are interpreted to be the deposits of a muddy tidal flat. Field observations indicate that these mixed carbonate-siliciclastic sediments have been variably affected by early lithification (numerous clasts and hardgrounds); mechanical compaction (fracturing, and compacted mudcracks and burrows); and chemical compaction (stylolites). The fabric-specific nature of many diagenetic features further indicates that diagenesis has only modified and enhanced original sedimentary structures of heterogeneous composition and texture (Table 7.1).

This chapter integrates field, polished slab, petrographic and cathode luminescence observations to assess the nature of lithification and compaction in parted limestones. From this data, a model is developed to explain the origin of parted limestones on the Port au Port Peninsula which has application to parted limestones present elsewhere in the rock record.

TABLE 7.1: COMPONENTS OF PARTED LIMESTONE

	LIMESTONE	ARGILLACEOUS DOLOSTONE
Lithologies		
	-silty mudstone and bioclastic wackestone; punctuated by flat-pebble conglomerates and bioclastic calcarenites	-argillaceous dolostone to dolomitic shale
Geometry and Thickness		
	-continuous and discontinuous beds -layers of nodules of cm-scale	-sub-continuous thin beds to partings drape over limestone beds and nodules
Bedding Structures		
	-ripple laminations, mudcracks, gutter casts, load structures runzelmarken, skip, and bounce marks, trace fossils	-compacted mudcracks and burrows -wavy laminations
Biota		
	-trilobites, echinoderms, phosphatic brachiopods	-minor trilobite fragments
Diagenesis		
	-precompaction lithification (synsedimentary and post-depositional) -hardgrounds, minor surface paleokarst -brittle deformation -pressure solution	-syn- and post-compaction lithification -dolomitization and dolomite cementation -squashing of poorly lithified sediment -pressure solution

7.2 PETROGRAPHY

The basic unit of parted limestone is the limestone-argillaceous dolostone or shale couplet. The following discussion is based primarily on type 1 parted limestones (limestone and argillaceous dolostone; see Chap. 3). These are volumetrically more important than type 2 (limestone and dolostone with grey shale; see Chap. 3) and are also the most variable in terms of composition and texture.

7.2.1 Limestones

Limestone beds and nodules are predominantly mudstone (including wackestone), consisting of micrite, microspar and pseudospar (Plate 22b; 24b). Carbonate grains include trilobite, echinoderm and inarticulate brachiopod fragments, peloids, intraclasts and radial ooids (grey oolite type). Silt-size quartz and feldspar are ubiquitous; while glauconite, ferroan dolomite and laths of mica are minor components. Horizontal clay-rich stringers with minor silt-size bioclasts and siliciclastic grains and ferroan dolomite are abundant and vary from less than 1 mm to 5 mm in thickness.

Distinctive V-shaped fractures may occur at the upper and/or lower surfaces of limestone beds, nodules or clasts (Plate 22f; 26b). Fractures are vertically to steeply inclined and are occluded by medium to coarse crystalline, non-ferroan blocky calcite and minor ferroan and non-ferroan dolomite. Some fractures are partially filled with argillaceous dolostone that is identical to interbedded argillaceous dolostone beds or partings. These fractures are best developed in

limestone that overlies irregularly shaped, limestone beds and nodules. Other thinner fractures filled with similar blocky calcite cut both limestone and argillaceous dolostone microfacies.

Two types of mudstone are recognized: (1) "homogeneous mudstone" and (2) "marginally-aggraded mudstone". These terms have been previously used by Coniglio (1985) to describe similar fabrics in deep-water ribbon and parted limestones of the Cambro-Ordovician Cow Head Group in western Newfoundland. Both types occur in beds and nodules, but only homogeneous mudstone occurs in conglomerate clasts.

7.2.1.1 Homogeneous Mudstone

Composed predominantly of ferroan or non-ferroan micrite, microspar (10-15 μm size crystals) and rare pseudospar (50-60 μm size crystals), these mudstones lack systematic changes in neospar fabric or composition. Coarser crystals are subhedral to anhedral and irregularly shaped with few inclusions. An intercrystalline matrix of clays(?) and organic matter(?) is obvious in pseudospar mosaics and individual crystals may be isolated from their neighbours. Patches of pseudospar, roughly circular in cross section and up to 2.5 mm in diameter, and pseudospar haloes around patches of ferroan dolomite are sporadically scattered throughout mudstones.

Mudstone present below surfaces interpreted to be hardgrounds, and mudstone and wackestone clasts in flat-pebble conglomerates are composed primarily of micrite and microspar (5-10 μm).

7.2.1.2 Marginally-Aggraded Mudstone

This type of mudstone is composed of neospar that is petrographically identical to homogeneous mudstone but is characterized by a gradual coarsening of micrite to microspar (commonly 10-15 μm size crystals) and rarely to pseudospar (up to 50-60 μm crystal size) toward the margins of mudstone beds and nodules (Plate 22b-f). This aggradation is accompanied by an increase in crystal spacing and in the amount of intercrystalline matrix; pseudospar crystals occasionally float in the matrix. Iron content in the calcite tends to increase overall in the coarser mosaic, but the most ferroan neospar occurs in millimeter thin bands that are parallel to and 1-2 mm from the margin (see description of cathode luminescence). Aggraded margins may occur at upper and lower bed boundaries, and concentrically around nodules. They are never seen in mudstone clasts in flat-pebble conglomerates. Aggrading neospar is also well developed in bioturbated mudstone where micrite and microspar coarsen toward dolomitized burrows to form pseudospar haloes, up to 1.5 mm wide (Plate 22a).

7.2.2 Argillaceous Dolostone Partings

This microfacies occurs interbedded with the above limestone beds, as horizontal and vertical partings, and irregular patches within the limestone beds and nodules, and as an internodular "matrix" in horizons of limestone nodules (Plate 22b; 23a). Two intergradational endmembers are recognized: (1) fine to medium crystalline, ferroan dolomite with an intercrystalline matrix of undetermined composition (possibly clay and/or organic material) is most prominantly developed in the

internodular matrix and (2) shale, with scattered rhombs of ferroan dolomite, is common to argillaceous interbeds. Quartz and feldspar silt are abundant, commonly concentrated in laminations, but dolostone without silt is also present. Silt-size opaques (probably pyrite), mica laths and glauconite are minor components and elongate grains tend to parallel bedding. Horizontally anastomosing partings of clay and other insoluble grains are present throughout. These argillaceous dolostone partings are compositionally similar to the matrix of flat-pebble conglomerates interbedded with parted limestones.

7.2.3 Lithologic Boundaries

The transition between limestone beds and nodules and argillaceous dolostone occurs over a distance of millimeters. At limestone margins, the proportion of neospar crystals rapidly decreases and scattered dolomite rhombs occur (Plate 25c); coarsening of neospar may or may not occur. Horizontal boundaries are either: (1) depositional or (2) diagenetic consisting of clay- and silt-rich seams or stylolites with accumulations of insoluble material. Lateral transitions between mudstone nodules (sedimentary, ambient and blocky varieties) and internodular dolostone generally lack the above diagenetic contacts, although rare microstylolite swarms are present.

Distinct changes in bedding structures commonly coincide with the lithologic changes, particularly at horizontal boundaries. Notable exceptions are limestone beds and nodules that contain dolostone, where the limestone-dolostone transition clearly cuts across sedimentary structures (Plate 26a, d).

7.2.4 Types Of Limestone Nodules

Five varieties of limestone nodules of centimeter-scale size which commonly occur in close vertical association, are recognized (Fig. 7.1): (1) sedimentary nodules (types 1 and 2); (2) mudstone nodules; (3) blocky nodules; and (4) fitted nodules. Lateral variations in nodule character are rare on the scale of an outcrop (hundreds of meters), and sedimentary and blocky nodules are volumetrically the most important types.

7.2.4.1 Sedimentary Nodules (Type 1)

Lenticular nodules in a matrix of shale or argillaceous dolostone include a variety of sedimentary structures (e.g. ripple laminations; ripple forms; gutter casts; and load structures -- Plate 1c; 23a). Laminations are not traceable into the laterally adjacent argillaceous matrix.

7.2.4.2 Sedimentary Nodules (Type 2)

These nodules have an obvious core consisting of burrows (Plate 23d), mudcracks (Plate 25a, b) or laminations of silt- and sand-size grainstone and siliciclastic siltstone. This type of nodule is distinct from type 1 sedimentary nodules because laminations may be traced into the adjacent dolomitic matrix and correlated between adjacent limestone nodules. Laminations in the nodules rarely converge at the margins even when the nodules thin laterally into clay-rich stringers (Plate 25e).

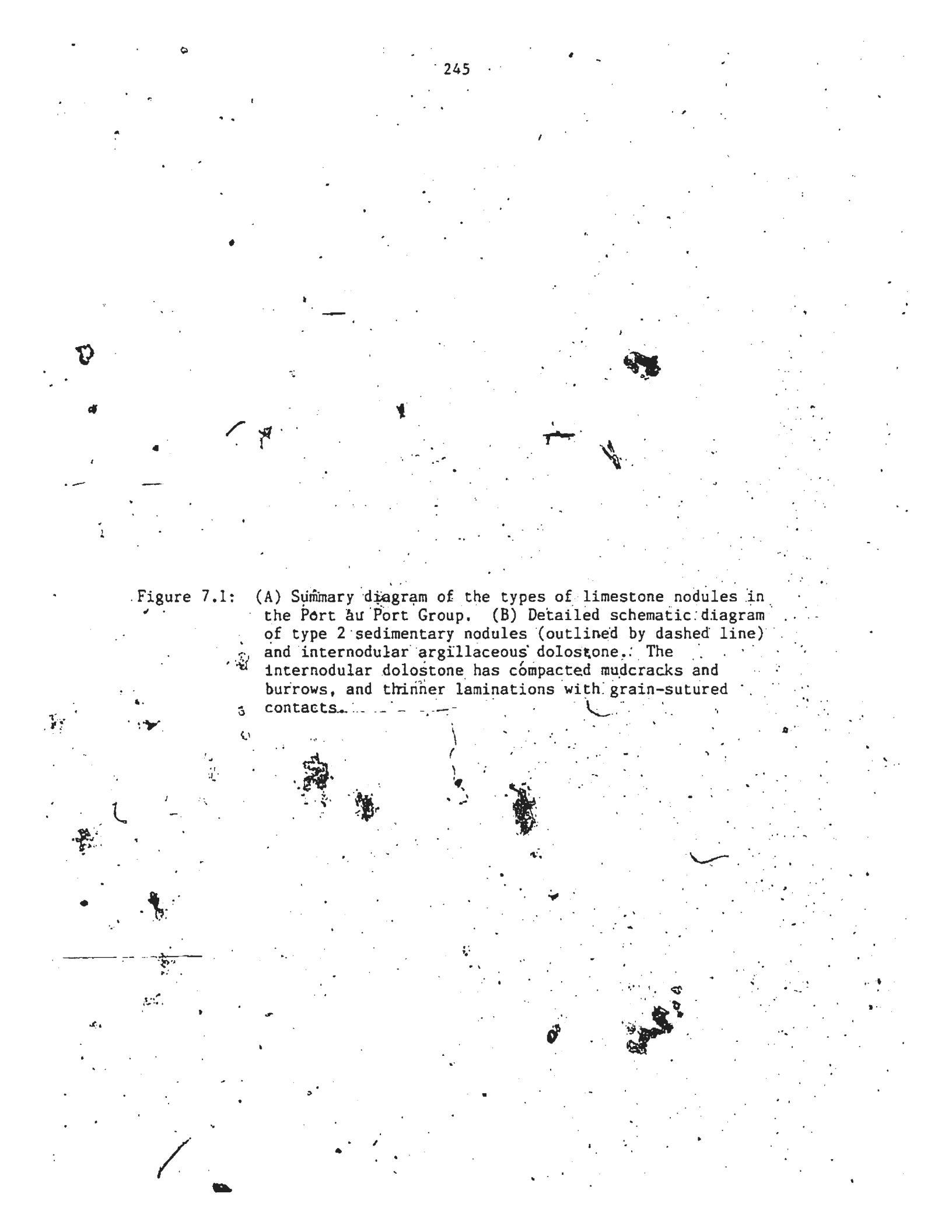

Figure 7.1: (A) Summary diagram of the types of limestone nodules in the Port au Port Group. (B) Detailed schematic diagram of type 2 sedimentary nodules (outlined by dashed line) and internodular argillaceous dolostone. The internodular dolostone has compacted mudcracks and burrows, and thinner laminations with grain-sutured contacts.

LIMESTONE NODULES

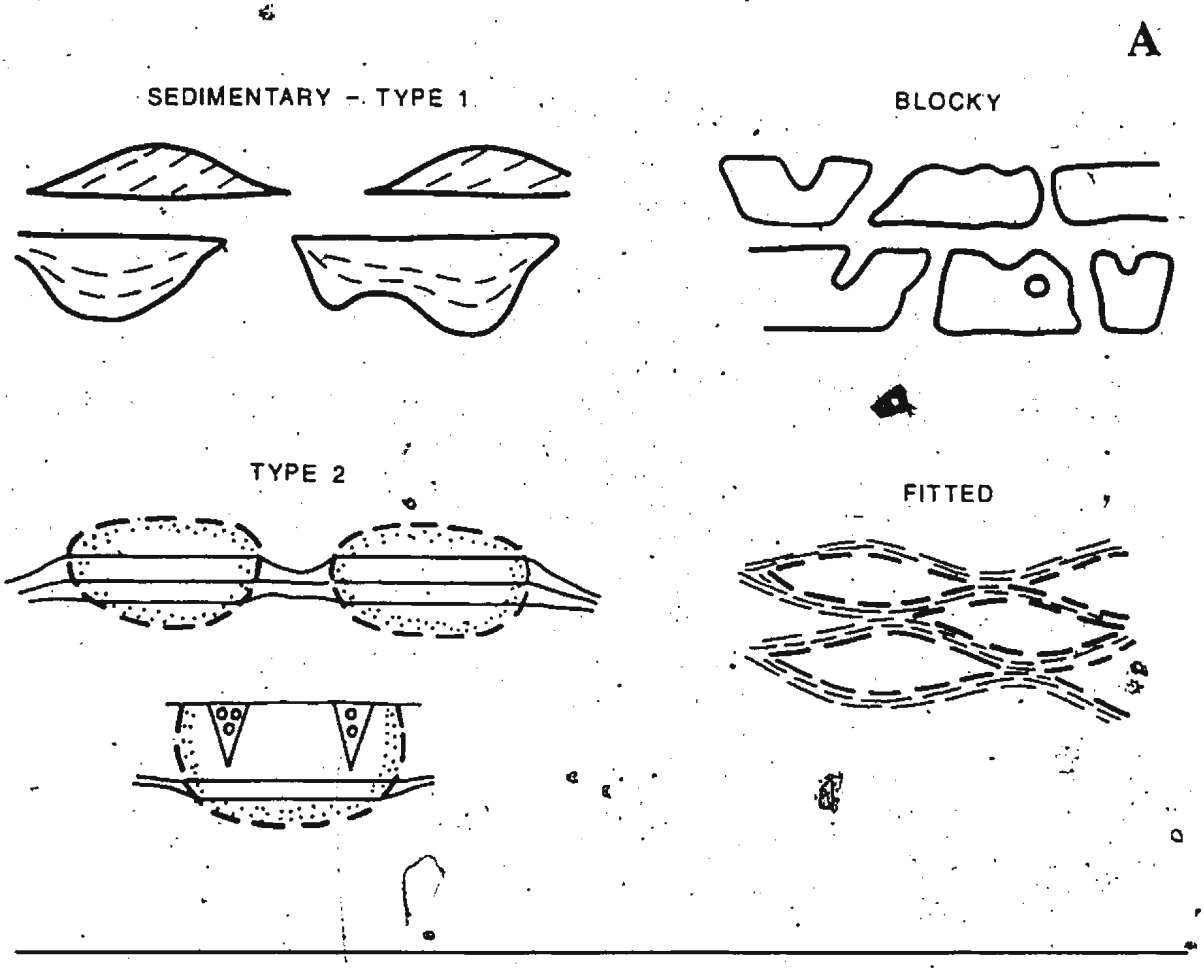

Grainy parted limestones of the Campbells Member of the Petit Jardin Formation contain particularly good examples of type 2 sedimentary nodules. Mudstone nodules contain oolitic and quartz sand-rich laminae that are readily traced into an "internodular matrix" of finely crystalline, ferroan dolostone (Plate 23b, c). The transition between laterally adjacent limestone and dolostone involves: (1) the rapid transition of mudstone into dolostone across an aggraded mudstone margin, accompanied by thinning of the dolostone and warping of underlying and overlying arenaceous beds and (2) oolitic laminae pass into dolostone where they thin and contain ferroan dolomite, corroded calcareous and siliciclastic grains, sutured grain contacts and microstylolites (Plate 25c, d).

Included in this group are amoeboid mudstone nodules that contain highly contorted silt laminations. These nodules are present in a matrix of silty, argillaceous dolostone with similarly distorted laminations.

7.2.4.3 Mudstone Nodules

These nodules are similar in shape to type 2 sedimentary nodules but lack obvious sedimentary structures. The mudstone is homogeneous and nodule margins are diffuse.

7.2.4.4 Blocky Nodules

In cross section, these equidimensional to horizontally elongate, rectangular-shaped nodules contain sedimentary structures that are

identical to those in continuous limestone beds (Plate 24a). Nodule margins commonly have micropits (1-5 mm deep) which in plan view are seen to be distinct dolomitized burrows (Plate 1e). Some nodules grade laterally into continuous limestone beds that have been fractured and slightly displaced.

7.2.4.5 Fitted Nodules

Millimeter- to centimeter-size, lense-shaped clots of limestone are arranged in a closely packed mosaic (Plate 24c; 27a). Clots are separated by thin, undulating argillaceous stringers containing scattered siliciclastic silt and opaque grains, and rare dolomite. Fitted nodules may grade vertically into laterally continuous limestone beds with horizontal argillaceous seams. Similar lateral variations have not been observed on an outcrop scale.

7.2.5 Trace Fossils

Abundant trace fossils are present in parted limestones, occurring in both limestones and argillaceous dolostone partings. Three varieties are recognized (Richards, 1984): (1) vertical burrows which include Skolithos and Monocraterion; (2) horizontal burrows such as Palaeophycus and Planolites; and (3) surface traces such as Monomorphichnus. Vertical burrows in argillaceous dolostone are clearly compacted; those in limestone are undeformed (Plate 23c; 25f).

Undolomitized burrows in cross section are circular structures containing microspar with minor silt, dolomite and opaque grains; they

may be partially occluded by prismatic or blocky calcite cements (Plate 10c). Occasionally present are burrows with microspar margins, up to 0.5 mm wide, and cores of pseudospar. Burrows in limestone may be subtly expressed, recognizable in some cases only by slight variations in sediment composition, such as an increase in the amount of siliciclastic silt or carbonate grains.

Burrows may also be completely replaced by ferroan dolomite identical to that in internodular argillaceous dolostone (refer to following section on "dolomite"; Plate 22a). These burrows are readily identifiable by their distinctive tan-coloured weathering.

7.3 INTERPRETATION

Field evidence presented and extensively discussed in Chapter 3 indicates that the limestone-argillaceous dolostone couplet is of primary depositional origin. Limestone beds are interpreted to have been deposited as rippled, fine carbonate sand and silt during periods of ebb- and flood-tide. These beds alternate rhythmically with organic-rich, siliciclastic and carbonate mudstone that is interpreted to have originally been: (1) mud that settled out of suspension during slack tide and/or (2) peloids that were deposited with weakening tidal currents.

Parted limestones with nodular fabrics in the Port au Port Group are in close vertical association with those containing more continuous limestone beds. Textural and compositional similarities between

limestone nodules and beds indicate that they are genetically related. There are several possible mechanisms for the formation of nodules: (1) laterally discontinuous primary sedimentary structures (isolated ripples; gutter casts); (2) disruption of bedding by synsedimentary process (e.g. loading; bioturbation); (3) pressure solution (e.g. Logan and Semeniuk, 1976; Wanless, 1979); and (4) local lithification (ie. concretion formation) of carbonate-rich sediment (e.g. Coniglio, 1985 and references cited therein).

Based upon field evidence, type 1 sedimentary nodules, with their distinct sedimentary structures are interpreted to be the result of primary depositional processes, such as soft-sediment loading and sediment transport. The abundance of burrows in this type of nodule and in the blocky nodules suggest that bioturbation is responsible for: (1) the chaotic fabric in both the nodules and matrix; (2) pitted surfaces of blocky nodules; and (3) disruption of continuous beds to form blocky nodules. Type 2 sedimentary nodules, whose margins crosscut laminations, and mudstone and fitted nodules, which lack obvious sedimentary structures, are interpreted to be mostly diagenetic in origin. These secondary nodules are discussed in the following sections.

7.4 DIAGENETIC FABRICS

Parted limestones have been modified by three major diagenetic processes which in the order of occurrence and importance are: (1) early

limestone lithification; (2) mechanical compaction; and (3) chemical compaction. Limestone and argillaceous dolostone exhibit distinct fabrics in response to these processes. Dolomitization, on the other hand, is of secondary importance because it appears to be governed primarily by pre-existing depositional and early lithification fabrics.

7.4.1 Limestone Lithification

7.4.1.1 Physical Evidence

The occurrence of uncompacted mudcracks and uncompacted burrows in limestones imply that limestone lithification occurred prior to extensive mechanical compaction (ie. during shallow burial conditions). The following observations also support this interpretation but are more equivocal: (1) laminations in limestone nodules do not converge at the nodule margins; (2) grainy sediment laminations in limestones have normal grain packing fabrics; and (3) mudstone layers are thicker than laterally equivalent argillaceous dolostone. The occurrence of structurally resistant limestone nodules (e.g. limestone haloes enclosing uncompacted mudcracks) in otherwise dolomitized and deformed beds further suggests that limestone lithification was occasionally localized.

Additional evidence indicates that some of this pre-compaction lithification of limestones occurred syndepositionally and resulted in the early formation of well lithified, structurally resistant beds and nodules on the sea-floor (refer to Chap. 5):

(1) Flat-pebble conglomerates with clasts identical in composition to underlying and adjacent limestone beds and nodules are present throughout parted limestone lithofacies. Argillaceous dolostone or shale clasts are absent.

(2) Flat-pebble conglomerates and the few calcarenites interbedded with parted limestone are partly cemented by fibrous calcite cement that is interpreted to be of synsedimentary marine origin.

(3) Rare deep cracks and pits with oversteepened sides, interpreted as karst features, are present in parted limestone.

(4) Horizons interpreted as hardgrounds have only been recognized in limestone beds.

7.4.1.2 Components of Limestone Lithification

The occurrence of coarse homogeneous mudstone and marginally aggraded mudstone in limestone beds and nodules, and their absence in conglomerates and hardground horizons suggest that limestone lithification was not completely synsedimentary. Limestone lithification apparently continued during shallow burial and may have been in part synchronous with mechanical compaction.

In limestone beds and nodules of the Port au Port Group, homogeneous mudstones with micrite to fine microspar mosaics are compositionally similar to mudstone clasts in flat-pebble conglomerates and hardground horizons. These homogeneous mudstones are interpreted to have been similarly subjected to synsedimentary lithification which sufficiently

reduced porosity and permeability to inhibit subsequent lithification. Sediment that is now coarser microspar and pseudospar in homogeneous mudstones is interpreted to have been only partially affected by synsedimentary lithification so that it was susceptible to post-sedimentary (shallow burial) lithification.

Applying the same reasoning to marginally aggraded mudstones, it is suggested that the cores of beds and nodules that are now micrite and fine microspar were lithified early. Structures such as burrows; mudcracks filled with coarse sediment and grainstone dikes (e.g. type 2 sedimentary nodules); or microscopic carbonate grains may have provided preferential sites of nucleation. In contrast, coarser microspar and pseudospar at bed and nodule boundaries formed during shallow burial lithification, nucleating on already consolidated sediment. Lithification progressed in an outward direction and would have been limited only by such factors as the porosity and permeability of adjacent argillaceous beds, the supply of calcium carbonate, and the availability of suitable nuclei.

These mudstones share many petrographic and CL similarities with mudstones in parted and ribbon limestones of the Cow Head Group. Mudstones examined in this study, however, do not have abundant coarse pseudospar (100-300 μm crystal size) as is present in the Cow Head Group (Coniglio, 1985), and contain abundant evidence for synsedimentary sea floor lithification that is not present in the Cow Head Group. Based upon field evidence, standard and CL petrography, and isotopic data, Coniglio (1985) similarly interpreted microspar and pseudospar to be the result of early, shallow-burial lithification.

7.4.1.3 Implications for Aggrading Neomorphism

Considerations of marginally aggraded mudstones in parted limestones have important implications for aggrading neomorphism in carbonates. As defined by Folk (1965) and extensively discussed in Coniglio (1985), this type of neomorphism involves the recrystallization of small crystals into coarser neospar by either coalescive or porphyroid neomorphism. Both processes result in the cannibalization and replacement of finer crystals.

Study of mudstones in the Cow Head Group by Coniglio (1985), however, indicates that these cannibilizing processes cannot be applied in the interpretation of all mudstones. Marginally aggraded neospar was interpreted by him to be the product of constructional aggrading neomorphism during shallow burial, based upon petrography, CL and stable isotopes. Petrographic and CL similarities between Cow Head mudstones and those of the Port au Port Group suggest that his interpretation of aggrading neomorphism may be applied to the Port au Port Group.

The following observations, obtained from CL microstratigraphy of marginally aggrading mudstones in the Port au Port Group (Plate 22c-f), in conjunction with interpretations from Coniglio (1985) suggest that aggrading neomorphism involved the marginal precipitation of calcite into micropores: (1) formation of neospar developed progressively marginward; (2) growth of marginal crystals occurred by the accretion of younger calcite preferentially on the marginward side of crystals (cf. Coniglio, 1985, Plate 35e); (3) smaller crystals in the cores of

mudstone beds and nodules are not cannibalized in the formation of larger marginal crystals (cf. Coniglio, 1985, Plate 35e); and (4) these smaller crystals also occur at the margin and are nuclei for coarser crystal growth. This interpretation of neospar formation is not aggrading neomorphism, as strictly defined by Folk (1965), as there is no evidence of crystal replacement or corrosion. Neomorphism in Port au Port mudstones resulted in synsedimentary and shallow burial lithification. The abundance and close packing of carbonate nuclei in mudstone layers probably prevented large crystal growth because of interference from adjacent crystals.

7.4.2 Dolomitization

7.4.2.1 Petrography

Finely crystalline, ferroan dolomite is a ubiquitous component of argillaceous beds and partings, burrows, internodular matrix and pressure solution seams. Dolomite also occurs as disseminated rhombs in limestone beds and nodules, and in blocky calcite-filled fractures (refer to Chap. 8; Plate 22f; 27d).

Dolomite rhombs are characterized by turbid, inclusion-rich cores and relatively inclusion-free rims, and in suitably thin thin-sections are observed to have curved crystal faces. The cores are brightly luminescent whereas the rims, usually ferroan, are non-luminescent (Plate 22d-f). Rhombs in internodular matrix adjacent to nodule margins, and in burrows and fractures in limestone are up to 250 μm in size and have non-luminescent rims that are 50-100 μm in width. Rhombs in the

central areas of internodular matrix and in argillaceous dolostone partings tend to be finer crystalline (50-100 μm in size) with narrower non-luminescent rims. In mudstones, dolomite rhombs may poikilotopically enclose neospar crystals or have serrated, presumably corroded, boundaries when adjacent to coarse neospar (Plate 29e).

7.4.2:2 Interpretation

The abundance of dolomite mosaics that crosscut primary depositional structures, (e.g. type 2 sedimentary nodules; limestone beds that contain irregular zones of dolomite) suggests that the distribution of dolomite was controlled in large part by diagenetic processes. Early limestone lithification, which occludes much of the original porosity in limestones, appears to be the most important factor. The paucity of dolomite within limestones relative to argillaceous sediments implies that: (1) dolomitization generally succeeded limestone lithification and (2) only poorly lithified, argillaceous sediments were susceptible to dolomitization. The corrosion of rhombs by coarse neospar in limestones, however, indicates that some dolomitization terminated prior to the latest event of limestone lithification. Mechanical and chemical compaction also affected dolomitization and is discussed in the following section on "burial compaction".

Following from the interpretation that dolomite formed preferentially in poorly lithified, argillaceous sediment, it is reasonable to suggest that this "dolomitization" may have involved the precipitation of dolomite cement into micropores, rather than the alteration of calcareous particles. This is further supported by: (1) the

preservation of calcareous grains, such as ooids and (2) the absence of recognizable nuclei in rhombs. The extent of rhomb growth was probably limited by the reduction in porosity and permeability due to compaction and dolomitization.

7.4.3 Burial Compaction

7.4.3.1 Current Understanding

Various workers such as Shinn et al. (1977), Pratt (1982), Shinn and Robbin (1983) have proposed that limestones undergo significant mechanical compaction during burial. The recognition of mechanical compaction is usually based on such criteria as grain breakage, grain rotation and plastic bending (e.g. Shinn et al., 1977; Meyers, 1980; Bathurst, 1980b). Also included are telescoping of burrows and mudcracks, and subtle features such as "stylolite-like" stringers and flattening of peloids and fenestrae.

Other workers (e.g. Stockdale, 1922; Logan and Semeniuk, 1976; Wanless, 1979, 1983; Buxton and Sibley, 1981) have supported the importance of post-lithification dissolution of limestones. Stylolites and grain contact suturing have long been recognized as the products of pressure solution (Sorby, 1879) but the variety of potential dissolution fabrics has only recently been recognized. Logan and Semeniuk (1976) and Wanless (1979) have proposed that such features as clay-rich surfaces, dolomite and nodular fabrics are the products of seam or pervasive pressure solution. Many of these fabrics interpreted as solution-related have also been interpreted by others as resulting from

mechanical compaction (e.g. Pratt, 1982).

In the Port au Port Group, obvious stylolites at bed boundaries attest to the pervasiveness of pressure solution. Field and petrographic evidence, however, indicates that sediment compaction was the joint product of mechanical deformation and pressure solution, and that mechanical compaction was the more important process (Table 7.2).

7.4.3.2 Evidence for Mechanical Compaction

Limestone and argillaceous dolostone in parted limestones exhibit distinct styles of mechanical deformation. The close association of brittle deformation fabrics and "squashed structures" in limestone and argillaceous dolostone, respectively, suggests that mechanical compaction may have occurred synchronously in these two microfacies. Similar conclusions were drawn by Goldhammer et al. (1985) in their study of thin-bedded Cambro-Ordovician carbonates in the central Appalachians; during compaction, lithified grainstones deformed brittly whereas unlithified mudstone behaved ductilely.

Limestones. These beds and nodules contain little evidence of extensive compaction. Abundant evidence for early limestone lithification, such as the occurrence of undistorted mudcracks and burrows, implies that significant compaction of mudstones was prevented by early lithification (e.g. Bathurst, 1975; Steinen, 1978; Shinn and Robbin, 1983). The most common deformation structures in limestones are: (1) V-shaped fractures on upper and lower surfaces of beds, nodules and horizontally disposed clasts that are prominently developed over

TABLE 7.2: EFFECTS OF COMPACTION

	MECHANICAL	CHEMICAL
Limestone	-V-shaped fractures in beds nodules and clasts	-stylolites, -grain-contact sutures -microstylolites -microstylolite swarms -clay seams
Argillacebus Dolostone	-squashed mudcracks and burrows -fractured bioclasts -injection structures -draping over limestone surfaces	-microstylolites -microstylolite swarms -clay seams

irregularities in underlying limestones (Plate 26b, c) and (2) fracturing of thin limestone beds and nodules into angular clasts that have not been significantly displaced (Plate 26b, e). Fractures are filled with argillaceous dolostone, blocky calcite and ferroan dolomite (Plate 22f; 27d).

Compaction fabrics in limestones are interpreted to be the products of brittle failure that resulted from the minor compression of competent beds, nodules and clasts and from the greater compaction of argillaceous dolostones.

Argillaceous Dolostones. These beds and partings, in contrast to mudstones, contain an abundance of extensively deformed primary and diagenetic fabrics: (1) distorted mudcracks and burrows (Plate 22c; 26a); (2) fractured bioclasts; (3) dolostone layers that are generally thinner than laterally equivalent limestone beds or nodules (Plate 25c, d; 26b); (4) probable "injection" structures in which argillaceous dolomite laminations are squeezed upwards into the internodular matrix (Plate 24b); and (5) draping of argillaceous dolostone partings over surface irregularities in limestone nodules.

These fabrics, together with the lack of evidence for early lithfication as is present in limestones, imply that volume reduction in argillaceous sediments was in large part the result of mechanical "squashing" of responsive sediments; more resistant components, such as calcareous and siliciclastic grains, underwent fracturing.

Dolomite growth was in part concomitant with mechanical compaction of argillaceous sediment. This is suggested by the progressive decrease in

rhomb size (and in the width of the non-luminescent rim) away from resistant limestone beds and nodules, as described in the section on "dolomite". Decreasing permeability in compacting argillaceous sediment probably inhibited the growth of large crystals. The joint effects of dolomitization and mechanical compaction resulted in lithification.

7.4.3 Evidence for Chemical Compaction

There are two types of solution surfaces, sutured and non-sutured, that occur in both limestones and argillaceous dolostones.

Sutured Solution Surfaces. Included in this group are stylolites and grain-contact sutures (Wanless, 1979). Stylolites generally have relief of less than 1 mm to several millimeters and concentrate insoluble particles such as clays, organics, dolomite, and silt-size siliciclastics and opaque particles. Horizontal stylolites are most prominently developed at boundaries between beds and nodules of grainy limestone and argillaceous dolostone; curved, vertical to steeply inclined stylolites are present throughout limestone beds and nodules, commonly dissecting them into millimeter-wide blocks that may be microfaulted (Plate 25f; 26b). Associated with some stylolites are discontinuous gashes or veins of fibrous calcite (less than one millimeter in width) in which crystals are perpendicular to the stylolites. Circumgranular stylolites and grain-sutured contacts are common in flat-pebble conglomerates and packstones (Plate 25c).

Non-Sutured Solution Surfaces (Wanless, 1979). The most common seam solution fabrics in parted limestone are microstylolites, microstylolite swarms[1], and clay seams up to 0.5 cm thick. These non-sutured surfaces occur within limestone and argillaceous dolostone and at boundaries between the two microfacies and contain clays, with less abundant micas and possible organics(?) [Plate 22a-c; 26a, b]. Siliciclastic silts, opaque grains, and variable amounts of fine crystalline, ferroan dolomite may be present along these surfaces. Non-sutured surfaces can be traced laterally from limestone nodules into dolostone matrix but more frequently these surfaces either: (1) "feather out" at the margin of limestone nodules and become very diffuse in the matrix or (2) become very thin swarms in the dolostone matrix. Siliciclastic and carbonate particles contained in these surfaces are corroded and are truncated by microstylolites. Burrows and mudcracks, however, tend to be resistant structures that can either deflect or be cut by microstylolite swarms and clay seams (Plate 23d; 27b).

Non-sutured solution surfaces occasionally isolate centimeter-scale, lenticular nodules of limestone to form "fitted nodules" (see previous description of limestone nodules). No other bedding structures are apparent in these nodular mudstones with the exception of isolated laminae (20-25 μm wide and up to 1 cm long) that are horizontal to gently inclined and composed of microspar that is slightly coarser than the surrounding sediment.

---

1. Following the terminology of Wanless (1979), a microstylolite is an undulose, clay-rich surface with relief of tens of micrometers; a microstylolite swarm is an anastomosing network of microstylolites around small mudstone clots.

Interpretation

Sutured solution surfaces are concentrated at lithological transitions and are widely accepted as being the products of stress-induced solution in structurally resistant rock units (Sorby, 1879; Stockdale, 1943; Bathurst, 1975 ; Logan and Semeniuk, 1976; Wanless, 1979). Horizontal stylolites resulted from overburden pressure whereas oblique stylolites are likely products of tectonic stress. The occurrence of calcite veins and gashes and the curved shape of some oblique stylolites indicate that these surfaces (and non-sutured solution seams described below) were the loci of minor movement related to later tectonic activity or changes in overburden pressure (Durney and Ramsay, 1973).

Non-sutured surfaces are also associated with carbonate and siliciclastic dissolution, but evidence suggests that they are not solely the products of pressure solution as proposed by Wanless (1979). Some of the thicker seams (microstylolite swarms and clay seams) in particular may have been primary clay-rich laminations along which later dissolution was concentrated (Garrison and Kennedy, 1977; Wanless, 1979, 1983). Similarly, the wispy microstylolites may have originally been organic stringers formed by mechanical compaction that later initiated dissolution and concentration of insolubles (Pratt, 1982; Shinn and Robbin, 1983).

7.4.3.4 Discussion

Timing of Dolomite

Petrography of dolomites in limestones and argillaceous sediment suggests that formation of much of the dolomite is subsequent to limestone lithification and in part concomitant with mechanical compaction of argillaceous sediments. The role of pressure solution, however, must be considered in light of the protracted history of dolomites in the Port au Port Group and the documentation of pressure solution-related dolomitization in other studies (e.g. Logan and Semeniuk, 1976; Wanless, 1979).

Truncated rhombs and crystal-sutured contacts commonly occur in solution surfaces in the Port au Port Group and could readily be considered as evidence for dolomite growth preceding pressure solution. Following arguments presented by Wanless (1983), however, the morphology of a dolomite crystal cannot be used to determine the timing of dolomite formation relative to pressure solution. By way of example, truncated dolomite rhombs could indicate that: (1) pre-existing dolomite was corroded during pressure solution or (2) dolomite precipitated concomitantly with pressure solution and was partially dissolved by continued pressure solution. Similarly, dolomite rhombs that have solution surfaces deformed around them could be interpreted to have formed during or after pressure solution. Comparison of crystal abundance between solution seams and zones of limestone unaffected by pressure solution has also been used as evidence for estimating the amount of pressure

solution-related dolomitization (e.g. Wanless, 1983). Use of this criterion is suspect, however, because an initial homogeneity for the rock must be assumed, which is doubtful.

Less equivocal evidence involves comparison of the crystal size and CL zoning. The similarity in CL zoning in rhombs in limestones and solution surfaces of the Port au Port Group, together with the following evidence, imply that dolomite in parted limestones generally preceded pressure solution and that Wanless' (1979) interpretation of pressure solution-related dolomitization is not applicable to Port au Port parted limestones:

(1) Larger dolomite rhombs are associated with limestone beds and nodules. If a pressure solution mechanism prevailed larger rhombs would be restricted to solution surfaces and to argillaceous sediment which contains more solution surfaces than laterally adjacent limestone.

(2) In limestone, dolomite rhombs commonly occur in fractures in association with blocky calcite which is identical to intergranular cements in calcarenites and calcirudites interbedded with parted limestones (refer to Chap. 5). These cements are crosscut by stylolites.

Additional Evidence for Origin of Nodules

As previously discussed, limestone nodules in Port au Port parted limestones are interpreted to be the products of primary sedimentary processes and/or early lithification. There is no equivocal evidence to indicate that they are solution remnants of originally continuous beds

(Wanless' [1979] non-sutured seam solution mechanism), as suggested by:

(1) Well preserved bedding plane structures such as trace fossils, runzelmarken, and tool marks are abundant. If pressure solution had been the sole process forming the nodules, these features would not have been preserved.

(2) Coarsening of neospar occurs toward the margins of limestone nodules. If these nodules were products of pressure solution, marginal crystals would have been preferentially dissolved rather than exhibiting evidence for precipitation away from the center of the nodule.

(3) Solution seams and accumulations of insoluble material are rare in the transition zone between nodules and laterally adjacent internodular matrix (Plate 22b). In some cases, non-sutured surfaces in limestone nodules "feather out" at the nodule margin and do not pass into the adjacent argillaceous dolostone.

(4) Laminations in nodules rarely converge at nodule margins. If pervasive pressure solution had been active, convergent laminations would accompany marginal thinning of nodules. Where convergent laminations are present at nodule margins, they are generally accompanied by marginally aggraded mudstone. This suggests that lithification was in part concomitant with compaction of adjacent argillaceous sediment, rather than indicating pressure solution effects.

Occasional occurrences of solution surfaces at the transition zone between limestones and laterally equivalent argillaceous dolostones as

well as within limestones and dolostones indicate that pressure solution did occur. This is well demonstrated in sedimentary nodules (type 2) where oolitic laminae that pass into dolostone from laterally adjacent limestone exhibit thinning, particle corrosion, sutured grain contacts and abundant microstylolites (Plate 25c).

7.5 DISCUSSION AND SUMMARY

7.5.1 Diagenetic Sequence

From the above description of the lithification and compaction of parted limestones, the following is the interpreted sequence of diagenesis:

(1) Synsedimentary lithification of sediment on the sea floor under submarine and/or strandline conditions forming well lithified sediments that were susceptible to reworking to form pebble conglomerates and hardgrounds.

(2) Minor soft-sediment deformation of unlithified or poorly lithified sediment, particularly peloids, under minimal overburden pressure.

(3) Shallow burial lithification of mudstone prior to extensive mechanical compaction, which in conjunction with synsedimentary lithification, formed resistant limestone.

(4) Mechanical deformation during burial resulting in significant compaction of responsive argillaceous sediments and brittle deformation

of mudstone.

(5) Formation of ferroan dolomite, in part contemporaneous with mechanical compaction, by: (a) precipitation in poorly lithified argillaceous sediment; (b) precipitation in fractures in brittly deformed mudstones; and (c) minor dolomitization of limestone beds and nodules.

(6) Some marginal aggradation of mudstones after formation of ferroan dolomite, resulting in corrosion of dolomite rhombs.

(7) Pressure solution with increasing burial depths which was influenced by both primary and earlier diagenetic fabrics, and modified and enhanced these same fabrics.

7.5.2 Diagenetic Overprint Model

Several diagenetic models have been proposed to explain rhythmically bedded sediments. The first type involves originally homogeneous sediment that has undergone either: (1) sediment unmixing in which carbonate is redistributed into discrete beds or nodules (Sujkowski, 1958; Hallam, 1964) or (2) pervasive or non-seam pressure solution that results in thinning of units, nodular fabrics and dolomitization (Wanless, 1979). In the second type of model, diagenetic processes have modified primary sediments that either contain original sedimentary structures (e.g. Shinn and Robbin, 1983; Coniglio, 1985) or are homogeneous with only porosity and permeability variations (Einsele, 1982; Eder, 1982).

Evidence, such as the preservation of delicate bedding plane structures (detailed in Chapter 3), for the primary depositional control of thin bedding in Port au Port parted limestones eliminates the possibililty of a purely diagenetic model. The abundance of early and late diagenetic fabrics, however, suggests that a model involving diagenetic overprinting of primary sedimentary fabrics is most applicable.

This model consists of the following four components which are interpreted to govern the fabric preserved in parted limestone in the Port au Port Group (Fig. 7.2): (1) deposition of rhythmically interbedded carbonate-rich and clay-rich sediment by periodic tidal processes; (2) precompaction lithification of carbonate-rich beds to form limestone; (3) mechanical compaction of clay-rich sediment; and (4) pressure solution. This is a simplified model as it deals only with the calcite system and does not consider more complex mineralogical transformations such as aragonite-to-calcite, Mg calcite-to-calcite, or pervasive dolomitization.

Muddy tidal flat sediments are deposited by tidal processes which form two compositionally distinct types of sediment (details are given in Chap. 3). Carbonate-rich sediment (deposited by tidal currents) is interbedded with clay-rich sediment (deposited during periods of slack tide). Episodic storm deposition of coarse calcarenites and flat-pebble conglomerates punctuate the tidal sequence. Variability in environmental conditions during sediment deposition result in a diverse assemblage of sedimentary structures, such as mudcracks, burrows and gutter casts which impart additional textural variability to parted

Figure 7.2: Diagenetic sequence for two parted limestones in the Port au Port Group, which involves: (1) deposition of rhythmically interbedded carbonate-rich and clay-rich sediment by periodic tidal processes; (2) precompaction lithification of the carbonate-rich beds to limestone (dashed lines); (3) brittle deformation of limestone (stippled area is marginally aggraded mudstone), and squashing and cementation by dolomite of clay-rich sediment; and (4) pressure solution. Details are provided in text.

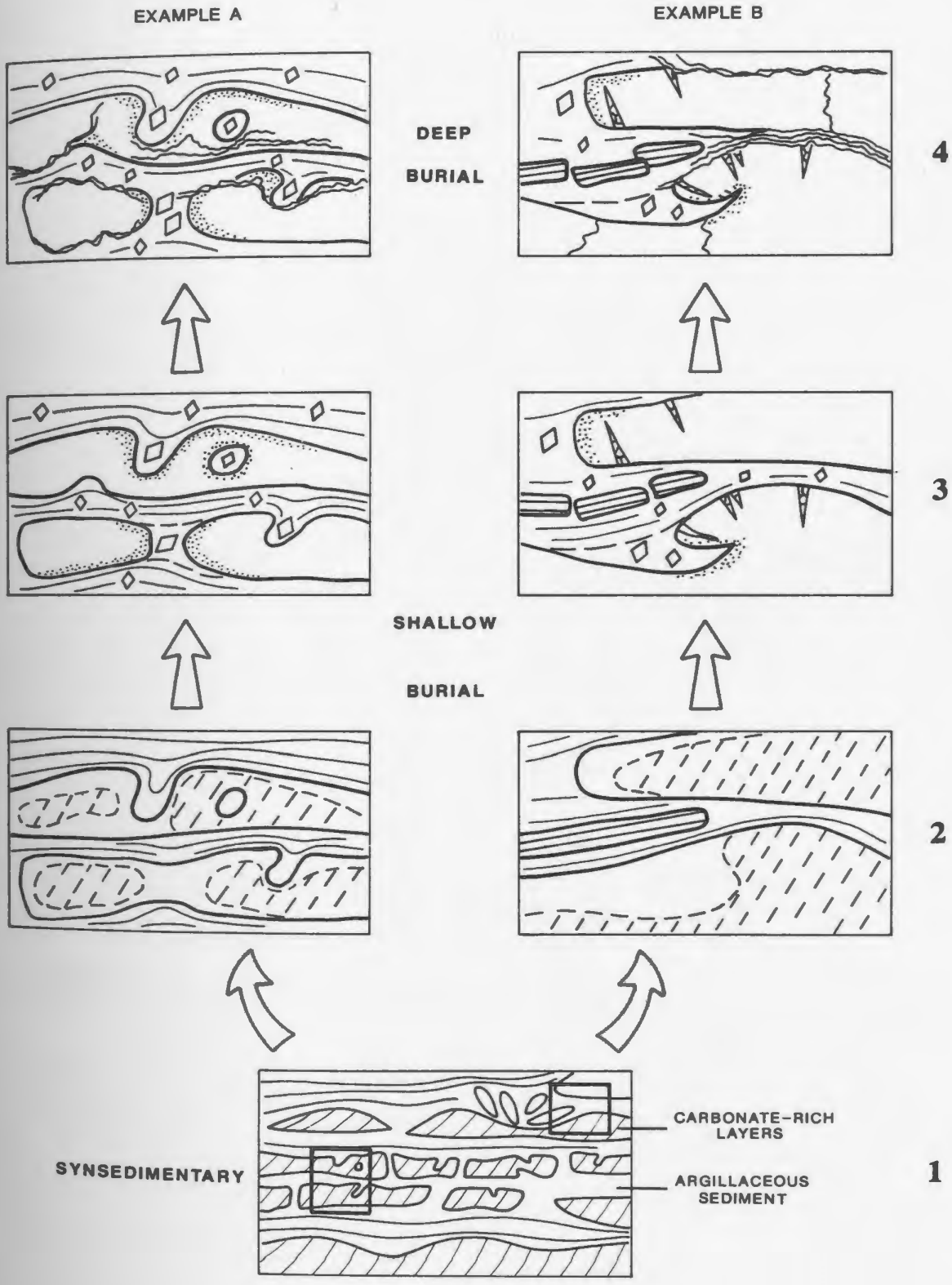
EXAMPLE A
EXAMPLE B
DEEP
BURIAL
4
3
SHALLOW
BURIAL
2
1
SYNSEDIMENTARY
CARBONATE-RICH
LAYERS
ARGILLACEOUS
SEDIMENT

limestones.

These primary heterogeneities with their inherent variations in porosity, permeability and organic content provide the template for diagenetic alterations. Precompaction lithification, which commences with synsedimentary cementation on the seafloor, is concentrated in carbonate sands and silts due to their higher porosity and permeability and the abundance of suitable carbonate nuclei; the degree of sediment heterogeneity governs whether lithification is pervasive or localized. This early lithification results in mudstones with micrite and fine microspar mosaics, most of which resist subsequent alteration.

Portions of these carbonate-rich layers, in particular their margins, continue to lithify during later diagenesis. Sediment and earlier cements become the focal points for continued growth of neospar by providing nucleation sites for calcite precipitation. The limiting factors are the availability of a calcite source(s), and sufficient porosity and permeability. Much of the microporosity is occluded prior to compaction but some neospar growth continues subsequent to mechanical deformation. The resulting mudstone is structurally resistant and is composed of coarse microspar and pseudospar.

Precompaction cementation little affects clay-rich sediment (now argillaceous dolostone beds and partings). With progressive burial, these very fine grained sediments are lithified by mechanical compaction and precipitation of dolomite into a porous argillaceous network. Previously lithified limestones only undergo minor brittle deformation as a result of mechanical compaction.

Although these clay-rich sediments are not altered by extensive early lithification, they may contribute to lithification of the above mudstones by providing a possible source of Ca and bicarbonate ions. Aerobic oxidation of organic matter may dissolve and remobilize carbonates in argillaceous sediments which are then reprecipitated into carbonate-rich beds (Sass and Kolodny, 1972). A similar mechanism of calcite redistribution has been proposed by Coniglio (1985) to explain the generation of parted and ribbon limestones in slope deposits of the Cow Head Group. Other possible sources for the ions include connate water, clay and feldspar alterations, and dewatering of deeper sediments (Irwin, 1980).

All of the above processes elicit responses in limestones and argillaceous dolostones that further emphasize the bipartite nature of parted limestone. Pressure solution, which is the latest stage considered in this model, is also governed by primary and earlier diagenetic structures. Apart from accentuating, masking or obliterating older features, such as hardgrounds and bedding contacts, no additional fabrics are interpreted to result from pressure solution.

7.5.3 Consideration of Original Mineralogy and Grain Size

Based upon petrography and CL, it is not possible to unequivocally interpret the original composition of mudstones in the Port au Port Group. Petrographically similar mudstones in other studies, however, have been interpreted by various workers (e.g. Raiswell, 1971; Coniglio, 1985) to have an original calcite mineralogy which suggests mudstones of the Port au Port Group may have had a similar mineralogy.

The above discussion of parted limestone diagenesis has been simplified by considering only a calcite system. In light of the uncertainty regarding original mudstone mineralogy, the possibility of aragonite and Mg calcite components requires that the alteration of these metastable minerals be considered in the mud to mudstone transformation: (1) wholesale aragonite dissolution under meteoric conditions (James and Choquette, 1984) which would provide additional sources of dissolved calcium carbonate for shallow burial lithification and (2) alteration of Mg calcite to calcite with preservation of microscopic textures (James and Choquette, 1984). The calcitization of aragonite components during shallow burial is not considered important as there is no evidence of calcitized particles.

In addition, the fine grain size of parted limestone components presents difficulties in differentiating the effects of synsedimentary submarine lithification from strandline lithification. Physical evidence indicates that mudstones were intermittently exposed to subaerial conditions (e.g. mudcracks) and were subjected to submarine exposure (e.g. eroded hardgrounds, glauconite) in a tidal flat setting. This suggests that synsedimentary limestone lithification occurred in both marine and strandline environments but provides no evidence for the relative importance of the different processes.

7.5.4 Implications for Other Parted Limestones

Parted or ribbon limestones (herein to be termed parted limestone) in other ancient shallow-marine sequences (e.g. Aitken, 1966, 1978;

Wanless, 1979; Demicco, 1983) are virtually identical in character to those of the Port au Port Group, and many have been similarly interpreted to be tidal flat deposits. Similar types of rhythmically bedded rocks are also common in deeper water sequences, such as slope deposits (e.g. Cook and Taylor, 1977; Coniglio, 1985) and intrashelf basins (e.g. Aitken, 1978; Markello and Read, 1981). Many of these deep-water parted limestones are macroscopically identical to tidal flat sediments and are differentiable from the shallow-water deposits on the basis of paleogeographic considerations; stratigraphic position; the absence of subaerial exposure features; and some sedimentary features such as Bouma sequences. Comparison of petrographic characteristics of Port au Port parted limestones with those of the Cow Head Group from Coniglio (1985) reveals fabrics common to both (e.g. marginally aggraded mudstones).

The striking physical and petrographic similarities between these shallow and deep water parted limestones suggests that some basic phenomena are common to parted limestones and govern the nature of their diagenesis. It is postulated that the primary rhythmic bedding of limestone and argillaceous sediment and early limestone lithification are the denominators linking these different parted limestones. Interbedded carbonate-rich and carbonate-poor bedding may result from a variety of depositional processes: (1) alternating periods of ebbing and flooding tides and slack water in tidal flats (e.g. this study; Demicco, 1983); (2) carbonate turbidite deposition alternating with terrigenous hemipelagites in slope deposits (e.g. Coniglio, 1985); and (3) storm generated deposition in the deep ramp of intrashelf basins (e.g.,

Markello and Read, 1981). Subsequent diagenetic process, although they may differ in shallow and deep water sequences, merely accentuate the rhythmic character of parted limestones.

Chapter 8

DOLOMITIZATION

8.1 INTRODUCTION

Dolomitization of limestone is an important aspect of diagenesis in the Port au Port Group. It is controlled stratigraphically and lithologically, and forms a spectrum of features ranging from pervasively dolomitized units, such as the Felix Member and the Berry Head Formation, to fabric-specific dolomites in limestone intervals. These dolomites are divided on the basis of their CL properties into three types -- red CL, dull CL and zoned dolomites -- that occur individually or together throughout the sequence. This simple division belies the variable nature and occurrence of the dolomites, which span synsedimentary, early and late diagenesis. This chapter integrates field and petrographic data from these dolomites, some of which were discussed in previous chapters. Co-existing limestone and dolomite also enable a determination of the timing of dolomitization relative to limestone diagenesis.

8.2 TYPES OF DOLOMITE

8.2.1 Red CL Dolomite

This type is composed predominantly of clear to inclusion-rich, aphanocrystalline to very finely crystalline rhombs (10-15 μm size). They are ferroan or non-ferroan and have bright to moderate red luminescence. Coarser crystals may have thin outer zones with dull luminescence.

Red CL dolomite is specific to interbedded dololaminites and dolomitized brown oolite. Sedimentary fabrics are well preserved in outcrop and hand specimen, and are identical to those in equivalent undolomitized rocks (see Chapter 3; Plate 21d). Microfabrics are also well preserved. Micritic cement and matrix, and grains (specifically ooids, echinoderm fragments, and oolitic and mudstone intraclasts) in undolomitized calcarenites and calcirudites may also be partially or completely replaced by aphanocrystalline dolomite (Plate 30a).

8.2.2 Zoned Dolomite

This type includes pervasively dolomitized intervals and is composed of hypidiotopic mosaics of finely to medium crystalline dolomite (30-250 μm size). Rhombs have cloudy cores with bright red luminescence and inclusion-poor rims with zoned moderate and dull luminescence (Plate 30a-e). Intercrystalline areas are filled with bright-luminescent

ferroan blocky calcite, a matrix of clays and (?) organic material (herein referred to as "argillaceous matrix"), or remain open as intercrystalline porosity. Preservation of original fabrics is generally poor, but vague grain outlines may be recognized due to inclusions in rhombs or by slight variations in crystal size (Plate 30b, d). Vuggy porosity in zoned dolomite may be occluded by bright-luminescent blocky calcite.

8.2.3 Dull CL Dolomite

This dolomite occurs in hypidiotopic mosaics of finely to coarsely crystalline rhombs (30-500 μm size) which exhibit sharp to undulose extinction. Crystals have slightly curved faces and are commonly zoned with small, inclusion-rich cores of bright orange luminescence and clear, ferroan rims of dull to nonluminescence. They are closely packed or float in an argillaceous, commonly pyritic matrix.

Dull CL dolomite is generally fabric-specific but does not preserve original fabrics, and occurs in: (1) argillaceous dolostone partings and internodular matrix in parted limestones; (2) burrows; (3) grains, such as ooids, micritic intraclasts, bioclasts and oncoids, where the dolomite replaces grains or occludes grain molds, and voids developed from grain deformation (refer to Chapter 6); (4) intergranular areas of calcarenites and flat-pebble conglomerates; (5) fenestral porosity in carbonate laminites; and (6) fractures that crosscut grains, neospar and earlier cements (Plates 22f; 29d). The last four occurrences are commonly associated with dull- and moderate-luminescent, ferroan blocky calcite and occasionally with bright-luminescent calcite. Dolomite

rhombs in contact with the first type of calcite have well-developed or serrated crystal faces and, when present in fractures, are first-stage cement. Rhombs adjacent to bright-luminescent calcite always have serrated faces (refer to the following section on dedolomites).

Fractures, vugs and breccia clasts in pervasively dolomitized rocks are commonly lined with very coarsely crystalline dull CL dolomite, followed by bright-luminescent, very coarsely crystalline blocky calcite (Plate 30f). This variety is less abundant than the finer crystalline dolomites and is characterized by rhombs with prominently curved crystal faces and undulose extinction. Crystals have inner, non-ferroan zones of alternating inclusion-rich and clear dolomite and an outer, ferroan rim that is commonly dedolomitized. This dolomite is commonly termed "baroque" or "saddle" dolomite (e.g. Mattes and Mountjoy, 1980; Radke and Mathis, 1980).

8.2.3.1 Argillaceous Dolostone Partings and Burrows

As described in Chapter 7, finely to medium crystalline dolomite is a pervasive component of burrows (Plate 22a) and the argillaceous dolostone microfacies in parted limestone (Plate 22d-f). The largest dolomite rhombs with wide non-luminescent rims occur in: (1) argillaceous dolostone adjacent to limestone beds and nodules (Plate 22b, e) and (2) burrows and fractures in limestone beds and nodules (Plate 22 d, f). Dolomitized burrows are either completely dolomitized or have variably dolomitized walls and cores of neospar or blocky calcite cement. They are generally closely associated with

undolomitized burrows, and are uncompacted in limestone beds and nodules.

8.2.3.2 Grains

Partially or completely dolomitized grains are composed of: (1) a single dolomite crystal, up to 0.8 mm size, in ooids (Plate 11d) or (2) a cluster of rhombs (Plate 28a, b). These grains commonly occur in close association with undolomitized grains. Dolomite tends to be contained within grain boundaries, obliterating much of the internal microfabric. Grains replaced by a mosaic of rhombs are most common and these rhombs may be present throughout the grain or may be concentrated at the core, near the margin or within micritic areas of the grain.

Dull CL dolomite commonly replaces ooid cortices in grey oolite but it is rare in brown oolite. In grey oolite, dolomitized ooids tend to be concentrated in laminations which alternate with laminations of calcareous ooids. Dolomite occurs in finely and coarsely preserved varieties of grey oolite (refer to Chapter 6) but some rhombs in coarsely preserved ooids have irregular contacts with later blocky calcite. Trilobite and echinoderm particles, and cement-filled molds forming nuclei for ooids and oncoids are generally undolomitized (Plate 28b).

In some calcarenites, echinoderm fragments and their syntaxial calcite overgrowths appear to be the loci of some unusual dolomitization patterns. Dull CL dolomite completely or partially replaced these components and is syntaxial with calcite relicts. It occurs in two

modes:

(1) When aphanocrystalline, red CL dolomite is present at grain margins, dull CL dolomite variably replaces syntaxial overgrowths, some of the adjacent matrix and any undolomitized echinoderm cores remaining after aphanocrystalline dolomitization. Original fabrics are generally well preserved (Plate 30a).

(2) Individual sand-size, calcareous echinoderm plates with thin calcite overgrowths and minor micritic matrix are completely or partially enclosed by a rhombic "band" of ferroan dolomite that is syntaxial with the echinoderm nucleus (Plate 28c, d).

8.2.3.3 Intergranular Dolomite

Dull CL dolomite occurs as intergranular cement in calcarenites, precipitating after such synsedimentary cements as isopachous micritic calcite (refer to Chapter 5; Plate 29c). It also replaces cements and micritic matrix and impinges upon (ie. partially replaced) adjacent grains, particularly siliciclastic and micritic grains (Plate 29a, b). Where dolomite crosscuts grain-matrix boundaries, grain outlines are preserved as relict inclusions within rhombs. Minor vuggy and intercrystalline porosity may occur with this variety of dolomite.

8.3 DISTRIBUTION OF DOLOMITES

Occurrences of red and dull CL dolomites are present throughout the

predominantly limestone units of the March Point Formation, and the Cape Ann, Big Cove, Campbells and Man O' War Members, but zoned dolomite is generally absent (Table 8.1). Red CL dolomite in interbedded dolomitized brown oolite and dololaminite is most prominent in the basal one-third of the Campbells and Felix Members, where grey oolite is rarely developed. Dull CL dolomite, in contrast, is widely distributed, occurring in all lithofacies throughout the sequence. Fabric-specific occurrences (ie. in argillaceous dolostone in parted limestones, burrows, grains, and as intergranular cements) however, tend to be best developed or preserved in the limestone units.

All three types of dolomite occur together in pervasively dolomitized intervals of the Felix Member and Berry Head Formation. In outcrop, a range of sedimentary structures are variably preserved, so that primary lithofacies are still identifiable. Petrography reveals two types of pervasive dolostones. The first type occurs most commonly in dolomitized brown oolite and bioclastic calcarenites, and is composed of: (1) red CL dolomite which preferentially replaces grains, preserving original fabrics and (2) an intergranular, zoned or dull CL dolomite with no fabric preservation (Plate 30a). Dull CL dolomite also occludes intercrystalline pores and dissolution vugs in the zoned dolomite. The second type lacks red CL dolomite and is composed only of zoned dolomite with occurrences of dull CL dolomite, as in the first type of dolostone (Plate 30b-e). Saddle dolomite is most abundant in the dolomitized Felix Member and Berry Head Formation in association with both types of pervasive dolostone.

Reconnaissance of other Port au Port sequences along the Great

TABLE 8.1: DISTRIBUTION OF DOLOMITES

	CL Types			
	RED	ZONED	DULL	
			(Finely to coarsely crystalline variety)	(Saddle dolomite variety)
STRATIGRAPHIC				
Berry Head Fm.	XX	XXX	X	XX
Man O' War Mbr.	X		XXX	
Felix Mbr.	XX	XXX	X	XX
Big Cove Mbr.	X		XXX	
Campbells Mbr.	XXX		XX	X
Cape Ann Mbr.	X		XXX	
March Point Fm.	X		XXX	
LITHOLOGIC				
Facies-specific (Carbonate laminite and brown polite)	XXX			
Fabric-specific	XX		XXX	
Non-fabric specific		XXX		XXX

(XXX - most abundant
X - least abundant)

Northern Peninsula (refer to Chapter 2) suggests that type 2 pervasive dolostone is also the dominant lithology in the Petit Jardin Formation in western Newfoundland. The restricted occurrence of this type of dolostone on the Port au Port Peninsula appears to be exceptional.

8.4 DEDOLOMITE

Blocky calcite has variably replaced all of the previously described dolomites, but it is most prominent in (ferroan) dull CL dolomite (Plate 28a; 29e; 30f). Rhombs may be partially or completely dedolomitized[1], with calcite occurring in irregular patches throughout the crystals, at rhomb margins, rhomb cores, or in ferroan zones.

CL reveals two zones of dedolomitization in rhombs: (1) an initial stage of bright yellow-luminescent calcite which preferentially occurs at rhomb margins and (2) a later stage of moderate to bright orange-luminescent calcite which occurs within the outer half of rhombs. The first type of calcite also occludes micropores adjacent to rhomb margins. Both calcite types have CL identical to that of the last cement stage, which partially occludes vuggy, intergranular and intercrystalline porosity in limestone and dolostone, and fills fractures that crosscut all lithologies.

---

1. The term, "dedolomitization" is used to refer to the diagenetic replacement of dolomite by calcite (after Morlot, 1947; in Bates and Jackson, 1980).

8.5 INTERPRETATION

The variety of dolomite and dolostone in the Port au Port Group and their variable stratigraphic occurrences indicate a complex history of dolomitization. Three stages are recognizable: syngenetic, early diagenetic and late diagenetic dolomitization.

8.5.1 Syngenetic Stage

A synsedimentary origin for the red CL dolomites in Port au Port dololaminites, interpreted to be supratidal deposits (Chapter 3), is collectively suggested by: (1) their facies-specific occurrence; (2) well-preserved sedimentary structures; (3) aphano- to very finely crystalline fabric; and (4) the abundance of dololaminite intraclasts in overlying undolomitized sediment. The fabric of these syngenetic dolomites (Friedman and Sanders, 1967) is analogous to penecontemporaneously dolomitized sediment in modern intertidal and supratidal carbonate environments, such as the Bahamian tidal flats (Shinn and Ginsburg, 1964; Bathurst, 1975) and Persian Gulf sabkhas (Illing et al., 1965; Bathurst, 1975). Red CL dolomites were relatively unaffected by subsequent dolomitization; only minor zoned and dull CL dolomite overgrowths are developed in very finely crystalline rhombs.

Red CL dolomite, which replaced carbonate grains in intertidal brown oolites and some bioclastic calcarenites that are closely associated with dololaminites, is also interpreted to be of synsedimentary origin.

This is based upon petrographic similarities (points 1 to 3, previously described) and identical CL to dololaminites. These dolomitized calcarenites are closely associated with dololaminites.

The absence of evidence for evaporites in both lithofacies suggests that seepage refluxion and evaporative pumping (summarized in Morrow, 1982b; Land, 1985) are unlikely dolomitization mechanisms for syngenetic dolomites. A more feasible process may involve the interaction of marine and meteoric waters in tidal environments (mixed-water model -- Land, 1973; Margaritz et al., 1980; Morrow, 1982b). This mechanism involves the near-surface, mixed marine-meteoric zone (James and Choquette, 1983) in which high bicarbonate concentrations in meteoric waters and a supply of Mg ions from seawater (Morrow, 1982a), in conjunction with reduced precipitation rates due to low salinities (Folk and Land, 1975; Kastner, 1984), favour dolomite precipitation.

8.5.2 Early Diagenetic Stage

The relationship of finely to coarsely crystalline, dull CL dolomites (ie. excluding saddle dolomite) with diagenetic limestone fabrics indicates that the time of dolomitization is bracketed by precompaction limestone lithification and the latest stage of bright-luminescent blocky calcite precipitation. This is suggested by the following evidence:

(1) Data provided by parted limestones (see Chapter 7) suggest that dolomites in burrows, internodular matrix and argillaceous dolostone partings formed after the lithification of mudstone components and was in part synchronous with mechanical compaction. Rhombs with serrated

boundaries, presumably corroded by adjacent neospar, imply that dolomitization preceded the last stages of mudstone lithification.

(2) Serrated contacts between rhombs and blocky calcite in coarsely preserved ooids suggest precipitation of dull CL dolomite occurred in part prior to the coarse alteration of ooids (refer to Chapter 6).

(3) The common association of dull CL dolomite and dull-luminescent blocky calcite cements in fractures and intergranular voids suggests that precipitation of these cements was closely associated. In some fractures, dolomite is the first cement stage indicating that it predated blocky calcite.

The timing of zoned dolomite is more problematical because the dolomite occurs only in pervasively dolomitized units. The formation of zoned dolomite, however, was earlier than dull CL dolomite and later than red CL dolomite, as evidenced by: (1) dull CL dolomite occluding intercrystalline and dissolution voids in zoned dolomite and (2) the bright-luminescent cores of zoned (and dull CL) dolomite rhombs that are identical in CL and size to red CL dolomite, suggesting that the latter provided nuclei for zoned and dull CL dolomitization.

Field and petrographic observations support only incomplete and often equivocal interpretations of zoned and dull CL dolomites. Complications arise from such factors as the variable occurrence of the dolomites and their overprinting of limestone diagenetic fabrics and earlier dolomites. In light of these uncertainties, evaluation of the possible mechanisms of dolomitization (including saddle dolomite discussed below) is not feasible. Several interpretations have been proposed for such

types of dolomite in other studies, but are difficult to assess due to the lack of modern analogues (Morrow, 1982b; Land 1980). They include: (1) mixed-water model -- similar to that described for red CL dolomite but occurring in a deep aquifer (e.g., Hanshaw et al., 1971; Sears and Lucia, 1980); (2) burial compaction model -- Mg-rich waters, derived from compacting fine-grained sediments, cause dolomitization during burial (e.g. Mattes and Mountjoy, 1980); and (3) dolomitization related to sulphate reduction resulting from bacterial oxidation of organics (e.g. Baker and Kastner, 1981; Coniglio, 1985).

8.5.3 Late Diagenetic Stage

The saddle dolomite variety of dull CL dolomite generally lines fractures and vugs that crosscut all limestone and dolomitized lithofacies and thus is interpreted to be of late diagenetic origin (epigenetic dolomite of Friedman and Sanders, 1967). Its occurrence as a cement rimming breccia clasts, in which stylolites are truncated by clast boundaries, also indicate that it precipitated subsequent to pressure solution. Saddle dolomite is followed by bright-luminescent blocky calcite cement, which is similar to calcites replacing all varieties of dolomite, suggesting that formation of saddle dolomite occurred prior to dedolomitization (discussed below).

Saddle dolomite has also been documented in other studies (e.g., Beales and Hardy, 1980; Mattes and Mountjoy, 1980; Radke and Mathis, 1980). Numerous mechanisms for the formation of this late stage dolomite have been proposed (listed above), but there has generally been little agreement amongst various workers (Morrow, 1982b). Restriction of saddle

dolomite in the Port au Port Group to late-stage fractures and breccias, however, suggests that the dolomite may be related to such fracture-related processes as mixing of near-surface fluids with deep burial brines along fractures (cf. Mattes and Mountjoy, 1980).

Calcitization of dolomites has often been interpreted to be the product of near-surface diagenesis, related to subaerial exposure horizons within the sequence or late-stage surficial weathering (reviewed in Budai et al., 1984). Port au Port Group dedolomites, however, are interpreted to have formed during late diagenesis and are not related to the synsedimentary paleokarst surfaces in the sequence, as suggested by: (1) the occurrence of dedolomite in all dolomite types; (2) similar CL properties in dedolomites and the last stage of blocky calcite cement; and (3) the stratigraphically widespread distribution of dedolomites.

Petrographic similarities with dedolomites in the St. George Group (Haywick, 1985) suggest that those in the Port au Port Group may have originated during Lower Mississippian karstification of uplifted Cambro-Ordovician strata on the Port au Port Peninsula (Dix, 1981). Various workers have recognized the importance of associated evaporites and dedolomite in ancient carbonates and have proposed that dedolomitization is driven by calcium sulphate-saturated solutions, derived from the dissolution of gypsum (e.g. Lucia, 1961; Back et al., 1983). This may be applicable to the Port au Port Group, where downward-percolating Mississippian/post-Mississippian groundwaters may have infiltrated and dissolved evaporites in the Mississippian Codroy Group (Dix, 1981). The fluids thus reached saturation with regards to

calcium sulphate and effected dedolomitization in the St. George and Port au Port Groups. Faults and fractures developed in Cambro-Ordovician strata during (?)Taconic and/or Acadian Orogenies (late Early to Middle Ordovician and Late Devonian respectively) were probable conduits for fluid flow; fractures occluded by bright-luminescent blocky calcite are commonly associated with dedolomites.

8.6 DISCUSSION

In the Port au Port Group, the formation of red CL dolomites is interpreted to be controlled by the intertidal and supratidal depositional environments. In contrast, the later dolomites are non-facies specific; variably occurring in all lithofacies: dull CL dolomite is stratigraphically widespread but fabric-specific; and zoned dolomites are stratigraphically restricted and non-fabric specific. These observations suggest that a diagenetic process, common to all lithofacies in the sequence, controlled later dolomitization. Synsedimentary and near-surface lithification is the most feasible possibility. The products of this selective, early lithification (e.g. intergranular cements, mudstone lithification) are of volumetric importance in all limestone lithofacies and resulted in occlusion of much original pore space (see Chapters 5 and 7). The distribution of early lithification products appears to have restricted the occurrence of later dolomites to more porous sediments and secondary voids (cf. Hardie et al., 1982).

The role of early lithification is apparent in the March Point Formation, Cape Ann, Campbells and Man O' War Cove Members but there is no unequivocal evidence for its importance in the pervasively dolomitized Felix Member and Berry Head Formation. Restriction of zoned dolomite, interpreted to predate dull CL dolomite and most blocky calcite cements, to these latter units, however, suggests that they were incompletely lithified or contained fractures that rendered them susceptible to dolomitization. This stage is not well developed in the other units due to pervasive early limestone lithification, which renders strata impermeable. Subsequent development of fractures, formed during the (?)Taconic and/or Acadian Orogenies, exposed much of the sequence to dull CL dolomitization. Earlier limestone lithification and zoned dolomitization, however, restricted this later dolomite to specifically replacing grains, argillaceous sediments, and occluding remaining original porosity and secondary fracture and vuggy porosity.

8.7 SUMMARY

The spectrum of dolomites in the Port au Port Group represents a protracted history of dolomitization. The three CL types of dolomite have variable stratigraphic and lithologic distributions, and occur individually in limestone intervals and together in pervasively dolomitized intervals. The syngenetic dolomite, red CL type, is specific to interbedded dololaminite and dolomitized brown oolite and has excellent fabric preservation. The mixed marine-meteoric waters in the supratidal-intertidal zone may have promoted the facies-specific

dolomitization. Early diagenetic dolomites, forming subsequent to early limestone lithification and prior to the last stage of blocky calcite cementation, show greater variability in their mode of occurrence and no fabric preservation. Zoned dolomite is restricted to the Felix Member and Berry Head Formations and crosscuts lithofacies boundaries. The later, finely to coarsely crystalline, dull CL dolomite is stratigraphically widespread and occurs in all lithofacies, but is fabric-specific. It is in part concomitant with dull-luminescent blocky calcite precipitation, the alteration of radial ooids and possibly mudstone lithification. These earlier dolomites are crosscut by late diagenetic saddle dolomite that lines fractures and vugs and postdates pressure solution. All dolomites were subjected to dedolomitization, probably related to Mississippian karstification and evaporite dissolution.

Chapter 9

SYNTHESIS: DIAGENETIC SEQUENCE, ISOTOPE GEOCHEMISTRY, AND IMPLICATIONS FOR A DEPOSITIONAL-DIAGENETIC MODEL

9.1 INTRODUCTION

It is readily apparent from previous chapters that the Port au Port Group is characterized by a wide spectrum of depositional and diagenetic features, reflecting the variable environmental conditions through which these sediments have passed. Peritidal sediment deposition took place under fluctuating submarine and strandline subaerial conditions and was controlled by local environmental changes which gave rise to meter-scale, oolite-laminite and parted limestone-shale assemblages. Superimposed on these local processes were changes in relative sea level which resulted in the formation of Grand Cycles (and possibly meter-scale assemblages). These primary depositional controls in turn affected the nature of synsedimentary and early meteoric diagenesis. Field and petrographic data indicate the importance of early lithification and its role in controlling later diagenesis. The purpose of this chapter is to: (1) synthesize the previously discussed carbonate diagenetic interpretations into an overall diagenetic model; (2) evaluate the carbon and oxygen isotopic geochemistry of the limestones

in light of field and petrographic evidence; and (3) to compare depositional models with the interpreted diagenetic sequence to determine a predictive depositional-diagenetic model.

9.2 SEQUENCE OF DIAGENESIS

Port au Port carbonates have a protracted diagenetic history in which two endmembers are readily recognizable: an initial stage of synsedimentary diagenesis and the late stages of deep burial and tectonically-related diagenesis. Figure 9.1 summarizes the interpreted diagenetic sequence, details of which are provided in Chapters 5 through 8.

Synsedimentary diagenesis is characterized by facies-specific lithification and erosion which occurred in shallow subtidal, intertidal and supratidal settings. Evidence of this early stage is preserved in nearly all lithofacies and includes: (1) interparticle cementation of shallow subtidal and intertidal calcarenites and calcirudites; (2) localized mudstone lithification in parted limestones; (3) dolomitization (red CL type) of supratidal carbonate laminites and intertidal brown oolite; and (4) peritidal erosion surfaces such as "hardgrounds" and "surface paleokarst" in grey oolite and parted limestone, and carbonate laminites respectively. Conglomerate clasts derived from these lithified sediments are also ubiquitous products of synsedimentary diagenesis.

The last two stages recognized in the diagenetic sequence involve

Figure 9.1: Summary of the diagenetic sequence of the Port au Port Group, Port au Port Peninsula.

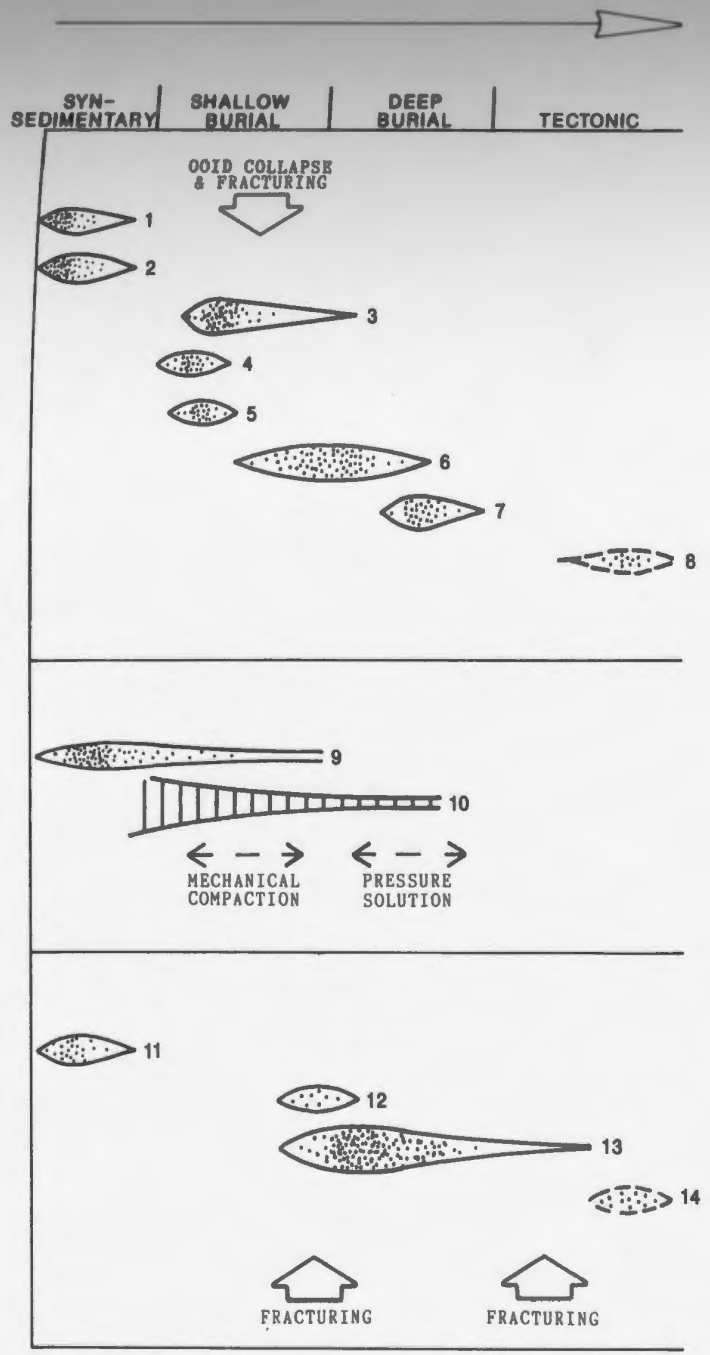

OOID CALCARENITES

1. Early submarine cementation by fibrous, isopachous micritic, syntaxial (?)Mg calcite/calcite; hardgrounds.
2. Early marine-vadose cementation by meniscus micritic calcite; beachrock.
3. Mixed marine-meteoric/meteoric cementation by prismatic clear calcite.
4. Meteoric alteration of Mg calcite ooids to finely preserved calcite ooids.
5. Meteoric dissolution & alteration of aragonite in ooids and bioclasts.
6. Alteration of finely to coarsely preserved ooids.
7. Deep burial cementation by dull CL blocky calcite in fractures, intergranular voids.
8. Cementation by bright CL blocky calcite in fractures, inter- & intragranular voids during re-exposure.

PARTED LIMESTONES

9. Early marine & meteoric mudstone lithification; hardgrounds.
10. Compaction of porosity: brittle deformation in mudstone; squashing of argillaceous sediment; pressure solution.

DOLOMITES

11. Marine-meteoric red CL dolomitization; karstification.
12. Deep phreatic zoned dolomitization.
13. Deep phreatic dull CL dolomitization.
14. Dedolomitization by meteoric groundwaters (?related to event 8).

processes that are non-facies specific but may be fabric specific. The deep burial stage (mesogenetic stage of Choquette and Pray, 1970) includes mechanical compaction; fracturing; cementation by dull-luminescent blocky calcite; dolomitization (zoned and dull CL types); and pervasive pressure solution. The tectonically-related or telogenetic stage (Choquette and Pray, 1970) includes fracturing; precipitation of bright-luminescent blocky calcite; and dedolomitization. This stage is unrelated to the earlier stages. Features of this last stage crosscut all above fabrics and probably formed as a result of Acadian (Late Devonian) uplift and faulting; Carboniferous karstification of the Cambro-Ordovician sequence on the Port au Port Peninsula; and alteration of Carboniferous carbonates and evaporites.

In addition to the readily interpreted early and late diagenetic end-members, several fabric-specific processes have been recognized that are interpreted to have occurred between the end-member stages: (1) dissolution of metastable sediments (aragonite and Mg calcite) to form fossil molds; (2) mineralogical transformations (Mg calcite and aragonite to calcite); (3) post-synsedimentary mudstone lithification in parted limestones; and (4) precipitation of prismatic clear calcite cements (distal stage). Their intermediate position in the sequence of diagenesis is compatible with a shallow-burial meteoric interpretation; there is no conclusive evidence, however, for either vadose or shallow phreatic meteoric diagenesis. The lack of unequivocal meteoric fabrics suggests that this intermediate stage either is difficult to recognize due to such factors as overprinting by late diagenesis or was poorly

developed, if at all, due to such factors as insufficient periods of subaerial exposure; the predominance of calcitic components; and the pervasiveness of synsedimentary lithification and dolomitization.

9.3 CALCITE STABLE ISOTOPE GEOCHEMISTRY

In recent years, carbon and oxygen stable isotope geochemistry has been used extensively in studies of carbonate diagenesis (e.g. Bathurst, 1975; Hudson, 1977; Anderson and Arthur, 1983). Isotopic data may supplement the assessment of paleoenvironments and provide information regarding such parameters as paleotemperature and the chemistry of pore-waters (e.g. Anderson and Arthur, 1983). As documented by numerous workers, limestones subjected to progressive burial diagenesis exhibit a trend toward lighter $\delta^{18}O$ values with burial, which is accompanied by little variation or a slight decrease in $\delta^{13}C$, as a result of increasing temperature and/or infiltration by meteoric water (summarized in James and Choquette, 1983). Increasing evidence, however, suggests that: (1) some ancient marine precipitates remain isotopically distinct from meteoric and deep burial products and (2) vadose- and phreatic-meteoric and mixed marine-meteoric zones may be differentiated on the basis of isotopes (e.g., Allan and Matthews, 1982; James and Choquette, 1983, 1984, and references cited therein).

In this study, carbon and oxygen isotope geochemistry is used to further assess the interpreted diagenetic sequence, previously determined on the basis of field and petrographic evidence. Isotopic

analyses of 35 limestone samples (cements, ooids and mudstones) were carried out by Teledyne Isotopes (New Jersey) using standard procedures. Sample descriptions and procedures, and a complete tabulation of isotope data are provided in Appendix D. Values are expressed in $\delta^{13}C$ and $\delta^{18}O$ in parts per mil (o/oo) relative to the PDB standard.

9.3.1 Summary of Analyses

Three types of components were extracted and analyzed: (1) finely and coarsely preserved radial ooids; (2) calcite cements including (a) prismatic calcite in conglomerate and occluding burrows in mudstone; (b) fibrous calcite from biohermal and biostromal limestones; and (c) blocky calcite from conglomerates, fractures and fossil molds; and (3) homogeneous neospar in conglomerate clasts, underlying parted limestone hardgrounds, and marginally aggraded neospar in parted limestone. Whole-rock analyses include grey oolite with fibrous and isopachous micritic calcite cements, and brown oolite with meniscus micritic calcite. Isotopic values for all samples cluster in a narrow zone between $\delta^{13}C$ of -0.6 and -2.4 o/oo and $\delta^{18}O$ of -7.3 and -10.4 o/oo (Figs. 9.2 to 9.4; Appendix D). Several notable values and groupings, however, are apparent:

(1) The heaviest $\delta^{18}O$ occurs in finely preserved ooids (-7.6 o/oo; "A" in Fig. 9.3), parted limestone hardgrounds (-7.3 o/oo; "H" in Fig. 9.4), and the center of a mudstone bed (-7.5 o/oo; "I" in Fig. 9.4).

(2) $\delta^{13}C$ and $\delta^{18}O$ values for all calcite cements, with the exception of

Figure 9.2: $\delta^{13}C$ versus $\delta^{18}O$ of calcite cements. Star indicates estimated marine carbonate $\delta^{18}O$ signature for inorganic precipitates from the Port au Port Group. Also plotted on this diagram are values for fibrous marine cements from the Middle Ordovician and Lower Cambrian (James and Choquette, 1983); radiaxial fibrous calcite from the Cow Head Group (Lower and Middle Ordovician; Coniglio, 1985); and Lower Ordovician wackestones (Haywick, 1985). Circled letters are referred to in text. See text for discussion.

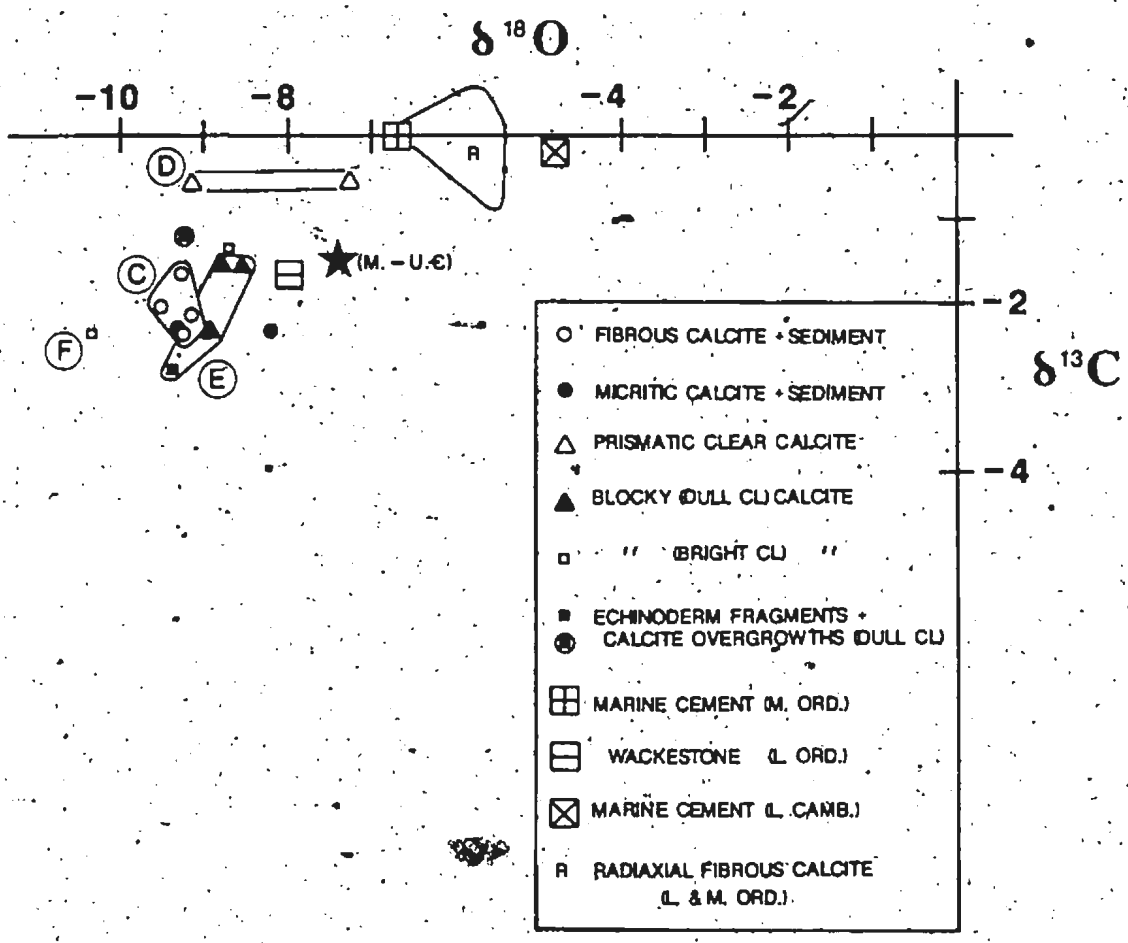
δ18O
−10
−8
−4
−2
R
D
C
F
E
(M. – U.€)
−2
−4
δ13C
FIBROUS CALCITE + SEDIMENT
MICRITIC CALCITE + SEDIMENT
PRISMATIC CLEAR CALCITE
BLOCKY (DULL CL) CALCITE
" (BRIGHT CL) "
ECHINODERM FRAGMENTS + CALCITE OVERGROWTHS (DULL CL)
MARINE CEMENT (M. ORD.)
WACKESTONE (L. ORD.)
MARINE CEMENT (L. CAMB.)
R RADIAXIAL FIBROUS CALCITE (L. & M. ORD.)

Figure 9.3: $\delta^{13}C$ versus $\delta^{18}O$ of ooids. Circled letters are referred to in text. See text for distussion.

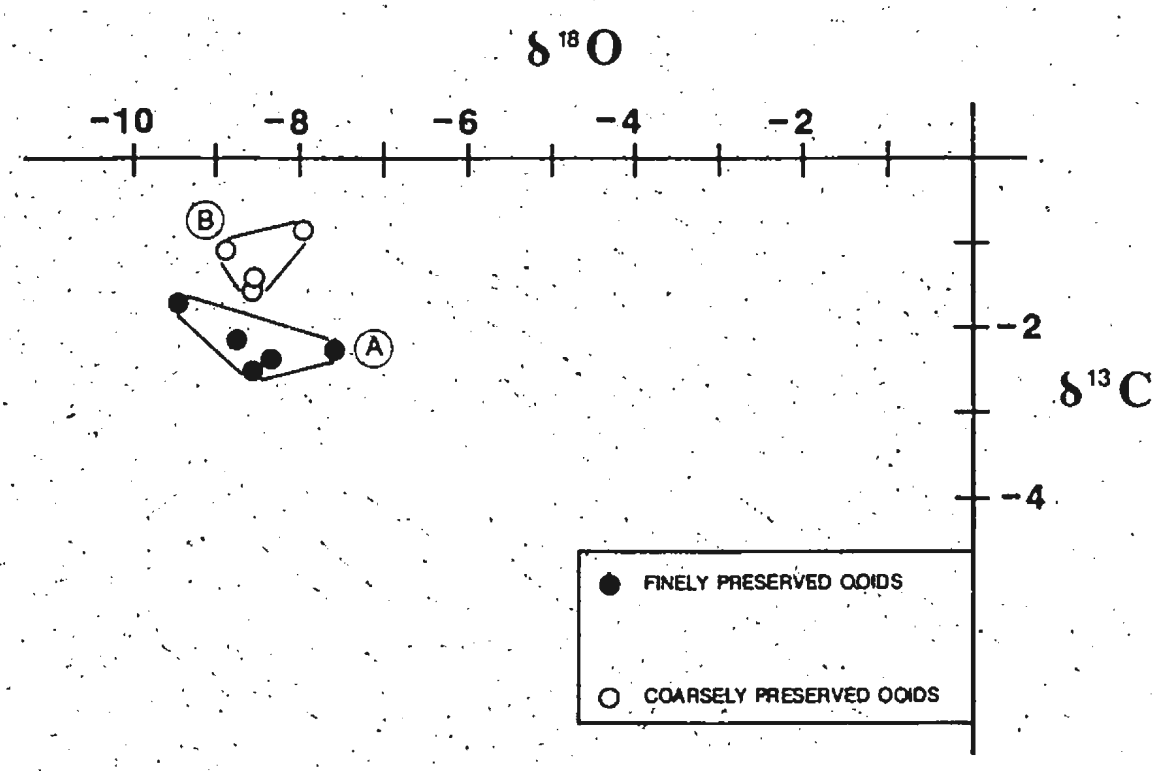
δ18O
-10
-8
-6
-4
-2
B
A
-2
δ13C
-4
FINELY PRESERVED OOIDS
COARSELY PRESERVED OOIDS

Figure 9.4: $\delta^{13}C$ versus $\delta^{18}O$ of mudstones. Circled letters are referred to in text. Numbers 1 and 2 refer to serial analyses of marginally aggraded mudstones. See text for discussion.

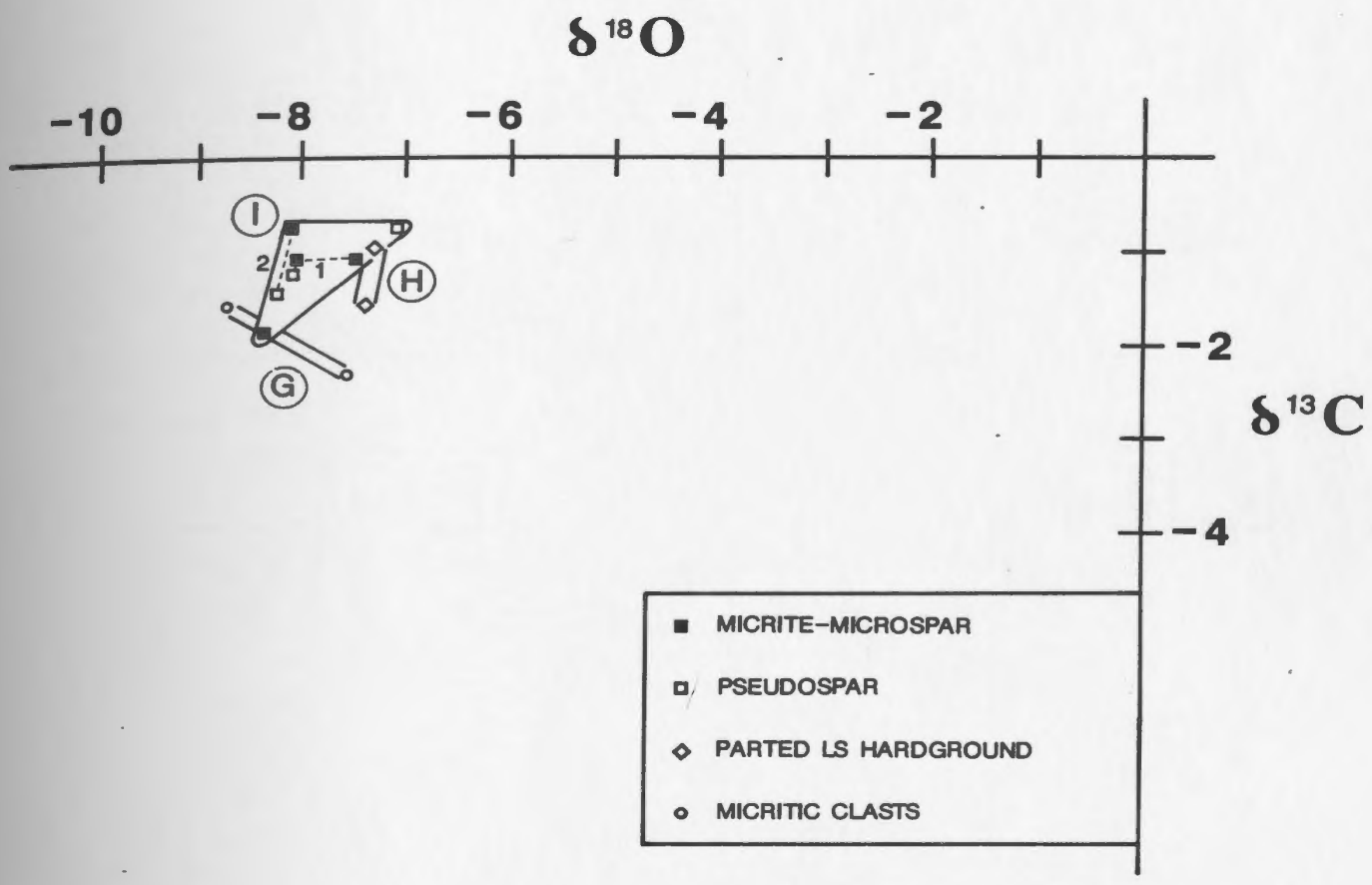
δ18O
-10
-8
-6
-4
-2
I
H
G
2
1
-2
-4
δ13C
MICRITE-MICROSPAR
PSEUDOSPAR
PARTED LS HARDGROUND
MICRITIC CLASTS

prismatic calcite, show considerable overlap ("C"-"F" in Fig. 9.2). Prismatic calcite has the heaviest $\delta^{13}C$ of -0.6 o/oo.

(3) Finely and coarsely preserved radial ooids have $\delta^{18}O$ clustered around -8.4 o/oo but show a two-fold division of $\delta^{13}C$ in which finely preserved ooids (average $\delta^{13}C$ of -2.1 o/oo; "A" in Fig. 9.3) are lighter than coarsely preserved ones (average $\delta^{13}C$ of -1.1 o/oo; "B" in Fig. 9.3).

(4) Two serial samples of the core and margins of mudstone nodules and beds that coarsen marginally have $\delta^{13}C$ of -1.1 to -1.5 and $\delta^{18}O$ of -7.5 to -8.2 ("I" in Fig. 9.4). These differences do not appear to be significant. This contrasts with Coniglio (1985), who demonstrated obvious isotopic differences from the center to the margin of some marginally coarsening mudstone beds.

9.3.2 Interpretation

9.3.2.1 $\delta^{18}O$ and the Middle and Upper Cambrian Marine Carbonate Signature

All analyzed samples are severely depleted in ^{18}O relative to modern sediments, a phenomenon which has been documented in other studies of Phanerozoic limestones (e.g. Veizer and Hoefs, 1976). Although higher ocean water temperatures in the past and post-depositional exchange with isotopically lighter fluids (e.g. meteoric waters) have been used to explain these highly negative values, growing evidence indicates that these values may in part be explained by secular variations in the

isotopic composition of sea water (summarized in Anderson and Arthur, 1983; James and Choquette, 1983). These systematic variations lend further support to the validity of isotopic "marine signatures" in ancient limestones (Choquette, 1968; James and Choquette, 1983). The heaviest $\delta^{18}O$ values usually occur in the best preserved components and thus are probably closest to an unmodified $\delta^{18}O$ (e.g. Given and Lohmann, 1985). Based upon the heaviest values from well-preserved Port au Port samples (Middle Cambrian hardground of -7.3 o/oo; Upper Cambrian radial ooids of -7.6 o/oo), a $\delta^{18}O$ value of approximately -7.5 o/oo is an estimate of the typical marine oxygen isotopic signature for inorganic precipitation in the Middle and Upper Cambrian (Fig. 9.2). This is compatible with other $\delta^{18}O$ estimates from other Lower Paleozoic sequences (e.g., -4.8 o/oo in the Lower Cambrian, western Newfoundland -- James and Klappa, 1983; -8.0 o/oo in the Lower Ordovician, western Newfoundland -- Haywick, 1985; -5.3 in Lower and Middle Ordovician, western Newfoundland -- Coniglio, 1985).

From field and petrographic observations, a spectrum of early and late diagenetic features has been recognized in Port au Port limestones. Yet, surprisingly, no oxygen isotopic trend accompanies progressive burial diagenesis; $\delta^{18}O$ values tend to cluster tightly between -8.0 and -9.5 o/oo. Assuming that the heaviest values (-7.3 to -7.6 o/oo) are closest to the original $\delta^{18}O$ of Cambrian inorganic precipitates, the slightly lighter $\delta^{18}O$ of most of the ooids, mudstones, and synsedimentary and burial cements may be due to several causes: (1) initial transformation of aragonite and Mg calcite sediment and early cements to calcite occurred during deep burial diagenesis (cf. Allan and Matthews,

1982); (2) sediments and early cements altered in a shallow-burial meteoric setting, and the meteoric calcite cements acquired and retained meteoric $\delta^{18}O$ values that are similar to $\delta^{18}O$ of deep-burial calcite cements (e.g., rock-dominated system; Meyers and Lohmann, 1985; Czerniakowski et al., 1984); and (3) re-equilibration at higher temperatures and/or with lighter $\delta^{18}O$ pore fluids at burial depths (e.g., Hudson, 1977; Dickson and Coleman, 1980).

The first possibility is rejected in light of previously discussed petrographic and CL evidence that suggests that initial alteration of ooids and synsedimentary cements; some mudstone lithification; and prismatic calcite cementation are possible shallow-burial meteoric events. The latter two possibilities are more feasible; available information, however, does not enable a choice to be made between these two alternatives.

9.3.2.2 $\delta^{13}C$

The $\delta^{13}C$ of Port au Port limestones is similar to that in Holocene and ancient shallow marine sediments (Veizer and Hoefs, 1976; Hudson, 1977; James and Choquette, 1983); Veizer and Hoefs (1976) reported whole-rock $\delta^{13}C$ values for Cambrian limestones of -3 to +1 o/oo. The narrow range of values (-0.6 to -2.4 o/oo) in the Port au Port Group suggests that either: (1) soil gas (e.g. Allan and Matthews, 1982) and bacterial oxidation of organics were not important sources of carbon (e.g. Irwin et al., 1977) -- in the lower Paleozoic, the role, if any, of soils is unresolved (however, see Beeunas and Knauth, 1985) or (2) diagenesis occurred in a rock-dominated system in which carbon is from remobilized

marine bicarbonate (e.g., Czerniakowski et al, 1984; Given and Lohmann, 1985; Meyers and Lohmann, 1985).

Two groupings, however, are apparent in the cluster of $\delta^{13}C$ values. The first grouping involves ooids in which finely preserved ooids are more ^{13}C-depleted than coarsely preserved ones by an average of approximately 1 o/oo. Both types of ooids are interpreted on the basis of petrography to have originated from the same Mg calcite precursors, and the clustering of $\delta^{13}C$ and $\delta^{18}O$ for each type of ooid further suggests alteration under slightly different pore-water conditions. The explanation for greater $\delta^{13}C$ of coarsely preserved ooids over finely preserved ooids is not straightforward. The differences may reflect inherent differences in the precursor ooids, and/or variations in carbon content in pore-water.

The second grouping includes two analyses of prismatic calcite which exhibit the heaviest $\delta^{13}C$ values in this study; their $\delta^{18}O$ values are variable. Based on petrographic evidence, which suggests these calcites are shallow-burial meteoric and possibly mixed marine-phreatic cements with an original calcite mineralogy, their relatively heavy $\delta^{13}C$ may be explained by either: (1) precipitation of this cement after dissolution or alteration of metastable sediments and cements which may have contributed marine carbon isotopes to pore-waters (cf. Dickson and Coleman, 1980) or (2) the influence of marine waters in the mixed marine-meteoric zone.

9.3.3 Summary

Interpretation of carbon and oxygen isotopic analyses of Port au Port limestones is inconclusive. These isotopic values do not independently illustrate the spectrum of early to late diagenetic fabrics interpreted on the basis of field and petrographic evidence. Values cluster between $\delta^{13}C$ of -0.6 and -2.4 o/oo and $\delta^{18}O$ of -7.3 and -10.4 o/oo and there are no obvious trends with progressive burial diagenesis.

The heaviest $\delta^{18}O$ values (approximately -7.5 o/oo) provide the closest estimate for the original marine signature of inorganic precipitates in Middle and Late Cambrian times. Most other $\delta^{18}O$ values are only slightly lighter than this estimate and the narrow range of $\delta^{18}O$ in early and late diagenetic calcites may be ascribed to factors such as re-equilibration at depth. The narrow range of $\delta^{13}C$ in Port au Port calcites is similar to that in modern and other ancient marine carbonates and suggests that organic sources of carbon were not important.

9.4 EARLY LITHIFICATION: IMPLICATIONS FOR A DEPOSITIONAL-DIAGENETIC MODEL

Previous chapters have demonstrated that the diagenetic pathway followed by carbonate sediments of the Port au Port Group is strongly controlled by the depositional environment and sediment composition. Considering the cyclical nature of the sequence, it would be logical to expect a consistent diagenetic pattern from which a predictive

depositional-diagenetic model could be constructed. A similar approach has been used by Heckel (1983) on Pennsylvanian cyclothems in Midcontinent North America. He demonstrated that: (1) basal, transgressive facies have a limited variety of diagenetic fabrics, suggesting that most diagenesis occurred under deep burial conditions and (2) upper, regressive facies exhibit a greater variety of features interpreted to indicate diagenesis in the marine phreatic and meteoric zones as well as under deep burial conditions.

Facies sequences in the Port au Port Group (described in Chap. 4) reveal no consistent diagenetic patterns. For meter-scale, oolite-laminite assemblages, this is not surprising in light of the unpredictable nature of these assemblages, postulated to be the result of rapidly migrating, peritidal environments. Parted limestone-shale cycles are meter-scale, shallowing-upward sequences which also do not exhibit any stratigraphic diagenetic patterns. Similar to oolite-laminite assemblages, they contain a variety of diagenetic features which are interpreted to be products of synsedimentary peritidal lithification; dolomitization and erosion; and later meteoric to burial diagenesis. Grand Cycles, composed of the above meter-scale assemblages, do not exhibit any systematic, large-scale variations in diagenetic features.

The widespread, peritidal conditions under which Port au Port sediments were deposited and modified appear to be the key factor behind the absence of small- and large-scale diagenetic patterns. Synsedimentary lithification prevailed in nearly all carbonate lithofacies, under widely fluctuating submarine and strandline subaerial

conditions. This process, along with shallow-burial lithification by prismatic clear calcite, formed the diagenetic framework for later compaction, deep-burial cementation, and dolomitization. This early lithification has been the recurring "diagenetic theme" throughout this study. Products of deeper burial are widespread, affecting all lithofacies, but are of secondary importance in determining the final appearance of the rocks. In summary, unlike Heckel's (1983) model, the depositional-diagenetic model for the Port au Port carbonates is characterized by the variability and facies- and fabric-specific nature of early lithification and dolomitization, and the diffuse overprint of later burial diagenesis. The absence of pervasive diagenetic patterns throughout the sequence further emphasizes the importance of early peritidal lithification and the interplay of submarine and strandline subaerial conditions in early Paleozoic shallow marine settings.

Chapter 10

CONCLUSIONS

The Middle and Upper Cambrian Port au Port Group in western Newfoundland is a sequence of carbonates and siliciclastics deposited on an outer pertidal platform on the south-facing margin of the Iápetus Ocean. These rocks display a spectrum of depositional and diagenetic structures that reflects their shallow-water origin and protracted diagenetic history.

10.1 STRATIGRAPHY

The Port au Port Group is provisionally divided into three formations which in ascending order are: (1) the March Point Formation (late Middle Cambrian age) composed predominantly of thinly interbedded mudstones, dolostones and shales; (2) the Petit Jardin Formation (late Middle to Late Cambrian age); a complex sequence of thick-bedded ooid grainstones and laminated dolostones interbedded with thin-bedded mudstones, dolostones, and shales; and (3) the Berry Head Formation (?latest Late Cambrian age) composed of dolomitized grainstones and stromatolites, and laminated dolostones. In the type area of the Port au Port Peninsula, the Petit Jardin Formation is further divisible into five members, in

ascending order: the Cape Ann, Campbells, Big Cove, Felix, and Man O' War Members.

From lithologic correlations between the type area and other Newfoundland outcrops to the north, the March Point and Berry Head Formations have relatively uniform lithologies and are readily recognized in all areas. The Petit Jardin Formation, in contrast, is lithologically more variable and forms two southwest-northeast trending facies belts: an easterly carbonate belt including White Bay and Goose Arm outcrops and a westerly, mixed carbonate and siliciclastic belt including the Port au Port Peninsula, Bonne Bay, Canada Bay and St. Barbe outcrops.

10.2 SEDIMENTOLOGY

Based on Port au Port Peninsula outcrops, six lithofacies are recognized:

Parted Limestones: Parted limestones, composed of thinly interbedded mudstone and argillaceous dolostone/grey shale, are interpreted to be muddy tidal flat deposits. They are texturally similar to some modern siliciclastic tidal flat sediments and are unlike modern carbonate tidal deposits. Limestones were deposited by peak ebb and flood tidal currents while dolostones and shales settled out of suspension during periods of slack high tide. Flaser, wavy and lenticular bedding are well preserved and represent shallow subtidal, intertidal and supratidal deposition respectively. Abundant interbedded flat-pebble conglomerates

are interpreted to be storm-derived.

Shales: Grey shales associated with parted limestones and variegated red and green shales interbedded with ooid calcarenites/carbonate laminites are interpreted to be intertidal to supratidal deposits. Grey shales are regarded as slack tide deposits on a muddy tidal flat; variegated shales are considered to be supratidal deposits on a carbonate sand shoal complex respectively. A nearshore supply of siliciclastic mud was probably reworked by high energy events (e.g. storms) or rising relative sea level, resulting in the sporadic deposition of these muds in carbonate-dominated environments. This intertidal-supratidal distribution of siliciclastic mud is in contrast to many comparable carbonate platform sequences in which the shales are interpreted to be deeper water deposits.

Ooid Calcarenites: The two types of ooid calcarenites, grey oolite and brown oolite, and the associated carbonate laminites are interpreted to have formed heterogenous, carbonate sand shoal complexes. Grey oolites, which lack mud and evidence of subaerial exposure, are interpreted to be deposits of a high energy, subtidal mobil sand fringe. Brown oolites, with intercalated mudcracked mudstone beds indicating intermittent subaerial exposure and fluctuating energy conditions, are interpreted to be intertidal sand flat deposits. This model is in contrast to Bahamian platform-rim ooid shoals, composed of long and narrow or spill-over type bars and tidal channels, and alongshore oolite deposits of the Persian Gulf.

Carbonate Laminites: Dolostone and limestone laminites, with abundant

evidence of subaerial exposure, are interpreted to be supratidal deposits. Dololaminites interbedded wth parted limestones represent supratidal deposition in muddy tidal flats during periods of low siliciclastic mud influx. Carbonate laminites interbedded with ooid calcarenites are interpreted to be the supratidal crest facies of carbonate sand shoals.

Stromatolite and Thrombolite Mounds: Stromatolites and thrombolites forming a plethora of biostromes and bioherms have variable shapes and internal composition. Morphology and inter-mound lithologies suggest that stromatolites grew in shallow subtidal, intertidal and supratidal zones of both carbonate shoal complexes and muddy tidal flats: hemispherical mounds in the subtidal to lower intertidal; columnar and digitate forms in the higher energy intertidal; and stratiform stromatolites in the upper intertidal to supratidal. Thrombolites are interpreted as algal patch reefs which, on the basis of the associated lithofacies, grew in shallow subtidal to intertidal environments.

Glauconitic Sandstones and Oolites: A bimodal grain-size of rounded siliciclastic sands and angular silts is present throughout. Silt-size quartz and feldspar are ubiquitous and interpreted to be eolian. Glauconitic, siliciclastic sandstones and arenaceous limestones at the base of the sequence are regarded as remobilized and reworked sediments of the underlying Hawke Bay siltciclastic sandstones that were deposited in a shallow subtidal environment. Sand-size quartz and feldspar in the Port au Port limestones and dolostones are associated with brown oolite, either as scattered grains or in thin beds; they are interpreted to have been reworked from a nearshore environment by storms or extreme tides

and trapped in the carbonate sand shoal complexes. The occurrence of glauconite with siliciclastic sands suggests extensive reworking and concentration of grains, possibly during low stands of sea-level.

The environmental conditions during Port au Port deposition were: (1) a tidal range of at least 2 m (mesotidal) -- indicated by flaser, wavy and lenticular bedding and thickness of sediment packages in parted limestones; (2) periodically high energy conditions on both muddy tidal flats and carbonate sand shoal complexes and good circulation with the open ocean --- suggested by the abundance of ooid calcarenites and well-developed bedding structures in parted limestones; (3) a humid climate — indicated by the well-developed paleokarst and absence of evidence of evaporites; and (4) deposition in very shallow subtidal, intertidal and supratidal environments -- evidence for extensive deep subtidal deposition is absent.

10.3 FACIES SEQUENCES

Small- and large-scale sedimentary assemblages are the most obvious sedimentary features of the Port au Port Group on the Port au Port Peninsula.

Predictable meter-scale, shallowing-upward cycles of parted limestone and shale are most reasonably accounted for by an autocyclic mechanism. These muddy tidal flat cycles are interpreted to be controlled in large part by variable rates of subtidal carbonate sedimentation under

conditions of constant sea-level rise and/or subsidence. Meter-scale, oolite-laminite assemblages, in contrast, are characterized by unpredictable lithofacies sequences. They are best explained by vertical accretion and frequent, rapid migration of the carbonate shoal complex in response to hydrographic factors, such as tidal variations and storms. Both assemblages are punctuated by sediments interpreted as storm deposits or "tempestites"; these include: (1) flat-pebble conglomerates and gutter casts in parted limestones; (2) grey oolite beds in parted limestones; and (3) occasional "waning energy" sequences in brown oolites.

Large-scale cycles or Grand Cycles are composed of a lower shaly half-cycle of parted limestone-shale cycles and an upper carbonate half-cycle of oolite-laminite assemblages. These cycles are variably developed in the mixed carbonate and siliciclastic belt. They are interpreted to represent: (1) inundation of the platform by shoreward-derived siliciclastic muds during a rapid marine transgression and (2) the gradual development of a carbonate shoal and leeward tidal flat during the period of waning siliciclastic influx and slowed transgression. Comparison with other North American Grand Cycles suggests a eustatic mechanism of formation, possibly involving variations in the rate of relative sea-level rise. Unlike the western North American examples, Newfoundland Grand Cycles are composed almost entirely of peritidal sediments; they are also thinner and have a smaller areal extent than those in the west. These differences may be due to such factors as narrower shelf widths; slower rates of sedimentation; and lower amplitudes of relative sea-level rise on the

now northeastern margin of the North American craton than on the western margin.

10.4 LITHIFICATION

Calcite cements in Port au Port sediments reflect a prolonged and convergent history of lithification involving: (1) facies-specific, fibrous and micritic calcites interpreted to be synsedimentary peritidal precipitates; (2) relatively rare, prismatic clear calcite considered to be possible shallow-burial meteoric cements; and (3) pervasive, blocky calcite interpreted to have precipitated during deep burial and subsequent re-exposure. Additional evidence for synsedimentary lithification is provided by a variety of conglomerate horizons, commonly flat-pebble conglomerates with mudstone and oolitic clasts; hardgrounds in parted limestones and grey oolites; and peritidal paleokarst in carbonate laminites.

The early cements and erosion surfaces indicate the collective influence of submarine and subaerial lithification, ie. peritidal lithification, in shallow marine deposits. The distribution and extent of this early lithification in Port au Port sediments appear to be the key factors governing the direction and extent of subsequent diagenesis.

10.5 ORIGIN AND DIAGENESIS OF OOIDS

Oolites of the Port au Port Group contain four types of facies-specific ooids that are interpreted to represent *in situ* precipitation and deposition in two distinct regimes in carbonate sand shoal complexes. Radial and radial-concentric ooids (grey oolite) of a subtidal mobile fringe were probably controlled in large part by the nature of grain transport (suspension versus bedload transport). The radial cortices are interpreted to have originally been entirely Mg calcite that underwent progressive burial alteration to give rise to a variety of ooid preservation styles.

Concentric and superficial radial ooids (brown oolite) are interpreted to have been deposited in an intertidal sand flat under fluctuating energy conditions. Cortices with concentric laminae are interpreted to have precipitated within the sand flat and to have been bimineralic: aragonitic laminae are now blocky calcite; and laminae of fibrous and micritic Mg calcite are well preserved as calcite. Radial ooids were transported from the mobile fringe and were originally Mg calcite.

The correlation between original mineralogy, morphology and environment of formation indicates that local physical conditions, such as turbulence and sea floor topography, influenced ooid formation in Cambrian times. This is absent in modern ooids suggesting that more widespread chemical and organic controls now prevail.

10.6 ORIGIN OF PARTED LIMESTONES

Parted limestones are most reasonably explained by diagenetic overprinting of primary sedimentary fabrics. The model consists of: (1) tidal deposition of rhythmically interbedded carbonate-rich and clay-rich sediments that were subject to burrowing and intermittent subaerial exposure; (2) synsedimentary and possible shallow-burial meteoric lithification of carbonate-rich beds to form mudstone; (3) "squashing" of clay-rich sediment and fracturing of mudstone; and (4) precipitation of ferroan dolomite, in part contemporaneous with mechanical compaction, in clay-rich sediment. Pressure solution accentuates or masks older primary and diagenetic features in parted limestones but does not result in additional fabrics.

Primary rhythmic bedding of carbonate-rich and clay-rich sediments appears to be the most significant factor controlling the nature of these parted limestones. This factor may be the denominator linking these rocks to lithologically similar parted limestones in other ancient platform and deeper marine sequences.

10.7 DOLOMITIZATION

The three CL types of dolomite occur individually in limestones and together in pervasively dolomitized limestones. Fabric-preserving,

syngenetic dolomite (red CL type) is specific to dololaminites and dolomitized brown oolites. Early diagenetic dolomites formed subsequent to early limestone lithification and prior to the last stage of blocky calcite cementation. These dolomites are non-facies specific and include: (1) zoned dolomite which is restricted to the Felix Member and Berry Head Formations and (2) the later, dull CL dolomite which is stratigraphically widespread. Their distribution is interpreted to have been controlled by the extent of synsedimentary and shallow-burial limestone lithification and later fracturing. The last stage of dolomitization, forming saddle dolomite, cross-cuts earlier dolomites; lines fractures and vugs; and postdates pressure solution. All dolomites were subjected to dedolomitization, probably related to Mississippian karstification and evaporite dissolution.

10.8 SUMMARY OF DIAGENESIS

The protracted sequence of diagenesis in Port au Port carbonates has three readily recognized components: (1) synsedimentary diagenesis characterized by facies-specific lithification, erosion and dolomitization under peritidal conditions; (2) late diagenesis which includes non-facies-specific deep burial cementation, dolomitization, and chemical and mechanical compaction; and (3) tectonically-related cementation and dedolomitization. Interpretation of intermediate processes, which include mineralogical transformations, mudstone lithification and cementation by prismatic clear calcite, is more difficult; petrography and their position between the synsedimentary and

late diagenetic stages, however, are compatible with a shallow-burial meteoric origin. The products of synsedimentary peritidal and minor shallow-burial lithification collectively determined the final appearance of the rocks; deeper burial and re-exposure events resulted in only a diffuse overprinting of all lithofacies. This diagenetic sequence is readily interpreted from field and petrographic evidence. Calcite stable carbon and oxygen isotopic analyses, however, do not reveal clear complementary trends.

10.9 SYNTHESIS

Platform carbonate and siliciclastic sediments of the Port au Port Group on the Port au Port Peninsula display a spectrum of sedimentary and diagenetic structures that enable interpretation of the history of these rocks and speculation about the ature of the Cambrian platform.

10.9.1 Paleogeographic and Depositional Setting

The Port au Port Group is part of the Cambro-Ordovician sequence that records the growth and destruction of a continental margin of the Iapetus Ocean. Paleogeographic reconstructions indicate that this margin was south-facing and situated at approximately 20-25 degrees S latitude, within the sub-tropical climate zone. Sedimentologic evidence, such as abundant surface paleokarst and absence of evidence for evaporites, further suggests relatively humid climatic conditions. The Port au Port Group represents deposition on the outer part of a narrow shelf,

estimated to be 200 km wide. Neither the cratonic shoreline nor the shelf-slope transition are exposed in western Newfoundland; inner shelf sediments are covered and coeval slope and basin sediments (ie. Cow Head and Curling Groups) are allochthonous, outcropping north of the Port au Port Peninsula.

Peritidal platform sediments of the Port au Port Group were deposited in two laterally adjacent mega-environments: (1) an extensive, outer ooid shoal complex deposited under high energy conditions and (2) muddy tidal flats situated cratonward of the shoal complex which probably pass landward into prograding terrestrial sediments. Bedding structures suggest a mesotidal range; good circulation with the open ocean; and frequent high energy conditions due to storms.

10.9.2 Synsedimentary Diagenesis

The Port au Port Group was subject to extensive peritidal lithification. In ooid shoal complexes, there was subtidal and intertidal cementation of oolites and algal biostromes; formation of hardgrounds in subtidal oolites; dolomitization and karstification of supratidal sediments; and the formation of abundant conglomerates. In muddy tidal flat settings, synsedimentary diagenesis resulted in lithification of carbonate-rich horizons in parted limestones; formation of hardgrounds in mudstones; cementation of algal bioherms and biostromes; and abundant flat-pebble conglomerates.

10.9.3 Depositional History

Mixed carbonate-siliciclastic sediments of the Port au Port Group represent the gradual transition from shallow-marine, siliciclastic deposition (Lower Cambrian Hawke Bay Formation) to predominantly carbonate accumulation (Lower Ordovician St. George Group). The sequence records the lateral migration of two mega-environments, ooid shoal complexes and muddy tidal flats, in response to a complex interplay of sea level eustasy, sedimentation rate and shelf morphology. On the Port au Port Peninsula, this interplay resulted in the generation of three large-scale cycles or Grand Cycles, each composed of a lower shaly half-cycle and an upper carbonate half-cycle. Superimposed on these Grand Cycles are meter-scale assemblages controlled mainly by variable rates of carbonate sedimentation.

The March Point Formation marks the beginning of the first shaly half-cycle, the base of Grand Cycle A. This formation records the onset of widespread, shallow subtidal conditions over much of the platform during rapid sea level rise. The siliciclastic sands at its base were probably derived from the subtidal reworking of siliciclastic sands from the underlying Hawke Bay Formation. Elsewhere in the March Point Formation, deposition of fine-grained carbonate sediments predominated to form parted limestones.

With continued sea level rise and advent of high energy conditions, the supply of siliciclastic muds derived from nearshore sources increased. This resulted in deposition of parted limestones and shales

of the overlying Cape Ann Member of the Petit Jardin Formation in a muddy tidal flat setting. Sedimentation generally kept pace with or exceeded sea level rise, resulting in the development of meter-scale, shallowing upward cycles. During storms, ooids were derived from a ooid shoal complex, located seaward of the tidal flat during deposition of the uppermost part of the Cape Ann Member.

As sea level rise slowed, the ooid shoal complex widened shelfward and encroached upon the adjacent tidal flat. Interbedded oolites and carbonate laminites of the Campbells Member were deposited, forming the carbonate half-cycle of Grand Cycle A, Storm and tidal processes caused frequent shifting of shoal deposits and resulted in unpredictable, meter-scale assemblages.

Renewed increase in the rate of sea level rise flooded inner portions of the platform, marking the onset of deposition of the Big Cove Member, the shaly half-cycle of Grand Cycle B. Muddy tidal flat conditions were re-established as sedimentation rates kept up with the rate of sea level rise. Deposition of mixed carbonate sediments and siliciclastic muds prevailed during this time, resulting in strata similar to that of the Cape Ann Member.

The seaward ooid shoal complex expanded laterally over the adjacent tidal flat once again as the rate of sea level rise decreased. This resulted in deposition of the Felix Member, the carbonate half-cycle of Grand Cycle B, which is composed of meter-scale assemblages similar to those of the Campbells Member. Near the end of this cycle, very shallow water conditions and reduced rates of carbonate sedimentation persisted

in the shoal complex, resulting in formation of the (sub-Elvinia unconformity). A slight increase in sea level rise temporarily re-established ooid shoal deposition at the end of this cycle.

A phase of rapid sea level rise flooded of the platform depositing the Man O' War Member, the shaly half-cycle of Grand Cycle C, but did not completely inundate the ooid shoal complex. The supply of remobilized siliciclastic mud was relatively small so that only the lowermost part of the member contains siliciclastic mud. Carbonate deposition in a muddy tidal flat environment was re-established and parted limestones characterize the rest of the member. Throughout this period, ooids were swept from the ooid shoal complex onto the muddy tidal flat.

With a decreasing rate of sea level rise, the ooid shoal complex expanded laterally, gradually blanketing most of what is now western Newfoundland and forming the Berry Head Formation.

10.9.4 Post-Depositional History

After deposition and synsedimentary diagenesis, carbonate sediments were altered during burial and tectonism. Shallow-burial (meteoric?) diagenesis affected all carbonate sediments and included the following processes: (1) dissolution of aragonite and Mg calcite to form molds; (2) transformation of Mg calcite and aragonite to calcite; (3) lithification of mudstone in parted limestones; and (4) precipitation of prismatic, clear calcite cements. The lack of conclusive evidence for meteoric diagenesis may be related to insufficient periods of subaerial exposure; the predominance of calcitic components; or the pervasiveness

of synsedimentary diagenesis.

Progressive burial to an estimated depth of 3-4 km resulted in continued alteration of these sediments. Diagenetic processes included: (1) mechanical compaction; (2) alteration of ooids to coarsely crystalline calcite; (3) multi-stage dolomitization; (4) fracturing (during Middle Ordovician Taconic Orogeny); and (5) cementation by blocky calcite.

The sediments were further altered during Late Devonian Acadian uplift and faulting; karstification during the Carboniferous; and diagenesis of Carboniferous carbonates and evaporites. This latest stage involved fracturing; cementation by blocky calcite; and dedolomitization.

REFERENCES

Ager, D.V., 1974, Storm deposits in the Jurassic of the Moroccan High Atlas: Paleogeography, Paleoclimatology, and Paleoecology, v. 15, p. 83-93.

Ahr, W.M., 1971, Paleoenvironment, algal structures and fossil algae in the Upper Cambrian of central Texas: Journal of Sedimentary Petrology, v. 41, p. 205-216.

Aigner, T., 1982, Calcareous tempestites: storm-dominated stratification in Upper Muschelkalk Limestones (Middle Trias, SW-Germany): in Einsele, G., and Seilacher, A., eds., Cyclic and Event Stratification, Springer-Verlag, New York, p. 180-198.

Aigner, T., and Futterer, E., 1978, Kolk-Topfe und - Rinnen (pot and gutter casts) in Muschelkalk - Anzeiger fur Wattenmeer?: Neues Jahrbuch fur Geologie und Palaontologie, Abh. 156, p. 285-304.

Aitken, J.D., 1966, Middle Cambrian to Middle Ordovician cyclic sedimentation, southern Rocky Mountains of Alberta: Bulletin of Canadian Petroleum Geology, v. 14, p. 405-441.

Aitken, J.D., 1967, Classification and environmental significance of cryptalgal limestones and dolostones, with illustrations from the Cambrian and Ordovician of SW Alberta: Journal of Sedimentary Petrology, v. 37, p. 1163-1178.

Aitken, J.D., 1978, Revised models for depositional grand cycles, Cambrian of the southern Rocky Mountains, Canada: Bulletin of Canadian Petroleum Geology, v. 26, p. 515-542.

Aitken, J.D., 1981, Generalizations about Grand Cycles: in Taylor, M.E., ed., Short Papers for the Second International Symposium on the Cambrian System, United States Department of the Interior, Geological Survey, Open File Report 81-743, p. 8-14.

Allan, J.R., and Matthews, R.K., 1982, Isotope signatures associated with early meteoric diagenesis: Sedimentology, v. 29, p. 797-817.

Amieux, P., 1982, La cathodoluminescence: Methode d'etude sedimentologique des carbonates: Bulletin de Centres Recherce Exploration-Production Elf-Aquitaine, v. 6, p. 437-483.

Anderson, E.J., and Goodwin, P.W., 1980, Application of the PAC hypothesis to limestones of the Helderberg Group: Society of Economic Paleontologists and Mineralogists, Eastern Section Guidebook, 32 p.

Anderson, E.J., Goodwin, P., and Sobieski, T., 1984, Episodic accumulation and the origin of formation boundaries in the Helderberg Group of New York State: Geology, v. 12, p. 120-123.

Anderson, T.F., and Arthur, M.A., 1983, Stable isotopes of oxygen and carbon and their implication to sedimentologic and paleoenvironmental problems: in Arthur, M.A., Anderson, T.F., Kaplan, I.R., Veizer, J., and Land, L.S., Stable Isotopes in Sedimentary Geology, Society of Economic Paleontologists and Mineralogists, Short Course no. 10, p. 1-1 - 1-151.

Assereto, R.L., and Kendall, C.G.St.C., 1971, Megapolygons in Landinian Limestones of Triassic of southern Alps: evidence of deformation by penecontemporaneous dessication and cementation: Journal of Sedimentary Petrology, v. 41, p. 715-723.

Assereto, R.L., and Kendall, C.G.St.C., 1977, Nature, origin and classification of peritidal tepee structures and related breccias: Sedimentology, v. 24, p. 153-210.

Back, W., Hanshaw, B.B., Plummer, N., Rahn, P.H., Rightmire, C.T., and Rubin, M., 1983, Process and rate of dedolomitization: mass transfer and ^{14}C dating in a regional carbonate aquifer: Geological Society of America Bulletin, v. 94, p. 1415-1429.

Ball, M.M., 1967, Carbonate sand bodies of Florida and the Bahamas: Journal of Sedimentary Petrology, v. 37, p. 556-591.

Baker, P.A., and Kastner, M., 1981, Constraints on the formation of sedimentary dolomite: Science, v. 213, p. 214-216.

Bates, R.L., and Jackson, J.A., eds., 1980, Glossary of Geology, second edition: American Geological Institute, Virginia.

Bathurst, R.G.C., 1967, Oolitic films on low energy carbonate sand grains, Bimimi Lagoon, Bahamas: Marine Geology, v. 5, p. 89-109.

Bathurst, R.G.C., 1975, Carbonate Sediments and their Diagenesis, second edition: Elsevier Scientific Publishing Company, New York, 658 p.

Bathurst, R.G.C., 1980a, Lithification of carbonate sediments: Science Progress, Oxford, v. 66, p. 451-471.

Bathurst, R.G.C., 1980b, The roles of mechanical and chemical compaction in the deformation and diagenesis of carbonate sediments: in Humbert, L., ed., Cristallization, Deformation, Dissolution des Carbonate, Institut de Geodynamique, Universite de Bordeaux III, p. 25-32.

Bathurst, R.G.C., 1983, Neomorphic spar versus cement in some Jurassic grainstones: significance for evaluation of porosity evolution and compaction: Journal of Geological Society, v. 140, p. 220-237.

Bauld, J., 1981, Geobiological role of cyanobacteria mats in sedimentary environments: production and preservation of organic matter: Bureau of Mineral Resources, Journal of Australian Geology and Geophysics, v. 6, p. 307-317.

Beales, F.W., and Hardy, J.L., 1980, Criteria for the recognition of diverse dolomite types with an emphasis on studies on host rocks for Mississippi Valley-type ore deposits: in Zenger, D.H., Dunham, J.B., and Ethington, R.L., eds., Concepts and Models of Dolomitization, Society of Economic Paleontologists and Mineralogists, Special Publication no. 28, p. 197-213.

Beeunas, M.A., and Knauth, L.P., 1985, Preserved stable isotopic signature by subaerial diagenesis in the 1.2-b.y. Mescal Limestone, central Arizona: implications for the timing and development of terrestrial plant cover: Gological Society of America, v. 96, p. 737-745.

Benson, L.V., and Matthews, R.K., 1971, Electron microprobe studies of magnesium distribution in carbonate cements and recrystallized skeletal grainstones from the Pleistocene of Barbados, West Indies: Journal of Sedimentary Petrology, v. 41, p. 1018-1025.

Betz, F., 1939, Geology and mineral deposits of the Canada Bay area, Northern Newfoundland: Geological Survey of Newfoundland Bulletin 16, 53 p.

Boyce, W.D., 1977, New Cambrian trilobites from western Newfoundland: unpublished B.Sc. thesis, Memorial University of Newfoundland, 66 p.

Boyce, W.D., 1979, Further developments in western Newfoundland biostratigraphy: in Mineral Development Division, Department of Mines and Energy, Government of Newfoundland and Labrador, Report 79-1, p. 7-10.

Bricker, O.P., 1971, Carbonate Cements: Johns Hopkins Press, Baltimore, 376 p.

Bromley, R.G., 1967, Some observations on burrows of thalassinidean Crustacea in Chalk hardgrounds: Quarterly Journal of the Geological Society of London, v. 123, p. 157-177.

Bromley, R.G., 1975, Trace fossils at omission surfaces: in Frey, R.W., ed., Study of Trace Fossils, Springer-Verlag, New York, p. 399-428.

Bromley, R.G., 1978, Hardground diagenesis: in Fairbridge, R.W., and Bourgeois, J., eds., Encyclopedia of Earth Sciences, v. VI, Dowden, Hutchinson & Ross Inc., Pennsylvania, p. 397-399.

Budai, J.M., Lohmann, K.C., and Owen, R.M., 1984, Burial dedolomite in the Mississippian Madison Limestone, Wyoming and Utah Thrust Belt: Journal of Sedimentary Petrology, v. 54, p. 276-288.

Buxton, T.M., and Sibley, D.F., 1981, Pressure solution features in a shallow buried limestone: Journal of Sedimentary Petrology, v. 51, p. 19-26.

Carozzi, A.V., 1963, Half-moon oolites: Journal of Sedimentary Petrology, v. 33, p. 633-645.

Carpenter, A.B., and Oglesby, T.W., 1976, A model for the formation of luminescently zoned calcite cements and its implications (abstract): Geological Society of America, Abstracts with Programs, v. 8, p. 469-470.

Cherns, L., 1982, Paleokarst, tidal erosion surfaces and stromatolites in the Silurian Eke Formation of Gotland, Sweden: Sedimentology, v. 29, p. 819-833.

Choquette, P.W., 1968, Marine diagenesis of shallow marine lime-mud sediments: insights from $\delta^{18}O$ and $\delta^{13}C$ data: Science, v. 161, p. 1130-1132.

Choquette, P.W., and Pray, L.C., 1970, Geologic nomenclature and classification of porosity in sedimentary carbonates: American Association of Petroleum Geologists Bulletin, v. 54, p. 207-250.

Coniglio, M., 1985, Origin and diagenesis of fine-grained slope sediments, Cow Head Group (Cambro-Ordovician), western Newfoundland: unpublished Ph.D. thesis, Memorial University of Newfoundland, 648 p.

Cook, H.E., and Taylor, M.E., 1977, Comparison of continental slope and shelf environments in the Upper Cambrian and Lowest Ordovician of Nevada: in Cook, H.E., and Enos, P., eds., Deep-Water Carbonate Environments, Society of Economic Paleontologists and Mineralogists, Special Publication no. 25, p. 51-81.

Cowie, J.W., and Cribb, S.J., 1978, The Cambrian System: in Cohee, G.V., et al., eds., Contribution to the Geologic Time Scale, American Association of Petroleum Geologists, Studies in Geology no. 6, p. 355-362.

Czerniakowski, L.A.; Lohmann, K.C., and Wilson, J.L., 1984, Closed-system marine burial diagenesis: isotopic data from the Austin Chalk and its components: Sedimentology, v. 31, p. 863-877.

Davies, G.R., 1970, Carbonate bank sedimentation, eastern Shark Bay, Western Australia: American Association of Petroleum Geologists Memoir 13, p. 85-168.

Davies, G.R., 1977, Former magnesian calcite and aragonite submarine cements in Upper Paleozoic reefs of the Canadian Arctic: a summary: Geology, v. 5, p. 11-15.

Davies, P.J., Bubela, B., and Ferguson, J., 1978, The formation of ooids: Sedimentology, v. 25, p. 703-731.

Davies, P.J., and Martin, K., 1976, Radial aragonite ooids, Lizard Island, Great Barrier Reef, Queensland, Australia: Geology, v. 4, p. 120-122.

Demicco, R.V., 1982, Upper Cambrian Conococheague Limestone: in Lyttle, P.T., ed., Central Appalchian Geology, NE-SE Geological Society of America, 1982 Field Trip Guidebooks, American Geological Institute, p. 217-266.

Demicco, R.V., 1983, Wavy and lenticular-bedded carbonate ribbon rocks of the Upper Cambrian Conococheague Limestone, central Appalachians: Journal of Sedimentary Petrology, v. 53, p. 1121-1132.

Dickson, J.A.D., 1983, Graphical modelling of crystal aggregates and its relevance to cement diagnosis: Philosophical Transactions of the Royal Society of London, v. A309, p. 465-502.

Dickson, J.A.D., and Coleman, M.L, 1980, Changes in carbon and oxygen isotope composition during limestone diagenesis: Sedimentology, v. 27, p. 107-118.

Dix, G.R., 1981, The Codroy Group (Upper Mississippian) on the Port au Port Peninsula, western Newfoundland: stratigraphy, paleontology, sedimentology and diagenesis: unpublished M.Sc. thesis, Memorial University of Newfoundland, 218 p.

Dixon, J., 1976, Pattern carbonate - a diagenetic feature: Bulletin of Canadian Petroleum Geology, v. 24, p. 450-456.

Donahue, J., 1978, Pisolite: in Fairbridge, R.W., and Bourgeois, J., eds., Encyclopedia of Earth Sciences, v. VI, Dowden, Hutchinson & Ross Inc., Pennsylvania, p. 582-583.

Donaldson, J.A. and Ricketts, B.D., 1979, Beachrock in Proterozoic dolostone of the Belcher Islands, N.W.T., Canada: Journal of Sedimentary Petrology, v. 49, p. 1287-1294.

Dott, R.H., Jr., 1983, 1982 SEPM Presidential Address: Episodic sedimentation - How normal is average?: Journal of Sedimentary Petrology, v. 53, p. 5-23.

Dott, R.H., Jr., and Bourgeois, J., 1982, Hummocky stratification: significance of its variable bedding sequences: Geological Society of America Bulletin, v. 93, p. 663-680.

Dott, R.H., Jr., and Byers, C.W., 1980, SEPM Research Conference on modern shelf and ancient cratonic sedimentation - The orthoquartzite-carbonate suite revisited: Journal of Sedimentary Petrology, v. 50, p. 329-346.

Dravis, J., 1979, Rapid and widespread generation of Recent oolitic hardgrounds on a high energy Bahamian platform, Eleuthera Bank, Bahamas: Journal of Sedimentary Petrology, v. 49, p. 195-208.

Dunham, R.J., 1962, Classification of carbonate rocks according to depositional texture: in Ham, W.E., ed., Classification of Carbonate Rocks, American Association of Petroleum Geologists, Memoir 1, p. 108-121.

Dunham, R.J., 1971, Meniscus cement: in Bricker, O.P., ed., Carbonate Cements, Johns Hopkins Press, Baltimore, Maryland, p. 297-300.

Durney, D.W., and Ramsay, J.G., 1973, Incremental strain measured by syntectonic crystal growths: in De Jong, K.A., and Cholten, R., eds., Gravity and Tectonics, John Wiley & Sons, New York, p. 67-96.

Eardley, A.J., 1938, Sediments of Great Salt Lake, Utah: Bulletin of American Association of Petroleum Geologists, v. 22, p. 1305-1411.

Eder, W., 1982, Diagenetic redistribution of carbonate, a process in forming limestone-marl alternations (Devonian and Carboniferous) Rheinisches Schiefergebirge, W. Germany: in Einsele, G., and Seilacher, A., eds., Cyclic and Event Stratification, Springer-Verlag, New York, p. 98-112.

Edwards, D., Bassett, M.G., and Rogerson, E.C.W., 1979, The earliest vascular land plants; continuing the search for proof: Lethaia, v. 12, p. 313-324.

Einsele, G., 1982, Limestone-marl cycles (periodites): diagnosis, significance, causes - a review: in Einsele, G., and Seilacher, A., eds., Cyclic and Event Stratification, Springer-Verlag, New York, p. 8-53.

Esteban, M., and Klappa, C.F., 1983, Subaerial exposure: in Scholle, P.A., Bebout, D.G., and Moore, C.H., eds., Carbonate Depositional Environments, American Association of Petroleum Geologists Memoir 33, p. 1-54.

Fairbridge, R.W., and Bourgeois, J., eds., Encyclopedia of Earth Sciences, v. VI: Dowden, Hutchinson & Ross Inc., Pennsylvania.

Ferguson, J., Bubela, B., and Davies, P.J., 1978, Synthesis and possible mechanism of formation of radial carbonate ooids: Chemical Geology, v. 22, p. 285-308.

Fischer, A.G., 1981, Climatic oscillations in the biosphere: in Nitecki, M.H., ed., Biotic Crises in Ecological and Evolutionary Time, Academic Press, New York, p. 103-133.

Folk, R.L., 1965, Some aspects of recrystallization in ancient limestones: Society of Economic Paleontologists and Mineralogists, Special Publication no. 13, p. 14-48.

Folk, R.L., 1974a, The natural history of crystalline calcium carbonate: effect of magnesium content and salinity: Journal of Sedimentary Petrology, v. 44, p. 40-53.

Folk, R.L., 1974b, Petrology of Sedimentary Rocks: Hemphill Publishing Co., Austin, Texas, 182 p.

Folk, R.L., Andrews, P.B., and Lewis, D.W., 1970, Detrital sedimentary rock classification and nomenclature for use in New Zealand: New Zealand Journal of Geology and Geophysics, v. 13, p. 937-968.

Folk, R.L., and Land, L.S., 1975, Mg/Ca ratio and salinity: two controls over crystallization of dolomite: American Association of Petroleum Geologists Bulletin, v. 59, p. 60-68.

Frank, J.R., Carpenter, A.B., and Oglesby, T.W., 1982, Cathodoluminescence and composition of calcite cement in the Taum Sauk Limestone (Upper Cambrian), Southeast Missouri: Journal of Sedimentary Petrology, v. 52, p. 631-638.

Friedman, G.M., Amiel, A.J., Braun, M., and Miller, D.S., 1973, Generation of carbonate particles and laminites in algal mats - examples from sea-marginal hypersaline pool, Gulf of Aqaba, Red Sea: Bulletin of American Association of Petroleum Geologists, v. 57, p. 541-557.

Friedman, G.M., and Saunders, J.E., 1967, Origin and occurrence of dolostones: in Chilingar, G.V., Bissel, H.J., and Fairbridge, R.W, eds., Carbonate Rocks, Developments in Sedimentology 9, Elsevier, Amsterdam, p. 267-348.

Fritz, W.H., 1972, Corner-of-the-Beach Formation: in St. Julian, P., Hubert, C., Skidmore, W.D., and Beland, J., Appalachian Structure and Stratigraphy in Quebec, Excursion A56-C56, XXIV International Geological Congress, Montreal, p. 72-74.

Fritz, W.H., 1975, Broad correlations of some Lower and Middle Cambrian strata in North American Cordillera: Geological Survey of Canada Paper 75-1, part A, p. 533-540.

Garrison, R.E., and Kennedy, W.J., 1977, Origin of solution seams and flaser structure in Upper Cretaceous chalks of southern England: Sedmentary Geology, v. 19, p. 107-137.

Ginsburg, R.N., 1971, Landward movement of carbonate mud: new model for regressive cycles in carbonates (abstract): American Association of Petroleum Geologists Bulletin, v. 55, p. 340.

Given, R.K., and Lohmann, K.C., 1985, Derivation of the original isotopic composition of Permian marine cements: Journal of Sedimentary Petrology, v. 55, p. 430-439.

Given, R.K., and Wilkinson, B.H., 1985, Kinetic control of morphology, composition, and mineralogy of abiotic sedimentary carbonates: Journal of Sedimentary Petrology, v. 55, p. 109-119.

Goldhammer, R.K., Hardie, L.A., and Nguyen, C., 1985, Compactional features in Cambro-Ordovician carbonates of Central Appalachians and their significance (abstract): American Association of Petroleum Geologists Bulletin, v. 69, p. 257-258.

Grotzinger, J.P., 1985, Evolution of Early Proterozoic passive-margin carbonate platform, Rocknest Formation, Wopmay Orogen, N.W.T., Canada: unpublished Ph.D. thesis, Virginia Polytechnic Institute and State University, 225 p.

Grover, G., Jr., and Read, J.F., 1983, Paleoaquifer and deep burial related cements defined by regional cathodoluminescent patterns, Middle Ordovician carbonates, Virginia: American Association of Petroleum Geologists Bulletin, v. 67, p. 1275-1303.

Hallam, A., 1964, Origin of the limestone-shale rhythm in the Blue Lias of England: a composite theory: Journal of Geology, v. 72, p. 157-169.

Hallam, A., 1977, Secular changes in marine inundation of the USSR and North America through the Phanerozoic: Nature, v. 269, p. 769-772.

Halley, R.B., 1977, Ooid fabric and fracture in the Great Salt Lake and the geologic record: Journal of Sedimentary Petrology, v. 47, p. 1099-1120.

Hanshaw, B.B., Back, W.E., and Deike, R.G., 1971, A geochemical hypothesis for dolomitization by groundwater: Economic Geology, v.66,p. 710-724.

Hardie, L.A., Mitchell, R.W., III, and Demicco, R.V., 1982, Influence of early cementation on dolomitization and compaction in Cambro-Ordovician carbonates of central Appalachians (abstract): American Association of Petroleum Geologists Bulletin, v.66, p. 577.

Hardie, L.A., and Garrett, P., 1977a, General environmental setting - Chapter 4: in Hardie, L.A., ed., Sedimentation on the Modern Carbonate Tidal Flats of Northwest Andros Island, Bahamas, The Johns Hopkins University Press, Baltimore, p. 12-49.

Hardie, L.A., and Garret, P., 1977b, Some miscellaneous implications and speculations: in Hardie, L.A., ed., Sedimentation on the Modern Carbonate Tidal Flats of Northwest Andros Island, Bahamas, The Johns Hopkins University Press, Baltimore, p. 184-187.

Hardie, L.A., and Ginsburg, R.N., 1977, Layering: the origin and environmental significance of lamination and thin bedding: in Hardie, L.A., ed., Sedimentation on the Modern Carbonate Tidal Flats of Northwest Andros Island, Bahamas, The Johns Hopkins University Press, Baltimore, p. 50-123.

Harms, J.C., Southard, J.B., Spearing, D.R., and Walker, R.G., 1975, Depositional environments as interpreted from primary sedimentary structures and stratification sequences: Society of Economic Paleontologists and Mineralogists, Short Course no., 2, 161 p.

Harris, P.M., 1979, Facies anatomy of a Bahamian ooid shoal: Sedimenta VII, The Comparative Sedimentology Laboratory, The University of Miami, 163 p.

Hawley, N., 1981, Flume experiments on the origin of flaser bedding: Sedimentology, v. 28, p. 699-712.

Haywick, D.W., 1985, Dolomites in the St. George Group (Lower Ordovician), western Newfoundland: unpublished M.Sc. thesis, Memorial University of Newfoundland.

Heckel, P.H., 1983, Diagenetic model for carbonate rocks in Midcontinent Pennsylvanian eustatic cyclothems: Journal of Sedimentary Petrology, v. 53, p. 733-759.

Heller, P.L., Komar, P.D., and Pevear, D.R., 1980, Transport processes in ooid genesis: Journal of Sedimentary Petrology, v. 50, p. 943-952.

Heyl, G.R., 1937, The geology of the Sops Arm area, White Bay, Newfoundland: Newfoundland Department of Natural Resources, Geology Section, Bulletin 8, 42 p.

Hoffman, P., 1976, Stromatolite morphogenesis in Shark Bay, Western Australia, in Walter, M.R., ed., Stromatolites, Elsevier, Amsterdam, p. 261-272.

Holland, C.H., ed, 1971, Cambrian of the New World: Wiley-Interscience, New York, 456 p.

Hudson, J.D., 1977, Stable isotopes and limestone lithification: Journal of Geological Society of London, v. 133, p. 637-660.

Illing, L.V., 1954, Bahamian calcareous sands: American Association of Petroleum Geologists Bulletin, v. 38, p. 1-95.

Irwin, H., 1980, Early diagenetic carbonate precipitation and pore fluid migration in the Kimmeridge Clay of Dorset, England: Sedimentology, v. 27, p. 577-591.

Irwin, H., Curtis, C., and Coleman, M., 1977, Isotope evidence for source of diagenetic carbonates formed during burial of organic-rich sediments: Nature, 269, p. 209-213.

James, N.P., 1972, Holocenne and Pleistocene calcareous crust (caliche) profiles; criteria for subaerial exposure: Journal of Sedimentary Petrology, v. 42, p. 817-836.

James, N.P., 1974, Diagenesis of scleractinian corals in the subaerial vadose environment: Journal of Paleontology, v. 48, p. 758-799.

James, N.P., 1981, Megablocks of calcified algae in the Cow Head Breccia, western Newfoundland: vestiges of a Cambro-Ordovician platform margin: Geological Society of America Bulletin, part 1, v. 92, p. 799-811.

James, N.P., 1984, Shallowing-upward sequences in carbonates: in Walker, R.G., ed., Facies Models, second edition, Geoscience Canada Reprint Series 1, p. 213-228.

James, N.P., and Choquette, P.W., 1983, Limestones - The sea floor diagenetic environment: Geoscience Canada, v. 10, p. 162-179.

James, N.P., and Choquette, P.W., 1984, Limestones - The meteoric diagenetic environment: Geoscience Canada, v. 11, p. 161-194.

James, N.P., and Ginsburg, R.N., 1979, The seaward margin of Belize barrier and atoll reefs: International Association of Sedimentologists, Special Publication no. 3.

James, N.P., Ginsburg, R.N., Marszalek, D.S., and Choquette, P.W., 1976, Facies and fabric specificity of early subsea cements in shallow Belize (British Honduras) reefs: Journal of Sedimentary Petrology, v. 46, p. 523-544.

James, N.P., and Klappa, C.F., 1983, Petrogenesis of Early Cambrian reef limestones, Labrador, Canada: Journal of Sedimentary Petrology, v. 53, p. 1051-1096.

James, N.P., Knight, I. , and Chow, N., 1983, Middle and Upper Cambrian platform carbonates, western Newfoundland: Anatomy of a high-energy shelf (abstract): Geological Association of Canada, Newfoundland Section, 1983 Annual Spring Meeting, St. Johns, Newfoundland.

James, N.P., and Kobluk, D.R., 1978, Lower Cambrian patch reefs and associated sediments: southern Labrador, Canada: Sedimentology, v. 25, p. 1-35.

James, N.P., and Stevens, R.K., 1982, Anatomy and evolution of a lower Paleozoic continental margin, western Newfoundland: 11th International Congress on Sedimentology, Field Guidebook 2B, Hamilton, 75 p.

Kahle, C.F., 1974, Ooids from Great Salt Lake, Utah - as an analogue for the genesis and diagenesis of ooids in marine limestone: Journal of Sedimentary Petrology, v. 44, p. 30-39.

Kalkowsky, E., 1908, Oolith und Stromatolith im norddeutschen Bundsandstein: Deutsche Geologische Gesellschaft, Zeitschrift, Bd. 60, p. 68-125.

Kastner, M., 1984, Origin of dolomite and its spacial and chronological distribution - a new insight (abstract): Reservoir (Canadian Society of Petroleum Geolgists), v. 11, p. 1-3.

Kaye, C.A., 1959, Shoreline features and Quaternary shoreline changes, Puerto Rico: United States Geological Survey Professional Paper 317-B, p. 1-140.

Kendall, A.C., 1977, Fasicicular-optic calcite: a replacement of bundled acicular carbonate cements: Journal of Sedimentary Petrology, v. 47, p. 1056-1062.

Kendall, C.G.St.C., and Schlager, W., 1981, Carbonates and relative changes in sea level: Marine Geology, v. 44, p. 181-212.

Kendall, C.G.St.C., and Skipwith, Sir P.A.d'E., 1968, Recent algal mats of a Persian Gulf lagoon: Journal of Sedimentary Petrology, v. 38, p. 1040-1058.

Kindle, C.H., and Whittington, H.B., 1965, New Cambrian and Ordovician fossil localities in western Newfoundland: Geological Society of America Bulletin, v. 76, p. 683-688.

Klappa, C.F., Opalinski, P.R., and James, N.P., 1980, Middle Ordovician Table Head Group of western Newfoundland: a revised stratigraphy: Canadian Journal of Earth Science, v. 17, p. 1007-1019.

Klein, G. de V., 1971, A sedimentary model for determining paleotidal range: Geological Society of America Bulletin, v. 82, p. 2585-2592.

Knight, I. , 1977, Cambro-Ordovician platformal rocks of the Northern Peninsula, Newfoundland: Mineral Development Division, Department of Mines and Energy, Government of Newfoundland and Labrador, Report 77-6, 27 p.

Knight, I. , 1978, Platformal sediments on the Great Northern Peninsula, stratigraphic studies and geological mapping of the North St. Barbe District: in Mineral Development Division, Department of Mines and Energy, Government of Newfoundland and Labrador, Report 78-1, p. 140-150.

Knight, I. , 1979, Cambro-Ordovician platformal rocks of the Roddickton map sheet: in Mineral Development Division, Department of Mines and Energy, Government of Newfoundland and Labrador, Report 79-7, p. 1-3.

Knight, I. , 1980a, Geological mapping of parts of the Eddies Cove, Salmon River and adjacent map areas: in Mineral Development Division, Department of Mines and Energy, Government of Newfoundland and Labrador, Report 80-1, p. 1-9.

Knight, I. , 1980b, Cambro-Ordovician carbonate stratigraphy of western Newfoundland; sedimentation, diagenesis and zinc-lead mineralization: summary of a paper given at CIMM 82nd Annual General Meeting, Toronto, 34 p.

Knight, I. , and Saltman, P., 1980, Platformal rocks and geology of the Roddickton map area, Great Northern Peninsula: in Mineral Development Division, Department of Mines and Energy, Government of Newfoundland and Labrador, Report 80-1, p. 10-28.

Kobluk, D.R., 1984, Coastal paleokarst near the Ordovician-Silurian boundary, Manitoulin Island, Ontario: Bulletin of Canadian Petroleum Geology, v. 32, p. 398-407.

Kobluk, D.R., Pemberton, S.G., Karolyi, M., and Risk, M.J., 1977, The Silurian-Devonian disconformity in southern Ontario: Bulletin of Canadian Petroleum Geology, v. 25, p. 1157-1186.

Koopman, B.J., Lees, A., Piessens, P., and Sarnthein, M., 1979, Skeletal carbonate sands and wind-derived silty marls off the Saharan coast: Baie due Levrier, Arguin Platform, Mauritania: Meteor Forsch.-Ergebnisse, Reihe C, no. 30, seite 15-57.

Kreisa, R.D., 1981, Storm-generated sedimentary structures in subtidal marine facies with examples from the Middle and Upper Ordovician of southwestern Virginia: Journal of Sedimentary Petrology, v. 51, p. 823-848.

Kreisa, R.D., and Bambach, R.K., 1982, The role of storm processes in generating shell beds in Paleozoic shelf environments: in Einsele, G. and Seilacher, A., eds., Cyclic and Event Stratification, Springer-Verlag, p. 200-207.

Land, L.S., 1967, Diagenesis of skeletal carbonates: Journal of Sedimentary Petrology, v. 37, p. 914-930.

Land, L.S., 1973, Holocene meteoric dolomitization of Pleistocene limestones, North Jamaica, Sedimentology, v. 20, p. 411-424.

Land, L.S., 1980, The isotopic and trace element geochemistry of dolomite: the state of the art: Society of Economic Paleontologists and Mineralogists, Special Publication no. 28, p. 87-110.

Land, L.S., 1985, The origin of massive dolomite: Journal of Geological Education, v. 33, p. 112-125.

Land, L.S., Behrens, E.W., and Frishman, S.A., 1979, The ooids of Baffin Bay, Texas: Journal of Sedimentary Petrology, v. 49, p. 1269-1279.

Land, L.S., and Moore, C.H., 1980, Lithification, micrititization and syndepositional diagenesis of biolithites on the Jamaican island slope: Journal of Sedimentary Petrology, v. 50, p. 357-370.

Lasemi, Z., and Sandberg, P.A., 1984, Transformation of aragonite-dominated lime muds to microcrystalline limestones: Geology, v. 12, p. 420-423.

Larsonneur, G., 1975, Tidal deposits, Mont Saint-Michel Bay, France: in Ginsburg, R.N., ed., Tidal Deposits, Springer-Verlag, New York, p. 21-30.

Levesque, R.J., 1977, Stratigraphy and sedimentology of Middle Cambrian to Lower Ordovician shallow water carbonate rocks, Western Newfoundland: unpublished M.Sc. thesis, Memorial University of Newfoundland, 276 p.

Lilly, H.D., 1961, Geology of the Goose Arm-Hughes Brook area: unpublished M.Sc. thesis, Memorial University of Newfoundland, 123 p.

Lindstrom, M., 1979, Diagenesis of Lower Ordovician hardgrounds in Sweden: Geologica et Palaeontologica, v. 13, p. 9-30.

Lippman, F., 1973, Sedimentary Carbonate Minerals: Springer, Berlin, 229 p.

Lochman, C., 1938, Middle and Upper Cambrian fauna from Western Newfoundland: Journal of Paleontology, v. 12, p. 461-477.

Lock, B.E., 1969, The Lower Paleozoic geology of western White Bay, Newfoundland: unpublished Ph.D. thesis, Cambridge University, Cambridge, England, 343 p.

Logan, B.W., Rezak, R., and Ginsburg, R.N., 1964, Classification and environmental significance of algal stromatolites: Journal of Geology, v. 72, p. 68-83.

Logan, B.W., and Semeniuk, V., 1976, Dynamic metamorphism; processes and products in Devonian carbonate rocks, Canning Basin, Western Australia: Geological Society of Australia, Special Publication no. 6, 138 p.

Logan, Sir, W.E., 1863, Geology of Canada: Geological Survey of Canada, Report of progress from its commencement to 1863, Dawson Brothers, Montreal, 983 p.

Lohmann, K.C., 1977, Causitive factors of the outer detrital belt House Embayment: a sedimentological examination of a terrigenous-carbonate depositional system, Early Upper Cambrian (Dresbachian), east-central Utah and west-central Nevada: unpublished Ph.D. thesis, State University of New York at Stony Brook, 185 p.

Lohmann, K.C., and Meyers, W.J., 1977, Microdolomite inclusions in cloudy prismatic calcites: Journal of Sedimentary Petrology, v. 47, p. 1075-1088.

Longman, M.W., 1980, Carbonate diagenetic textures from nearsurface diagenetic environments: American Association of Petroleum Geologists Bulletin, v. 64, p. 461-487.

Longman, M.W., 1982, Depositional environments: in Sprinkle, J., ed., Echinoderm faunas from the Bromide Formation (Middle Ordovician) of Oklahoma, University of Kansas, Paleontological Contributions, Monograph 1.

Loreau, J.-P., and Purser, B.H., 1973, Distribution and ultrastructure of Holocene ooids in the Persian Gulf: in Purser, B.H., ed., Persian Gulf, Springer-Verlag, New York, p. 279-328.

Lowenstam, H., 1963, Biological problems relating to the composition and diagenesis of sediments: in Donnelly, T.W., ed., The Earth Sciences, University of Chicago Press, p. 137-195.

Lucia, F.J., 1961, Dedolomitization in the Tansill (Permian) Formation: Geological Society of America Bulletin, v. 72, p. 1107-1110.

MacIntyre, I.G., 1977, Distribution of submarine cements in a modern Caribbean fringing reef, Galeta Point, Panama: Journal of Sedimentary Petrology, v. 47, p. 503-516.

MacKenzie, F.T., and Pigott, J.D., 1981, Tectonic controls of Phanerozoic sedimentary rock cycling: Journal of Geological Society of London, v. 138, p. 183-196.

Macqueen, R.W., Ghent, E.D., and Davies, G.R., 1974, Magnesium distribution in living and fossil specimens of the echinoid Peronella lesceuric Agassiz, Shark Bay, western Australia: Journal of Sedimentary Petrology, v. 44, p. 60-69.

Margaritz, M., Goldenberg, L., Kafri, U., and Arad, A., 1980, Dolomite formation in the seawater-freshwater interface: Nature, v. 287, p. 622-624.

Markello, J.R., and Read, J.F., 1981, Carbonate ramp-to-deeper shale shelf transitions of an Upper Cambrian intrashelf basin, Nolichucky Formation, southwest Virginia Appalachians: Sedimentology, v. 28, p. 573-597.

Marshall, J.F., and Davies, P.J., 1975, High magnesium calcite ooids from the Great Barrier Reef: Journal of Sedimentary Petrology, v. 45, p. 285-291.

Mattes, B.W., and Mountjoy, E.W., 1980, Burial dolomitization of the Upper Devonian Mette buildup, Jasper National Park, Alberta: Society of Economic Paleontologists and Mineralogists, Special Publication no. 28, p. 259-320.

Matti, J.C., and McKee, E.D., 1976, Stable eustasy, regional subsidence and a carbonate factory: self-generating model for onlap-offlap cycles in shallow water carbonate sequences (abstract): Geological Society of America, Abstracts with Programs, v. 8, p. 1000-1001.

Mazzullo, S.J., 1977, Shrunken (geopetal) ooids: evidence of origin unrelated to carbonate-evaporite diagenesis: Journal of Sedimentary Petrology, v. 47, p. 392-397.

Mazzullo, S.J., and Cys, J.M., 1977, Submarine cements in Permian boundstones and reef-associated rocks, Guadelupe Mountains, west Texas and southeastern New Mexico: Society of Economic Paleontologists and Mineralogists, Permian Basin Section, Guidebook 77-16/1, p. 151-200.

Mazzullo, S.J., and Cys, J.M., 1979, Marine aragonite sea-floor growths and cements in Permian phylloid algal mounds, Sacramento, New Mexico: Journal of Sedimentary Petrology, v. 49, p. 917-936.

Medwedeff, D.A., and Wilkinson, B.H., 1983, Cortical fabrics in calcite and aragonite ooids: in Peryt, T.M., ed., Coated Grains, Springer-Verlag, Berlin, p. 109-115.

Meyers, W.J., 1974, Carbonate cement stratigraphy of the Lake Valley Formation (Mississippian) Sacramento Mountains, New Mexico: Journal of Sedimentary Petrology, v. 44, p. 837-861.

Meyers, W.J., 1978, Carbonate cements: their regional distribution and interpretation in Mississippian limestones of southwestern New Mexico: Sedimentology, v. 25, p. 371-400.

Meyers, W.J., 1980, Compaction in Mississippian skeletal limestones, southwestern New Mexico: Journal of Sedimentary Petrology, v. 50, p. 457-474.

Meyers, W.J., and Lohmann, K.C., 1978, Microdolomite-rich syntaxial cements: proposed meteoric-marine mixing zone phreatic cements from Mississippian limestones, New Mexico: Journal of Sedimentary Petrology, v. 48, p. 475-488.

Meyers, W.J., and Lohmann, K.C., 1985, Isotope geochemistry of regionally extensive calcite cement zones and marine components in Mississippian limestones, New Mexico: in Schneidermann, N., and Harris, P.M., eds., Carbonate Cements, Society of Economic Paleontologists and Mineralogists, Special Publication no. 36, p. 223-239.

Milliman, J.D., and Barretto, H.T., 1975, Relict magnesian calcite oolite and subsidence of the Amazon shelf: Sedimentology, v. 22, p. 137-145.

Mitterer, R.M., 1968, Amino acid composition of organic matrix in calcareous oolites: Science, v. 162, p. 1498-1499.

Morner, N., 1976, Eustasy and geoid changes: Journal of Geology, v. 84, p. 123-151.

Morner, N., 1983, Sea levels: in Gardner, R., and Scoging, H., eds., Mega-Geomorphology, Oxford University Press, p. 74-91.

Morrow, D.W., 1982a, Dolomite: Geoscience Canada, v. 9, p. 5-13.

Morrow, D.W., 1982b, Dolomitization models and ancient dolostones: Geoscience Canada, v. 9, p. 95-107.

Mossop, G.D., 1979, The evaporites of the Ordovician Baumann Fiord Formation, Ellesmere Island, Arctic Canada: Geological Survey of Canada Bulletin 298, 52 p.

Mount, J.F., and Rowland, S.M., 1981, Grand Cycle A (Lower Cambrian of the southern Great Basin: a product of differential rates of relative sea-level rise: in Taylor, M.E., ed., Short Papers for the 2nd International Symposium on the Cambrian System, United States Department of the Interior, Geological Survey, Open File Report 81-743, p. 143-146.

Newell, N.D., Purdy, E.G., and Imbrie, J., 1960, Bahamian oolitic sand: Journal of Geology, v. 68, p. 481-497.

Nicols, R.A.H., 1967, The "...sparite" complex: eosparite vs. neosparite: Journal of Sedimentary Petrology, v. 37, p. 1247-1248.

North, F.K., 1971, The Cambrian of Canada and Alaska: in Holland, C.H., ed., Cambrian of the New World, Wiley-Interscience, New York, p. 219-324.

North American Commision on Stratigraphic Nomenclature, 1983, North American Stratigraphic Code: American Association of Petroleum Geologists Bulletin, v. 67, p. 841-875.

Palmer, A.R., 1960, Some aspects of the early Upper Cambrian stratigraphpy of White Pine County, Nevada and vicinity: Intermountain Association of Petroleum Geologists, 11th Annual Field Conference, p. 53-58.

Palmer, A.R., 1969, Cambrian trilobite distributions in North America and their bearing on Cambrian paleogeography of Newfoundland: American Association of Petroleum Geologists Memoir 12, p. 139-144

Palmer, A.R., 1971, The Cambrian of the Appalachian and eastern New England regions, eastern United States: in Holland, C.H., ed., Cambrian of the New World, Wiley-Interscience, New York, p. 169-217.

Palmer, A.R., 1972, Problems of Cambrian biogeography: in 24th International Geological Congress, Paleontology, section 7, p. 310-315.

Palmer, A.R., 1981a, On the correlatability of Grand Cycle tops: in Taylor, M.E., ed., Short Papers for the 2nd International Symposium on the Cambrian System, United States Department of the Interior, Geological Survey, Open File Report 81-743, p. 156-159.

Palmer, A.R., 1981b, Subdivision of the Sauk sequence: in Taylor, M.E., ed., Short Papers for the 2nd International Symposium on the Cambrian System, United States Department of the Interior, Geological Survey, Open File Report 81-743, p. 160-162.

Palmer, A.R., and Halley, R.B., 1979, Physical stratigraphy and trilobite biostratigraphy of the Carrara Formation (Lower and Middle Cambrian) of the southern Great Basin: United States Geological Survey Professional Paper 1047, 131 p.

Palmer, A.R., and James, N.P., 1979, The Hawke Bay Event: a circum-Iapetus regression near the Lower-Middle Cambrian boundary: I.G.C.P. Meeting, Blacksburg, Virginia, p. A3.

Pettijohn, F.J., 1975, Sedimentary Rocks: Harper and Row Publishers, New York, 628 p.

Pfeil, R.W., and Read, J.F., 1980, Cambrian carbonate platform margin facies, Shady Dolomite, Southwestern Virginia, U.S.A.: Journal of Sedimentary Petrology, v. 50, p. 91-116.

Pigott, J.D., and MacKenzie, F.T., 1979, A signature of paleocean and atmospheric chemistry: Geological Society of America, Abstracts with Programs, 1979 Annual Meeting, p. 495-496.

Pingitore, N.E., Jr., 1976, Vadose and phreatic diagenesis: processes, products, and their recognition in corals: Journal of Sedimentary Petrology, v. 46, p. 985-1006.

Pingitore, N.E., Jr., 1978, The behaviour of Zn and Mn during carbonate diagenesis: theory and applications: Journal of Sedimentary Petrology, v. 48, p. 799-814.

Pingitore, N.E., Jr., 1982, The role of diffusion during carbonate diagenesis: Journal of Sedimentary Petrology, v. 52, p. 27-39.

Pitman, W.C., III, 1978, Relationship between eustacy and stratigraphic sequences of passive margins: Geological Society of America Bulletin, v. 89, p. 1389-1403.

Postma, H., 1961, Transport and accumulation of suspended matter in the Dutch Wadden Sea: Netherland Journal of Sea Research, v. 1, p. 148-190.

Powers, D.W., and Easterling, R.G., 1982, Improved methodology for using embedded Markov chains to describe cyclical sediments: Journal of Sedimentary Petrology, v. 52, p. 913-923.

Pratt, B.R., 1979, The St. George Group (Lower Ordovician), western Newfoundland: sedimentology, diagenesis and cryptalgal structures: unpublished M.Sc. thesis, Memorial University of Newfoundland, 254 p.

Pratt, B.R., 1982, Limestone response to stress: pressure solution and dolomitization - discussion and examples of compaction in carbonate sediments: Journal of Sedimentary Petrology, v. 52, p. 323-334.

Pratt, B.R., and James, N.P., 1982, Cryptalgal-metazoan bioherms of early Ordovican age in the St. George Group, western Newfoundland: Sedimentology, v. 29, p. 543-569.

Pratt, B.R., and James, N.P., in press, The St. George Group (Lower Ordovician) of western Newfoundland: tidal flat island model for carbonate sediments in epeiric seas: Sedimentology.

Purser, B.H., ed., 1973, The Persian Gulf: Springer-Verlag, New York, 471 p.

Purser, B.H., and Loreau, J.-P., 1973, Aragonitic, supratidal encrustations on the Trucial coast, Persian Gulf: in Purser, B.H., ed., The Persian Gulf, Springer-Verlag, New York, p. 343-376.

Radke, B.M., and Mathis, R.L., 1980, On the formation of saddle dolomite: Journal of Sedimentary Petrology, v. 50, p. 1149-1168.

Raiswell, R., 1971, Cementation in some Cambrian concretions, South Wales: in Bricker, O.P., ed., Carbonate Cements, The Johns Hopkins Press, Baltimore, Maryland, p. 196-197.

Read, J.F., 1976, Calcretes and their distinction from stromatolites: in Walters, M.R., ed., Stromatolites, Elsevier, Amsterdam, p. 55-71.

Read, J.F, and Grover, G.A., Jr., 1977, Scalloped and planar erosion surfaces, Middle Ordovician limestones, Virginia: analogues of Holocene exposed karst or tidal rock platforms: Journal of Sedimentary Petrology, v. 47, p. 956-972.

Read, J.F., and Pfeil, R.W., 1983, Fabrics of allochthonous reefal blocks, Shady Dolomite (Lower to Middle Cambrian), Virginia Appalachians: Journal of Sedimentary Petrology, v. 53, p. 761-779.

Reineck, H.E., 1975, German North Sea tidal flats: in Ginsburg, R.N., ed., Tidal Deposits, Springer-Verlag, New York, p. 5-12.

Reineck, H.E., and Singh, I.B., 1980, Depositional Sedimentary Environments, second edition: Springer-Verlag, New York, 439 p.

Reineck, H.E., and Wunderlich, F., 1968, Classification and origin of flaser and lenticular bedding: Sedimentology, v. 11, p. 99-104.

Rich, M., 1982, Ooid cortices composed of neomorphic pseudospar: possible evidence for ancient originally aragonite ooids: Journal of Sedimentary Petrology, v. 52, p. 843-847.

Richards, N., 1984, Ichnology of the March Point Formation (Middle Cambrian), Port au Port Peninsula, western Newfoundland: unpublished B.Sc. thesis, Queen's University, Kingston, Ontario, 48 p.

Richter, D.K., 1974, Zur subaerischen Diagenese von Echinidenskeletten und das relative Alter pleistozaner Karbonatterassen bei Korinth (Griechenland): Neues Jahrbuch fur Geologie und Palaohtologie Abh., v. 46, p. 51-77.

Richter, D.K., 1980, Former magnesian-calcite ooids in Paleozoic to Recent sediments (abstract): International Association of Sedimentologists, 1st European Regional Meeting 1980, Bochum, Germany.

Richter, D.K., and Fuchtbauer, H., 1978, Ferroan calcite replacement indicates former magnesian calcite skeletons: Sedimentology, v. 25, p. 843-860.

Richter, D.K., von Detlev, K., and Zinkernagel, U., 1981, Advances in cathode-luminescence in carbonate petrography: Sonderdruck aus der Geologischen Rundschau Band 70, p. 1276-1302.

Ritter, D.F., 1978, Process Geomorphology: Wm. C. Brown, Dubuque, Iowa, p. 465-511.

Robison, R.A., 1960, Lower and Middle Cambrian stratigraphy of the eastern Great Basin: in Geology of east-central Nevada, Intermountain Association of Petroleum Geologists, 11th Annual Field Conference Guidebook, p. 43-52.

Robinson, R.B., 1967, Diagenesis and porosity development in Recent and Pleistocene oolites from southern Florida and the Bahamas: Journal of Sedimentary Petrology, v. 37, p. 355-364.

Rodgers, J., 1965, Long Point and Clam Bank Formations, western Newfoundland: Geological Association of Canada Proceedings, v. 16, p. 83-94.

Rodgers, J., 1968, The eastern edge of the North American continent during the Cambrian and Early Ordovician: in Zen, E., White, W.S., Hadley, J.B., and Thompson, J.B., eds., Studies of Appalachian Geology: Northern and Maritime, John Wiley & Sons, New York, p. 141-150.

Rodgers, J., and Neale, E.R.W., 1963, Possible Taconic klippen in western Newfoundland: American Journal of Science, v. 261, p. 713-730.

Ross, R.J., Jr., Jaanusson, V., and Friedman, I., 1975, Lithology and origin of Middle Ordovician calcareous mudmound at Meiklejohn Peak, southern Nevada: United States Geological Survey Professional Paper 871, 48 p.

Rusnak, G.A., 1960, Some observations of recent oolites: Journal of Sedimentary Petrology, v. 30, p. 471-480.

Sandberg, P.A., 1975, New interpretations of Salt Lake ooids and of ancient non-skeletal carbonate mineralogy: Sedimentology, v. 22, p. 497-537.

Sandberg, P.A., 1983, An oscillating trend in Phanerozoic non-skeletal carbonate mineralogy: Nature, v. 305, p. 19-22.

Sandberg, P.A., and Popp, B.N., 1981, Pennsylvanian aragonite from southeastern Kansas - environmental and diagenetic implications (abstract): American Association of Petroleum Geologists Bulletin, v. 65, p. 985.

Sander, B., 1951, Contributions to the study of depositional fabric: translated by Knopf, E.B., American Association of Petroleum Geologists, 207 p.

Sass, E., and Kolodny, Y., 1972, Stable isotopes, chemistry and petrology of carbonate concretions (Mishash Formation, Israel): Chemical Geology, v. 10, p. 261-286.

Schneider, J.F., 1975, Recent tidal deposits, Abu Dhabi, UAE, Arabian Gulf: in Ginsburg, R.N., ed., Tidal Deposits, Springer-Verlag, New York, p. 209-214.

Scholle, P.A., and Halley, R.B., 1985, Burial diagenesis: out of sight, out of mind: in Schneiderman, N., and Harris, P.M., eds., Carbonate Cements, Society of Economic Paleontologists and Mineralogists, Special Publication no. 36, p. 309-334.

Schroeder, J.H., 1979, Carbonate diagenesis in Quaternary beachrock of Uyombo, Kenya - sequences of processes and coexistance of heterogenic products: Geologische Rundschau, v. 68, p. 894-919.

Schuchert, C., and Dunbar, C.O, 1934, Stratigraphy of Western Newfoundland: Geological Society of America, Memoir 1, 123 p.

Scotese, C.R., Bambach, R.K., Van der Voo, R., and Zeigler, A.M., 1979, Paleozoic base maps: Journal of Geology, v. 87, p. 217-268.

Sears, S.O., and Lucia, F.J., 1980, Dolomitization of northern Michigan Niagara reefs by brine refluxion and freshwater/seawater mixing: in Zenger, D.H., Dunham, J.B., and Ethington, R.L, eds., Concepts and Models of Dolomitization, Society of Economic Paleontologists and Mineralogists, Special Publication no. 28, p. 215-235.

Seilacher, A., 1982, General remarks about event deposits: in Einsele, G., and Seilacher, A., eds., Cyclic and Event Stratification, Springer-Verlag, p. 161-174.

Sepkoski, J.J., 1982, Flat-pebble conglomerates, storm deposits and the Cambrian bottom fauna; in Einsele, G., and Seilacher, A., eds., Cyclic and Event Stratification, Springer-Verlag, New York, p. 371-385.

Shearman, D.J., Twyman, J., and Karimi, M.Z., 1970, The genesis and diagenesis of oolites: Geological Association Proceedings, v. 81, p. 561-576.

Shinn, E.A., 1969, Submarine lithification of Holocene carbonate sediments in the Persian Gulf: Sedimentology, v. 12, p. 109-144.

Shinn, E.A., 1975, Polygonal cement sutures from the Holocene - a clue to recognition of submarine diagenesis (abstract): American Association of Petroleum Geologists, Society of Economic Paleontologists and Mineralogists Annual Meeting Abstracts, v. 2, p. 68.

Shinn, E.A., and Ginsburg, R.N., 1964, Formation of Recent dolomite in Florida and the Bahamas (abstract): Bulletin of American Association of Petroleum Geologists, v. 48, p. 547.

Shinn, E.A., Halley, R.B., Hudson, J.H., and Lidz, B.H., 1977, Limestone compaction: an enigma: Geology, v. 5, p. 21-24.

Shinn, E.A., Lloyd, R.M., and Ginsburg, R.N., 1969, Anatomy of a modern carbonate tidal flat, Andros Island, Bahamas: Journal of Sedimentary Petrology, v. 39, pl. 1202-1228.

Shinn, E.A., and Robbin, D.M., 1983, Mechanical and chemical compaction in fine-grained shallow-water limestones: Journal of Sedimentary Petrology, v. 53, p. 595-618.

Simone, L., 1981, Ooids: a review: Earth Science Reviews, v. 16, p. 319-355.

Sloss, L.L., 1963, Sequences in the cratonic interior of North America: Geological Society of America Bulletin, v. 74, p. 93-114.

Smit, D.E., 1971, Stratigraphy and sedimentary petrology of the Cambrian and Lower Ordovician shelf sequence in Western Newfoundland: unpublished Ph.D. thesis, University of Iowa, 192 p.

Smyth, W.R., 1981, Lower Paleozoic geology of southwestern White Bay: in Mineral Development Division, Department of Mines and Energy, Government of Newfoundland and Labrador, Report 81-1, p. 70-79.

Smyth, W.R., and Schillereff, H.S., 1982, The pre-Carboniferous geology of southwest White Bay: in Mineral Development Division, Department of Mines and Energy, Government of Newfoundland and Labrador, Report 82-1, p. 78-98.

Sommer, S.E., 1972, Cathodoluminescence of carbonates, 1. characterization of cathodoluminescence from carbonate solid solutions: Chemical Geology, v. 9, p. 257-273.

Sorby, H.C., 1879, On the structure and origin of limestones: in Summerson, C.H., ed., Sorby on Sedimentation, A Collection of Papers from 1851 to 1908 by Henry Clifton Sorby, Geological Milestones, v. 1, 1976, Comparative Sedimentology Laboratory, University of Miami, p. 59-113.

Stehli, F.G., 1965, Shell mineralogy of Paleozoic invertebrates, Science, v. 123, p. 1031.

Steinen, R.P., 1978, On the diagenesis of lime mud: scanning electron microscopic observations of subsurface material from Barbadoes, W.I.: Journal of Sedimentary Petrology, v. 48, p. 1139-1148.

Stevens, R.K., 1970, Cambro-Ordovician flysch sedimentation and tectonics in west Newfoundland and their possible bearing on a Proto-Atlantic Ocean: in Lajoie, J., ed., Flysch Sedimentology in North America, Geological Association of Canada, Special Paper no. 7, p. 165-177.

Stockdale, P.B., 1922, Stylolites: their nature and origin: Indiana University Studies, no. 55, vol. IX, 97 p.

Stockdale, P.B., 1943, Stylolites: primary or secondary?: Journal of Sedimentary Petrology, v. 13, p. 3-12.

Stouge, S., 1981, Cambrian-Middle Ordovician stratigraphy of Salmon River region, southwest Hare Bay, Great Northern Peninsula: in Mineral Development Division, Department of Milnes and Energy, Government of Newfoundland and Labrador, Report 81-1, p. 1-16.

Stouge, S., and Boyce, W.D., 1983, Fossils of northwestern Newfoundland and southeastern Labrador: conodonts and trilobites: Mineral Development Division, Department of Mines and Energy, Government of Newfoundland and Labrador, Report 83-3, 55 p.

Suess, E., 1970, Interaction of organic compounds with calcium carbonate - I, Phenomena and geochemical implications: Geochemica et Cosmochimica Acta, v. 34, p. 157-168.

Suess, E., and Futterer, D., 1972, Aragonitic ooids: experimental precipitation from seawater in the presence of humic acids: Sedimentology, v. 19, p. 129-139.

Sujkowski, Z.L, 1958, Diagenesis: American Association of Petroleum Geologists Bulletin, v. 42, p. 2692-2717.

Sweeting, M.M., 1972, Karst Landforms: Macmillan Publishing Co. Ltd., London, 362 p.

Swett, K., and Smit, D.E., 1972, Paleogeography and depositional environments of the Cambro-Ordovician shallow-marine facies of the North Atlantic: Geological Society of America Bulletin, v. 83, p. 3223-3248.

Taft, W.H., Arrington, F., Hainovitz, A., Macdonald, C., and Woolheater, C., 1968, Lithification of modern carbonate sediments at Yellow Bank, Bahamas: Bulletin of Marine Science Gulf Caribbean, v. 18, p. 762-828.

Teichert, C., 1970, Runzelmarken (wrinkle marks): Journal of Sedimentary Petrology, v. 40, p. 1056-1057.

Teiglar, D.J., and Towe, K.M., 1973, Microstructure and composition of the trilobite exoskeleton: in Martinsson, A., ed., Evolution and Morphology of the Trilobita, Trilobitoidea and Merostomata, Fossils and Strata no. 4, p. 137-151.

Thompson, R.W., 1975, Tidal-flat sediments of the Colorado River Delta, northwestern Gulf of California: in Ginsburg, R.N., ed., Tidal Deposits, Springer-Verlag, New York, p. 57-65.

Towe, K.M., and Hemleben, C., 1976, Diagenesis of magnesian calcite; evidence from miliolacean foraminifera: Geology, v. 4, p. 337-339.

Troelsen, J.C., 1947, Geology of the Bonne Bay-Trout River area, Newfoundland: unpublished Ph.D. thesis, Yale University, 289 p.

Tucker, M.E., 1984, Calcitic, aragonitic and mixed calcitic-aragonitic ooids from the mid-Proterozoic Belt Supergroup, Montana: Sedimentology, v. 31, p. 627-644.

Vail, P.R., Mitchum, R.M., and Thompson, S., III, 1977, Seismic stratigraphy and global changes of sea level, Part 3: Relative changes of sea level from coastal onlap: in Payton, C., ed., Seismic stratigraphy - applications to hydrocarbon exploration, American Association of Petroleum Geologists Memoir 26, p. 63-81.

Van Houten, F.B., and Purucker, M.E., 1984, Glauconitic peloids and chamositic ooids - favorable factors, constraints, and problems: Earth Science Reviews, v. 20, p. 211-243.

Veizer, J., and Hoefs, J., 1976, The nature of $^{18}O/^{16}O$ and $^{13}C/^{12}C$ trends in sedimentary carbonate rocks: Geochimica et Cosmochimica Acta, v. 40, p. 1387-1395.

Walker, R.G., 1984, Shelf and shallow marine sands: in Walker, R.G., ed., Facies Models, second edition, Geoscience Canada Reprint Series 1, p. 141-170.

Walthier, T.M., 1949, Geology and mineral deposits of the area between Corner Brook and Stephenville, Part I; and Geology and mineral deposits of the area between Lewis Hills and Bay St. George, western Newfoundland, Part II: Newfoundland Geological Survey, Bulletin no. 35, 87 p.

Wanless, H.R., 1979, Limestone response to stress: pressure solution and dolomitization: Journal of Sedimentary Petrology, v. 49, p. 437-462.

Wanless, H.R., 1983, Burial diagenesis in limestones: in Parker, A., and Sellwood, B.W., eds., Sediment Diagenesis, Reidel Publishing Co., Boston, p. 379-417.

Weimer, R.J., Howard, J.D., and Lindsay, D.R., 1982, Tidal flats: in Scholle, P.A., and Spearing, D.R., eds., Sandstone Depositonal Environments, American Association of Petroleum Geologists Memoir 31, p. 191-254.

Whitaker, J.H. McD., 1973, "Gutter casts" a new name for scour-and-fill stsructures: with examples from the Llandoverian of Ringerlike and Malmoya : Norsk. Geol. Tidsskr., v. 53, p. 403-417.

Whittington, H.B., and Kindle, C.H., 1966, Middle Cambrian strata at the Strait of Belle Isle, Newfoundland: Geological Society of America Abstracts, p. 46.

Whittington, H.B., and Kindle, C.H., 1969, Cambrian and Ordovician stratigraphy of western Newfoundland: in Kay, M., ed., North Atlantic Geology and Continental Drift, American Association of Petroleum Geologists Memoir 12, p. 655-664.

Wilkinson, B.H., 1979, Biomineralization, paleo-oceanography, and the evolution of calcareous marine organisms: Geology, v. 7, p. 524-527.

Wilkinson, B.H., 1982, Cyclic cratonic carbonates and Phanerozoic calcite seas: Journal of Geological Education, v. 30, p. 189-203.

Wilkinson, B.H., Buczynski, C., and Owen, R.M., 1984, Chemical control of carbonate phases: implications from Upper Pennsylvanian calcite-aragonite ooids of southeastern Kansas: Journal of Sedimentary Petrology, v. 54, p. 932-947.

Wilkinson, B.H., Janecke, S.U., and Brett, C.E., 1982, Low-magnesian calcite marine cement in Middle Ordovician hardgrounds from Kirkfield, Ontario: Journal of Sedimentary Petrology, v. 52, p. 47-57.

Wilkinson, B.H., Landing, E., 1978, "Eggshell diagenesis" and primary radial fabric in calcite ooids: Journal of Sedimentary Petrology, v. 48, p. 1129-1138.

Wilkinson, B.H., Owen, R.M., and Carroll, A.R., 1985, Submarine hydrothermal weathering, global eustasy, and carbonate polymorphism in Phanerozoic marine oolites: Journal of Sedimentary Petrology, v. 55, p. 171-183.

Williams, A., and Wright, A.D., 1970, Shell structure of the Craniacea and other calcareous inarticulate Brachiopods: Palaeontological Association of London, Special Paper no. 7, 51 p.

Williams, H., 1976, Tectonic stratigraphic subdivision of the Appalachian Orogen (abstract): Geological Society of America, Abstracts with Program, v. 8, p. 300.

Williams, H., 1979, Appalachian Orogen in Canada: Canadian Journal of Earth Science, v. 16, p. 792-807.

Williams, H., and Stevens, R.K., 1974, The ancient continental margin of eastern North America: in Burke, C.A., and Drake, C.L., eds., The Geology of Continental Margins, Springer-Verlag, New York, p. 781-796.

Wilson, J.L., 1975, Carbonate Facies in Geologic History: Springer-Verlag, New York, 471 p.

Wong, P.K., and Oldershaw, A.E., 1980, Causes of cyclicity in reef interior sediments, Kaybob reef, Alberta: Bulletin of Canadian Petroleum Geology, v. 28, p. 411-424.

Wood, H.M., 1983, Clay mineralogy of Middle Cambrian to Lower Ordovician sediments, Port au Port, Newfoundland: unpublished B.Sc. thesis, Memorial University of Newfoundland, 46 p.

ADDENDUM

Illing, L.V., Wells, A.J., and Taylor, J.C.M., 1965, Penecontemporary dolomite in the Persian Gulf: in Pray, L.C. and Murray, R.C., eds., Dolomitization and Limestone Diagenesis: a Symposium, Society of Economic Paleontologists and Mineralogists, Special Publication 13, p. 89-111.

Schillereff, S. and Williams, H., 1979, Geology of the Stephenville map area, Newfoundland: in Current Research, Part A, Geological Survey of Canada, Paper 79-1A, p. 327-332.

PLATES

All thin section photomicrographs are taken in plane-polarized light unless otherwise indicated.

PLATE 1: PARTED LIMESTONE LITHOFACIES

a, b: Parted limestone (type 1) with thin beds and nodules of mudstone (medium grey in photo) interbedded with thin beds and partings of tan-weathering, argillaceous dolostone (light grey in photo). Ripples (arrow) and gutter casts (G) are well developed in mudstone. A flat-pebble conglomerate bed (F) is present in middle of "a". Stratigraphic top is up. Man O' War Member; Felix to Man O' War Coves section, Bed 17.

c: Resistant weathering, ripple laminated mudstone interbedded with recessive-weathering, argillaceous dolostone and shale (type 2). Arrow points to isolated mudstone ripple. Stratigraphic top is up. Cape Ann Member; March Point section, Bed 10.

d: Grey, blocky mudstone nodules in a tan weathering, argillaceous dolostone matrix. Scale is lense cap in upper right of photo. Stratigraphic top is up. March Point Formation, Degras section, Bed 5.

e: Bedding plane view of dolomitized burrows in parted limestone similar to "d" above. March Point Formation; March Point section, Bed 5.

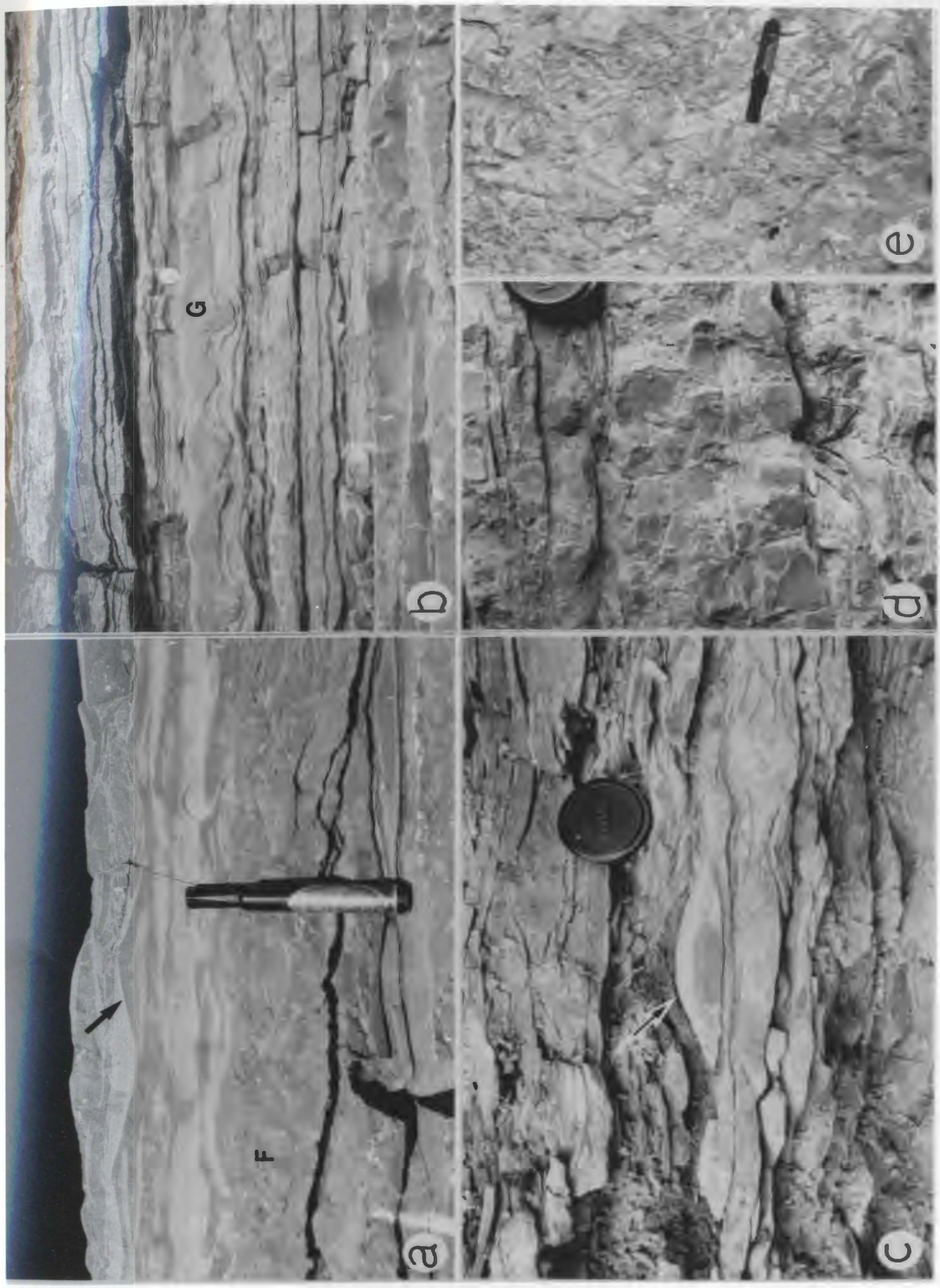
a
F
b
G
c
d
e

PLATE 2: PARTED LIMESTONE LITHOFACIES

a: Parted limestone-shale cycles, each consisting of: (A) lower, ripple cross-laminated limestone, and flaser-bedded parted limestone (type 2); (B) wavy-bedded parted limestone; and (C) upper, lenticular-bedded parted limestone, and grey shale. Cape Ann Member, March Point section, Bed 10.

b: Parted limestone-shale cycle similar to "a" above, but with type 1 parted limestone and an uppermost bed of tan-weathering dololaminite. Man O' War Member, Felix to Man O' War Coves section, Bed 18.

c: Transition interval between shaly half-cycle (dark grey in photo), composed predominantly of recessive-weathering parted limestone; and overlying carbonate half-cycle (light grey in photo), composed predominantly of resistant-weathering ooid calcarenite and dololaminite. Arrow points to the contact between the Cape Ann Member (shaly half-cycle) and the overlying Campbells Member (carbonate half-cycle). Scale bar is 2 m. Stratigraphic top is up. March Point section.

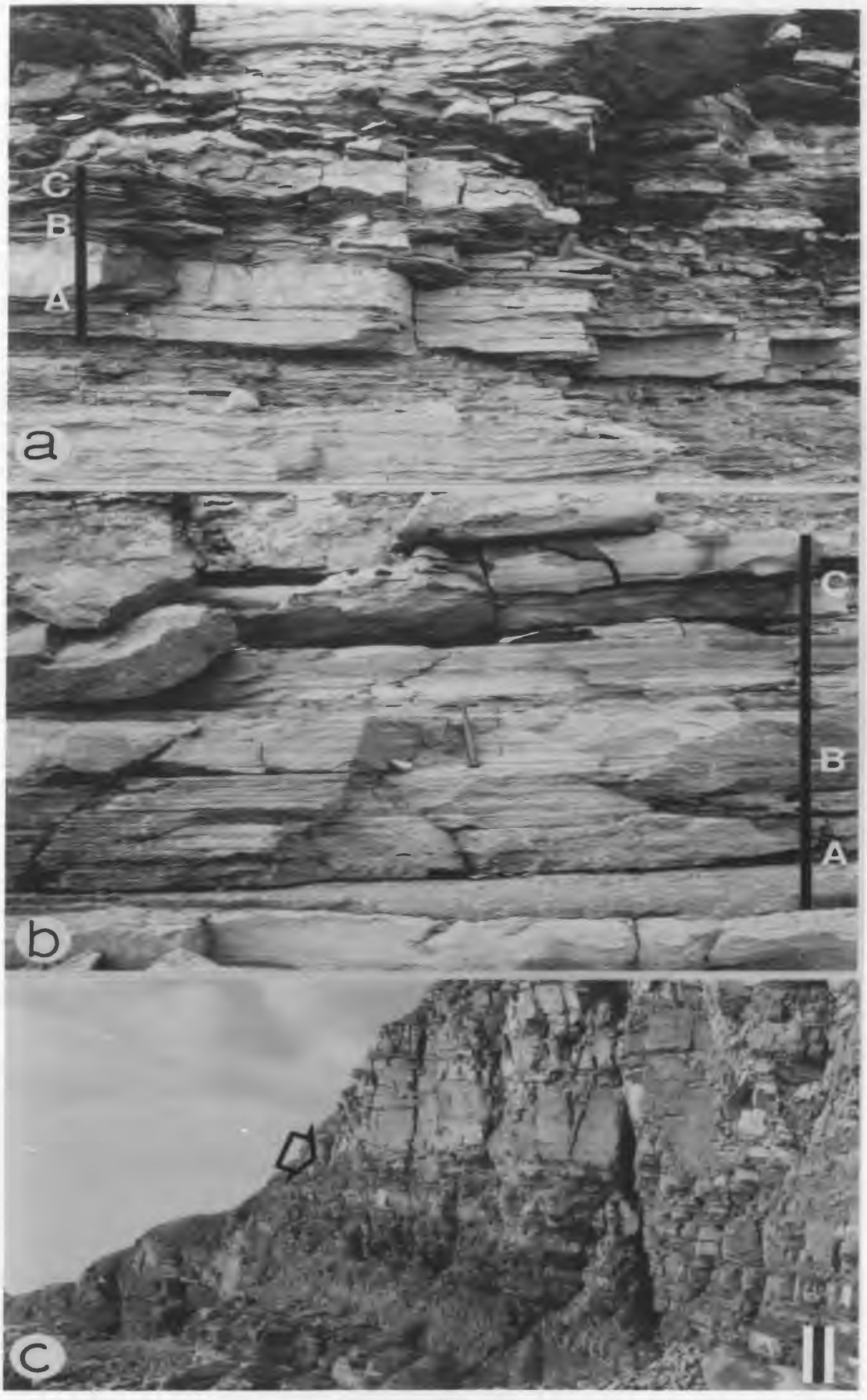
C
B
A
a
C
B
A
b
c

PLATE 3: OOID CALCARENITE LITHOFACIES

a: Resistant weathering sea cliffs of interbedded grey oolite (dark grey in photo), brown oolite and carbonate laminite (light grey in photo). Range pole is 1.2 m (arrow). Stratigraphic top is up. Campbells Member, March Point section, Beds 10-11.

b: Bedding plane view of grey oolite with large, flat-topped ripples, which have preferentially silicified crests (dark grey in photo). Range pole is 1 m. Man O' War Member, Felix to Man O' War Coves section, Bed 18.

c: Grey oolite composed of thin beds of resistant weathering pisoids (P) and ooids (O), which are preferentially dolomitized. Stratigraphic top is up. Man O' War Member, Felix to Man O' War Coves member, Bed 17.

d: Grey oolite (arrow) interbedded with parted limestone. Lower surface of oolite is gently undulose and erodes underlying parted limestone. Range pole is 1.2 m. Stratigraphic top is up. Big Cove Member, March Point section, Bed 6.

a
b
c
d

PLATE 4: OOID CALCARENITE LITHOFACIES

a: Dolomitized flat-pebble conglomerate in interbedded ooid calcarenites and dololaminites. Tabular clasts are horizontally to vertically disposed and are composed of grey oolite. Stratigraphic top is up. Felix Member, March Point section, Bed 3.

b: Thick-bedded brown oolite with herringbone cross-bedding, dolomitized mudstone clasts and thin, mudcracked beds (arrow) of the same lithology. Stratigraphic top is up. Campbells Member, March Point section, Bed 11.

c: Dolomitized brown oolite similar to "b" above. Mudcracked mudstone beds (light grey in photo) and underlying ripple forms of ooid calcarenite are pronounced. Felix Member, March Point section, Bed 5.

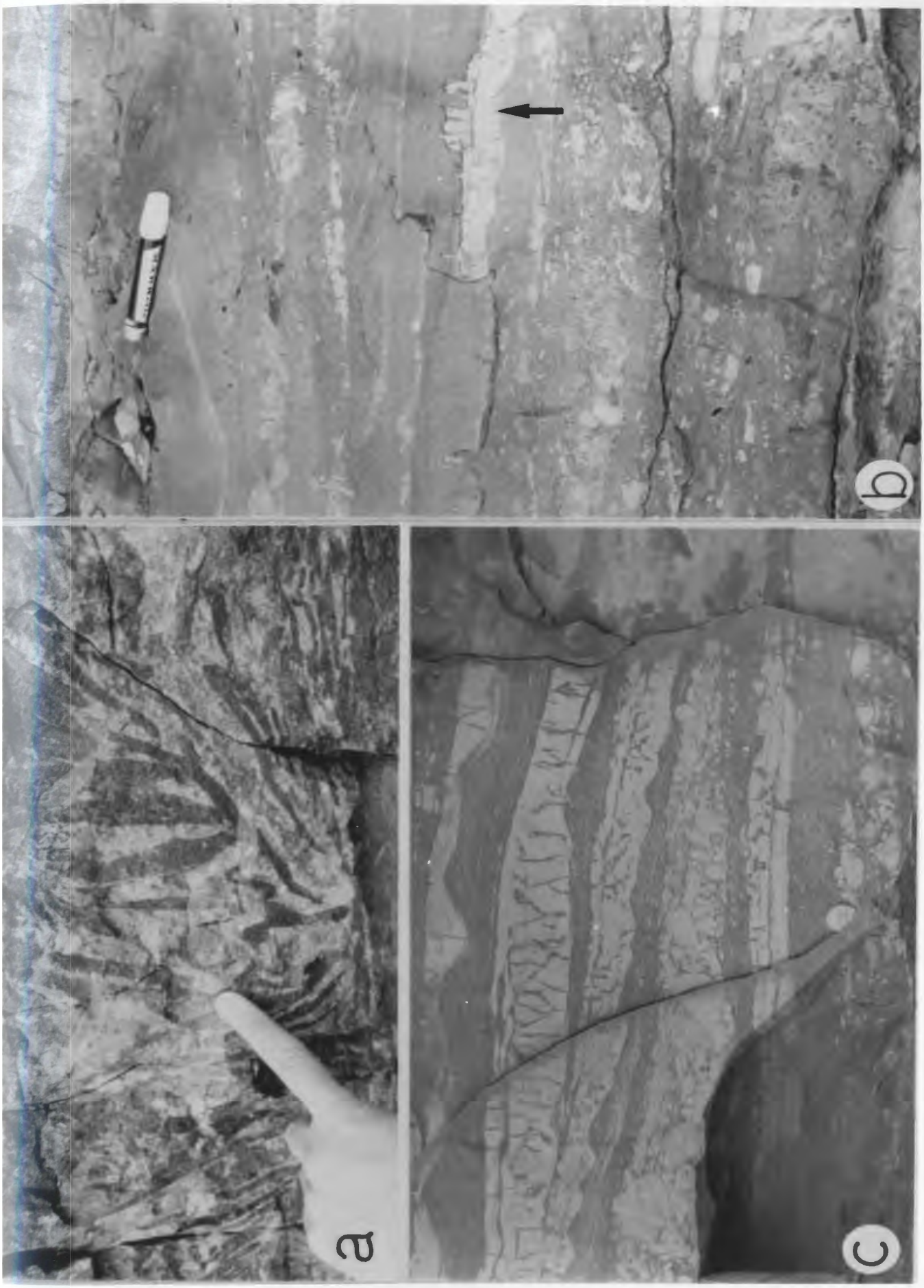
a
b
c

PLATE 5: CARBONATE LAMINITE LITHOFACIES

a: Tan weathering, thin-bedded and laminated dolostone (type 1) with abundant distorted mudcracks. Stratigraphic top is up. Berry Head Formation, Little Coney Arm section, Bed 3.

b: Thin-bedded and laminated patterned dolostone (type 3). Dark flecks in photo are disseminated pyrite (arrows). Stratigraphic top is up. Berry Head Formation, Little Coney Arm section, Bed 16.

c: Tan weathering, cryptalgalaminated dolostone (type 2) with wavy and crenulated laminations, and rip-up clasts (arrow). Stratigraphic top is up. Campbells Member, March Point section, Bed 1.

d: Bedding plane and cross-sectional view of prism cracks in cryptalgalaminated dolostone. Stratigraphic top is up. Felix Member, Felix to Man O' War Coves section, Bed 2.

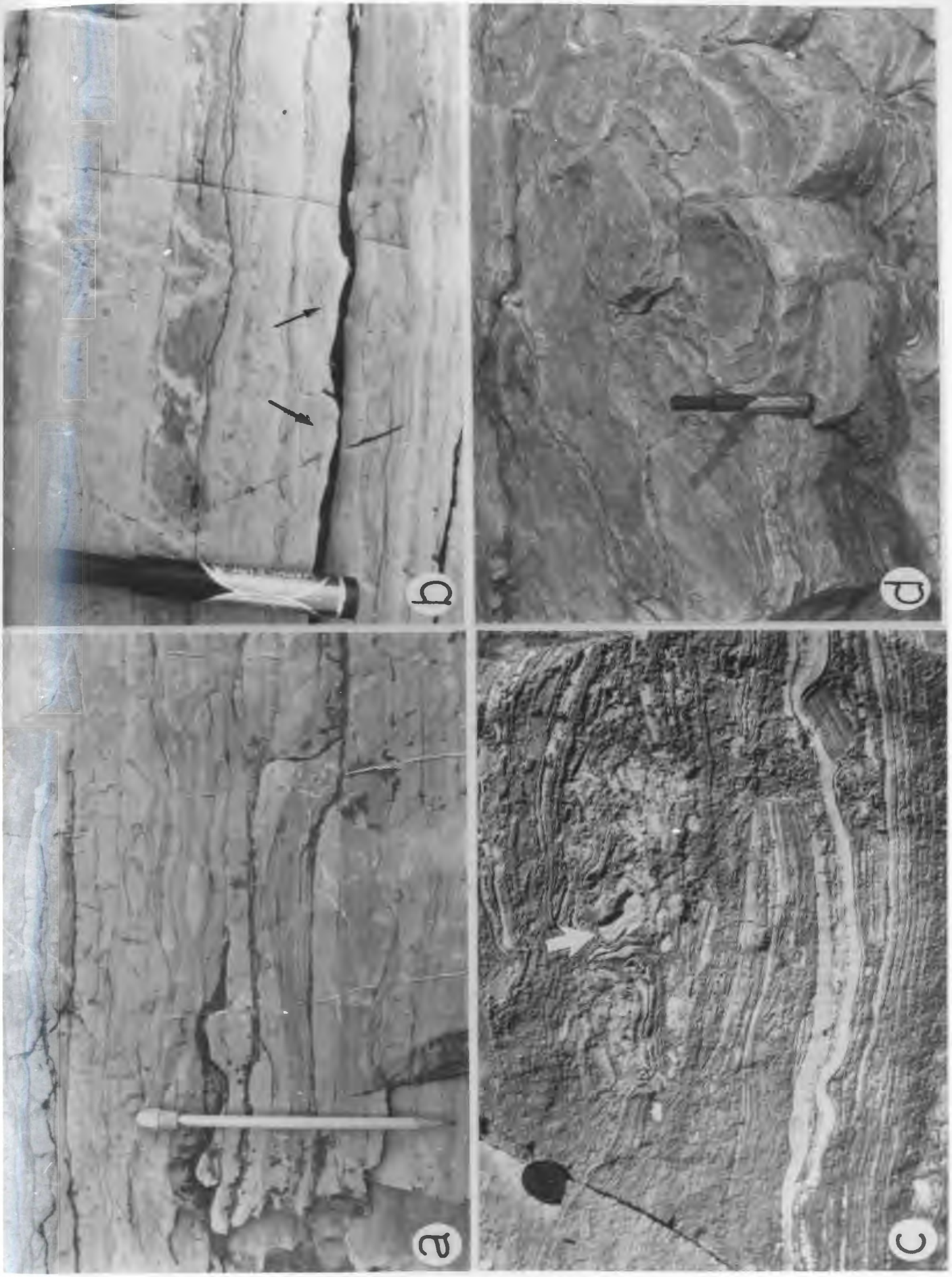
b
d
a
c

PLATE 6: STROMATOLITE AND THROMBOLITE MOUNDS

a: Bioherm complex (3) and underlying biostromes (1, 2) composed of coalesced stromatolite-thrombolite mounds. The bioherm directly overlies biostrome "2". Intermound sediment is parted limestone and dololaminite. Upper surface of bioherm is shown in Plate 14.f. Range pole is 1 m (arrow). Stratigraphic top is up. Cape Ann Member, Degras section, Beds 12-13.

b: Partially dolomitized thrombolite horizon composed of superimposed mounds. The lower mounds (1) are coalesced and have planar upper surfaces. The upper mound (2) is oblate and has a dolomitized core and undolomitized outer margin with a clotted texture. Arrow points to contact between core and margin. Range pole is 1.2 m. Stratigraphic top is up. Man O' War Member, headland east of Man O' War Cove, Bed 17.

c: Dolomitized mound composed of two upward-coalescing, bulb-shaped mounds (1 and 2). Intermound sediment is parted limestone (P). Large divisions on range pole are 10 cm. Stratigraphic top is up. Man O' War Member, headland east of Man O' War Cove, Bed 17.

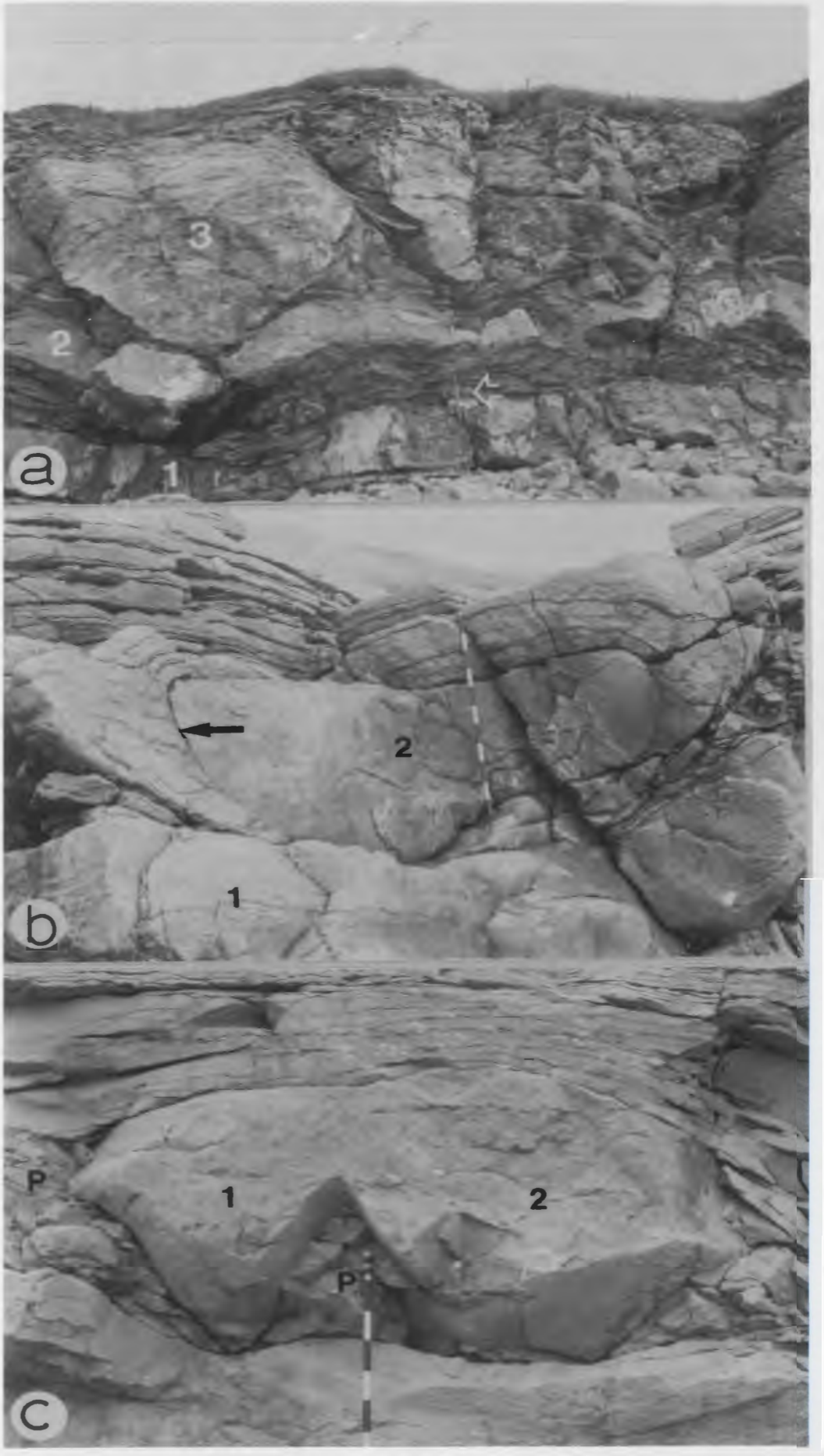
3
2
a
1
2
b
1
P
1
2
P
c

PLATE 7: STROMATOLITE AND THROMBOLITE MOUNDS

a: Thrombolite mound composed of three stages (light grey in photo), separated by and overlying fissile grey shale. This biostromal horizon is correlative with biostrome "1" in Plate 6.a. Divisions on range pole are 2 cm. Stratigraphic top is up. Cape Ann Member, March Point section, Bed 10.

b: Dolomitized upward-branching, digitate stromatolites (dark grey in photo; arrows) present in dolomitized brown oolite. Stratigraphic top is up. Felix Member, March Point section, Bed 5.

c: Mound composed of digitate stromatolites, which are preferentially dolomitized (light grey in photo). Man O' War Member, headland east of Man O' War Cove, Bed 18.

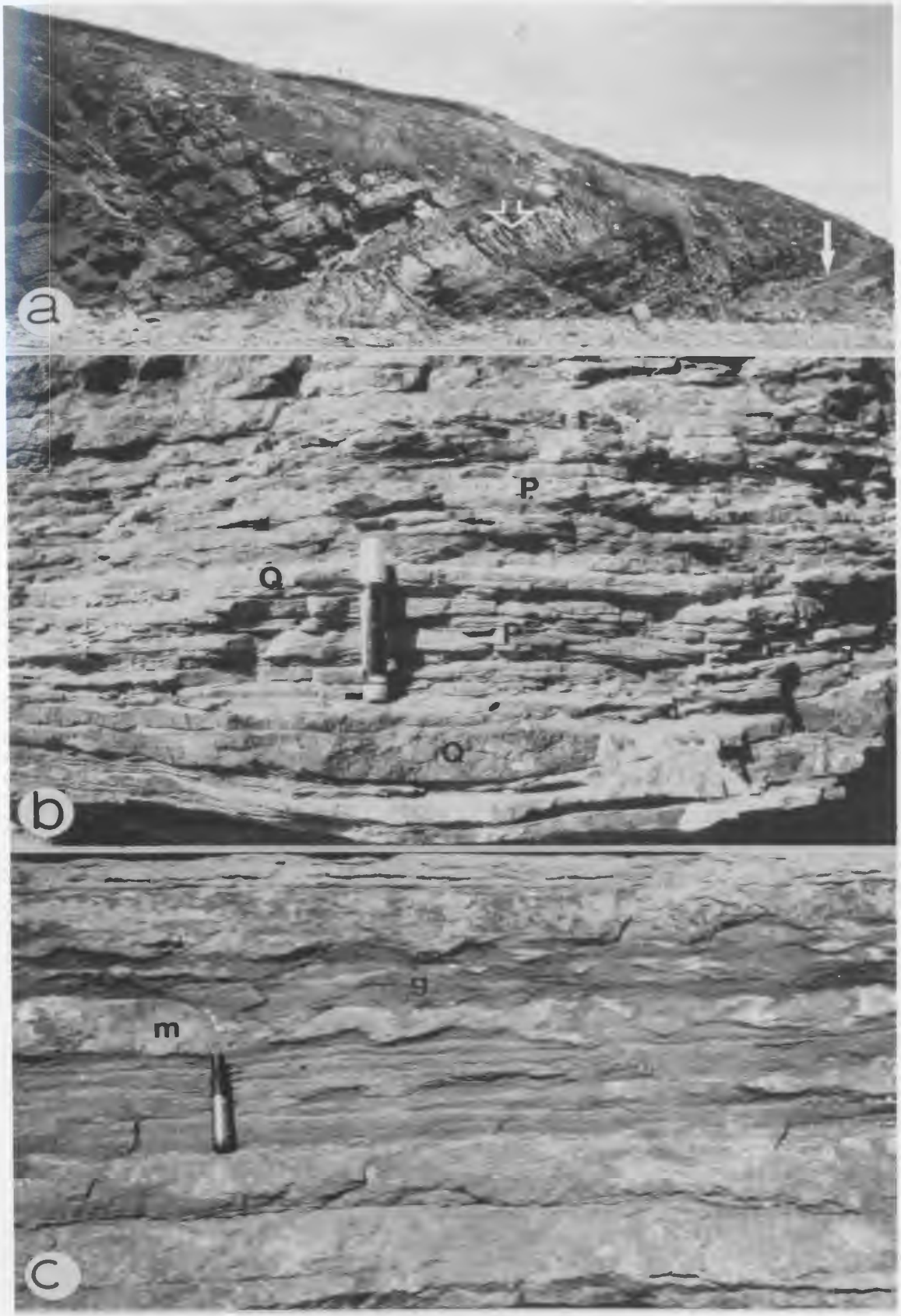
a
P
Q
P
Q
b
g
m
c

PLATE 8: GLAUCONITIC SANDSTONE LITHOFACIES

a: View of basal March Point Formation. White arrow points to the top of Hawke Bay Formation, which is composed of quartzarenite. Open arrow points to 1 m thick quartzarenite which is underlain by thin-bedded grey shale and overlain by thinly interbedded glauconite-rich siliciclastic siltstone and sandstone, and parted limestone. Stratigraphic top is to upper left of photo. Degras section, Beds 1-4.

b: Recessive weathering, parted limestone (P) interbedded with resistant weathering, glauconitic-rich, calcareous quartzarenite to arenaceous mudstone (Q). Stratigraphic top is up. March Point Formation, Degras section, Bed 4.

c: Greenish-grey weathering, glauconitic, siliciclastic silt-rich mudstone (g) with irregular nodules of grey, siliciclastic silt-rich mudstone (m). Stratigraphic top is up. March Point Formation, March Point section, Bed 5.

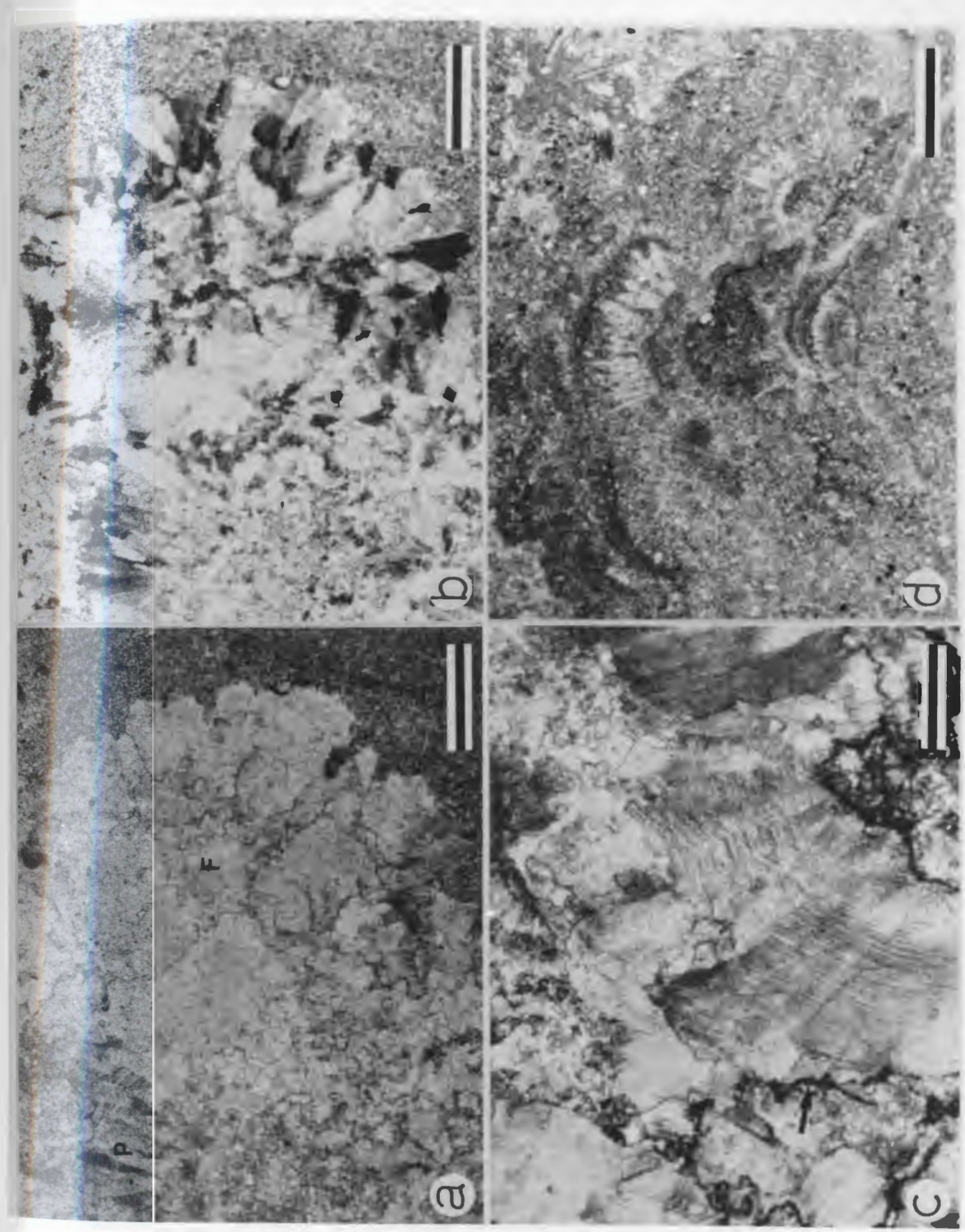
P
E
a
b
c
d

PLATE 9: BIOHERM-BIOSTROME CEMENTS

a, b: Plane and cross polarized light photomicrographs of fan-like arrays of fibrous calcite (type 1; F) forming rinds in thrombolitic-stromatolitic mounds. Prismatic calcite (P) is closely associated with this type of calcite. Scale bar is 500 μm. Bioherm complex; Cape Ann Member, Degras section, Bed 13, sample NC-83-64a.

c: Thin section photomicrograph of prismatic calcite (type 2) in thrombolite. Crystal terminations are commonly truncated by microstylolites (arrow). Scale bar is 500 μm. Bioherm complex; Cape Ann Member, Degras section, Bed 13, sample NC-83-64a.

d: Thin section photomicrograph of prismatic calcite (type 2) in stromatolite. Crystals have distinct scalenohedral terminations and are interlaminated with siliciclastic silt-rich micrite. Adjacent crystals are commonly separated by micrite. Scale bar is 500 μm. Stratigraphic top is up. Cape Ann Member, Match Point section, Bed 10, sample NC-82-162a.

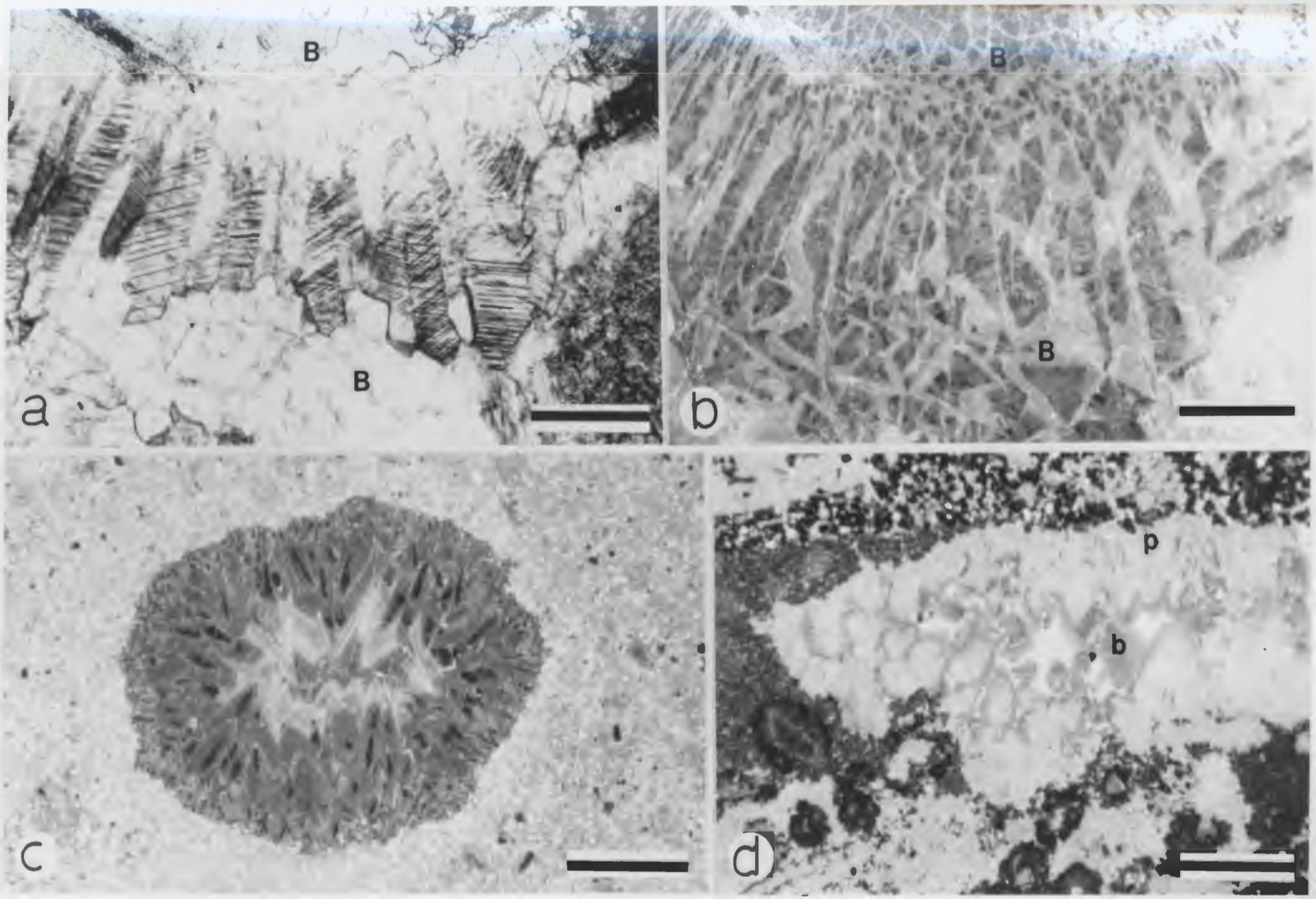
B
B
a
B
B
b
c
p
b
d

PLATE 10: PRISMATIC CLEAR CALCITE CEMENT

a, b: Plane light and CL photomicrographs of prismatic clear calcite cement rimming bioclast. Crystals (B) at top and base of fringe are cross-sectional views of prismatic calcite. Scale bar is 500 μm. Stratigraphic top is up. March Point Formation, Degras section, Bed 6, sample NC-83-28.

c: CL photomicrograph of burrow in parted limestone occluded by distinctly zoned, prismatic clear calcite. Scale bar is 640 μm. Berry Head Formation, Isthmus Bay section, Bed 27, sample NC-82-139a.

d: CL photomicrograph of intergranular pore in conglomerate that is occluded by prismatic clear calcite (p) with moderate luminescence which passes gradationally into blocky calcite (b) with dull and bright luminescence. Scale bar is 500 μm. Campbells Member, March Point section, Bed 2, sample NC-83-278.


a
b
c
d

PLATE 11: BLOCKY CALCITE CEMENT

a: Cross-polarized light photomicrograph of ooid-bioclastic calcarenite with syntaxial calcite overgrowths (black) on echinoderm fragments (E) and blocky ooids (O). Scale bar is 500 μm. Campbells Member, March Point section, Bed 8, sample NC-83-290.

b: CL photomicrograph of dull-luminescent blocky calcite (B) and non-luminescent argillaceous dolostone (D) filling shelter porosity and fractures in flat-pebble conglomerate (c - clasts). Scale bar is 1.2 mm. Man O' War Member, Felix to Man O' War Coves section, sample NC-82-45.

c: CL photomicrograph of blocky calcite occluding moldic porosity in bioclastic calcarenite. Zoning in calcite consists of a moderate- to dull-luminescent phase (d) and a bright-luminescent phase (b). Scale bar is 1 mm. Man O' War Member, headland east of Man O' War Cove, Bed 17, sample NC-83-55.

d: CL photomicrograph of ooid molds in grey oolite, filled by blocky calcite cement (b) with zoned bright to non-luminescence and partially replaced by single crystals of weak red-luminescent, ferroan dolomite (D). Scale bar is 700 μm. Campbells Member, March Point section, Bed 9, sample NC-83-328.

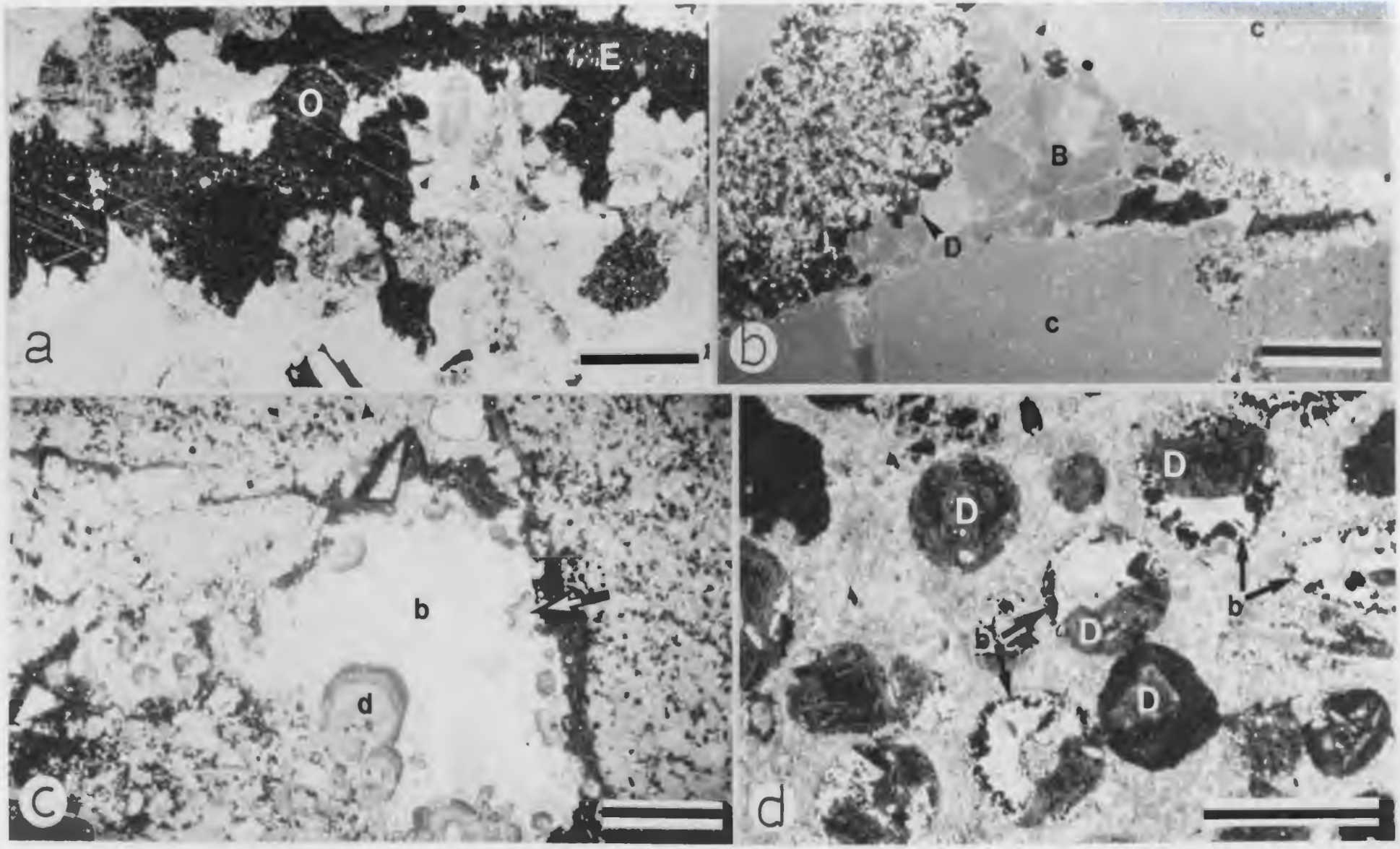
a
O
E
b
B
C
D
c
C
b
d
d
D
D
D
D
b
b

PLATE 12: CONGLOMERATES

a: Flat-pebble conglomerate interbedded with parted limestone. Mudstone clasts are enclosed in an argillaceous dolostone matrix. Stratigraphic top is up. Man O' War Member, Felix to Man O' War Coves section, Bed 17.

b: Bedding plane view of flat-pebble conglomerate, composed of horizontally to vertically disposed clasts. Arrows point to possible borings in clasts. March Point Formation, Degras section, Bed 5.

c: Thin section negative print of flat-pebble conglomerate composed of laminated and massive mudstone. Possible borings (arrow) are present in some clasts. Scale bar is 900 μm. March Point Formation, Degras section, Bed 5, sample NC-82-15A.

d: Thin section photomicrograph of oolitic conglomerate. Ooids (O), fibrous calcite cements (F) and micritic matrix (m) in clasts are truncated at clast boundaries. Scale bar is 500 μm. Campbells Member, March Point section, Bed 10, sample NC-82-227.

e: Thin section negative print of hardground (arrow) on flat-pebble conglomerate. Hardground truncates clasts and is overlain by parted limestone. White patches are pyrite. Scale bar is 900 μm. Stratigraphic top is up. Campbells Member, March Point section, Bed 6, sample NC-83-284B.

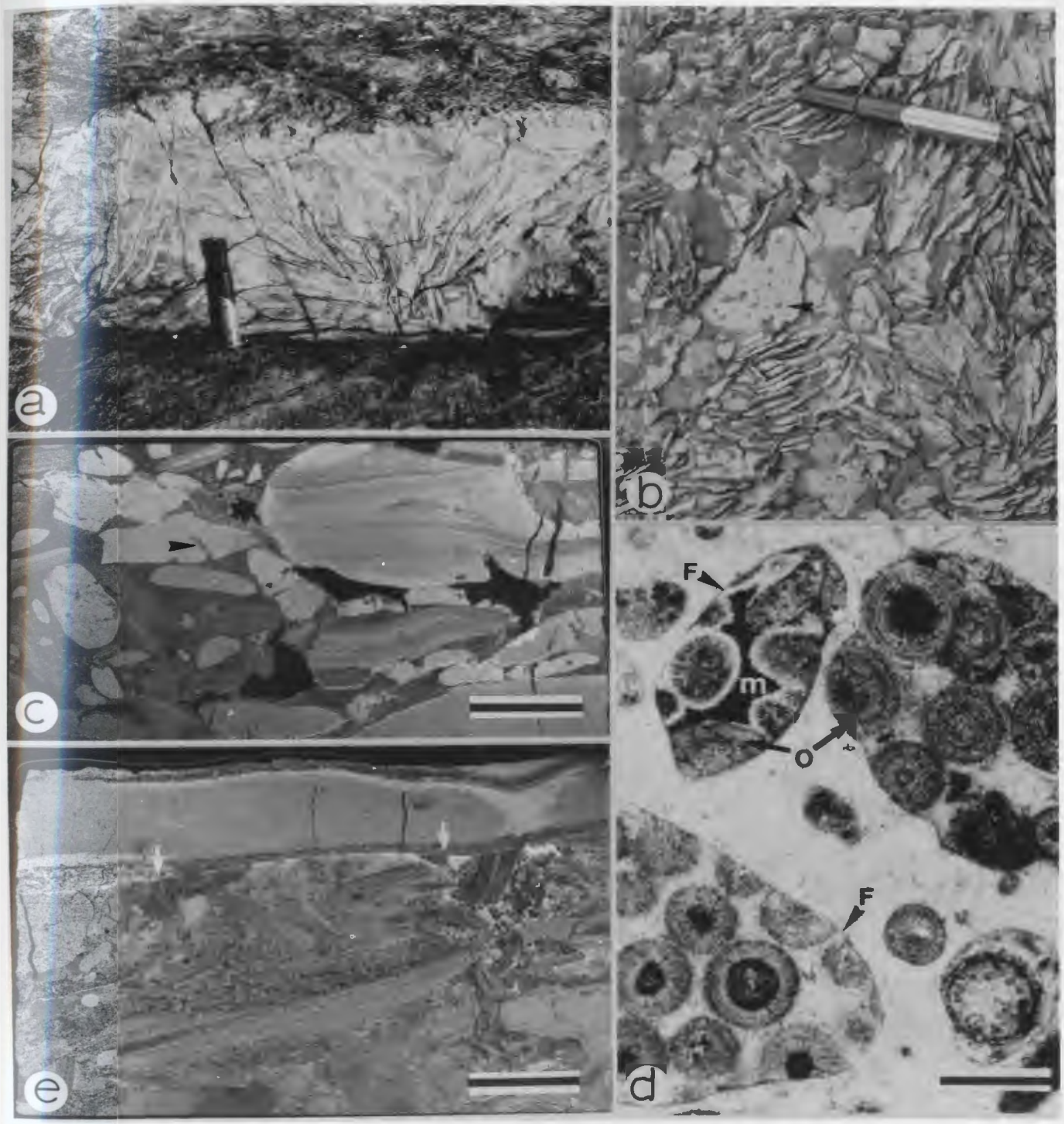
a
b
c
F
m
o
F
d
e

PLATE 13: HARDGROUNDS

a: Hardground (below marker) in parted limestone forms resistant-weathering ledges with distinctive bluish-grey colouration. Stratigraphic top is up. March Point Formation, Degras section, Bed 5.

b: Slab of hardground similar to that in "a" above. Irregular pits and cracks in upper surface are filled with intraclastic calcarenite. Pyrite (arrow) penetrates mudstone and rims pits and cracks. Stratigraphic top is up. March Point Formation, March Point section, Bed 6, sample NC-83-18.

c: Thin section negative print of multiple hardgrounds in bioclast-intraclast calcarenite (arrows). Conglomerate fill of lowermost hardground is also truncated by a hardground (C). White rim is pyrite. Scale bar is 7 mm. Stratigraphic top is up. Man O' War Member, Felix to Man O' War Coves section, Bed 17, sample NC-82-259.

d: Thin section photomicrograph of hardground in grey oolite, overlain by interlaminated fibrous calcite and micrite. Borings (B) are impregnated with pyrite and truncate fibrous calcite crystals. Scale bar is 500 μm. Stratigraphic top is up. Man O' War Member, Felix to Man O' War Coves section, Bed 17, sample NC-82-255a.

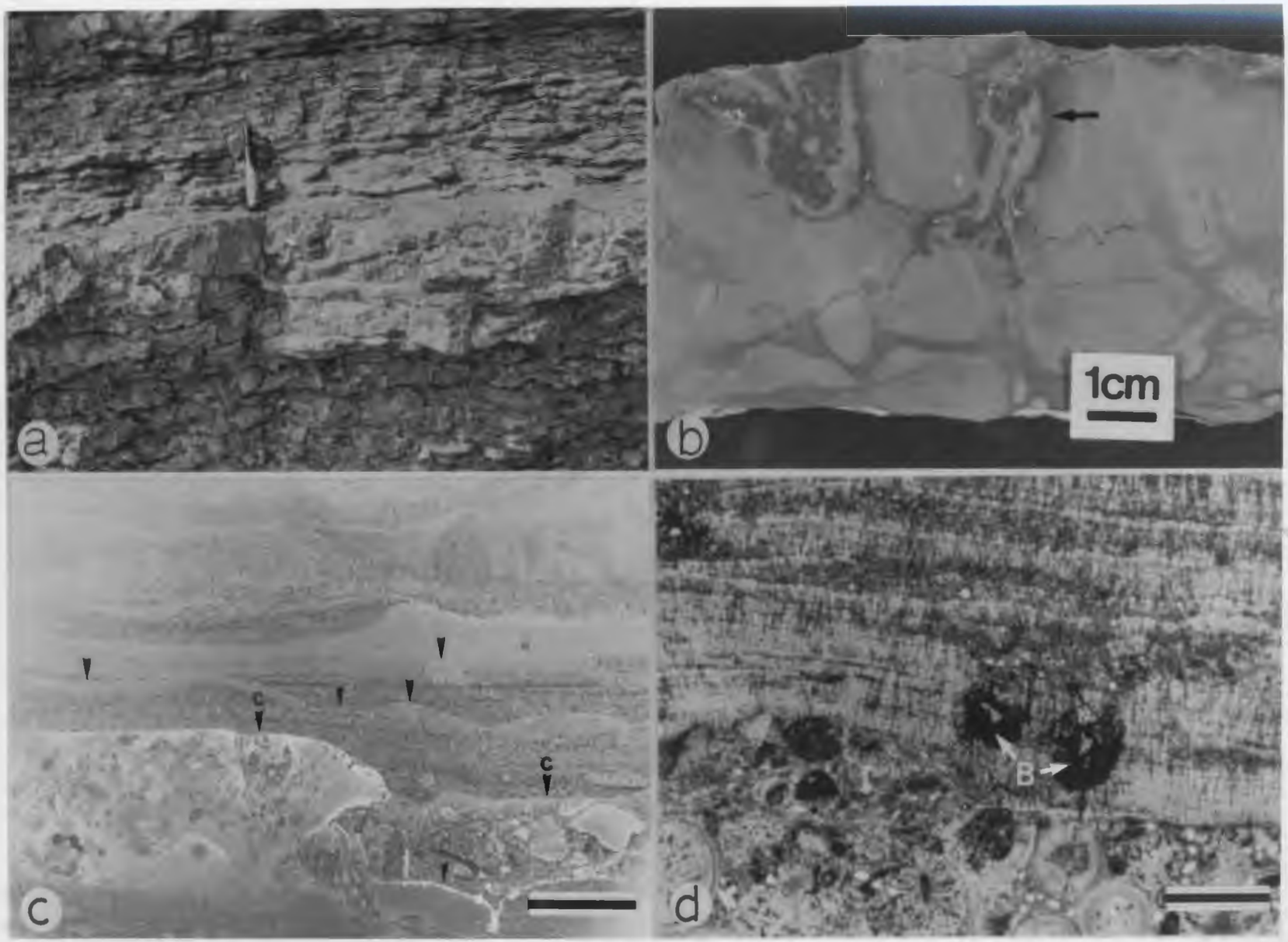
a
b
1cm
c
c
c
d
B

PLATE 14: SURFACE PALEOKARST

a: Fractures and brecciation in dololaminite. Lamellar stromatolite (arrow), 2-5 mm thick, is present on upper surface of breccia blocks. Stratigraphic top is up. Felix Member, March Point section, Bed 4.

b: Undulose upper surface of dololaminite (arrow) overlain by dolomitized grey oolite with a planar upper surface. Flanks of "highs" in dololaminite contain abundant intraclast calcirudites. Range pole is 1.2 m. Stratigraphic top is up. Felix Member, March Point section, Bed 3.

c: Rounded, overhanging margin (arrows) of flat-bottomed depression in dololaminite. Range pole is 1.0 m. Stratigraphic top is up. Berry Head Formation, Isthmus Bay East section, Bed 3.

d: Undulose surface in dolomitized calcarenite (C), overlain and draped by dololaminite (D). Berry Head Formation, Isthmus Bay East section, Bed 2.

e: Cross-sectional view of dolomitized algal mounds with planar upper surfaces (arrow), which are capped by lamellar stromatolite (S), 1-5 cm thick, and dololaminite. Intermound sediment is also truncated by surfaces. Stratigraphic top is up. Man O' War Member, Man O' War Cove section, Bed 17.

f: Bedding plane view of bioherm complex with planar upper surface. Darker grey laminations are iron-oxide staining which penetrates to several millimeters below the surface. Cape Ann Member, Degras section, Bed 13.

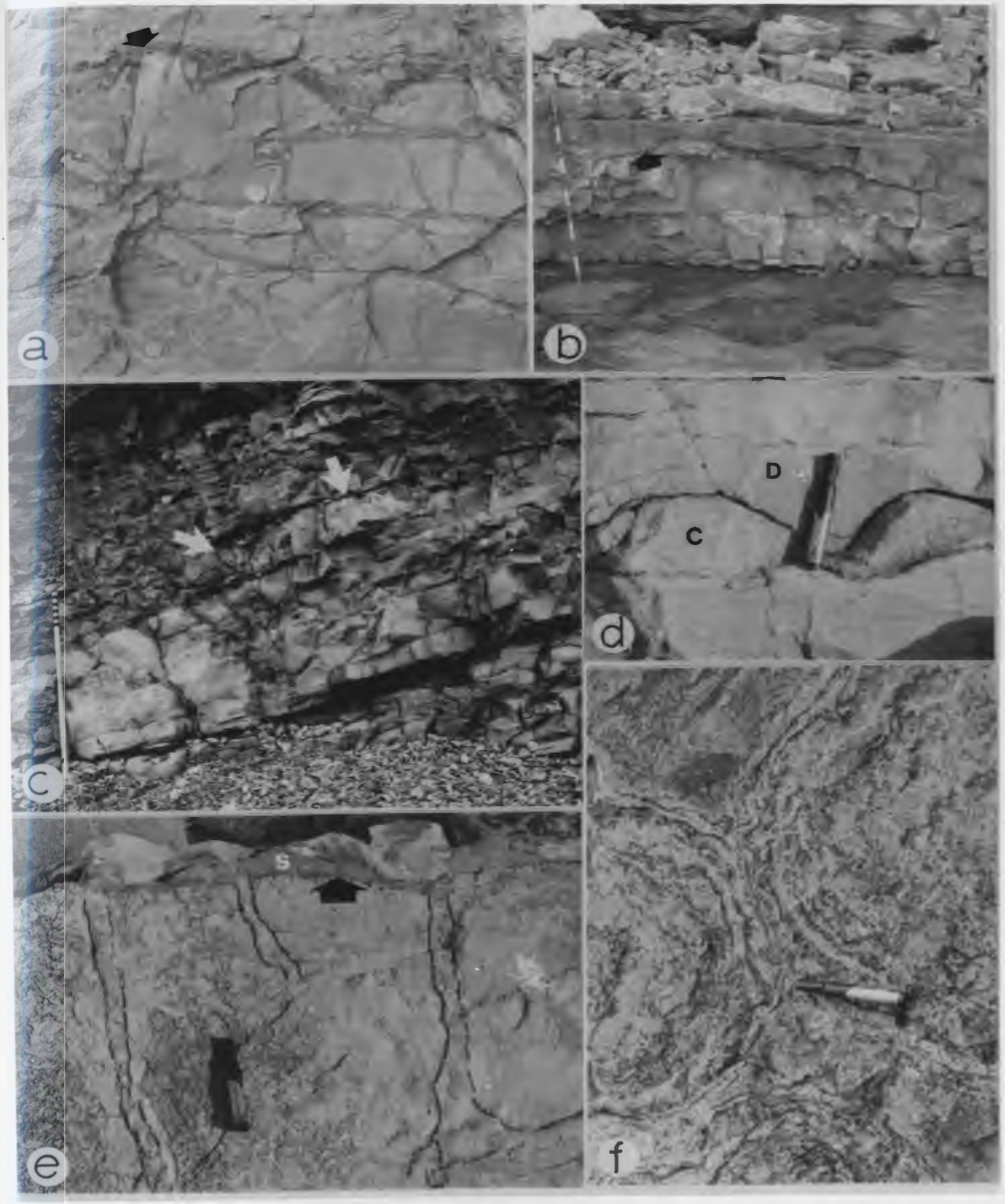
a
b
c
D
C
d
S
e
f

PLATE 15: SURFACE PALEOKARST

a: Scalloped surface (arrows) in dololaminite with rounded-bottom pits filled by angular clasts and thin beds of dololaminite. One division on range pole is 10 cm. Stratigraphic top is up. Campbells Member, March Point section, Bed 10.

b: Scalloped surface in dololaminite with flat-bottomed pits (up to 30 cm deep) and flat-top ridges (arrow). Surface is overlain by dolomitized intraclast-bioclast calcirudite and dololaminite. Stratigraphic top is up. Felix Member, Felix to Man O' War Coves section, Bed 3.

c: Slab illustrating scalloped surface in massive dolostone. Iron-oxide staining coats and penetrates surface and overhanging flanks of pit (arrows). Intraclasts overlying the surface are identical in composition to dolostone. Stratigraphic top is up. Felix Member, Felix to Man O' War Coves section, Bed 5, sample NC-82-235.

d: Thin section negative print of scalloped surface in mudstone. Pit is filled by tabular mudstone intraclasts. Surface is draped by lamellar stromatolite (arrow). Borings (B) penetrate scalloped surface, conglomerate and stromatolite. Scale bar is 5 mm. Stratigraphic top is up. Campbells Member, March Point section, Bed 10, sample NC-83-240a.

e: CL photomicrograph of "d" above, illustrating the progressively brighter luminescence downward from the scalloped surface (large arrow points to surface). Borings (B) are the bright-luminescent patches. Details are given in text. Mudstone is cross-cut by two fractures filled by dull-luminescent blocky calcite (small arrows). Scale bar is 800 μm. Stratigraphic top is up. Campbells Member, March Point section, Bed 10, sample NC-83-240a.

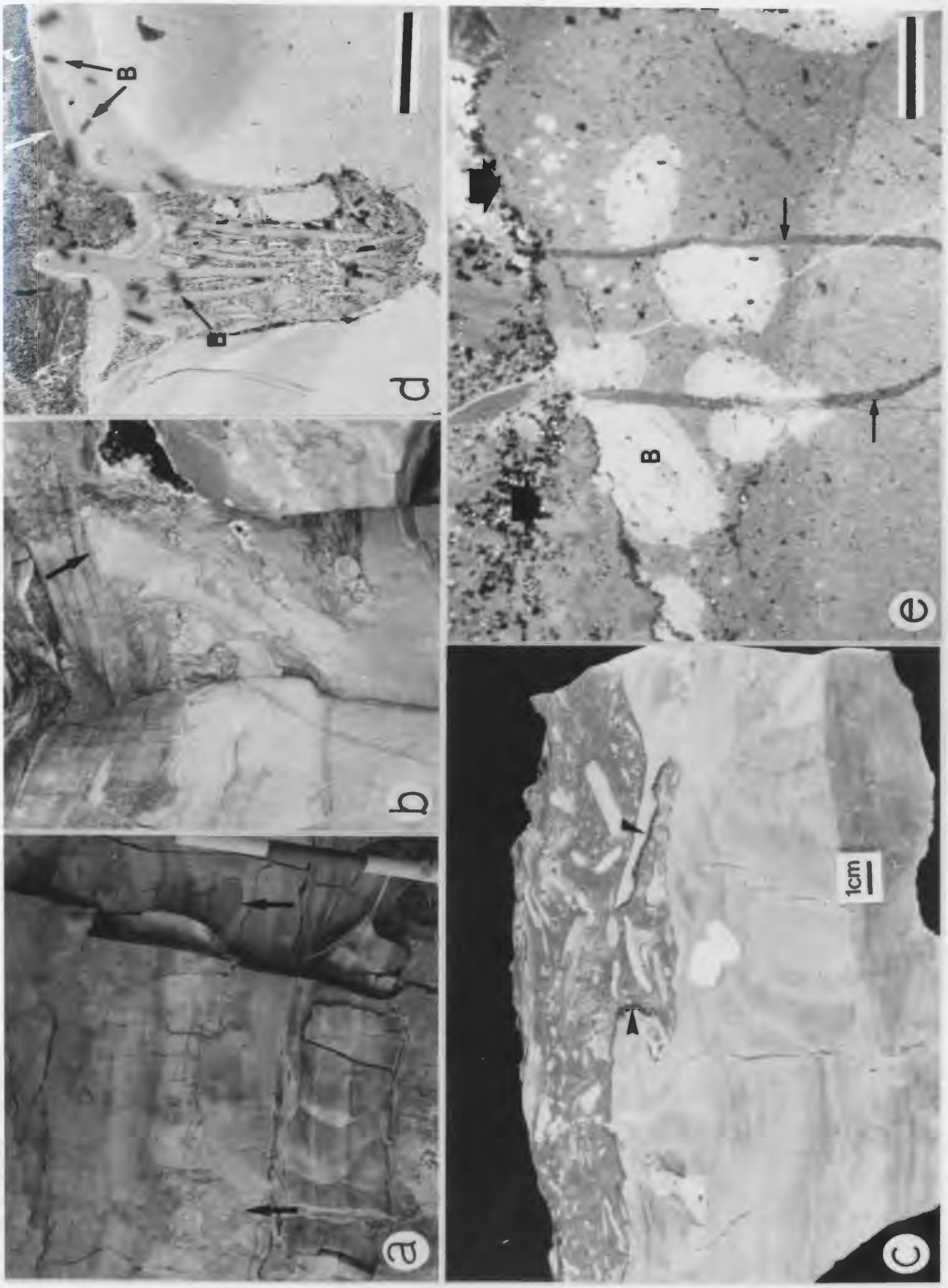
a
b
c
d
e
B
B
B
1cm

PLATE 16: RADIAL OOIDS

a: Thin section photomicrograph of radial ooids cemented by fibrous calcite with polygonal sutures (arrows). Echinoderm fragments (E) have syntaxial calcite overgrowths. Scale bar is 500 μm. Campbells Member, March Point section, Bed 6, sample NC-82-96E.

b: Thin section photomicrograph of radial ooids with isopachous micritic cement. Remaining interparticle porosity is occluded by blocky calcite. Scale bar is 375 μm. Campbells Member, March Point section, Bed 9, sample NC-82-61.

c: SEM photograph of radial ooid cortex (lower third of photo) cemented by fibrous calcite (middle of photo) and blocky calcite (upper third of photo). Crystallites of cortex contain abundant holes. Arrow points to the surface of the ooid. Scale bar is 19 μm. Campbells Member, March Point section, Bed 7, sample NC-83-288.

d: CL photomicrograph of radial ooids with concentric zones of dull and moderate luminescence. Arrows point to dull-luminescent fibrous calcite cement. Scale bar is 320 μm. Campbells Member, March Point section, Bed 7, sample NC-83-288.

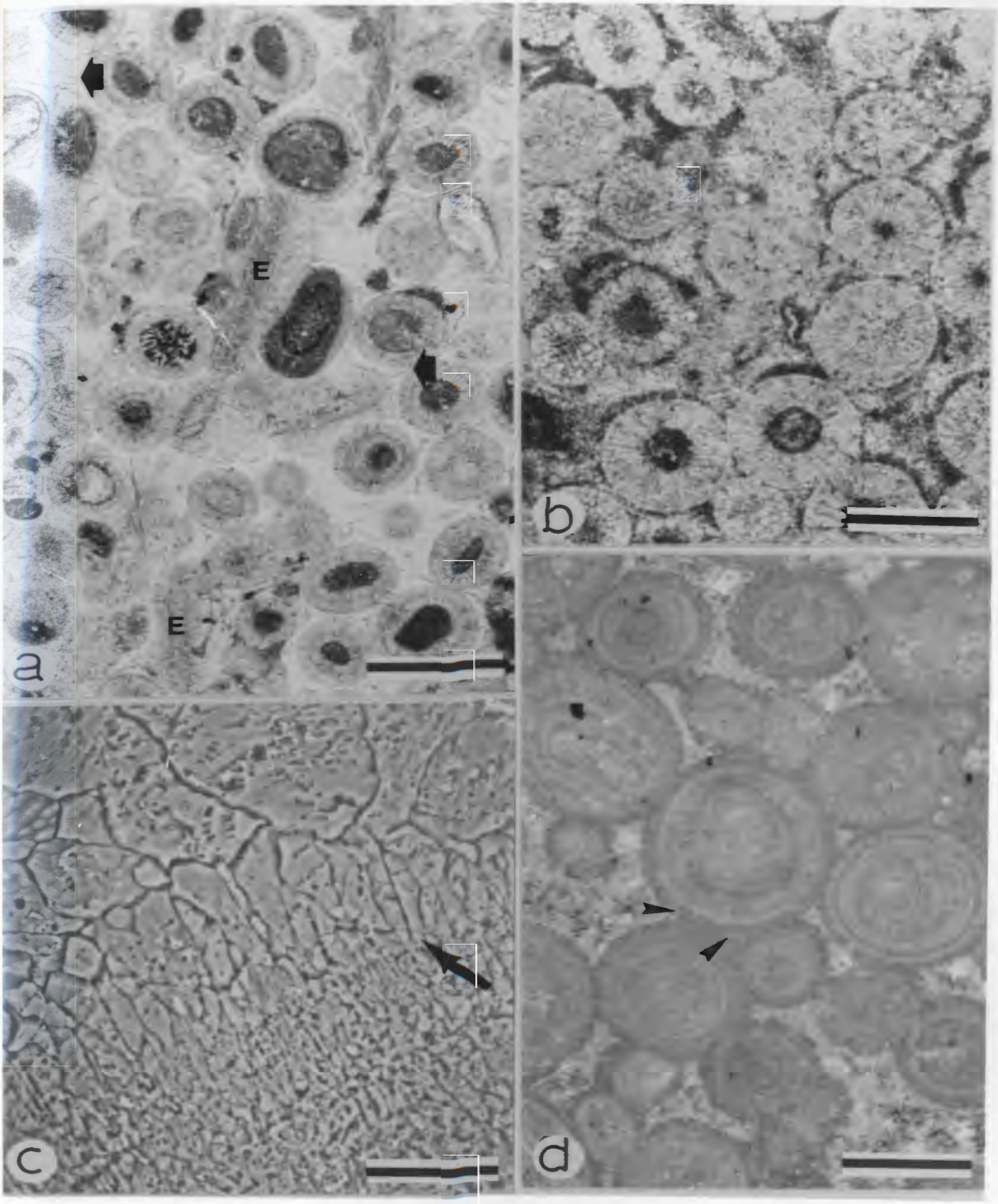
E
E
a
b
c
d

PLATE 17: RADIAL-CONCENTRIC OOIDS

a: Thin section photomicrograph of radial-concentric ooids with thin fringe of fibrous calcite cement (arrow) and a matrix of micrite (m), silt-size peloids and siliciclastic silts. Scale bar is 500 μm. Campbells Member, March Point section, Bed 8, sample NC-83-290.

b: Thin section photomicrograph of distorted radial-concentric ooids. Concentric laminae have collapsed and separated, and resulting voids are occluded by blocky calcite (arrows). Radial cores are relatively undistorted. Scale bar is 500 μm. Man O' War Member, Felix to Man O' War Coves section, Bed 18, sample NC-82-267.

c: Thin section photomicrograph of radial-concentric ooids with deformed concentric laminae. Some radial cores of ooids are partially dissolved and contain distinct micrite rays. Scale bar is 500 μm. Berry Head Formation, Isthmus Bay East section, Bed 24, sample NC-82-127A.

d: Thin section negative print of "b" above, illustrating ooid calcarenite with bimodal distribution of ooids. Small ooids are radial (large arrow) and larger ones are radial-concentric that are commonly distorted (similar to "b" above) or have multiple-ooid nuclei (m). Some ooids are preferentially silicified (black particles in upper third of photo). Scale bar is 2.7 mm. Man O' War Member, Felix to Man O' War Coves section, Bed 18, sample NC-82-267.

e: Thin section photomicrograph of asymmetrical radial-concentric and radial ooids ("16c" above) in micritic matrix. Micritic rays and patches in ooids contain concave laminae (arrows) that are continuous with those in radial parts of the cortex. Scale bar is 500 μm. Campbells Member, March Point section, Bed 7, sample NC-83-288.

f: Thin section photomicrograph of complex radial-concentric ooid with irregular fringe of fibrous calcite cement and micritic matrix. Scale bar is 500 μm. Campbells Member, March Point section, Bed 7, sample NC-83-288.

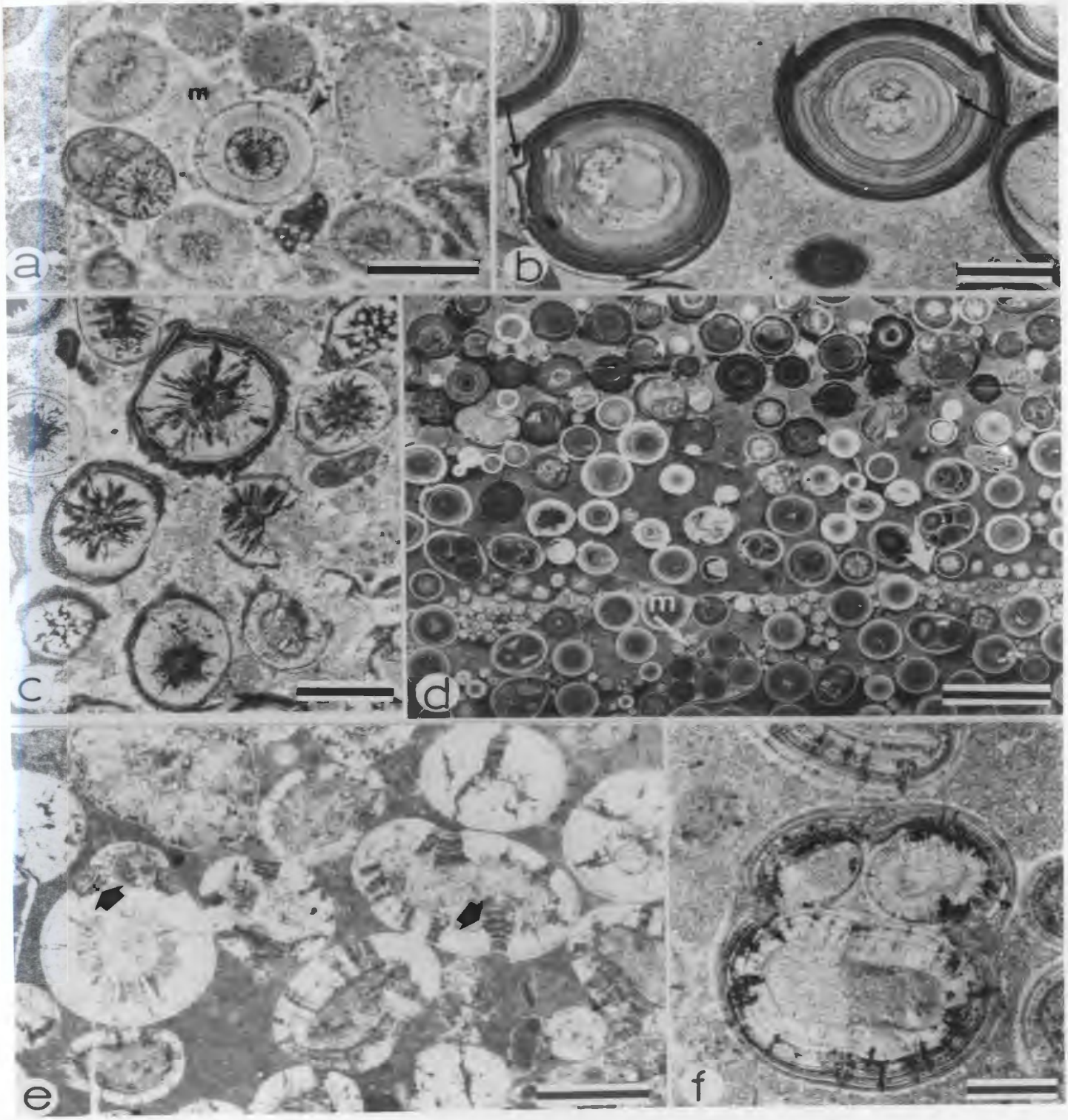
a
m
b
c
d
m
e
f

PLATE 18: COARSELY PRESERVED OOIDS, SPARRY RADIAL OOIDS IN GREY OOLITE

a: Thin section photomicrograph of ooid calcarenite containing finely preserved radial ooids (R), sparry radial (s), and blocky ooids (b). Scale bar is 500 µm. Campbells Member, March Point section, Bed 9, sample NC-82-61.

b: Thin section photomicrograph of sparry radial ooids with cortices of rice-shaped calcite. Indistinct concentric banding is present in some ooids. Scale bar is 500 µm. Campbells Member, March Point section, Bed 8, sample NC-83-290.

c: SEM photograph of rice-shaped, calcite crystallites in sparry radial ooids. Scale bar is 16 µm. Campbells Member, March Point section, Bed 2, sample NC-83-275.

d: Thin section photomicrograph of sparry radial ooids with cortices of prismatic crystallites of calcite. Scale bar is 500 µm. Cape Ann Member, west of Campbells Cove section, sample NC-83-339.

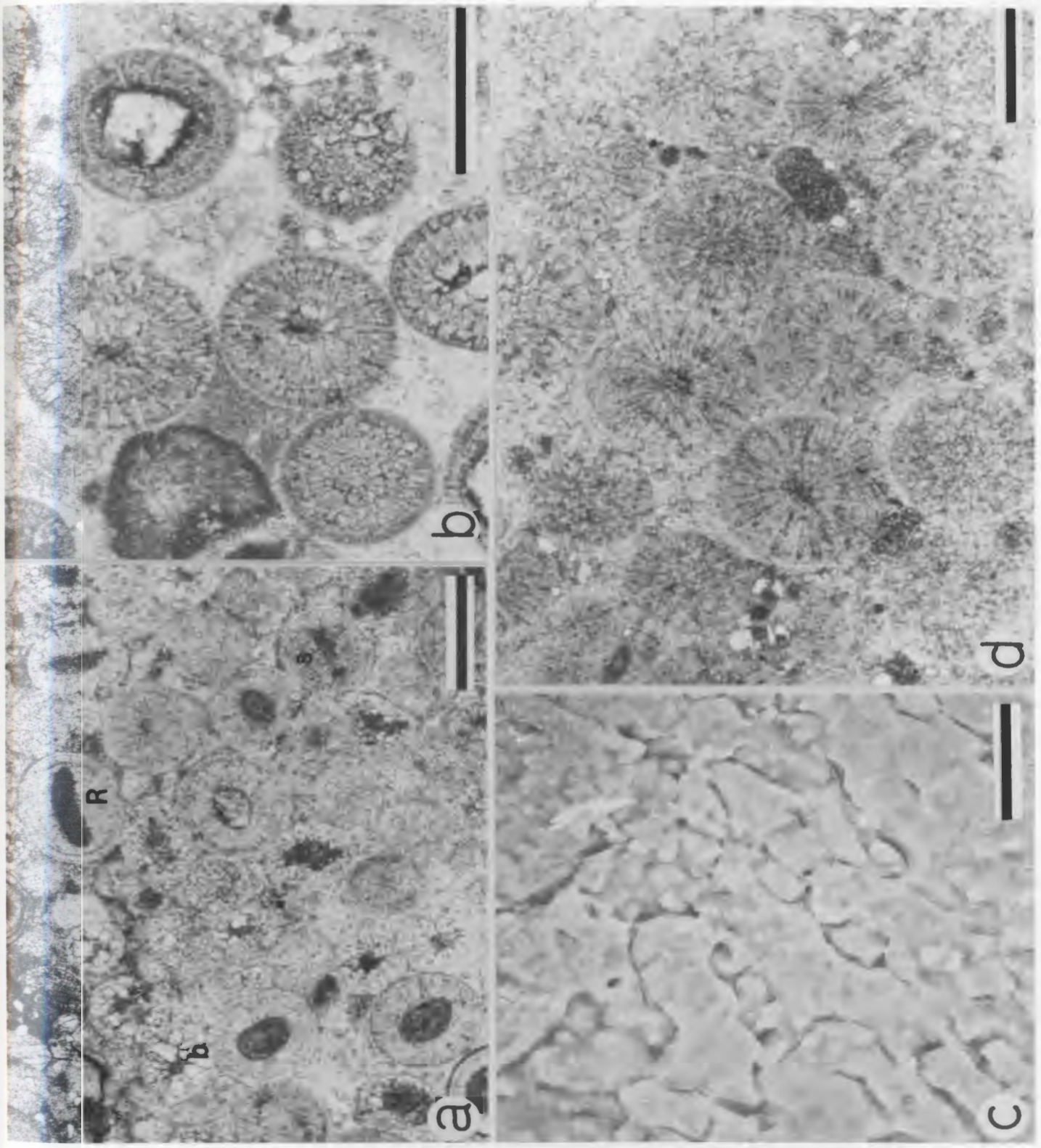
a
b
c
d
R
S
B

PLATE 19: RADIAL-BLOCKY OOIDS IN GREY OOLITE

a: Thin section photomicrograph of radial-blocky ooids with inner cortices of blocky calcite (B) and rims of sparry radial calcite (prismatic [P] or rice-shaped [R]). Scale bar is 500 μm. Campbells Member, March Point section, Bed 2, sample NC-82-55.

b: CL photomicrograph of radial-blocky ooids. Outer cortices of sparry radial calcite have indistinct concentric zones of moderate and bright luminescence (O), and occasionally inward-directed, scalenohedral crystal terminations (large arrow). Inner cortices of blocky calcite are dull luminescent (i). Non-luminescent crystals are ferroan dolomite (D). Scale bar is 400 μm. Campbells Member, March Point section, Bed 2, sample NC-83-275.

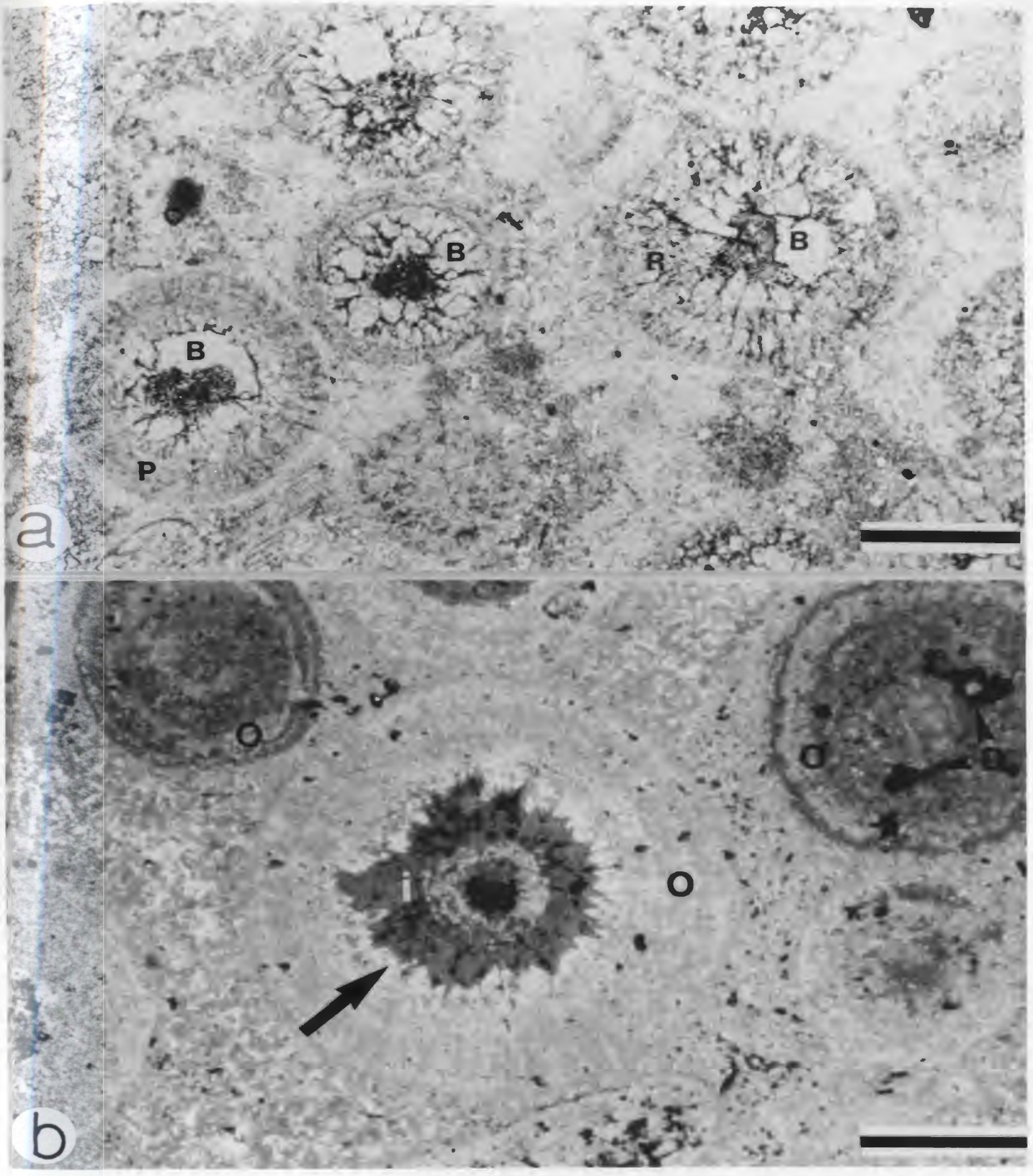
B
B
B
B
P
a
O
O
O
b

PLATE 20: BLOCKY OOIDS IN GREY OOLITE

a: Thin section photomicrograph of blocky ooids (B) composed of ferroan calcite with argillaceous and pyritic intercrystalline matrix. Sparry radial ooids (S) are present in lower half of photo. Clast (C) is partially replaced by ferroan dolomite. Scale bar is 500 μm. Campbells Member, March Point section, Bed 8, sample NC-83-290.

b: CL photomicrograph of dull-luminescent blocky ooids similar to those in "a" above. Some ooids have indistinct, dull- and moderate-luminescent zones (arrow). The white and black specks are silt-size feldspar and quartz, respectively, in a micritic matrix. Scale bar is 500 μm. Campbells Member, March Point section, Bed 8, sample NC-82-160.

c: Thin section photomicrograph of blocky ooids adjacent to fractures occluded by blocky calcite. Ooid nuclei are commonly preserved and may be displaced from the core of the ooid (arrows). Scale bar is 500 μm. Campbells Member, March Point section, Bed 6, sample NC-82-96E.

d: CL photomicrograph of same sample as "c" above, illustrating dull luminescence of blocky ooids and inward growth of calcite crystals (arrow). Ooids in upper right of photo are partially occluded by non-luminescent ferroan dolomite (D). Scale bar is 320 μm. Campbells Member, March Point section, Bed 6, sample NC-82-96E.

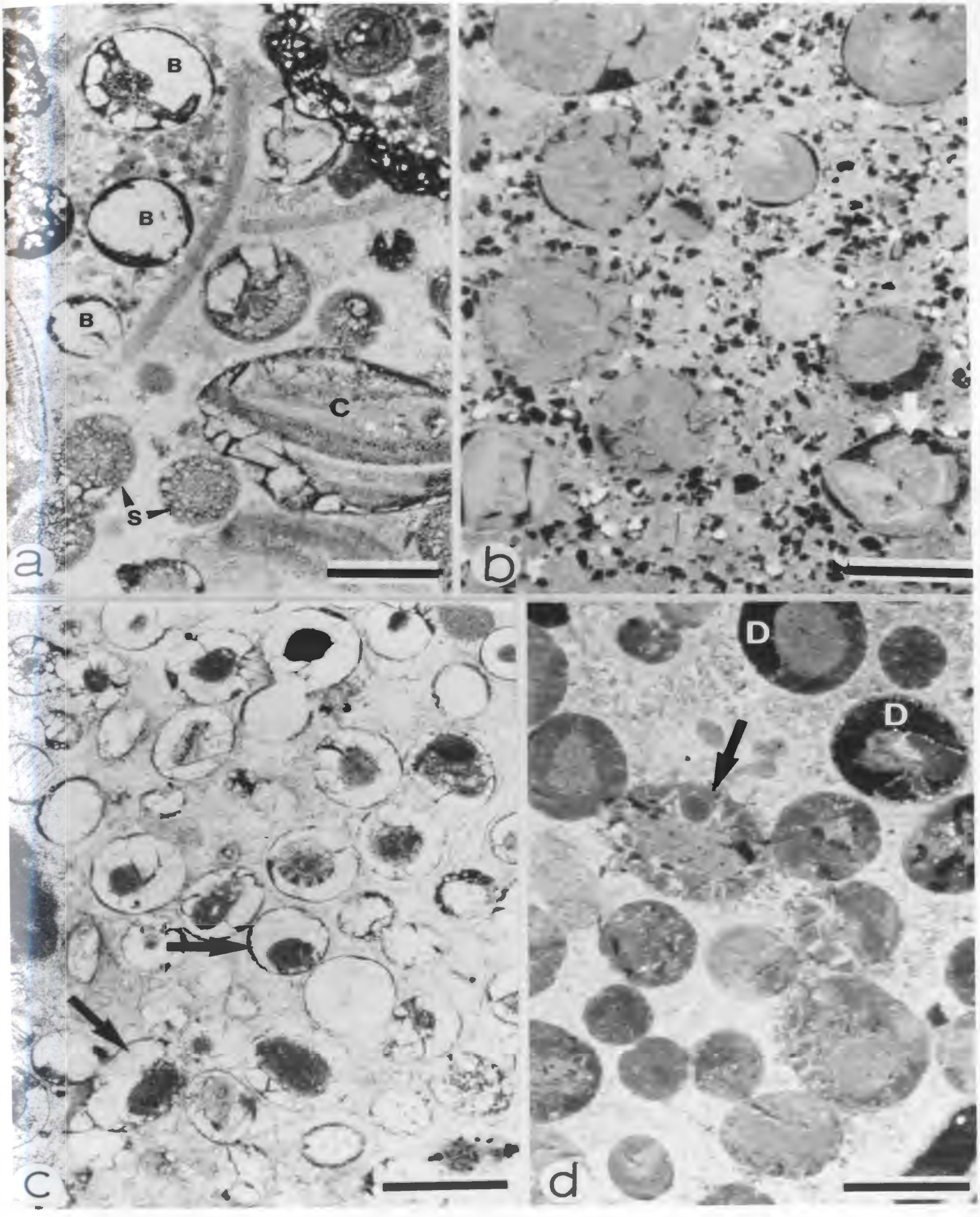
B
B
B
C
S
a
b
c
D
D
d

PLATE 21: CONCENTRIC AND SUPERFICIAL RADIAL OOIDS IN BROWN OOLITE

a: Thin section photomicrograph of ooid calcarenite composed of concentric ooids. Thin beds of undistorted ooids (upper half of photo) are cemented by fibrous calcite. Thin beds of distorted ooids (lower half of photo) have minor blocky calcite cement and micritic matrix and cement. Scale bar is 500 μm. Campbells Member, March Point section, Bed 11, sample NC-82-67.

b: Thin section photomicrograph of concentric ooids in "a" above with laminae of micritic (m), radial fibrous (r) and blocky (b) calcite. Interparticle porosity is occluded by fibrous calcite cement which forms polygonal sutures (arrow). Scale bar is 200 μm. Campbells Member, March Point section, Bed 11, sample NC-82-67.

c: Thin section photomicrograph of concentric ooids and intraclasts cemented by meniscus micritic calcite (M), and fibrous and blocky (b) calcites. Scale bar is 500 μm. Campbells Member, March Point section, Bed 10, sample NC-82-65.

d: Thin section photomicrograph of dolomitized concentric ooids (C) and radial ooids (R) with well preserved fabrics. Scale bar is 500 μm. Campbells Member, March Point section, Bed 1, sample NC-82-51.

e: Thin section photomicrograph of superficial ooids with peloidal nuclei and thin inclusion-rich cortices (C). Interparticle porosity is occluded by thin fringes of inclusion-poor, fibrous calcite cement (F) and micritic matrix (M). Scale bar is 100 μm. Campbells Member, March Point section, Bed 11, sample NC-83-245B.

f: Thin section photomicrograph of superficial radial ooids with cortices of prismatic calcite. Fibrous calcite cement (F) is poorly developed and micritic matrix (M) is abundant. Scale bar is 100 μm. Campbells Member, March Point section, Bed 10, sample NC-82-203C.

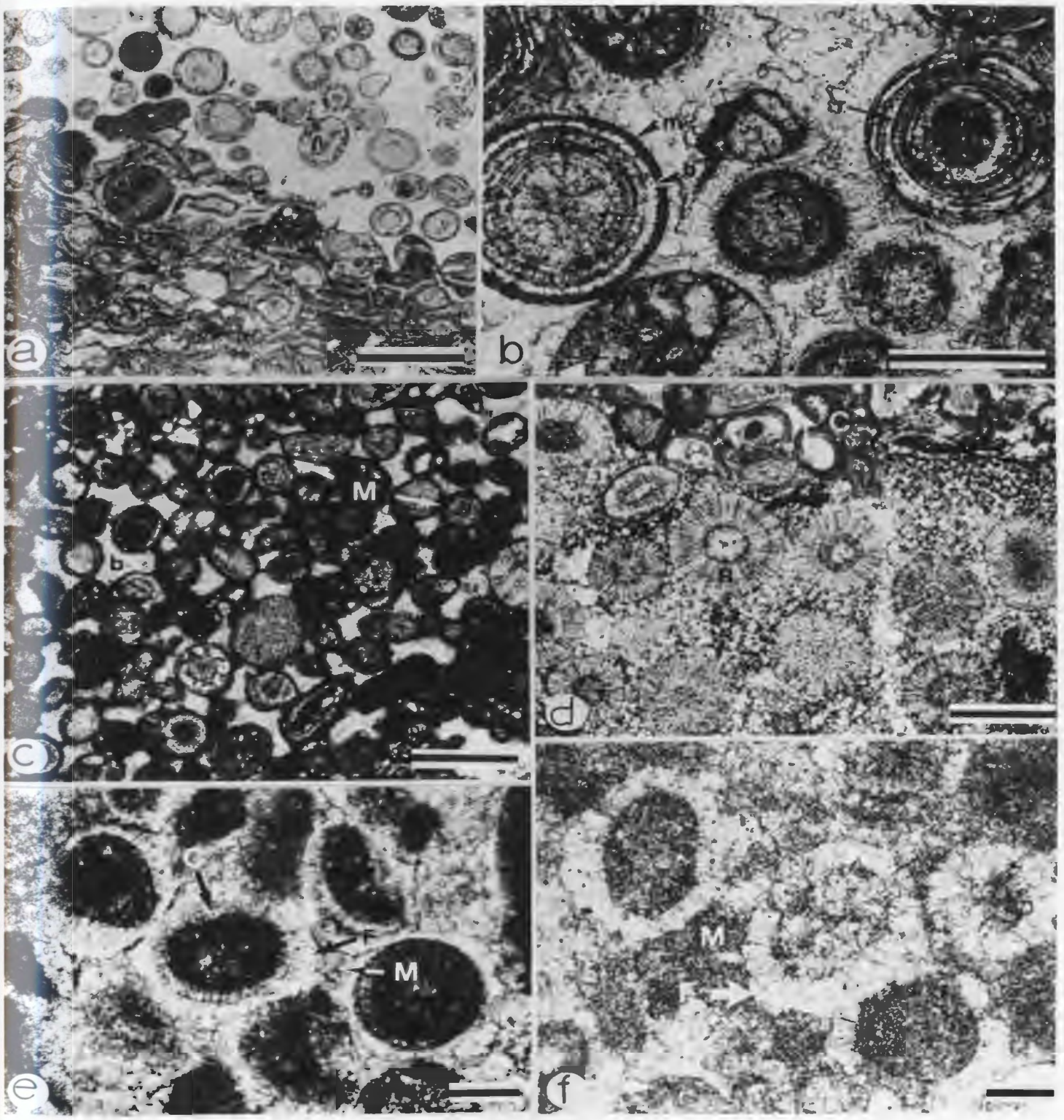
a
b
M
b
c
d
M
e
f
M

PLATE 22: MARGINALLY AGGRADED MUDSTONES IN PARTED LIMESTONE

a: Thin section negative print of aggraded mudstone (dark grey) encircling dolomitized burrows (B). White lines are microstylolite swarms. Scale bar is 820 µm. Stratigraphic top is up. March Point Formation, Degras section, Bed 5, sample NC-82-4A.

b: Thin section negative print of blocky mudstone nodules (M). Marginally aggraded neospar (dark grey fringe in photo; arrows) occurs adjacent to burrows (b) and in the side margins of nodules. The internodular matrix of argillaceous dolostone (I) is more dolomitic than the argillaceous interbeds (speckled grey and white in photo). Microstylolites and microstylolite swarms (white in photo) roughly parallel nodule margins and are present in argillaceous interbeds but absent in the transition areas between nodules and internodular matrix. Scale bar is 7.9 mm. Stratigraphic top is up. Man O' War Member, Felix to Man O' War Coves section, Bed 17, sample NC-83-220.

c: CL photomicrograph of marginally aggraded mudstone with zones of alternating moderate and bright luminescence that are truncated by a microstylolite swarm (arrow). Black area on right of photo is argillaceous dolostone. Scale bar is 1.2 mm. Man O' War Member, Felix to Man O' War Coves section, Bed 17, sample NC-83-219.

d: CL photomicrograph of CL zoning in marginally aggraded mudstone (M) developed concentrically around argillaceous dolostone embayment (D) in margin of mudstone nodule. Scale bar is 1.2 mm. Man O' War Member, Felix to Man O' War Coves section, Bed 17, sample NC-82-260.

e: Closeup of "d" above, showing the progressive development of outer CL zones. Dark grey and black area on right of photo is argillaceous dolostone. Scale bar is 700 µm. Man O' War Member, Felix to Man O' War Coves section, Bed 17, sample NC-82-260.

f: CL photomicrograph of fracture in marginally aggraded mudstone (M), filled by dull-luminescent blocky calcite (B) and ferroan, non-luminescent dolomite (D). Smaller dolomite rhombs are present in the overlying argillaceous dolostone (d). Scale bar is 700 µm. Stratigraphic top is up. Man O' War Member, Felix to Man O' War Coves section, Bed 17, sample NC-82-260.

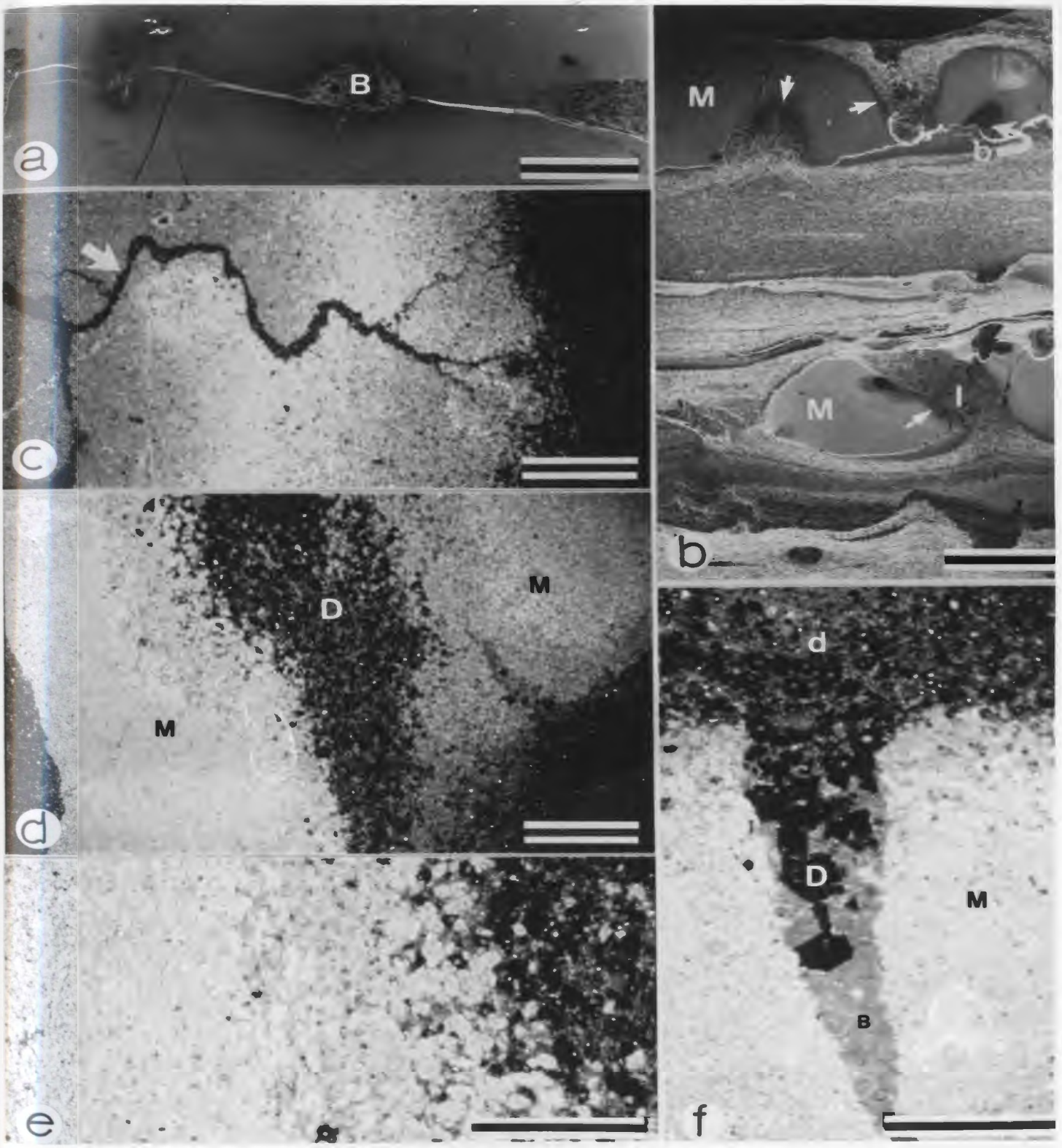
a
B
M
b
b
M
I
c
d
D
M
M
e
d
D
M
B
f

PLATE 23: NODULES IN PARTED LIMESTONE

a: Thin beds and nodules of mudstone (light grey in photo) interbedded with tan weathering, argillaceous dolostone (medium grey in photo). Gutter casts (G) composed of mudstone are abundant. Stratigraphic top is up. Man O' War Member, headland east of Man O' War Cove, Bed 17.

b: Laminated nodules ("type 2 sedimentary nodules") of mudstone and arenaceous ooid grainstone (light grey in photo; arrows) interbedded with argillaceous dolostone (medium and dark grey in photo). Mudcracks in the dolostone are distorted (arrowhead). Campbells Member, March Point section, Bed 8.

c: Slab of "b" above illustrating two limestone nodules (medium grey; arrows) in the upper half of the photo. Laminations of ooid grainstone (dark grey in photo) are readily traceable into the adjacent dolostone (light grey in photo). In the dolostone, laminations are thinner and warped, and burrows (B) and mudcracks (m) are deformed. Campbells Member, March Point section, Bed 8, sample NC-83-256.

d: Thin section negative print of Skolithos (S) preserved as vertically elongate mudstone nodule ("type 2 sedimentary nodule") in argillaceous dolostone. The nodule has vertical fractures filled by blocky calcite (black in photo). The nodule on the right of the photo contains a vertical, grainstone-filled crack (arrow). Microstylolites (white in photo) cut across all structures. Scale bar is 870 μm. Stratigraphic top is up. Campbells Member, March Point section, Bed 8, sample NC-83-293.

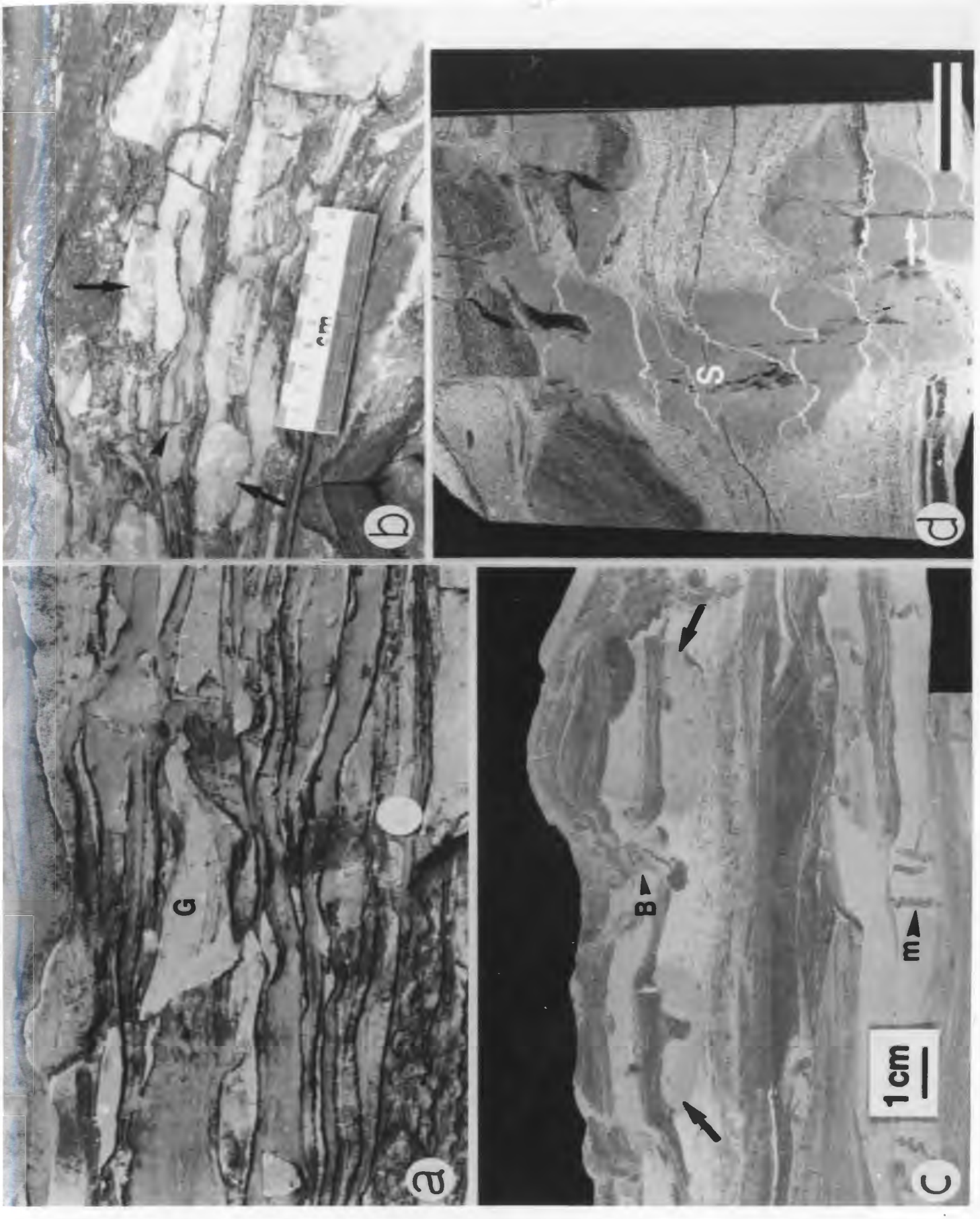
a
G
b
c
d
S
C
B
m
1cm

PLATE 24: NODULES IN PARTED LIMESTONE

a: Resistant weathering, blocky nodules of mudstone with an internodular matrix of recessive weathering, argillaceous dolostone. Abundant dolomitized burrows on bedding surfaces of mudstone layers (Plate 1.e) suggest that these nodules are primarily the product of burrowing activity. Stratigraphic top is up. March Point Formation, east of Campbells Cove section.

b: Slab illustrating blocky mudstone nodules (M) interbedded with argillaceous dolostone. Siliciclastic silt-rich lamination (arrow) in argillaceous dolostone is warped upwards into internodular matrix. Stratigraphic top is up. March Point section, Degras section, Bed 5, sample NC-82-241.

c: Thin mudstone beds and nodules ("fitted") of irregular thickness are parted with wispy, tan weathering, argillaceous dolostone (light grey in photo). Stratigraphic top is up. Man O' War Member, headland east of Man O' War Coves, Bed 17.

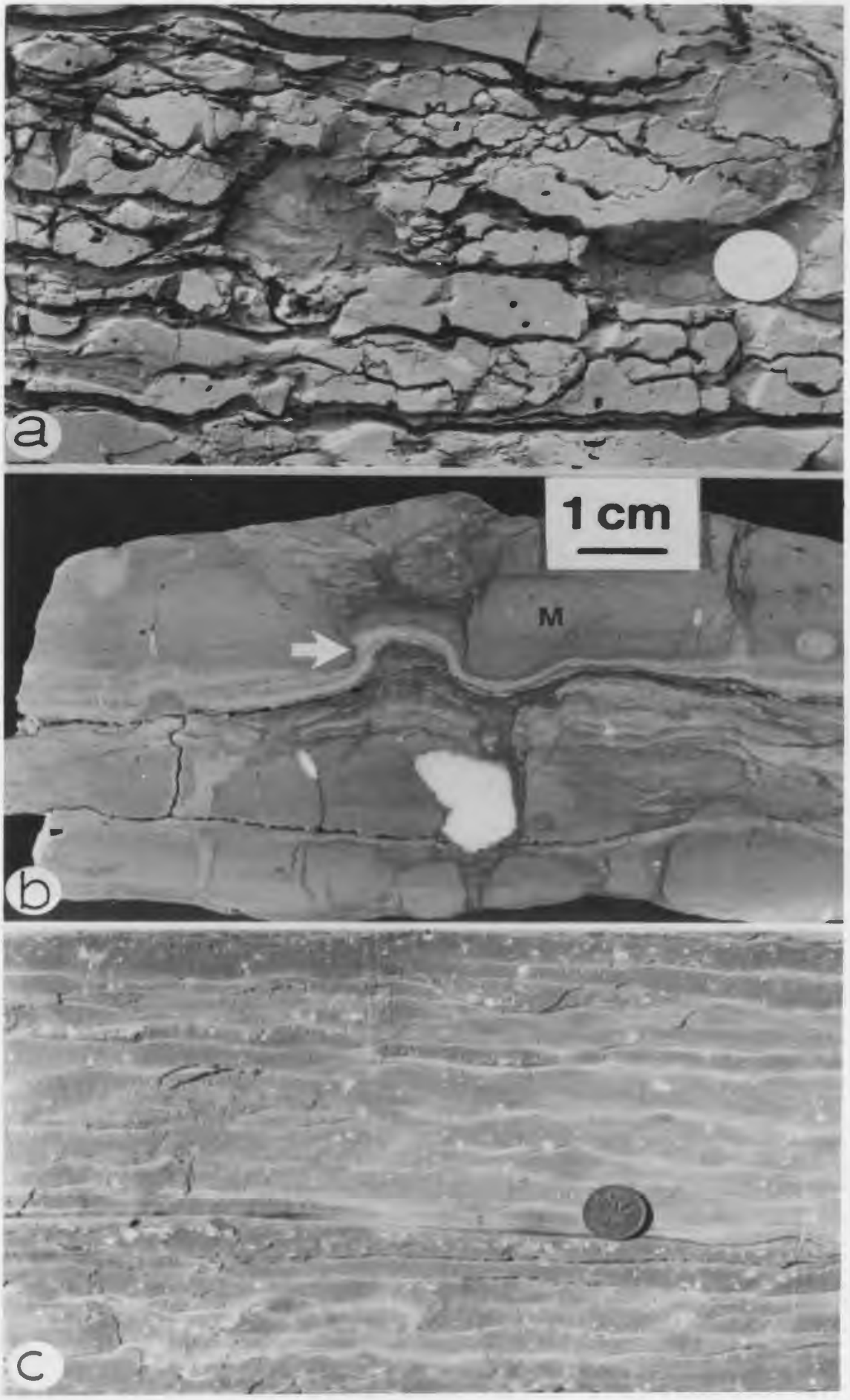
a
1 cm
M
b
c

PLATE 25: LIMESTONE-DOLOSTONE RELATIONSHIPS IN PARTED LIMESTONE

a: Bedding plane view of polygonal mudcracks, filled by ooid calcarenite, in finely crystalline dolostone. The mudcracks have distinct haloes of mudstone (arrow). Cape Ann Member, March Point section, sample NC-83-297.

b: Slab of "a" above, illustrating cross-sectional view of two mudcracks (top of photo) with mudstone halo (arrows). Scale bar is 1 cm. Stratigraphic top is up. Cape Ann Member, March Point section, sample NC-83-297.

c, d: Plane light and CL photomicrographs showing detail of transition from limestone nodule (right) to "internodular matrix" of dolostone (left) in Plate 22c, d. The transition from marginally aggraded mudstone (M) to thinner argillaceous dolostone (D) is accompanied by thinning of arenaceous calcarenite laminae (C) with pervasive grain-contact sutures. Black particles in "c" are pyritized ooids. Scale bars are 500 μm and 1.8 mm respectively. Stratigraphic top is up. Campbells Member, March Point section, Bed 8, sample NC-83-184B, -256B.

e: Thin section negative print of siliciclastic silt-rich grainstone nodule in calcareous, siliciclastic siltstone. Solid arrows point to upper and lower surfaces of the nodule. Parallel laminations in the nodule thin abruptly in the transition to siltstone (open arrow). Laminations in the siltstone are warped around the nodule. Scale bar is 9 mm. Stratigraphic top is up. March Point Formation, March Point section, Bed 8, sample NC-82-224.

f: Thin section negative print of packstone-filled burrow (b) which is deformed in argillaceous dolostone (D) and undeformed in mudstone (M). Clay-rich solution seams bend around the burrow and rim its lower quarter (arrow). The vertical, white lines are stylolites. Scale bar is 1.2 cm. Stratigraphic top is up. Man O' War Member, Felix to Man O' War Coves section, Bed 17, sample NC-82-258.

a
b
c
M
D
C
C
C
C
C
d
M
D
e
f
M
D

PLATE 26: LIMESTONE-DOLOSTONE RELATIONSHIPS IN PARTED LIMESTONE

a: Thin section negative print of grainy parted limestone with bed composed of argillaceous dolostone (speckled grey in photo; D) and mudstone (medium grey, M). A solution seam follows the limestone-dolostone contact (white line). Arrow points to a deformed mudcrack in argillaceous dolostone. Scale bar is 9.6 mm. Stratigraphic top is up. Campbells Member, March Point section, Bed 8, sample NC-83-256A.

b: Thin section negative print of mudstone beds and intraclasts (medium grey in photo) interbedded with argillaceous dolostone (speckled grey and white in photo). Disrupted clasts (C) and vertical fractures filled with blocky calcite and ferroan dolomite (black in photo; arrows) are restricted to mudstone. Argillaceous dolostone (D) exhibits thinning relative to laterally equivalent mudstone. Clay-rich solution seams (white in photo) are concentrated at lithologic boundaries. Scale bar is 6.7 mm. Stratigraphic top is up. Man O' War Member, Felix to Man O' War Coves section, Bed 17, sample NC-83-208A.

c: Slab of flat-pebble conglomerate with matrix of argillaceous dolostone. Clasts of laminated mudstone are fractured and bent. Stratigraphic top is up. March Point Formation, Degras section, Bed 6, sample, NC-82-242.

d: Irregular vertical contact (arrow) between grey mudstone (M) and tan weathering, argillaceous dolostone (D). Laminations cannot be traced between mudstone and dolostone. Stratigraphic top is up. Man O' War Member, headland east of Man O' War Cove section, Bed 18.

e: Thin beds of laminated mudstone (arrow) composed of microfaulted blocks and with irregular bed thicknesses. Overlying mudstone bed has irregular lower surface. Man O' War Member, Felix to Man O' War Coves, Bed 17.

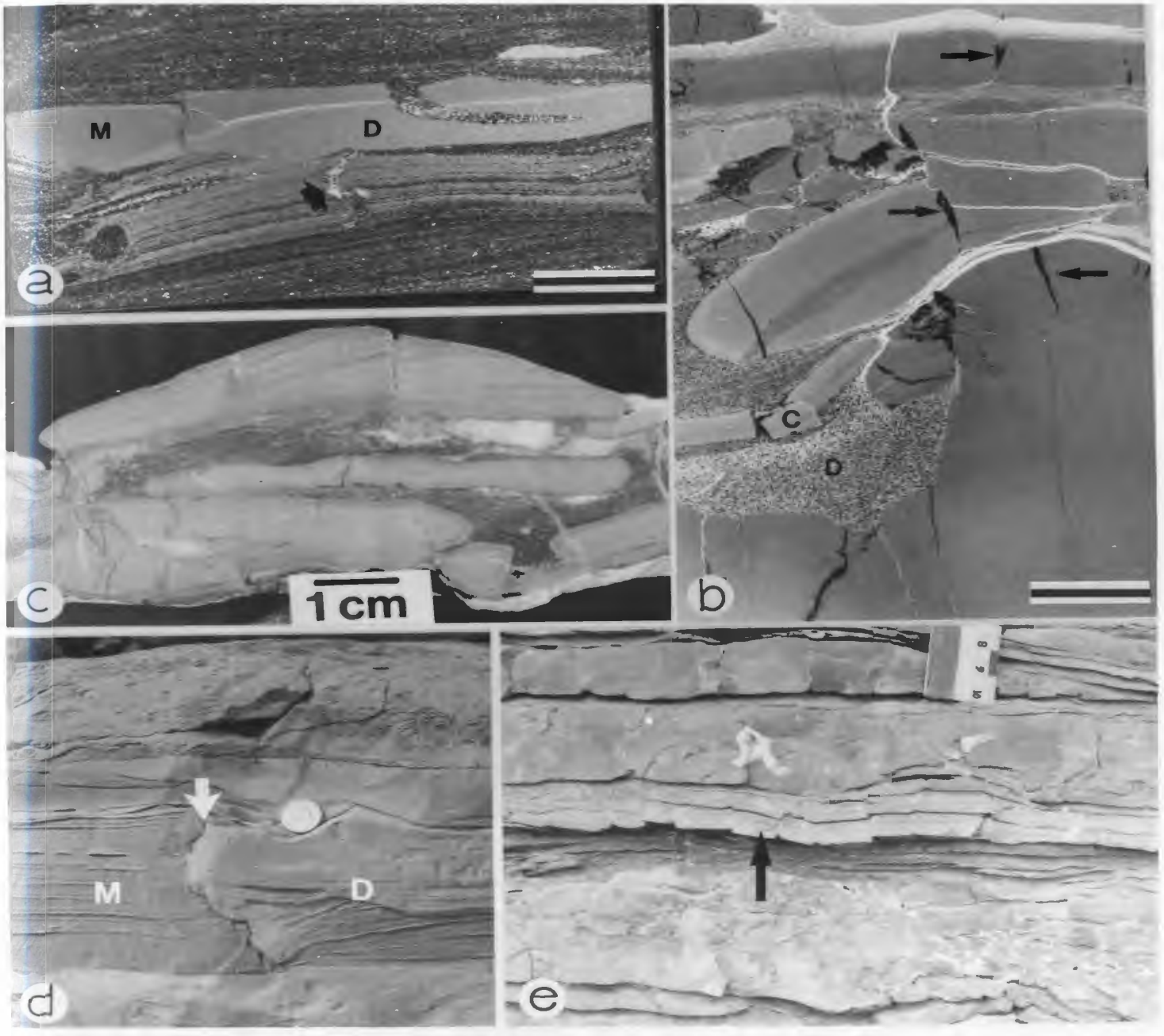
M
D
a
C
D
b
1 cm
c
M
D
d
e

PLATE 27: SOLUTION SURFACES IN PARTED LIMESTONE

a: Thin section negative print of microstylolite swarms (white in photo) which commonly have small limestone clots (fitted nodules). The upper swarm encloses vertical, blocky calcite burrows (black in photo; arrow). Scale bar is 5 mm. Stratigraphic top is up. Man O' War Member, Felix to Man O' War Member, Bed 18, sample NC-83-182.

b: Thin section photomicrograph detailing burrows in "a" above. Microstylolites warp around and cut through burrows. Scale bar is 500 μm. Stratigraphic top is up. Man O' War Member, Bed 18, sample NC-83-182.

c: Thin section photomicrograph of microstylolite swarm at contact between mudstone and peloidal, siliciclastic siltstone. Scale bar is 500 μm. Stratigraphic top is up. March Point Formation, March Point section, Bed 6, sample NC-82-27A.

d: Thin section photomicrograph of microstylolite truncating V-shaped fracture filled with dull-luminescent blocky calcite (C) and ferroan dolomite (D). Scale bar is 500 μm. March Point Formation, March Point section, Bed 6, sample NC-82-27A.

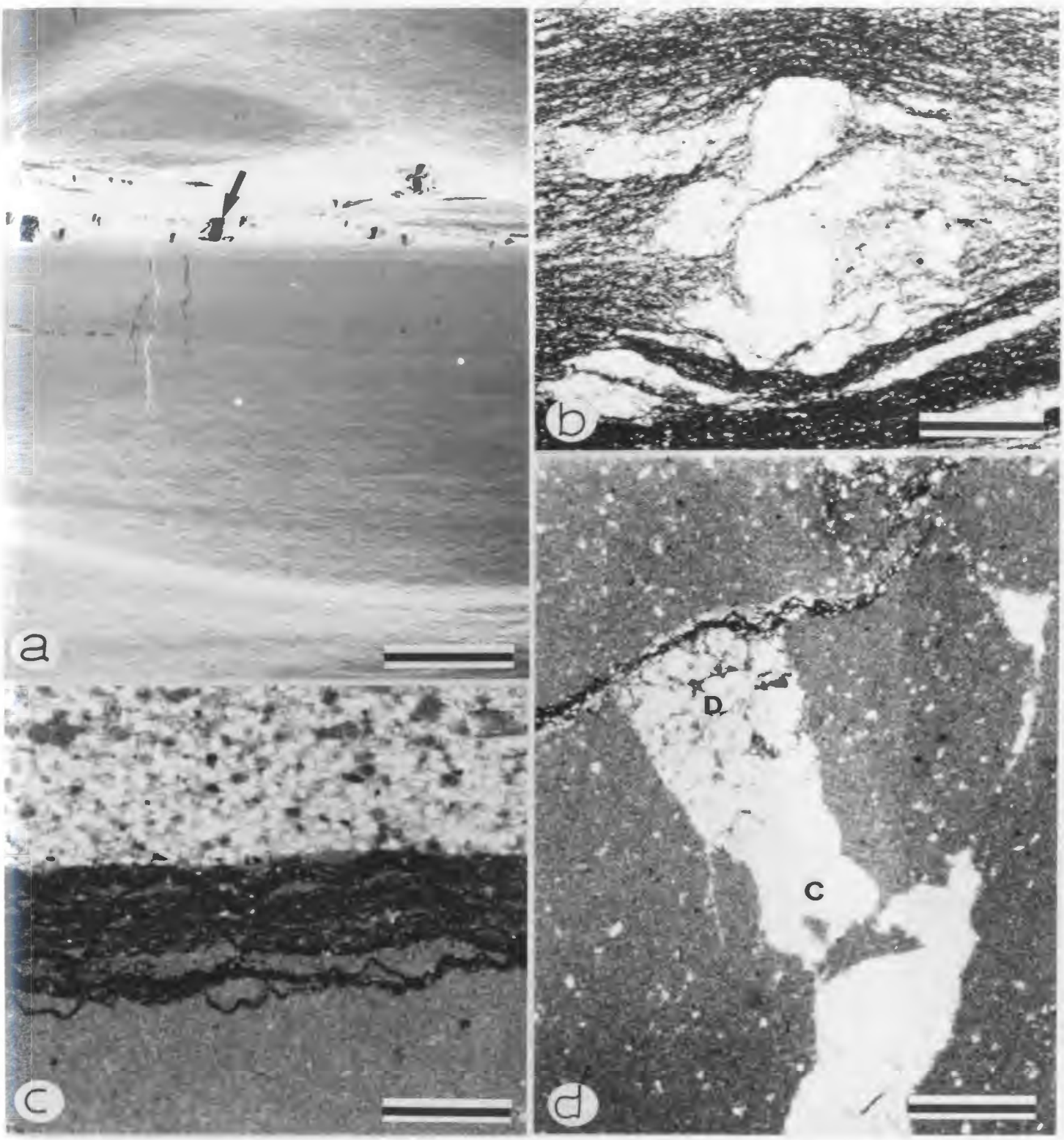
a
b
c
d
D
C

PLATE 28: DULL CL DOLOMITE

a: CL photomicrograph of dull-luminescent radial-blocky ooids in grey oolite, which are partially replaced by euhedral, non-luminescent (ferroan) dolomite rhombs (solid arrows). Rhombs are partially replaced by bright-luminescent blocky calcite (white in photo; open arrow). Scale bar is 730 μm. Man O' War Member, Felix to Man O' War Coves section, Bed 17, sample NC-83-32.

b: CL photomicrograph of micritic intraclasts and oncoid (center of photo) preferentially replaced by non-luminescent ferroan dolomite (D). Bioclastic nucleus (N) of oncoid is undolomitized. Scale bar is 730 μm. March Point Formation, March Point section, Bed 5, sample NC-83-17.

c, d: Plane light and CL photomicrographs of bioclast calcarenite matrix in flat-pebble conglomerate. Echinoderm fragments (E), syntaxial calcite overgrowths (O) and some micrite matrix (m) are preferentially rimmed by rhombic "band" of non-luminescent ferroan dolomite (black in photo, d). Scale bar is 650 μm. Big Cove Member, March Point section, sample NC-82-36.

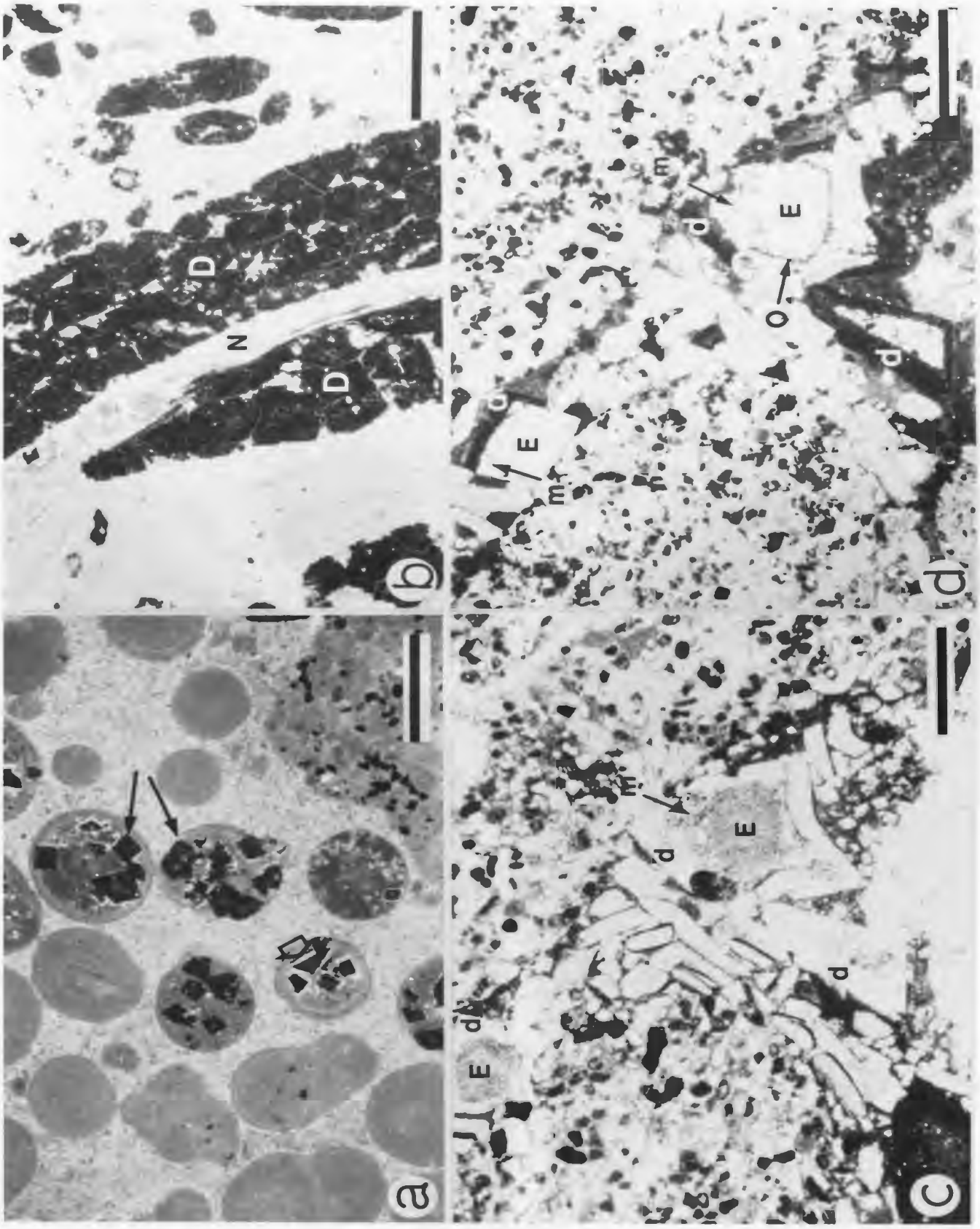
a
b
D
N
D
c
E
d
m
d
d
E
d
d
d
E
m
d
d
E
O
p
p

PLATE 29: DULL CL DOLOMITE

a, b: Plane light and CL photomicrographs of intraclast calcirudite (c - clast) with matrix replaced by dull-luminescent ferroan dolomite (D) that partially replaces grain margins. Grain outlines are preserved by inclusions within dolomite rhombs (arrows). Scale bar is 500 μm. Felix Member, Felix to Man O' War Coves section, sample NC-82-211B.

c: CL photomicrograph of brown oolite with intergranular porosity occluded by non-luminescent ferroan dolomite (black in photo). Particles are rimmed by undolomitized micritic calcite (diffuse grey fringe in photo; arrows). Scale bar is 500 μm. Campbells Member, March Point section, Bed 11, sample NC-83-246.

d: CL photomicrograph of fracture filled by dull-luminescent blocky calcite (B) and ferroan dolomite rhombs (D) with zoned dull luminescence. Rhombs appear to have grown inward toward center of fracture. Scale bar is 500 μm. Campbells Member, March Point section, Bed 11, sample NC-83-249C.

e: CL photomicrograph of non-luminescent ferroan dolomite floating in a micritic matrix. Rhombs have been partially replaced by at least two stages of bright-luminescent blocky calcite. (dedolomitized) and have serrated contacts with adjacent matrix (arrow). Scale bar is 300 μm. March Point Formation, east of Campbells Cove section, sample NC-83-22.

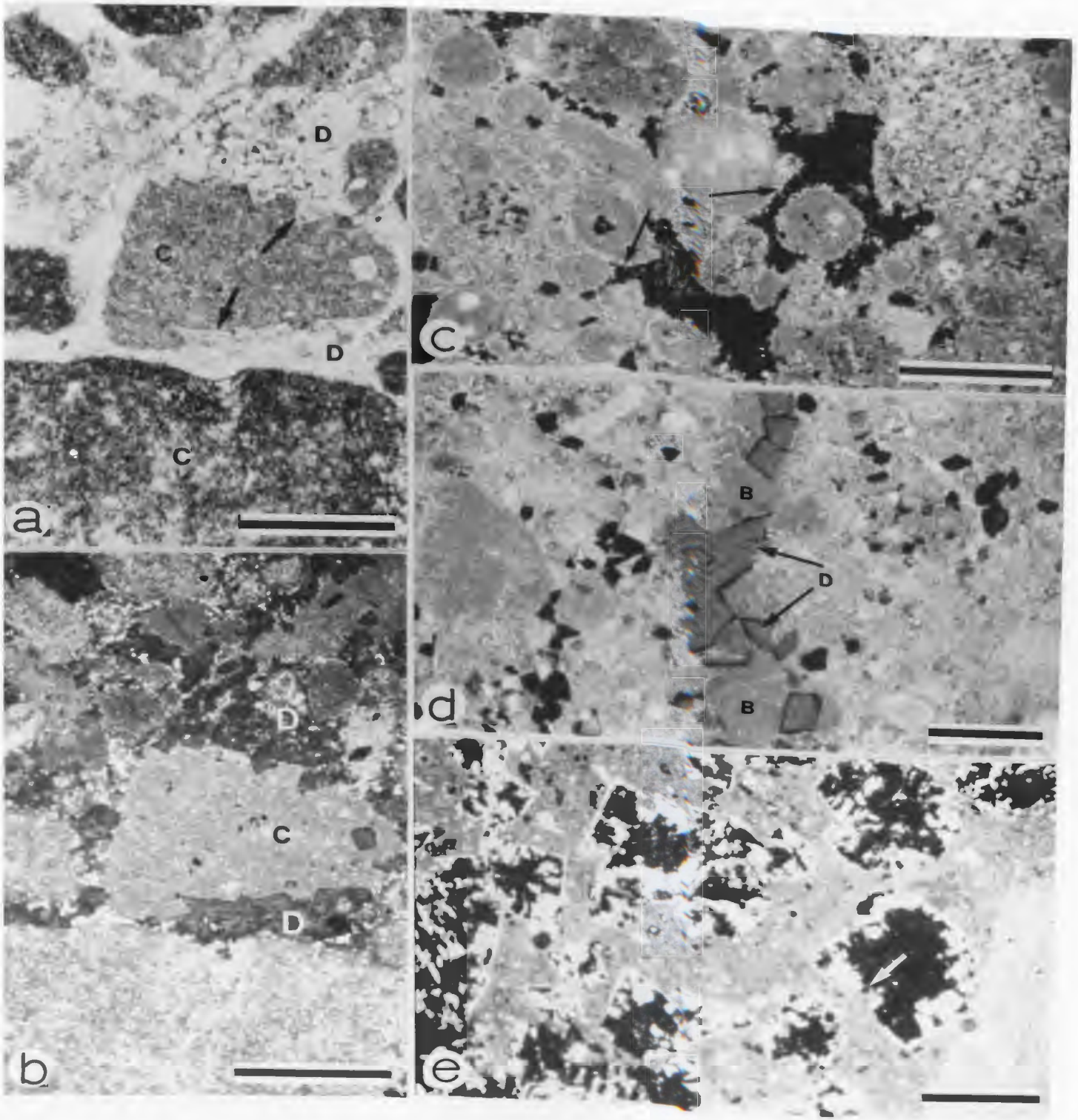
D
C
D
C
a
C
D
C
D
b
B
D
B
d
e

PLATE 30: ZONED DOLOMITE AND PERVASIVE DOLOSTONE

a: CL photomicrograph of dolomitized bioclast calcarenite composed predominantly of echinoderm fragments and overgrowths, which are replaced by: (1) bright red CL dolomite (light grey in photo); and (2) zoned bright and non-luminescent dolomite. Scale bar is 570 μm. Campbells Member, March Point section, Bed 9, sample NC-82-193.

b, c: Plane light and CL photomicrographs of dolomitized ooid calcarenite (type 2 pervasive dolostone) with ooid textures preserved by inclusions in zoned, bright red luminescent dolomite rhombs (0). Scale bar is 300 μm. Berry Head Formation, Isthmus Bay East section, Bed 3, sample NC-82-101.

d: CL photomicrograph of dolomitized calcarenite (type 1 pervasive dolostone) composed of: (1) particles with excellent fabric preservation that are replaced by bright red luminescent dolomite; and (2) interparticle matrix replaced by zoned bright-luminescent and non-luminescent dolomite. Patches of coarse crystalline dolomite in center of photo have sharp boundaries (arrows). Scale bar is 900 μm. Felix Member, March Point section, Bed 2, sample NC-82-73D.

e: Thin section photomicrograph of type 2 pervasive dolostone with no original fabric preservation and composed of bright red luminescent dolomite. Vuggy pore in center of photo is occluded by distinctly zoned, bright to non-luminescent rhombs. Scale bar is 500 μm. Berry Head Formation, Isthmus Bay East section, Bed 13, sample NC-82-121.

f: CL photomicrograph of saddle dolomite lining fracture in dololaminite. Outer ferroan zone with dull to non-luminescence is partially replaced by bright-luminescent blocky calcite (arrow). Remaining fracture porosity is occluded by very coarse crystalline, bright-luminescent blocky calcite cement (b). Scale bar is 900 μm. Berry Head Formation, Isthmus Bay East section, Bed 3, sample NC-82-226.

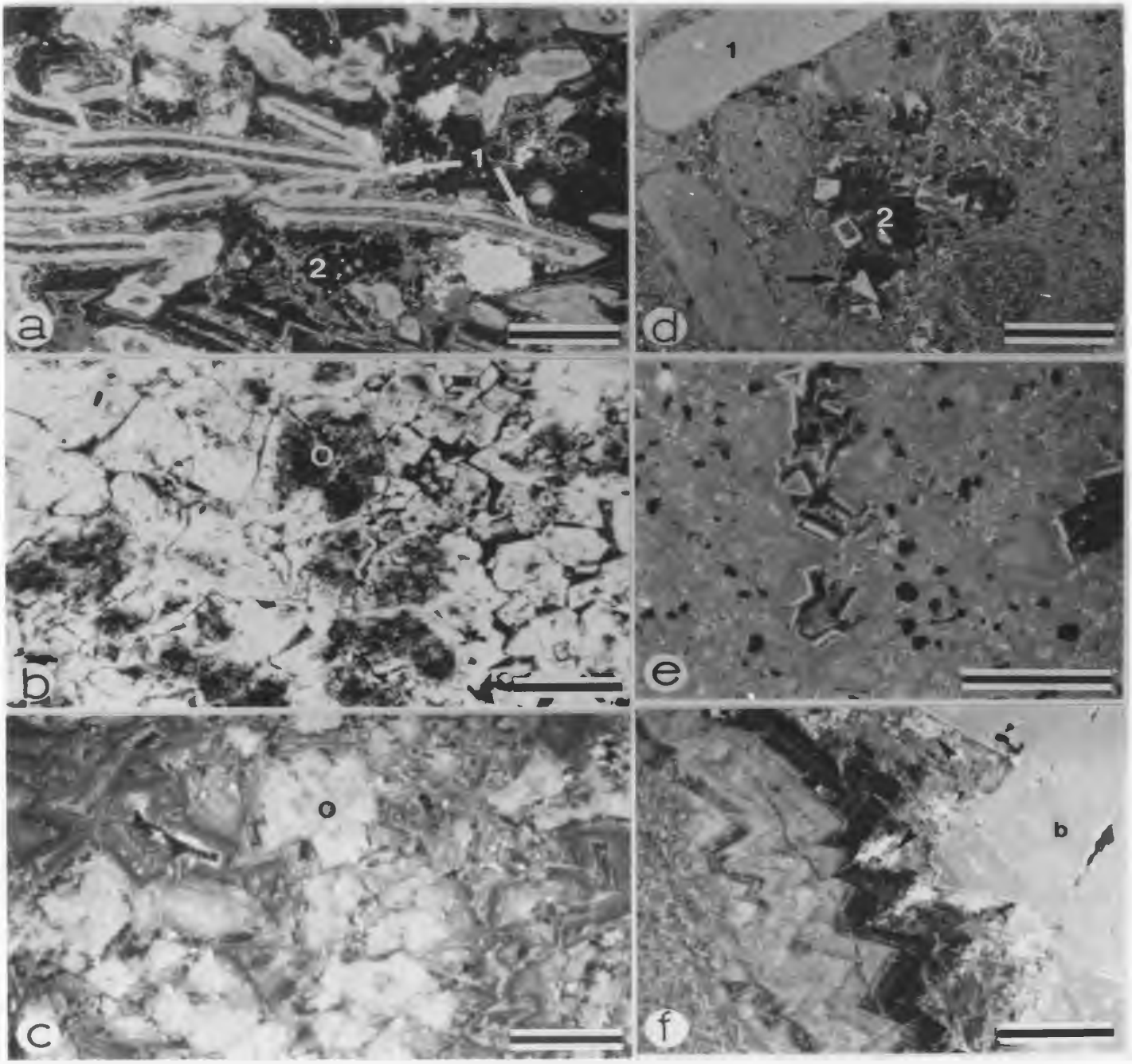
a
1
2
d
1
2
b
o
e
c
o
f
b

Appendix A

REVISION OF STRATIGRAPHIC TERMINOLOGY

A.1 Introduction

Examination of the stratigraphy of Middle and Upper Cambrian platform strata in western Newfoundland reveals a need for re-evaluation of the stratigraphic terminology. The "March Point formation" and "Petit Jardin formation" proposed by Lochman (1938) in the type area of the Port au Port Peninsula are well ensconced in the literature (refer to Chapters 1 and 2), but are based solely on trilobite data of Schuchert and Dunbar (1934). Furthermore, recent studies (Kindle and Whittington, 1965; Levesque, 1977) have revealed that: (1) strata from Cape St.George to Big Cove Brook (Cambrian type section of Schuchert and Dunbar, and Lochman) are an incomplete Cambrian sequence; and (2) strata from Jerrys Nose to east of Gravels Ponds (part of the Ordovician St. George series of Schuchert and Dunbar) are of Cambrian age. Numerous studies of equivalent strata have also been undertaken on the Great Northern Peninsula, but separate, informal stratigraphic units have generally been proposed for each area (see Chapter 1). Nor has correlation of these outcrops with those on the Port au Port Peninsula been attempted

due to the predominance of dolostone and paucity of fossils in the more northerly outcrops.

The purpose of this section is to recount the revised stratigraphic terminology used in this study that will eventually be formalized by publication.

A.2 Proposed Stratigraphy

Incorporating the stratigraphic divisions proposed by Levesque (1977), the Middle to Upper Cambrian sequence will be named the Port au Port Group and divided into three formations: March Point, Petit Jardin, and Berry Head. These laterally traceable and mappable units will be formally defined on the Port au Port Peninsula.

Each revised or newly proposed formation or member is described as recommended by the North American Stratigraphic Code (1983) and includes: (1) formation or member stratotype location; (2) lithologic description; (3) thickness; (4) lower and upper boundaries; (5) geologic age; (6) synonymy; and (7) characteristic fossils.

PORT AU PORT GROUP

Well exposed outcrops of the Port au Port Group are located along the west coast of Newfoundland, from the Port au Port Peninsula in the south to the St. Barbe coast in the north. The group is composed of a sequence of thinly interbedded carbonate mudstones, shales and

argillaceous dolostones and thick-bedded ooid and skeletal packstones to grainstones and laminated dolostones. The sequence is frequently punctuated by stromatolites and thrombolites and flat-pebble conglomerates. The carbonates and siliciclastics of the Port au Port Group unconformably overly sandstones of the Hawke Bay Formation (Labrador Group) and conformably underly limestones and dolostones of the Lower Ordovician St. George Group.

MARCH POINT FORMATION

Formation Stratotype - Degras (grid reference NTS 12B/6 UD 351707); cliff exposure and wave-cut platform approximately 0.5 km southwest of the town of Cape St. George.

Lithologic Character - Glauconitic, silty limestone to calcareous siltstone and interbedded limestone and shale in lower 15 m with rest of unit consisting of interbedded limestone and dolostone. Limestones composed of lime mudstone, peloidal and bioclastic packstone to wackestone, and flat pebble conglomerates. Increasing shale content toward top.

Thickness - 55 m.

Lower Boundary - Defined at stratotype by junction between massive sandstones of the underlying Lower Cambrian Hawke Bay Formation and thin-bedded limestones, dolostones and shales.

Upper Boundary - Defined at base of first thick black shale and lime mudstone bed that concordantly overlies limestones and dolostones of the

March Point Formation. At the stratotype the boundary is marked by a distinctive round-pebble conglomerate bed.

Age - Trilobites identified by Lochman (1938), Levesque, 1977) and Boyce (pers. comm., 1984) indicate that the formation is mainly of late Middle Cambrian age, with fauna from the Bathyuriscus-Elrathina and Bolaspidella zones.

Synonymy - Beds 6 to 12(?) of March Point formation as defined by Schuchert and Dunbar (1934) and re-examined by Lochman (1938); approximately the lower 55 m of the lower shaly member of the March Point Formation of Levesque (1977).

Characteristic Fossils - inarticulate brachiopods, trilobites, echinoderm fragments.

Remarks - Formation can be correlated to more northerly outcrops in west Newfoundland and has relatively uniform composition.

PETIT JARDIN FORMATION

The Petit Jardin Formation contains a wide spectrum of lithologies. In the type area of the Port au Port Peninsula, it is composed of repeated packages of thick-bedded carbonates, and thin-bedded carbonates and shales, and is divisible into five members. Equivalent strata on the Great Northern Peninsula also have a variety of lithologies, but tend to be predominantly dolostone.

Cape Ann Member

Member Stratotype - Degras (grid reference NTS 12B/6 UD 348706); wave-cut platform and cliff exposure approximately 0.5 km southwest of town of Cape St. George.

Lithologic Character - Recessive weathering, thinly bedded dark grey shale, limestone and dolostone. Limestone is composed of peloidal packstone to wackestone. Large algal mound horizons present in upper 15 m of stratotype.

Thickness - 36 m.

Lower Boundary - Defined as base of first thickly interbedded black shale and limestone; at stratotype distinct, 10 to 15 cm, rounded pebble conglomerate bed of underlying March Point Formation marks junction.

Upper Boundary - Defined as highest occurrence of interbedded silty limestone, dolostone and shale underlying thick-bedded dolostones of the Campbells Member.

Age - *Bolaspidella* zone - late Middle Cambrian (Lochman, 1938; Levesque, 1977).

Synonymy - Bed 13 of March Point formation of Schuchert and Dunbar (1934) and Lochman (1938); the upper 36 m of the lower shaly member of the March Point Formation as proposed by Levesque (1977).

Characteristic Fossils - trilobites, inarticulate brachiopods.

Campbells Member

Member Stratotype - March Point (grid reference NTS 12B/11 UD 434742); cliff exposure directly east of March Point to approximately 1 km northeast of March Point.

Lithologic Character - Resistant weathering, thick-bedded dark grey and light coloured ooid packstones to grainstones and laminated limestones and dolostones punctuated by algal mound horizons and minor parted limestones. Carbonate laminites dominant at base with oolites dominating top of unit.

Thickness - 95.9 m.

Lower Boundary - At the stratotype defined as the junction between thin-bedded limestones and dolostones of the Cape Ann Member and the overlying thick-bedded dolostones.

Upper Boundary - Defined as the highest occurrence of thick-bedded oolitic limestones and dolostones.

Age - Trilobites indicate that the member is early Late Cambrian in age (early Dresbachian), with fauna from the Cedaria-Crepicephalus zones (Boyce, pers. comm., 1984).

Synonymy - Beds 14 to 22 of March Point formation of Schuchert and Dunbar (1934) and Lochman (1938); informally named upper massive member of March Point Formation by Levesque (1977).

Characteristic Fossils - trilobites.

Big Cove Member

Member Stratotype - March Point (grid reference NTS 12B/11 UD 442746); cliff exposure approximately 1 km northeast of March Point.

Lithologic Character - Interbedded parted limestone, oolite grainstone and red and green shale at base developing upward into thinly bedded dark grey shales, dolostones and limestones. Shale content decreases toward upper boundary. Limestones comprised of silty lime mudstone to peloidal packstone.

Thickness - 51 m.

Lower Boundary - Defined at stratotype as junction between thick-bedded dolostones and oolitic limestones of the Campbells Member and the overlying thin-bedded limestones and shales.

Upper Boundary - Defined as highest occurrence of thin-bedded limestones, dolostones and shales underlying the thick-bedded dolostones of the Felix Member.

Age - Trilobites of the Cedaria zone (Lochman, 1938) indicate earliest Late Cambrian age (Dresbachian).

Synonymy - Beds 23 to 27 of the March Point formation of Schuchert and Dunbar (1934); Beds 23 to 27 of the Petit Jardin formation as proposed

by Lochman (1938); corresponds to lower shaly member of Petit Jardin Formation of Levesque (1977).

Characteristic Fossils - trilobites; inarticulate brachiopods.

Felix Member

Member Stratotype - March Point (grid reference NTS 12B/11 UD 445747); cliff exposure approximately 2.5 km northeast of March Point.

Lithologic Character - Resistant weathering, thick-bedded laminated dolostones, oolites and algal mound horizons. Although most of unit has been dolomitized, it is apparent that it is similar in composition to Campbells Member.

Thickness - 65 m.

Lower Boundary - Defined as junction between thin-bedded limestones and dolostones of underlying Big Cove Member and thick-bedded laminated dolostones.

Upper Boundary - At stratotype defined as contact between dominantly thick-bedded dolostones of the Felix Member and overlying shales, dolostones and limestones.

Age - In the upper 15 m of the unit, trilobites of the Crepicephalus, Aphelaspis, Dicanthopyge, Prehousia and Dunderbergia zones have been collected indicating a Dresbachian age (early Late Cambrian) [Levesque,

1977].

Synonymy - Beds 28 to 30 of Schuchert and Dunbar's (1934, p. 34) March Point formation; upper 65 m of Petit Jardin formation (Beds 28 to 30) of Lochman (1938, p. 463); middle dolostone member of Petit Jardin Formation proposed by Levesque (1977).

Characteristic Fossils - trilobites.

Man O' War Member

Member Stratotype - Felix Cove to Man O' War Cove (grid reference NTS 12B/10 UD 695770); cliff exposure and wave-cut platform located 0.5 km east of Felix Cove to approximately 0.5 km west of Man O' War Cove; upper 25 m are repeated in headland east of Man O' War Cove.

Lithologic Description - Dominantly thin-bedded limestone and dolostone with minor shale beds. Excellent flat pebble conglomerates, algal mound horizons and oolitic-bioclastic grainstones to packstones punctuate unit.

Thickness - 69 m.

Lower Boundary - Defined as highest occurrence of thick-bedded dolostones of the Felix Member and the first appearance of interbedded shales, dolostones and limestones.

Upper Boundary - At stratotype defined as junction between thin-bedded

limestones and dolostones and overlying massive dolostones of the Berry Head Formation.

Age - Trilobites collected near the base of the member indicate an Elvinia zone age and those in the uppermost shale bed indicate a Taenicephalus zone age (Franconian - middle Late Cambrian age) [Levesque, 1977].

Synonymy - Corresponds to Bed 3 and part of Bed 2 of the type section of the St. George series defined by Schuchert and Dunbar (1934, p. 48 to 50); upper shaly member of the Petit Jardin Formation proposed by Levesque (1977).

Characteristic Fossils - gastropods, trilobites.

BERRY HEAD FORMATION

Formation Stratotype - east of Isthmus Bay (grid reference NTS 12B/10 UD 744788); wave-cut platform on the southern shore 0.6 to 1.6 km east of Gravels Pond.

Lithologic Description - Interbedded laminated dolostone and dolomitized oolites and stromatolites near base, with interbedded dolostone and limestone near top. Limestones are composed of oolites and lime mudstones to wackestones. Chert nodules and bands are abundant in the upper two thirds of the unit. Stromatolite mounds are present throughout the Formation.

Thickness - 196 m.

Lower Boundary - Defined as first occurrence of thick-bedded pinkish coloured dolostones overlying thin-bedded limestones and dolostones of the Man O' War Member.

Upper Boundary - Defined as junction between thick-bedded limestones and dolostones and overlying mottled limestones and dolostones of the St. George Group (refer to Pratt, 1979).

Age - No zone trilobites have been collected to date. Preliminary conodont examination has yielded a latest Late Cambrian age (F. O'Brien, pers. comm., 1983).

Synonymy - Beds 4 and 5 of the St. George series type section of Schuchert and Dunbar (1934, p.48, 50); Beds 1 to 4 of the lower cyclic member of the St. George Formation as revised by Levesque (1977).

Characteristic Fossils - trilobites.

Appendix B

MEASURED STRATIGRAPHIC SECTIONS

This section includes detailed descriptions and measurements of five stratigraphic sections in western Newfoundland: Degras (Fig. B.1), March Point (Fig. B.2), Felix to Man O'War Coves (Fig. B.3) on the Port au Port Peninsula; Isthmus Bay East (Fig. B.6); and Little Coney in White Bay (Fig. B.7). Supplemental sections measured at Abrahams Cove and Campbells Cove on the Port au Port Peninsula are shown in Figures B.4 and B.5 respectively. The legend to symbols used in the graphic sections is provided in Table B.1.

TABLE B.1: LEGEND TO MEASURED STRATIGRAPHIC SECTIONS

CARBONATE ROCK TYPES

DOLOSTONE
LIMESTONE
PARTED LIMESTONE
M Mudstone
W Wackestone
P Packstone
G Grainstone

SILICICLASTIC ROCK TYPES

Q SANDSTONE
SILTSTONE
SHALE

PARTICLES

OOIDS
PISOIDS
ONCOIDS
INTRACLASTS
TABULAR PEBBLES
PYRITE
GLAUCONITE
CHERT
PHOSPHATE

FOSSILS

TRILOBITES
GASTROPODS
BRACHIOPODS
STROMATOLITES
THROMBOLITES
UNDIFFERENTIATED MOUNDS

SEDIMENTARY STRUCTURES

FENESTRAE
HERRINGBONE CROSS-BEDDING
RIPPLES
MUDCRACKS
PRISM CRACKS
GUTTER CASTS
RÜNZELMARKEN
P PATTERNED DOLOSTONE
TEPEE STRUCTURES
BIOTURBATION
MOTTLING

OTHER

BRECCIA
FAULT
COVERED INTERVAL

OUTCROP MAPS

A B LOCATION OF SECTION FROM BASE (A) TO TOP (B)
M.PT. MARCH POINT FM.
C.A. PETIT JARDIN FM.: CAPE ANN MBR.
CAMP. CAMPBELLS MBR.
B.C. BIG COVE MBR.
FEL. FELIX MBR.
M.O.W. MAN O' WAR MBR.
B.H. BERRY HEAD FM.
UNIT CONTACTS (EXPOSED)
UNIT CONTACTS (COVERED)
FAULTS

B.1 Degras, Port au Port Peninsula

This section was measured along the southern shore of the Port au Port Peninsula, 0.5 km west of the town of Cape St. George. Unit numbers and thicknesses from James (pers. comm., 1982).

Unit	Description	Thickness (m) Unit	Total from base
	PETIT JARDIN FORMATION Cape Ann Member		
17	Shale, dolomitic, variegated red and green; interbedded with dolostone, buff weathering, laminated; minor thin-bedded, flat-pebble conglomerate beds composed of tabular mudstone clasts, horizontally to vertically disposed.	...12.0	92.8
16	Dolostone, argillaceous, to dolomitic shale, variegated red and green; thin-bedded, well developed prism cracks and tepee structures.	...2.5	80.8
15	Limestone, ooid calcarenite, dark grey; thick-bedded, (30-40 cm in thickness), cross-laminated, with minor shale-partings; interbedded with: Limestone, mudstone, medium grey; thin-bedded, ripple cross-laminations; thinly interbedded with dolostone, argillaceous, tan weathering.	...2.3	78.3
14	Dolostone, argillaceous, to dolomitic shale, variegated red and green; thin- to thick-bedded, fissile. Stromatolite mounds are 30 cm in height, LLH, and overly flat-pebble conglomerate.	...2.8	76.0
13	Limestone, stromatolite/thrombolite mounds, grey; biostromal mounds, 0.3-1.0 m in thickness, overly flat-pebble conglomerate; coalesce upward into bioherm complex with planar, reddish-brown stained surface, overlain by 1-2 cm thick pustulose mat. Intermound sediment is grey, laminated mudstone.	...11.0	73.2

12 Limestone, stromatolite/thrombolite mounds, grey; three biostromal layers composed of mounds, 30-50 cm in height, commonly rooted on flat-pebble conglomerate; abundant trilobite hash. Intermound sediment is thin-bedded grey, green and red shale and grey mudstone. ...7.6 62.2

MARCH POINT FORMATION

11 Limestone, mudstone, medium grey; thin-bedded to nodular, ripple cross-laminated, parted with dark grey shale, calcareous; runzelmarken and mudcracks; recessively weathering. Distinctive round-pebble conglomerate occurs at top of unit. ...5.3 54.6

10 Limestone, parted with dark grey shale, as above. Lenticular beds (20-50 cm in thickness) of flat-pebble conglomerate and bioclast (trilobite) calcarenite are common. ...2.0 49.3

9 Limestone, mudstone, as above; interbedded with bioclast calcarenite, up to 50 cm thick, ripple cross-bedded, vugs. Shale partings to thin beds become more abundant at top of unit. ...5.6 47.3

8 Limestone, mudstone, as above; interbedded with argillaceous dolostone and rare shale partings; resistant weathering. Quartz-filled vugs are common. ...5.6 41.7

7 Limestone interbedded with shale and argillaceous dolostone, as above; percentage of shale increases upward in unit. Abundant flat-pebble conglomerate beds occur throughout. ...4.7 36.1

6 As above, interbedded with abundant bioclast wackestone to packstone, ripple cross-laminated, abundant trilobite hash. ...5.0 31.4

5 As above, with multiple horizons of distinctive, thin beds of flat-pebble conglomerate, 5-10 cm thick and lenticular; tabular mudstone clasts, up to 10 cm in diameter, are horizontally to vertically disposed, and cut by cracks and possible borings. ...9.0 26.4

4	Sandstone, quartzose, to arenaceous limestone, greenish-grey, medium to coarse sand-size grains; thick-bedded, planar to low-angle cross-bedding; glauconitic, phosphatic pebbles; Skolithos. Above 6 m, glauconitic sandstone with rhombohedral ripples, is thinly interbedded with limestone, shale and argillaceous dolostone, as above; mudcracks.	...10.6	17.4
3	Shale, dark grey, fissile.	...0.4	6.8
2	Sandstone, quartzose, reddish-brown weathering, medium to coarse sand-size grains; large-scale, low angle cross-bedding, and runzelmarken, straight ripples, and mudcracks on bedding planes; burrows.	...1.4	6.4
1	Limestone, siliciclastic silt-rich, to calcareous siltstone, medium grey; occur as centimeter- to decimeter-scale channels (gutter casts) with wavy laminations, load casts, small dikes, and pebble clasts; interbedded with shale, black, fissile.	...5.0	5.0

B.2 March Point, Port au Port Peninsula

This section was measured from March Point eastward to a fault zone west of Big Cove Brook.

Unit	Description	Thickness (m) Unit	Total from base
	PETIT JARDIN FORMATION Man O' War Member		
6	Unit consists of three interbedded lithologies: Dolostone, mauve-buff, finely to medium crystalline; thick-bedded (1.0–1.5 m), mudcracks, relict ooid calcarenite texture; resistant weathering. Shale, dolomitic, variegated red and green; thick-bedded, fissile; grey weathering. Dolostone, light brown, very finely crystalline; thin-bedded, laminations; silty; resistant weathering. Only the lower 2 m are accessible.	...10	
	Felix Member		
5	Unit consists of four lithofacies: Dolostone, mauve-brown, finely to medium crystalline; thick-bedded (1.0–1.5 m), herringbone cross-bedding, mudcracked finely crystalline layers (2–5 cm thick), finely crystalline intraclasts, relict ooid calcarenite texture; pinhole porosity; glauconitic, rounded sand-size quartz grains; resistant weathering. At 10 m from base, thin-bedded dolostone, reddish-brown; mudcracks; glauconitic, silty, rounded coarse sand-size quartz grains. Dolostone, light grey, very finely crystalline; thick-bedded (50–60 cm), laminations, mudcracks; resistant weathering. Dolostone, dark grey, medium crystalline; thick-bedded (50–70 cm), relict ooid calcarenite texture; glauconitic; resistant weathering; most common near base of unit.		

Dolostone, stromatolitic, reddish-brown; hemispheroidal mounds and digitate clusters, 10-30 cm in height, composed of LLH and SH; occur at 1 m, 6.2 m, 16.9 m, 20.9 m, 22 m from base of unit. ...25.1 54.8

4 Dolostone, as above. At base, laminated dolostone has irregular brecciated and fractured upper surfaces. Stromatolites occur at base on brecciated dolostone, and at 6.2 m. ...8.1 29.7

3 Dolostone, as above. Mauve-brown dolostone is most abundant. Irregular bedding contacts between laminated and dark grey dolostone.
Conglomerate, medium grey, near base of unit, composed of tabular clasts of laminated dolostone up to 5 cm in length and horizontally to vertically disposed, 20 cm in thickness. ...14.6 21.6

2 Dolostone, as above. Conglomerate, as above, 10 cm thick, occurs at base. ...4.1 7.0

1 Dolostone, light grey, very finely crystalline; planar to wavy laminations, prism cracks, minor ooids, vuggy porosity.
Thrombolite mounds occur at 1.2 m from base, overlying grainy dolostone. ...2.9 2.9

Big Cove Member

6 Unit consists of three lithologies, which in order of decreasing abundance are:
Limestone, medium grey, mudstone; ripple cross-laminations, gutter casts, load casts, skip and bounce marks, mudcracks; grey weathering, trace fossils; parted or thinly interbedded with:
Shale, calcareous, medium grey; fissile, mudcracks; most abundant in lower half of unit; or,
Dolostone, argillaceous, medium grey, very finely crystalline; laminations, mudcracks; tan weathering; trace fossils.
Limestone, ooid-bioclast calcarenite, dark grey, medium sand-size; thick-bedded (10-30 cm), rippled surface; occurs near top of unit.
Limestone, conglomeratic, medium grey; thick-bedded (5-20 cm in thickness, planar to lenticular; tabular pebbles composed of grey mudstone, horizontally to vertically disposed.
Limestone, stromatolitic, medium grey; hemispheroidal mounds, up to 50 cm in height. ...10.5 45.2

5	Limestone, medium grey, mudstone and conglomerate, as above; parted with: Dolostone, argillaceous, as above. Grey shale, 5 cm in thickness, is rare.	...4.5	35.2
4	Limestone, as above; abundant runzelmarken, mudcracks; 10 cm thick, bioclastic calcarenite at 2.0 m above base; interbedded with partings to thick-beds of: Shale, calcareous, dark grey; fissile, mudcracks. Poorly exposed.	...17.5	30.7
3	Covered.	...2.0	13.2
2	Limestone interbedded with shale, as above. Poorly exposed.	...2.2	11.2
1	Unit consists of interbedded: Shales, variegated red and green; thin-bedded to thick-bedded, fissile. Limestone, ooid-bioclast calcarenite, reddish-grey; thick-bedded, irregular upper bedding surfaces; mudstone intraclasts; light grey weathering; trilobite fragments. Limestone, as above; thinly interbedded with shale, as above. Limestone, conglomeratic, medium grey; thick-bedded; tabular clasts of ooid calcarenite and mudstone, horizontally to vertically disposed. At 7.0 m from the base is stromatolite horizon composed of three superimposed mounds, hemispheroidal, 15-20 cm in height, LLH to SH.	...9.0	9.0

Campbells Member

11	Unit consists of four main lithologies, which in order of decreasing abundance are: Limestone, ooid calcarenite, light to dark brown; thick-bedded (1.0-1.5 m), herringbone cross-bedding; dolomitic mudstone clasts and mudcracked layers; buff weathering. Limestone, ooid calcarenite, dark grey; thick-bedded (30-50 cm), bedding contacts with above limestone generally irregular, upper bed surfaces may have ripple to megaripple forms. Beds occasionally capped by thombolite mounds, 4-5 cm in height. Limestone, mudstone, grey; with argillaceous partings, green, mudcracked. Small thrombolite mounds occur at 3.4 m from base, 10-15 cm in height and 20 cm wide.		

Limestone, dolomitic, to calcareous limestone, buff to light brown; thick-bedded (0.5-1.0 m), laminations, mudcracks; oolitic and mudstone clasts. ...18.5 95.5

10 Limestone, dolomitic, to calcareous dolomite, as above; prism cracks, irregular upper surfaces. Stromatolite (LLH)/thrombolite mound horizons occur at 0.6 m, 1.2 m, 4.5 m, 5.3 m from base; hemispheroidal to cap-shaped, 30-100 cm in height and 30-40 cm in width; occasionally have planar upper surfaces; interbedded with:
Limestone, ooid calcarenite, dark grey, as above; minor mudstone clasts; trilobite hash occasionally at top of beds. Minor brown ooid calcarenite.
Above 4.5 m, ooid calcarenite is interbedded with green calcareous shale, partings to thin beds, and grey mudstone, thin-bedded. ...8.2 77.0

9 Limestone, dolomitic, to calcareous dolomite, as above; interbedded with:
Limestone, brown ooid calcarenite and minor dark grey ooid calcarenite, as above, and calcareous grey-green shale. Occasional thick beds of trilobite-rich grainstone. Near top of unit, thinly interbedded grey mudstone and tan weathering dolostone is abundant. Thrombolite mound horizons occur near base of unit, at 15.1 m and 16 m; 20-50 cm in height and up to 1 m in width; occasionally have planar upper surface and overlain by fractured dolomitic limestone. ...18.8 68.8

8 Unit consists of interbedded:
Limestone; mudstone to ooid calcarenite, medium grey; thin-bedded; interbedded to interlaminated with dolostone, argillaceous, medium grey; compacted mudcracks, burrows; tan weathering. Thrombolite mounds are approximately 30 cm in height and 20-30 cm in width.
Limestone, ooid-bioclast calcarenite, dark grey, as above; tabular oolitic clasts.
Limestone, dolomitic, as above; occasionally contain stromatolites, digitate, 2-5 cm in height. ...9.7 50.0

7 Limestone, ooid calcarenite, dark grey and brown types, as above; minor laminated dolomitic limestone, as above. Stromatolite mounds occur in brown ooid calcarenite, LLH-C, 0.10 m in height and 1 m in width. ...4.8 40.3

6	Limestone, mudstone, thinly interbedded with tan weathering dolostone, as above. Stromatolite/thrombolite mounds occur at 1.2 m and 3.0 m from base, hemispheroidal, 50-80 cm in height and 1-1.5 m. in width. Limestone, ooid calcarenite, dark grey and brown types, as above, minor abundance; trilobite fragments. Digitate stromatolites, occur in grey ooid calcarenite, 5 cm in height.	...6.8	35.5
5	Limestone, ooid calcarenite, light brown, as above; minor dark grey ooid calcarenite; interbedded with: Limestone, dolomitic to calcareous dolomite, as above; occasional horizons of breccia overlain by thin lamellar stromatolites. Large vugs up to 20 cm in width, filled by very coarsely crystalline calcite crystals and mudstone.	...4.3	28.7
4	Limestone, ooid calcarenite, light brown, as above; glauconitic; possible thrombolite mound horizon, 1-1.5 m thick, near base of unit. Limestone, conglomeratic, grey; thick-bedded; tabular clasts, horizontally disposed, of mudstone and ooid calcarenite; occur at base and 4.0 m.	...4.8	24.4
3	Limestone, dolomitic to calcareous dolomite, light green-grey, mottled; laminations to thin-beds, mudcracks; mudstone clasts; interbedded with: Shale, variegated red-green; thin-bedded; mudcracked.	...5.8	19.6
2	Unit consists of interbedded: Limestone, ooid calcarenite, dark grey and brown types, as above; commonly glauconitic. Limestone, light green-grey, as above; prism cracks, bioturbated; occasional cryptalgal laminations.	...5.6	13.8
1	Dolostone, calcareous, light grey; thick-bedded, laminations (occasionally cryptalgal), domed, low relief stromatolites (LLH) occur throughout; buff weathering; with minor interbeds of: Dolostone, calcareous to dolomitic limestone, ooid calcarenite, light grey-brown, as described for brown ooid calcarenite above. Abundance and percentage of limestone increases upward in unit. Shale, dolomitic, green; thin-bedded. Minor stromatolite mound horizons interbedded with ooid calcarenite, 50 cm in height.	...8.2	8.2

Cape Ann Member

14 Shale, dolomitic, variegated red-green; interbedded with: Dolostone, calcareous, light grey; thin-bedded, laminations, prism cracks. ...4.6 68.9

13 Limestone, ooid calcarenite, dark grey; thick-bedded; interbedded with: Limestone, mudstone, medium grey; thin-bedded to nodular, ripple cross-laminations; thinly interbedded with tan weathering, argillaceous dolostone; as above. Abundant flat-pebble conglomerates composed of mudstone clasts, horizontally to vertically disposed. ...3.0 64.3

12 Shale, interbedded with laminated to thin-bedded dolostone, as above. ...1.0 61.3

11 Interbedded mudstone and argillaceous dolostone, dark grey ooid calcarenite and minor shale, as above. Ooid calcarenite, 1 m above base of unit and 15 cm in thickness, has well-developed herringbone cross-bedding. ...4.0 60.3

10 Interbedded limestone, mudstone, medium grey, as above; interbedded with grey shale, calcareous; partings to thick beds (up to 40 cm), mudcracks. Stromatolite/thrombolite mound horizons at 1.8 m, 6.0 m, and 8.0 m above base of unit; hemispheroidal, 30-80 m in height; correlative with bioherm complex in Degras section. ...12.0 56.3

MARCH POINT FORMATION

9 Interbedded grey mudstone and shale, as above; percentage of shale increases upward in unit. Distinctive pebble conglomerate, 10-15 cm in thickness, occurs at top of unit. ...12.0 44.3

8 Interbedded grey mudstone, argillaceous dolostone, and grey shale, as above; percentage of shale increases upward (up to 5 cm in thickness; abundant flat-pebble conglomerates and minor bioclast calcarenites, 10 cm in thickness. At 3.6 m above base is an oncoid-intraclast calcirudite, 30 cm in thickness. ...10.4 32.2

7	Interbedded grey mudstone and argillaceous dolostone; minor shaly partings. Flat-pebble conglomerate and mudstone beds occasionally have bluish-grey veneer on upper surface; resistant weathering.	...6.8	21.9
6	Cover	...0.3	15.1
5	Quartzose sandstone, calcareous, to arenaceous limestone, greenish-grey; thick-bedded, low-angle cross-stratification; rounded, coarse-sand size quartz, phosphatic clasts up to 2 cm in length), glauconitic; interbedded with: Limestone to siliciclastic siltstone, calcareous, greenish-grey; thick-bedded (10-20 cm); glauconitic; Skolithos. Minor thin beds of flat-pebble conglomerates and grey shale partings; mudcracks occur throughout. At 10 m is oncoid-intraclast calcirudite, 20 cm thick. Interbedded grey mudstone and argillaceous dolostone occurs at 11-12 m.	...12.0	14.8
4	Quartzose sandstone, as above; abundant trace fossils.	...0.75	2.85
3	Shale, dark grey; fissile, runzelmarken; micaceous; interbedded with: Limestone, mudstone; grey; thin-bedded; abundant siliciclastic silt. Poorly exposed.	...0.5	2.1
2	Cover	...1.0	1.6
1	Quartzose sandstone, as above.	...0.6	0.6

B.3 Felix to Man O War Coves, Port au Port Peninsula

This section was measured along the southern shore of the Port au Port Peninsula from Felix Cove to Man O' War Cove.

Unit	Description	Thickness (m) Unit	Total from base
	PETIT JARDIN FORMATION **Man O' War Member**		
22	Limestone, stromatolitic, grey; two superimposed mound horizons at base, each mound is 50-70 m in height, 1-2 m in width and with a planar upper surface; composed of SH; overlain by pustulose mat and cap-shaped stromatolites (LLH), 10 cm in height. Dolostone, grey, very finely crystalline; laminated, mudcracks; tan weathering; interbedded with: Shale, variegated red and green; thin- to thick-bedded.	...6.8	126.5
21	Shale, variegated red and green.	...1.0	119.7
20	Limestone, dolomitic, grey; composed of two superimposed stromatolite/thrombolite mound horizons at base, each approximately 80 cm thick; overlain by 10 cm LLH stromatolites; mudcracks. Dolostone, laminated, as above, with minor thin beds of mudstone.	...1.9	118.7
19	Shale, variegated red and green; thinly interbedded with laminated dolostone (5-15 cm thick); minor flat-pebble conglomerates and prism cracks, mudcracks.	...2.2	116.8
18	Unit composed of interbedded: Limestone, mudstone, grey; thin-bedded, ripple cross-laminations; parted to interbedded with argillaceous laminated dolostone, mudcracks and tepee structures. Limestone, flat-pebble conglomerate, grey; thin- to thick-bedded; occasionally lenticular; tabular, mudstone and oolitic clasts are horizontally to vertically disposed.		

Limestone, ooid-intraclast calcarenite, dark grey; 10-30 cm in thickness; occasional herringbone cross-bedding. Bed at 11.3 m from base, has upper surface with large ripples with silicified crests.
Dolostone, calcareous, greenish-grey; thick-bedded, laminations, prism cracks; tan weathering.
Stromatolite mound horizons abundant, commonly overlying conglomerate beds. At 0.5 m from base of unit is 1.5 m thick horizon of columnar thrombolite (up to 50 cm in width) with planar upper surface. Stromatolite mounds at 3.2 m, 7.1 m, 8.5 m, 9.7 m, 10.5 m, 11.3 m, 13.2 m, 15.6 m are generally hemispheroidal, 20-50 cm in height and up to 1.5 m in width. ...16.0 114.6

17 Unit consists of interbedded:
Limestone, mudstone; interbedded with argillaceous dolostone, as above.
Limestone, flat-pebble conglomerate, as above; commonly overlying or underlying dark grey ooid calcarenite, as above. Pisolite bed, 50 cm thick, occurs at 10.3 m, and is partly dolomitized and inversely graded.
Dolostone, calcareous, greenish-grey; thick-bedded, laminations, prism cracks; tan weathering.
Shale, dark grey, red and green; laminated to thin-bedded, mudcracks and runzelmarken.
Stromatolite mound horizons occur near base of unit, at 9.1 m, and near top of unit; vary from hemispheroidal and elongate mounds, 0.1-1.5 m in height, to digitate stromatolites (LLH to SH), 20 cm in height and up to 3 m in lateral extent. ...25.4 98.6

16 Dolostone, pinkish-grey weathering; thick-bedded, mottled; overlain by:
Dolostone, stromatolitic; two superimposed mounds, 20-30 cm in height with indistinct digitate internal structure; intermound sediment is tan- to grey-weathering dolostone; mudcracked. ...2.0 73.2

15 Dolostone, calcareous, greenish-grey, very finely crystalline; thick-bedded, laminations, cryptalgal in places, reddish-brown weathering; interbedded with:
Limestone, mudstone, interbedded with argillaceous dolostone, as above.
Limestone, flat-pebble conglomerate; up to 30 cm in thickness, lenticular with convex upper surface and near-planar lower surface. ...3.0 71.2

14 Dolostone, buff to pink weathering, finely to medium crystalline; stromatolite mounds, up to 1.5 m in height, indistinct internal structure, occur at base, 2.0 m, and 2.9 m. Mound horizons interbedded with:
Shale, variegated red and green; 50 cm thick; and dolostone, laminated, as above. ...6.4 68.2

Felix Member

13 Dolostone, pinkish-grey weathering, finely to medium crystalline; thick-bedded, oolitic(?); interbedded with variegated red and green shale, containing minor lenses of dolostone. ...4.6 61.8

12 Dolostone to dolomitic limestone, oolitic, brownish-grey, finely to medium crystalline; thick-bedded (1-2 m), abundant clasts and mudcracked layers of dololutite; rounded sand-size quartz (20-30 % by volume). Minor interbedded grey mudstone and argillaceous dolostone. ...9.4 27.2

11 Unit consists of interbedded:
Shale, greenish grey; thick-bedded (80 cm bed at base of unit).
Dolostone, laminated, as above; may underly, overly, or pass laterally into flat-pebble conglomerate.
Dolostone, oolitic, brownish grey, as above.
Limestone, oolitic, dark grey; 20 cm in thickness.
Limestone, stromatolite mound horizon; digitate, 20 cm in thickness, indistinct internal structure; overly flat-pebble conglomerate at 1.0 m from base of unit.
Sandstone, quartzarenite, coarse-grained, rusty grey-brown; 20 cm thick, overlies above stromatolite; calcareous, glauconitic. ...6.1 47.8

10 Interbedded grey mudstone and argillaceous dolostone, as above; compacted mudcracks in dolostone. Flat-pebble conglomerate, 10-20 cm in thickness, occurs at top of unit; irregular lower bedding surface. ...0.8 41.7

9 Dolostone, oolitic, pinkish-grey; as above. At base of unit is brecciated layer. At top of unit, stromatolite mounds overly dolomitized oolite; 30 cm in height and 50 cm in width, hemispheroidal with indistinct digitate structures; passes laterally into laminated dolostone.
Limestone, oolitic, dark grey; as above; glauconitic. ...6.5 40.9

8 Limestone, dolomitic, to calcareous dolostone, oolitic, grey-buff; thick-bedded, herringbone cross-bedding; mudstone intraclasts and mudcracked layers; interbedded with:
Limestone, oolitic, dark grey; thick-bedded. Bed at 2.3 m from base has upper surface with large ripple forms.
Dolostone, grey, finely crystalline; laminated to thin-bedded; recessive weathering. ...3.6 34.4

7 Unit consists of interbedded:
Dolostone, oolitic, light grey; thick-bedded, abundant clasts and mudcracked layers, tepee structures.
Dolostone, flat-pebble conglomerate; 5-10 cm thick, irregular upper surface with thin, dark brown coating. ...2.9 30.8

6 Unit is composed of:
Thinly interbedded grey mudstone and argillaceous dolostone, as above; 50-80 cm thick; occur at base and top of unit.
Limestone, oolitic, dark grey, as above; 20-30 cm thick; abundant stylolites.
Limestone, oolitic, light grey-buff, as above; 50 cm thick.
Dolostone, laminated, grey; thick-bedded, laminations; contains thin-beds of grainy dolomite (oolitic?) and dome-shaped, lamellar stromatolites, 20 cm thick. ...4.3 27.9

5 Dolostone to limestone, oolitic, dark grey; 10-15 cm in thickness, upper surface commonly has large ripples; oolitic clasts; interbedded with:
Dolostone, laminated, light grey; 40-50 cm in thickness; parted with dolomitic shale, fissile, less than 10 cm thick.
Stromatolite mound horizon at 5.1 m; mounds are 50 cm in height and up to 2 m in width with vague digitate structures; intermound sediment is laminated dolostone. Stromatolite/thrombolite mound horizon at 6.4 m overlies grey oolite; mounds are 30 cm in height and up to 1 m in width; vuggy porosity; intermound sediment is thinly interbedded grey mudstone and argillaceous dolostone. ...7.0 23.6

4 Dolostone, light buff-grey oolite, with minor dark grey oolite and laminated to patterned dolostone, as above. Laminated dolostone generally has irregular upper bedding surface when overlain by grey oolite.

Stromatolite mound horizon occurs at 3.0 m from base in buff oolite; 20 cm thick, developed on flat-pebble conglomerate and overlain by laminated dolostone and pustulose mat. ...9.8 16.6

3 Dolostone, interbedded dark grey oolite, buff-grey oolite and laminated dolostone. as above. Possible stromatolitic horizon occurs at 3.3 m from base. ...3.8 6.8

2 Dolostone, stromatolite mound horizons, light grey; 2 m thick; indistinct digitate structures; lower 1 m is columnar mounds, approximately 20 cm in width, overlain by dome-shaped mounds, 1 m in width. Intermound and overlying sediment is laminated dolostone with well-developed prism cracks. ...3.0 3.0

Big Cove Member

1 Interbedded mudstone and argillaceous dolostone, as above; stromatolite mound horizons.
Accessible only at very low tide; poorly exposed.

B.4 Isthmus Bay East Section

This section was measured along the south shore, 0.6-1.6 km east of the Gravels on the Port au Port Peninsula. Unit thicknesses are from James (pers. comm., 1982).

Unit	Description	Thickness (m) Unit	Thickness (m) Total from base
	ST. GEORGE GROUP		
	Limestone, dolomitic, mudstone to packstone, dark grey; dolomite partially replaces burrows and mounds. Only the basal 26 m are exposed.		
	BERRY HEAD FORMATION		
28	Limestone, mudstone to packstone, partially dolomitic, light grey; 30-50 cm thick beds, burrowed, stylobedded; occasional thin beds to partings of tan weathering, argillaceous dolostone. Stromatolite horizons occur in upper 4 m of unit, ranging from digitate forms, 10-30 cm in height, to pancake-shaped mounds, 10 cm in height and surrounded by flat-pebble conglomerate. Chert occurs as nodules and outlining stromatolites.	...12.2	196.4
27	Unit consists of interbedded: Dolostone, grey, medium crystalline; laminated, patterned aspect, burrowef; minor brecciated horizons, 5-10 cm thick, and shaly partings. Dolostone, light grey, medium crystalline; thick-bedded, abundant finely crystalline dolostone intraclasts and mudcracked layers; sand-size quartz grains. Limestone, oolitic and peloidal, dark grey; thick-bedded, burrows. Stromatolites occur at top of unit; mounds are 1.5 m in height, composed of digitate and lamellar forms; horizon has planar upper surface; intermound sediment is thin-bedded mudstone. Yellow-weathered chert outlines stromatolites and occurs as nodules.	...6.5	184.2

26	Dolostone, light grey, finely crystalline; laminated to massive, cryptalgal in places; commonly with patterned aspect; mudcracks, bioturbated; tan weathering. Limestone, mudstone, medium grey; thin-bedded, ripple cross-laminated; parted with tan weathering, argillaceous dolostone; abundant burrows, mudcracks; flat-pebble conglomerates. Stromatolite horizon occurs at top of unit; 50 cm thick, dome-shaped; intermound sediment is mudcracked, laminated dolostone. Brown-weathering chert occurs in stromatolites.	...8.4	177.7
25	Dolostone, as above, with minor interbeds of thin-bedded mudstone and dolostone, as above.	...7.0	169.3
24	Unit consists of three lithologies interbedded, which in decreasing abundance are: Limestone, stromatolite mound horizons; 50-60 cm in height and up to 50 cm in width; composed of digitate and lamellar stromatolites, planar upper surface. Intermound sediment is thin-bedded mudstone and dolostone and conglomerate; overlain by pustulose mat, 10 cm thick. Dark grey chert occurs as irregular nodules. Dolostone, tan weathering, finely crystalline; laminated as above. Limestone, oolitic, dark grey; 30 cm thick, large flat-topped ripples, clasts; partly silicified; draped by thin, mudcracked mudstone.	...9.0	162.3
23	Dolostone, grainy, pinkish-grey; mottled, bioturbated.	...1.0	153.3
22	Cover	...10.1	152.3
21	Dolostone, pinkish-grey; medium crystalline; possibly stromatolitic, minor clasts.	...1.0	142.2
20	Cover	...8.8	141.2
19	Dolostone, as above.	...1.0	153.3
18	Cover	...5.7	131.4
17	Dolostone, reddish-grey; medium crystalline; massive, mudcracks, indistinct digitate structures (possibly stromatolitic), irregular upper surface; minor sand-size quartz grains.	...3.8	125.7

16 Dolostone, grey, finely crystalline; patterned to laminated; occasional laminated clasts. ...5.9 121.9

15 Dolostone, medium brown, medium crystalline; 1.5 m thick, abundant clasts, possibly oolitic; interbedded with mottled, pinkish-grey dolostone, finely crystalline. ...3.3 116.0

14 Dolostone, grey, finely crystalline; laminated to patterned; interbedded with mottled, buff dolostone. Stromatolite mounds occur at top of unit; 50 cm thick, dome-shaped; rooted on flat-pebble conglomerate and flanked by laminated dolostone. ...11.5 112.7

13 Interbedded brown dolostone, 50-60 cm in thickness, and laminated and patterned dolostone, as above. At 6.3 m are abundant mudcracks with rounded sand-size quartz grains; tepee structures. ...9.8 101.2

12 Unit consists of interbedded:
Limestone, mudstone, grey; parted to thinly interbedded with argillaceous dolostone; mudcracks; local occurrences of rounded sand-size quartz grains.
Limestone, oolitic, dark grey; thick-bedded, abundant burrows and clasts.
Limestone, packstone to wackestone, medium grey; thick-bedded, abundant clasts and peloids; trilobite fragments.
Stromatolite horizon occurs at base of unit; 50 cm in height and greater than 1 m in width; upward branching, digitate structure. Intermound sediment is dolomitic, intraclast wackestone. ...3.2 91.4

11 Limestone, mudstone, grey, thin-bedded to nodular; parted to thinly interbedded with argillaceous dolostone, as above; interbedded with:
Limestone, oolitic, medium brown and dark grey types, as above. ...8.9 88.2

10 Interbedded mudstone and argillaceous dolostone, as above. ...0.8 88.2

9 Unit consists of interbedded:
Dolostone, oolitic, medium brown; 30-50 cm in thickness, ripple and herringbone cross-bedding, intraclasts and discontinuous mudcracked layers, burrows.
Dolostone, oolitic, dark grey; up to 40 cm in thickness.

	Dolostone, grey, finely crystalline; laminated, mudcracks, bioturbated. Local occurrences of rounded, sand-size quartz grains at top of unit.	..14.8	78.5
8	Dolostone, composed of interbedded brown oolite and laminated dolostone, as above; tepee structures, localized quartz sand; minor occurrences of grey oplite. Near top of unit are small, low-relief stromatolites.	...5.8	63.7
7	Dolostone of interbedded brown oolite and laminated dolostone, as in unit 8; minor occurrences of conglomerate with laminated dolostone clasts.	...21.9	57.9
6	Dolostone, grainy, grey-brown; highly shattered with indistinct fabric.	...1.5	36.0
5	Dolostone, as in unit 9.	...11.1	34.5
4	Dolostone, brown-grey weathering, finely crystalline; laminated to thin-bedded, tepee structures, fractured; common flat-pebble conglomerates. Upper bedding surface of dolostone occasionally very irregular and overlain by small, low-relief stromatolites, at base of unit. Stromatolite mound horizon present near base of unit, 50 cm thick, with indistinct digitate structure, vuggy porosity; undulose bed overlying tepee-like structures.	....8.7	23.4
3	Dolostone, buff to pinkish-grey weathering; finely to medium crystalline; laminated to thin-bedded, occasional patterned aspect; vuggy porosity partly filled with pink and white calcite and buff dolomite. At base of unit are several beds with undulose upper and lower surfaces; wavelengths vary from 10-20 cm and relief of 5-10 cm cutting into underlying thin bed of grainy brown dolostone, to meter-scale depressions.	...5.0	14.7
2	Unit consists of interbedded: Dolostone, pinkish-grey weathering, finely crystalline; 30-40 cm thick, laminated. Dolostone, stromatolitic, 0.5-1.0 m thick; indistinct structure, occasional vague digits. Dolostone, pinkish-grey weathering, finely crystalline; massive; fractures and vugs filled by pink and white calcite and dolomite.	...9.7	9.7

1 Dolostone, pinkish-grey weathering, massive, as above. Only upper few meters are accessible in sea-cliff.

B.5 Little Coney Arm, White Bay

This section was measured along the wave-cut platform of the northern shore of Little Coney Arm in White Bay.

Unit	Description	Thickness (m) Unit	Thickness (m) Total from base
	BERRY HEAD FORMATION		
23	Limestone, dolomitic, dark grey; thick-bedded (1 m in thickness), laminations; medium grey weathering; upper bedding surfaces occasionally brecciated and mudcracked; prism cracks; wispy stylolites; white-yellow weathering chert nodules and stringers; interbedded with: Limestone, dolomitic, medium grey; thick-bedded, mottled; pitted weathering surface; abundant in upper 10 m of unit. Unit is faulted and cut by calcite veins.	...19.3	461.5
22	Unit consists of interbedded: Dolostone, calcareous, dark grey; thick-bedded, laminations (in place cryptalgal), tepee structures; minor shaly partings, chert nodules; grey-brown weathering. Dolostone, calcareous, dark grey; laminated to thin-bedded, mudcracks, low-angle cross-bedding, irregular upper bedding surfaces; abundant wispy stylolites, fractures and brecciation, chert nodules.	...15.3	442.2
21	Dolostone, medium grey, finely crystalline; thick-bedded, mottled; stromatolite mounds at 1.5 m from base, with indistinct digitate structures; chert nodules, as above; interbedded with: Limestone, medium grey; thick-bedded, ripple cross-laminations, compacted mudcracks; thin shale partings.	...14.7	426.9

20 Unit consists of interbedded:
Dolostone, medium grey, very finely crystalline; 50 cm in thickness, laminated (in places cryptalgal); light grey-brown weathering.
Dolostone, medium grey; 50 cm thick beds, vague wavy laminations; light grey-white weathering.
Dolostone, calcareous, very finely crystalline, to dolomitic limestone, dark grey; thick-bedded, wavy laminations, abundant clasts and thin, discontinuous layers, mudcracks; stringers of white calcite.
Chert, as above; occurs in all lithologies. ...17.3 412.2

19 Unit is composed two lithologies interbedded:
Dolostone, light grey; 1-2 m thick, mottled; minor argillaceous partings and thin, discontinuous beds of dark grey dolomite with mudcracks; fractures at high angle to bedding.
Dolostone, calcareous, to dolomitic limestone, dark grey, very finely crystalline, thick-bedded, mudcracks; shaly partings to thin beds; white quartz veins throughout. ...10.7 394.9

18 Dolostone, calcareous, dark grey, as above; ripple cross-laminations; minor conglomerates, less than 5 cm thick, and grainy beds, 20 cm thick. Occasional massive dolomite beds, 50 cm in thickness, with undulose upper surfaces. ...13.5 384.2

17 Dolostone, light grey; highly fractured; indistinct fabrics. ...1.5 370.7

16 Dolostone, light grey; laminated to thin-bedded, patterned aspect to some layers, bioturbated, mudcracked. ...6.1 369.2

15 Dolostone, light grey; massive, indistinct mottling; occasional thin beds of medium grey dolostone, bioturbated; cut by thin, coarsely crystalline dolomite veins and fractures. ...5.0 363.1

14 Dolostone, medium grey; thick-bedded, mottled, abundant clasts and thin mudcracked layers; interbedded with:
Dolostone, grey; laminated to thin-bedded, tepee structures. ...17.4 358.1

13 Limestone, dark grey, finely crystalline; irregular small lenses of white to light grey limestone, laminated. ...5.8 340.7

12 Unit composed of interbedded:
Dolostone, grey, finely crystalline; laminated to thin-bedded, ripple cross-laminations, mottled. At top of unit, white dolostone, lenses to thin-bedded, occurs with grey dolostone.
Dolostone, grey; laminated, possibly cryptalgal in places; tan weathering.
Limestone, conglomeratic, at 1.5 m from base, tabular clasts of grey dolostone horizontally to vertically disposed. Chert, reddish to white weathering; wispy stringers to nodules throughout above lithologies. ...19.5 334.9

11 Dolostone, dark grey, finely crystalline; laminated, mottling; minor thin, dolomitic shale, local parallel-to-bedding cleavage. ...3.2 315.4

10 Dolostone, purplish-grey; laminated to thin-bedded, mottled, highly fractured. At 7.8 m from base, irregular light brown chert lenses. Unit has irregular upper surface, which appears to be downcut by overlying dolostone. ...9.9 312.2

9 Unit consists of interbedded:
Dolostone, purplish-grey, finely crystalline; laminated to patterned (pyritic) dolostone, mottled; fractures, minor thin beds of white, laminated dolostone.
Dolostone, dark grey, as above. ...20.8 302.3

8 Dolostone, purplish-grey, as above; with minor dark grey dolostone, as above. Bedding contact between these two lithologies is undulose. At 1 m from top of unit, dolostone is brecciated; 20-30 cm thick. ...18.0 281.5

7 Unit composed of three major lithologies interbedded:
Dolostone, medium grey, coarsely crystalline; irregular thickness (average 20-30 cm), bedding contacts are undulose; finely crystalline clasts.
Dolostone, grey-brown; approximately 1 m thick beds, laminated to patterned aspect, small-scale tepee structures, occasional grainy dolostone layers.
Dolostone, medium grey, finely to medium crystalline; mottled, cut by high-angle-to-bedding fractures; occasional clasts and laterally discontinuous, mudcracked layers up to 4 cm thick; locally coarsely crystalline and minor shaly laminations.
Breccia horizon at 3-5 m from top of unit.
...34.5 263.5

6	Dolostone, medium grey; laminated, commonly cryptalgal; interbedded with: Dolostone, grey; massive, mottled, irregular upper surfaces common. Shale, dolomitic; occurs in upper 60 cm of unit, mudcracks.	...5.2	229.0
5	Dolostone, dark grey; thin-bedded to laminated, compacted mudcracks; dolomitic shale partings occur near top of unit.	...4.0	223.8
4	Dolostone, medium grey, finely crystalline; indistinct laminations, mottled; shaly partings (less than 5 cm thick).	...12.8	219.8
3	Unit composed of interbedded: Phyllite, medium grey; 2.5-3 m thick, cleavage parallel to bedding, mudcracks; abundant quartz and calcite veins; tan-rust weathering. Limestone, medium grey, fine to medium crystalline, with irregular partings of tan weathering, argillaceous dolostone; up to 1.5 m thick.	...45.3	207.0
2	Dolostone, light to medium grey, finely crystalline; thick-bedded, mottled; light brown argillaceous partings; in part recrystallized to variegated white and brown marble; interbedded with: Limestone, medium grey; thin-bedded to nodular; with partings to thin beds of laminated, calcareous shale to argillaceous mudstone or argillaceous dolostone; up to 2.5 m thick; recessive weathering. Flat-pebble conglomerate occurs near top of unit.	...19.7	161.7
1	Dolostone, light to medium grey, finely crystalline; thick-bedded, indistinct laminations and mottling, rare large-scale cross-bedding; white weathering. At top of unit is stromatolite? mounds, 50 cm thick, overlying flat-pebble conglomerate. Only upper 15 m are well exposed; rest of unit is heavily covered by vegetation. Estimated thickness of	..142	142

Appendix C

OOIDS: REVIEW OF PREVIOUS STUDIES

The interpretation of fossil ooids has been strongly influenced by studies of modern ooids. The classic Bahamian ooids with cortices of tangentially-arranged aragonite have been extensively studied (e.g., Illing, 1954; Newall et al., 1960; Bathurst, 1975) and have been widely cited as a modern analogue for various ancient ooids. It was not until the 1960's that modern ooids with radial-fibrous aragonite coatings were recognized (e.g., Laguna Madre, Mexico; Rusnak, 1960). Since then radial aragonite ooids have been documented in sediments from Great Salt Lake, Utah (Eardley, 1938; Kahle, 1974; Halley, 1977; Sandberg, 1975); Shark Bay, Western Australia (Davies, 1970); the Gulf of Aquaba in the Red Sea (Friedman et al., 1973); the Persian Gulf (Loreau and Purser, 1973); and the Great Barrier Reef province, Australia (Davies and Martin, 1976). Relict Mg calcite ooids have been examined on the Amazon Shelf, Brazil (Milliman and Barretto, 1975) and off the Great Barrier Reef, Queensland (Marshall and Davies, 1975). Bimineralic ooids of calcite and aragonite have been found in Baffin Bay, Texas (Land et al., 1979).

Ancient ooids, which now have a dominantly radial calcite cortex, were long considered to have been tangential ooids that had undergone complex diagenesis (e.g., Newall et al., 1960; Shearman et al., 1970). Sorby in

1879, proposed that Jurassic calcitic ooids had not changed extensively and had retained their original mineralogy and structure. This interpretation was not widely accepted until the 1970's when Sandberg (1975) interpreted ancient radial cortices in Great Salt Lake ooids as primary calcitic features based on comparison with biogenic particles. Subsequent studies, such as Wilkinson and Landing (1978), Heller et al. (1980) and James and Klappa (1983), have further substantiated this concept. In contrast, originally aragonitic ooids are generally interpreted to have been replaced by sparry calcite with poor fabric retention (e.g. Rich, 1982).

Numerous mechanisms of ooid formation have been proposed in past years and can be divided into four categories: (1) mechanical accretion of calcium carbonate mud "snowball style" (Sorby, 1879); (2) purely organic precipitation of calcium carbonate (Rothpletz, in Simone, 1981); (3) purely inorganic precipitation (Link, in Simone, 1981); and (4) biochemical precipitation influenced by bacteria, amino acids and other organic material (Mitterer, 1968; Suess and Futterer, 1972; Ferguson et al., 1978; and Davies et al., 1978). At present it is generally believed that the formation of ooids involves a complex interplay of inorganic processes and catalyzing organic effects (summarized in Simone, 1981).

The original mineralogies and fabrics of modern ooids are considered to be governed by several environmental factors, most of which are probably applicable to ancient ooids as well: (1) energy conditions (Loreau and Purser, 1973; Land et al., 1979; Simone, 1981; Heller et al., 1980); (2) water chemistry, in particular ratios of Ca^{+2}/CO_3^{-2} and Mg^{+2}/Ca^{+2} (Lippman, 1973; Sandberg, 1975); (3) atmospheric composition, in

particular CO_2 levels (Mackenzie and Pigott, 1981; Sandberg, 1983); (4) organic matter; and (5) seafloor topography and temperature (Wilkinson et al., 1984). No unequivocal conclusions have yet been reached as to the relative importance of these factors.

Appendix D

GEOCHEMICAL ANALYSES

D.1 Cathode Luminescence

A Nuclide Corporation ELM-2A Luminoscope and Leitz MO400 microscope were used to examine cathode luminescence of selected polished thin sections. A beam diameter of approximately 1 cm, accelerating voltage of 16 kv, and a beam current of 0.6 ma were used. Photography was carried out on a Wild Photoautomat System, using Ektachrome 400 daylight slide film.

D.2 Stable Isotopic Geochemistry

Representative calcite samples for carbon and oxygen isotope analysis were selected from sections on the Port au Port Peninsula. Samples, washed with distilled water and methanol, were spot sampled using a vibrating engraver under a binocular microscope. To reduce contamination, rubber gloves were worn during all stages of sample preparation and extraction.

Powdered samples were analyzed by Teledyne Isotopes (New Jersey).

Samples were reacted with 100% phosphoric acid at 50 degrees C and isotopes were measured on a mass spectrometer. Analytical uncertainty, based on eight replicate measurements for each sample, is 0.01-0.13 o/oo for $\delta^{13}C$ and $\delta^{18}O$.

Brief sample descriptions are provided below and analytical results are listed in Tables D.1 and D.2.

Sample Descriptions

OOIDS

NC-82-55: Blocky-radial ooids in grey oolite [Campbells Member, March Point section].

-82-61: Finely preserved radial ooids in grey oolite [Campbells Member, March Point section, Bed 9].

-82-66: Concentric ooids in brown oolite [Campbells Member, March Point section].

-82-68: Finely preserved radial ooids in grey oolite [Campbells Member, March Point section].

-82-160a: Blocky ooids in parted limestone [Campbells Member, March Point section, Bed 8].

-83-1: Finely preserved radial-concentric ooids in grey oolite [Man O' War Member, east of Big Cove Brook].

-83-201: Finely preserved radial-concentric ooids in grey oolite [Man O' War Member, Felix to Man O' War Coves section, Bed 17].

-83-290: Sparry radial ooids in grey oolite [Campbells Member, March Point section, Bed 8].

CEMENTS

NC-82-36, -15: Bright-luminescent blocky calcite in flat-pebble conglomerate [Big Cove Member, March Point section; March Point Formation, Degras section].

-82-36, -15: Dull-luminescent blocky calcite in flat-pebble conglomerate [Big Cove Member, March Point section; March Point Formation, Degras section].

-82-45: Dull-luminescent blocky calcite in flat-pebble conglomerate [Man O' War Member, Felix to Man O' War Coves section].

-82-65: Meniscus micritic calcite and concentric ooids in brown oolite [Campbells Member, March Point section, Bed 10].

-82-96e: Dull-luminescent blocky calcite occluding fractures and ooid molds in grey oolite [Campbells Member, March Point Formation, Bed 6].

-82-161b: Echinoderm and syntaxial calcite overgrowths with a later micritic matrix in ooid-bioclast grainstone [Campbells Member, March Point section, Bed 6].

-82-195f: Echinoderms and syntaxial calcite overgrowths in bioclast calcarenite [Campbells Member, March Point section, Bed 9].

-82-246c: Fibrous calcite in biostromal limestone [Cape Ann Member, March Point section].

-83-28: Prismatic clear calcite in bioclastic calcarenite interbedded with parted limestones [March Point Formation, Degras section].

NC-83-51: Bright-luminescent blocky calcite in dololaminite [Man O' War Member, headland east of Man O' War Cove].

-83-63c: Fibrous calcite in biohermal limestone [Cape Ann Member, Degras section, Bed 13].

-83-64a: Fibrous calcite (fascicular optic calcite) cement in biohermal limestone [Cape Ann Member, Degras section, Bed 13].

-83-140: Prismatic clear calcite in burrows in parted limestone [Campbells Member, March Point section, Bed 6].

-83-233: Fibrous calcite and finely preserved radial ooids in grey oolite [Man O' War Member, headland east of Man O' War Member, Bed 18].

-83-237a: Fibrous calcite and finely preserved radial ooids in grey oolite [Campbells Member, March Point section, Bed 10].

-83-237b: Isopachous micritic calcite and radial ooids in grey oolite [Campbells Member, March Point section, Bed 10].

MUDSTONES

NC-82-4a: Parted limestone hardground [March Point Formation, Degras section].

-82-27a: Parted limestone hardground [March Point Formation, March Point section].

-82-36a: Mudstone clast in flat-pebble conglomerate [Big Cove Member, March Point section].

-82-242: Mudstone clast in flat-pebble conglomerate [March Point Formation, Degras section, Bed 6].

-83-182: Homogeneous mudstone in parted limestone [Man O' War Member, Felix to Man O' War Coves section, Bed 18].

-83-208a: Two serial samples of core and margin of mudstone bed that coarsens marginally (from microspar to pseudospar) in parted limestone [Man O' War Member, Felix to Man O' War Coves section, Bed 17].

-83-220: Three serial samples of core and margin of mudstone nodules that coarsen marginally (from micrite/microspar to pseudospar) in parted limestone [Man O' War Member, Felix to Man O' War Coves Member, Bed 17].

TABLE D.1: Calcite Stable Isotope Analyses -- Single Samples

Sample	$\delta^{13}C$	$\delta^{18}O$	Lot
NC-82-4a	-1.59	-7.41	1
-82-27a	-0.99	-7.31	1
-82-36a	-1.45	-8.74	1
-82-45	-2.29	-8.95	2
-82-55	-1.02	-8.89	1
-82-61	-2.11	-8.76	1
-82-65	-2.28	-8.22	2
-82-66	-2.32	-8.34	1
-82-68	-2.47	-8.57	1
-82-96e	-1.51	-8.58	1
-82-160a	-1.41	-8.54	1
-82-161b	-1.19	-9.26	2
-82-195f	-2.78	-9.35	2
-82-242	-2.33	-7.54	1
-82-246c	-2.13	-9.19	2
NC-83-1	-1.70	-9.50	1
-83-28	-0.58	-7.25	2
-83-51	-2.37	-10.36	2
-83-63c	-2.03	-9.54	2
-83-64a	-1.65	-9.29	2
-83-140	-0.60	-9.14	2
-83-182	-1.89	-8.35	1
-83-201	-2.24	-7.60	1
-83-233	-1.68	-9.30	2
-83-237a	-2.33	-9.26	2
-83-237b	-2.29	-9.32	2
-83-290	-0.84	-7.97	1

TABLE D.2: Calcite Stable Isotope Analysis -- Serial Samples

Sample	$\delta^{13}C$	$\delta^{18}O$	Lot
NC-83-220:			
[1] core	-1.08	-7.53	1
[2]	-1.11	-8.04	1
[3] margin	-1.26	-8.09	1
NC-83-208a:			
[1] core	-1.11	-8.10	1
[2] margin	-1.48	-8.25	1
NC-82-36, -15:			
[1] dull CL	-1.52	-8.81	2
[2] bright CL	-1.38	-8.72	2

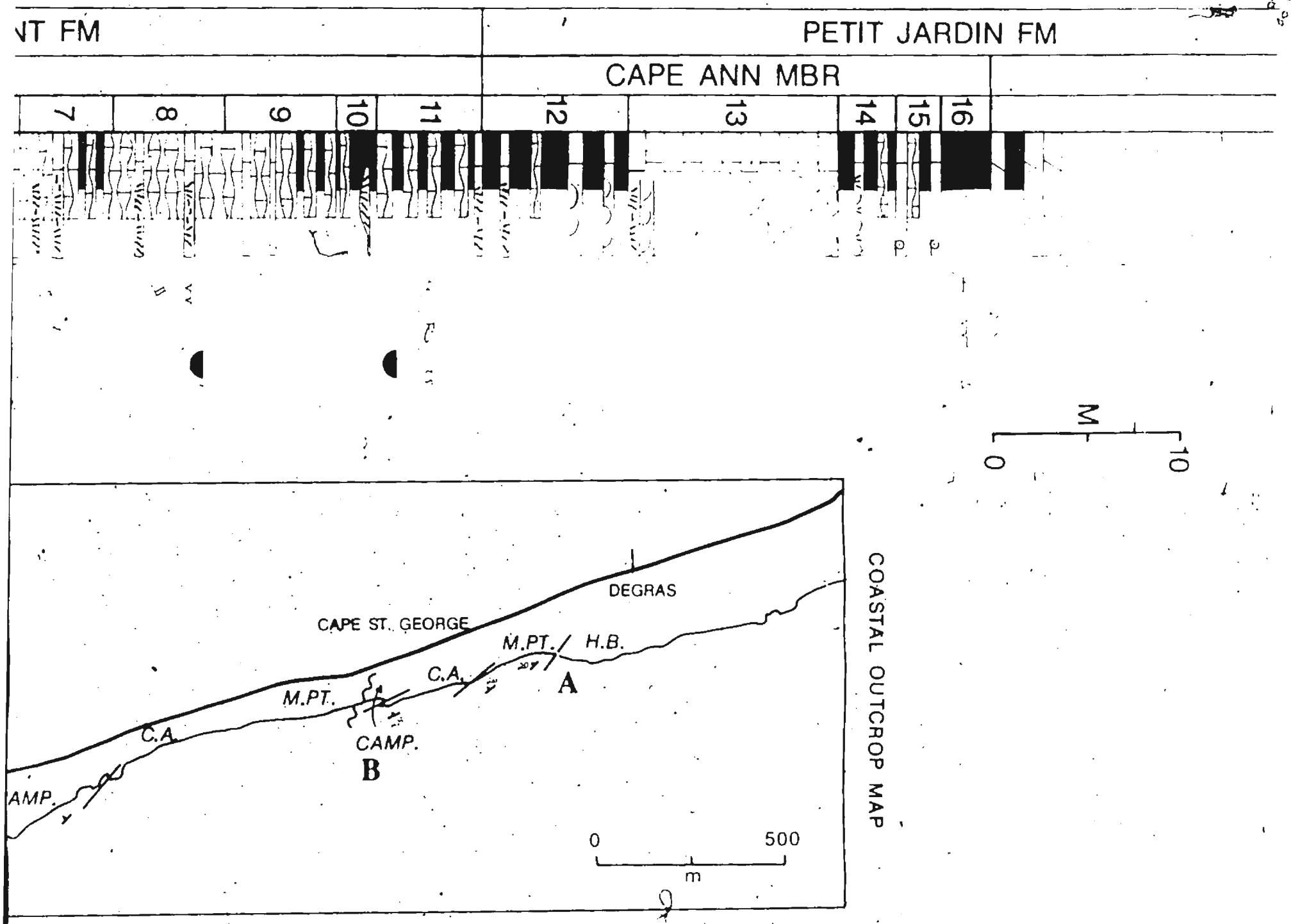
NT FM
PETIT JARDIN FM
CAPE ANN MBR
7
8
9
10
11
12
13
14
15
16
M
0
10
DEGRAS
CAPE ST. GEORGE
M.PT. / H.B.
C.A.
A
M.PT.
C.A.
CAMP.
B
AMP.
0
500
m
COASTAL OUTCROP MAP

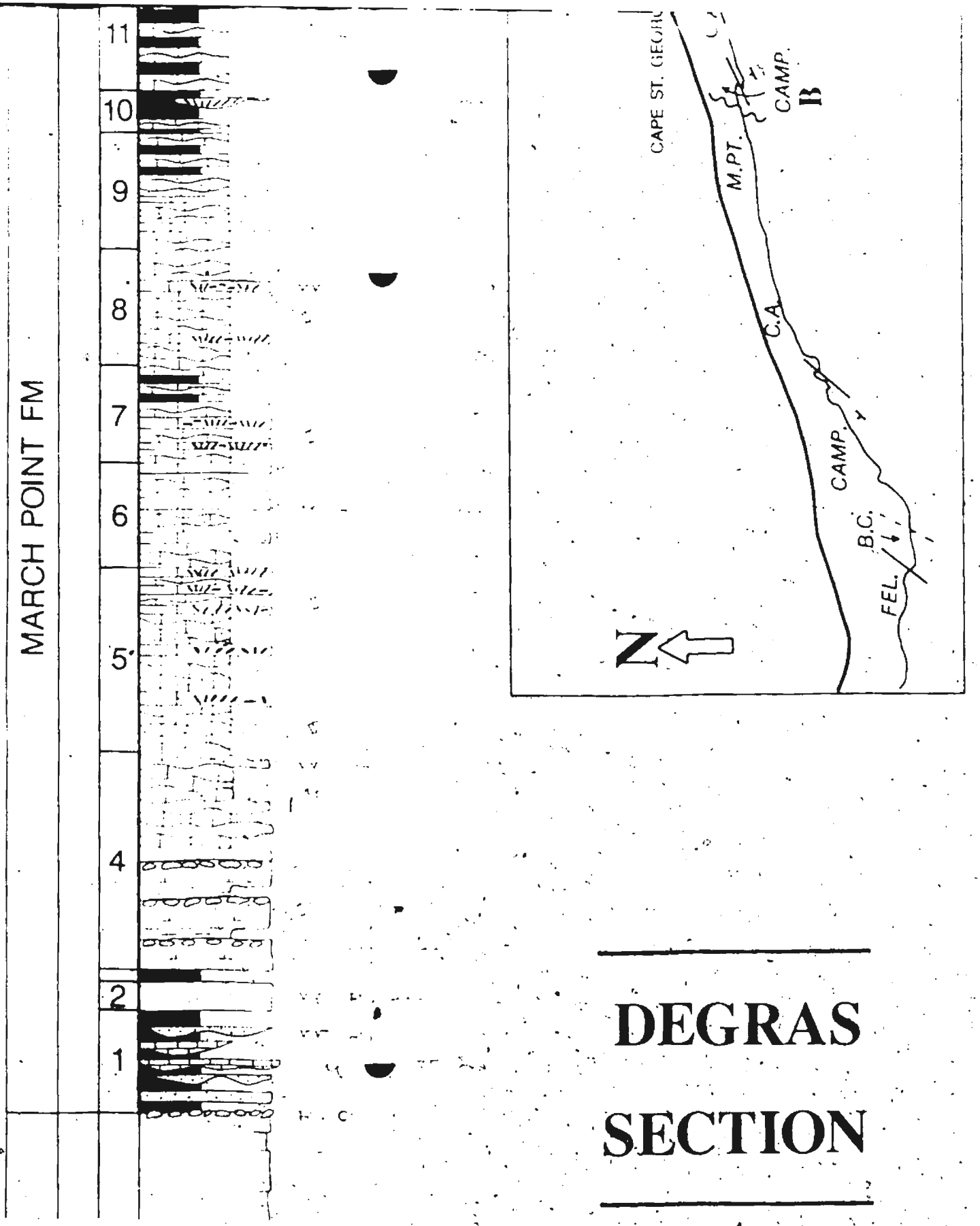

DEGRAS SECTION

FIG. B.1

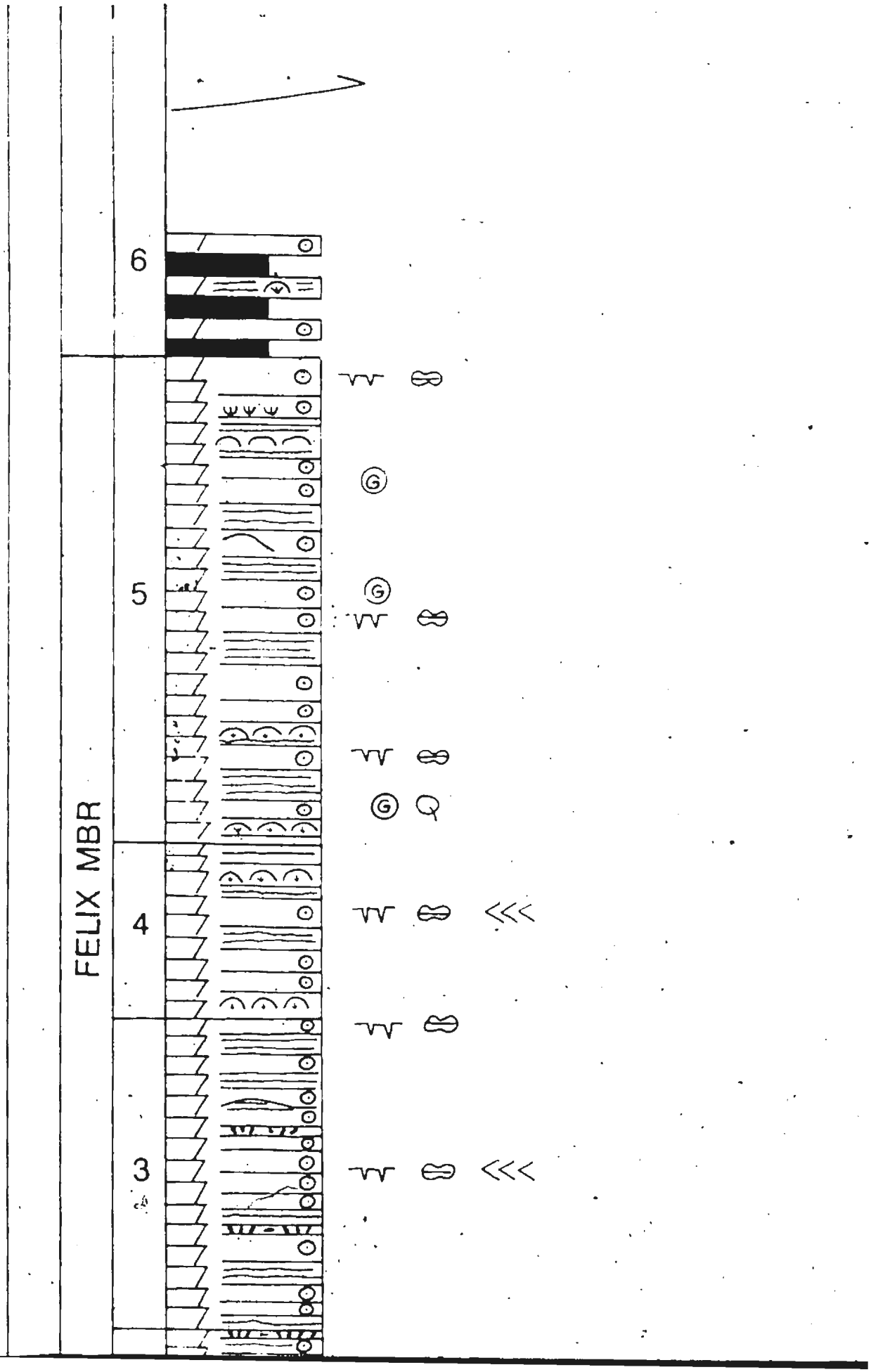
FELIX MBR
6
5
4
3

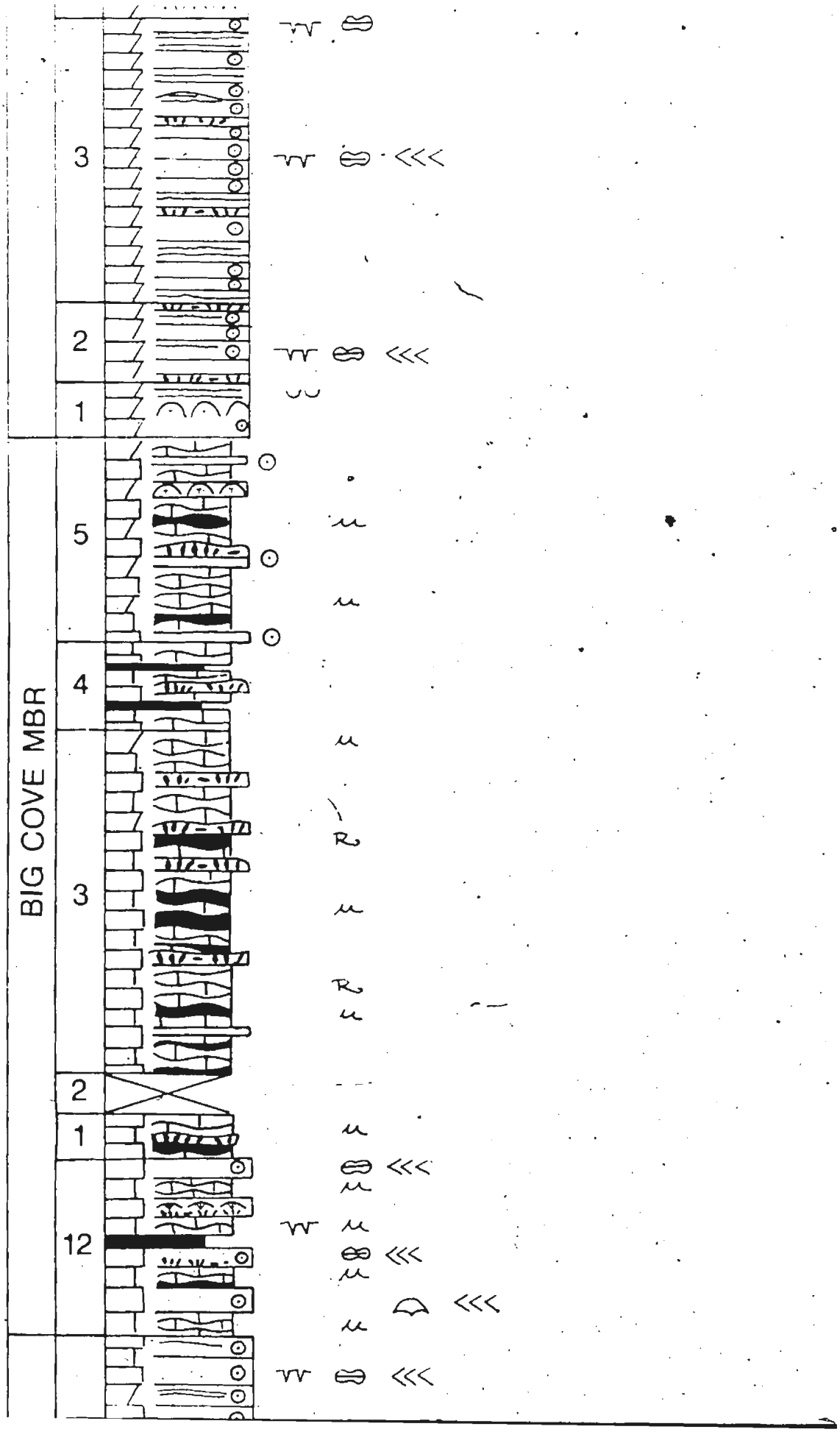
BIG COVE MBR
3
2
1
5
4
3
2
1
12

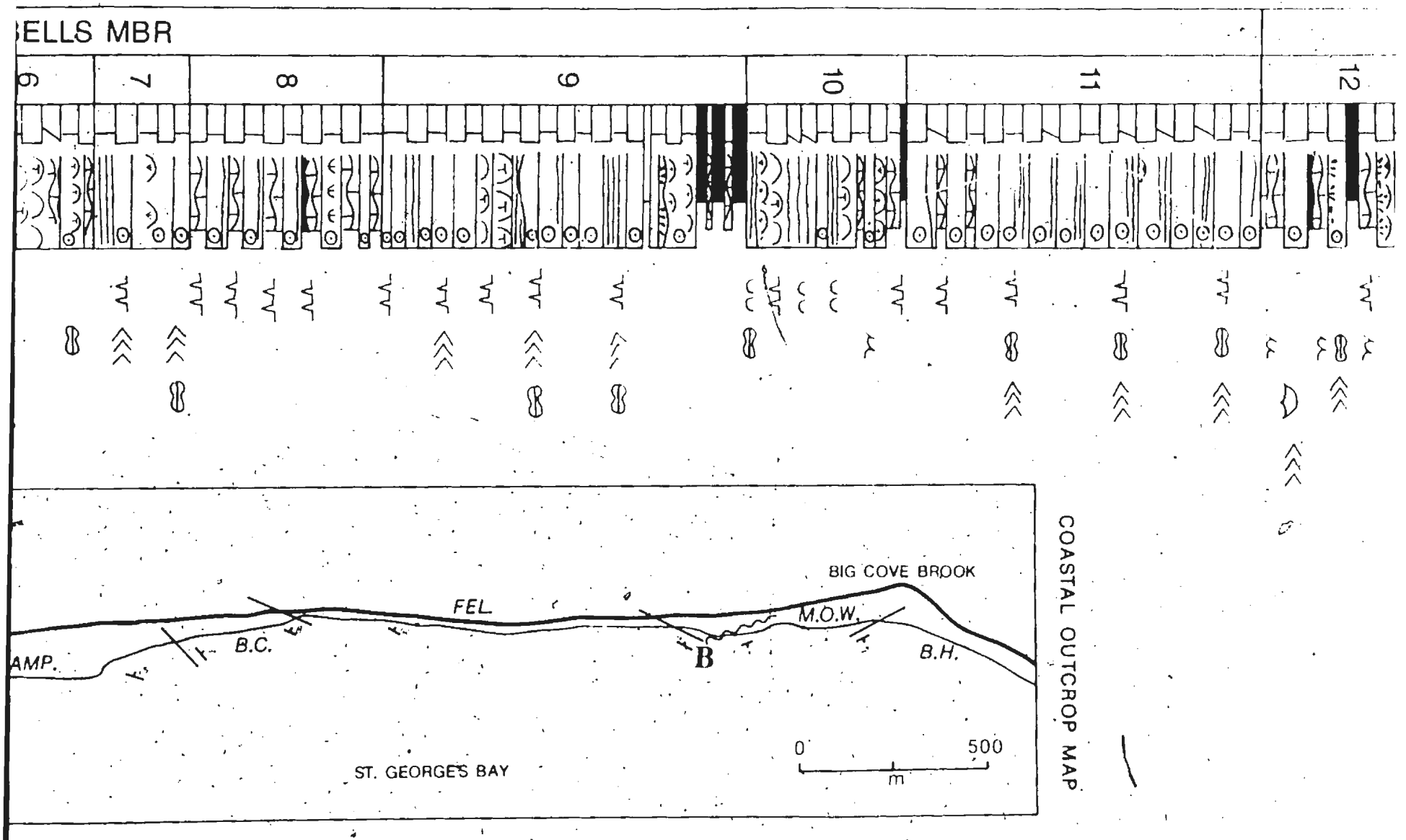
ELLS MBR
6
7
8
9
10
11
12
BIG COVE BROOK
FEL
M.O.W.
B.C.
B.H.
B
AMP.
ST. GEORGES BAY
0
500
m
COASTAL OUTCROP MAP

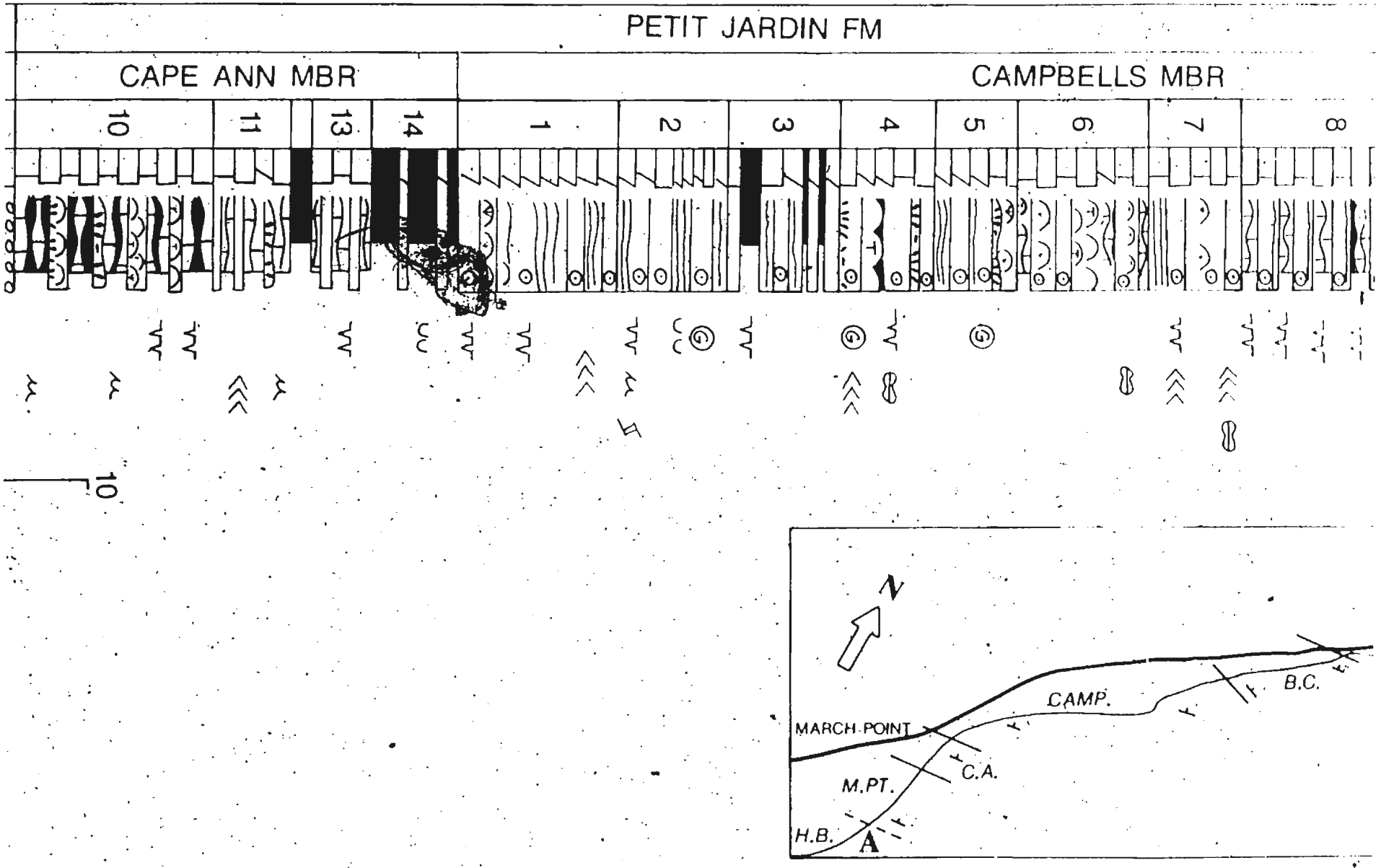
PETIT JARDIN FM
CAPE ANN MBR
CAMPBELLS MBR
10
11
13
14
1
2
3
4
5
6
7
8
10
N
MARCH POINT
CAMP.
B.C.
C.A.
M.PT.
H.B.
A

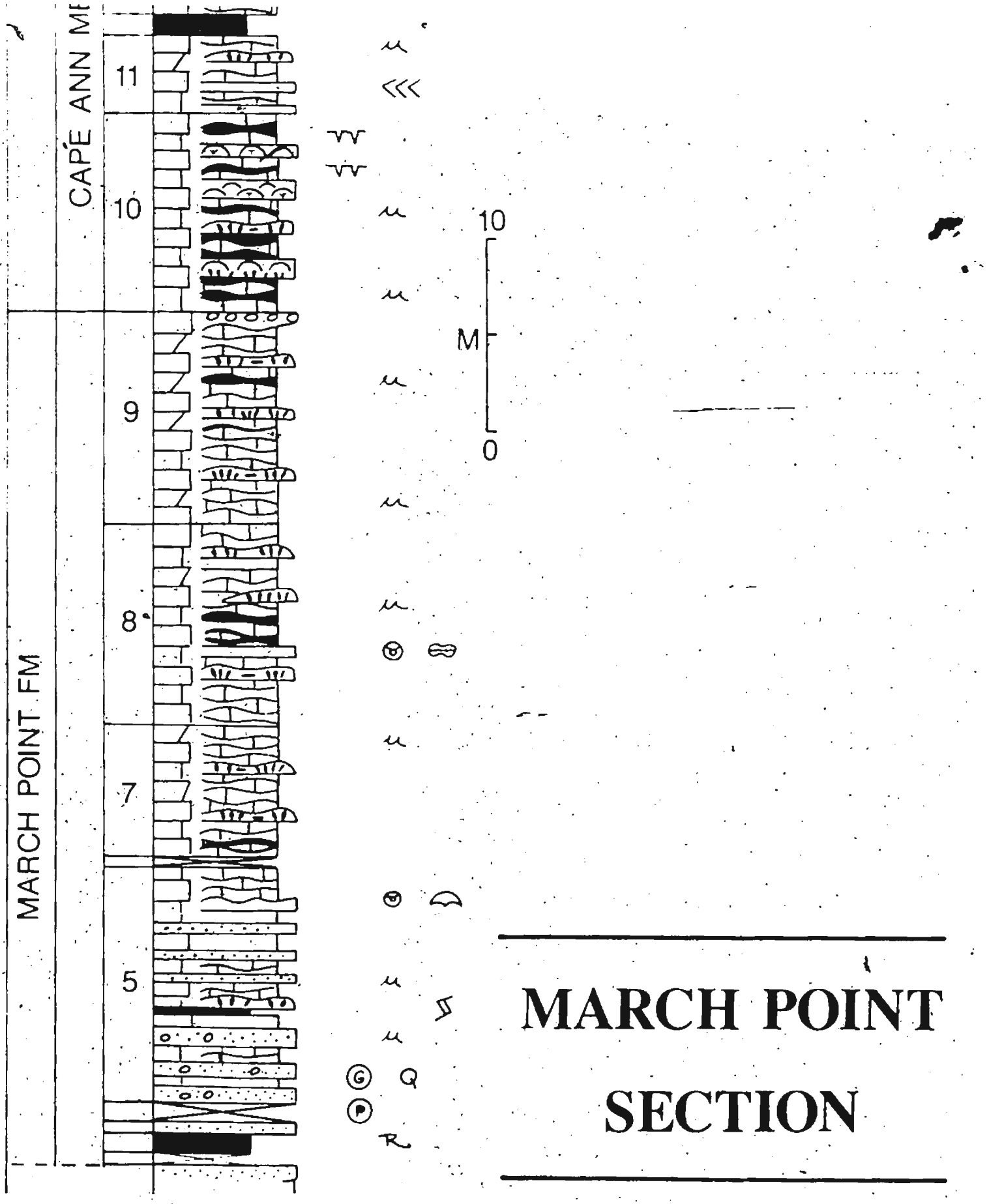

MARCH POINT SECTION

FIG. B.2

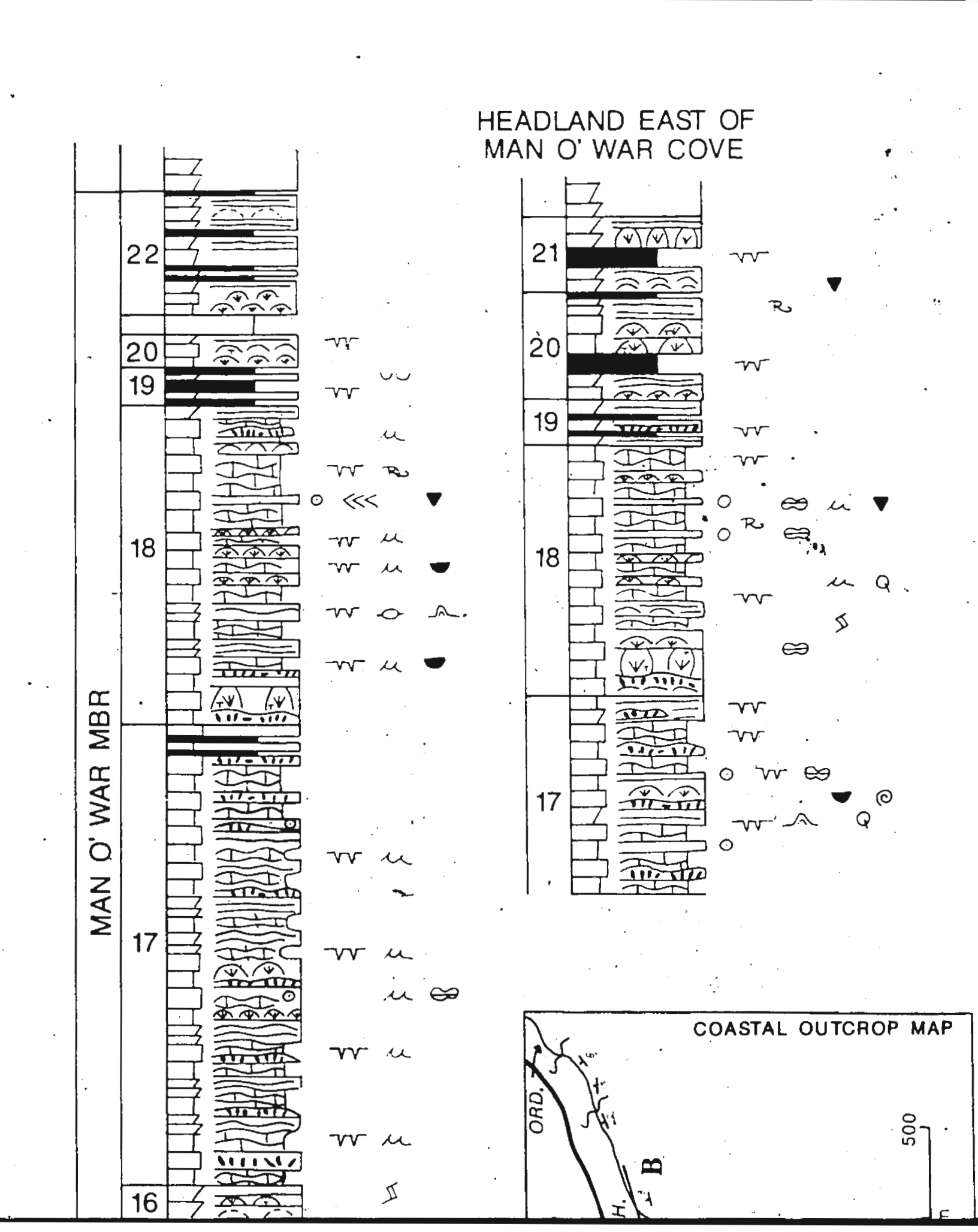
HEADLAND EAST OF
MAN O' WAR COVE
MAN O' WAR MBR
22
21
20
19
18
17
16
COASTAL OUTCROP MAP
ORD.
B
500

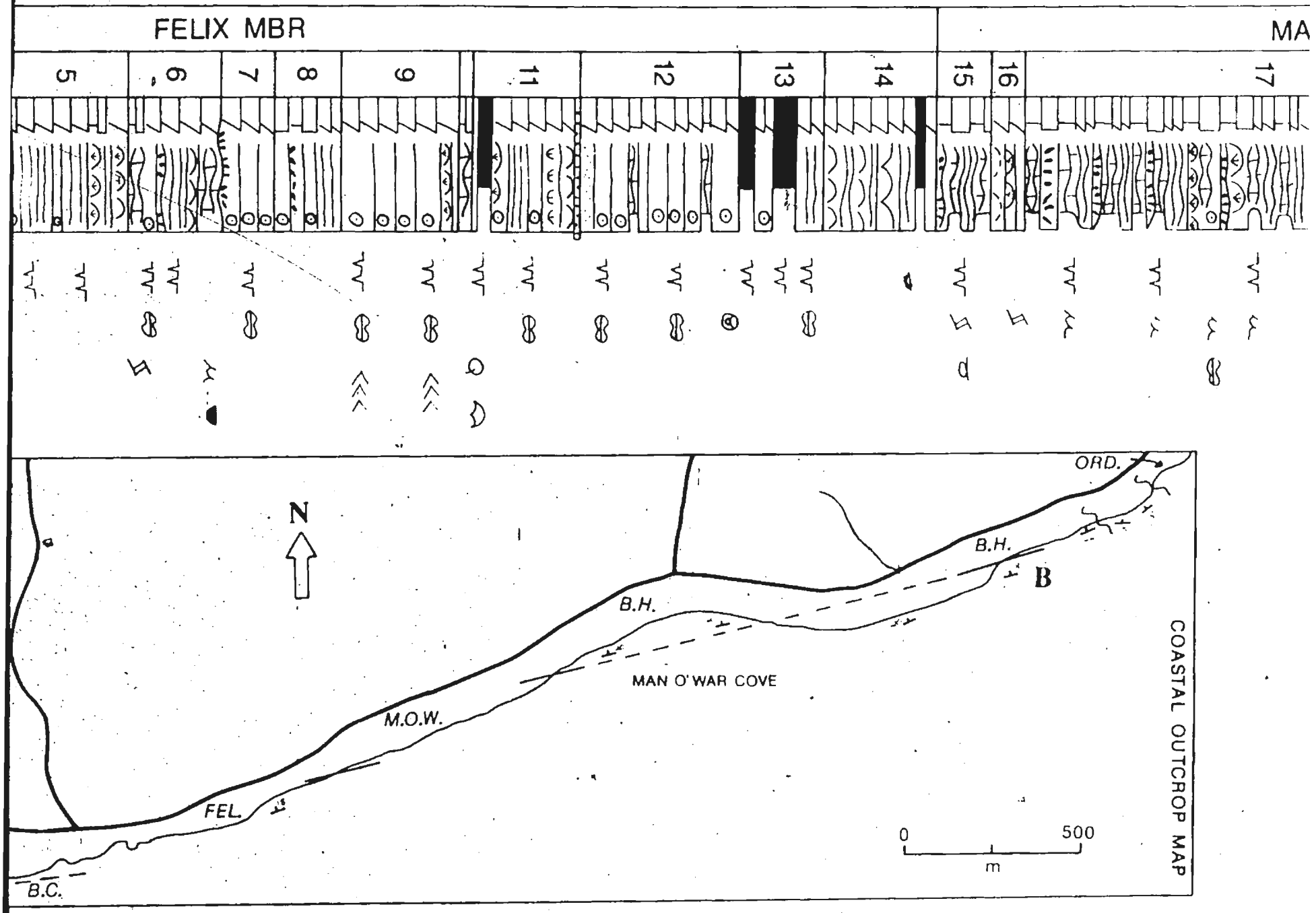
FELIX MBR
MA
5
6
7
8
9
11
12
13
14
15
16
17
N
ORD.
B.H.
B
B.H.
MAN O'WAR COVE
M.O.W.
FEL.
B.C.
0
500
m
COASTAL OUTCROP MAP

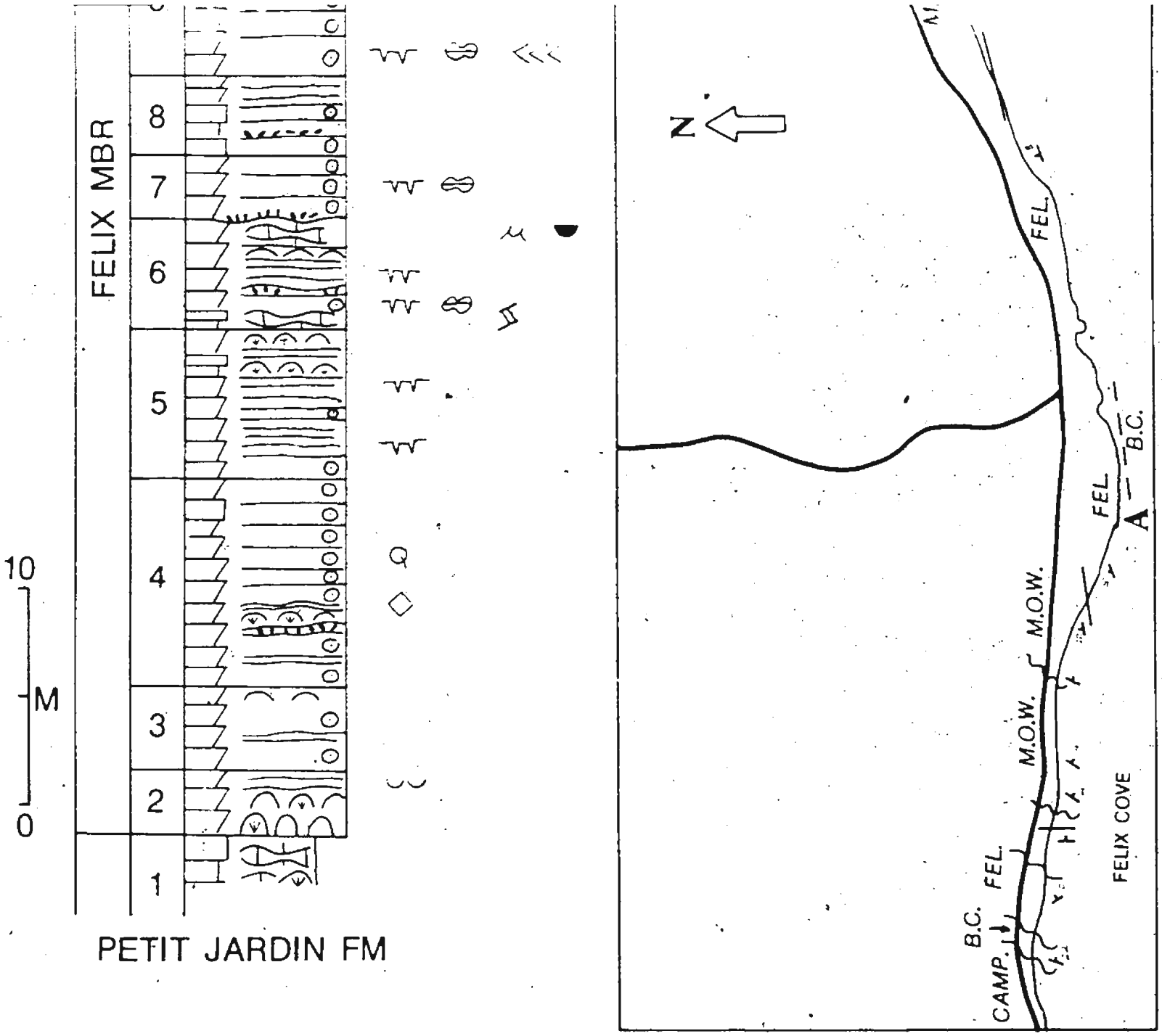

FELIX TO MAN' O WAR COVES

SECTION

FIG. B.3

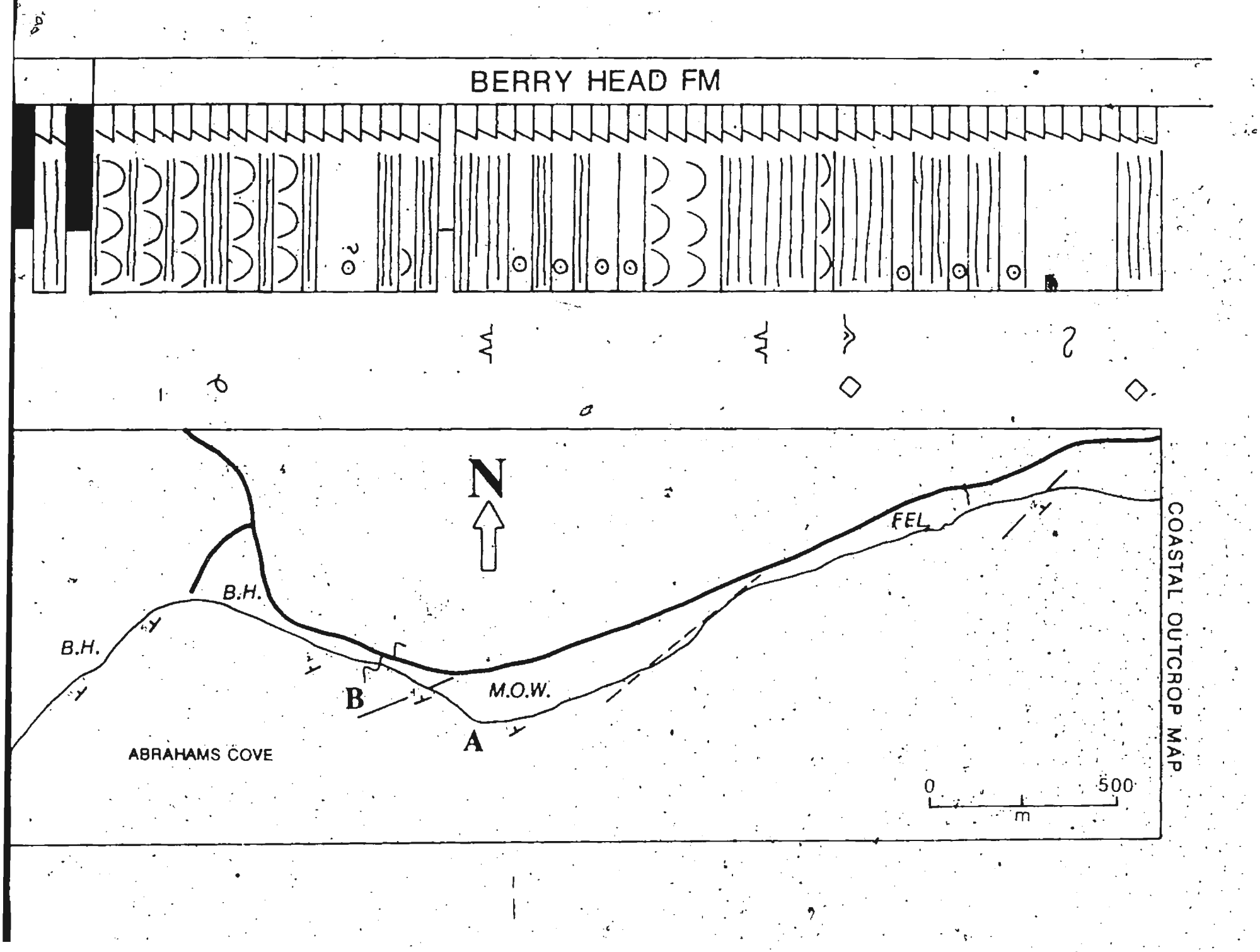
BERRY HEAD FM
N
B.H.
B.H.
B
M.O.W.
A
FEL
ABRAHAMS COVE
0
500
m
COASTAL OUTCROP MAP

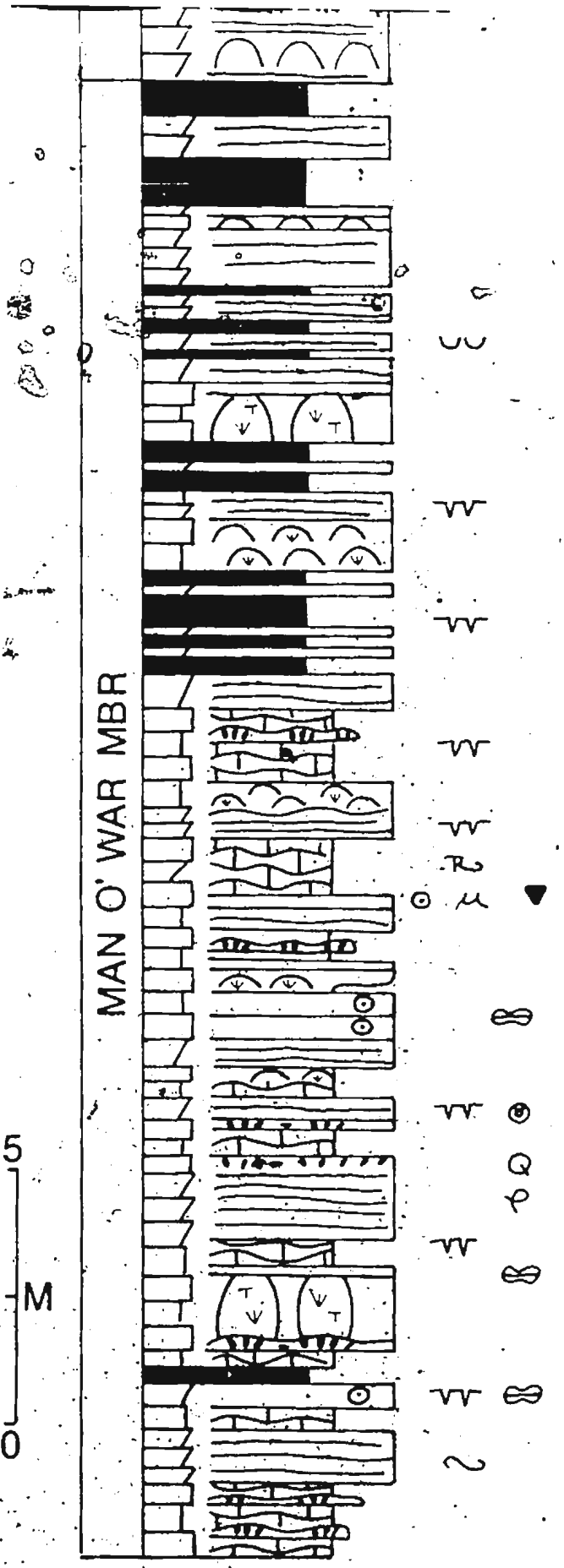

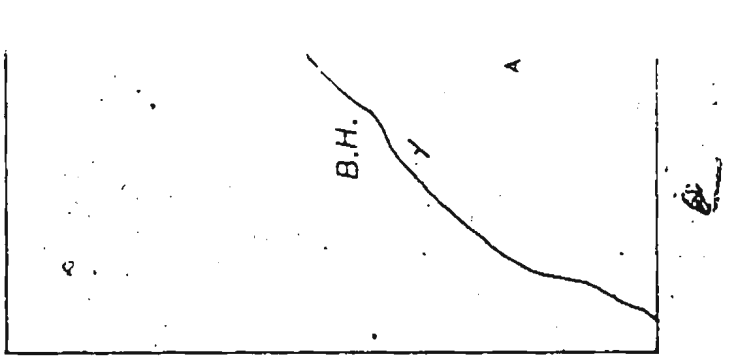

ABRAHAMS COVE SECTION

FIG. B.4

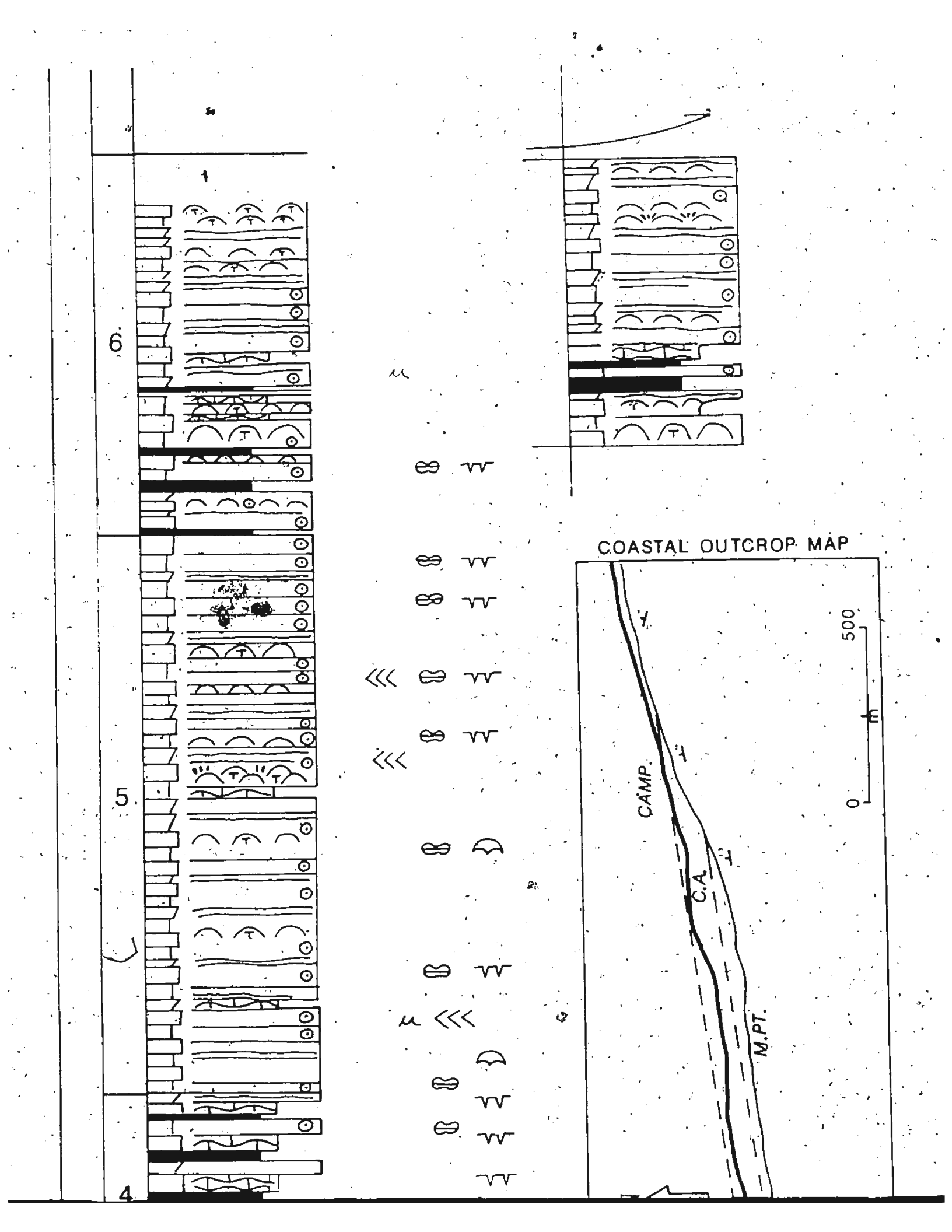
6
5
4
COASTAL OUTCROP MAP
500
0
CAMP.
C.A.
M.PT.

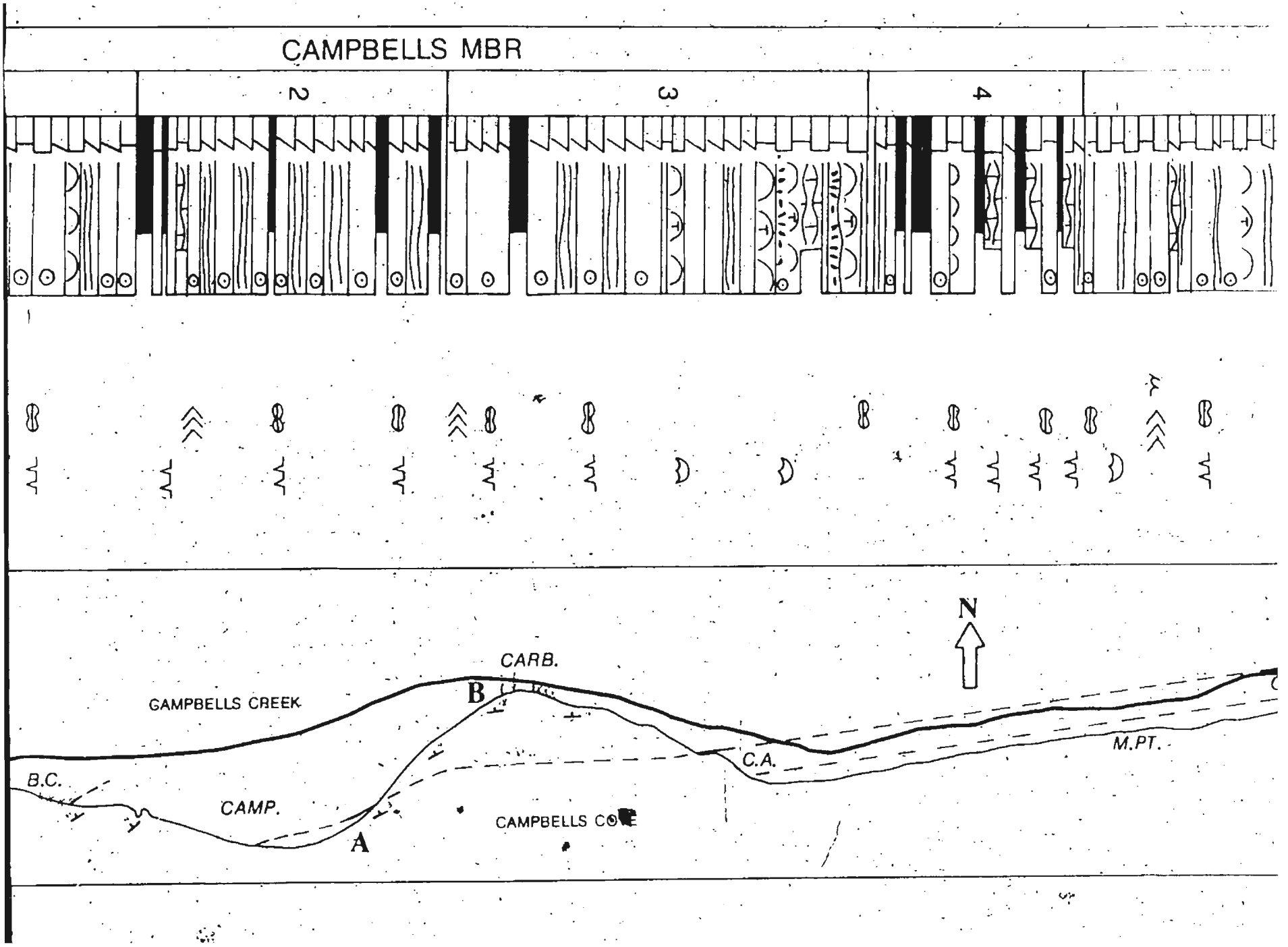
CAMPBELLS MBR
2
3
4
N
CARB.
B
GAMPBELLS CREEK
B.C.
CAMP.
A
CAMPBELLS COVE
C.A.
M.PT.

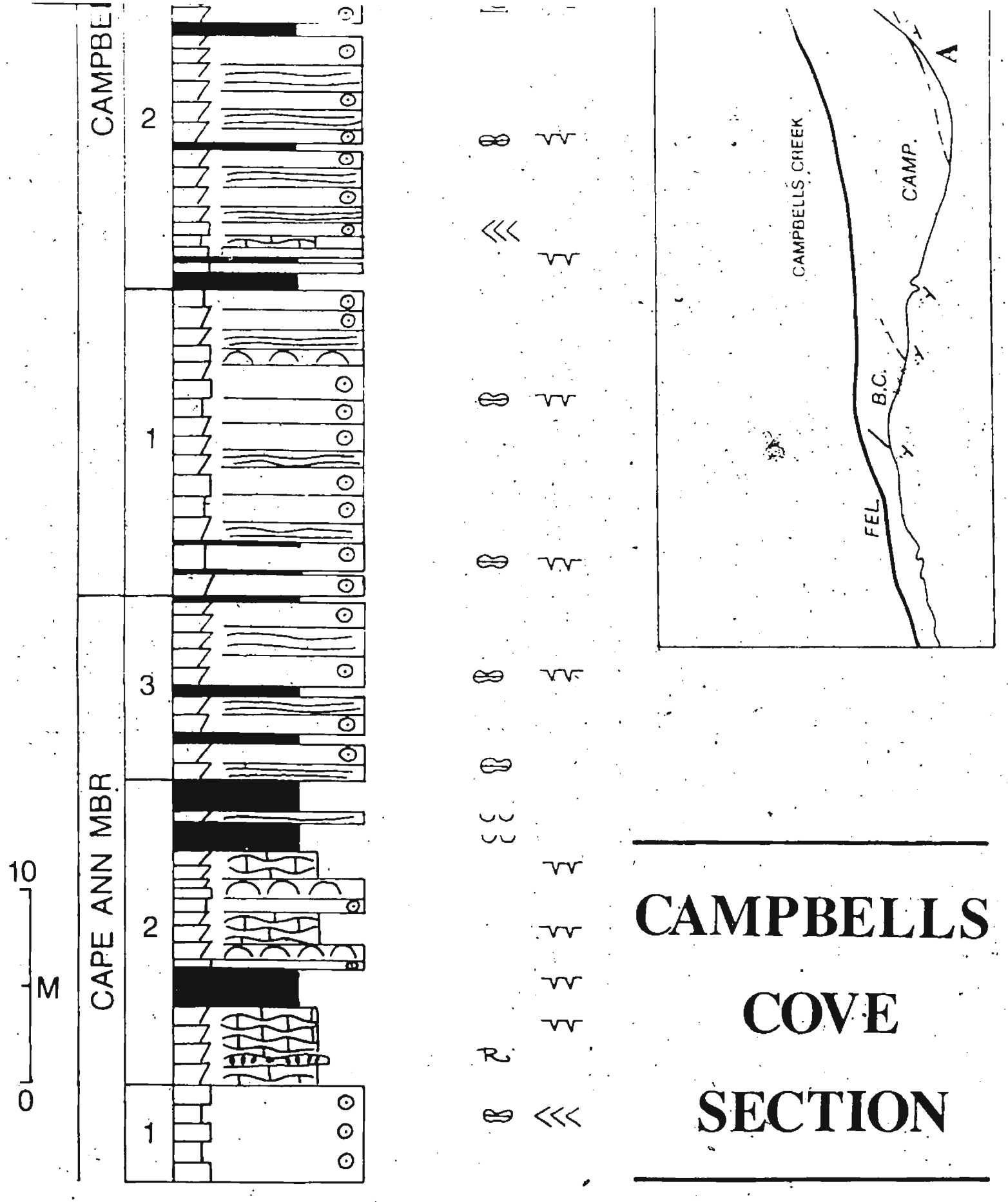
CAMPBELLS CREEK
CAMP.
A
B.C.
FEL
CAMPBELLS
COVE
SECTION
CAMPBELLS
2
1
CAPE ANN MBR
3
2
1
10
M
0
PETIT JARDIN FM

FIG. B.5

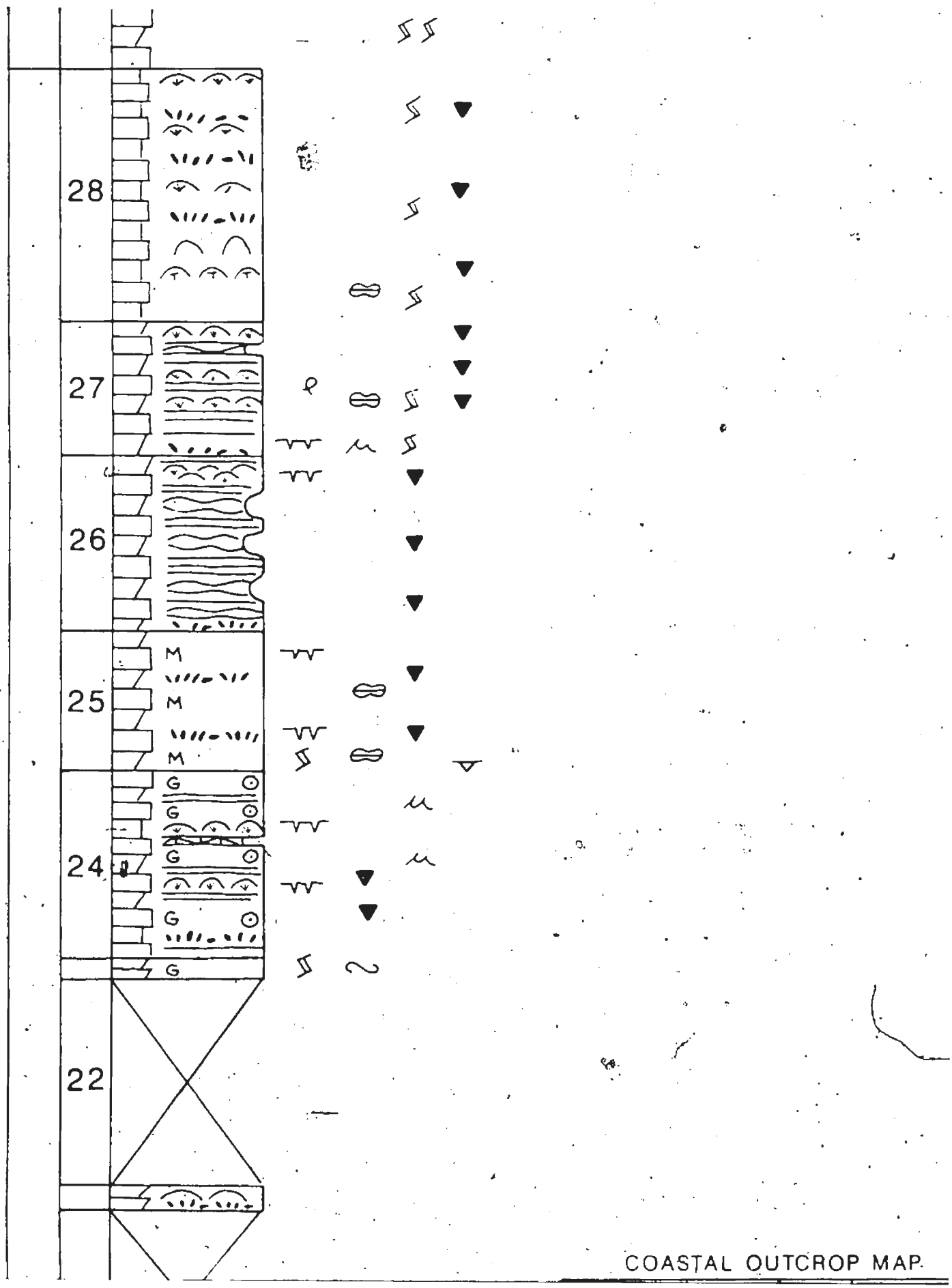

COASTAL OUTCROP MAP

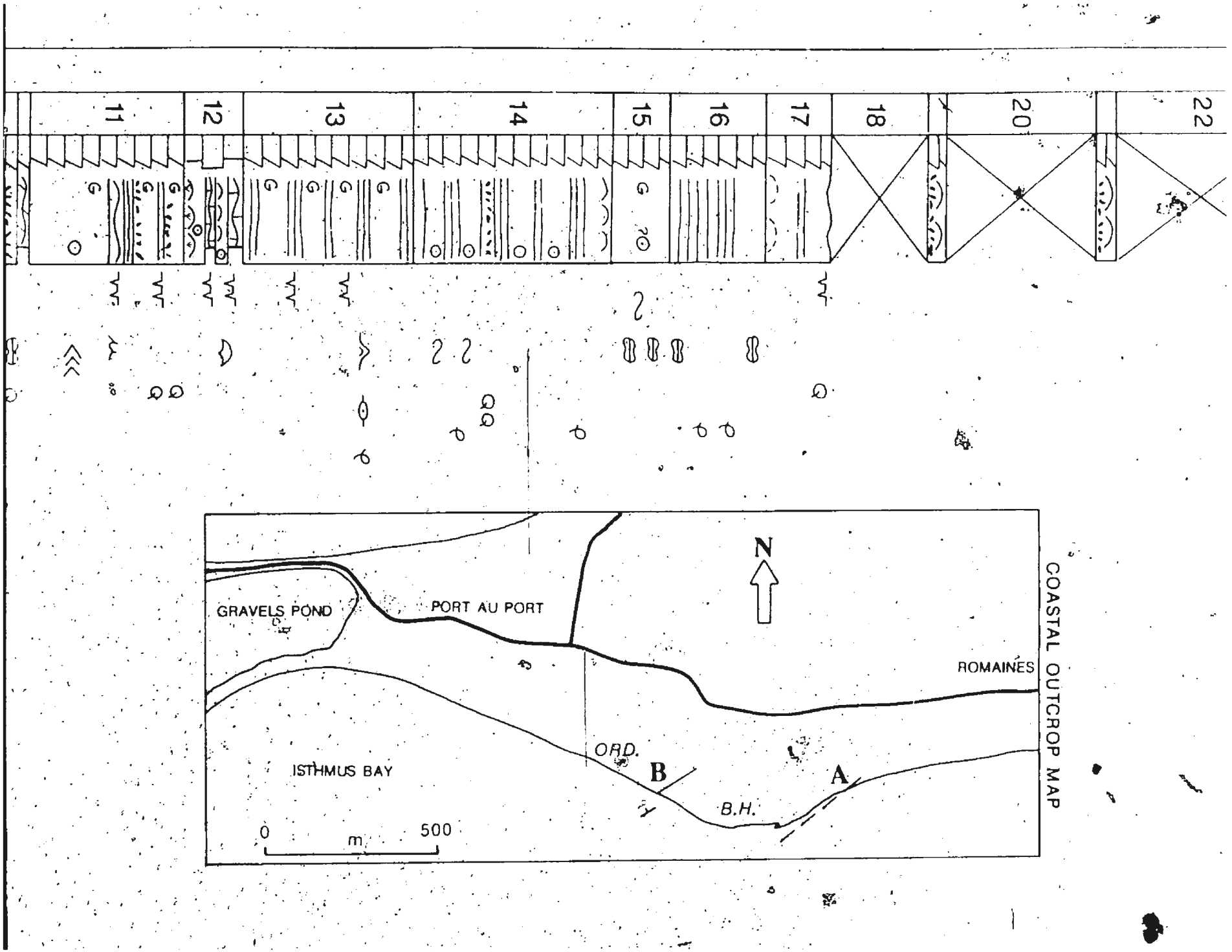
11
12
13
14
15
16
17
18
20
22
GRAVELS POND
PORT AU PORT
ROMAINES
N
ISTHMUS BAY
ORD.
B
A
B.H.
0
m
500
COASTAL OUTCROP MAP

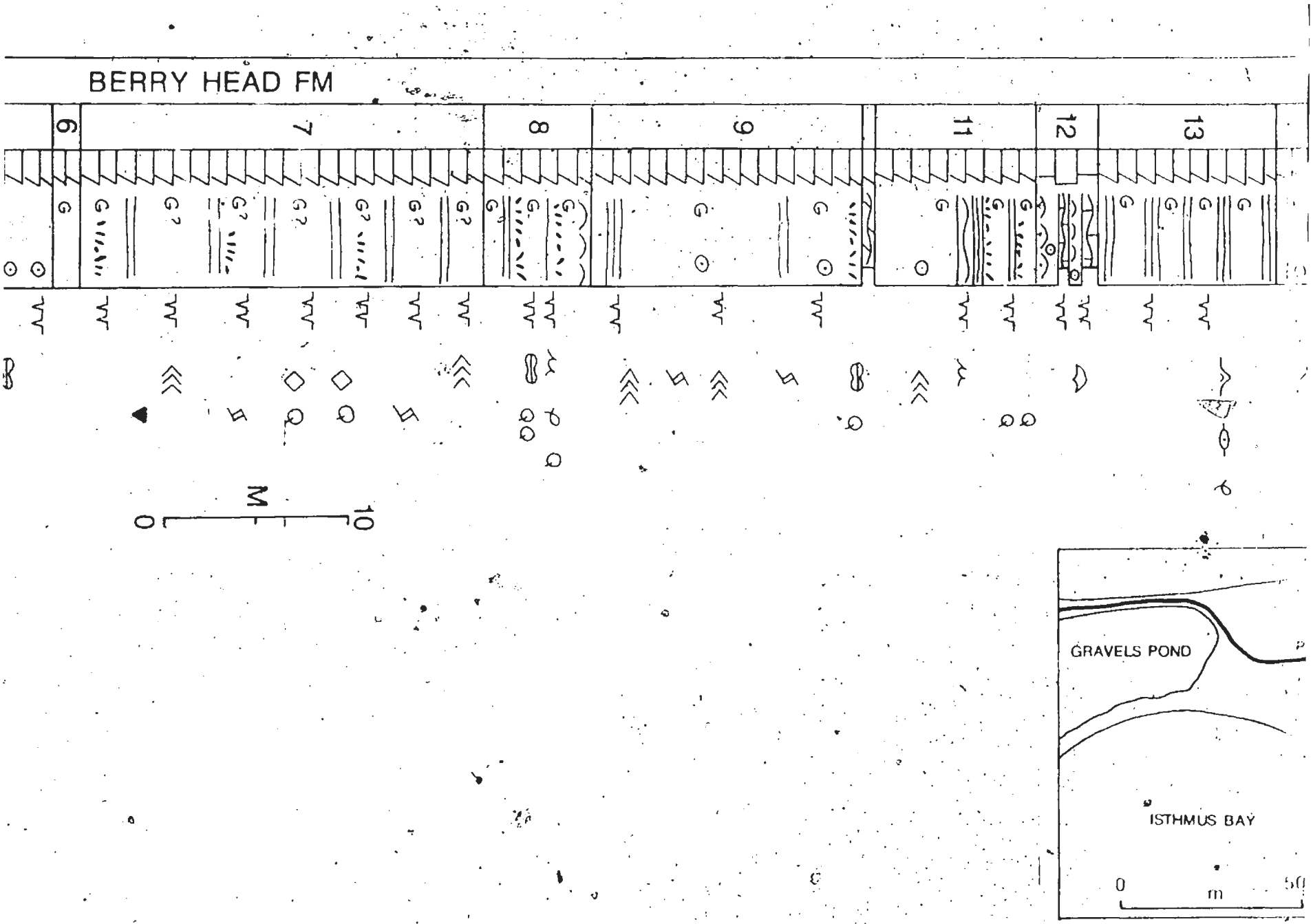
BERRY HEAD FM
6
7
8
9
11
12
13
G
G?
Q
0
M
10
GRAVELS POND
ISTHMUS BAY
0
m
50

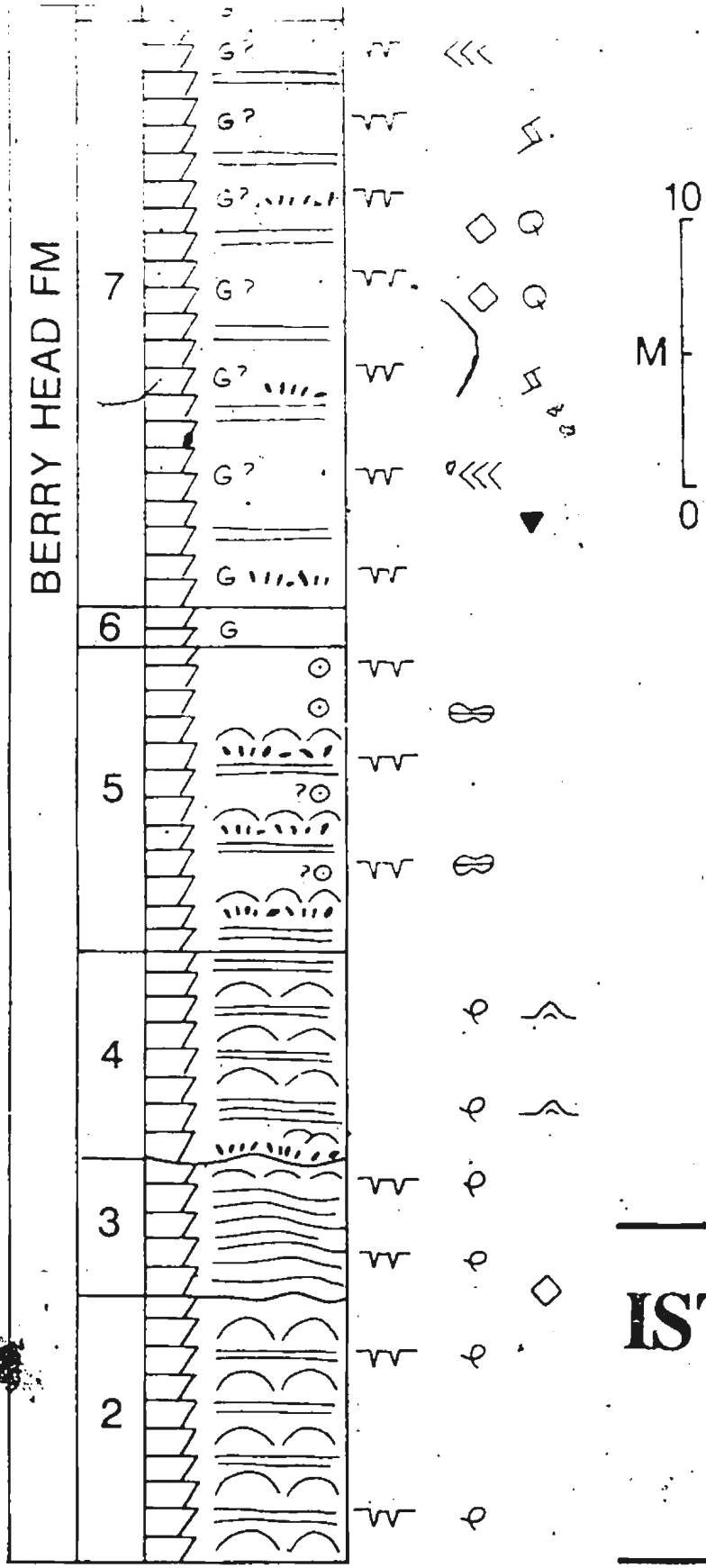

ISTHMUS BAY EAST SECTION

FIG. B.6

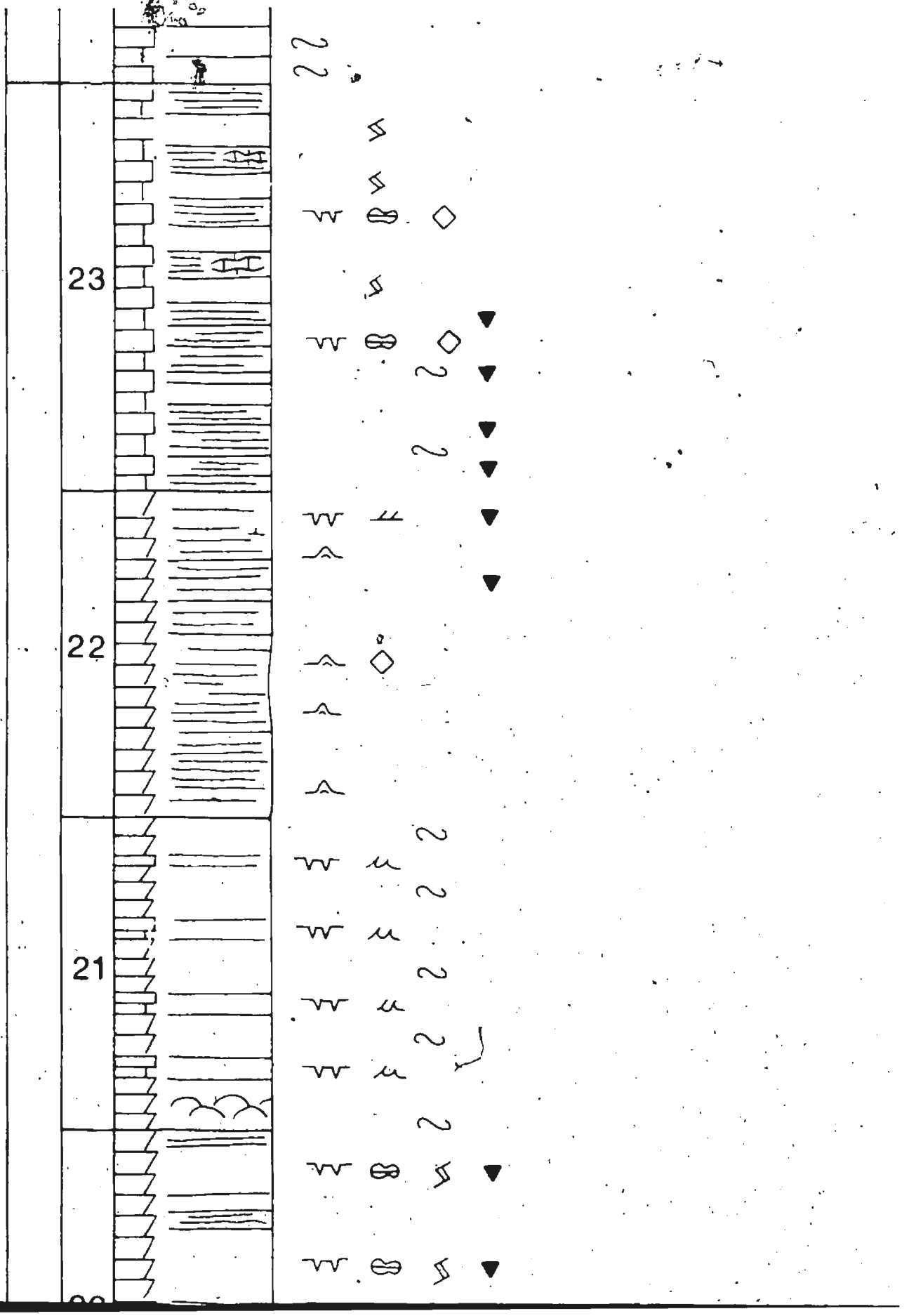
23
22
21

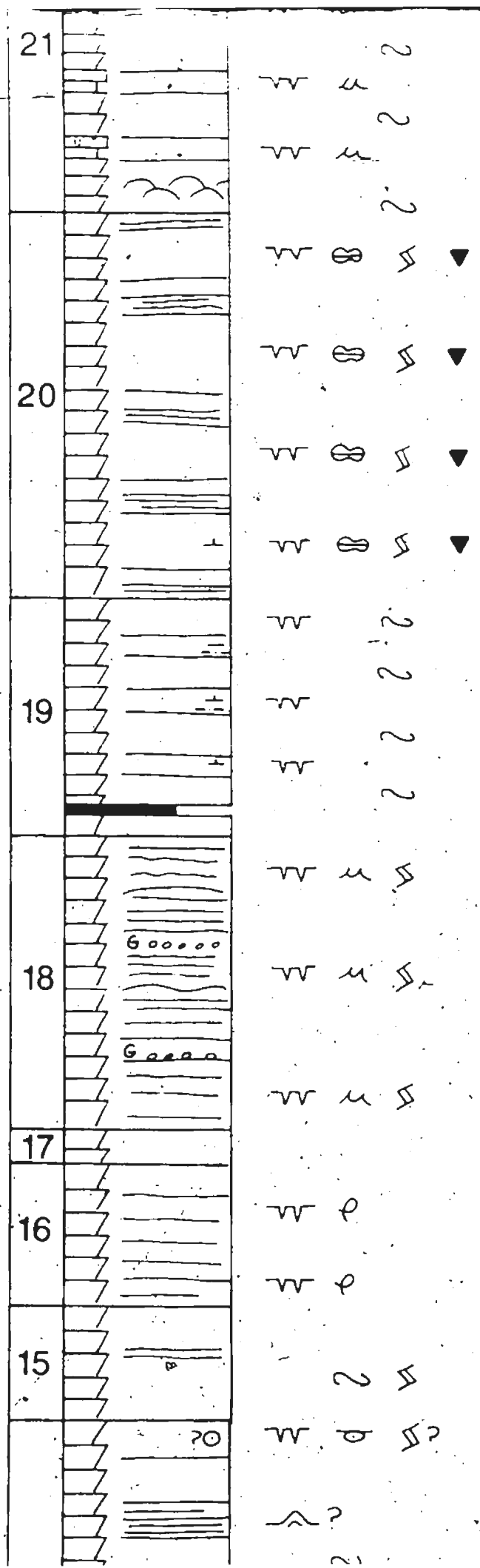
21
20
19
18
17
16
15
G
G
?

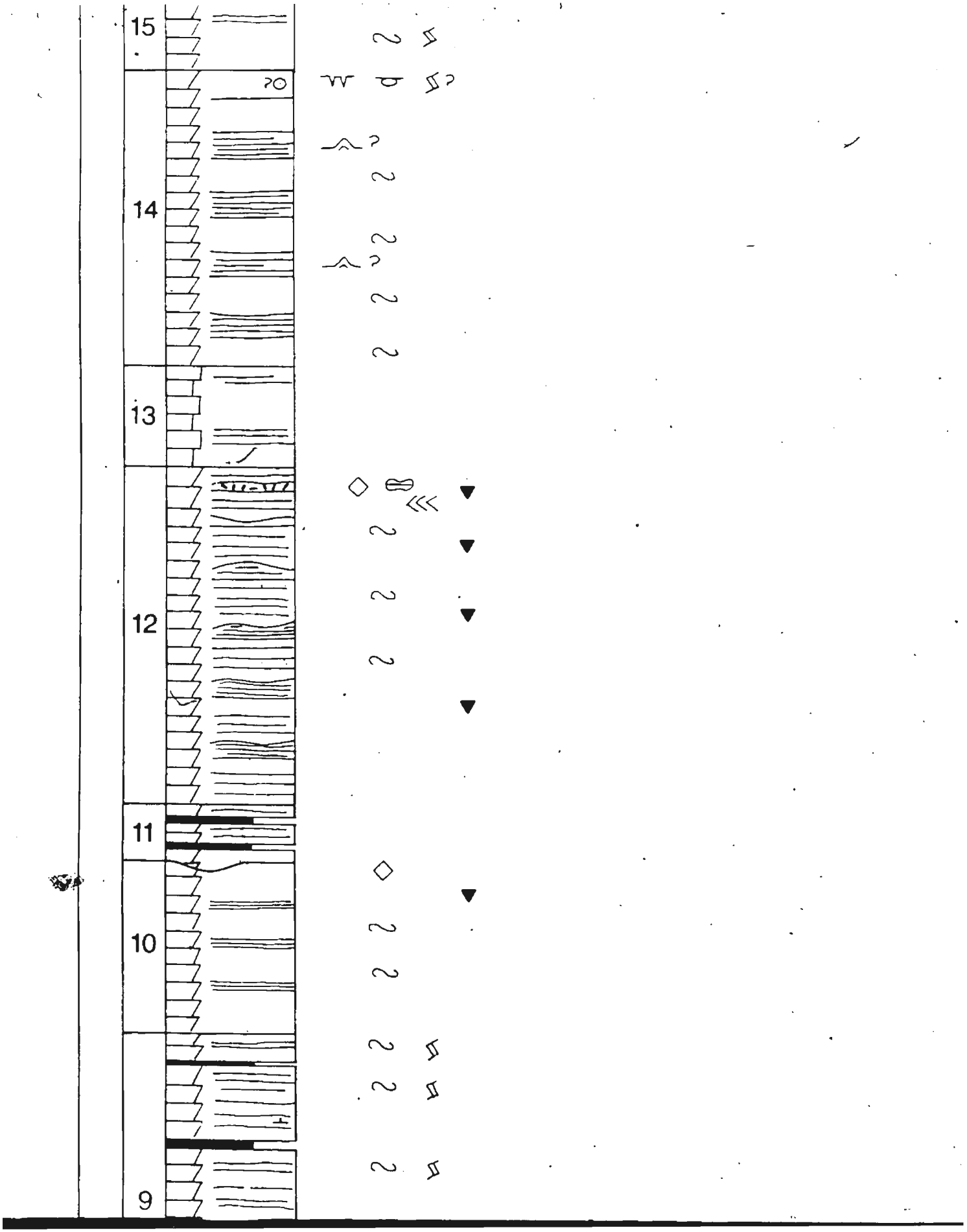
15
14
13
12
11
10
9

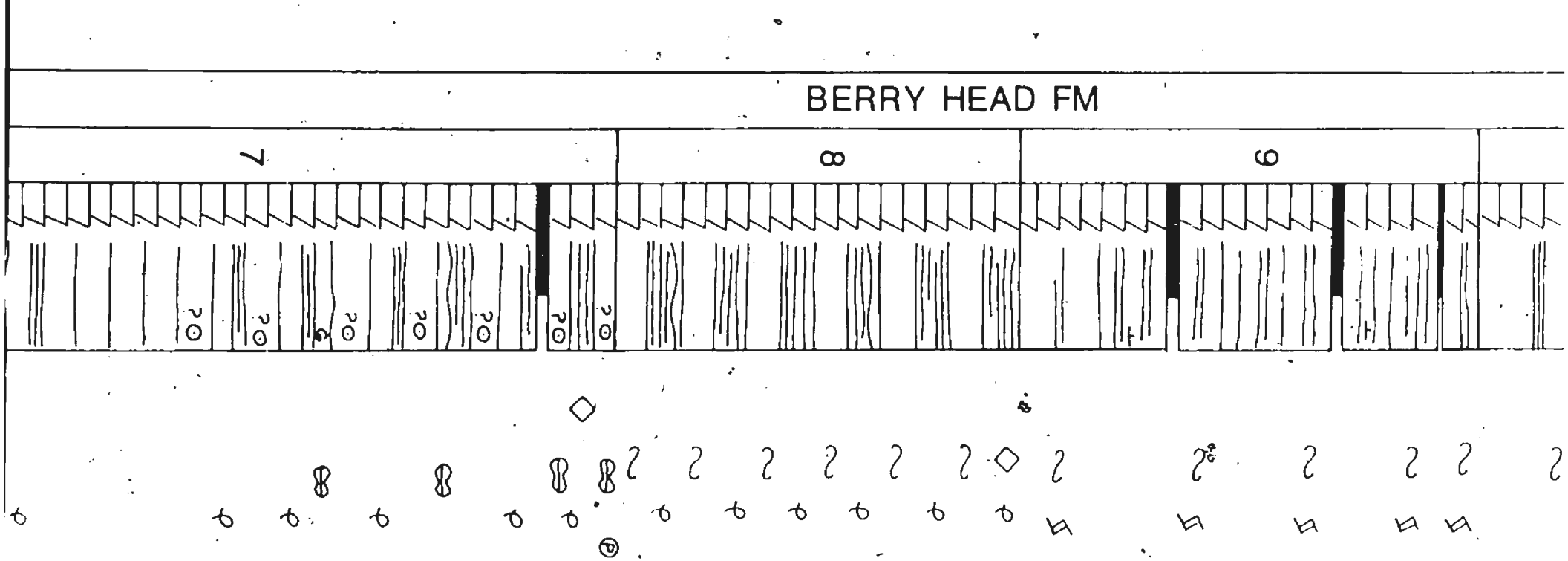
BERRY HEAD FM
7
8
9

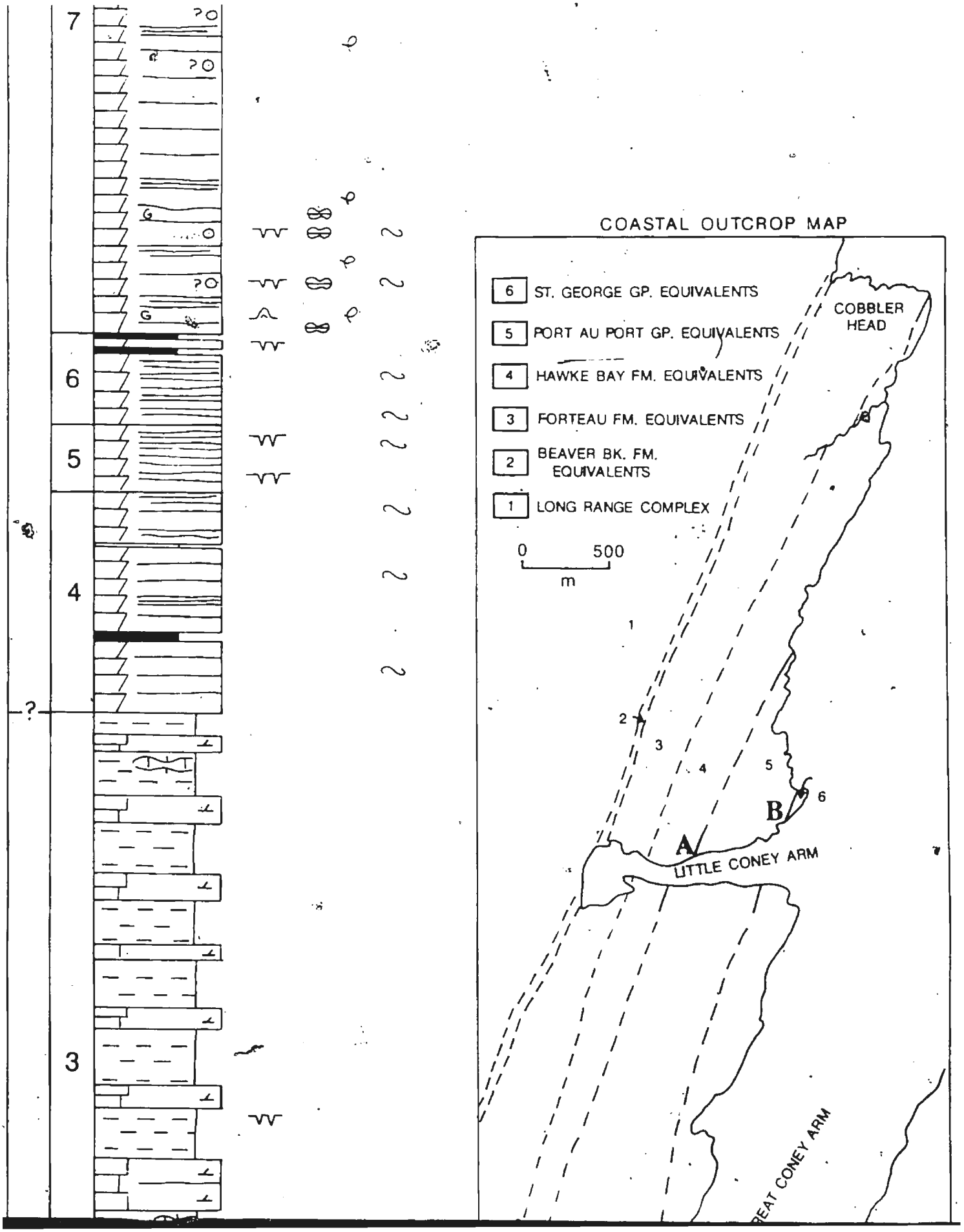
7
6
5
4
3
?
COASTAL OUTCROP MAP
6 ST. GEORGE GP. EQUIVALENTS
5 PORT AU PORT GP. EQUIVALENTS
4 HAWKE BAY FM. EQUIVALENTS
3 FORTEAU FM. EQUIVALENTS
2 BEAVER BK. FM. EQUIVALENTS
1 LONG RANGE COMPLEX
0 500
m
COBBLER HEAD
1
2
3
4
5
6
A
B
LITTLE CONEY ARM
GREAT CONEY ARM

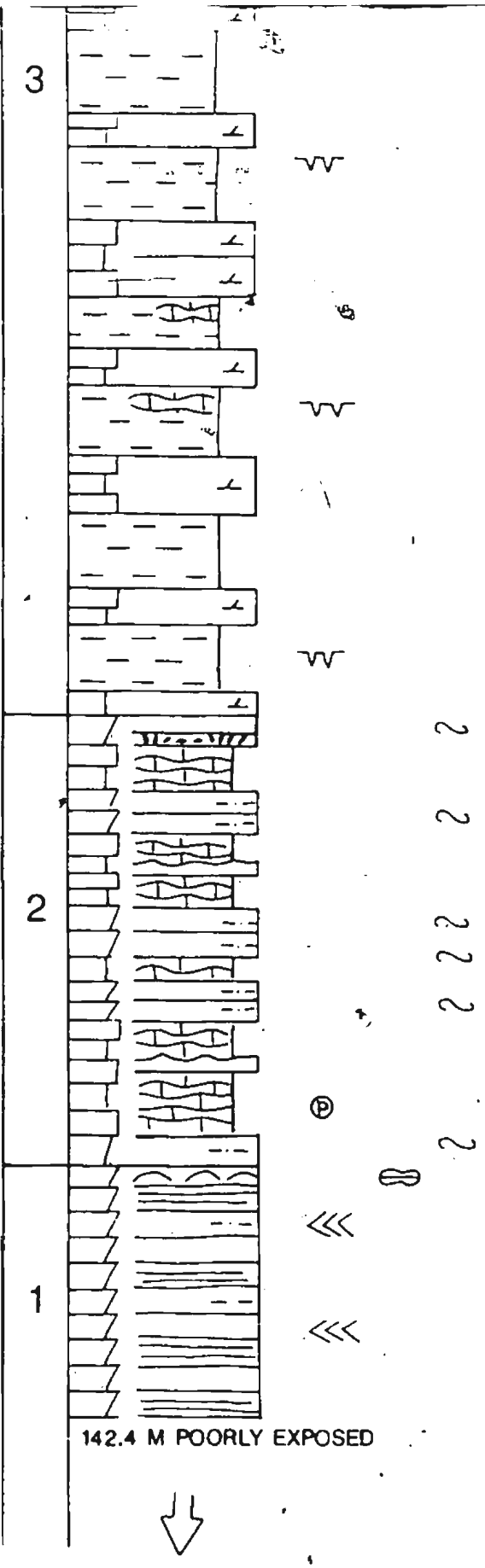

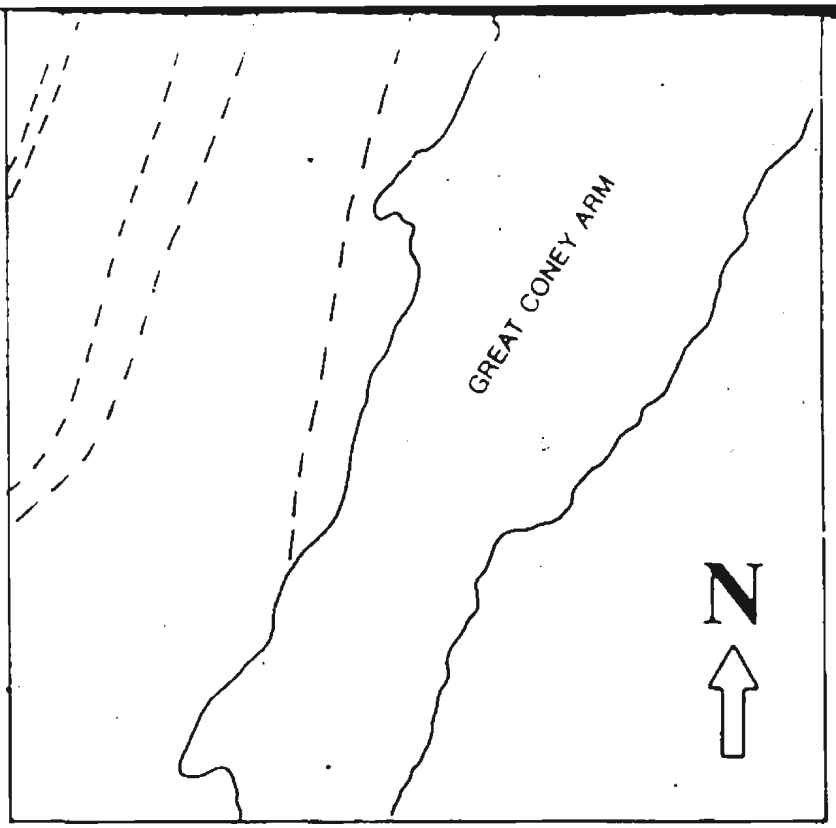

(after Smyth & Schillereff, 1981)

LITTLE CONEY ARM SECTION

WHITE BAY

FIG. B.7

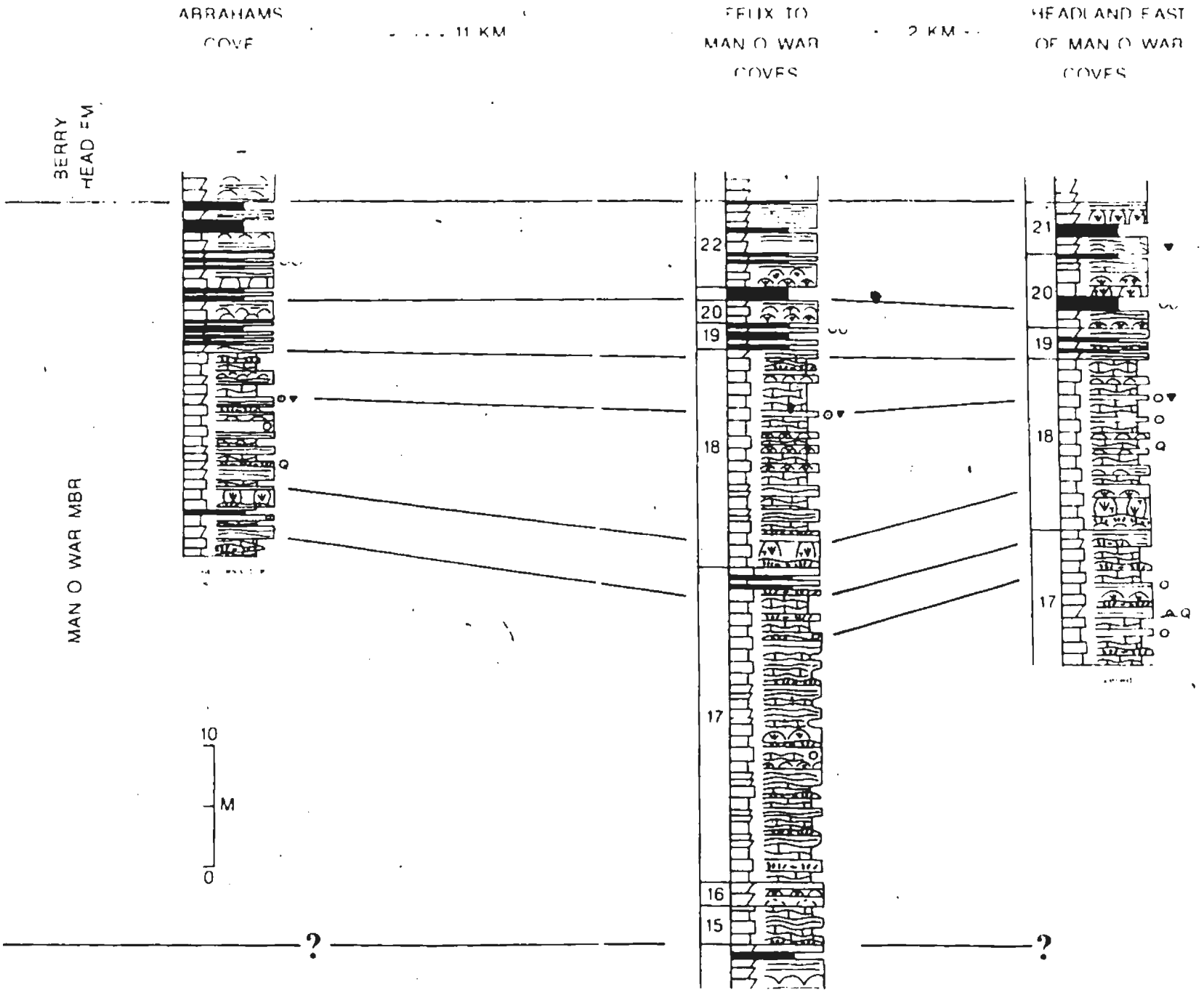

FIG. B.8

FIG. B.8. Correlation of Man O' War Member, Petit Jardin Formation, Port au Port Peninsula

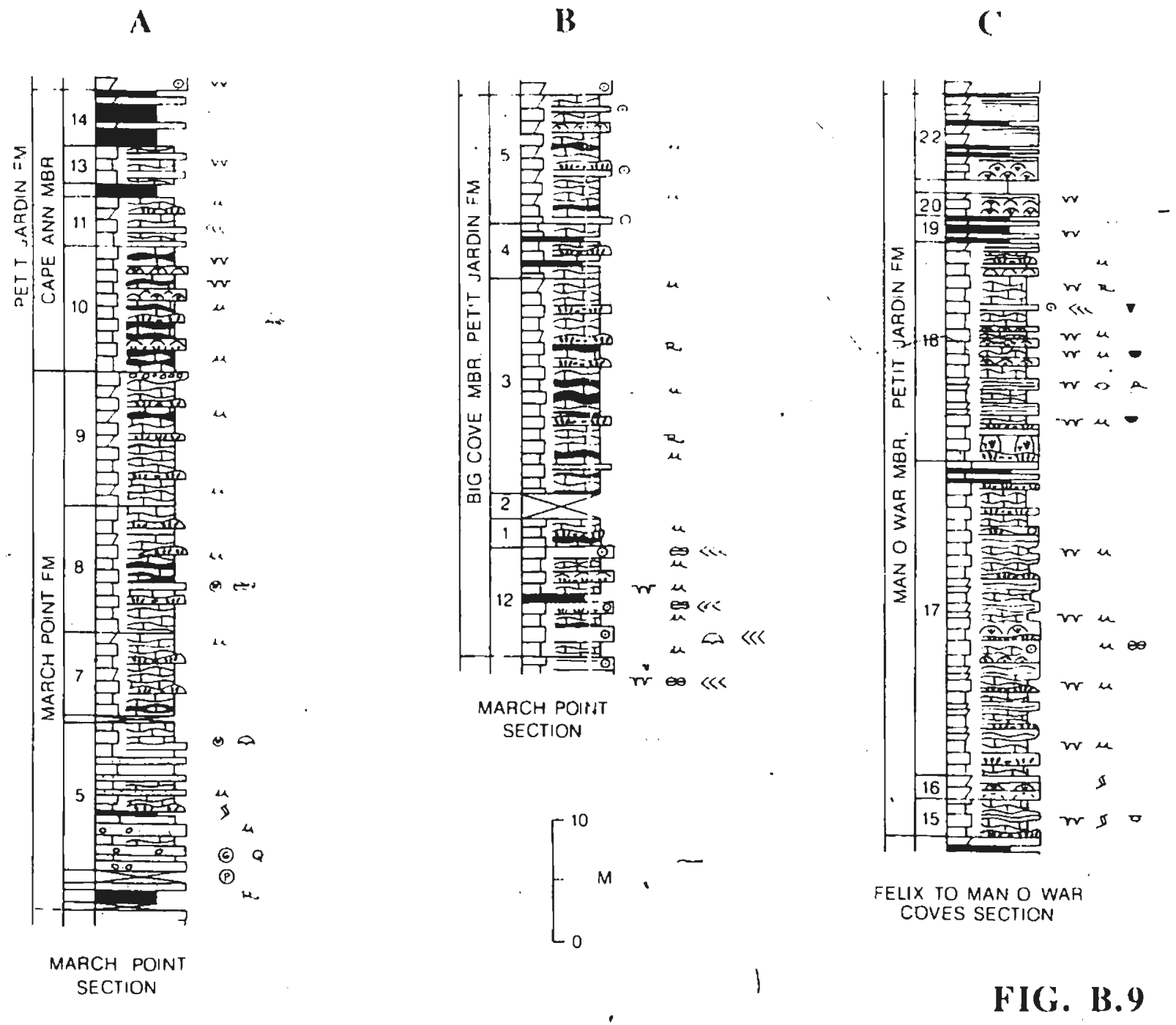

FIG. B.9

FIG. B.9. Shaly Half-Cycles of Grand Cycles A, B, and C, Port au Port Peninsula